THE PERIPHERAL NERVOUS SYSTEM: INJURY AND DISEASE

Tessa Gordon

A thesis submitted to the University of Birmingham for the degree of

DOCTOR OF SCIENCE

School of Clinical and
Experimental Medicine,
University of Birmingham
November 2015

UNIVERSITY OF
BIRMINGHAM

University of Birmingham Research Archive

e-theses repository

This unpublished thesis/dissertation is copyright of the author and/or third parties. The intellectual property rights of the author or third parties in respect of this work are as defined by The Copyright Designs and Patents Act 1988 or as modified by any successor legislation.

Any use made of information contained in this thesis/dissertation must be in accordance with that legislation and must be properly acknowledged. Further distribution or reproduction in any format is prohibited without the permission of the copyright holder.

Dedication

This thesis is dedicated to Phil, Karen, Tanya, David, Maya and Ellie, my wonderful family.

Acknowledgements

My grateful thanks are extended to the 1) University of Birmingham where I received my graduate training and my degree of Doctor of Philosophy under the wonderful supervision of Dr. Gerta Vrbova, 2) the University of Alberta, Alberta, Canada where I received my post-graduate training under the excellent supervision of Dr. Richard Stein and where, subsequently, I was a member of the Faculty of Medicine and Dentistry as a Heritage Foundation for Medical Research Scholar, Senior Scholar, Scientist, Senior Scientist and finally, a Senior Investigator over a period of 33 years, 3) The Hospital for Sick Children where I am currently a senior scientist in the Department of Surgery and where I would like to extend my grateful thanks to Dr. Gregory H Borschel for his friendship and continuing collaboration and, finally 4) to the support and love of my husband, children and grandchildren who are ‘the best’.

Abstract

Poor functional outcomes are frequent after peripheral nerve injuries despite the regenerative support of Schwann cells. Whilst motoneurons and to a lesser extent, sensory neurons survive the injuries, outgrowth of axons across the injury site is slow and the neuronal regenerative capacity is progressively reduced when neurons remain without targets and chronically denervated Schwann cells fail to support axon growth. Strategies including brief low frequency electrical stimulation that accelerates axon outgrowth and, in turn, target reinnervation and functional recovery, have excellent potential for translation to human patients. Other strategies including the insertion of cross-bridges between a donor nerve and a recipient denervated nerve stump, are effective in promoting functional outcomes after complete injuries. During muscle reinnervation the properties of the motoneurons and muscle fibers that they supply are rematched that provide some control of muscle force even when regenerating axons are misdirected to foreign targets. Axon sprouting from intact nerves is effective, although limited, in reinnervating denervated muscle fibers after incomplete injuries and in poliomyelitis. Studies in mouse models of amyotrophic lateral sclerosis however, indicate that sprouting is very limited with rapid and preferential loss of the largest and fastest contracting motor units during the asymptomatic phase of the disease.

Table of contents

I. **Introduction**

II. **Peripheral nerve injury**

1. **Transient regenerative potential of injured neurons**
2. **The molecular bases for the reduced regenerative capacity after delayed nerve repair**
3. **Brief electrical stimulation accelerates growth of axons across the site of injury and surgical repair**

   3.1 Staggered axon regeneration

   3.2 Preferential reinnervation of motor and sensory nerve branches

   3.3 Brief electrical stimulation accelerates axon outgrowth

   3.4 Mechanisms by which electrical stimulation accelerates axon outgrowth

   3.5 Electrical stimulation is effective in promoting nerve regeneration even after delayed nerve surgery in rats and humans
4. **Rematching of the properties of motoneurons and their muscle fibers after nerve injury**

   4.1 The size principle in the motor system is restored after reinnervation

   4.2 Misdirection of regenerating motor nerve fibers with random reinnervation of target muscles
5. **Axonal sprouting after motoneuron loss in partial nerve injuries and after motoneuron death in amyotrophic lateral sclerosis** and **poliomyelitis**

   5.1. Axon sprouting and upper limits of compensation for partial denervation

   5.2 Axon sprouting occurs close to the muscle fibers that the motor nerve innervates

   5.3 Regeneration rather than sprouting through nerve autografts placed end-to-side

   5.4 Excess neuromuscular activity is deleterious for sprouting and retention of enlarged motor units

   5.5 Preferential loss of fast motor units in a transgenic mouse model of amyotrophic lateral sclerosis

Synopsis

I. Introduction

Peripheral nerve regeneration is the growth of lost axons from the stump of the remaining crushed or transected nerve: regenerating axons grow into the denervated nerve stumps where the axons undergo Wallerian degeneration and the remaining Schwann cells in the empty endoneurial sheaths support axon regeneration (Fu and Gordon, 1997[1]). Motor axon sprouting describes axonal outgrowth from intact intramuscular nerve sheaths to reinnervate partially denervated muscles. Yet functional outcomes are frequently poor after nerve injuries particularly for injuries that are sustained at short distances from the cell bodies of motoneurons in the spinal cord and lower brainstem and from the nerves with their cell bodies in the dorsal root ganglia alongside the spinal cord. This is despite the well-recognized capacity for Schwann cells, the myelinating glial cells of the peripheral nervous system, to support axon regeneration. Our major contributions to this field include findings that 1) the long delays incurred during axon regeneration through denervated distal nerve stumps result in progressive decline in the regenerative capacity of the neurons and of the regenerative support of the Schwann cells (Fu and Gordon, 1995[2,3]; Gordon et al., 2011[4]); 2) the elucidation of the molecular bases for reduced regenerative capacity of chronically injured neurons and of Schwann cell support in the nerve stumps that account for poor functional recovery; 3) brief low frequency electrical stimulation of injured neurons elevates cAMP and growth associated genes to accelerate axon outgrowth of motor and sensory neurons (Al-Majed et al., 2000[5,6]; Brushart et al., 2002[7]; Al-Majed et al., 2004[8]; Geremia et al., 2007[9]; Aglah et al., 2008[10]). In turn, the stimulation promotes earlier contact of the regenerated axons with denervated targets and enhanced functional recovery in rats and humans after both immediate and delayed nerve repair (Eberhardt et al., 2006[11]; Gordon et al., 2010[12]; Elzinga et al., 2015[13]). The same stimulation regimen promotes axon outgrowth of injured central axons of rat sensory nerves (Udina et al., 2008[14]); 4) the matching properties of motoneurons and their muscle fibers are

restored after nerve injury, axon regeneration and muscle reinnervation; and 5) axonal sprouting allows some reinnervation of denervated muscle fibers after partial nerve injuries and in patients suffering motoneuron diseases that include poliomyelitis and amyotrophic lateral sclerosis. The capacity is normally limited and is more so in neuromuscular disease (Tam et al, 2001[15]; Hegedus et al, 2007[16]; 2008[17]). In this synopsis of my work, I elaborate briefly on these contributions to the biology of peripheral nerve injury, axon regeneration and sprouting, describing these contributions within the context of a large body of literature which I have reviewed in several published reviews. These include Fu and Gordon, 1997[1]; Gordon et al, 2004[18]; Gordon, 2009[19]; Gordon and English, 2015[20].

II. Peripheral nerve injury

1. Transient regenerative potential of injured neurons

Peripheral nerve crush and transection injuries disrupt axonal continuity that isolates the axons from their cell bodies. W*allerian degeneration* ensues with denervated Schwann cells that had myelinated the large axons, proliferating and taking part in the removal or phagocytosis of myelin and axon debris. The cells form elongated processes within the vacated endoneurial tubes that, in turn guide and support axons as they regenerate toward denervated end-organs. I have reviewed these processes in several reviews that include Fu and Gordon, 1997[1] and Gordon and English, 2015[20]. Yet functional recovery is frequently poor when time and distance isolate injured neurons from targets (chronic axotomy) and leave the distal nerve stump and target organs chronically denervated for long periods.

We demonstrated in 1995 that it is *not* the progressive fat replacement of chronically denervated end-organs that accounts for the poor functional recovery with time and distance as has been, and still is claimed (Fu and Gordon, 1995[2-3]). We used a cross-suture paradigm with and without the insertion of a nerve autograft to prolong either neuronal axotomy, Schwann cell denervation, or muscle denervation, demonstrating definitively that the regenerative ability of chronically axotomized

motoneurons *and* the capacity of chronically denervated Schwann cells to support axonal regeneration each decline exponentially; the sum of the effects account for progressive failure of nerve regeneration and target reinnervation (Fu and Gordon, 1995[2-3]; Boyd and Gordon, 2002[21]; 2003[22]; Gordon et al., 2011[4]). We determined the success of axon regeneration quantitatively at least four months after the nerve repair by first, recording the contractile forces of muscle and their motor units elicited by stimulation of the regenerated nerve and of single motor axons in dissected ventral root filaments (Fu and Gordon, 1995[2-3]; Gordon et al., 2011[4]) and second, by using fluorescent dyes to backlabel and count the motoneurons that regenerated their axons into the distal nerve stump (Sulaiman and Gordon, 2000[23]; Boyd and Gordon, 2001[24]; 2002[21]; 2003[22]). The finding that regenerated axons were myelinated *and* recovered their normal dimensions demonstrated that the normal interaction of regenerating axons and surviving Schwann cells leads to their myelination despite the 'hostile' growth environment provided by the chronically denervated nerve stumps (Sulaiman and Gordon, 2000[23]). These few nerves reinnervated three-four times as many muscle fibers as they did formerly, demonstrating their capacity to survive and to accept innervation (Fu and Gordon, 1995[3]). The muscle recovery likely involved satellite muscle cells that restored muscle fibers albeit smaller in diameter that in turn was explained by limited available numbers of these cells (Fu and Gordon, 1995[3]; Gordon et al., 2011[4]).

2. The molecular bases for the reduced regenerative capacity after delayed nerve repair

Neurons that are normally in a transmitting mode, releasing neurotransmitters that convey information from nerve to nerve and nerve to muscle (Fu and Gordon, 1997[1]; Gordon and English, 2015[16]). After injury, the neurons enter into a growth permissive state in which we demonstrated with *in situ* hybridization that they express many growth associated genes of which some transcribe neurotrophic factors and their receptors (Al-Majed et al., 2000[6]) and cytoskeletal proteins that include actin and tubulin (Al-Majed et al., 2004[8]; Gordon and English, 2015[20]). The upregulation is transient however, the genes being downregulated with time (Gordon et al., 2015[20]). The genes are

upregulated again when the proximal nerve stump is cut or refreshed for surgical repair but the expression is either reduced in magnitude or declines more rapidly than after the first injury (Gordon et al., 2015[25]). The fact that a refreshment injury of axotomized neurons leads to the re-expression of growth associated genes shows the signal for the upregulation of the genes is not related to the isolation of the nerves from their targets but rather, is directly associated with the nerve injury itself (Gordon et al., 2015[25]). The expression of growth associated genes in the distal nerve stump is also transient with neurotrophic factors and their p75 receptor declining from the peak reached within a week to pre-operative levels within one to two months (Hoke et al., 2002[26]; You et al., 1997[27]; Gordon et al., 2015[25]). Hence the progressive decline in regenerative capacity of axotomized neurons and of the regenerative support of the denervated Schwann cells is linked to the transient expression of their growth associated genes that culminates in limited and disappointing functional recovery over time.

3. Brief electrical stimulation accelerates growth of axons across the site of injury and surgical repair

3.1 Staggered axon regeneration

Whilst axon regeneration was reputed to proceed at a rate of 1-3 mm/day after a latent period of a few days, our use of backlabeling at several time points after transection and microsurgical repair of rat femoral nerve demonstrated that axon regeneration is asynchronous: the numbers of motoneurons that regenerated their axons increased progressively with all the neurons regenerating axons over a distance of 25 mm 8-10 weeks after the repair (Al-Majed et al., 2000[5]). As *all* the neurons were expected to regenerate their axons over the distance within 2-3 weeks, the lengthy time period was a surprise. We surmised that the long period for all the nerves to regenerate from the suture site was due to ‘staggered’ outgrowth of axons across the site. This was indeed the explanation. By applying a retrograde fluorescent dye to regenerated axons 1.5 mm from the suture site, we counted the motoneurons whose axons had regenerated across the suture site after four to 28 days (Brushart et al., 2002[7]). We

found that the numbers of neurons increased progressively to a maximum over a protracted period of three to four weeks during which the outgrowing axons 'wandered' across the suture site concurrent with a progressive but slow entry of Schwann cells through disorganized extracellular matrix (Brushart et al., 2002[7]). Hence axons grow out from the proximal nerve stump in an asynchronous fashion and 'stagger' across the suture site prior to entering into the endoneurial tubes.

3.2 Preferential reinnervation of motor and sensory nerve branches

In the first two weeks after femoral nerve repair, retrograde labelling of the motoneurons regenerating axons into the motor branch to the quadriceps muscle and into the sensory saphenous nerve branch to the skin revealed that the motoneurons regenerated their axons randomly into the two branches (Al-Majed et al., 2000[5]). Thereafter, *all* the motoneurons regenerated their axons into the appropriate endoneurial tubes of the motor nerve, demonstrating delayed but preferential motor reinnervation of appropriate endoneurial tubes (Al-Majed et al., 2000[5]). Similarly there is also preferential reinnervation of appropriate sensory pathways by sensory nerves (reviewed in Gordon and English, 2015[20]). In my invited perspective of the findings of Hoke and Brushart and their colleagues in the same journal that Schwann cells of motor and sensory endoneurial tubes express different neurotrophic factors, I calculated that preferential entry of motor and sensory axons into the appropriate motor and sensory pathways, respectively, occurs concomitant with the upregulation of the growth factors in the specific pathways (Gordon, 2014[28]). To date, this explanation is the most plausible for the emergence of preferential reinnervation after the initial random reinnervation.

3.3 Brief electrical stimulation accelerates axon outgrowth

In the same experiments of 2000, we implanted a stimulator with which to continuously stimulate the transected and repaired femoral nerve (Al-Majed et al., 2000[5]). We found that a two week period of continuous 20 Hz electrical stimulation

profoundly shortened the time course of the reinnervation of the nerve branches; all motoneurons grew their axons into the nerve branches within three weeks with electrical stimulation as compared to 8-10 weeks with sham stimulation. Further, we demonstrated that this stimulation period could be shortened to one hour with the same effect. The efficacy of the one hour 20 Hz electrical stimulation generated considerable attention and many studies followed, using several different nerves to verify this efficacy of the one hour period of low frequency stimulation (see references in Elzinga et al., 2015[13]). Moreover, the brief electrical stimulation accelerated target reinnervation and functional recovery (Eberhardt et al., 2006[11]) as we subsequently demonstrated in a human study of patients after carpal tunnel surgical release of the compressed median nerve (Gordon et al., 2010[29]). The efficacy of the brief period of stimulation in the animal and human studies is not only important for clinical application of the technique but, the finding that a one hour stimulation period immediately after surgical repair was serendipitous in the sense that we found that *only* a one hour period was effective in promoting the regeneration of sensory nerves; longer time periods were ineffective because prolonged sensory nerve stimulation downregulates receptors for neurotrophic factors (Geremia et al., 2007[9]).

Another three experiments were described with findings of seminal importance. The first was that tetrodotoxin block of action potential conduction to the cell bodies of the neurons eliminated the effect of the stimulation (Al-Majed et al., 2000[5]; Geremia et al., 2007[9]). Second, the brief electrical stimulation accelerated axon outgrowth across a suture site but did *not* accelerate the rate of axon growth within the endoneurial tubes (Brushart et al., 2002[7]). Third, we found that the same one hour period of 20Hz electrical stimulation promotes axon outgrowth in the central nervous system when the central and not the peripheral process of the bipolar sensory neurons was transected (Udina et al., 2008[14]).

3.4 Mechanisms by which electrical stimulation accelerates axon outgrowth

Having demonstrated that the effect of the electrical stimulation was mediated via the neuronal soma (Al-Majed et al., 2000[5]), we went on to show that the stimulation

accelerated the upregulation of growth associated genes that included the neurotrophic factors and their receptors in the stimulated neurons (Geremia et al., 2007[9]; Al-Majed et al., 2000[6]) followed by the upregulation of genes that transcribe cytoskeletal proteins and growth associated proteins (Al-Majed et al., 2004[8]). Later findings that drugs that elevated cAMP increased neurite outgrowth from motoneurons in culture (Aglah et al, 2010[10]) and, that rolipram mediated elevation of intracellular cAMP mimicked the effect of electrical stimulation in accelerating axon outgrowth regeneration *in vivo* (Udina et al., 2010[30]), established cAMP as a mediator upstream of the neurotrophic factors.

3.5 Electrical stimulation is effective in promoting nerve regeneration even after delayed nerve surgery in rats and humans

Surgical repair of injured nerves almost invariably involves delays and hence, reduced regenerative capacity of the nerves and their growth environment (Fu and Gordon, 1997[1]). It was therefore essential to establish whether the brief electrical stimulation that we had shown to be so effective in accelerating nerve regeneration and functional recovery after immediate nerve repair (Al-Majed et al., 2000[5]; Eberhardt et al., 2006[11]), could be efficacious for nerve regeneration over time and distance. In a proof of principle study, we selected patients undergoing carpal tunnel release surgery who had suffered the loss of ~50% of their median motor nerve supply to the muscles of the thenar eminence in the hand (Gordon et al., 2010[12]). The number of functional motor units in the thenar eminence was estimated by electromyography pre- and post-operatively from the ratio of the amplitudes of the compound muscle action potential recorded in response to median nerve stimulation and, of the mean unitary muscle action potential recorded in response to stimulation of single median axons (Gordon et al., 2010[12]). In half the patients, we inserted wires above the carpal tunnel for the one hour period of 20 Hz continuous electrical stimulation of the median nerve proximal to the site of nerve injury.

The results were striking because the electrically stimulated neurons regenerated *all* their axons and reinnervated the thenar eminence within 6-8 months to restore movement and sensation in stark contrast to the small but insignificant increase in the

numbers of motor nerves that reinnervated the target muscles in the absence of electrical stimulation (Gordon et al., 2010[12]). These findings were particularly remarkable given that the injuries were incurred years before the recordings and the surgery and that, even over the 100 mm distance from the injury site to the thenar eminence, the time of regeneration and target reinnervation is slow.

Our later rat study demonstrated that the same brief stimulation regimen is effective in significantly increasing the regenerative capacity of both motor and sensory neurons and of accelerating target reinnervation after chronic axotomy of the injured neurons and/or chronic denervation of the distal nerve stumps (Elzinga et al., 2015[13]). Indeed, the brief electrical stimulation was as effective in promoting nerve regeneration after chronic injuries it is after immediate nerve repair (e.g Al-Majed et al., 2000[5]).

Our findings that exogenous nerve growth factors, including brain and glial derived neurotrophic factors delivered to the injury site significantly improve nerve regeneration after chronic axotomy (Boyd and Gordon, 2002[21]; 2003[22]) argue that the positive effect of the electrical stimulation arises at least in part, from the elevated expression of regeneration associated genes in the neurons (Al-Majed et al., 2000[6]; Al-Majed et al, 2004[8]). Since regenerating axons release mitogens, it is likely that these promoted Schwann cell proliferation as they normally do, culminating in significantly improved nerve regeneration and target reinnervation after chronic nerve injury. We are currently improving our local delivery of growth factors as well as tacrolimus (FK506) to the surgical repair site, both of which have been shown to improve nerve regeneration after chronic axotomy (Boyd and Gordon, 2002[21]; Boyd and Gordon, 2000[22]; Sulaiman et al., 2002[31]).

4. Rematching of the properties of motoneurons and their muscle fibers after nerve injury

4.1 The size principle in the motor system is restored after reinnervation

There is normally a direct relationship between the size of motoneurons and the contractile force generated by the muscle fibers that each motoneuron supplies (Gordon

and Stein, 1982[32]). Because motoneurons are activated in order of their size, the progressive increase in contractile force generated by the muscle ensures sufficient muscular contraction for controlled movement, the so-called size principle of Henneman (Gordon et al., 2004[33]). We carried out a number of studies of nerve regeneration and muscle reinnervation in the cat to examine the properties of regenerated hindlimb nerves and reinnervated muscles as well as the properties of single motor nerves and the muscle fibers that they reinnervated after nerve injury (Gordon and Stein, 1982[32]). These experiments were unique in the sense that nerve regeneration had not formally been examined from the point of view of the organization of motor unit properties and that, using chronic recording electrodes implanted into the cat hindlimb, we were able to follow the events over time. Our primary findings were 1) that the nerves proximal to the injury site decrease in diameter as evaluated electrophysiologically from unitary action potentials recorded on the nerve; they recover only when functional contacts are remade, an important finding that clarified the determinants of nerve fiber size (Gordon and Stein, 1982[32]). Second, we found that the size relationships that we found between motor nerves and the muscle fibers they supply prior to injury. did not return immediately after muscle reinnervation because, after transection injuries, regenerating nerves do not reinnervate the muscle fibers that they formerly supplied (Gordon and Stein, 1982[32]; Tötösy de Zepetnek et al., 1992[34]). Nonetheless the size relationships are restored with time as the size of the motor nerves and the muscle fibers recovered (Gordon and Stein, 1982[32]; Gordon et al., 2004[33]), and 3) because the size of the motoneurons that are regenerating their nerves was found to determine the number of denervated muscle fibers that each neuron reinnervated in a similar manner as in the normal neuromuscular system, the size principle was re-established (Tötösy de Zepetnek et al., 1992[34]). The same size-dependent branching of nerves with preservation of the size principle was demonstrated 4) when intact nerves sprout axons to reinnervate denervated muscle fibers in partially denervated muscles, increasing motor unit contractile forces 5-8 fold without changing the size of the nerves (Rafuse et al, 1992[35]; Gordon and Rafuse 2001[36]) and 5) when reduced numbers of motor nerves regenerated and reinnervated many more muscle fibers than normal, the reinnervation process again obeyed the size principle with the size of the motor nerves determining

the contractile force and the number of reinnervated muscle fibers (Rafuse et al, 1992[35]). Finally 6) evidence that the conversion of the properties of the motoneurons as well as those of the muscle fibers that they reinnervate by electrically stimulating the nerves for a total of 12 hours per day in an on-off manner throughout each day for periods of time of up to a year, provided the ultimate evidence of the resilience of the size principle (Gordon et al., 1997[37]; Munson et al., 1997[38]). Under these conditions, the motoneurons became more similar to one another in their properties and the range of contractile forces and contractile speeds of the motor units decreased. Even so, the diversity of the neuromuscular properties was sufficient to demonstrate the relationship between motoneurons and their muscle fibers. When the nerve to the muscle was transected and surgically repaired prior to the onset of the daily electrical stimulation, again for long periods of time during and after muscle reinnervation, the size relationships were also re-established (Gordon et al., 2004[33]).

These many lines of evidence for the resilience of the size principle demonstrate that the size relationships are not restored because of the different daily patterns or amounts of activity. Rather, it is the size of the motoneurons per se, or more probably, the properties of the neurons that are size dependent and in turn, determine the matching of motoneurons and muscle properties that characterize the neuromuscular system and play a central role in the control of movement.

4.2 Misdirection of regenerating motor nerve fibers with random reinnervation of target muscles

The failure of regenerating motor axons to ‘find’ their original muscle fibers during muscle reinnervation is a generalized finding. In a rat model of nerve injury in which the common nerve to the lateral gastrocnemius and soleus muscles was cut and surgically repaired, we showed that the regenerating nerves did *not* find their original muscles with the distribution of the reinnervation being random (Gillespie et al., 1986[39]). The reinnervation of hand muscles in patients after median nerve transection and surgical repair was also found to be random, a finding that explained the loss of the normal fine control of hand movements (Thomas et al., 1987[40]). These findings are of considerable

importance because the inability of regenerating nerves to grow back into their original endoneurial tubes leads to random reinnervation of appropriate and inappropriate targets. This in turn, accounts for return of poor sensation and the frequent difficulties in movement that may be inappropriate for the given task (Thomas et al, 1987[40]; Tötösy de Zepetnek et al., 1992[34]).

5. Axonal sprouting after motoneuron loss in partial nerve injuries and after motoneuron death in amyotrophic lateral sclerosis and poliomyelitis

I have had a long-term interest in amyotrophic lateral sclerosis (ALS), the disease in which most affected patients die within 2 to 5 years of their diagnosis as well as in the survival of reinnervated neuromuscular junctions in adults who contracted the disease of poliomyelitis in early life. My work in this area has been funded continuously, initially by Muscular Dystrophy Association of Canada (MDAC) and thereafter by the ALS society after the MDAC ceased to fund operating grants. Initially, our interest was axon sprouting in a model of the partial muscle denervation that the patients suffer as motoneurons progressively die. Later we used transgenic mice that express the mutant form of superoxide dismutase (SOD1) as the model of ALS. Our work on partial denervation in rats and cats, established 1) the upper limits of reinnervation of muscles by axon sprouting, and that 2) most of the axon sprouts from intramuscular intact motor nerves are nodal sprouts emanating from the last node of Ranvier between myelin sheaths on the nerves, 3) that excess neuromuscular activity is deleterious to the process of axon sprouting, and 4) that neuromuscular activity also promotes withdrawal of the sprouts in a mouse model of post-polio syndrome. Our work on the SOD1 transgenic mouse model of ALS demonstrated the there is a progressive loss of intact motor units that occurs during the presymptomatic phase of disease with the fast fatigable motor units being the most susceptible.

5.1 Axon sprouting and upper limits of compensation for partial denervation

Whilst it was known that the intact motor nerves can enlarge their field of innervation within partially denervated muscles and thereby compensate for partial loss of motor nerve innervation, it was not until we used electrophysiological methods of determining the extent of partial denervation of muscles, motor unit forces and the number of muscle fibers innervated by single motor axons in cat and rat models of partial muscle denervation, that the upper limits of axon sprouting were defined (Rafuse et al, 1992[35]; Gordon and Tyreman, 2010[41]). Recordings of muscle contractile forces in response to stimulation of each of the three ventral roots supplying motor axons to the muscle, provided the relative contribution of each root to the innervation of the muscle and thereby, the loss of innervation that results from the transection of one ventral root to partially denervate the muscle on the contralateral side of the animal (Rafuse et al, 1992[35]; Tam et al., 2001[15]; Tam et al., 2002[42]; Tam et al., 2003[43]; Gordon and Tyreman, 2010[41]). The enlargement of motor units, namely the increased numbers of muscle fibers innervated per motoneuron, was established by recording from at least 30% of the hundred(s) and ~40-90 motor units in cat and rat muscles, respectively, and from counts of glycogen depleted muscle fibers of one motor unit in each rat after exhaustive stimulation of an isolated motor nerve to the muscle fibers (Gordon and Tyreman, 2010[41]). We established that there was an upper limit of motor unit enlargement of 4-5-fold and 5-8-fold by the axon sprouting in partially denervated rat and cat muscles, respectively (Rafuse et al., 1992[35]; Gordon and Tyreman, 2010[41]). This upper limit corresponds with the sprouting capacity demonstrated in partially denervated muscles of humans (Yang et al 1990[44]) and the involvement of all motor units in the enlargement, *all* motor units, small and large enlarging in a similar fashion (Rafuse et al., 1992[31]; Tam et al., 2001[15]; Yang et al., 1990[44]). Interestingly, the reduced neuromuscular activity generated in the enlarged motor units of spinal cord injured patients did not impact on the capacity of the motor units to enlarge to compensate for the loss of motoneurons at the location of the spinal cord injury (Yang et al., 1990[44]).

5.2 Axon sprouting occurs close to the muscle fibers that the motor nerve innervates

Using silver stain to visualize motor nerves and α-bungarotoxin staining of the acetylcholine receptors at the muscle endplates where the nerves innervate the muscle fibers, we demonstrated that axon sprouts emerge from intramuscular nerves very close to their innervation of intact endplates to reinnervate denervated endplates within the vicinity (Tam et al., 2001[15]; Gordon and Tyreman, 2010[41]). Using glycogen depletion to visualize muscle fibers innervated by one motor nerve in intact and partially denervated muscles, we provided a parsimonious explanation for the limit to sprouting (Gordon and Tyreman, 2010[41]). Muscle fibers of a single innervated motor unit that were previously found contained within a defined territory in muscle cross-sections are each surrounded by 5-6 non-unit muscle fibers (Gordon and Tyreman, 2010[41]). Axonal sprouts reinnervate denervated muscle fibers close or adjacent to their own muscle fibers within the 'territory'. The upper limit of a 4-6 fold increase in numbers of muscle fibers per nerve that allows for reinnervation of all the denervated muscle fibers in partially denervated rat muscles is reached when all or most of the denervated muscle fibers within the 'territory' are reinnervated by the sprouts (Gordon and Tyreman, 2010[41]).

5.3 Regeneration rather than sprouting through nerve autografts placed end-to-side

Although claims were made that axons sprout from nodes of Ranvier of an intact nerve to cross through nerve autografts into an adjacent denervated peripheral nerve stump, our recent study that used retrograde tracing of the motor and sensory neurons that sent their axons across these autografts, demonstrated that sprouting was rare (Gordon et al, 2015[45]). Depending on the size of a window cut into the perineurium of a rat hindlimb nerve, we found that the donor nerves regenerate axons through nerve autografts that bridge between the donor nerve and a recipient denervated nerve stump. The advantage of the small number of donor nerves that grow in both directions either side of three autografts, is that they appeared to sustain growth support for axons that regenerated through the autograft after delayed surgery. In addition, an end-to-side transfer of a sensory nerve to the rat facial nerve that also improved regeneration through a 'protected' nerve stump, anticipates translation to facial nerve surgery in patients (Gordon et al, 2015[45]; Placheta et al, 2015[46]).

5.4 Excess neuromuscular activity is deleterious for sprouting and retention of enlarged motor units

Our experiments in rats demonstrated that excessive exercise is counterproductive after partial nerve injuries because high levels of neuromuscular activity by exercise or electrical nerve stimulation prevents the 'bridging' of Schwann cell processes between innervated and denervated endplates that normally occurs after partial denervation; the 'bridging' is responsible for 'leading' axon sprouts from intramuscular nerves to reinnervate denervated muscles (Tam and Gordon 2001[15]; Tam and Gordon, 2003[43]) Furthermore, our experiments demonstrated that excessive exercise is also counterproductive in in post-polio patients because, in a rat model of post-polio syndrome, the exercise exacerbates the progressive age-dependent destabilization of enlarged motor units (Tam et al., 2002[42]). As a result, age-dependent loss of motor units increased with accompanying muscle weakness and fatigue. These findings indicate that excessive exercise and/or physiotherapy may be detrimental after partial nerve injuries and in post-polio patients.

5.5 Preferential loss of fast motor units in a transgenic mouse model of amyotrophic lateral sclerosis

In addressing the question of whether axon sprouting can compensate, even partially, for loss of functional motor units in ALS, we examined the time course of loss of these motor units in the SOD1 transgenic mouse model of the disease. We were surprised to find that, at the onset of symptomatic disease at 90 days of age when significant motoneuron death begins, extensive loss of functionally intact motor units was already evident in hindlimb fast-twitch muscles (Hegedus et al., 2007[16]; Hegedus et al., 2008[17]). Indeed we found that there was already significant loss of these units at 40 days of age. Slow in contrast to fast motor units were relatively resistant to this phenomenon of 'die-back' of the axons and histochemical analysis of muscle fiber types

revealed the preferential denervation of the most fatigable muscle fibers (Hegedus et al., 2007[16]). Interestingly, the remaining intact nerves fail to sprout to compensate for loss of motor units so that the number of denervated muscle fibers increases with the loss of functional motor units. The loss of the fast motor units suggested the possibility that conversion of the most fatigable and forceful fast motor units to a more fatigue resistant phenotype might allow more intact motor units to survive. This was indeed the case, there being significantly more intact motor units that survived when their neuromuscular activity was increased by partial denervation (Hegedus et al., 2007a[47]). Hence strategies to promote conversion of muscle phenotype by moderate neuromuscular activity may have some role in 'saving' functional motor units in neuromuscular diseases.

List of References

1. Fu,S.Y. and T.Gordon. 1997. The cellular and molecular basis of peripheral nerve regeneration. *Mol Neurobiol* 14:67-116.

2. Fu,S.Y. and T.Gordon. 1995. Contributing factors to poor functional recovery after delayed nerve repair: prolonged axotomy. *J Neurosci* 15:3876-3885.

3. Fu,S.Y. and T.Gordon. 1995. Contributing factors to poor functional recovery after delayed nerve repair: prolonged denervation. *J Neurosci* 15:3886-3895.

4. Gordon,T., N.Tyreman, and M.A.Raji. 2011. The basis for diminished functional recovery after delayed peripheral nerve repair. *J Neurosci* 31:5325-5334.

5. Al-Majed,A.A., C.M.Neumann, T.M.Brushart, and T.Gordon. 2000. Brief electrical stimulation promotes the speed and accuracy of motor axonal regeneration. *J Neurosci* 20:2602-2608.

6. Al-Majed,A.A., T.M. Brushart, and T.Gordon. 2000. Electrical stimulation accelerates and increases expression of BDNF and trkB mRNA in regenerating rat femoral motoneurons. *Eur J Neurosci* 12:4381-4390.

7. Brushart,T.M., P.N.Hoffman, R.M.Royall, B.B.Murinson, C.Witzel, and T.Gordon. 2002. Electrical stimulation promotes motoneuron regeneration without increasing its speed or conditioning the neuron. *J Neurosci* 22:6631-38.

8. Al-Majed,A.A., S.L.Tam, and T.Gordon. 2004. Electrical stimulation accelerates and enhances expression of regeneration-associated genes in regenerating rat femoral motoneurons. *Cell Mol Neurobiol* 24:379-402.

9. Geremia,N.M., T.Gordon, T.M.Brushart, A.A.Al-Majed, and V.M.Verge. 2007. Electrical stimulation promotes sensory neuron regeneration and growth-associated gene expression. *Exp Neurol* 205:347-359.

10. Aglah,C., T.Gordon, and E.I.Posse De Chaves. 2008. cAMP promotes neurite outgrowth and extension through protein kinase A but independently of Erk activation in cultured rat motoneurons. *Neuropharmacol* 55:8-17.

11. Eberhardt,K.A., A.Irintchev, A.A.Al-Majed, O.Simova, T.M.Brushart, T.Gordon, and M.Schachner. 2006. BDNF/TrkB signaling regulates HNK-1 carbohydrate expression in regenerating motor nerves and promotes functional recovery after peripheral nerve repair. *Exp. Neurol.* 198:500-510.

12. Gordon,T., N.Amirjani, D.C.Edwards, and K.M.Chan. 2010. Brief post-surgical electrical stimulation accelerates axon regeneration and muscle reinnervation without affecting the functional measures in carpal tunnel syndrome patients. *Exp Neurol* 223:192-202.

13. Elzinga,K., N.Tyreman, A.Ladak, B.Savaryn, J.Olson, and T.Gordon. 2015. Brief electrical stimulation improves nerve regeneration after delayed repair in Sprague Dawley rats. *Exp Neurol* 269:142-153.

14. Udina,E., M.Furey, S.Busch, J.Silver, T.Gordon, and K.Fouad. 2008. Electrical stimulation of intact peripheral sensory axons in rats promotes outgrowth of their central projections. *Exp Neurol* 210:238-247.

15. Tam,S.L., V.Archibald, N.Tyreman, B.Jassar, and T.Gordon. 2001. Increased neuromuscular activity reduces sprouting in partially denervated muscles. *J Neurosci* 21:654-667.

16. Hegedus,J., C.T.Putman, and T.Gordon. 2007. Time course of preferential motor unit loss in the SOD1(G93A) mouse model of amyotrophic lateral sclerosis. *Neurobiol Dis* 28:154-164.

17. Hegedus,J., C.T.Putman, N.Tyreman, and T.Gordon. 2008. Preferential motor unit loss in the $SOD1^{G93A}$ transgenic mouse model of amyotrophic lateral sclerosis. *J Physiol* 586:3337-3351.

18. Gordon, T, J.Hegedus, and S.L.Tam. 2004 Adaptive and maladaptive motor axonal sprouting in aging and motoneuron disease. Invited review. Neurol Res 26:174-185.

19. Gordon, T. 2009 The role of neurotrophic factors in nerve regeneration. Invited review. Neurosurgical Focus, 26: E3.

20. Gordon,T. and A.W.English. 2015. Strategies to promote peripheral nerve regeneration: electrical stimulation and/or exercise. *Eur J Neurosci*. *Epub.*

21. Boyd,J.G. and T.Gordon. 2002. A dose-dependent facilitation and inhibition of peripheral nerve regeneration by brain-derived neurotrophic factor. *Eur J Neurosci* 15:613-626.

22. Boyd,J.G. and T.Gordon. 2003. Glial cell line-derived neurotrophic factor and brain-derived neurotrophic factor sustain the axonal regeneration of chronically axotomized motoneurons in vivo. *Exp Neurol* 183:610-619.

23. Sulaiman,O.A.R. and T.Gordon. 2000. Effects of short- and long-term Schwann cell denervation on peripheral nerve regeneration, myelination, and size. *GLIA* 32:234-246.

24. Boyd,J.G. and T.Gordon. 2001. The neurotrophin receptors, trkB and p75, differentially regulate motor axonal regeneration. *J Neurobiol.* 49:314-325.

25. Gordon, T, S.You, S.I.Cassar, and W.Tetzlaff W 2015. Reduced expression of regeneration associated genes in chronically axotomized facial motoneurons. *Exp Neurol* 264: 26-32.

26. Hoke,A., T.Gordon, D.W.Zochodne, and O.A.R.Sulaiman. 2002. A decline in glial cell-line-derived neurotrophic factor expression is associated with impaired regeneration after long-term Schwann cell denervation. *Exp Neurol* 173:77-85.

27. You, S., T.Petrov, P.H.Chung, and T.Gordon. 1997. The expression of the low affinity nerve growth factor receptor in long-term denervated Schwann cells. *GLIA* 20:87-100.

28. Gordon,T, 2014. Neurotrophic factor expression in denervated motor and sensory Schwann cells: Relevance to specificity of peripheral nerve regeneration. *Exp Neurol* 254:99-108.

29. Gordon,T, N.Amirjani, D.C.Edwards,DC, and K.M.Chan. 2010. Brief post-surgical electrical stimulation accelerates axon regeneration and muscle reinnervation without affecting the functional measures in carpal tunnel syndrome patients. *Exp Neurol* 223: 192-202.

30. Udina,E., A.Ladak, M.Furey, T.Brushart, N.Tyreman, and T.Gordon. 2010. Rolipram-induced elevation of cAMP or chondroitinase ABC breakdown of inhibitory proteoglycans in the extracellular matrix promotes peripheral nerve regeneration. *Exp. Neurol* 223:143-152.

31. Sulaiman,O.A.R., J.Voda, B.G.Gold, and T.Gordon. 2002. FK506 increases peripheral nerve regeneration after chronic axotomy but not after chronic Schwann cell denervation. *Exp Neurol* 175:127-137.

32. Gordon,T. and R.B.Stein. 1982. Time course and extent of recovery in reinnervated motor units of cat triceps surae muscles. *J Physiol* 323:307-323.

33. Gordon,T., C.K.Thomas, J.B.Munson, and R.B.Stein. 2004. The resilience of the size principle in the organization of motor unit properties in normal and reinnervated adult skeletal muscles. *Can J Physiol Pharmacol* 82:645-661.

34. Tötösy de Zepetnek,J.E., H.V.Zung, S.Erdebil, and T.Gordon. 1992. Innervation ratio is an important determinant of force in normal and reinnervated rat tibialis anterior muscles. *J Neurophysiol* 67:1385-1403.

35. Rafuse,V.F., T.Gordon, and R.Orozco. 1992. Proportional enlargement of motor units after partial denervation of cat triceps surae muscles. *J Neurophysiol* 68:1261-1275.

36. Gordon, T. and V.R.Rafuse. (2001) Size of myelinated nerve fibres is not increased by expansion of the peripheral field in cats. *J Physiol* 532: 835-850.

37, Gordon,T, N.Tyreman, V.F.Rafuse, and J.B.Munson. 1997. Fast-to-slow conversion following chronic low-frequency activation of medial gastrocnemius muscle in cats .1. Muscle and motor unit properties. *J Neurophysiol* 77:2585-2604.

38. Munson,J.B., R.C.Foehring, L.M.Mendell, and T.Gordon. 1997. Fast-to-slow conversion following chronic low-frequency activation of medial gastrocnemius muscle in cats. II. Motoneuron properties. *J Neurophysiol* 77:2605-2615.

39. Gillespie,M.J., T.Gordon, and P.R.Murphy. 1986. Reinnervation of the lateral gastrocnemius and soleus muscles in the rat by their common nerve. *J Physiol* 372:485-500.

40. Thomas,C.K., R.B.Stein, T.Gordon, R.G.Lee, and M.G.Elleker. 1987. Patterns of reinnervation and motor unit recruitment in human hand muscles after complete ulnar and median nerve section and resuture. *J Neurol Neurosurg Psychiatry* 50:259-268.

41. Gordon,T. and N.Tyreman. 2010. Sprouting capacity of lumbar motoneurons in normal and hemisected spinal cords of the rat. *J Physiol* 588:2745-2768.

42. Tam, S.L., V.Archibald, N.Tyreman, and T.Gordon. 2002 Effect of exercise on stability of chronically enlarged units. *Muscle & Nerve* 25: 359-369.

43.Tam,S.L. and T.Gordon. 2003. Neuromuscular activity impairs axonal sprouting in partially denervated muscles by inhibiting bridge formation of perisynaptic Schwann cells. *J. Neurobiol.* 57:221-234.

44. Yang,J.F., R.B.Stein, J.Jhamandas, and T.Gordon. 1990. Motor unit numbers and contractile properties after spinal cord injury. *Ann Neurol* 28:496-502.

45 Gordon T, H.M.Hendry, C.A.Lafontaine, H.Carter, J.J.Zhang, and G.H.Borschel. 2015. Nerve cross-bridging to enhance nerve regeneration in a rat model of delayed nerve repair. *PLOSONE* #19410: e0127397.

46. Placheta, E, M.D.Wood, C.Lafontaine, E.H.Liu, J.M.Hendry, D.N.Angelov, M.Frey, T. Gordon, and G.H.Borschel. 2015. Enhancement of facial nerve motoneuron

regeneration through cross face nerve grafts by adding end-to-side sensory axons *Plastic Reconstr Surg* 135:460-471.

47. Gordon, T, N.Tyreman, S.Li, C.T.Putman, and J. Hegedus. 2010 Functional overload saves motor units in the SOD1-G93A transgenic mouse model of amyotrophic lateral sclerosis (ALS). *Neurobiol Dis* 37: 412-422.

Molecular Neurobiology
Copyright © 1997 Humana Press Inc.
All rights of any nature whatsoever reserved.
ISSN0893-7648/97/14(1): 67–116/$20.50

The Cellular and Molecular Basis of Peripheral Nerve Regeneration

Susan Y. Fu[1] and Tessa Gordon*,[2]

[1]Department of Biochemistry; and [2]Department of Pharmacology and Division of Neuroscience, University of Alberta, Edmonton, Canada T6G 2S2

Abstract

Functional recovery from peripheral nerve injury and repair depends on a multitude of factors, both intrinsic and extrinsic to neurons. Neuronal survival after axotomy is a prerequisite for regeneration and is facilitated by an array of trophic factors from multiple sources, including neurotrophins, neuropoietic cytokines, insulin-like growth factors (IGFs), and glial-cell-line-derived neurotrophic factors (GDNFs). Axotomized neurons must switch from a transmitting mode to a growth mode and express growth-associated proteins, such as GAP-43, tubulin, and actin, as well as an array of novel neuropeptides and cytokines, all of which have the potential to promote axonal regeneration. Axonal sprouts must reach the distal nerve stump at a time when its growth support is optimal. Schwann cells in the distal stump undergo proliferation and phenotypical changes to prepare the local environment to be favorable for axonal regeneration. Schwann cells play an indispensable role in promoting regeneration by increasing their synthesis of surface cell adhesion molecules (CAMs), such as *N*-CAM, Ng-CAM/L1, N-cadherin, and L2/HNK-1, by elaborating basement membrane that contains many extracellular matrix proteins, such as laminin, fibronectin, and tenascin, and by producing many neurotrophic factors and their receptors. However, the growth support provided by the distal nerve stump and the capacity of the axotomized neurons to regenerate axons may not be sustained indefinitely. Axonal regeneration may be facilitated by new strategies that enhance the growth potential of neurons and optimize the growth support of the distal nerve stump in combination with prompt nerve repair.

Index Entries: Nerve regeneration; axotomy; neuronal death; Schwann cells; basal lamina; macrophages; growth-associated proteins; neuropoietic cytokines; neurotrophic factors; cell adhesion molecules.

The Journal of Neuroscience, May 1995, *15*(5): 3876–3885

Contributing Factors to Poor Functional Recovery after Delayed Nerve Repair: Prolonged Axotomy

Susan Y. Fu and Tessa Gordon

Department of Pharmacology and Division of Neuroscience, University of Alberta, Edmonton, Alberta, Canada T6G 2S2

The contribution of prolonged motoneuron axotomy to the poor functional recovery after delayed nerve repair was determined by means of a nerve cross-anastomosis paradigm in the rat. The tibial nerve was axotomized up to 12 months before it was cross-sutured to the distal stump of the freshly cut common peroneal nerve to innervate the freshly denervated tibialis anterior muscle. Three to 17 months later, muscle and motor unit (MU) forces were measured to quantify the number of axons that had successfully regenerated and reinnervated the muscle. The extent of axonal branching was estimated by the innervation ratio (IR) (i.e., the number of muscle fibers innervated by each axon), which was obtained directly by counting muscle fibers in a single glycogen-depleted MU in each muscle and indirectly by calculation. The total number of MUs in each muscle significantly decreased with progression of axotomy and was only 35% of the control when axotomy was prolonged more than 3 months. Concurrently, MU force and IR increased exponentially, with a mean increase of threefold when axotomy was more than 3 months, which largely compensated for the reduction in the number of axons that reinnervated the muscle. Consequently, muscles reinnervated by tibial motor axons that had been axotomized up to 12 months produced as much force as those reinnervated by freshly axotomized tibial motor axons. Muscle weight, size, and muscle fiber size were similar to those after immediate nerve suture. Although prolonged axotomy does not compromise the number of muscle fibers innervated by each axon, it does reduce the capacity of motor axons to regenerate and thus is an important contributing factor to the poor functional recovery in delayed nerve repair.

[Key words: long-term axotomy, regeneration, reinnervation, motor units, innervation ratio, branching]

The Journal of Neuroscience, May 1995, *15*(5): 3886–3895

Contributing Factors to Poor Functional Recovery after Delayed Nerve Repair: Prolonged Denervation

Susan Y. Fu and Tessa Gordon

Department of Pharmacology and Division of Neuroscience, University of Alberta, Edmonton, Alberta, Canada T6G 2S2

The effects of prolonged denervation, independent from those of prolonged axotomy, on the recovery of muscle function were examined in a nerve cross-anastomosis paradigm. The tibialis anterior muscle was denervated for various durations by cutting the common peroneal nerve before a freshly cut tibial nerve was cross-sutured to its distal stump. Nerve regeneration and muscle reinnervation were quantified by means of electrophysiological and histochemical methods. Progressively fewer axons reinnervated the muscle with prolonged denervation; for example, beyond 6 months the mean (±SE) motor unit number was 15 ± 4, which was far fewer than that after immediate nerve suture (137 ± 21). The poor regeneration after prolonged denervation is not due to inability of the long-term denervated muscle to accept reinnervation because each regenerated axon reinnervated three- to fivefold more muscle fibers than normal. Rather, it is due to progressive deterioration of the intramuscular nerve sheaths because the effects of prolonged denervation were simulated by forcing regenerating axons to grow outside the sheaths. Fewer regenerated axons account for reinnervation of less than 50% of the muscle fibers in each muscle and contribute to the progressive decline in muscle force. Reinnervated muscle fibers failed to fully recover from denervation atrophy: muscle fiber cross-sectional area being 1171 ± 84 μm^2 as compared to 2700 ± 47 μm^2 after immediate nerve suture. Thus, the primary cause of the poor recovery after long-term denervation is a profound reduction in the number of axons that successfully regenerate through the deteriorating intramuscular nerve sheaths. Muscle force capacity is further compromised by the incomplete recovery of muscle fibers from denervation atrophy.

[Key words: prolonged denervation, regeneration, reinnervation, motor units, intramuscular nerve sheath]

The Journal of Neuroscience, April 6, 2011 • 31(14):5325–5334 • 5325

Development/Plasticity/Repair

The Basis for Diminished Functional Recovery after Delayed Peripheral Nerve Repair

Tessa Gordon, Neil Tyreman, and Mukaila A. Raji
Centre for Neuroscience, Department of Medicine and Dentistry, University of Alberta, Edmonton, Alberta T6G 2S2, Canada

The postsurgical period during which neurons remain without target connections (chronic axotomy) and distal nerve stumps and target muscles are denervated (chronic denervation) deleteriously affects functional recovery. An autologous nerve graft and cross-suture paradigm in Sprague Dawley rats was used to systematically and independently control time of motoneuron axotomy, denervation of distal nerve sheaths, and muscle denervation to determine relative contributions of each factor to recovery failure. Tibial (TIB) nerve was cross-sutured to common peroneal (CP) nerve via a contralateral 15 mm nerve autograft to reinnervate the tibialis anterior (TA) muscle immediately or after prolonging TIB axotomy, CP autograft denervation, or TA muscle denervation. Numbers of motoneurons that reinnervated TA muscle declined exponentially from 99±15 to asymptotic mean (±SE) values of 35 ± 1, 41 ± 10, and 13 ± 5, respectively. Enlarged reinnervated motor units fully compensated for reduced motoneuron numbers after prolonged axotomy and autograft denervation, but the maximal threefold enlargement did not compensate for the severe loss of regenerating nerves through chronically denervated nerve stumps and for failure of reinnervated muscle fibers to recover from denervation atrophy. Muscle force, weight, and cross-sectional area declined. Our results demonstrate that chronic denervation of the distal stump plays a key role in reduced nerve regeneration, but the denervated muscle is also a contributing factor. That chronic Schwann cell denervation within the nerve autograft reduced regeneration less than after the denervation of both CP nerve stump and TA muscle, argues that chronic muscle denervation negatively impacts nerve regeneration.

The Journal of Neuroscience, April 1, 2000, *20*(7):2602–2608

Brief Electrical Stimulation Promotes the Speed and Accuracy of Motor Axonal Regeneration

Abdulhakeem A. Al-Majed,[1] Catherine M. Neumann,[1] Thomas M. Brushart,[2] and Tessa Gordon[1]

[1]*Department of Pharmacology, Division of Neuroscience, University of Alberta, Edmonton, Alberta T6G 2S2, Canada, and* [2]*Departments of Orthopedic Surgery and Neurology, Johns Hopkins Medical School, Baltimore, Maryland*

Functional recovery is often poor despite the capacity for axonal regeneration in the peripheral nervous system and advances in microsurgical technique. Regeneration of axons in mixed nerve into inappropriate pathways is a major contributing factor to this failure. In this study, we use the rat femoral nerve model of transection and surgical repair to evaluate (1) the effect of nerve transection on the speed of regeneration and the generation of motor-sensory specificity, (2) the efficacy of electrical stimulation in accelerating axonal regeneration and promoting the reinnervation of appropriate muscle pathways by femoral motor nerves, and (3) the mechanism of action of electrical stimulation. Using the retrograde neurotracers fluorogold and fluororuby to backlabel motoneurons that regenerate axons into muscle and cutaneous pathways, we found the following. (1) There is a very protracted period (10 weeks) of axonal outgrowth that adds substantially to the delay in axonal regeneration (staggered regeneration). This process of staggered regeneration is associated with preferential motor reinnervation (PMR). (2) One hour to 2 weeks of 20 Hz continuous electrical stimulation of the parent axons proximal to the repair site dramatically reduces this period (to 3 weeks) and accelerates PMR. (3) The positive effect of short-term electrical stimulation is mediated via the cell body, implicating an enhanced growth program. The effectiveness of such a short-period low-frequency electrical stimulation suggests a new therapeutic approach to accelerate nerve regeneration after injury and, in turn, improve functional recovery.

Key words: electrical stimulation; staggered regeneration; motoneuron; TTX; PMR; retrograde labeling



European Journal of Neuroscience, Vol. 12, pp. 4381–4390, 2000 © *Federation of European Neuroscience Societies*

Electrical stimulation accelerates and increases expression of BDNF and trkB mRNA in regenerating rat femoral motoneurons

Abdulhakeem A. Al-Majed,[1] Thomas M. Brushart[2] and Tessa Gordon[1]
[1]Department of Pharmacology, Division of Neuroscience, 513 Heritage Medical Research Center, University of Alberta, Edmonton, Alberta T6G 2S2, Canada
[2]Departments of Orthopaedic Surgery and Neurology, Johns Hopkins Medical School, Baltimore, MD, USA

Keywords: *in situ* hybridization, intramuscular labelling, motor axonal regeneration, neurotrophin.

Abstract

Electrical stimulation promotes the speed and accuracy of motor axonal regeneration. The positive effects of stimulation are mediated at the cell body. Here we characterize the effect of electrical stimulation on motoneuronal expression of BDNF and its receptor, trkB, two genes whose expression levels in motoneurons correlate with regeneration and are regulated by electrical activity in a variety of neurons. We used semiquantitative *in situ* hybridization to measure expression of mRNA encoding BDNF and the full-length trkB receptor at intervals of 8 h, 2 days and 7 days after unilateral femoral nerve cut, suture, and stimulation. Expression in regenerating motoneurons was compared to that of contralateral intact motoneurons. BDNF and trkB signals were not significantly upregulated 8 h and 2 days after femoral nerve suture and sham stimulation. By 7 days, there was a 2-fold increase in both BDNF and trkB mRNA expression. In contrast, stimulation of cut and repaired nerves for only 1 h led to rapid upregulation of BDNF and trkB mRNA by 3-fold and 2-fold, respectively, within the first 8 h. The stimulation effect peaked at 2 days with 6-fold and 4-fold increases in the signals, respectively. Thereafter, the levels of BDNF and trkB mRNA expression declined to equal the 2-fold increase seen at 7 days after nerve repair and sham-stimulation. We conclude that brief electrical stimulation stimulates BDNF and trkB expression in regenerating motoneurons. Because electrical stimulation is known to accelerate axonal regeneration, we suggest that changes in the expression of BDNF and trkB correlate with acceleration of axonal regeneration.



The Journal of Neuroscience, August 1, 2002, *22*(15):6631–6638

Electrical Stimulation Promotes Motoneuron Regeneration without Increasing Its Speed or Conditioning the Neuron

Thomas M. Brushart,[1,2] **Paul N. Hoffman,**[2,3] **Richard M. Royall,**[4] **Beth B. Murinson,**[2] **Christian Witzel,**[1] **and Tessa Gordon**[5]

Departments of [1]*Orthopaedics,* [2]*Neurology, and* [3]*Opthalmology, Johns Hopkins School of Medicine, and Department of* [4]*Biostatistics and Statistics, Bloomberg School of Public Health, Johns Hopkins University, Baltimore Maryland 21287, and* [5]*Department of Pharmacology, Division of Neuroscience, University of Alberta, Alberta T6G 2S2, Canada*

Motoneurons reinnervate the distal stump at variable rates after peripheral nerve transection and suture. In the rat femoral nerve model, reinnervation is already substantial 3 weeks after repair, but is not completed for an additional 7 weeks. However, this "staggered regeneration" can be temporally compressed by application of 20 Hz electrical stimulation to the nerve for 1 hr. The present experiments explore two possible mechanisms for this stimulation effect: (1) synchronization of distal stump reinnervation and (2) enhancement of regeneration speed. The first possibility was investigated by labeling all motoneurons that have crossed the repair at intervals from 4 d to 4 weeks after rat femoral nerve transection and suture. Although many axons did not cross until 3–4 weeks after routine repair, stimulation significantly increased the number crossing at 4 and 7 d, with only a few crossing after 2 weeks. Regeneration speed was studied by radioisotope labeling of transported proteins and by anterograde labeling of regenerating axons, and was not altered by stimulation. Attempts to condition the neuron by stimulating the femoral nerve 1 week before injury were also without effect. Electrical stimulation thus promotes the onset of motor axon regeneration without increasing its speed. This finding suggests a combined approach to improving the outcome of nerve repair, beginning with stimulation to recruit all motoneurons across the repair, followed by other treatments to speed and prolong axonal elongation.

Key words: electrical stimulation; peripheral nerve; anterograde tracing; BDNF; conditioning; neurobiotin

Cellular and Molecular Neurobiology, Vol. 24, No. 3, June 2004 (© 2004)

Electrical Stimulation Accelerates and Enhances Expression of Regeneration-Associated Genes in Regenerating Rat Femoral Motoneurons

Abdulhakeem A. Al-Majed,[1] Siu Lin Tam,[1] and Tessa Gordon[1,2]

Received July 28, 2003; accepted September 22, 2003

SUMMARY

1. In this study we investigated whether electrical stimulation accelerates the upregulation of T_α1-tubulin and GAP-43 (regeneration-associated genes; RAGs) and the downregulation of the medium-molecular-weight neurofilament (NFM), in concert with stimulation-induced acceleration of BDNF and trkB gene expression and axonal regeneration.

2. Two weeks prior to unilateral femoral nerve transection and suture, fluorogold (Fluorochrome Inc., Denver) or fluororuby (Dextran tetramethylrhodamine, Mol. Probes, D-1817, Eugene, OR) was injected into quadriceps muscles of the left and right hindlimbs to label the femoral motoneuron pools as previously described. Over a period of 7 days, fresh spinal cords were processed for semiquantitation of mRNA by using in situ hybridization.

3. There was an increase in T_α1-tubulin and GAP-43 mRNA and a decline in the NFM mRNA at 7 days after nerve suture and sham stimulation but not in intact nerves. In contrast, 1-h stimulation of sutured but not intact nerves dramatically accelerated the changes in gene expression: mRNA levels of T_α1-tubulin and GAP-43 were significantly elevated above control levels by 2 days while NFM mRNA was significantly reduced by 2 days in the sutured nerves. Thereby, the neurofilament/tubulin expression ratio was reduced at 2 days after suture and stimulation, possibly allowing more tubulin to be transported faster into the growing axons to accelerate the elongation rate following stimulation. Importantly, the changes in RAGs and NFM gene expression were delayed relative to the accelerated upregulation of BDNF and trkB mRNA by electrical stimulation.

4. The temporal sequence of upregulation of BDNF and trkB, altered gene expression of RAGs and NFM, and accelerated axonal outgrowth from the proximal nerve stump are consistent with a key role of BDNF and trkB in mediating the altered expression of RAGs and, in turn, the promotion of axonal outgrowth after electrical stimulation.

KEY WORDS: rat; peripheral nerve regeneration; electrical stimulation; neurofilament; tubulin; growth-associated proteins.

[1] Centre of Neuroscience, Division of Physical Medicine and Rehabilitation, Faculty of Medicine and Dentistry, University of Alberta, Edmonton, Canada.

[2] To whom correspondence should be addressed at Centre of Neuroscience, Division of Physical Medicine and Rehabilitation, Faculty of Medicine and Dentistry, Room 513, Heritage Medical Research Centre, University of Alberta, Edmonton, Alberta, Canada T6G 2S2; e-mail: tessa.gordon@ualberta.ca.

0272-4340/04/0600-0379/0 © 2004 Plenum Publishing Corporation

Available online at www.sciencedirect.com
ScienceDirect
Experimental Neurology 205 (2007) 347–359
Experimental Neurology
www.elsevier.com/locate/yexnr

Electrical stimulation promotes sensory neuron regeneration and growth-associated gene expression

Nicole M. Geremia [a,1], Tessa Gordon [b], Thomas M. Brushart [c], Abdulhakeem A. Al-Majed [b,2], Valerie M.K. Verge [a,*]

[a] Department of Anatomy and Cell Biology, Cameco MS/Neuroscience Research Center University of Saskatchewan, Saskatoon City Hospital Room 5800, 701 Queen Street, Saskatoon, Saskatchewan, Canada S7K 0M7
[b] Division of Physical Medicine and Rehabilitation, Division of Neuroscience, Faculty of Medicine and Dentistry, University of Alberta, Edmonton, Alberta, Canada T6G 2S2
[c] Departments of Orthopaedics and Neurology, Johns Hopkins School of Medicine, Johns Hopkins University, Baltimore, MD 21287, USA

Received 15 September 2006; revised 16 January 2007; accepted 19 January 2007
Available online 21 February 2007

Abstract

Brief electrical stimulation enhances the regenerative ability of axotomized motor [Nix, W.A., Hopf, H.C., 1983. Electrical stimulation of regenerating nerve and its effect on motor recovery. Brain Res. 272, 21–25; Al-Majed, A.A., Neumann, C.M., Brushart, T.M., Gordon, T., 2000. Brief electrical stimulation promotes the speed and accuracy of motor axonal regeneration. J. Neurosci. 20, 2602–2608] and sensory [Brushart, T. M., Jari, R., Verge, V., Rohde, C., Gordon, T., 2005. Electrical stimulation restores the specificity of sensory axon regeneration. Exp. Neurol. 194, 221–229] neurons. Here we examined the parameter of duration of stimulation on regenerative capacity, including the intrinsic growth programs, of sensory neurons. The effect of 20 Hz continuous electrical stimulation on the number of DRG sensory neurons that regenerate their axons was evaluated following transection and surgical repair of the femoral nerve trunk. Stimulation was applied proximal to the repair site for 1 h, 3 h, 1 day, 7 days or 14 days at the time of nerve repair. Following a 21-day regeneration period, DRG neurons that regenerated axons into the muscle and cutaneous sensory nerve branches were retrogradely identified. Stimulation of 1 h led to a significant increase in DRG neurons regenerating into cutaneous and muscle branches when compared to 0 h (sham) stimulation or longer periods of stimulation. Stimulation for 1 h also significantly increased the numbers of neurons that regenerated axons beyond the repair site 4 days after lesion and was correlated with a significant increase in expression of growth-associated protein 43 (GAP-43) mRNA in the regenerating neurons at 2 days post-repair. An additional indicator of heightened plasticity following 1 h stimulation was elevated expression of brain-derived neurotrophic factor (BDNF). The effect of brief stimulation on enhancing sensory and motoneuron regeneration holds promise for inducing improved peripheral nerve repair in the clinical setting.
© 2007 Elsevier Inc. All rights reserved.

Keywords: Sensory neuron; Electrical stimulation; Regeneration; Peripheral nerve; Injury; Neurotrophin; Plasticity

Introduction

Peripheral nerve regeneration, although more successful than central nervous system regeneration, is fraught with challenges when reinnervation is not exact or when debilitating neuropathic pain develops. Despite surgical repair to guide regenerating axons to their appropriate target, axonal regeneration often fails to achieve significant functional recovery (Sunderland, 1978; Kline and Hudson, 1995). One reason is that regenerating axons frequently grow long distances to reach denervated target organs and the rate of regeneration is slow.

Abbreviations: BDNF, brain-derived neurotrophic factor; GAP-43, growth-associated protein 43; DRG, dorsal root ganglia; ATF3, activated transcription factor 3; TTX, tetrodotoxin; FR, fluororuby; FG, fluorogold.

* Corresponding author. Fax: +1 306 655 8709.
E-mail address: valerie.verge@usask.ca (V.M.K. Verge).
[1] Present address: BioTherapeutics Research Group, Robarts Research Institute, London, Ontario, Canada N6A 5K8.
[2] Present address: Department of Pharmacology, College of Pharmacy, King Saud University, P.O. Box 2457, Riyadh 11451, Saudi Arabia.

0014-4886/$ - see front matter © 2007 Elsevier Inc. All rights reserved.
doi:10.1016/j.expneurol.2007.01.040

Rapidly regenerating axons grow at 1–3 mm/day with a latent period of 3–7 days for axons to cross the surgical site (Sunderland, 1978; Kline and Hudson, 1995). By the time regenerating axons enter the distal nerve stumps, the growth potential of axotomized neurons and the permissive growth environment of the distal nerve stumps has begun to deteriorate (Fu and Gordon, 1995a,b; Whitworth et al., 1996). As a result regenerating axons may fail to reach their target end-organs.

Strategies to improve peripheral nerve regeneration are aimed at inducing and maintaining strong growth states in the maximum number of neurons. The signals that modulate these programs in sensory neurons involve disconnection from peripheral target tissue (Richardson and Issa, 1984; Richardson and Verge, 1987) and induction of regeneration-associated gene (RAG) expression (Richardson and Issa, 1984; Richardson and Verge, 1987; Bevan and Winter, 1995; Doster et al., 1991; Andersen and Schreyer, 1999; Fernandes et al., 1999; Al-Majed et al., 2004). Acceleration of these programs can be achieved in sensory neurons by a conditioning lesion (Richardson and Verge, 1987), which is effective, but not clinically desirable. Studies by Al-Majed et al. (2000b) demonstrate that 1 h of 20 Hz electrical stimulation (alternating current) of the nerve proximal to the site of surgical repair enhances motor axonal regeneration across the surgical gap (Brushart, 1988) and shortens the time frame required for motor axons to select the correct motor nerve branch by 3-fold. This effect is correlated with increased expression of injury/regeneration-associated genes (GAP-43 and Tα1 tubulin), the neurotrophin BDNF and its receptor trkB (Al-Majed et al., 2000a, 2004). Thus, brief electrical stimulation holds tremendous clinical promise for axonal regeneration of motoneurons after surgical repair. In addition, recent evidence demonstrates that 1 h stimulation improves the specificity of sensory neuron regeneration 21 days post-repair (Brushart et al., 2005). However, whether this duration of electrical stimulation is optimal and whether it alters the intrinsic growth programs of sensory neurons is unknown.

We hypothesize that electrical stimulation increases the intrinsic regenerative capacity of sensory neurons. The present study evaluates the effect of duration of electrical stimulation on the regeneration of sensory neurons contributing to the femoral nerve following transection and repair. Our findings demonstrate that the beneficial effects of electrical stimulation observed for motoneurons extend to sensory neurons as evidenced by the increased number of sensory neurons that regenerate their axons in response to the stimulation and the pronounced effect on expression of injury/regeneration-associated genes. Portions of this work have been published in abstract form (Geremia et al., 2002, 2005).

Materials and methods

Experimental design

Experiments were performed on the adult rat femoral nerve in which regenerating motor axons preferentially reinnervate muscle pathways (Brushart and Seiler, 1987). The femoral nerve contains cutaneous sensory fibers that branch to innervate the skin via the saphenous nerve. These fibers are intermingled in the femoral nerve with sensory and motor fibers that innervate the quadriceps muscle via the quadriceps muscle nerve branch (Fig. 1A). One third of the axons derive from the α-motoneurons that innervate the skeletal muscle fibers (Brushart and Seiler, 1987). Experiments were approved by a local ethical committee (University of Alberta Health Science Laboratory Animal Services) under the Canadian guidelines for animal experimentation.

Nerve repair

Experiments were performed under aseptic conditions on the left femoral nerves of young adult (220–240 g) female Sprague Dawley rats that were anesthetized with somnitol (65 mg/kg, i.p.). The proximal femoral nerve was sharply cut 20 mm proximal to the bifurcation of the cutaneous and muscle nerves. The proximal and distal stumps were then carefully aligned and surgically joined within a 4-mm-long silastic nerve cuff (0.03 mm inner diameter; Dow Corning) by placing a single stitch of 9-0 silk (Ethicon) through the epineurium of the proximal and distal stumps under 40× magnification (Fig. 1B).

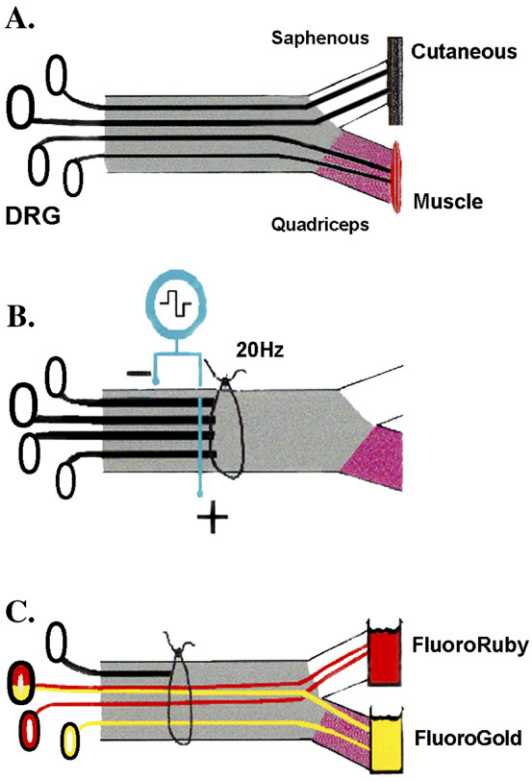


Fig. 1. Diagrammatic representation of the regeneration model employed (as adapted from Al-Majed et al., 2000b). (A) The femoral nerve has two branches: one to the quadricep muscle via the quadricep muscle nerve (motor and sensory axons) and one to the skin (cutaneous branch) via the saphenous nerve (sensory axons). (B) Bipolar electrodes were placed proximal to the site of nerve transection and surgical repair. Stimulation was a continuous train of 20 Hz for various times. (C) Retrograde tracers were applied 21 days after nerve repair to assess the number of sensory neurons that had regenerated axons into the muscle and cutaneous branches of the femoral nerve.

Electrical stimulation of cut and repaired femoral nerve

Two insulated stainless steel wires (Cooner A 5632) were bared of insulation for 2–3 mm, twisted to form a small loop to secure on either side of the femoral nerve stump proximal to the suture site and positioned proximal to the suture repair site for electrical stimulation. The cathode was sutured alongside the femoral nerve just below its exit from the peritoneal cavity, whereas the anode was sutured to muscle more distally, close to the nerve and just proximal to the suture repair site. The wires were connected to a custom-made biocompatible implantable stimulator that was encased in epoxy resin and covered with biocompatible silastic and contained a light-sensitive diode, which turned the stimulator on and off by an external light flash. Stimulation commenced immediately after nerve repair with supramaximal pulses (100 μs; 3 V) delivered in a continuous 20-Hz train by the implantable stimulator. The nonstimulated control group underwent nerve transection and repair alone ($n=7$). In the sham group of rats, the nerve was transected and repaired and the electrodes were implanted, but the stimulator was not activated ($n=13$). The stimulated axotomized sensory neurons and their regenerating axons were subject to short-term (1 h, $n=19$) or long-term (3 h, $n=6$; 1 day, $n=3$; 7 day, $n=4$; or 14 day, $n=5$) periods of continuous low-frequency electrical stimulation.

Tetrodotoxin (TTX) application

We used TTX at a dose of 60 μg/ml to block the propagation of action potentials back to the cell body as described previously (Al-Majed et al., 2000b). A sterile piece of absorbent cotton soaked with a 60 μg/ml dose of TTX was applied to the femoral nerve proximal to the position of the stimulating electrodes prior to the femoral nerve transection, repair and the 1 h stimulation period (Fig. 6A). The electrodes and the TTX were removed before closing the wound site ($n=6$).

Retrograde labeling of sensory neurons

In three naïve control animals or in animals at the end of a 21-day regeneration period, the muscle and cutaneous branches of the left femoral nerve were isolated, cut and backlabeled with neurotracers to identify the sensory neurons innervating each branch. Fluorogold (FG; Fluorochrome Inc., Denver, CO) and fluororuby (FR; dextran tetramethylrhodamine, D-1817; Molecular Probes, Eugene, OR) were employed because they are effectively endocytosed and retrogradely transported (Schmued and Fallon, 1986). The muscle and cutaneous branches were cut 5 mm distal to the femoral bifurcation (25 mm from the repair site). In each rat, one branch was labeled with FG and the other with FR (the dye application was alternated between animals to control for possible differences in retrograde uptake and transport of the dyes). Backlabeling with FG was done by exposing the tip of the severed branch to 4% FG in 0.1 M cacodylic acid for 1 h in a Vaseline well, after which it was extensively irrigated and reflected to a distant portion of the wound. Backlabeling with FR was done by placing the tip of the severed branch above a small weighing paper with FR crystals for 2 h and then irrigating the nerve and placing it in the opposite corner of the wound to prevent cross-contamination by diffusion of tracers. Animals were kept for 72 h after tracer application to allow the retrograde tracers to travel back to the neuronal cell bodies.

Backlabeling of femoral nerve axons just distal to the repair site

Experiments were performed on the femoral nerves of young adult (250 g) female Sprague Dawley rats ($n=11$). The animals were anesthetized by intramuscular injection of ketamine (87 mg/kg) and xylazine (13 mg/kg). Both femoral nerves of each rat were transected and repaired, but only one repair was stimulated. The femoral nerve was sharply transected 1 mm distal to the iliacus branch, carefully aligned and sutured with 11-0 nylon under 20–40× magnification. Stimulation was delivered intraoperatively for 1 h with animals under the same anesthetic. A Grass (Quincy, MA) SD-9 stimulator delivered continuous 20-Hz stimulation (100 μs, 3–5 V) to fine silver wires placed at (anode) and just proximal to (cathode) the repair.

As described previously for motoneurons (Brushart, 1988), backlabeling of axons just distal to the repair site was used to identify the sensory neurons that regenerated their axons across the surgical repair site. After a 4 day regeneration period, the femoral nerve was exposed and crushed 1.5 mm distal to the suture line with a narrow microforceps. A micropipette was introduced through the epineurium and perineurium distal to the crush and advanced intraneurally to the crush zone. Approximately 0.5 μl of 5 % FR was injected with a Picospritzer (Parker Hannefin, Fairfield, NJ) to restore the flattened crush zone to its normal rounded contour (Fig. 5A). Animals were kept for 48 h after tracer application, the time required for the tracer to reach the neuronal cell body.

Tissue fixation by cardiac perfusion

All rats were deeply anesthetized (somnitol, 80 mg/kg) and perfused through the left ventricle prior to further histological analysis as described below. A warm saline flush (100 ml) was followed by 500 ml of ice cold 4% paraformaldehyde. L3 DRGs were dissected ipsilaterally, cryoprotected in 20–30% sucrose overnight, embedded in OCT compound (Tissue Tek, Miles INC, Elkhart, IN) in a cryomold (Tissue Tek), frozen in isopentane cooled to −70 °C and stored at −80 °C until further processing.

Quantification of the number of regenerated sensory neurons

The L3 DRG were serially sectioned at 10 μm using a Microm HM500 cryostat (Zeiss, Canada) and mounted on glass slides. Each section was visualized at 20–40× under ultraviolet fluorescence at barrier filters of 580 nm for FR and 430 nm for FG. Sensory neurons containing both FR and FG were visualized using both filters. The observer who was unaware of experimental condition and which branch had received FG or FR counted the backlabeled sensory neurons. Only DRG neu-

rons with a visible nucleus were counted. The number of backlabeled sensory neurons was determined by counting every other section to minimize the possibility of counting large neurons more than once.

In situ hybridization

Following a 2 day regeneration period, L3 DRG were harvested from cardiac perfused rats subjected to 0 h (sham, $n=3$), 1 h ($n=3$) or 3 h ($n=3$) stimulation at the time of nerve repair. The L3 DRGs were cryoprotected, embedded as above and stored at −80 °C until further processing. Serial DRG sections were cut at 6 μm using a Microm HM500 cryostat (Zeiss, Canada), thaw mounted onto Probe-ON$^+$ slides (Fisher Scientific, Canada) and stored with desiccant at −20 °C until hybridization.

In situ hybridization was carried out on tissue using a 48 base pair oligonucleotide probe (University Core DNA Services, Calgary, AB, Canada) complementary to and selective for GAP-43 mRNA (complementary to bases 70–117; Karns et al., 1987). The probe was checked against the GenBank database (NIH, Bethesda, MD) to ensure that no greater than 75% homology was found to sequences other than the cognate. The probe was labeled at the 3′-end with α-[^{35}S]dATP (New England Nuclear, Boston, MA) using terminal deoxynucleotidyl-transferase (Amersham Biosciences, Piscataway, NJ) in a buffer containing 10 mM $CoCl_2$, 1 mM dithiothreitol (DTT), 300 mM Tris base and 1.4 M potassium cacodylate, pH 7.2, and purified through Bio-Spin Disposable Chromatograph Columns (Bio-Rad Laboratories, Hercules, CA) containing 200 mg of NENSORB PREP Nucleic Acid Purification Resin (DuPont NEN, Boston MA). Dithiothreitol was added to a final concentration of 10 nM.

In situ hybridization was carried out according to published procedures (Dagerlind et al., 1992). Briefly, the sections were hybridized at 43 °C for 14–18 h in a buffer containing 50% formamide (Sigma Aldrich, Oakville, Ontario, Canada), 4× SSC (1× SSC = 0.15 M NaCl, 0.015 M sodium citrate), 1× Denhardt's solution (0.02% bovine serum albumin and 0.02% Ficoll), 1% sarcosyl (*N*-laurylsarcosine), 0.02 M phosphate buffer, pH 7.0, 10% dextran sulfate, 500 μg/ml heat-denatured sheared salmon sperm DNA, 200 mM dithiothreitol and 10^7 cpm/ml of probe. After hybridization, the slides were washed 4 × 15 min in 1× SSC at 55 °C, dehydrated in ascending alcohols, processed for radioautography as per Karchewski et al. (2002) and exposed for 7 days before developing in D-19 (Kodak, Rochester, NY).

The specificity of hybridization signal for the probe was ascertained by hybridization of labeled probe, labeled probe with a 1000-fold excess of cold probe (signal abolished) or labeled probe with a 1000-fold excess of a dissimilar cold probe of the same length and similar G-C content (signal unchanged).

Immunohistochemistry

The L3 DRG sections were cut at 6 μm on a cryostat, thaw mounted onto Probe-ON$^+$ slides (Fisher Scientific) and processed for immunohistochemistry. To detect activating transcription factor 3 (ATF3) protein expression, sections were washed 3 × 10 min in 0.1 M TBS and blocked in 10% goat serum in TBS for 1 h at room temperature. Primary antibody rabbit anti-ATF3 (1:300; cat# sc-188, Santa Cruz Biotech Inc., Santa Cruz, CA) in TBS was left on tissue overnight at 4 °C. The next day, sections were washed at 3 × 10 min in TBS and then incubated in secondary antibody, biotinylated goat anti-rabbit IgG (1:300; Vector, Burlington, Ontario, Canada) in TBS. The ATF3 immunoreactivity was visualized using standard ABC procedure (Vector, Burlington, Ontario, Canada). To detect BDNF protein expression, immunohistochemistry was performed as previously described by Karchewski et al., 2002. The primary antibody, rabbit anti-BDNF (1:500; gift from Cindy Wetmore, Mayo Clinic, Rochester, MN, USA; Wetmore and Olson, 1995), was left on tissue overnight at 4 °C. The next day, sections were incubated in secondary antibody Cy3-conjugated donkey anti-rabbit IgG (1:300; Jackson, Westgrove, PA) for 1 h in the dark at room temperature. Slides were coverslipped with glycerol/PBS.

Control for antibody specificity: Control sections were processed in the same manner, but with blocking solution or undiluted normal rabbit serum replacing the primary antibody. Additional control sections were also processed using BDNF antibody preabsorbed overnight with a 50× excess of BDNF protein. All of these resulted in only background levels of immunoreactivity with no specific signal being observed (Fig. 2). To verify that anti-ATF3 was only labeling injured sensory neurons, 2 animals underwent partial injury of the sciatic nerve with only the peroneal branch being injured and backlabeled with 4% FG in 0.1 M cacodylic acid. Two days later, the animals were perfused, L5 DRG removed, serially sectioned at 6 μm and processed for ATF3 immunohistochemistry as described above. Microscopic analysis confirmed that only those neurons backlabeled with fluorogold and with a visible nucleus were immunoreactive for ATF3 (Fig. 2). A previous study confirmed by Western blot analysis that this antibody is selective for ATF3 (Takeda et al., 2000).

In situ hybridization quantification and analysis

Not all L3 DRG neurons contribute to the femoral nerve at the level of the nerve injury performed in this study. Neurons with transected axons were identified by processing sections for immunohistochemistry to detect ATF3, which is expressed *de novo* in axotomized sensory neurons (Tsujino et al., 2000). The adjacent section was processed for *in situ* hybridization to detect GAP-43 mRNA, and all neurons with a detectable nucleus were identified in the serial sections and labeled as axotomized or intact based on whether or not nuclear ATF3 expression was detected. This allowed alterations in GAP-43 mRNA hybridization signal to be quantified in the axotomized (those with the potential to regenerate) versus the nonaxotomized intact neurons. DRG sections from each experimental group were mounted on the same slide to ensure that slide to slide variability in hybridization signal did not impact the relative difference in hybridization signal for each experi-

mental group. Quantitative analysis was performed on DRG sections from all 2 day post-repair animals ($n=9$ sections analyzed one from each of the 9 experimental animals) to detect the density of GAP-43 mRNA hybridization signal in ATF3-positive and -negative neurons after 0 h (sham; 772 neuronal profiles analyzed), 1 h (895 neuronal profiles analyzed) and 3 h (831 neuronal profiles analyzed) of electrical stimulation. Photomontages of each section to be analyzed were prepared and all neurons with a visible nucleus were identified. Using a 63× light objective, the cross-sectional areas of individual neurons identified as ATF3-positive or -negative and the percentage of cytoplasmic area covered by silver grains were measured for all neurons in each DRG. The area per grain was kept constant for all neurons and a correction for grain overlap was made to obtain a parameter linearly related to density of silver grains (Richardson et al., 1989). Northern Eclipse, Version 7.0 (Empix Imaging, Mississauga, ON, Canada), Microsoft Office Excel 2003 (Microsoft Corporation, Redmond, WA) and Prizm 4.0 (Graph Pad Software, San Diego, CA) were the software utilized for the analysis. Cells were considered labeled if they had more than five times background levels of silver grains, as determined by averaging grain densities over defined areas of the neuropil devoid of positively labeled cell bodies. This cut-off corresponds to the level of hybridization signal that must be present in order to confidently declare the neuron labeled when observed under 63× oil immersion.

Statistical analysis

A Kruskal–Wallis nonparametric ANOVA (Prism v.2.01, GraphPad Software Inc., San Diego, CA) was used to compare the number of sensory neurons projecting axons to cutaneous and muscle branches within each group and to ascertain statistical significance for level of GAP-43 expression in ATF3-positive and -negative neurons 2 days post-repair and electrical stimulation. A Mann–Whitney *U* test (Prism v.2.01) was used to compare the number of sensory neurons extending an axon across the surgical repair site 4 days after repair with or without 1 h stimulation at the time of repair. Statistical significance was accepted at <0.05 level.

Results

The effect of duration of electrical stimulation on regeneration of sensory neurons in vivo

In the transected and surgically repaired rat femoral nerve, a 1 h period of continuous 20 Hz electrical stimulation was as effective as periods of 1 day to 2 weeks of electrical stimulation in significantly enhancing motor axonal regeneration (Al-Majed et al., 2000b). The identical stimulation protocol was employed to assess which duration(s) of stimulation beneficially impact sensory neuron regeneration.

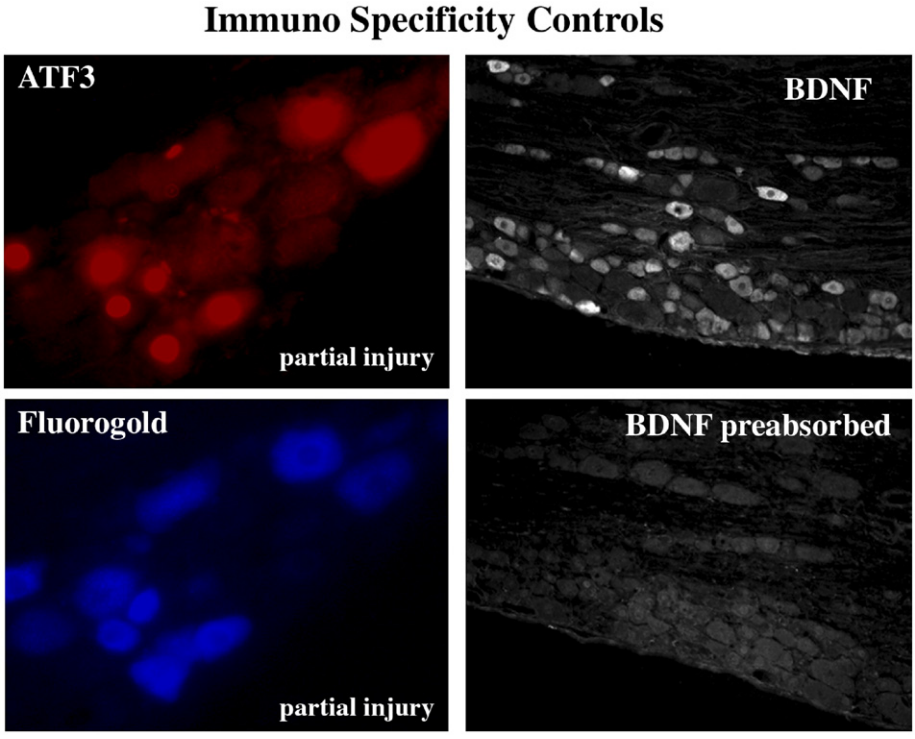


Fig. 2. Antibody control experiments. Left: Fluorescent photomicrographs of adjacent DRG sections processed for ATF3 immunohistochemistry (top) or identifying neurons that had been injured and retrogradely labeled with fluorogold (bottom). Note that only the injured neurons (i.e., those that are fluorogold labeled) are ATF3 positive. Right: Fluorescence photomicrographs of adjacent DRG sections processed for BDNF immunohistochemistry using either BDNF antibody alone (top) or BDNF antibody preabsorbed overnight with 50× BDNF protein (bottom). Note that preabsorbing the antibody abolished the positive signal observed with antibody alone.

The total number of L3 DRG neurons that regenerated their axons into the cutaneous or the muscle branch of the femoral nerve 21 days after nerve repair and experimental treatment was assessed by backlabeling with FR in one branch and FG in the other (Fig. 1C). The total number of DRG neurons that regenerated their axons down each branch was determined. Experimental control groups included nerve injury and repair (0 h stimulation) and the nerve injury and repair plus placement of electrodes for 1 h without turning on the stimulator (0 h stimulation sham group). No significant differences were found between the control groups, so the data from the two groups were pooled and comprised the 0 h group (Fig. 3). Stimulation of the femoral nerve for 1 h after nerve transection and repair resulted in a significant increase in the number of sensory neurons that regenerated axons into either the cutaneous or muscle branch (Fig. 3; Table 1).

The increase in the number of sensory neurons that regenerated their axons into the cutaneous or muscle branch was not due to an increased incidence of double labeled neurons, i.e., those that sent axonal collaterals to both branches, as the numbers of neurons remained relatively unchanged among treatment groups (210±45 SEM (0 h) versus 206± 27 SEM (1 h)) (Fig. 3). When factoring in the number of double labeled neurons, the total number of L3 DRG neurons that regenerated following nerve injury and repair was approximately 777 with 0 h stimulation versus 1643 with 1 h stimulation. The total number of L3 DRG neurons that contribute to the femoral nerve at the level where the backlabeling was performed in naïve animals is 1727 (±139 SEM) with an

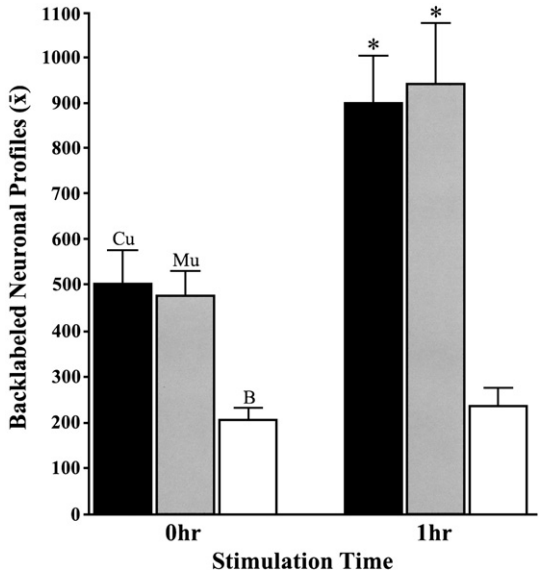


Fig. 3. Electrical stimulation for 1 h significantly improves sensory axon regeneration. The mean number ($\bar{X}$±SEM) of backlabeled sensory neurons that regenerated their axons into the muscle (mu—gray bar), cutaneous branch (cu—black bar) or both (B—open bar) after femoral nerve repair with no stimulation (0 h, $n=20$) or brief stimulation (1 h, $n=19$) delivered in a continuous 20-Hz train at time of nerve repair as indicated. Note: Stimulation of 1 h significantly increases the number of sensory neurons regenerating into the cutaneous and muscle branches after nerve transection and repair (asterisk $p<0.05$, Kruskal–Wallis nonparametric ANOVA).

Table 1
Influence of stimulation duration on number of regenerating sensory neurons ($\bar{X}$±SEM)

Stimulation time	Cutaneous	Muscle
0 h	507±73	480±54
1 h	904±103 *	945±133 *
3 h	757±53	709±130
1 day	437±331	548±277
7 days	409±118	411±133
14 days	456±131	558±138

* $p<0.001$ Kruskal–Wallis nonparametric ANOVA.

incidence of double labeling of 30 (±13 SEM). Thus, 1 h stimulation at time of repair results in approximately 97% of these L3 neurons regenerating at 21 days post-repair versus 46% with repair alone.

The duration of electrical stimulation at the time of nerve repair was extended beyond 1 h to assess whether regeneration of sensory neurons might be further enhanced. Stimulation for continuous periods of 3 h, 1 day, 7 days or 14 days was less effective than 1 h stimulation at enhancing the number of sensory neurons that regenerated into either the muscle or cutaneous branches 21 days after nerve repair. None of these additional stimulation paradigms were significantly different from the 0 h control group (Fig. 4; Table 1).

The effect of brief electrical stimulation on the ability of sensory neurons to regenerate beyond the repair site

We next examined whether the enhanced sensory nerve regeneration observed in response to 1 h stimulation at the time of femoral nerve repair was due to an accelerated growth of axons across the repair site into the distal nerve stump as observed for motor axons (Brushart, 1988). All sensory neurons that regenerated axons beyond the repair site by 4 days post-repair were identified using retrograde labeling just distal to the surgical reunion of the nerve stumps in 0 h and 1 h stimulated rats (Fig. 5A). The number of backlabeled neuronal profiles after 1 h stimulation group (758±75 SEM) was significantly greater than the 0 h control group (461±103 SEM), representing a 64% increase in the number of DRG neurons that rapidly regenerated axons across the repair site (Fig. 5B).

Influence of action potential blockade on sensory neuron regeneration following brief electrical stimulation

To assess whether the effect of electrical stimulation on sensory neuron regeneration was due to increased electrical activity of the sensory neurons and not solely an indirect affect on the nonneuronal components of the nerve at the site of stimulation, retrograde conduction of action potentials was blocked using a TTX-mediated blockade of sodium channels proximal to the stimulating electrode (Fig. 6A). As expected from the corresponding motoneuron data (Al-Majed et al., 2000b), TTX application abolished the positive influence of 1 h electrical stimulation on sensory axon regeneration (Fig. 6B). There was no significant difference on the regenerative response

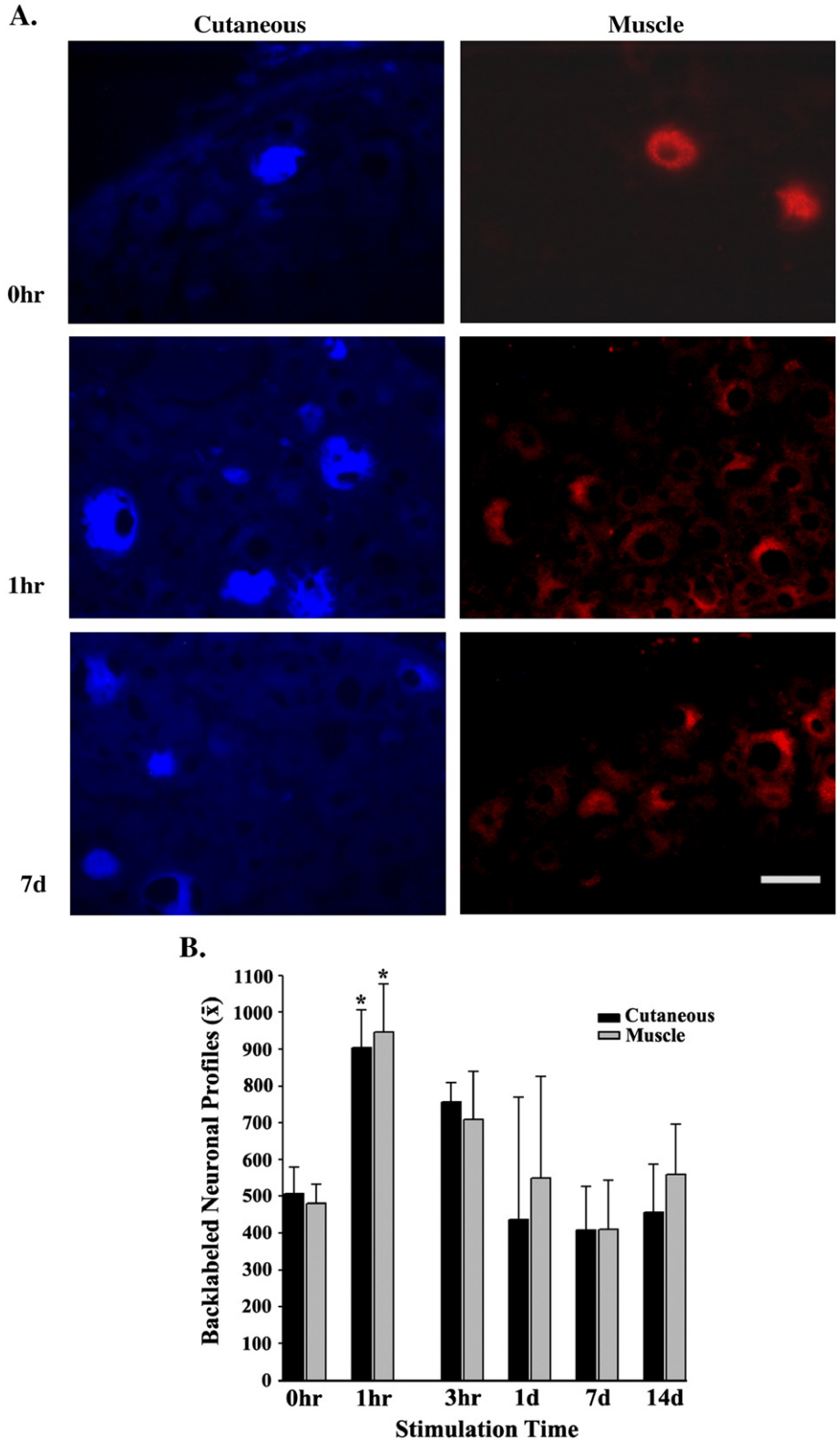


Fig. 4. Long-term stimulation is less effective than short-term stimulation in promoting axonal regeneration of sensory neurons. (A) Fluorescence photomicrographs of retrogradely labeled sensory neurons that regenerated into the muscle branch or cutaneous branch, 21 days after femoral repair with 0 h, 1 h or 7 days (d) of 20 Hz continuous electrical stimulation. Scale bar = 50 μm. (B) The mean number ($\bar{X} \pm$ SEM) of backlabeled sensory neurons that regenerated their axons into the cutaneous or muscle branches after femoral repair with continuous 20 Hz stimulation delivered at time of repair for 0 h ($n=20$), 1 h ($n=19$), 3 h ($n=6$), 1 d ($n=3$), 7 d ($n=4$) or 14 d ($n=5$) durations as indicated. Note: One hour stimulation is the only time point where there is a significant improvement in regeneration ($p<0.05$, Kruskal–Wallis nonparametric ANOVA).

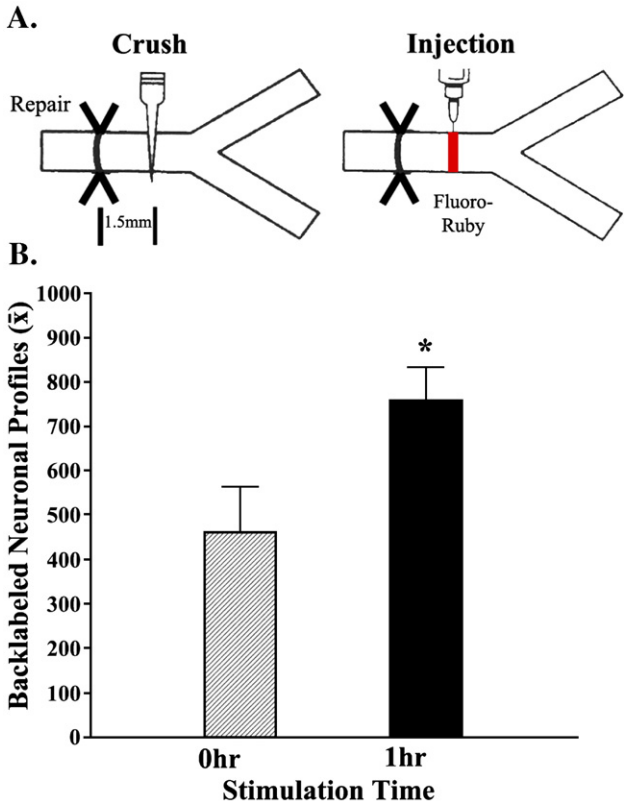


Fig. 5. One hour of 20 Hz continuous electrical stimulation significantly increases the number of sensory neurons extending axons across the repair site 4 days (d) following nerve transection. (A) Diagrammatic representation of distal labeling (as adapted from Brushart, 1988). Axons were labeled just distal to the repair to identify the sensory axons that crossed the repair site. (B) The mean number ($\bar{X}\pm$SEM) of backlabeled sensory neurons that regenerated axons beyond the repair site 4 d after injury and repair with no stimulation (0 h, $n=9$) or 1 h ($n=9$) continuous 20 Hz stimulation delivered at time of repair (asterisk $p<0.05$, Mann–Whitney U test).

of sensory neurons into either nerve branch for the stimulated +TTX-treated group when compared to the 0 h control group.

Abolishing sodium channel activity with TTX did not alter the incidence of regenerating sensory neurons extending axons down both the motor and cutaneous nerve branches (double-labeled neurons; 237±40 SEM) when compared to the 0 h (210±45 SEM) and the 1 h electrical stimulation groups (206±27 SEM; Fig. 6B).

The effect of short-term electrical stimulation on the cell body response of sensory neurons

To assess whether brief electrical stimulation at the time of femoral nerve repair results in elevated expression of the injury/regeneration-associated genes GAP-43 and BDNF, L3 DRG were removed 2 days following femoral nerve transection and repair with 0 h (sham), 1 h or 3 h electrical stimulation and expression of these markers was evaluated. The shorter 2 day regeneration time was selected for examination rather than the previous 21-day regeneration period because the electrical stimulation promotes the outgrowth of axons across the suture site within 4 days, and by 21 days post-repair discernible differences in expression of these markers are no longer evident (NMG, unpublished observations).

At 2 days post-nerve repair, 1 h stimulation resulted in an elevated level of GAP-43 mRNA expression in some but not all L3 sensory neurons when compared to the L3 sensory neurons that received 0 h or 3 h stimulation at the time of nerve repair (Fig. 7). Since only a proportion of L3 DRG neurons send their axons to the femoral nerve at the level of the nerve section and repair, we expected such a partial effect. To specifically identify axotomized neurons, we processed serial sections of the L3 DRGs for ATF3 immunoreactivity or GAP-43 mRNA in situ hybridization. ATF3 serves as a marker for sensory neurons that are axotomized (Tsujino et al., 2000) and allows identification of the neurons that have the potential to regenerate. Using serial sections, the same DRG neurons were identified in the adjacent sections and allowed quantification of GAP-43 mRNA hybridization signal over ATF3-positive (injured) versus the ATF3-negative (noninjured) neuronal subpopulations of the L3 DRG (Fig. 7).

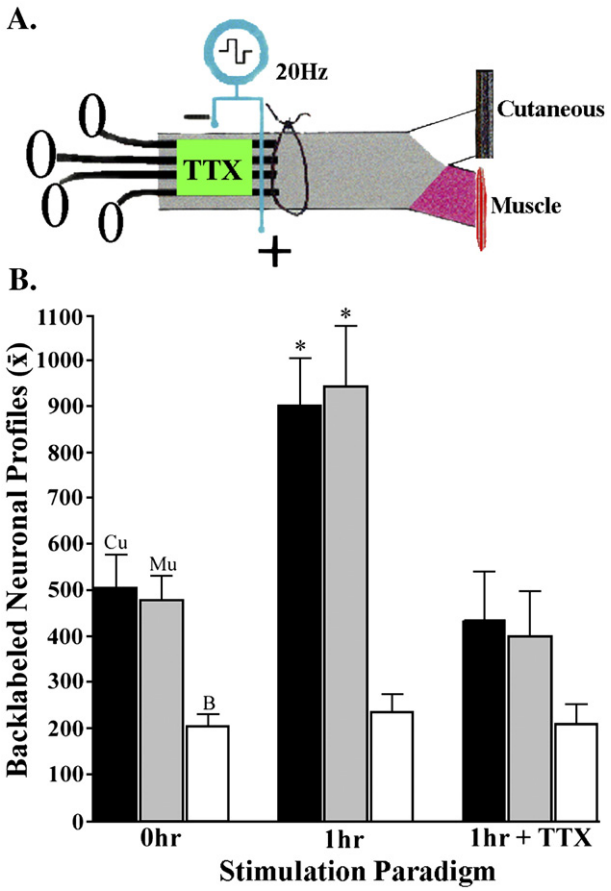


Fig. 6. TTX blocks the effect of 1 h of 20 Hz continuous electrical stimulation on 21 days of regeneration after nerve transection and surgical repair. (A) Diagrammatic representation of the application of TTX (60 μg/ml; as adapted from Al-Majed et al., 2000b). (B) The mean number ($\bar{X}\pm$SEM) of backlabeled sensory neurons that regenerated their axons into the cutaneous (cu—black bar), muscle (mu—gray bar) branches or both branches (B—open bar) after nerve transection and repair with continuous 20 Hz stimulation delivered for 0 h ($n=20$), 1 h ($n=19$) or 1 h in the presence of TTX ($n=6$) as indicated. Note: There is no significant difference between 1 h stimulation+TTX and 0 h stimulation (Kruskal–Wallis nonparametric ANOVA).

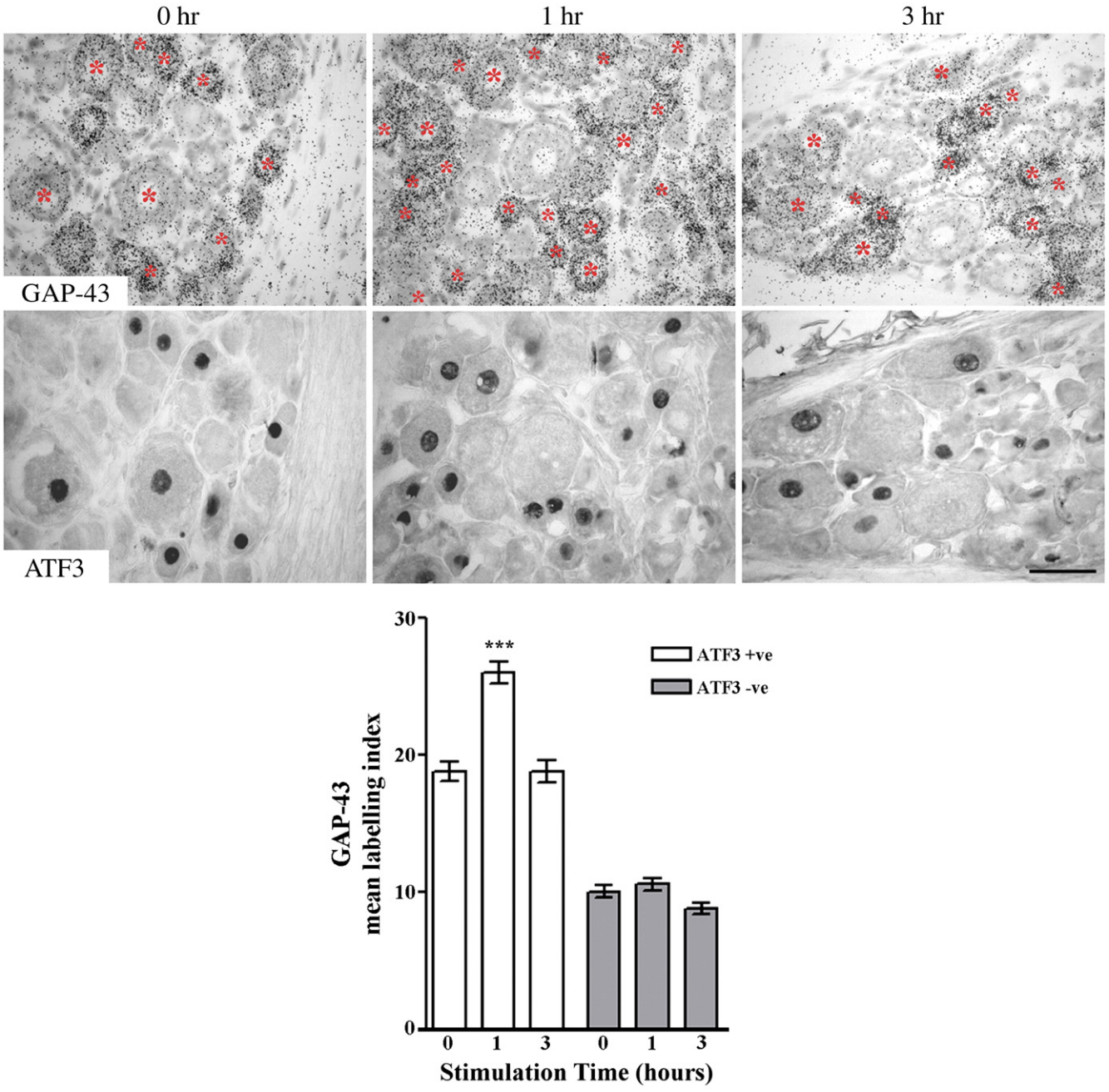


Fig. 7. Brief electrical stimulation results in increased GAP-43 expression in injured but not in uninjured sensory neurons. (A) Bright-field photomicrographs depicting levels of GAP-43 mRNA in L3 DRG in response to 0 h, 1 h or 3 h electrical stimulation. ATF3 is used as a marker to identify injured sensory neurons in slides adjacent to those processed by *in situ* hybridization to detect GAP-43 mRNA. The ATF3-positive neurons are indicated by red asterisks in the adjacent GAP-43 section. Note the elevated expression of GAP-43 in ATF3-positive neurons in response to 1 h stimulation. Scale bar=50 μm. (B) Mean labeling indices of GAP-43 mRNA hybridization signal over individual neurons identified as injured (ATF3-positive) or uninjured (ATF3-negative) for stimulation times as indicated (n=295–489 neurons quantified per condition). Labeling index refers to the ratio of silver grain density over the neuronal cytoplasm to silver grain density over areas of the neuropil devoid of positive hybridization signal. Note: 1 h stimulation results in a significant increase in the GAP-43 mRNA mean labeling index in ATF3-positive neurons when compared to either 0 h or 3 h time points ($p<0.001$, Kruskal–Wallis nonparametric ANOVA).

Quantification of the GAP-43 mRNA hybridization signal over the individual ATF3-negative neurons revealed that moderate to high levels of signal (>10× background) were detected almost exclusively over small- to medium-sized intact DRG neurons (data not shown). This distribution of GAP-43 mRNA in the ATF3-negative (noninjured) neurons is similar to the pattern of expression of GAP-43 mRNA previously described for intact sensory neurons (Verge et al., 1990). Stimulation for either 1 or 3 h at the time of femoral nerve transection and repair had no significant effect on the mean level of GAP-43 mRNA expression measured in noninjured, ATF3-negative sensory neurons when compared to the 0 h control group (Fig. 7).

In injured, ATF3-positive neurons, GAP-43 mRNA hybridization signal was elevated when compared to expression

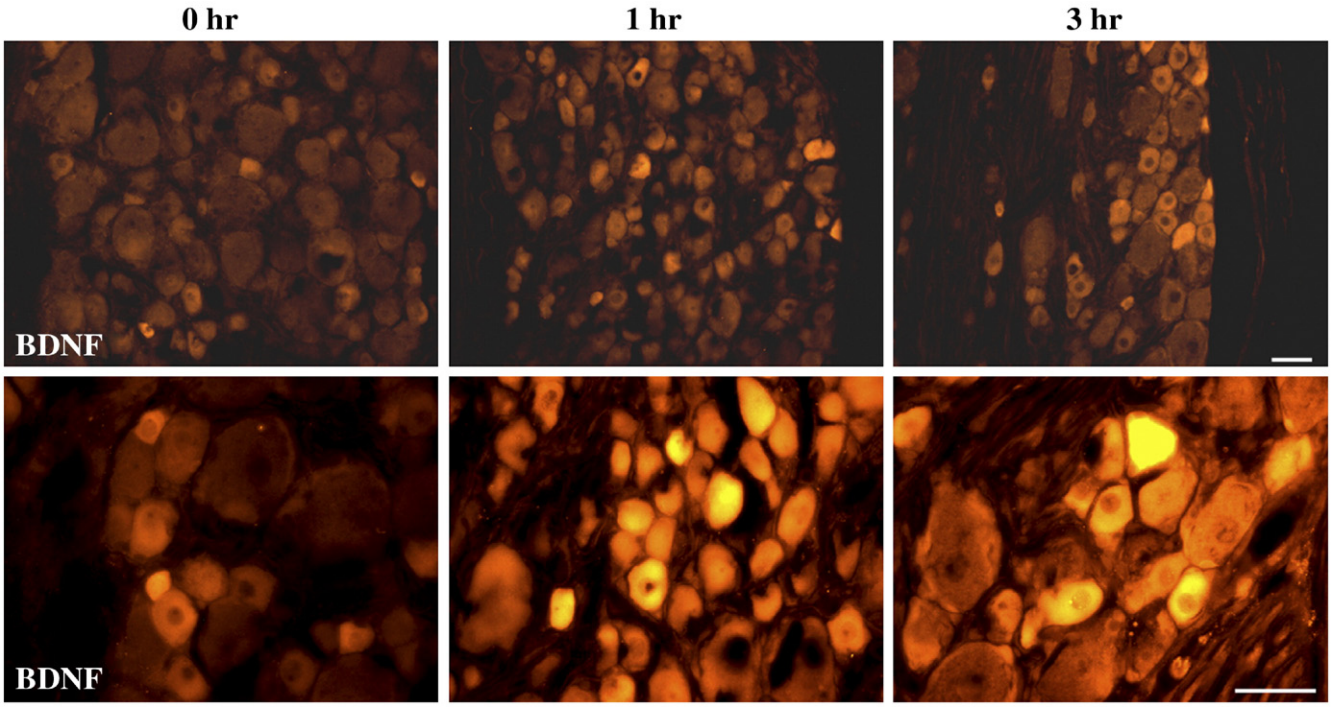


Fig. 8. Brief electrical stimulation results in elevated BDNF expression. Fluorescence photomicrographs taken at low (top) or high power (bottom) depict BDNF-LI in response to 0 h, 1 h or 3 h electrical stimulation. Note: One hour stimulation results in elevated neuronal BDNF-LI that appears to be enhanced in the 3 h group. Scale bar=50 μm.

levels in ATF3-negative neurons (Fig. 7A). This pattern of elevated GAP-43 mRNA expression is normally observed in response to peripheral axotomy in sensory neurons (Verge et al., 1990). Quantification revealed that 1 h stimulation at the time of repair results in significantly elevated GAP-43 hybridization signal over ATF3-positive neurons when compared to the 0 h control group. While the mean neuronal labeling index was significantly elevated in the 1 h stimulated neurons, this response was abolished in the 3 h stimulated group (Fig. 7B). Brief electrical stimulation also had a marked influence on the level of BDNF protein expression detected in sensory neurons supplying the femoral nerve. Immunohistochemical analysis revealed that 2 days following 1 h electrical stimulation at the time of femoral nerve repair, BDNF-like immunoreactivity (LI) was elevated across all size ranges of neurons, but most apparent over small- to medium-sized neurons (Fig. 8). BDNF-LI was still slightly elevated in the 1 h stimulated group 4 days following nerve repair but did not differ from the 0 h stimulated group by 21 days post-repair (NMG, data not shown). However, 3 h electrical stimulation further elevated BDNF-LI when compared to 0 h or 1 h stimulation (Fig. 8).

Discussion

The present study assessed the effect of electrical stimulation on regeneration of sensory neurons following transection and repair of the rat femoral nerve under conditions that promote maximal and appropriate motoneuron regeneration. We present the novel findings that continuous electrical stimulation at 20 Hz for 1 h significantly increases the number of regenerating sensory fibers, promotes early regeneration across the repair site and induces an enhanced regeneration-associated cell body response in the affected sensory neurons. However, extending the duration of stimulation beyond 1 h resulted in less effective repair, unlike what has been observed for motoneurons.

Brief electrical stimulation promotes sensory neuron regeneration in the injured peripheral nerve

Brief electrical stimulation applied immediately after surgical repair of the transected femoral nerve was effective in significantly enhancing sensory axonal regeneration with over twice the number of neurons regenerating compared to repair alone. Though electrical stimulation (alternating current) has been shown to enhance motoneuron regeneration of the peripheral nerve (Nix and Hopf, 1983; Al-Majed et al., 2000b), this is the first study examining the effect of various durations of electrical stimulation on the intrinsic regenerative response of sensory neurons. Stimulation for 1 h was optimal for sensory neuron regeneration, while longer periods of stimulation were not as effective. Brief electrical stimulation significantly increased the number of regenerating sensory axons; however, there was no change in double-labeled neurons within each treatment group. The fact that the number of neurons extending axon collaterals to both branches remains unchanged suggests that a select subpopulation of regenerating sensory neurons is predisposed to do so regardless of treatment (Langford and Coggeshall, 1981; Taylor and Pierau, 1982; Taylor et al., 1983). To resolve this requires further character-

ization of the subpopulation of double-labeled neurons and is beyond the scope of this study.

The increase in sensory axonal regeneration in response to brief electrical stimulation correlated with an enhanced cell body response. Peripheral nerve axotomy induces a regenerative state in sensory neurons (Richardson and Issa, 1984; Richardson and Verge, 1986; Aigner and Caroni, 1993, 1995; Tetzlaff et al., 1989) and is correlated with a cell body response that includes upregulation in expression of injury/regeneration-associated genes such as GAP-43, Tα1 tubulin and BDNF (Verge et al., 1990; Schreyer and Skene, 1991, 1993; Mohiuddin and Tomlinson, 1997; Michael et al., 1999; Zhou et al., 1999; Karchewski et al., 2002). Brief electrical stimulation at the time of nerve repair induced a more robust response with respect to GAP-43 and BDNF expression in the affected sensory neurons and this correlated with an enhanced propensity for axonal regeneration. Stimulation for longer periods (3 h) was found to decrease the levels of GAP-43 injury/regeneration-associated gene expression and this was correlated with decreased axonal regeneration.

The significant increase in sensory axonal regeneration is different from the findings of another study examining the effect of 1 h electrical stimulation on the specificity of sensory neuron regeneration. Brushart et al. (2005) found that 1 h of 20 Hz electrical stimulation enhanced the specificity of target reinnervation to the muscle but did not significantly increase the overall numbers of regenerating neurons (Brushart et al., 2005). Importantly, brief electrical stimulation appropriately redistributed the regenerating sensory neurons to their original targets, decreasing the number of regenerating sensory neurons to the muscle and increasing those to the cutaneous branch (Brushart et al., 2005). This is different from our current study where we show significant improvement in the overall numbers of neurons regenerating to either branch. The difference may be related to cell count strategy. To determine specificity, Brushart et al. (2005) counted all neurons contributing to the femoral nerve, including contributions from L2, L3 and some L4 DRG neurons. Our study focused on the effect of stimulation duration on sensory neuron regeneration and impact on injury/regeneration-associated gene response. As a result, we only examined L3 DRG neurons. The increased number of sensory neurons regenerating to the muscle, observed in this study, may be reflective of the L3 DRG neuron population. We found that this significant increase in L3 sensory neurons regenerating in response to1 h electrical stimulation was consistent in three separate experiments and correlated with an upregulation of injury/regeneration-associated genes.

Benefits of brief electrical stimulation: reducing the staggered regeneration

Femoral nerve axons regenerating at a rate of 1–3 mm/day (Gutmann et al., 1942) would take 2–3 weeks to regenerate from the repair site to the target tissue. This is the rate of the fastest growing axons and does not take into account the lag period of days or weeks before axons enter the distal nerve stump (Al-Majed et al., 2000b). Electrical stimulation might enhance regeneration by decreasing the delay before axons begin to elongate and therefore compress the 'staggered' regeneration period. Brushart (1988) found brief stimulation significantly compressed this staggered regeneration period for motoneurons. We find the same stimulation protocol led to a significant increase in the number of sensory axons that regenerate across the repair site. It remains undetermined whether electrical stimulation forces quiescent neurons more rapidly into their regeneration program or whether that program has been modified to facilitate crossing the repair gap (see Brushart, 1988).

Potential mechanism

The increase in injury/regeneration-associated gene expression in response to brief electrical stimulation suggests that the beneficial effects of stimulation impact the cell body response. Blocking action potentials with TTX abolished this response in both sensory (present study) and motoneurons (Al-Majed et al., 2000b). Blocking membrane depolarization prevents the opening of voltage dependent calcium channels and calcium influx (Ming et al., 2001), thereby impairing upregulation of immediate early genes, intracellular cAMP (Ming et al., 2001; Kocsis et al., 1994), elevated BDNF and trkB expression (Shieh et al., 1998; Tao et al., 1998; Kingsbury et al., 2003) and increased neurite outgrowth (Kocsis et al., 1994). In addition, in response to an increase in neuronal activity BDNF is rapidly released (Lever et al., 2001), trkB receptors are recruited to the cell membrane (Meyer-Franke et al., 1998; Goldberg et al., 2002) and intracellular signaling and transcriptional events are altered (Fields et al., 1997; Itoh et al., 1997; Eshete and Fields, 2001).

We observed an increase in BDNF expression with electrical stimulation. A similar response was observed in motoneurons (Al-Majed et al., 2000a) and was correlated with an elevated expression of Tα1-tubulin and GAP-43 mRNAs (Al-Majed et al., 2004). BDNF likely plays a role in regeneration in sensory neurons, as it is induced in ~80% of sensory neurons immediately following injury (Karchewski et al., 2002). Antagonizing endogenous BDNF during peripheral nerve repair has been linked to impairment of injury/regeneration-associated gene expression (Geremia et al., 2003, 2004), reduction in axonal sprouting (Streppel et al., 2002) and growth and myelination deficits (Zhang et al., 2000; Geremia et al., 2004). Though electrical stimulation elevated BDNF in the sensory neurons, future studies will determine whether it is the underlying mechanism. Another effect of electrical stimulation is an increase in intracellular cAMP, which can overcome MAG-associated inhibition of axonal growth in the distal stump of an injured peripheral nerve (Cai et al., 2001; Neumann et al., 2002; Qiu et al., 2002). However, whether cAMP plays a key role in altering the cell body response of sensory neurons is less clear (Han et al., 2004; Andersen et al., 2000). One cannot exclude that there is also an impact of electrical stimulation on the nonneuronal cells in the vicinity of the stimulating electrodes previously shown *in vitro* to alter Schwann cell phenotype (Stevens and Fields, 2000). In the present paradigm where TTX was applied upstream of the site of injury and

stimulation, nonneuronal cells at the site of lesion would still be under the influence of stimulation but the action potentials going back to the sensory neuron cell bodies are blocked. Because this abolished the positive effect of brief electrical stimulation on regeneration of the sensory neurons, it suggests that the impact of the stimulation on the nonneuronal cells alone is not sufficient to effect this response.

Even though brief stimulation significantly improved the regeneration of both sensory and motor axons, there was a discrepancy between these two populations in response to long-term stimulation. Whereas stimulation for 1 h, 1 day, 7 days or 14 days was equally effective in increasing the numbers of regenerating motoneurons (Al-Majed et al., 2000b), 1 h stimulation is optimal for sensory neuron regeneration. Longer periods of stimulation were ineffective in significantly enhancing sensory axonal regeneration. The differential response may be related to trkB expression in response to injury and prolonged exposure to BDNF. Motoneurons respond to injury by elevating trkB expression (Al-Majed et al., 2000a). However, peripheral injury results in an overall decrease in trkB expression in sensory neurons and perineuronal cells (Karchewski et al., 1999) and prolonged exposure to high levels of BDNF can downregulate trkB expression in sensory neurons (Geremia and Verge, 2001). Stimulation for 1 h resulted in an upregulation of BDNF-immunoreactivity in sensory neurons. While stimulation for 3 h resulted in enhanced BDNF immunoreactivity, this was associated with decreased sensory axon regeneration and GAP-43 injury/regeneration-associated gene expression. Thus, long-term stimulation could potentially chronically expose these cells to elevated BDNF and lead to desensitization of the sensory neuron to this ligand by downregulation of trkB expression.

Significance

When nerve repair is delayed, there are disappointing regenerative outcomes (Fu and Gordon, 1995a,b). A more robust regeneration of injured axons across the repair site would counteract the delay in reinnervation of pathways and enhance functional recovery. The ability of brief electrical stimulation of the nerve to significantly enhance the cell body response, the number of sensory neurons that regenerate, regeneration specificity (Brushart et al., 2005) and the growth of motor axons into the appropriate muscle pathway of the transected femoral nerve (Al-Majed et al., 2000b; Brushart, 1988) has important implications for the design of therapeutic strategies to improve peripheral nerve repair following injury.

Acknowledgments

We are indebted to JM Johnston, S Bocking and N Tyreman for excellent technical and editorial assistance. This work was supported by grants to VMKV and TG from the Canadian Institutes of Health Research (CIHR), Neurotrauma Partners of Canada and Saskatchewan Regional Partnership Program. NMG is supported by a U.S. College of Medicine Graduate Scholarship. TMB is supported by NIH RO1 NS034484-07. TG is an Alberta Heritage Foundation for Medical Research (AHFMR) Scientist.

Appendix A. Supplementary data

Supplementary data associated with this article can be found, in the online version, at doi:10.1016/j.expneurol.2007.01.040.

References

Aigner, L., Caroni, P., 1993. Depletion of 43-kD growth-associated protein in primary sensory neurons leads to diminished formation and spreading of growth cones. J. Cell Biol. 123, 417–429.

Aigner, L., Caroni, P., 1995. Absence of persistent spreading, branching, and adhesion in GAP-43-depleted growth cones. J. Cell Biol. 128, 647–660.

Al-Majed, A.A., Brushart, T.M., Gordon, T., 2000a. Electrical stimulation accelerates and increases expression of BDNF and trkB mRNA in regenerating rat femoral motoneurons. Eur. J. Neurosci. 12, 4381–4390.

Al-Majed, A.A., Neumann, C.M., Brushart, T.M., Gordon, T., 2000b. Brief electrical stimulation promotes the speed and accuracy of motor axonal regeneration. J. Neurosci. 20, 2602–2608.

Al-Majed, A.A., Tam, S.L., Gordon, T., 2004. Electrical stimulation accelerates and enhances expression of regeneration-associated genes in regenerating rat femoral motoneurons. Cell. Mol. Neurobiol. 24, 379–402.

Andersen, L.B., Schreyer, D.J., 1999. Constitutive expression of GAP-43 correlates with rapid, but not slow regrowth of injured dorsal root axons in the adult rat. Exp. Neurol. 155, 157–164.

Andersen, P.L., Webber, C.A., Kimura, K.A., Schreyer, D.J., 2000. Cyclic AMP prevents an increase in GAP-43 but promotes neurite growth in cultured adult rat dorsal root ganglion neurons. Exp. Neurol. 166, 153–165.

Bevan, S., Winter, J., 1995. Nerve growth factor (NGF) differentially regulates the chemosensitivity of adult rat cultured sensory neurons. J. Neurosci. 15, 4918–4926.

Brushart, T.M., 1988. Preferential reinnervation of motor nerves by regenerating motor axons. J. Neurosci. 8, 1026–1031.

Brushart, T.M., Seiler, W.A.t., 1987. Selective reinnervation of distal motor stumps by peripheral motor axons. Exp. Neurol. 97, 289–300.

Brushart, T.M., Jari, R., Verge, V., Rohde, C., Gordon, T., 2005. Electrical stimulation restores the specificity of sensory axon regeneration. Exp. Neurol. 194, 221–229.

Cai, D., Qiu, J., Cao, Z., McAtee, M., Bregman, B.S., Filbin, M.T., 2001. Neuronal cyclic AMP controls the developmental loss in ability of axons to regenerate. J. Neurosci. 21, 4731–4739.

Dagerlind, A., Friberg, K., Bean, A.J., Hokfelt, T., 1992. Sensitive mRNA detection using unfixed tissue: combined radioactive and non-radioactive in situ hybridization histochemistry. Histochemistry 98, 39–49.

Doster, S.K., Lozano, A.M., Aguayo, A.J., Willard, M.B., 1991. Expression of the growth-associated protein GAP-43 in adult rat retinal ganglion cells following axon injury. Neuron 6, 635–647.

Eshete, F., Fields, R.D., 2001. Spike frequency decoding and autonomous activation of Ca2+-calmodulin-dependent protein kinase II in dorsal root ganglion neurons. J. Neurosci. 21, 6694–6705.

Fernandes, K.J., Fan, D.P., Tsui, B.J., Cassar, S.L., Tetzlaff, W., 1999. Influence of the axotomy to cell body distance in rat rubrospinal and spinal motoneurons: differential regulation of GAP-43, tubulins, and neurofilament-M. J. Comp. Neurol. 414, 495–510.

Fields, R.D., Eshete, F., Stevens, B., Itoh, K., 1997. Action potential-dependent regulation of gene expression: temporal specificity in ca2+, cAMP-responsive element binding proteins, and mitogen-activated protein kinase signaling. J. Neurosci. 17, 7252–7266.

Fu, S.Y., Gordon, T., 1995a. Contributing factors to poor functional recovery after delayed nerve repair: prolonged denervation. J. Neurosci. 15, 3886–3895.

Fu, S.Y., Gordon, T., 1995b. Contributing factors to poor functional recovery after delayed nerve repair: prolonged axotomy. J. Neurosci. 15, 3876–3885.

Geremia, N.M., Verge, V.M.K., 2001. Role of BDNF in inducing an injury phenotype in intact sensory neurons. Abstr.-Soc. Neurosci. 595.20.

Geremia, N.M., Gordon, T., Al-Majed, A.A., Brushart, T.M., Verge, V.M.K., 2002. Brief electrical stimulation promotes regeneration of sensory fibers into cutaneous and muscle branches of femoral nerve. Abstr.-Soc. Neurosci. 535.14.

Geremia, N.M., Pettersson, L.M.E., Danielsen, N., Verge, V.M.K., 2003. Endogenous BDNF regulates injury/regeneration-associated gene expression in adult sensory neurons. Abstr.-Soc. Neurosci. 38.4.

Geremia, N.M., Pettersson, L.M.E., Hryciw, T., Schreyer, D.J., Danielsen, N., Verge, V.M.K., 2004. Antagonizing BDNF alters the growth capabilities of injured sensory neurons and signalling pathways. Abstr.-Soc. Neurosci. 39.1.

Geremia, N.M., Gordon, T., Al-Majed, A.A., Brushart, T.M., Verge, V.M.K., 2005. Brief electrical stimulation promotes sensory neuron regeneration and intrinsic growth-associated gene expression. Abstr.-Soc. Neurosci. 28.6.

Goldberg, J.L., Espinosa, J.S., Xu, Y., Davidson, N., Kovacs, G.T., Barres, B.A., 2002. Retinal ganglion cells do not extend axons by default: promotion by neurotrophic signaling and electrical activity. Neuron 33, 689–702.

Gutmann, E., Gutmann, L., Medawar, P.B., Young, J.Z., 1942. The rate of regeneration. J. Exp. Biol. 19, 14–44.

Han, P.J., Shukla, S., Subramanian, P.S., Hoffman, P.N., 2004. Cyclic AMP elevates tubulin expression without increasing intrinsic axon growth capacity. Exp. Neurol. 189, 293–302.

Itoh, K., Ozaki, M., Stevens, B., Fields, R.D., 1997. Activity-dependent regulation of N-cadherin in DRG neurons: differential regulation of N-cadherin, NCAM, and L1 by distinct patterns of action potentials. J. Neurobiol. 33, 735–748.

Karchewski, L.A., Kim, F.A., Johnston, J., McKnight, R.M., Verge, V.M., 1999. Anatomical evidence supporting the potential for modulation by multiple neurotrophins in the majority of adult lumbar sensory neurons. J. Comp. Neurol. 413, 327–341.

Karchewski, L.A., Gratto, K.A., Wetmore, C., Verge, V.M., 2002. Dynamic patterns of BDNF expression in injured sensory neurons: differential modulation by NGF and NT-3. Eur. J. Neurosci. 16, 1449–1462.

Karns, L.R., Ng, S.C., Freeman, J.A., Fishman, M.C., 1987. Cloning of complementary DNA for GAP-43, a neuronal growth-related protein. Science 236, 597–600.

Kingsbury, T.J., Murray, P.D., Bambrick, L.L., Krueger, B.K., 2003. Ca(2+)-dependent regulation of TrkB expression in neurons. J. Biol. Chem. 278, 40744–40748.

Kline, D.G., Hudson, A.R., 1995. Nerve injuries: operative results for entrapments and tumors. Saunders, Philadelphia.

Kocsis, J.D., Rand, M.N., Lankford, K.L., Waxman, S.G., 1994. Intracellular calcium mobilization and neurite outgrowth in mammalian neurons. J. Neurobiol. 25, 252–264.

Langford, L.A., Coggeshall, R.E., 1981. Branching of sensory axons in the peripheral nerve of the rat. J. Comp. Neurol. 203, 745–750.

Lever, I.J., Bradbury, E.J., Cunningham, J.R., Adelson, D.W., Jones, M.G., McMahon, S.B., Marvizon, J.C., Malcangio, M., 2001. Brain-derived neurotrophic factor is released in the dorsal horn by distinctive patterns of afferent fiber stimulation. J. Neurosci. 21, 4469–4477.

Meyer-Franke, A., Wilkinson, G.A., Kruttgen, A., Hu, M., Munro, E., Hanson Jr., M.G., Reichardt, L.F., Barres, B.A., 1998. Depolarization and cAMP elevation rapidly recruit TrkB to the plasma membrane of CNS neurons. Neuron 21, 681–693.

Michael, G.J., Averill, S., Shortland, P.J., Yan, Q., Priestley, J.V., 1999. Axotomy results in major changes in BDNF expression by dorsal root ganglion cells: BDNF expression in large trkB and trkC cells, in pericellular baskets, and in projections to deep dorsal horn and dorsal column nuclei. Eur. J. Neurosci. 11, 3539–3551.

Ming, G., Henley, J., Tessier-Lavigne, M., Song, H., Poo, M., 2001. Electrical activity modulates growth cone guidance by diffusible factors. Neuron 29, 441–452.

Mohiuddin, L., Tomlinson, D.R., 1997. Impaired molecular regenerative responses in sensory neurones of diabetic rats: gene expression changes in dorsal root ganglia after sciatic nerve crush. Diabetes 46, 2057–2062.

Neumann, S., Bradke, F., Tessier-Lavigne, M., Basbaum, A.I., 2002. Regeneration of sensory axons within the injured spinal cord induced by intraganglionic cAMP elevation. Neuron 34, 885–893.

Nix, W.A., Hopf, H.C., 1983. Electrical stimulation of regenerating nerve and its effect on motor recovery. Brain Res. 272, 21–25.

Qiu, J., Cai, D., Dai, H., McAtee, M., Hoffman, P.N., Bregman, B.S., Filbin, M.T., 2002. Spinal axon regeneration induced by elevation of cyclic AMP. Neuron 34, 895–903.

Richardson, P.M., Issa, V.M., 1984. Peripheral injury enhances central regeneration of primary sensory neurones. Nature 309, 791–793.

Richardson, P.M., Verge, V.M., 1986. The induction of a regenerative propensity in sensory neurons following peripheral axonal injury. J. Neurocytol. 15, 585–594.

Richardson, P.M., Verge, V.M., 1987. Axonal regeneration in dorsal spinal roots is accelerated by peripheral axonal transection. Brain Res. 411, 406–408.

Richardson, P.M., Verge, V.M.K., Riopelle, R.J., 1989. Quantitative radio-autography for NGF receptors. In: Rush, R.A. (Ed.), Nerve Growth Factors. John Wiley & Sons, England, pp. 315–326.

Schmued, L.C., Fallon, J.H., 1986. Fluoro-Gold: a new fluorescent retrograde axonal tracer with numerous unique properties. Brain Res. 377, 147–154.

Schreyer, D.J., Skene, J.H., 1991. Fate of GAP-43 in ascending spinal axons of DRG neurons after peripheral nerve injury: delayed accumulation and correlation with regenerative potential. J. Neurosci. 11, 3738–3751.

Schreyer, D.J., Skene, J.H., 1993. Injury-associated induction of GAP-43 expression displays axon branch specificity in rat dorsal root ganglion neurons. J. Neurobiol. 24, 959–970.

Shieh, P.B., Hu, S.C., Bobb, K., Timmusk, T., Ghosh, A., 1998. Identification of a signaling pathway involved in calcium regulation of BDNF expression. Neuron 20, 727–740.

Stevens, B., Fields, R.D., 2000. Response of Schwann cells to action potentials in development. Science 287, 2267–2271.

Streppel, M., Azzolin, N., Dohm, S., Guntinas-Lichius, O., Haas, C., Grothe, C., Wevers, A., Neiss, W.F., Angelov, D.N., 2002. Focal application of neutralizing antibodies to soluble neurotrophic factors reduces collateral axonal branching after peripheral nerve lesion. Eur. J. Neurosci. 15, 1327–1342.

Sunderland, S., 1978. Nerve and Nerve Injuries. Churchill Livingstone, London.

Takeda, M., Kato, H., Takamiya, A., Yoshida, A., Kiyama, H., 2000. Injury-specific expression of activating transcription factor-3 in retinal ganglion cells and its colocalized expression with phosphorylated c-Jun. Invest. Ophthalmol. Visual Sci. 41 (9), 2412–2421.

Tao, X., Finkbeiner, S., Arnold, D.B., Shaywitz, A.J., Greenberg, M.E., 1998. Ca2+influx regulates BDNF transcription by a CREB family transcription factor-dependent mechanism. Neuron 20, 709–726.

Taylor, D.C., Pierau, F.K., 1982. Double fluorescence labelling supports electrophysiological evidence for dichotomizing peripheral sensory nerve fibres in rats. Neurosci. Lett. 33, 1–6.

Taylor, D.C., Pierau, F.K., Schmid, H., 1983. The use of fluorescent tracers in the peripheral sensory nervous system. J. Neurosci. Methods 8, 211–224.

Tetzlaff, W., Zwiers, H., Lederis, K., Cassar, L., Bisby, M.A., 1989. Axonal transport and localization of B-50/GAP-43-like immunoreactivity in regenerating sciatic and facial nerves of the rat. J. Neurosci. 9, 1303–1313.

Tsujino, H., Kondo, E., Fukuoka, T., Dai, Y., Tokunaga, A., Miki, K., Yonenobu, K., Ochi, T., Noguchi, K., 2000. Activating transcription factor 3 (ATF3) induction by axotomy in sensory and motoneurons: a novel neuronal marker of nerve injury. Mol. Cell. Neurosci. 15, 170–182.

Verge, V.M., Tetzlaff, W., Richardson, P.M., Bisby, M.A., 1990. Correlation between GAP43 and nerve growth factor receptors in rat sensory neurons. J. Neurosci. 10, 926–934.

Wetmore, C., Olson, L., 1995. Neuronal and nonneuronal expression of neurotrophins and their receptors in sensory and sympathetic ganglia suggest new intercellular trophic interactions. J. Comp. Neurol. 353, 143–159.

Whitworth, I.H., Brown, R.A., Dore, C.J., Anand, P., Green, C.J., Terenghi, G., 1996. Nerve growth factor enhances nerve regeneration through fibronectin grafts. J. Hand Surg., Br. 21, 514–522.

Zhang, J.Y., Luo, X.G., Xian, C.J., Liu, Z.H., Zhou, X.F., 2000. Endogenous BDNF is required for myelination and regeneration of injured sciatic nerve in rodents. Eur. J. Neurosci. 12, 4171–4180.

Zhou, X.F., Chie, E.T., Deng, Y.S., Zhong, J.H., Xue, Q., Rush, R.A., Xian, C.J., 1999. Injured primary sensory neurons switch phenotype for brain-derived neurotrophic factor in the rat. Neuroscience 92, 841–853.

Neuropharmacology 55 (2008) 8–17

Contents lists available at ScienceDirect

Neuropharmacology

journal homepage: www.elsevier.com/locate/neuropharm

cAMP promotes neurite outgrowth and extension through protein kinase A but independently of Erk activation in cultured rat motoneurons

C. Aglah [b], T. Gordon [b,*], E.I. Posse de Chaves [a,**]

[a] Department of Pharmacology and Centre for Neuroscience, University of Alberta, 928 Medical Sciences Building, Edmonton, Alberta, Canada T6G 2H7C
[b] Division of Physical Medicine and Rehabilitation, Centre for Neuroscience, University of Alberta, 525 Heritage Medical Research Centre, Edmonton, Alberta, Canada T6G 2S2

ARTICLE INFO

Article history:
Received 19 October 2007
Received in revised form 19 February 2008
Accepted 8 April 2008

Keywords:
cAMP
PKA
Motoneurons
Neurite outgrowth
ERK1/2
BDNF

ABSTRACT

It is well established that cAMP counteracts myelin inhibition to permit axon regeneration in the central nervous system. On the other hand, the role of cAMP in axonal growth on permissive substrates remains controversial because the evidence available is contradictory. In view that elevation of cAMP represents an attractive therapeutic target to promote nerve regeneration in vivo, we investigated the effect of cAMP on neurite outgrowth and extension in motoneurons. We manipulated cAMP levels pharmacologically in cultured motoneurons and investigated targets downstream of cAMP of neurite outgrowth and extension on a permissive substrate. Reduction of cAMP by the adenylyl cyclase inhibitor SQ22536 inhibited, and elevation of cAMP by forskolin, dibutyryl cAMP, IBMX and rolipram increased outgrowth and extension of neurites. The cAMP-mediated effects occur via activation of protein kinase A (PKA) and were reduced by the inhibitors, H89 and Rp-cAMP. However, cAMP elevation did not lead to Erk activation that is an essential downstream component of neurotrophin signaling. These findings provide evidence for a key role of cAMP in promoting peripheral nerve regeneration after nerve injuries and indicate that this effect is unusual in not being mediated via Erk phosphorylation.

© 2008 Published by Elsevier Ltd.

1. Introduction

cAMP is implicated in several neuronal processes such as neuronal differentiation (Fujioka et al., 2004), axonal guidance (Song et al., 1997), neuronal survival (Hanson et al., 1998; Meyer-Franke et al., 1998) and neurite outgrowth and axonal regeneration in the central nervous system (CNS) (Cai et al., 1999; Neumann et al., 2002; Roisen et al., 1972). Central axon regeneration is normally inhibited by Nogo-A protein, oligodendrocyte-myelin glycoprotein and myelin-associated glycoprotein (MAG), all of which bind to the common Nogo receptor to mediate axon growth inhibition (Liu et al., 2006; McKerracher and Winton, 2002). Elevation of cAMP and activation of the cAMP-signaling cascade converts the repulsive turning of growth cones and inhibition of neurite outgrowth by these myelin-associated inhibitors to attraction and neurite extension (Cai et al., 1999; Song et al., 1998). The finding that high levels of cAMP in neonatal dorsal root ganglion (DRG) neurons permit neurite extension on CNS myelin both in vivo and in vitro, provided supportive evidence that cAMP plays a role in neurite outgrowth and/or axonal regeneration on a non-permissive growth substrate (Cai et al., 1999).

On the other hand, the role of cAMP in the growth of neurites on a permissive substrate is unclear. Consistent with in vivo evidence obtained in the 1980s for a role of cAMP in the regeneration of sensory nerve axons in the peripheral nervous system (PNS) (Carlsen, 1982, 1983), Neumann et al. (2002) found that intraganglionic injection of a membrane permeable analog of cAMP, dbcAMP, increases the rate of neurite outgrowth in DRG neurons cultured on permissive substrate. However, Qiu et al. (2002) did not observe any effect of dbcAMP on neurite outgrowth on a permissive substrate, in contrast to an increased outgrowth on a non-permissive substrate following dbcAMP injection. Similarly, dbcAMP and the protein kinase A (PKA) activator Sp-cAMP, did not enhance neurite outgrowth of retinal ganglion cells (RGC) grown on the same permissive substrate, and the cAMP antagonist Rp-cAMP did not inhibit DRG neurite outgrowth on the permissive substrate (Cai et al., 2001). Inhibition of the most important target of cAMP, protein kinase A (PKA) also did not prevent the outgrowth of neurites from DRG neurons cultured on permissive substrate (Cai et al., 2001; Qiu et al., 2002). All together the evidence indicates that while cAMP elevation enhances axonal regeneration on a non-permissive substrate, cAMP cannot be considered 'a priori' as a neurite growth enhancer on

* Corresponding author. Tel.: +780 492 1668; fax: +780 492 1716.
** Corresponding author. Tel.: +1 780 492 5966; fax: +1 780 4924325.
E-mail addresses: tessa.gordon@ualberta.ca (T. Gordon), echaves@pmcol.ualberta.ca (E.I. Posse de Chaves).

0028-3908/$ – see front matter © 2008 Published by Elsevier Ltd.
doi:10.1016/j.neuropharm.2008.04.005

a permissive substrate (Teng and Tang, 2006). In motoneurons, elevation of intracellular cAMP level is sufficient to support neuronal survival (Hanson et al., 1998), but the role of cAMP on neurite outgrowth has not been studied in this neuronal type. Low frequency 1 h electrical stimulation of the peripheral nerve elevates cAMP in motoneurons and DRG neurons but this elevation has not been linked directly to the pronounced increase in axonal outgrowth that was observed in both motor and DRG sensory neurons (Al-Majed et al., 2000; Brushart et al., 2002, 2005; Geremia et al., 2007). The studies we present here address specifically the issue of whether cAMP mediates neurite outgrowth in motoneurons.

The signaling pathways downstream of cAMP responsible for neurite outgrowth have been identified for neurons on non-permissive substrates. Filbin and colleagues demonstrated that elevated neuronal cAMP levels and activation of PKA are pivotal to axon outgrowth in cerebellar and DRG neurons (Cai et al., 1999; Qiu et al., 2002). In many circumstances cAMP exerts its cellular effects through regulation of extracellular signal-regulated kinases (Erks) (Dumaz and Marais, 2005; Stork and Schmitt, 2002). Significantly, cAMP-induced activation of Erk is essential to overcome neurite growth inhibition by MAG (Gao et al., 2003). The question as to whether Erks are involved in cAMP-mediated neurite outgrowth on a permissive substrate remains unanswered.

In this study, we have purified embryonic motoneurons in order to determine whether cAMP plays a central role in neurite outgrowth on a permissive substrate and to establish the downstream molecular mediators of cAMP. We demonstrate that cAMP is required for neurite outgrowth in cultured primary motoneurons grown on a permissive substrate. We present evidence that neurite outgrowth is mediated by PKA but that Erks are not activated downstream of cAMP.

Our studies are important to identify cAMP as a valid target for regulation of axonal regeneration in the peripheral nervous system.

2. Methods

2.1. Animals

Timed pregnant Sprague–Dawley Rats were bred at the University of Alberta and all procedures were approved by the Animal Welfare Committee of the Institution. The timing of pregnancies was determined from the appearance of sperm plugs in the breeding cages. The morning of detection of the sperm plug was considered the day 0 of the pregnancy. Incision was made across the lower abdomen and rat embryos (E15) were delivered under halothane anaesthesia (1.25–1.5% delivered in 95% O_2 and 5% CO_2). The embryos were transferred into an ice-cold PBS (pH 7.4) and the spinal cord dissected.

2.2. Motoneuron purification and culture

Establishment of pure motoneuron cultures was carried out as described (Arce et al., 1999; Raoul et al., 2005). Briefly motoneurons from day 15 embryonic rats (E15) were purified to >90% homogeneity using an antibody against surface receptor $p75^{NTR}$ (Yan and Johnson, 1988). Motoneurons bound to anti-p75 antibody were then separated by immunoaffinity using magnetically labeled IgG microbeads and a magnetized column (Miltenyi Biotech, USA). The purified motoneurons were seeded on polyornithine/laminin-coated dishes at 200 cells per 96-well dishes for survival and neurite outgrowth determinations, and at 30,000 per 24-well dishes for cAMP determination and immunoblotting studies. The culture medium used was neurobasal medium (Gibco) supplemented with the B27 supplement (Gibco), L-glutamine (0.5 mM), 2-mercaptoethanol (25 μM), L-glutamate (25 μM), hereafter called complete neurobasal medium.

The purity of the cultures was assessed by immunofluorescence using antibodies to several neuronal markers, which are selectively expressed by embryonic spinal motoneurons. These include Islet 1/2 (Arce et al., 1999; Ericson et al., 1992), choline acetyltransferase (ChAT) (Bataille et al., 1998), SMI-32 (Carriedo et al., 1996; Rao and Weiss, 2004), or p75 (Camu and Henderson, 1992). In our cultures, over 90% of the cells were motoneurons.

2.3. Assessment of neuronal survival

Survival of cultured motoneurons was determined by measuring the reduction of MTT [3-(4,5-dimethylthiazol-2-yl)-2,5-diphenyl tetrazolium bromide]. The MTT survival assay was performed as described by (Mosmann, 1983). MTT solution (5 mg/ml) was added to the culture well (1:9) and incubated at 37 °C for 1 h. Live cells with active mitochondria convert the tetrazolium salt into a visible dark blue formazan reaction product (Berridge and Tan, 1993). The live (blue) and dead (clear) neurons in each well were counted by bright-field microscopy. All values are given as the mean ± SEM of at least three cultures. All experiments were repeated at least three times.

2.4. Detection of cell death

Cell death was identified by nuclear staining with Hoechst 33258. Neurons were fixed with 4% paraformaldehyde in PBS for 20 min and stained with 500 ng/ml Hoechst 33258 for 10–20 min. The percentage of apoptotic neurons was estimated by counting condensed and/or fragmented nuclei versus evenly stained nuclei. Neurons were visualized using a Nikon TE300 inverted fluorescence microscope equipped with a Nikon digital camera DXM-1200 (Nikon Canada, Toronto ON). Images were analyzed using Northern Elite V6.0 image capture and analysis software (Empix Imaging, Mississauga, ON). About 500–1000 neurons per treatment were counted by an observer 'blinded' to the neuronal treatment. Data were analyzed by One Way ANOVA with Newman–Keuls Multiple range test. The level of statistical significance selected was a P-value < 0.05.

2.5. Motoneuron treatments

Appropriate agents were applied to modulate intracellular cAMP levels. To elevate cAMP we used the membrane permeable analog of cAMP, dibutyryl cAMP (Calbiochem), and forskolin (Sigma), which activates adenylyl cyclase to convert adenosine triphosphate (ATP) to cAMP. In order to prevent the metabolism of cAMP, 1-Isobutyl-3-methylxanthine (IBMX) (Calbiochem) a general phosphodiesterase inhibitor and Rolipram (AG Scientific), a phosphodiesterase type-4 inhibitor were used. To reduce intracellular cAMP levels, SQ22536 (Calbiochem), a soluble adenylate cyclase inhibitor that prevents conversion of ATP to cAMP, was applied. H89 (Calbiochem) a specific PKA inhibitor, and the soluble cAMP antagonist Rp-cAMP (Calbiochem) were used to inhibit PKA action. The doses used for the various agents were based on concentrations used in vitro in other neuronal cells and on the dose responses obtained in motoneurons for these agents. Unless otherwise stated motoneuron treatments started at the time of plating and continued for up to 24 h.

2.6. Parameters of neurite outgrowth

The number of neurons with neurites and the length of the longest neurite were determined from images captured using the Nikon TE300 inverted microscope equipped with the Nikon digital camera DXM-1200 (Nikon Canada). The images were analyzed using Northern Eclipse Elite V6.0 image capture and analysis software (Empix Imaging, Canada). The motoneurons with processes >10 μm were counted as neurons with neurites from 10 randomly selected fields per well performed in triplicate and the percent of neurons with neurites was calculated. Neurite length was determined by tracing the longest neurite from the cell body of the neuron and following the entire length of the neurite in 100–150 neurons per experimental point. In all cases the experiments were done in triplicate and repeated three times ($n = 3$).

2.7. Measurement of cAMP in cultured motoneurons

Quantification of cAMP in cultured motoneurons was carried out using a commercially available ELISA kit (R&D Systems). After treatment of the motoneurons the culture media were aspirated and 350 μl of 0.1 N HCl added and incubated at 37 °C for 10 min to lyse neurons and prevent degradation of cAMP by phosphodiesterases. The resulting solution was centrifuged at 15,000 rpm for 5 min. The supernatant was used for cAMP determination. The pellets were dissolved in RIPA buffer and the protein determined using the Bicinchoninic Acid BCA kit (Pearce, USA). The amount of cAMP was expressed as pmol/μg of protein.

2.8. Immunoblotting

After experimental treatment motoneurons were washed with ice-cold PBS containing 1 mM sodium orthovanadate and 10 mM sodium fluoride and harvested in RIPA buffer. An aliquot was taken for protein determination. Buffer containing 40 mM Tris–HCl pH 6.8, 1% sodium dodecyl sulfate (SDS), 4% 2-mercaptoethanol, 10% glycerol and 0.002% bromophenol blue was added to the sample and boiled for 2 min. Equal amount of proteins (20 μg) were separated by SDS-PAGE on 10% polyacrylamide gels containing 0.1% SDS and transferred overnight at 4 °C to PVDF membranes in 25 mM Tris:192 mM glycine, 16% methanol buffer, pH 8.3, containing 0.1% SDS. Membranes were blocked for 1 h in TBS, 0.1% Tween-20 (TTBS) containing 5% non-fat milk and incubated overnight in the primary antibody solution prepared in TTBS containing 5% bovine serum albumin. The primary antibodies used were anti-phospho-ERK1/2 (1:1000) and anti-total ERK1/2 (1:1000) from Cell Signaling Technology (Beverly, MA, USA), and anti phospho-specific $PKA_{RII\beta}$(pS114) (1:1000) and anti $PKA_{RII\beta}$ (1:1000) from BD Transduction Laboratories. Membranes were washed for 20 min with TTBS, 20 min with TBS and then 20 min with TTBS and incubated for 1 h with the correspondent secondary antibodies (1:2000) in blocking

buffer at room temperature with gentle agitation. Immunoreactivity was detected by Enhanced Chemo Luminescence (ECL-Plus, Amersham Biosciences).

2.9. Statistics

Where indicated the data were analyzed using the Graphpad Instat software. The statistical significance was determined where indicated by Student's *t*-test and/or One Way Analysis of Variance with Newman–Keuls Multiple range test. The data are presented as the mean ± standard error (SEM).

3. Results

We investigated whether: (1) the levels of intracellular cAMP in embryonic motoneurons are sufficient to promote neurite outgrowth on a permissive substrate, and (2) elevation or decline of cAMP levels promotes and reduces axon outgrowth as predicted for this role.

3.1. Intracellular cAMP is required for neurite outgrowth in motoneurons

Physiologically, cAMP is produced from ATP when adenylyl cyclase is activated by the G_s subunit of heterotrimeric G-proteins (Houslay, 1998). We used the readily soluble and potent adenylyl cyclase inhibitor SQ22536 (Harris et al., 1979) in order to reduce intracellular cAMP levels and to ask whether reduction in cAMP inhibits neurite outgrowth in cultured motoneurons. We first established the range of SQ22536 concentrations at which motoneuron survival was unaffected (Fig. 1A), and then we determined the effective concentrations of SQ22536 in reducing intracellular cAMP in motoneurons (Fig. 1B). SQ22536 rapidly reduced intracellular cAMP levels in motoneurons at concentrations similar to those used for cerebellar neurons and PC12 cells (Gomes et al., 1999; Gysbers and Rathbone, 1996).

As levels of intracellular cAMP decreased upon SQ22536 treatment, the percent of motoneurons that extended neurites dramatically declined (Fig. 1C), and the length of neurite extension progressively fell (Fig. 1D). The greatest effect of SQ22536 was observed at 500 μM. At this inhibitor concentration the levels of intracellular cAMP were reduced by 50–60% and only 5% of motoneurons extended neurites. The effect of SQ22536 was reversible, with the majority of the neurons extending neurites upon discontinuation of the treatment (not shown). Concentrations of SQ22536 above 500 μM were neurotoxic, resulting in obvious morphological

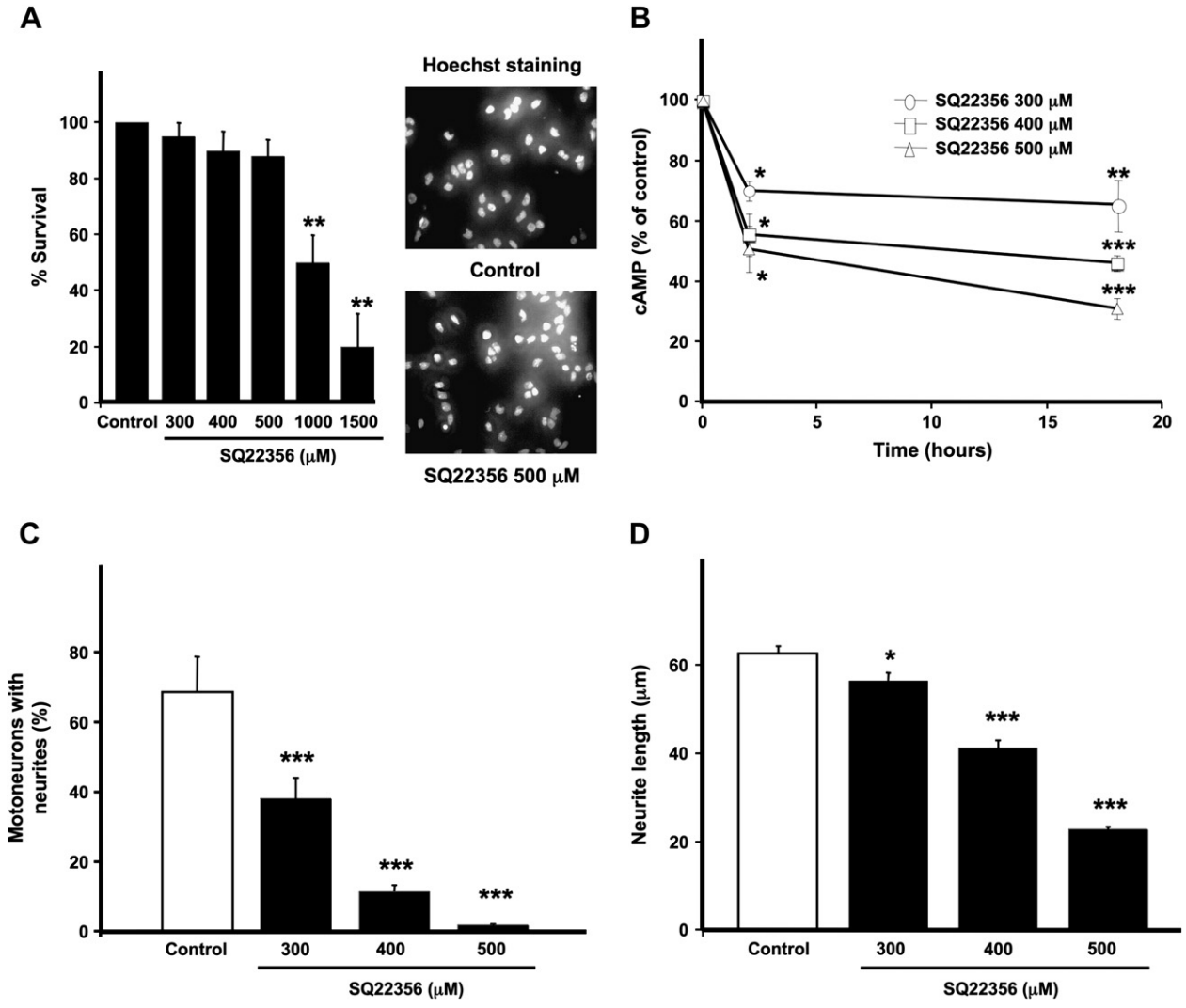


Fig. 1. AMP is required for neurite outgrowth and extension in motoneurons. Motoneurons were cultured at a density of 200 cells per 96-well dish or 30,000 per 24-well dish and treated with SQ22536 (300–1500 μM) at the time of plating. (A) Survival of motoneurons was examined after 18 h using MTT. In parallel, Hoechst staining was performed. (B) Intracellular cAMP was determined after 2 and 18 h. The percent of motoneurons which extended neurites (C), and neurite length (D) were determined 18 h after treatment. The data represent the Mean ± SEM. The experiment was performed in triplicates and repeated three times. Data were analyzed by One Way ANOVA with Newman–Keuls Multiple range test. Significance is indicated with respect to the untreated control $^{*}p < 0.05$, $^{**}p < 0.01$, $^{***}p < 0.001$.

changes characteristic of cell death. The correlation between reduced levels of intracellular cAMP, percentage of motoneurons with neurites and their neurite length, strongly indicate that intrinsic intracellular cAMP levels are necessary and sufficient for axon outgrowth in motoneurons growing on permissive substrate.

3.2. Elevation of cAMP enhances outgrowth of neurites in motoneurons

The question now arises as to whether cAMP levels can be increased pharmacologically and result in increased neurite outgrowth in motoneurons. We first investigated the effect of exogenous soluble analog of cAMP, dibutyryl cAMP (dbcAMP) on neurite outgrowth and extension. We treated the motoneurons with dbcAMP at 1 mM at the time of cell plating. The number of motoneurons that extended neurites (Fig. 2A, C) and the mean length of the longest neurites (Fig. 2B, C) were significantly increased in medium containing 1 mM of dbcAMP.

Next, we increased the endogenous levels of cAMP pharmacologically using forskolin, which stimulates adenylyl cyclase. We determined the concentrations of forskolin that did not compromise neuronal viability (Fig. 3A), and we investigated the effect of forskolin on intracellular cAMP (Fig. 3B). At a very early time (2 h) neuronal survival was not affected by any concentration of forskolin used (not shown) and there was a dose-dependent increase on cAMP in cultured motoneurons (Fig. 3B). Longer treatments with forskolin at concentrations of 7 μM or higher resulted in motoneuronal death (Fig. 3A). Hence, to assure the health of the neurons, we used 3 μM forskolin for further experiments. The increase in intracellular cAMP elicited by 3 μM forskolin resulted in significantly increased numbers of motoneurons that extended neurites at 24 h (Fig. 3C), and increased mean length of the longest neurites after 12 and 24 h (Fig. 3D, E). The percent of motoneurons that extended neurites did not change between 12 and 24 h in untreated motoneurons; however, it increased significantly in forskolin-treated neurons. This suggests that between 12 and 24 h more motoneurons are induced to extend neurites in response to forskolin-mediated elevation of cAMP.

An alternative way to increase intracellular cAMP is to inhibit its degradation. Under physiological conditions cAMP is quickly degraded by cAMP phosphodiesterases (Houslay, 1998). Therefore, we used the general phosphodiesterase inhibitor isobutyl-3-methylxanthine (IBMX) and the type-4 phosphodiesterase inhibitor rolipram. Rolipram is the archetypal inhibitor of the type-4 phosphodiesterases (Houslay and Kolch, 2000), which are the most abundant group of the phosphodiesterases in neuronal tissues (Jin et al., 1999). Rolipram has been used in vitro at concentrations ranging from 0.1 to 100 μM, which were effective in increasing cAMP levels and removing MAG inhibition to promote neurite outgrowth on a non-permissive substrate (Gao et al., 2003). Similarly, IBMX has been used at concentrations ranging between 50 and 100 μM to inhibit cAMP phosphodiesterases in several neuronal types including motoneurons (Hanson et al., 1998; Ivins et al., 2004). However, the effect of the cAMP phosphodiesterase inhibitors on neurite outgrowth has not been examined in motoneurons.

Cultured motoneurons were treated with Rolipram (10 μM) or IBMX (50 μM) at the time of plating, and cAMP was measured over time. Both inhibitors were effective in increasing intracellular cAMP (Fig. 4A). The increased levels of intracellular cAMP by IBMX and Rolipram resulted in significantly increased number of motoneurons that extended neurites (Fig. 4B) and increased mean length of the longest neurites (Fig. 4C) at 12 and 24 h. As indicated for neurons treated with forskolin, the number of Rolipram- or IBMX-treated motoneurons that extended neurites was greater at 24 h than at 12 h. At the doses used for these studies some significant differences exist between Rolipram and IBMX at 24 h. While

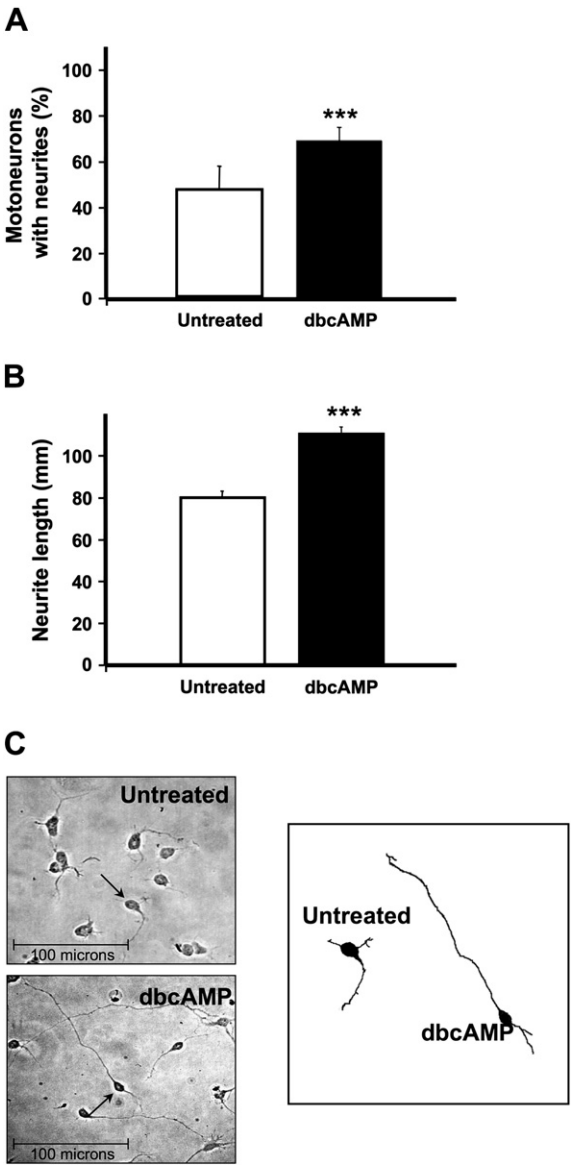


Fig. 2. Exogenous cAMP stimulates neurite outgrowth in motoneurons. Motoneurons were plated at 200 cells per well of a 96-well dish and treated with 1 mM of dbcAMP at the time of seeding. (A) The percent of neurons with neurites and (B) the mean length of the longest neurites were determined after 24 h in culture. The experiment was done in triplicate and repeated three times. The differences between treated and untreated controls were determined by Student's *t*-test. The results are presented as Mean ± SEM, $n = 3$, $^{***}p < 0.001$. (C) Representative phase-contrast micrographs of neurons cultured with and without dbcAMP, accompanied by drawings of neurons indicated by black arrows. Neurons drawing were performed using the Empix software.

Rolipram caused a more substantial increase in the number of neurons with neurites, the neurites were longer in neurons treated with IBMX. Although interesting, the studies required for understanding these differences depart from the focus of our work.

3.3. Activation of PKA by cAMP is required for neurite outgrowth in motoneurons

The most common intracellular target of cAMP is PKA. PKA activation is responsible for many of the actions attributed to cAMP (Houslay and Kolch, 2000), including neurite outgrowth of DRG neurons on non-permissive substrate (Qiu et al., 2002). Nonetheless there are other systems in which cAMP-induced neurite outgrowth is independent of PKA activation (Charles et al., 2003).

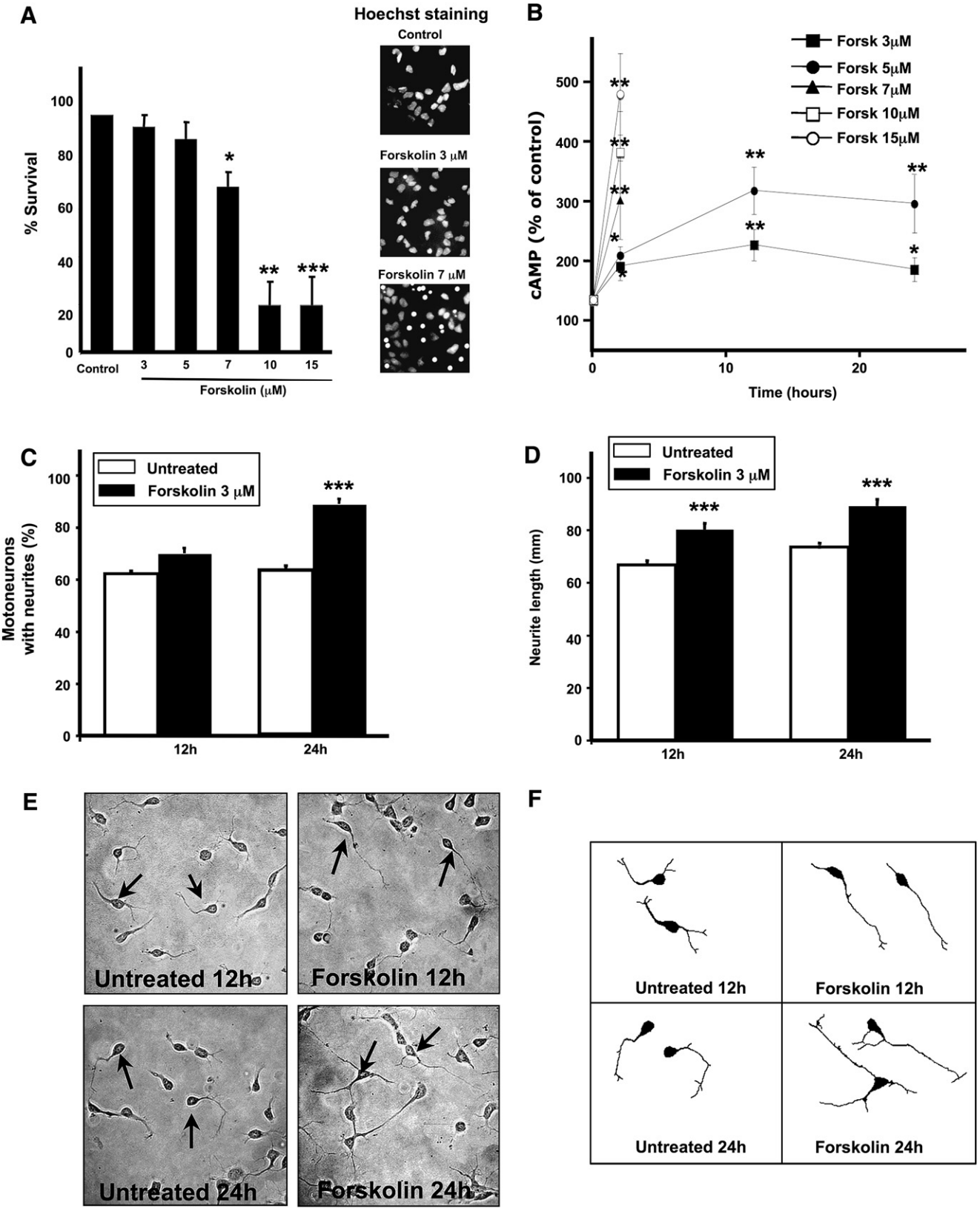


Fig. 3. Activation of adenylyl cyclase by forskolin increases cAMP and promotes neurite outgrowth. Motoneurons were cultured at a density of 200 cells per 96-well dish or 30,000 per 24-well dish and treated with various concentrations of forskolin at the time of plating. (A) Survival of motoneurons detected by MTT after 24 h of treatment with the indicated concentrations of forskolin. In parallel Hoechst staining was used to detect nuclear fragmentation. (B) Intracellular cAMP levels were determined at selected time points. The experiment was discontinued with forskolin concentrations $\geq$7 μM due to reduced neuronal survival. (C) The percent of motoneurons that extend neurites, and (D) the mean length of the longest neurites after 12 and 24 h in culture are shown. The data represent the Mean ± SEM. Significance is indicated with respect to the untreated control $^{*}p < 0.05$, $^{**}p < 0.01$, $^{***}p < 0.001$. (E) Representative phase-contrast micrographs of neurons cultured with and without forskolin, accompanied by drawings of neurons indicated by black arrows. Neurons drawing were performed using the Empix software.

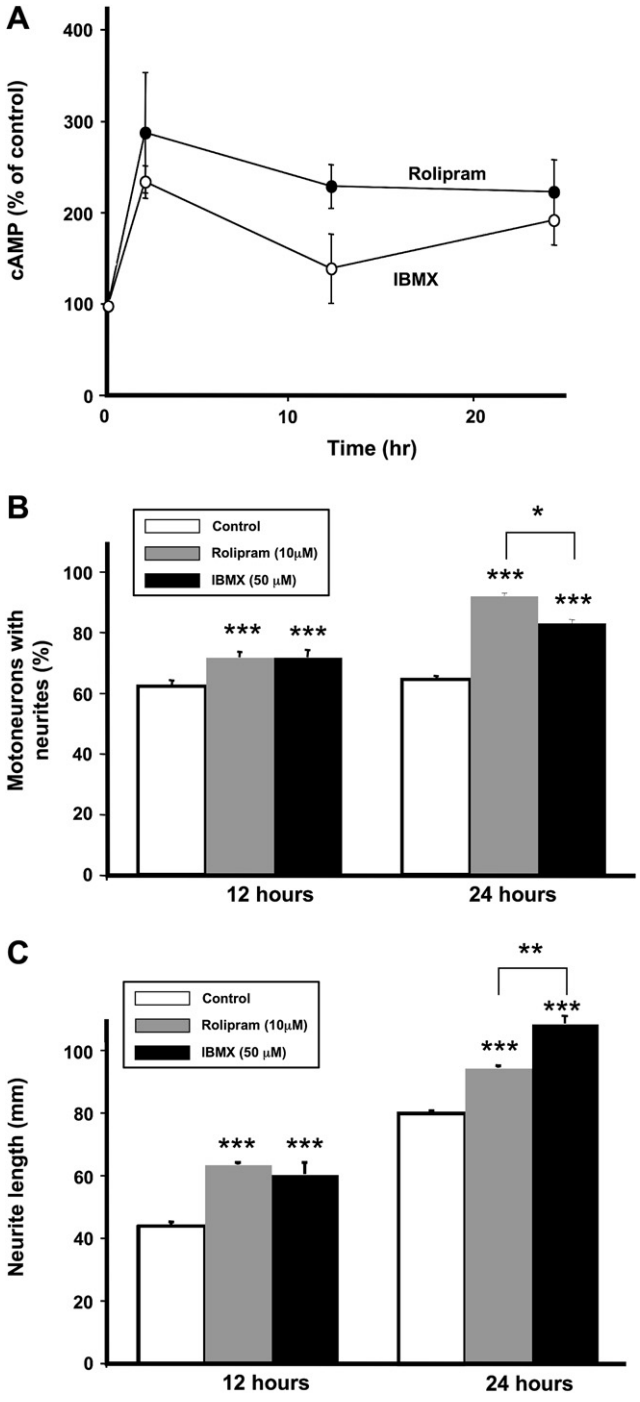


Fig. 4. Inhibition of phosphodiesterases raises intracellular cAMP and promotes neurite outgrowth. Motoneurons cultured at a density of 200 cells per 96-well dish or 30,000 per 24-well dish were treated with Rolipram (10 μM) or IBMX (50 μM) at the time of plating. (A) cAMP was measured at 2 h, 12 h and 24 h. (B) Percent of motoneurons that extended neurites (C) and the mean length of longest neurites over the 24 h period. The data represent the Mean ± SEM. Data were analyzed by One Way ANOVA with Newman–Keuls Multiple range test. Significance is indicated: $^{***}p < 0.001$ (with respect to the untreated control); $^{**}p < 0.01$ and $^{*}p < 0.05$ (between Rolipram and IBMX).

We therefore investigated if PKA activation is required for cAMP-mediated neurite extension in motoneurons cultured on a permissive substrate. We first tested the activation or inhibition of PKA in neurons in which cAMP elevation has been induced, and in neurons treated with the PKA inhibitors H89 and Rp-cAMP. As expected, treatment of motoneurons with forskolin- and dbcAMP-induced PKA activation as demonstrated by the cAMP-dependent phosphorylation of $PKA_{RII\beta}$ subunit (Fig. 5A). Conversely, H89 and Rp-cAMP inhibited PKA basal activity and significantly reduced forskolin- and dbcAMP-induced PKA activation (Fig. 5A). The inhibitory effects of H89 and Rp-cAMP were not due to general toxic effects since motoneurons remained healthy and did not show signs of cell death upon the indicated treatments (Fig. 5B).

Next, we examined the role of PKA activation in neurite extension in motoneurons. We found that H89 caused a substantial and significant decrease in neurite length at concentrations between 10 and 20 μM after 24 h (Fig. 6A). This result indicates that intrinsic intracellular cAMP-regulated neurite outgrowth in motoneurons is mediated through PKA. H89 was also able to prevent neurite outgrowth elicited by treatment with forskolin (3 μM) or dbcAMP (1 mM) (Fig. 6B, C). The involvement of PKA in cAMP-induced neurite outgrowth was confirmed using the cAMP competitive inhibitor Rp-cAMP. Rp-cAMP (500 μM) reduced basal and forskolin-induced neurite extension (Fig. 6D). These experiments show that the increase in neurite outgrowth in motoneurons that follows elevation of cAMP above basal levels is also mediated by PKA.

3.4. Cyclic AMP does not activate the Erk pathway in motoneurons

Several signaling mechanisms can be activated or inhibited downstream of PKA. Among them, Erks represent important targets involved in cAMP-induced proliferation and growth (Stork and Schmitt, 2002), activity-dependent neuronal function (Grewal et al., 2000), and differentiation (Chu et al., 2006; Kiermayer et al., 2005). Hence, we examined Erk activation in motoneurons under conditions in which the levels of cAMP and neurite outgrowth were effectively modulated. Although a basal level of Erk2 phosphorylation was present even in untreated motoneurons, agents that increase (dbcAMP, forskolin) or decrease cAMP (SQ22536) did not affect Erk activation by phosphorylation (p-Erk) (Fig. 7A, B). Accordingly, the PKA inhibitors H89 and Rp-cAMP were also unable to regulate Erk activation. In contrast, the neurons responded robustly to BDNF (50 ng/ml) with Erk phosphorylation in the same period of incubation (Fig. 7A, B). This later process was mediated by tyrosine kinase because the tyrosine kinase inhibitor K252a prevented Erk phosphorylation (not shown).

4. Discussion

The results of this study demonstrate for the first time in embryonic motoneurons that intracellular cAMP is essential for neurite outgrowth and extension. These findings are very relevant in view of the conflicting data regarding the role of cAMP in neurite growth on permissive substrate. This ambiguity has led to the recent proposal that cAMP may work by modulating the response to myelin-associated inhibitors rather than being a neurite growth enhancer per se (Teng and Tang, 2006). Extensive evidence indicates that cAMP regulates differently neurite growth and extension on permissive and non-permissive substrates. Addition of dbcAMP to cerebellar neurons plated onto monolayers of MAG-expressing CHO cells (non-permissive substrate) resulted in dramatic increase in neurite length of neurons, but it did not affect neurite outgrowth of neurons grown on control cells (permissive substrate) (Cai et al., 2002, 1999). Similarly, only neurite growth on non-permissive substrate but not on a permissive substrate was increased when dbcAMP was delivered by injection 1 day prior to dissection of DRG neurons and cultured on permissive and non-permissive substrate (Qiu et al., 2002), and when cAMP was elevated by treatment of cerebellar neurons with neurotrophic factors (Cai et al., 1999). Moreover, PKA inhibition blocked neurite growth of young (P1) DRG neurons cultured on non-permissive substrate without affecting neurite growth of neurons on permissive

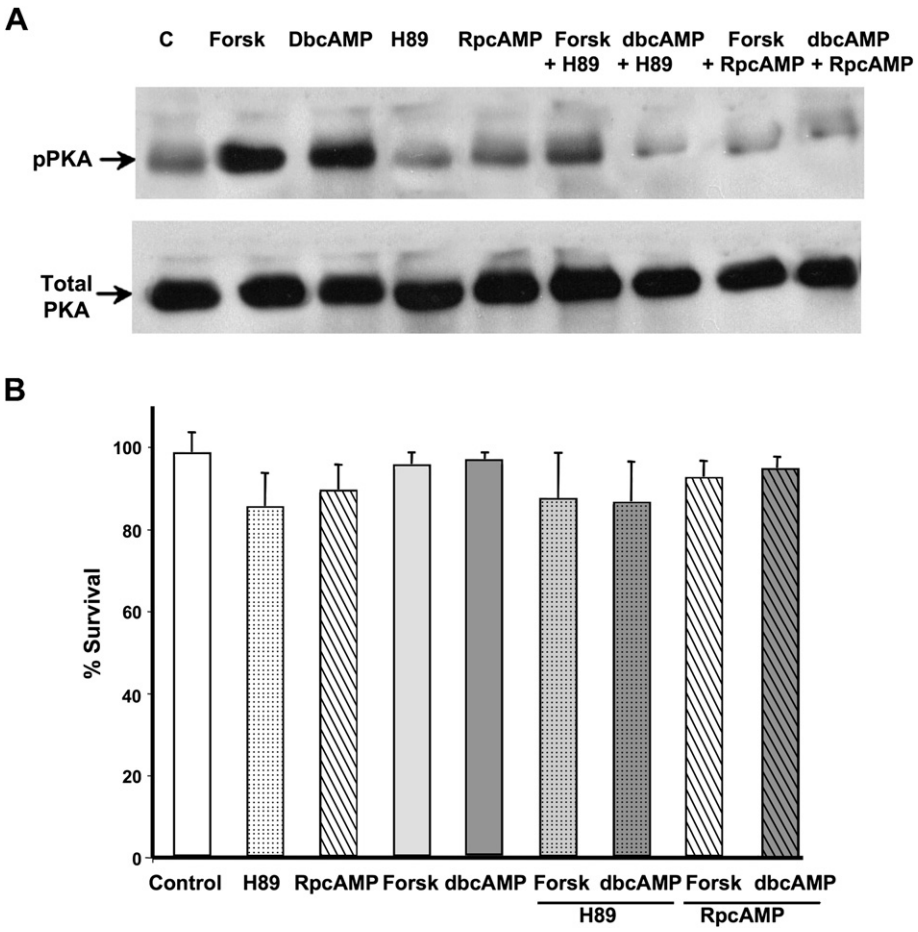


Fig. 5. Regulation of PKA in motoneurons. Motoneurons cultured at a density of 30,000 cells per 24-well dish were treated at the time of plating with forskolin (3 μM), dbcAMP (1 mM), H89 (20 μM), Rp-cAMP (500 μM), as well as forskolin or dbcAMP together with H89 or Rp-cAMP. (A) PKA activation was examined by detecting the phosphorylated form of the PKA regulatory subunit RII. (B) Neuronal survival measured with MTT assay was determined after 24 h. No significant differences were found according One Way ANOVA with Newman–Keuls Multiple range test.

substrate (Cai et al., 2001). On the other hand, Neumann et al. (2002) offered convincing evidence of the enhancement of axon outgrowth by cAMP in sensory neurons growing on permissive substrate. Nevertheless, the majority of the evidence for a role of cAMP in neurite outgrowth on a permissive substrate has been obtained from cell lines such as PC12 cells (Hansen et al., 2003) and therefore the data rather indicate that cAMP activates cell differentiation. In motoneurons, cAMP is able to support survival but to our knowledge the role in neurite outgrowth and extension has not been investigated previously.

Here, we demonstrate that pharmacological reduction of cAMP levels inhibits and elevation of cAMP promotes neurite outgrowth. We have performed quantitative analysis of neurite outgrowth in motoneurons. A reduction of cAMP levels with SQ22536 induced a dramatic decrease in both the number of neurons with neurites and the length of the neurites indicating that endogenous cAMP is required for neurite outgrowth. Under the conditions used SQ22536 did not affect neuronal survival. Conversely, we found that elevation of cAMP by diverse treatments including dbcAMP, forskolin, IBMX or Rolipram resulted in an increase of 20–40% in neurite length after 24 h. At this time, the percentage of neurons that extended neurites was also increased by 25–45% upon cAMP elevation. In untreated neurons the proportion of neurons extending neurites remained constant after 12 h suggesting that under basal culture conditions the process of neuritogenesis has been completed at that time. In neurons treated with forskolin, Rolipram or IBMX the percentage of neurons with neurites was significantly elevated at 12 h but increased even more between 12 and 24 h. These results suggest that elevation of cAMP not only stimulates neurite extension but it also prolongs neuritogenesis. The enhancement of neurite outgrowth and neurite extension by elevation of cAMP is remarkable considering that the basal culture conditions (substrate, culture medium, etc.) had been optimized for motoneuron growth.

PKA is the most important downstream signaling target of cAMP. We used the PKA inhibitor H89 and the cAMP antagonist Rp-cAMP to examine the role of PKA in motoneurons. Both agents effectively reduced PKA activity as demonstrated by the decreased phosphorylation of the PKA RII subunit. Under conditions of PKA inhibition forskolin and dbcAMP were unable to induce neurite extension indicating that PKA is required. Moreover, H89 and Rp-cAMP significantly reduced neurite outgrowth in untreated neurons supporting the notion that at least part of the basal neurite extension in motoneurons is mediated by cAMP. Although our experiments cannot exclude other cAMP-independent pathways, our finding that inhibition of PKA by H89 and Rp-cAMP and inhibition of all cAMP-mediated pathways by SQ22536 had similar effects on neurite extension suggests that the effects of cAMP are mediated via PKA. The contribution of other cAMP downstream pathways is therefore unlikely.

The role of PKA in cAMP-induced neurite outgrowth has been previously demonstrated in several neuronal types including DRG,

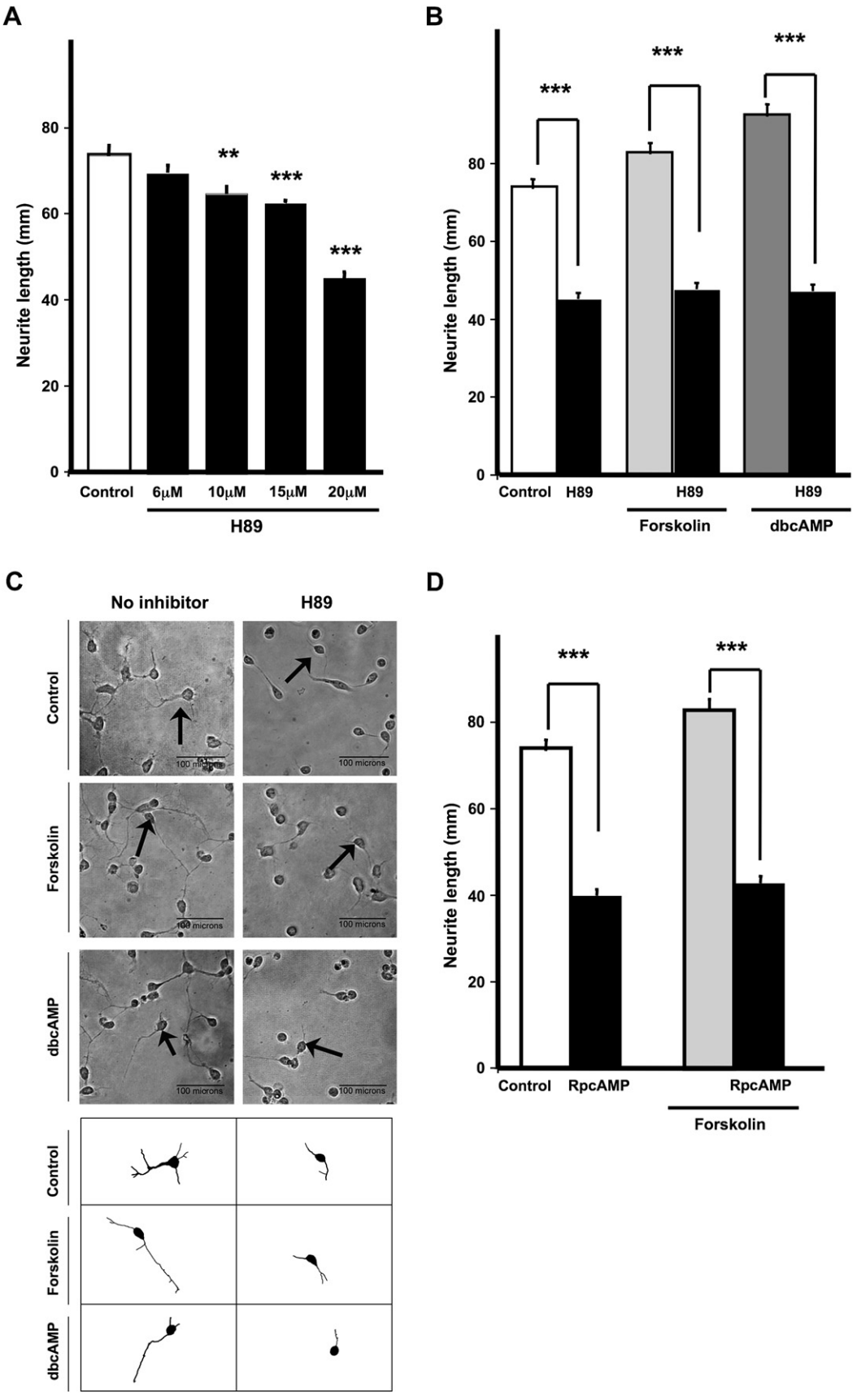


Fig. 6. PKA mediates neurite outgrowth in motoneurons. Motoneurons cultured at a density of 2000 cells per 96-well dish were treated at the time of plating with (A) H89 at concentrations of 6 to 20 μM or (B) forskolin (3 μM) or dbcAMP (1 mM) in the presence or absence of H89 (20 μM) and neurite length was measured after 24 h. (C) Phase-contrast images of motoneurons treated as indicated in (B), accompanied by drawings of neurons marked by black arrows. Neurons drawing were performed using the Empix software. (D) Motoneurons were treated with Rp-cAMP (500 μM) alone or together with forskolin and the length of neurite lengths measured. The experiments were done in triplicate and repeated three times. Data were analyzed by One Way ANOVA with Newman–Keuls Multiple range test. The results are presented as Mean ± SEM. Significance is indicated with respect to the untreated control $^{**}p < 0.01$, $^{***}p < 0.001$.

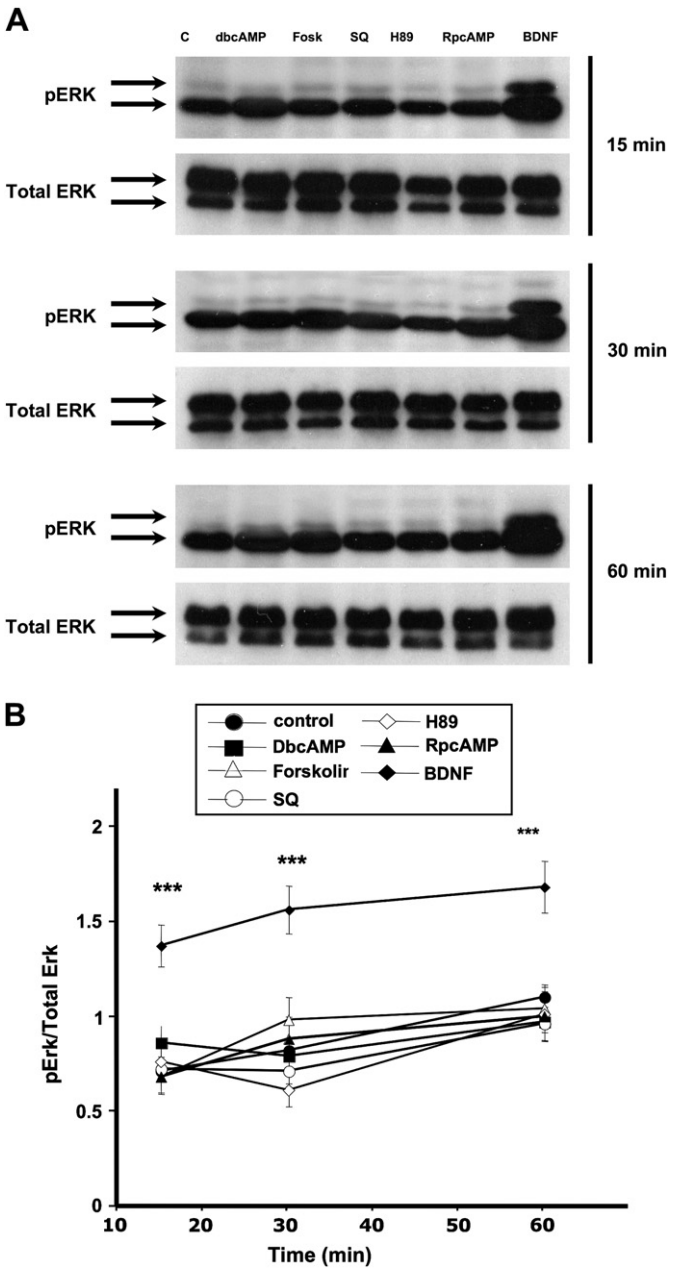


Fig. 7. Cyclic AMP does not regulate Erk activation in motoneurons. Motoneurons were cultured at a density of 30,000 per 24-well dish and treated for different times with dbcAMP (1 mM), forskolin 3 μM, SQ22536 (500 μM), H89 (20 μM), Rp-cAMP (500 μM) or BDNF (50 ng/ml). (A) Equal amounts of protein from cell lysates of each treatment were separated by SDS-PAGE and immunoblot analysis for Erk activation was performed as described in Section 2. The figure is a representative of at least three independent experiments. (B) Active Erk and total Erk was quantified using UN-SCAN-IT software and the correspondent values for the ratio p-Erk/total Erk was plotted. The results are presented as Mean ± SEM. Significance is indicated with respect to the untreated control $^{***}p < 0.001$.

cerebellar and retinal ganglion neurons (Cai et al., 2001). Nevertheless some differences exist between the motoneurons and the other neuronal types. Newborn DRG neurons (P1) extend neurites both on permissive and non-permissive substrate, however, only neurite outgrowth on a non-permissive substrate is blocked by PKA inhibitors and cAMP antagonists (Cai et al., 2001). In contrast, our results demonstrate that PKA downstream of cAMP regulates neurite outgrowth and extension of motoneurons on a permissive substrate and by analogy, may regulate motor axonal regeneration in the PNS.

Several targets downstream of PKA mediate cAMP cellular effects. Among them cAMP regulation of the Erk cascade offers and important crosstalk between hormones and growth factor signaling (Dumaz and Marais, 2005; Stork and Schmitt, 2002). Sustained Erk activation occurs in growth factor-mediated neurite growth (Kaplan and Miller, 2000). cAMP can activate or inhibit Erk in a cell-specific manner (Stork and Schmitt, 2002); activation of Erk by cAMP in neurons might depend of the developmental stage (Vogt Weisenhorn et al., 2001).

Our data indicate that the treatments used to increase cAMP namely forskolin and dbcAMP did not cause Erk activation in motorneurons. Under basal culture conditions some Erk2 activation was evident, however, the reduction of cAMP with SQ22536 or PKA inhibition by H89 or Rp-cAMP did not alter Erk2 phosphorylation suggesting that basal Erk2 activation is independent of cAMP. As expected, BDNF induced sustained and significant Erk activation in motoneurons. Identical results were obtained after 12 h of incubation with the different agents or growth factors (not shown). Taken together these results indicate that Erk activation is not an essential component of the effectiveness of cAMP in promoting axon growth in motoneurons in the PNS.

Our results are important for several reasons. First, they demonstrate in conjunction with evidence for the role of cAMP in axon outgrowth in sensory neurons in the PNS and the CNS, that elevation of cAMP and activation of PKA represent a fundamental mechanism in axon outgrowth in the nervous system. Second, they provide evidence that the downstream pathways of cAMP–PKA that control gene transcription and in turn, axon outgrowth are not common to all neurons. This is consistent with the many downstream targets for PKA and with the differential control of transcription of the growth associated genes for axon outgrowth (Andersen and Schreyer, 1999; Bradbury et al., 2000; Teng and Tang, 2006).

References

Al-Majed, A.A., Neumann, C.M., Brushart, T.M., Gordon, T., 2000. Brief electrical stimulation promotes the speed and accuracy of motor axonal regeneration. J. Neurosci. 20, 2602–2608.

Andersen, L.B., Schreyer, D.J., 1999. Constitutive expression of GAP-43 correlates with rapid, but not slow regrowth of injured dorsal root axons in the adult rat. Exp. Neurol. 155, 157–164.

Arce, V., Garces, A., de Bovis, B., Filippi, P., Henderson, C., Pettmann, B., deLapeyriere, O., 1999. Cardiotrophin-1 requires LIFRbeta to promote survival of mouse motoneurons purified by a novel technique. J. Neurosci. Res. 55, 119–126.

Bataille, S., Portalier, P., Coulon, P., Ternaux, J.P., 1998. Influence of acetylcholinesterase on embryonic spinal rat motoneurones growth in culture: a quantitative morphometric study. Eur. J. Neurosci. 10, 560–572.

Berridge, M.V., Tan, A.S., 1993. Characterization of the cellular reduction of 3-(4, 5-dimethylthiazol-2-yl)-2,5-diphenyltetrazolium bromide (MTT): subcellular localization, substrate dependence, and involvement of mitochondrial electron transport in MTT reduction. Arch. Biochem. Biophys. 303, 474–482.

Bradbury, E.J., McMahon, S.B., Ramer, M.S., 2000. Keeping in touch: sensory neurone regeneration in the CNS. Trends Pharmacol. Sci. 21, 389–394.

Brushart, T.M., Hoffman, P.N., Royall, R.M., Murinson, B.B., Witzel, C., Gordon, T., 2002. Electrical stimulation promotes motoneuron regeneration without increasing its speed or conditioning the neuron. J. Neurosci. 22, 6631–6638.

Brushart, T.M., Jari, R., Verge, V., Rohde, C., Gordon, T., 2005. Electrical stimulation restores the specificity of sensory axon regeneration. Exp. Neurol. 194, 221–229.

Cai, D., Deng, K., Mellado, W., Lee, J., Ratan, R.R., Filbin, M.T., 2002. Arginase I and polyamines act downstream from cyclic AMP in overcoming inhibition of axonal growth MAG and myelin in vitro. Neuron 35, 711–719.

Cai, D., Qiu, J., Cao, Z., McAtee, M., Bregman, B.S., Filbin, M.T., 2001. Neuronal cyclic AMP controls the developmental loss in ability of axons to regenerate. J. Neurosci. 21, 4731–4739.

Cai, D., Shen, Y., De Bellard, M., Tang, S., Filbin, M.T., 1999. Prior exposure to neurotrophins blocks inhibition of axonal regeneration by MAG and myelin via a cAMP-dependent mechanism. Neuron 22, 89–101.

Camu, W., Henderson, C.E., 1992. Purification of embryonic rat motoneurons by panning on a monoclonal antibody to the low-affinity NGF receptor. J. Neurosci. Methods. 44, 59–70.

Carlsen, R.C., 1982. Comparison of adenylate cyclase activity in segments of rat sciatic nerve with a condition/test or test lesion. Exp. Neurol. 77, 254–265.

Carlsen, R.C., 1983. Delayed induction of the cell body response and enhancement of regeneration following a condition/test lesion of frog peripheral nerve at 15 °C. Brain Res. 279, 9–18.
Carriedo, S.G., Yin, H.Z., Weiss, J.H., 1996. Motor neurons are selectively vulnerable to AMPA/kainate receptor-mediated injury in vitro. J. Neurosci. 16, 4069–4079.
Charles, M.P., Adamski, D., Kholler, B., Pelletier, L., Berger, F., Wion, D., 2003. Induction of neurite outgrowth in PC12 cells by the bacterial nucleoside N6-methyldeoxyadenosine is mediated through adenosine A2a receptors and via cAMP and MAPK signaling pathways. Biochem. Biophys. Res. Commun. 304, 795–800.
Chu, M.S., Chang, C.F., Yang, C.C., Bau, Y.C., Ho, L.L., Hung, S.C., 2006. Signalling pathway in the induction of neurite outgrowth in human mesenchymal stem cells. Cell. Signal. 18, 519–530.
Dumaz, N., Marais, R., 2005. Integrating signals between cAMP and the RAS/RAF/MEK/ERK signalling pathways. Based on The Anniversary Prize of the Gesellschaft für Biochemie und Molekularbiologie Lecture delivered on 5 July 2003 at the Special FEBS Meeting in Brussels. FEBS J. 272, 3491–3504.
Ericson, J., Thor, S., Edlund, T., Jessell, T.M., Yamada, T., 1992. Early stages of motor neuron differentiation revealed by expression of homeobox gene Islet-1. Science 256, 1555–1560.
Fujioka, T., Fujioka, A., Duman, R.S., 2004. Activation of cAMP signaling facilitates the morphological maturation of newborn neurons in adult hippocampus. J. Neurosci. 24, 319–328.
Gao, Y., Nikulina, E., Mellado, W., Filbin, M.T., 2003. Neurotrophins elevate cAMP to reach a threshold required to overcome inhibition by MAG through extracellular signal-regulated kinase-dependent inhibition of phosphodiesterase. J. Neurosci. 23, 11770–11777.
Geremia, N.M., Gordon, T., Brushart, T.M., Al-Majed, A.A., Verge, V.M., 2007. Electrical stimulation promotes sensory neuron regeneration and growth-associated gene expression. Exp. Neurol. 205, 347–359.
Gomes, F.C., Maia, C.G., de Menezes, J.R., Neto, V.M., 1999. Cerebellar astrocytes treated by thyroid hormone modulate neuronal proliferation. Glia 25, 247–255.
Grewal, S.S., Horgan, A.M., York, R.D., Withers, G.S., Banker, G.A., Stork, P.J., 2000. Neuronal calcium activates a Rap1 and B-Raf signaling pathway via the cyclic adenosine monophosphate-dependent protein kinase. J. Biol. Chem. 275, 3722–3728.
Gysbers, J.W., Rathbone, M.P., 1996. Neurite outgrowth in PC12 cells is enhanced by guanosine through both cAMP-dependent and -independent mechanisms. Neurosci. Lett. 220, 175–178.
Hansen, T.O., Rehfeld, J.F., Nielsen, F.C., 2003. KCl potentiates forskolin-induced PC12 cell neurite outgrowth via protein kinase A and extracellular signal-regulated kinase signaling pathways. Neurosci. Lett. 347, 57–61.
Hanson Jr., M.G., Shen, S., Wiemelt, A.P., McMorris, F.A., Barres, B.A., 1998. Cyclic AMP elevation is sufficient to promote the survival of spinal motor neurons in vitro. J. Neurosci. 18, 7361–7371.
Harris, D.N., Asaad, M.M., Phillips, M.B., Goldenberg, H.J., Antonaccio, M.J., 1979. Inhibition of adenylate cyclase in human blood platelets by 9-substituted adenine derivatives. J. Cyclic Nucleotide Res. 5, 125–134.
Houslay, M.D., 1998. Adaptation in cyclic AMP signalling processes: a central role for cyclic AMP phosphodiesterases. Semin. Cell Dev. Biol. 9, 161–167.
Houslay, M.D., Kolch, W., 2000. Cell-type specific integration of cross-talk between extracellular signal-regulated kinase and cAMP signaling. Mol. Pharmacol. 58, 659–668.
Ivins, J.K., Parry, M.K., Long, D.A., 2004. A novel cAMP-dependent pathway activates neuronal integrin function in retinal neurons. J. Neurosci. 24, 1212–1216.
Jin, S.L., Richard, F.J., Kuo, W.P., D'Ercole, A.J., Conti, M., 1999. Impaired growth and fertility of cAMP-specific phosphodiesterase PDE4D-deficient mice. Proc. Natl. Acad. Sci. U.S.A. 96, 11998–12003.
Kaplan, D.R., Miller, F.D., 2000. Neurotrophin signal transduction in the nervous system. Curr. Opin. Neurobiol. 10, 381–391.
Kiermayer, S., Biondi, R.M., Imig, J., Plotz, G., Haupenthal, J., Zeuzem, S., Piiper, A., 2005. Epac activation converts cAMP from a proliferative into a differentiation signal in PC12 cells. Mol. Biol. Cell 16, 5639–5648.
Liu, B.P., Cafferty, W.B., Budel, S.O., Strittmatter, S.M., 2006. Extracellular regulators of axonal growth in the adult central nervous system. Philos. Trans. R. Soc. Lond., B: Biol. Sci. 361, 1593–1610.
McKerracher, L., Winton, M.J., 2002. Nogo on the go. Neuron 36, 345–348.
Meyer-Franke, A., Wilkinson, G.A., Kruttgen, A., Hu, M., Munro, E., Hanson Jr., M.G., Reichardt, L.F., Barres, B.A., 1998. Depolarization and cAMP elevation rapidly recruit TrkB to the plasma membrane of CNS neurons. Neuron 21, 681–693.
Mosmann, T., 1983. Rapid colorimetric assay for cellular growth and survival: application to proliferation and cytotoxicity assays. J. Immunol. Methods 65, 55–63.
Neumann, S., Bradke, F., Tessier-Lavigne, M., Basbaum, A.I., 2002. Regeneration of sensory axons within the injured spinal cord induced by intraganglionic cAMP elevation. Neuron 34, 885–893.
Qiu, J., Cai, D., Dai, H., McAtee, M., Hoffman, P.N., Bregman, B.S., Filbin, M.T., 2002. Spinal axon regeneration induced by elevation of cyclic AMP. Neuron 34, 895–903.
Rao, S.D., Weiss, J.H., 2004. Excitotoxic and oxidative cross-talk between motor neurons and glia in ALS pathogenesis. Trends Neurosci. 27, 17–23.
Raoul, C., Abbas-Terki, T., Bensadoun, J.C., Guillot, S., Haase, G., Szulc, J., Henderson, C.E., Aebischer, P., 2005. Lentiviral-mediated silencing of SOD1 through RNA interference retards disease onset and progression in a mouse model of ALS. Nat. Med. 11, 423–428.
Roisen, F.J., Murphy, R.A., Braden, W.G., 1972. Neurite development in vitro. I. The effects of adenosine 3′5′-cyclic monophosphate (cyclic AMP). J. Neurobiol. 3, 347–368.
Song, H., Ming, G., He, Z., Lehmann, M., McKerracher, L., Tessier-Lavigne, M., Poo, M., 1998. Conversion of neuronal growth cone responses from repulsion to attraction by cyclic nucleotides. Science 281, 1515–1518.
Song, H.J., Ming, G.L., Poo, M.M., 1997. cAMP-induced switching in turning direction of nerve growth cones. Nature 388, 275–279.
Stork, P.J.S., Schmitt, J.M., 2002. Crosstalk between cAMP and MAP kinase signaling in the regulation of cell proliferation. Trends Cell Biol. 12, 258.
Teng, F.Y., Tang, B.L., 2006. Axonal regeneration in adult CNS neurons-signaling molecules and pathways. J. Neurochem. 96, 1501–1508.
Vogt Weisenhorn, D.M., Roback, L.J., Kwon, J.H., Wainer, B.H., 2001. Coupling of cAMP/PKA and MAPK signaling in neuronal cells is dependent on developmental stage. Exp. Neurol. 169, 44–55.
Yan, Q., Johnson Jr., E.M., 1988. An immunohistochemical study of the nerve growth factor receptor in developing rats. J. Neurosci. 8, 3481–3498.

Available online at www.sciencedirect.com
SCIENCE DIRECT®
Experimental Neurology 198 (2006) 500–510
Experimental Neurology
www.elsevier.com/locate/yexnr

BDNF/TrkB signaling regulates HNK-1 carbohydrate expression in regenerating motor nerves and promotes functional recovery after peripheral nerve repair

Kirsten A. Eberhardt [a,1], Andrey Irintchev [a,1], Abdulhakeem A. Al-Majed [b], Olga Simova [a], Thomas M. Brushart [c], Tessa Gordon [b], Melitta Schachner [a,*]

[a] Zentrum für Molekulare Neurobiologie, Universität Hamburg, Martinistr 52, D-20246 Hamburg, Germany
[b] Department of Pharmacology, Division of Neuroscience, 513 Heritage Medical Research Center, University of Alberta, Edmonton, Alberta, Canada T6G 2S2
[c] Department of Orthopedic Surgery and Neurology, Johns Hopkins Medical School, Baltimore, MD 21218, USA

Received 15 October 2005; revised 5 December 2005; accepted 19 December 2005
Available online 7 February 2006

Abstract

Functional recovery after peripheral nerve injury is often poor despite high regenerative capacity of peripheral neurons. In search for novel treatments, brief electrical stimulation of the acutely lesioned nerve has recently been identified as a clinically feasible approach increasing precision of axonal regrowth. The effects of this stimulation appear to be mediated by BDNF and its receptor, TrkB, but the down-stream effectors are unknown. A potential candidate is the HNK-1 carbohydrate known to be selectively reexpressed in motor but not sensory nerve branches of the mouse femoral nerve and to enhance growth of motor but not sensory axons in vitro. Here, we show that short-term low-frequency electrical stimulation (1 h, 20 Hz) of the lesioned and surgically repaired femoral nerve in wild-type mice causes a motor nerve-specific enhancement of HNK-1 expression correlating with previously reported acceleration of muscle reinnervation. Such enhanced HNK-1 expression was not observed after electrical stimulation in heterozygous BDNF or TrkB-deficient mice. Accordingly, the degree of proper reinnervation of the quadriceps muscle, as indicated by retrograde labeling of motoneurons, was reduced in TrkB+/− mice compared to wild-type littermates. Also, recovery of quadriceps muscle function, evaluated by a novel single-frame motion analysis approach, and axonal regrowth into the distal nerve stump, assessed morphologically, were considerably delayed in TrkB+/− mice. These findings indicate that BDNF/TrkB signaling is important for functional recovery after nerve repair and suggest that up-regulation of the HNK-1 glycan is linked to this phenomenon.
© 2006 Elsevier Inc. All rights reserved.

Keywords: BDNF; Femoral nerve; HNK-1 carbohydrate; Motion analysis; Motoneuron; Mouse; Regeneration; TrkB

Introduction

Injured peripheral neurons in mammals, in contrast to nerve cells in the central nervous system, can regenerate their axons over long distances. Despite this potential, functional recovery after surgical repair is often poor (Fu and Gordon, 1997; Lundborg, 2003). Choice of appropriate pathways by regenerating axons is considered to be a major determinant of successful functional recovery. A favorable model system to study appropriate reinnervation of denervated targets is the femoral nerve which bifurcates into two branches, the quadriceps motor nerve and the saphenous cutaneous branch (Fig. 1). After transection of this nerve proximal to the bifurcation, motor neurons preferentially reinnervate the quadriceps branch, when given equal access to both branches (Brushart, 1988, 1993; Brushart and Seiler, 1987; Brushart et al., 1998; Madison et al., 1996; Robinson and Madison, 2003, 2005).

In search of the cellular and molecular determinants underlying preferential motor reinnervation, we previously found that an unusual acidic glycan recognized by the monoclonal antibody HNK-1 is associated with myelin profiles of motor axons, but not of sensory axons in the mouse (Martini and Schachner, 1986; Martini et al., 1992, 1994). During development, HNK-1 is expressed by all premyelinating or non-myelinating Schwann cells and is down-regulated during early postnatal periods in these cells to then become up-

* Corresponding author. Fax: +49 40 42803 6248.
E-mail address: melitta.schachner@zmnh.uni-hamburg.de (M. Schachner).
[1] These authors contributed equally to this work.

0014-4886/$ - see front matter © 2006 Elsevier Inc. All rights reserved.
doi:10.1016/j.expneurol.2005.12.018

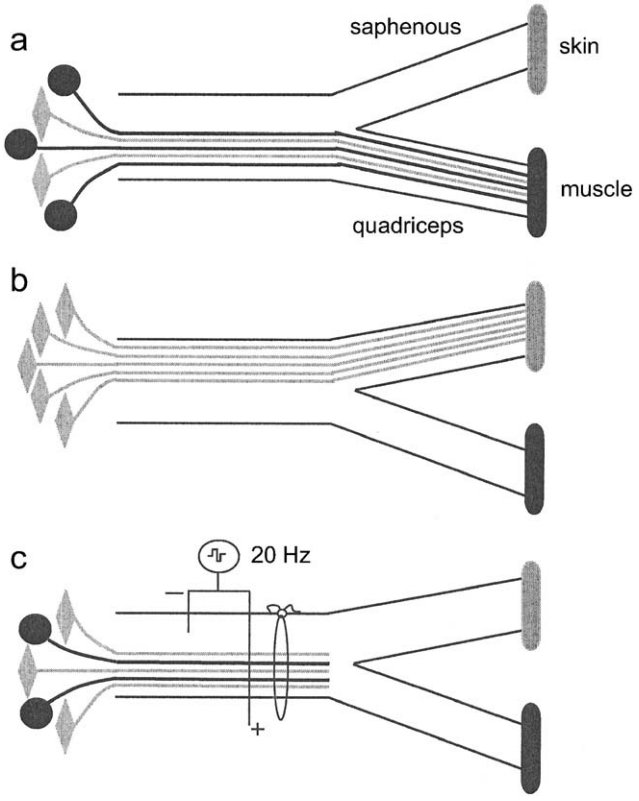


Fig. 1. Diagrammatic representation of the femoral nerve with its quadriceps (a) and saphenous branches (b). In intact animals, the quadriceps branch contains axons of motoneurons (black circles) innervating the quadriceps muscle as well as axons of sensory neurons (gray rhombuses) innervating muscle spindles and tendon organs. The saphenous branch is populated by axons of sensory neurons innervating the skin. The position of the bipolar electrode used to stimulate the transected nerve is shown in panel c.

regulated again in the myelin sheaths associated exclusively with motor axons. The HNK-1 carbohydrate is carried by or binds to different neural recognition molecules including the myelin associated glycoprotein MAG (Kruse et al., 1985), highly acidic glycolipids, several laminin isoforms (Hall et al., 1993), amphoterin (Mohan et al., 1992), the neural cell adhesion molecule (NCAM) and P0 (for reviews, see Kleene and Schachner, 2004; Schachner and Martini, 1995). These observations led to the hypothesis that the HNK-1 carbohydrate, which is detectable in compact myelin, basal lamina and at the cell surface of Schwann cells, the sites that motor axons follow as they regenerate after peripheral nerve damage, could be specifically involved in motor axon regrowth. This view was supported by in vitro experiments showing that substrate-coated HNK-1 carbohydrate enhances neurite outgrowth from motoneurons, but not from sensory neurons (Martini et al., 1992).

Previous work has shown that continuous low-frequency (20 Hz) electrical stimulation of the proximal nerve stump, performed immediately after nerve transection for a period as short as 1 h, dramatically reduces the period of protracted axonal regrowth and increases precision of reinnervation in the rat (Al Majed et al., 2000a). The accelerated preferential motor reinnervation after stimulation is associated with an accelerated and enhanced up-regulation of the neurotrophin BDNF and its cognate receptor TrkB in motor neurons (Al Majed et al., 2000b, 2004). Here, we tested the hypothesis that TrkB signaling exerts its effects on preferential motor reinnervation via modulation of HNK-1 epitope expression. The results described here show that TrkB signaling is important for functional recovery after injury and suggest that TrkB-dependent HNK-1 expression mediates these beneficial functions.

Materials and methods

Animals

To investigate the effect of electrical stimulation on HNK-1 expression, femoral nerve repair was performed in 72 C57BL/6J mice obtained from the breeding unit of the University Hospital Hamburg. To define the contribution of BDNF to this process, we used 18 heterozygous BDNF-deficient mice (Korte et al., 1995) kindly provided by Martin Korte (Max-Planck-Institute for Neurobiology, Martinsried). Sixteen wild-type littermate mice were used as controls for these experiments. Further experiments were performed on 28 heterozygous TrkB-deficient mice kindly provided by Louis F. Reichardt (University of California, San Francisco). Sixteen wild-type littermates served as controls. Half of the animals mentioned above were subjected to electrical stimulation after transection of the femoral nerve (see below). Additional 16 TrkB-deficient mice and 16 wild-type littermates were used for analysis of functional recovery after nerve repair and for subsequent morphological analyses of retrogradely labeled motoneurons and regenerated nerves. None of the animals in this group was subjected to electrical stimulation of the femoral nerve.

Breeding and genotyping of animals

Heterozygous BDNF and wild-type mice on a C57BL/6J background were bred in the animal facility of the University Hospital Hamburg and genotyped by standard polymerase chain reaction (PCR) assay at the Max-Planck-Institute for Neurobiology, Martinsried (Korte et al., 1995). Heterozygous TrkB mutants and wild-type littermates (C57BL/6J genetic background) were derived from heterozygous breeding and genotyped by PCR as described previously (Xu et al., 2000a,b).

Experimental paradigm

In the intact quadriceps branch of the femoral nerve, sensory and motor fibers are intermingled to innervate the skeletal muscles (Fig. 1a). The saphenous branch contains only sensory fibers that innervate the skin (Fig. 1b). Although after nerve injury motor axons preferentially reinnervate muscle pathways, many motor axons fail to find the appropriate muscle branch and regrow into the saphenous branch (Martini et al., 1992, 1994; Brushart et al., 1998; Robinson and Madison, 2005). Electrical stimulation of the proximal nerve stump after femoral nerve transection and surgical repair (Fig. 1c) causes accelerated regrowth of larger numbers of motor axons, as compared to

sham-stimulation, into the appropriate motor nerve branch (Al Majed et al., 2000a).

Nerve repair

Experiments were performed under antiseptic conditions on femoral nerves of adult mice anesthetized with sodium pentobarbital (Somnotol, MTC Pharmaceuticals, Cambridge, Ontario, Canada, 30 mg/kg) or with fentanyl (Fentanyl-Janssen, Janssen, Neuss, Germany, 0.4 mg/kg), droperidol (Dehydrobenzperidol, Janssen, 20 mg/kg) and diazepam (Valium 10 Roche, Hoffman-La Roche, Grenzach-Wyhlen, Germany, 5 mg/kg) by intraperitoneal injection. The proximal femoral nerve was cut 3–4 mm proximal to the bifurcation into saphenous and quadriceps nerve branches. The proximal and distal stumps were inserted into a 4-mm-long silastic nerve cuff (0.37 mm inner diameter; Dow Corning, Midland, Michigan, USA). Using single stitches of 11-0 Nylon suture thread (Ethicon, Peterborough, ON, Canada) through the epineurium, the stumps were fixed so that their ends were separated by a gap of 2 mm. Surgery was performed unilaterally in all animals. Experiments were either approved by a local ethical committee (Health Science Laboratory Animal Services) under the Canadian guidelines for animal experimentation or were approved by the State of Hamburg animal care committee and conformed to EC and NIH guidelines.

Electrical stimulation

In experiments in which transected and repaired femoral nerves were electrically stimulated, two insulated Teflon-coated stainless steel wires (A5632; Cooner Wire Company, Chatsworth, CA) were bared of insulation for 2–3 mm, and each was twisted to form a small loop to secure on either side of the nerve stump proximal to the suture site (Fig. 1c). The cathode was sutured alongside the femoral nerve just below its exit from the peritoneal cavity, whereas the anode was sutured to the muscle close to the nerve, just proximal to the suture repair site. The wires were connected to a SD9 Square Pulse Stimulator (Grass Instrument Co., Quincy, MA, USA) to commence stimulation (20 Hz, single square pulses of 0.1 ms duration and 3 V amplitude) immediately. We chose a low stimulus frequency because it is the physiologically relevant frequency of hind limb motoneuron discharge (Loeb et al., 1987). A stimulation period of 1 h was selected in view of the equal effectiveness of 1 h stimulation and up to 2-week stimulation periods in accelerating axonal regeneration and preferential motor reinnervation (Al Majed et al., 2000a). In the sham-stimulated group of mice, the electrodes were implanted, but the stimulator was not switched on.

Immunohistochemistry

After survival time-periods of 1, 2 or 3 weeks, the animals were sacrificed by an overdose of Somnotol. The nerves were quickly removed, embedded in Tissue Tec® (Sakura, Tokyo, Japan) and frozen in liquid nitrogen as previously described by Bartsch et al. (1989). The embedded femoral nerves were cut into 10-μm thick cross-sections on a cryostat (CM3050, Leica). The sections were dried overnight, washed three times in phosphate-buffered saline (PBS, pH 7.4) for 10 min each, blocked with 2% bovine serum albumin (BSA, Sigma, Deisenhofen, Germany) for 2 h, washed again three times for 10 min each in PBS and incubated for 1 h with the rat monoclonal antibody 412 raised against the HNK-1 carbohydrate (Kruse et al., 1984, dilution 1:100). After incubation, the sections were washed in PBS, incubated for 1 h in PBS containing the secondary fluorescent antibody (Cy3-conjugated anti-rat IgG, Dianova, Hamburg, Germany; 1:500), washed again in PBS and coverslipped with Aqua Polymount (Polysciences, Warrington, PA).

Analysis of HNK-1 carbohydrate expression

Data were collected by two independent procedures. In one procedure, the number of HNK-1 positive profiles was evaluated using images obtained with a laser scanning microscope (LSM 510, Zeiss, 40× objective). Number of HNK-1 positive profiles per nerve cross-section was evaluated using confocal images (LSM 510 microscope, Zeiss, 40× objective) and an image processing program (Analysis, Zeiss). At least 5 sections cut distal from the bifurcation per nerve branch were analyzed. In the same sample, average relative fluorescence intensity was measured using the intensity measuring module of the microscope.

Analysis of motor function

Functional recovery was assessed by a novel single-frame motion analysis (SFMA) approach recently developed in our laboratory (Irintchev et al., 2005). To evaluate quadriceps muscle function during ground locomotion prior to operation, mice were trained to perform a classical beam walking test. In this test, the animals walk unforced from one end of a horizontal beam (length 1000 mm, width 38 mm) towards their home cage located at the other end of the beam. For all mice, a rear view of one walking trial was captured prior to the operation with a Panasonic NV-DS12 camera (Panasonic Deutschland, Hamburg, Germany) at 25 frames per second and recorded on videotape (video recorder SVL-SE 830, Sony Deutschland, Cologne, Germany). The recordings were repeated 1, 2, 4, 8 and 12 weeks after nerve transection. The video sequences were digitized and examined with VirtualDub software (available at http://www.virtualdub.org). Selected frames in which the animals were seen in defined phases of the step cycle (see below) were used for measurements performed with UTHSCSA ImageTool 2.0 software (University of Texas, San Antonia, TX, USA, http://ddsdx.uthscsa.edu/dig/). Two parameters were measured: the foot-base angle (FBA, Figs. 2a, b) and the heels-tail angle (HTA, Figs. 2c, d). The foot-base angle, measured at toe-off position, is defined by a line dividing the sole surface into two halves and the horizontal line, and is measured with respect to the medial aspect. The heels-tail angle is measured when one leg is in the single support phase and the contralateral

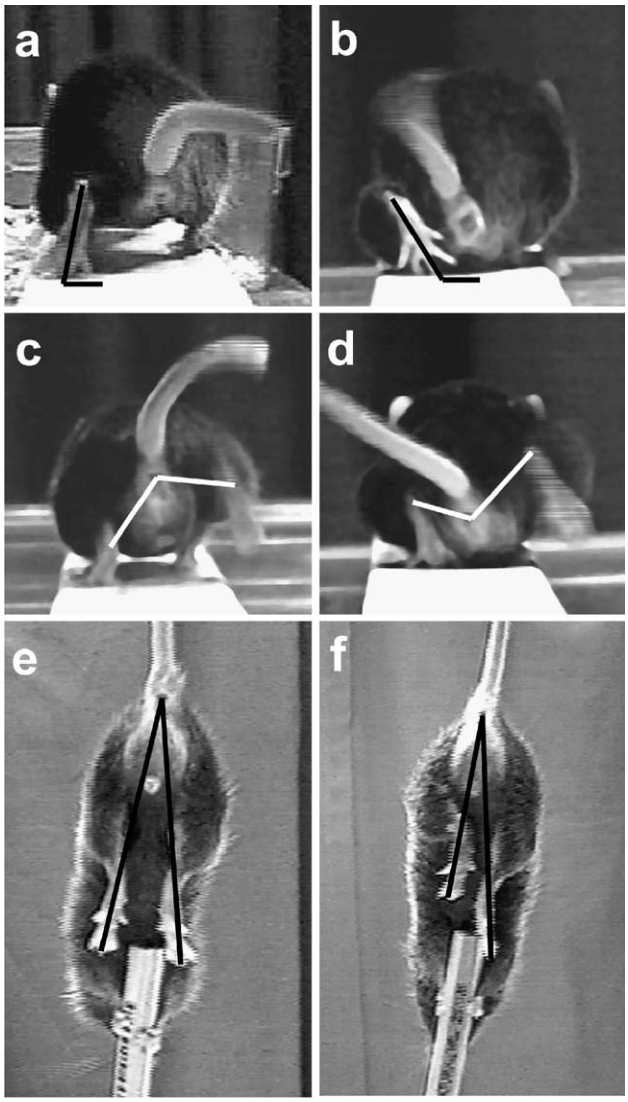


Fig. 2. Single video frames from recordings of beam walking (a–d) and limb protractions (e, f). Shown are intact animals (a, c, e) and animals with transection of the left femoral nerve at 7 days after lesion (b, d, f). The lines drawn in the video frames show the foot-base angle (FBA, a, b), the heels-tail angle (HTA, b, d) and the limb lengths used for calculation of the limb protraction length ratio (PLR, e, f). Note that HTA is measured always with respect to the dorsal aspect, FBA with respect to the medial aspect. For further explanations, see the main text.

extremity has maximum swing altitude, and is defined by the lines connecting the heels with the anus. The angle is measured with respect to the dorsal aspect. Compared to intact animals (Figs. 2a, c), the two angles change significantly after lesion of the femoral nerve (Figs. 2b, d). Both parameters are directly related to the ability of the quadriceps muscle to keep the knee joint extended during contralateral swing phases (see Irintchev et al., 2005). As a relative measure of functional recovery at 4 and 12 weeks after lesion, we calculated the stance recovery index which is a mean of the recovery index (RI) for the HTA and the FBA. The index is calculated, in percent, as:

$$\mathrm{RI} = [(X_{\mathrm{reinn}} - X_{\mathrm{den}})/(X_{\mathrm{pre}} - X_{\mathrm{den}})] \times 100,$$

where X_{pre}, X_{den} and X_{reinn} are values prior to operation, during the state of denervation (7 days after injury), and at 4 or 12 weeks of reinnervation, respectively.

A third parameter, the limb protraction length ratio (PLR), was evaluated from video recordings of voluntary pursuit movements of the mice (Figs. 2e, f). The mouse, when held by its tail and allowed to grasp a pencil with its fore paws, tries to catch the object with its hind paws and extends simultaneously both hind limbs. In intact animals, the relative length of the two extremities, as estimated by lines connecting the most distal mid-point of the extremity with the anus, is approximately equal and the PLR (ratio of the right to left limb length) is close to 1 (Fig. 2e). After denervation, the limb cannot extend maximally (left side of the animal shown in Fig. 2f) and the PLR increases significantly above 1.

Retrograde labeling of motor neurons

Three months after nerve transection, the animals were anaesthetized with fentanyl, droperidol and diazepam. After exposing the left femoral nerve, a piece of Parafilm (Pechiney Plastic Packaging, Chicago, IL, USA) was laid underneath the nerve trunks distal to the bifurcation, and the two nerve branches were transected 5 mm distal to the bifurcation. Fluorescence retrograde tracers were applied to the cut nerve ends in the form of powder: Fluoro-Ruby (tetramethylrhodamine dextran, Molecular Probes, Eugene, Oregon, USA) to the muscle branch, Fast-Blue (EMS-Chemie GmbH, Großumstadt, Germany) to the cutaneous branch. Thirty minutes after dye application, the nerve stumps were rinsed thoroughly with PBS and gently blotted with filter paper. The wound was surgically closed. Seven days later, the mice were deeply anaesthetized with sodium pentobarbital and transcardially perfused with PBS for 1 min followed by 4% formaldehyde in 0.1 M cacodylate buffer, pH 7.4, for 20 min. The lumbar spinal cord was removed, postfixed overnight at 4°C in the same fixative and cut transversely (serial section of 50 μm thickness) on a Leica VT 1000 M Vibratome (Leica). The sections were coverslipped with Fluoromount-G (SouthernBiotech, Birmingham, AL, USA) and examined under an Axiophot 2 microscope (Zeiss) with filter sets appropriate for Fluoro-Ruby and Fast-Blue. About 45–50 serial cross-sections contained retrogradely labeled cells. All sections were examined and all single- and double-labeled cells were counted except for those profiles visible on top of sections. The application of this simple stereological principle prevents double counting of labeled cells and allows an unbiased evaluation of cell numbers which does not rely on assumptions or require corrections.

Histological analysis of regenerated nerves

The common femoral nerve trunk was removed with both branches, postfixed in osmium tetroxide and embedded in Epon according to a routine protocol. Semithin (1 μm) transverse sections were cut from the nerve branches on a Reichert Ultracut UCT (Leica) and stained with 1% Toluidine blue/1% borax. The

number of myelinated axons in the muscle and cutaneous nerve branches was counted on an Axioskop microscope (Zeiss) equipped with a motorized stage and Neurolucida software-controlled computer system (MicroBrightField Europe, Magdeburg, Germany) using a 100× objective.

Statistical analyses

Data were analyzed using appropriate parametric or non-parametric tests as indicated in the text and figure legends. The accepted level of significance was 5%. Throughout the text and in the figures data are presented as mean values ± standard error of mean (SEM).

Results

In intact mice, the HNK-1 carbohydrate is detectable by indirect immunofluorescence in myelin sheaths of large-diameter axons in the femoral nerve prior to its bifurcation and in the motor branch, but barely in the sensory branch beyond the bifurcation point (Martini et al., 1992, 1994). One to three weeks after nerve transection, a similar staining pattern is observed in the proximal nerve stump in which the structural integrity of axons and myelin is largely preserved (Fig. 3b, compare with the negative staining control shown in Fig. 3a). In the distal nerve branches, the staining pattern is changed as a result of axon and myelin degeneration (Wallerian degeneration) and subsequent Schwann cell proliferation and axonal regrowth from the proximal nerve stump (compare the motor nerve branch on the right-hand side in Fig. 3c with the proximal nerve stump shown in Fig. 3b). Note higher expression of the HNK-1 epitope in the motor branch compared to the sensory nerve branch following nerve transection (Fig. 3c). The staining pattern and intensity in electrically stimulated nerves (Fig. 3d) appeared to be altered as compared to sham-stimulated nerves (Fig. 3c). To verify the existence of differences, we evaluated quantitatively staining intensities and counted numbers of HNK-1 positive structures in the regenerating nerve branches at 1, 2 and 3 weeks after nerve injury.

HNK-1 expression in electrically stimulated and sham-stimulated nerves of C57BL/6J mice

In the quadriceps branch, the density of HNK-1 positive structures 1 to 3 weeks after nerve transection was significantly lower in sham-stimulated nerves (12 mice per time-point studied) compared to intact contralateral nerves (Fig. 4a). This injury-induced decline in HNK-1 immunoreactive structures was not found in electrically stimulated nerves (12 mice per time-point studied) in which the numbers were similar to control

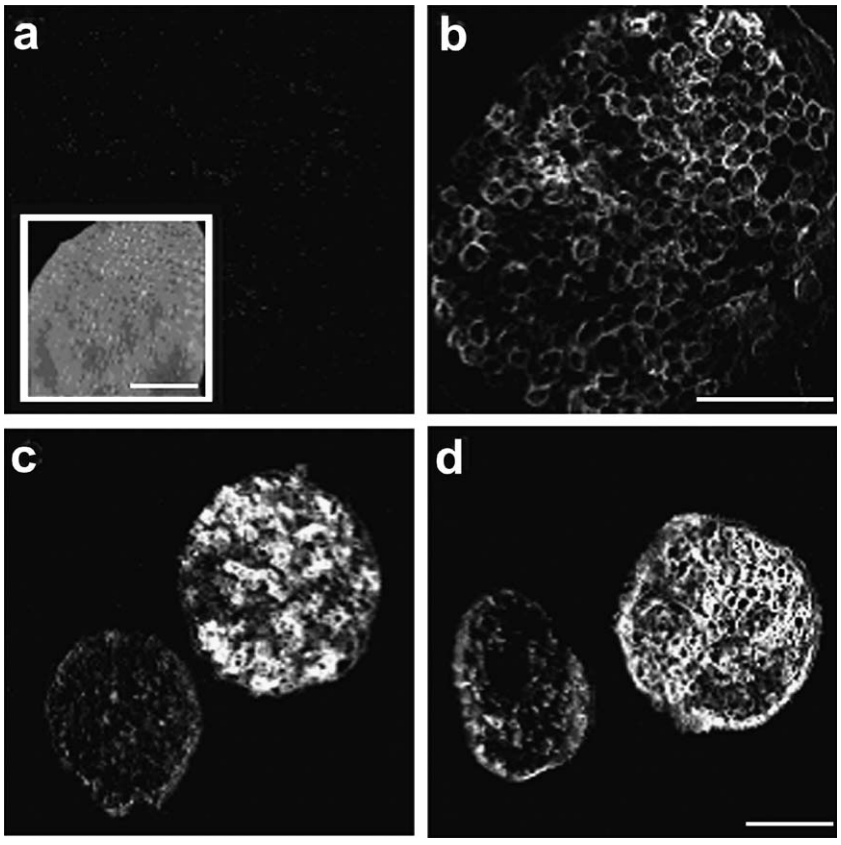


Fig. 3. HNK-1 expression in the femoral nerve and its branches. Shown are cross-sections from the femoral nerve proximal to the transection site (a, b) and immediately distal to the bifurcation (c, d) of a sham-stimulated (a–c) and an electrically stimulated animal (d) studied 1 week after surgery. The quadriceps branch is seen on the right hand side in panels c and d. Panel a shows a negative control section (omission of primary antibody) and a phase-contrast view (insert) of the section observed with epi-fluorescence in panel a. Scale bars shown in the insert, in panels b and d, indicate 100 μm for the insert, panels a, b and c, d, respectively.

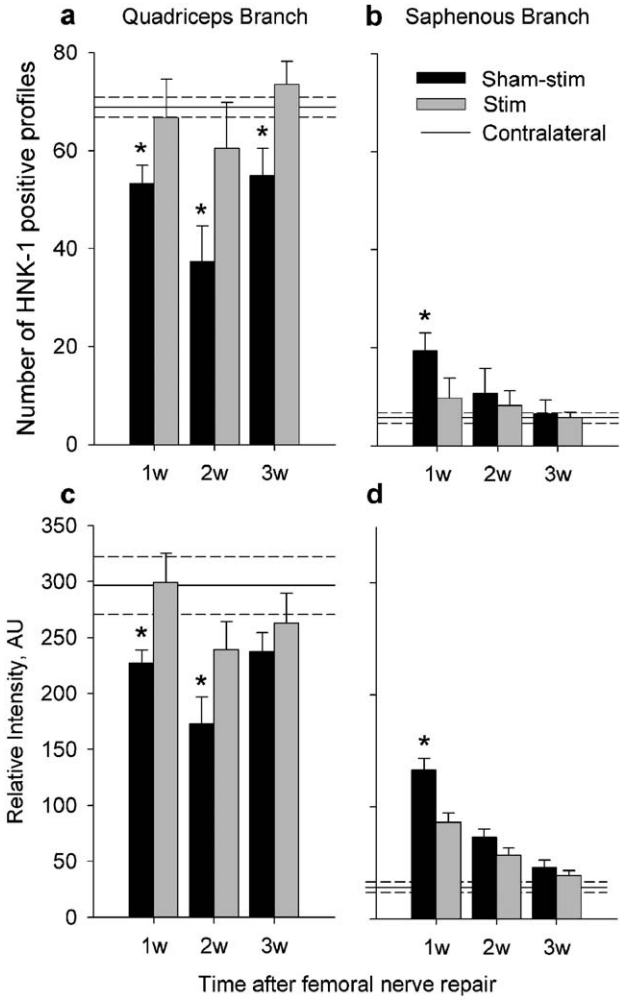


Fig. 4. Numbers of HNK-1 positive profiles (a, b) and relative intensity of HNK-1 immunofluorescence (c, d) in the quadriceps (a, c) and in the saphenous (b, d) branches of femoral nerves studied 1 to 3 weeks after nerve transection followed by electrical stimulation (black columns) or sham-stimulation (white columns). The values for the contralateral untreated nerves are shown as horizontal lines. Asterisks indicate significant differences between stimulated and non-stimulated nerves at a given time-period ($P < 0.05$, non-parametric Kruskal–Wallis analysis of variance, ANOVA, with Dunn's post hoc test). In the same tests, the sham-stimulated groups for the quadriceps branch at 1 to 3 weeks, and the saphenous branch at 1 week differed from contralateral control nerve values shown in panels a and b. For the data shown in panels c and d, the sham-stimulated groups for the quadriceps branch at 2 weeks and both experimental groups for the saphenous branch at 1 and 2 weeks differed from contralateral control nerve values.

values and significantly higher compared to sham-stimulated nerves (Fig. 4a). Measurements of the relative fluorescence intensities yielded similar results (Fig. 4c).

Femoral nerve injury and sham stimulation induced enhanced HNK-1 expression in the saphenous branch, contrary to the quadriceps branch in the same mice, at 1 week after surgery as compared to intact nerves which gradually declined to control levels at 3 weeks (Figs. 4b, d). Similar to the motor branch, however, electrical stimulation counteracted the injury-induced changes and significantly reduced the up-regulation of HNK-1 expression at 1 week after surgery (Figs. 4b, d).

These results show that nerve damage causes opposite changes in the two femoral nerve branches: a decrease in the high expression level in the quadriceps branch and an increase of the normally low HNK-1 expression in the saphenous branch. The injury-induced reduction in the chemical polarization of the two nerve branches is counteracted by electrical stimulation. It should be noted that, without electrical stimulation, the HNK-1 expression level in the motor nerve branch 1 week after lesion is reduced by some 25% only compared to intact nerves (Figs. 4a, c). The expression level is still 2- to 3-fold higher compared with the saphenous branch at 1 week and the ratio increases thereafter in parallel to the previously documented gradual increase in preferential motor reinnervation.

Effects of electrical stimulation on HNK-1 expression in TrkB- and BDNF-deficient mice

We studied the expression of the HNK-1 epitope in mice heterozygous and thus partially deficient in the expression of BDNF or its receptor TrkB. Without electrical stimulation, reduction in HNK-1 expression in the quadriceps branch and increase of this expression in the saphenous branch were found at 2 and 3 weeks after surgery in both BDNF (4 mice per time-point studied) and TrkB-deficient mice (7 per group), as well as in a group of simultaneously treated wild-type littermates (8 per group) (Figs. 5a, b). In this latter group of control animals, we again found that electrical stimulation significantly increased HNK-1 expression in the quadriceps branch and decreased this expression in the saphenous branch (Figs. 5a, b). The effects of electrical stimulation in both BDNF (5 mice per group) and TrkB-deficient mice (7 per group) were, however, not significant indicating that alterations in HNK-1 expression induced by electrical stimulation are strongly dependent on TrkB signaling.

Preferential motor reinnervation in TrkB-deficient mice and wild-type littermates

If TrkB signaling and HNK-1 expression are causally related to preferential motor reinnervation, one should expect that reduced levels of TrkB expression will compromise selectivity of reinnervation. To test this hypothesis, we performed double retrograde labeling of motoneurons that had reinnervated either the saphenous or the quadriceps branch only or both branches 3 months after nerve surgery. In TrkB-deficient mice (TrkB+/−, $n = 8$, Fig. 6a), equal numbers of motoneurons had innervated either the motor or sensory branch, and a minority had innervated both branches. While numbers of motoneurons labeled via the sensory branch alone or via both nerve branches were similar in wild-type mice (TrkB+/+, $n = 8$, Fig. 6a) and TrkB+/− littermates, neurons innervating the motor branch were significantly more numerous in TrkB+/+ versus TrkB+/− mice ($P < 0.05$, t test). These findings show a preferential motor reinnervation of the quadriceps nerve branch in TrkB+/+ mice (index of preferential motor reinnervation, PMR, bar pair to the

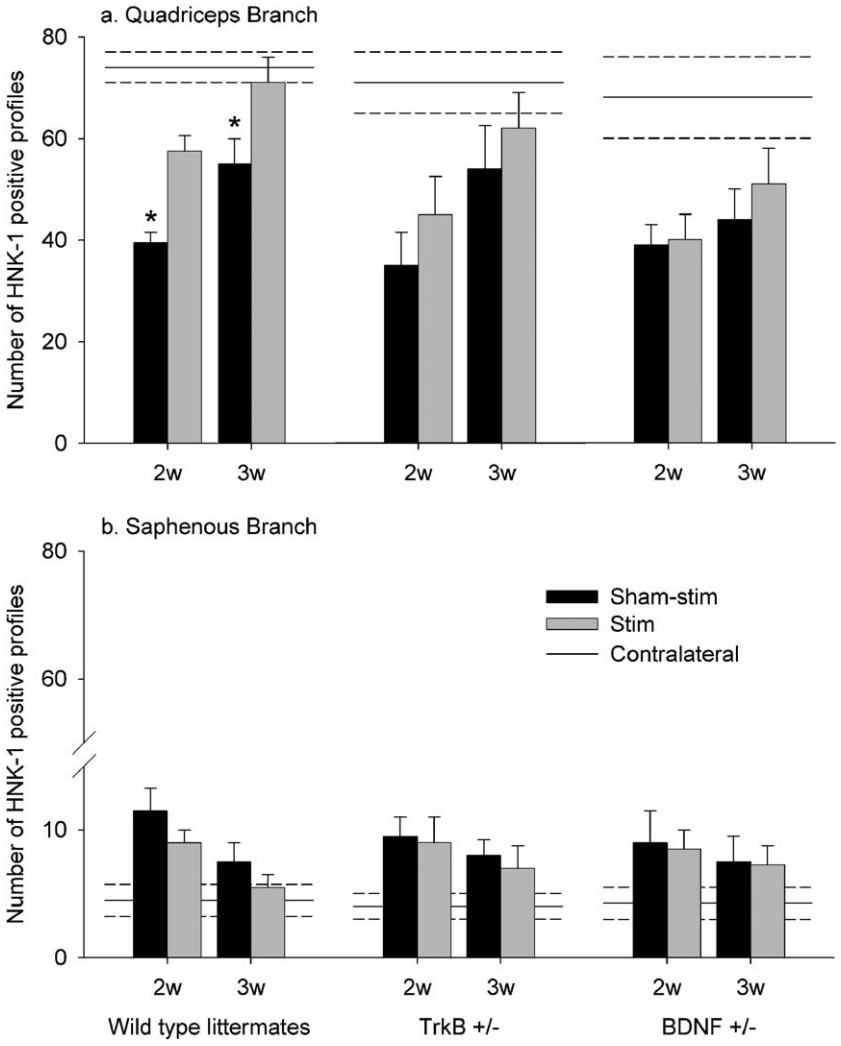


Fig. 5. Numbers of HNK-1 positive profiles in the quadriceps (a) and in the saphenous (b) branches of femoral nerves of wild-type animals (group of bars on the left-hand side), TrkB+/− mice (group of bars in the middle) and BDNF+/− mice (group of bars to the right). The animals were studied 2 and 3 weeks after nerve transection followed by electrical stimulation (black columns) or sham-stimulation (white columns). The values for the contralateral untreated nerves are shown as horizontal lines. Asterisks indicate significant differences between stimulated and non-stimulated nerves at given time-period ($P < 0.05$, non-parametric Kruskal–Wallis analysis of variance, ANOVA, with Dunn's post hoc test). In the same test, the stimulated and sham-stimulated groups for both branches at 2 weeks differed from contralateral control nerve values.

right-hand side in Fig. 6a), but not in TrkB+/− mice (Fig. 6a, $P < 0.05$ compared to TrkB+/+ littermates, *t* test).

To estimate the number of motoneurons normally innervating the quadriceps muscle in TrkB+/+ and TrkB+/− mice, we transected the femoral nerve in 4 animals of each genotype, applied tracer and perfused the animals 1 week later. No difference in the size of the quadriceps motoneuron pool was found between TrkB+/− mice (184 ± 13 motoneurons) and TrkB+/+ littermates (187 ± 11, not significant, *t* test). Compared with these control values, the total number of retrogradely labeled motoneurons after a regeneration period of 3 months (Fig. 6a) was reduced by 30% and 20% in TrkB+/− and TrkB+/+ mice, respectively ($P < 0.05$ for both genotypes, *t* test). Finally, we should note that the total number of motoneurons that had regenerated their axons into the motor nerve branch, i.e. neurons labeled through the motor branch plus double-labeled neurons, was significantly lower in the TrkB+/− mice (71 ± 6) versus TrkB+/+ mice (93 ± 9, $P < 0.05$, *t* test). These numbers represent only 39% and 50%, respectively, of the motoneurons which normally innervate the quadriceps muscle (around 180 motoneurons found in control animals of both genotypes, see above), a finding important with regard to the degree of functional recovery achieved after nerve injury (see below).

Numbers of myelinated axons in regenerated nerves in TrkB-deficient and wild-type littermate mice

One month after nerve transection, numbers of myelinated axons in both motor and sensory nerve branches were lower (by 33% and 24%, respectively) in TrkB+/− versus TrkB+/+ littermates (Fig. 6b, $P < 0.05$ for both branches, *t* test, 8 mice per genotype). While the values for TrkB+/+ mice did not change between 1 and 3 months of reinnervation (differences of

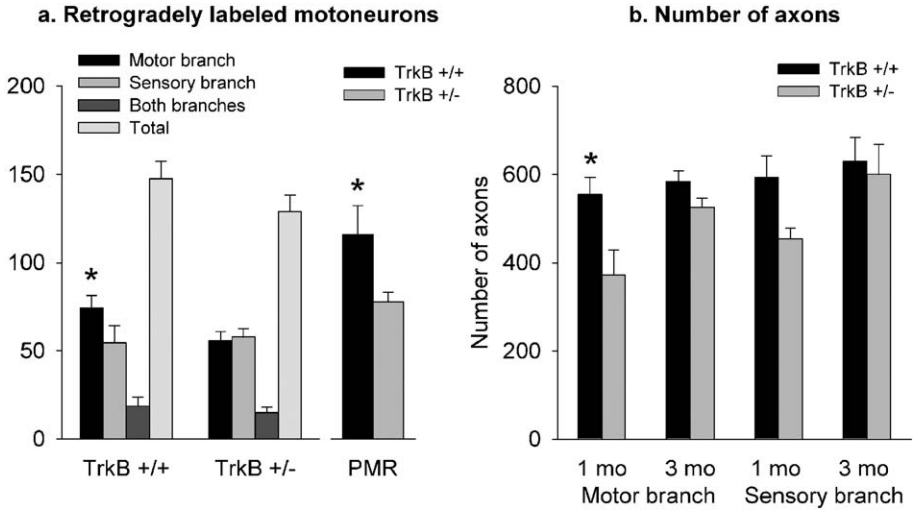


Fig. 6. Morphological evaluation of muscle reinnervation (a) and nerve regeneration (b) after nerve transection in TrkB+/+ and TrkB+/− mice. The two groups of bars on the left hand side in panel a show numbers of motoneurons innervating the motor (M) or sensory (S) branches only, or both branches (B), as well as the total number of regenerated motoneurons (T) 3 months after nerve lesion. The number of motoneurons with axons regenerated into the motor branch only (M, black bars) is significantly higher in TrkB+/+ ($n = 74 \pm 7$) compared to TrkB+/− ($n = 56 \pm 5$, asterisk, $P < 0.05$, t test) mice while no significant differences were found for the other categories of regenerated neurons (t test). The degree of preferential motor reinnervation (bar pair on the right hand side, values multiplied by 100 to fit the scaling), calculated as ratio of the number of motoneurons regenerated into the motor branch only (M) to those regenerated into the sensory branch (S), is also significantly higher in TrkB+/+ animals (dark gray bar) compared to TrkB+/− (gray bar, $P < 0.05$, t test) mice. (b) Numbers of myelinated axonal profiles in semithin sections from the motor and the sensory nerve branches 1 and 3 months after nerve transection in TrkB+/+ ($n = 555 \pm 37$ and 584 ± 24, respectively) and TrkB+/− mice ($n = 373 \pm 56$/ 534 ± 22, respectively). The asterisk indicates significant difference between the mean group values ($P < 0.05$, t test).

about 5% for both nerve branches, Fig. 6b), numbers of myelinated axons in TrkB+/− nerves increased to reach near-control levels at 3 months (Fig. 6b, 8 mice per genotype). Therefore, partial deficiency in TrkB expression causes a significant delay in axonal regrowth and myelination.

Recovery of motor function in TrkB-deficient mice and wild-type littermates

The finding of delayed and less precise reinnervation in the TrkB+/− mice raised the question as to whether also motor function recovery is delayed and/or less complete in TrkB+/− compared to TrkB+/+ mice. Using a novel single-frame motion analysis approach, we have recently provided evidence that TrkB deficiency causes impairment of functional recovery at early time-periods after nerve injury (Irintchev et al., 2005). To confirm this result and extend the observations to long-term recovery periods, we evaluated the extensor function of the quadriceps muscle in mice of both genotypes (16 mice per group) prior to nerve transection, and at 1, 2, 4, 8 and 12 weeks after surgery (Figs. 7a–c). Three parameters were used for evaluation, the foot-base angle (FBA, Figs. 2a, b, 7a), the heels-tail angle (HTA, Figs. 2b, c, 7b) and the limb protraction length ratio (PLR, Figs. 2e, f, 7c). The first two parameters, evaluated from video recordings of beam walking trials, reflect the abilities of the quadriceps muscle to keep the knee extended during single support phases of the gate cycle and, for the FBA, to counteract in addition the rotational moments in the hip caused by the swing of the contralateral extremity. These abilities were severely compromised after femoral nerve injury as seen from the changes in the angle values at 7 days after nerve transection compared to the preoperative values (day 0) of the same animals (Figs. 7a, b). Multifactor analysis of variance (MANOVA) for repeated measurements showed that both genotypes (TrkB+/+ versus TrkB+/−) and recovery period have a strong impact on the two parameters, with a significant interaction between the two factors. This shows that functional recovery is affected by reduced TrkB expression. As indicated by multiple comparisons between mean group values using the stringent post hoc test of Tukey, the most pronounced difference was observed at 4 weeks after lesion, when motor function recovery in TrkB+/− animals was by far less than in TrkB+/+ littermates (Figs. 7a, b, asterisks). The large difference between the two groups at 4 weeks is even more apparent for the stance recovery index (Fig. 7d, see Material and methods for calculation of the index). Functional improvement at 3 months after injury in both groups of animals (Fig. 7d) is remarkable in view of the fact that by that time the quadriceps muscle is reinnervated by only 50% and 39% of the intact motoneuron pool in TrkB+/+ and TrkB+/− mice, respectively (see results of retrograde tracing experiments above). The high degree of recovery despite low numbers of motoneurons is likely to be associated with enlargement of reinnervated motor units that compensates for their reduced numbers (Rafuse and Gordon, 1996). There was a tendency for less complete recovery of FBA in TrkB+/− versus TrkB+/+ littermates.

In addition to the FBA and HTA, which evaluate quadriceps function during ground locomotion, we studied a third functional parameter, the limb protraction length ratio (PLR). This parameter estimates the ability to stretch the knee joint during target-reaching movements performed without body weight support. Denervation-induced functional impairment, which is similar in both genotypes, was found also for these

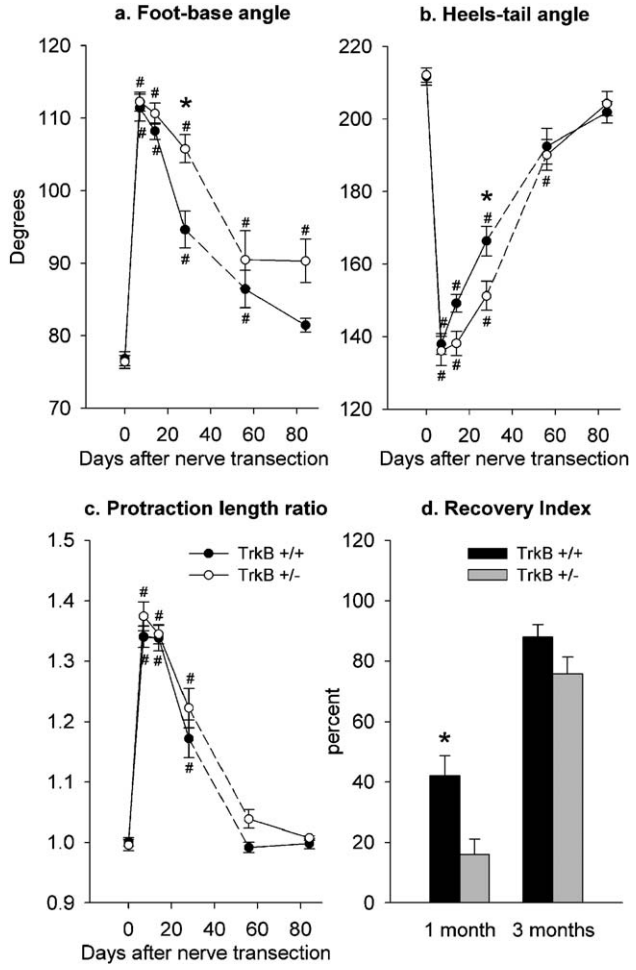


Fig. 7. Functional evaluation of quadriceps muscle reinnervation. Functional performance of TrkB+/+ (open circles and gray bars) and TrkB+/− mice (black circles and bars) was evaluated by measuring foot-base angle (FBA, a), heels-tail angle (HTA, b) and limb protraction length ratio (PLR, c) before lesion (day 0) and during 3 months after nerve transection. Ten TrkB+/+ and nine TrkB+/− animals were studied over a period of 1 month, additional 6 mice per genotype were followed up to 3 months after nerve transection. Statistically significant differences by post hoc Turkey's test analysis performed after multifactor analysis of variance (MANOVA) for repeated measurements are also indicated for group mean values different from: (#) the within-group preoperative value or (*) from both the within-group preoperative value and the corresponding postoperative value of the other group. (d) Stance recovery index, an overall estimate of quadriceps muscle function during stance, at 1 and 3 months after nerve transection in the TrkB+/+ (black bars) and TrkB+/− (gray bars) mice shown in panels a–c. The asterisk shown in panel d indicates a statistically significant difference between the two groups ($P < 0.05$, t test).

parameters (Fig. 7c, compare values at 0 and 7 days). As indicated by MANOVA analysis, PLR was significantly affected by recovery period but not by genotype. Thus, recovery of the ability to use the limb without bearing body weight was not compromised in TrkB+/− versus TrkB+/+ littermates.

Discussion

We have previously shown that the HNK-1 carbohydrate is specifically expressed in motor, but not sensory, axon pathways and proposed that this expression contributes to the preferential motor reinnervation of the quadriceps as opposed to the saphenous branch of the femoral nerve in rodents (Martini et al., 1992, 1994). Recent work has provided direct evidence for the importance of the HNK-1 carbohydrate in motor reinnervation (O. Simova, A. Irintchev, M. Schachner and colleagues, unpublished observations). Application of a HNK-1 peptide mimic to the transected femoral nerve of wild-type mice enhanced preferential motor innervation, HNK-1 carbohydrate expression in the motor nerve branch, survival of quadriceps motoneurons and functional recovery compared to three control groups. In accord with this findings, preliminary results from studies on mice deficient in the expression of the HNK-1 sulfotransferase indicate that HNK-1 deficiency causes enhanced loss of motoneurons after facial nerve injury (D.N. Angelov, O. Guntinas-Lichius, A. Irintchev and M. Schachner, unpublished observations). Here, we show that the expression of the HNK-1 epitope is strongly enhanced by short-term electrical stimulation applied to the nerve immediately after transection, a procedure that also leads to improved reinnervation (Al Majed et al., 2000a). Furthermore, we demonstrate that the stimulation-induced HNK-1 up-regulation is dependent on BDNF and its receptor TrkB. Finally, we show that even partially reduced expression of TrkB leads to compromised preferential motor reinnervation, delayed axonal regrowth into the distal nerve stump and delayed functional recovery after femoral nerve injury. In conjunction with previous data, these results show that TrkB signaling is a major factor regulating the functional outcome after nerve injury and that the HNK-1 carbohydrate plays an essential role in the TrkB signaling pathway.

The analysis of HNK-1 expression was based on quantitative immunohistochemistry. Our previous experience showed that immunochemical methods are not applicable for quantification of HNK-1 expression levels. The HNK-1 epitope is carried by both glycoproteins and glycolipids in the femoral nerve branches (Löw et al., 1994) and this makes extraction of small amounts of material that can be obtained from the peripheral nerves from one mouse technically impossible. To verify the reliability of the estimates, we simultaneously used two approaches, counts of immunoreactive profiles and measurements of relative intensities, which produced similar results. In addition, counting of profiles in two different experimental sets of animals indicated the reliability of our measurements. Thus, our data provide sound evidence that electrical stimulation strongly enhances HNK-1 carbohydrate expression in the motor nerve stump and reduces its posttraumatic up-regulation in the sensory nerve branch. This result is remarkable since we stimulated the proximal nerve stump after nerve transection and observed effects in the distal nerve stumps. We cannot rule out the possibility that, in a small animal like the mouse, current from the proximally located stimulation electrode may indirectly, via the surrounding tissue, reach the nerve trunk distal to the transection. Such stimulation of the distal nerve segment may have direct influences early after transection, such as enhancement of Wallerian degeneration and subsequent faster axonal regrowth. Yet, we may propose that the effects of electrical stimulation are dependent

on action potential firing and propagated electrical activity in the motoneuron cell bodies and not simply local depolarization of cells in the nerve trunk as shown in rats (Al Majed et al., 2000a). Regrowth of motor axons leads to contact of axons with Schwann cells coincident with up-regulation of HNK-1 immunoreactivity in lesioned nerves (Martini et al., 1992, 1994). It is therefore possible that accelerated up-regulation of HNK-1 expression is the consequence of an accelerated outgrowth of axons from the proximal nerve stump and temporarily earlier contacts of the regrowing axons with Schwann cells (Brushart et al., 2002). Motor axons are likely to induce HNK-1 expression in Schwann cells by direct surface contact or by supply of growth factors from the growth cone. Also, electrical stimulation may improve the capacity of regenerating axons to induce changes favoring regeneration in the denervated nerve environment. In accordance, enhanced expression of both BDNF and TrkB in electrically stimulated motoneurons (Al Majed et al., 2000b) has been found. Enhanced expression of BDNF might induce Schwann cells to up-regulate HNK-1 expression in the quadriceps branch and reduce it in the saphenous branch, via paracrine mechanisms involving the secretion of BDNF from regenerating axons. This functionally meaningful opposite regulation of HNK-1 expression in the motor and sensory pathways might be possible because the Schwann cells that originally have been in contact with motor versus sensory axons respond differently to regeneration-related cues of motor and sensory axons (Martini et al., 1994). Schwann cells during development and after a lesion express different neurotrophin receptors, including the low affinity p75 receptor and the truncated TrkB receptor (Ernfors et al., 1989; Funakoshi et al., 1993). Differential expression of receptors in the two nerve branches and/or different signaling pathways in motor versus sensory axon-associated Schwann cells may explain the opposite effects seen in the motor and sensory nerve branches.

Neurotrophins like NGF have been shown to influence expression of adhesion molecules, such as the potent neurite outgrowth promoting molecule L1 in neurons (Lee et al., 1981). Up-regulation of neurotrophin expression in neurons and possibly in Schwann cells may be essential for regulating speed of axonal regrowth. It is interesting in this respect that regulation of L1 synthesis can be affected by both neurotrophins and electrical stimulation (Seilheimer and Schachner, 1987; Scherer et al., 1992; Itoh et al., 1995, 1997). The fact that L1 expression is conducive to axon growth when expressed and up-regulated not only in neurons, but also in glial cells of the peripheral and central nervous system (Mohajeri et al., 1996; Yazaki et al., 1996) points to concerted actions of neurotrophins and electrical activity in nerve regeneration: generally expressed adhesion molecules provide the overall conducive environment for axon growth, glycans carried by these molecules or by glycolipids then provide the fine tuning of pathway choices at points of target decision. Recent findings indicate that a glycan, polysialic acid, attached to the cell adhesion molecule NCAM, a HNK-1 binding partner (Cole and Schachner, 1987), is essential for selective targeting of regenerating motoneurons in the mouse femoral nerve paradigm (Franz et al., 2005). These observations further strengthen the importance of recognition molecules and, in particular their associated glylcans, as regulators of peripheral nerve regeneration. It will be important to further investigate the molecular mechanisms promoting regeneration and functional recovery in the peripheral nervous system via growth- and survival-conducive adhesion molecules and associated glycans, since these could provide guides to understanding and manipulating recovery of function in patients after peripheral nerve lesions.

Acknowledgments

The authors are grateful to Drs. Louis F. Reichardt (University of California, San Francisco) and Martin Korte (Max-Planck-Institute for Neurobiology, Martinsried) for BDNF and TrkB-deficient mice, to Drs. Udo Bartsch and Maren von der Ohe for many helpful discussions, Emanuela Szpotowicz and Neil Tyreman for technical assistance, and the Roechling and Hertie Foundations, Erika and Condrad W. Schnyder-Stiftung, the Deutsche Forschungsgemeinschaft (Scha 185/28-1,2 to M. S.), the Canadian Institutes of Health Research (CIHR cg 37534 to T. G.) and the National Institutes of Health (NIH RO1 NS034484-8 to T.M.B.) for support.

References

Al Majed, A.A., Brushart, T.M., Gordon, T., 2000a. Electrical stimulation accelerates and increases expression of BDNF and trkB mRNA in regenerating rat femoral motoneurons. Eur. J. Neurosci. 12, 4381–4390.

Al Majed, A.A., Neumann, C.M., Brushart, T.M., Gordon, T., 2000b. Brief electrical stimulation promotes the speed and accuracy of motor axonal regeneration. J. Neurosci. 20, 2602–2608.

Al Majed, A.A., Tam, S.L., Gordon, T., 2004. Electrical stimulation accelerates and enhances expression of regeneration-associated genes in regenerating rat femoral motoneurons. Cell. Mol. Neurobiol. 24, 379–402.

Bartsch, U., Kirchhoff, F., Schachner, M., 1989. Immunohistological localization of the adhesion molecules L1, N-CAM, and MAG in the developing and adult optic nerve of mice. J. Comp. Neurol. 284, 451–462.

Brushart, T.M., 1988. Preferential reinnervation of motor nerves by regenerating motor axons. J. Neurosci. 8, 1026–1031.

Brushart, T.M., 1993. Motor axons preferentially reinnervate motor pathways. J. Neurosci. 13, 2730–2738.

Brushart, T.M., Seiler, W.A., 1987. Selective reinnervation of distal motor stumps by peripheral motor axons. Exp. Neurol. 97, 289–300.

Brushart, T.M., Gerber, J., Kessens, P., Chen, Y.G., Royall, R.M., 1998. Contributions of pathway and neuron to preferential motor reinnervation. J. Neurosci. 18, 8674–8681.

Brushart, T.M., Hoffman, P.N., Royall, R.M., Murinson, B.B., Witzel, C., Gordon, T., 2002. Electrical stimulation promotes motoneuron regeneration without increasing its speed or conditioning the neuron. J. Neurosci. 22, 6631–6638.

Cole, G.J., Schachner, M., 1987. Localization of the L2 monoclonal antibody binding site on chicken neural cell adhesion molecule (NCAM) and evidence for its role in NCAM-mediated cell adhesion. Neurosci. Lett. 78, 227–232.

Ernfors, P., Henschen, A., Olson, L., Persson, H., 1989. Expression of nerve growth factor receptor mRNA is developmentally regulated and increased after axotomy in rat spinal cord motoneurons. Neuron 2, 1605–1613.

Franz, C.K., Rutishauser, U., Rafuse, V.F., 2005. Polysialylated neural cell adhesion molecule is necessary for selective targeting of regenerating motor neurons. J. Neurosci. 25, 2081–2091.

Fu, S.Y., Gordon, T., 1997. The cellular and molecular basis of peripheral nerve regeneration. Mol. Neurobiol. 14, 67–116.

Funakoshi, H., Frisen, J., Barbany, G., Timmusk, T., Zachrisson, O., Verge, V.M., Persson, H., 1993. Differential expression of mRNAs for neurotrophins and their receptors after axotomy of the sciatic nerve. J. Cell Biol. 123, 455–465.

Hall, H., Liu, L., Schachner, M., Schmitz, B., 1993. The L2/HNK-1 carbohydrate mediates adhesion of neural cells to laminin. Eur. J. Neurosci. 5, 34–42.

Irintchev, A., Simova, O., Eberhardt, K.A., Morellini, F., Schachner, M., 2005. Impacts of lesion severity and TrkB deficiency on functional outcome of femoral nerve injury assessed by a novel single-frame motion analysis in mice. Eur. J. Neurosci. 22, 802–808.

Itoh, K., Stevens, B., Schachner, M., Fields, R.D., 1995. Regulated expression of the neural cell adhesion molecule L1 by specific patterns of neural impulses. Science 270, 1369–1372.

Itoh, K., Ozaki, M., Stevens, B., Fields, R.D., 1997. Activity-dependent regulation of N-cadherin in DRG neurons: differential regulation of N-cadherin, NCAM, and L1 by distinct patterns of action potentials. J. Neurobiol. 33, 735–748.

Kleene, R., Schachner, M., 2004. Glycans and neural cell interactions. Nat. Rev., Neurosci. 5, 195–208.

Korte, M., Carroll, P., Wolf, E., Brem, G., Thoenen, H., Bonhoeffer, T., 1995. Hippocampal long-term potentiation is impaired in mice lacking brain-derived neurotrophic factor. Proc. Natl. Acad. Sci. U. S. A. 92, 8856–8860.

Kruse, J., Mailhammer, R., Wernecke, H., Faissner, A., Sommer, I., Goridis, C., Schachner, M., 1984. Neural cell adhesion molecules and myelin-associated glycoprotein share a common carbohydrate moiety recognized by monoclonal antibodies L2 and HNK-1. Nature 311, 153–155.

Kruse, J., Keilhauer, G., Faissner, A., Timpl, R., Schachner, M., 1985. The J1 glycoprotein—A novel nervous system cell adhesion molecule of the L2/HNK-1 family. Nature 316, 146–148.

Lee, V.M., Greene, L., Shelanski, M.L., 1981. Identification of neural and adrenal medullary surface membrane glycoproteins recognized by antisera to cultured rat sympathetic neurons and PC12 pheochromocytoma cells. Neuroscience 6, 2773–2786.

Loeb, G.E., Marks, W.B., Hoffer, J.A., 1987. Cat hindlimb motoneurons during locomotion: IV. Participation in cutaneous reflexes. J. Neurophysiol. 57, 563–573.

Löw, K., Orberger, G., Schmitz, B., Martini, R., Schachner, M., 1994. The L2/HNK-1 carbohydrate is carried by the myelin associated glycoprotein and sulphated glucuronyl glycolipids in muscle but not cutaneous nerves of adult mice. Eur. J. Neurosci. 6, 1773–1781.

Lundborg, G., 2003. Richard P. Bunge memorial lecture. Nerve injury and repair—A challenge to the plastic brain. J. Peripher. Nerv. Syst. 8, 209–226.

Madison, R.D., Archibald, S.J., Brushart, T.M., 1996. Reinnervation accuracy of the rat femoral nerve by motor and sensory neurons. J. Neurosci. 16, 5698–5703.

Martini, R., Schachner, M., 1986. Immunoelectron microscopic localization of neural cell adhesion molecules (L1, N-CAM, and MAG) and their shared carbohydrate epitope and myelin basic protein in developing sciatic nerve. J. Cell Biol. 103, 2439–2448.

Martini, R., Xin, Y., Schmitz, B., Schachner, M., 1992. The L2/HNK-1 carbohydrate epitope is involved in the preferential outgrowth of motor neurons on ventral roots and motor nerves. Eur. J. Neurosci. 4, 628–639.

Martini, R., Schachner, M., Brushart, T.M., 1994. The L2/HNK-1 carbohydrate is preferentially expressed by previously motor axon-associated Schwann cells in reinnervated peripheral nerves. J. Neurosci. 14, 7180–7191.

Mohajeri, M.H., Bartsch, U., van der, P.H., Sansig, G., Mucke, L., Schachner, M., 1996. Neurite outgrowth on non-permissive substrates in vitro is enhanced by ectopic expression of the neural adhesion molecule L1 by mouse astrocytes. Eur. J. Neurosci. 8, 1085–1097.

Mohan, P.S., Laitinen, J., Merenmies, J., Rauvala, H., Jungalwala, F.B., 1992. Sulfoglycolipids bind to adhesive protein amphoterin (P30) in the nervous system. Biochem. Biophys. Res. Commun. 182, 689–696.

Rafuse, V.F., Gordon, T., 1996. Self-reinnervated cat medial gastrocnemius muscles: I. Comparisons of the capacity for regenerating nerves to form enlarged motor units after extensive peripheral nerve injuries. J. Neurophysiol. 75, 268–281.

Robinson, G.A., Madison, R.D., 2003. Preferential motor reinnervation in the mouse: comparison of femoral nerve repair using a fibrin sealant or suture. Muscle Nerve 28, 227–231.

Robinson, G.A., Madison, R.D., 2005. Manipulations of the mouse femoral nerve influence the accuracy of pathway reinnervation by motor neurons. Exp. Neurol. 192, 39–45.

Schachner, M., Martini, R., 1995. Glycans and the modulation of neural-recognition molecule function. Trends Neurosci. 18, 183–191.

Scherer, M., Heller, M., Schachner, M., 1992. Expression of the neural recognition molecule L1 by cultured neural cells is influenced by K+ and the glutamate receptor agonist NMDA. Eur. J. Neurosci. 4, 554–562.

Seilheimer, B., Schachner, M., 1987. Regulation of neural cell adhesion molecule expression on cultured mouse Schwann cells by nerve growth factor. EMBO J. 6, 1611–1616.

Xu, B., Gottschalk, W., Chow, A., Wilson, R.I., Schnell, E., Zang, K., Wang, D., Nicoll, R.A., Lu, B., Reichardt, L.F., 2000a. The role of brain-derived neurotrophic factor receptors in the mature hippocampus: modulation of long-term potentiation through a presynaptic mechanism involving TrkB. J. Neurosci. 20, 6888–6897.

Xu, B., Zang, K., Ruff, N.L., Zhang, Y.A., McConnell, S.K., Stryker, M.P., Reichardt, L.F., 2000b. Cortical degeneration in the absence of neurotrophin signaling: dendritic retraction and neuronal loss after removal of the receptor TrkB. Neuron 26, 233–245.

Yazaki, T., Martuza, R.L., Rabkin, S.D., 1996. Expression of L1 in primary astrocytes via a defective herpes simplex virus vector promotes neurite outgrowth and neural cell migration. Brain Res. Mol. Brain Res. 43, 311–320.

Experimental Neurology 223 (2010) 192–202

Contents lists available at ScienceDirect

Experimental Neurology

journal homepage: www.elsevier.com/locate/yexnr

Brief post-surgical electrical stimulation accelerates axon regeneration and muscle reinnervation without affecting the functional measures in carpal tunnel syndrome patients

Tessa Gordon, Nasim Amirjani, David C. Edwards, K. Ming Chan *

Division of Physical Medicine and Rehabilitation/Center for Neuroscience, University of Alberta, 525 Heritage Medical Research Centre, Edmonton, Alberta, Canada T6G 2S2

ARTICLE INFO

Article history:
Received 1 April 2009
Revised 23 September 2009
Accepted 25 September 2009
Available online 1 October 2009

Keywords:
Electrical stimulation
Motor unit numbers
Peripheral nerve injury
Reinnervation
Motor evoked potential
Sensory evoked potential
Hand muscles
Human
Behavior

ABSTRACT

Electrical stimulation (ES) of injured peripheral nerves accelerates axonal regeneration in laboratory animals. However, clinical applicability of this intervention has never been investigated in human subjects. The aim of this pilot study was to determine the effect of ES on axonal regeneration after surgery in patients with median nerve compression in the carpal tunnel causing marked motor axonal loss. A randomized control trial was conducted to provide proof of principle for ES-induced acceleration of axon regeneration in human patients. Carpel tunnel release surgery (CTRS) was performed and in the stimulation group of patients, stainless steel electrode wires placed alongside the median nerve proximal to the surgical decompression site for immediate 1 h 20 Hz bipolar ES. Subjects were followed for a year at regular intervals. Axonal regeneration was quantified using motor unit number estimation (MUNE) and sensory and motor nerve conduction studies. Purdue Pegboard Test, Semmes Weinstein Monofilaments, and Levine's Self-Assessment Questionnaire were used to assess functional recovery. The stimulation group had significant axonal regeneration 6–8 months after the CTRS when the MUNE increased to 290 ± 140 (mean $\pm$ SD) motor units (MU) from 150 ± 62 MU at baseline ($p<0.05$). In comparison, MUNE did not significantly improve in the control group ($p>0.2$). Terminal motor latency significantly accelerated in the stimulation group but not the control group ($p>0.1$). Sensory nerve conduction values significantly improved in the stimulation group earlier than the controls. Other outcome measures showed a significant improvement in both patient groups. We conclude that brief low frequency ES accelerates axonal regeneration and target reinnervation in humans.

© 2009 Elsevier Inc. All rights reserved.

Introduction

It is well known that, in man, functional recovery after peripheral nerve injuries is frequently poor despite the regenerative capacity of injured neurons and the permissive growth environment provided by the Schwann cells in the distal nerve stumps (Fu and Gordon., 1997; Gordon et al., 2003, 2009; Kline and Kim, 2008). Although poor functional recovery especially after proximal nerve injuries has generally been attributed to irreversible denervation atrophy of targets (Kline and Kim, 2008; Sunderland, 1978), progressive decline in the capacities of the neurons and Schwann cells to regenerate and support regeneration are now recognized for decline to ~5% in numbers of neurons that regenerate over time and distance (Fu and Gordon, 1995a,b; Sulaiman and Gordon, 2000; You et al., 1997).

Axon outgrowth is another factor that delays axon regeneration with a surprisingly long period of ~1 month required for all motoneurons to regenerate their axons across a surgical repair site in rats (Brushart et al., 2002). This "staggered axonal regeneration" with wandering of axons within the poorly organized extracellular matrix of the suture site into which Schwann cells migrate, culminates in many weeks for all neurons to regenerate their axons within the distal nerve stumps (Al Majed et al., 2000a; Witzel et al., 2005). Given the sluggish movement of Schwann cells in humans, the delayed outgrowth at the suture site may be even longer (Wood and Bunge, personal communication).

A 1-h period of low frequency electrical stimulation (ES) of surgically repaired rat hindlimb nerves accelerates axon outgrowth to promote regeneration of all motor axons within 3 rather than 8–10 weeks and with similar effect on sensory nerve regeneration (Al Majed et al., 2000b; Brushart et al., 2002, 2005; Geremia et al., 2007). Similar effects of ES in mice have been reported (Ahlborn et al., 2007; English et al., 2007). The important unanswered question that remains is whether this acceleration translates into earlier target reinnervation. More rapid recovery of muscle contractile force and evoked withdrawal reflexes after ES of crushed nerves are consistent with the accelerating ES effect on axon outgrowth but these outcome measures failed to distinguish whether ES promotes early axon regeneration of more neurons or it promotes sprouting and in turn,

* Corresponding author. Fax: +1 780 492 1617.
E-mail address: ming.chan@ualberta.ca (K.M. Chan).

0014-4886/$ – see front matter © 2009 Elsevier Inc. All rights reserved.
doi:10.1016/j.expneurol.2009.09.020

earlier muscle force recovery through reinnervation (Nix and Hopf, 1983; Pockett and Gavin, 1985).

In this study, we asked whether ES accelerates nerve regeneration and target reinnervation in a human model of median nerve crush injury, carpal tunnel syndrome (CTS). In selected patients with clear evidence of at least 50% axonal loss, motor unit number estimation (MUNE) was used to evaluate how many axons reinnervated target thenar muscles over time, electrophysiological recordings to evaluate time course of regeneration of sensory as well as motor axons, and behavioral measures to evaluate functional outcomes. A randomized controlled pilot study was carried out to provide proof of principle that electrical stimulation accelerates axon regeneration and promotes more rapid reinnervation of denervated targets by the regenerating axons.

Materials and methods

This was a randomized controlled clinical trial that complied with the guidelines of and was approved by the Human Research Ethics Board at the University of Alberta. All subjects gave their informed consent.

Participants

Patients with carpal tunnel syndrome (CTS) were recruited from a university hospital electromyography clinic. The inclusion criterion used in this study was the presence of at least one of the following constellation of symptoms: (1) numbness and tingling in the median nerve distribution, (2) precipitation of these symptoms by repetitive hand activities and relieved by resting, rubbing, and shaking the hand, (3) nocturnal awakening by such sensory symptoms and (4) weakness of thumb abduction and thenar muscle atrophy. Subsequently, the presence of median nerve compression was confirmed by electrophysiological studies. Conventionally, confirmation of the diagnosis of CTS and classification of its severity are commonly based on nerve conduction results (Padua et al., 1997). Based on those criteria, patients with moderate and severe CTS who had not responded to conservative treatments were recruited for this study. Patients with electrophysiological evidence of conduction block across the carpal tunnel were excluded because in those cases, changes in MUNE cannot be meaningfully interpreted. Other exclusion criteria were presence of other neurological conditions and previous carpal tunnel release surgery (CTRS). We evaluated these factors through interviews and clinical examination. When indicated, further electrophysiological studies and investigations were carried out. The ulnar and superficial radial nerves were evaluated through clinical examination and electrophysiological studies to rule out other peripheral neuropathies which may have contributed to the hand symptoms.

Conventional nerve conduction study

All sensory and motor nerve conduction studies were performed on patients using a Viking Select EMG machine (Nicolet Biomedical, Minneapolis). Sensory and motor nerve conduction studies of the median nerve were done using standard techniques (Dumitru, 1995).

Median sensory nerve conduction study

The hand was cleansed with rubbing alcohol and the skin temperature was maintained at 32–34 °C with an infrared heatlamp. Disposable silver/silver chloride surface strip electrodes (Nicolet VIASYS Healthcare), measuring 1×2.5 cm, were used. The recording electrode was placed on the proximal interphalangeal joint (G1) and the reference electrode on the distal interphalangeal joint of the third digit (G2) (Fig. 1). A ground electrode (Gd) was placed on the dorsum of the hand. The median nerve was stimulated in mid palm and also just proximal to the distal wrist crease at Sw and Sp. The transcarpal sensory conduction velocity and the negative peak amplitude of the sensory nerve action potential (SNAP) were measured.

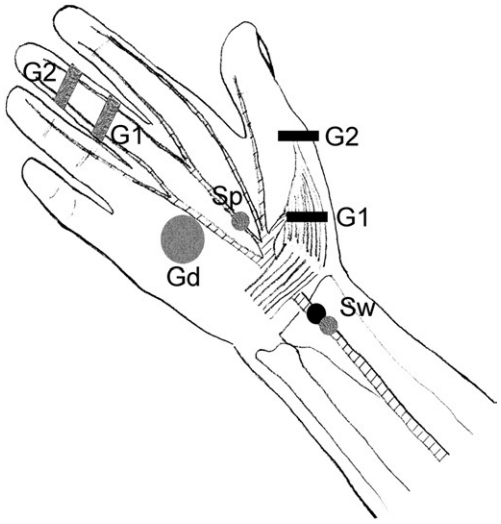


Fig. 1. Experimental setup for the nerve conduction studies. G1 is the recording electrode, G2 the reference electrode. Gd is the ground electrode placed on the dorsum of the hand. The sensory nerves were stimulated at the wrist (Sw) and at the palm (Sp). The stimulating and recording electrodes used for the motor conduction study are shown in solid black color while those used for the sensory conduction study are shown in stippled grey color. Detailed descriptions of the methods are given in the text.

Median motor nerve conduction study

A disposable recording surface strip electrode was placed over the motor point on the thenar eminence muscles with a reference electrode placed over the dorsal aspect of the first metacarpophalangeal joint (Fig. 1). The median nerve was stimulated at supramaximal intensity at the wrist (Sw) (8 cm proximal to the recording electrode) and also at the elbow. The negative peak amplitude of the maximal compound muscle action potential, terminal motor latency and conduction velocity in the forearm were measured. The median nerve was also stimulated at the palm (Sp). Those patients with evidence of conduction block across the carpal tunnel were excluded from the study.

Motor unit number estimation (MUNE)

MUNE was performed on all patients using the multiple point stimulation technique to determine the number of motoneurons that regenerate their axons and innervate thenar muscles (Doherty et al., 1995). This was done using proprietary software on an Advantage EMG machine (Neurosoft, Virginia).

Recording

Disposable, self-adhesive surface electrodes over the thenar muscles of the thumb were used to detect the maximum compound muscle action potential (CMAP) and surface-detected motor unit action potential (S-MUAP) (Fig. 2). Placement of the electrodes was the same as that used for motor nerve conduction study. A 3×3 cm metal plate was positioned on the back of the hand as a ground. The bandpass filter was set at 5–2000 Hz.

Stimulation

Electrical stimulation of the nerve was performed with a hand-held constant-current bipolar surface bar stimulator. The maximum CMAP of the median nerve was evoked by stimulating the median nerve at the wrist at 10 % above the maximal intensity with a stimulus duration of 0.01 ms (Fig. 2B). The course of the median nerve was mapped from the elbow to the axilla by advancing the bar

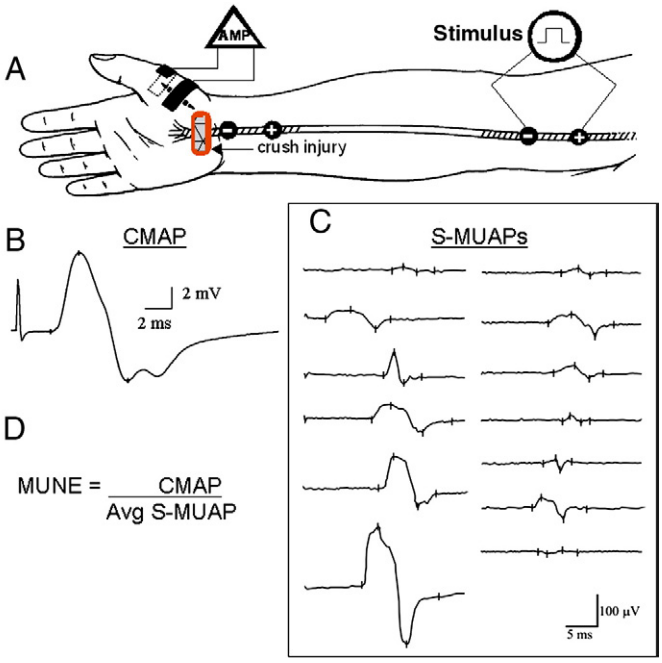


Fig. 2. The experimental setup for motor unit number estimation. (A) Placement of the recording and reference electrodes depicted are identical to those used for the motor conduction study in Fig. 1. Shaded stretches of the median nerve are the superficial portions at the wrist and between the elbow and axilla used for multiple point stimulation. (B) The maximal compound motor action potential (CMAP) was recorded in response to maximal electrical stimulation of the median nerve. (C) A collection of 13 surface recorded motor unit action potentials (S-MUAPs) was activated by stimulation of the median nerve along the arm with finely graded, low intensity threshold stimulation. (D) A motor unit number estimation (MUNE) was then calculated by dividing the CMAP by the average S-MUAP.

stimulator over the medial aspect of the arm at 1–2 cm intervals (Fig. 2A). Because the median and ulnar nerves are in close proximity in the upper arm, it was necessary to avoid co-stimulation of the ulnar nerve while mapping the course of the median nerve. Co-activation of the ulnar nerve was recognized by (1) an initial positive deflection of the CMAP, (2) abduction of the fifth digit, and (3) the radiation of an electrical sensation into the fourth and fifth digits. In earlier experiments, we also co-recorded from the hypothenar eminence and found that when the above conditions were avoided, there was no detectable action potential generated by the hypothenar muscles.

Using the same recording electrodes, S-MUAPs with the lowest stimulus thresholds were elicited by stimulating the median nerve at multiple sites where the nerve is more superficially located at the wrist and between the elbow and the axilla (Fig. 2C). Stimulation was performed at 1 Hz with gradually increasing intensity until the first reproducible, "all-or-none" S-MUAP was evoked. To increase the yield, the next higher threshold S-MUAP could sometimes be obtained through template subtraction. By this means, up to a maximum of 3 S-MUAPs were acquired at each site and a total of 13 to 20 S-MUAPs was stored in computer memory. The mean peak-to-peak amplitude of this sample of S-MUAPs was calculated using "datapoint-by-datapoint" summation. All S-MAUPs were temporally aligned at the same onset latency before they were averaged. The motor unit number estimate was obtained using the following equation:

$$\frac{\text{Peak–to–peak amplitude of the maximum CMAP}}{\text{Peak–to–peak amplitude of the average S–MUAP}}$$

Behavioral measures

(1) *Levine's Self-Assessment Questionnaire for CTS.* To assess the subjective symptoms, patients were asked to complete the Levine's Self-Assessment Questionnaire for CTS symptom severity before and at intervals after the surgery (Levine et al., 1993). This questionnaire consisted of two parts: (1) symptom severity scale comprised of 11 items scored on a Likert scale inquiring about pain, paraesthesia, numbness, weakness, nocturnal symptoms and overall functional status, and (2) functional status scale comprised of 8 questions regarding activities of daily life commonly affected by CTS. The symptom severity scores ranged from 1 to 5 with 1 representing no symptoms and 5, very severe symptoms. The functional status scores also ranged from 1: no difficulty to do a task, to 5: inability to do a task. The patients were asked to rate the severity of the symptoms on the hand that was to be operated on.

(2) *Semmes Weinstein Monofilaments (SWM).* As sensory complaints are prominent in CTS, we used a test kit of 20 SWM (Sammons Preston Rolyan, Canada) to assess the impact of the CTS with and without electrical stimulation (ES) treatments on hand sensation. This tool, which examines the sensation threshold, has proven reliability (Bell-Krotoski and Tomancik, 1987) and is utilized in the clinical evaluation of peripheral nerve diseases such as diabetic neuropathy (Imai et al., 1989; Lee et al., 2003). Since pressure sensation involves primarily small, unmyelinated or poorly myelinated nerve fibers, this test complements the convention sensory nerve conduction study well because the latter only evaluates large myelinated sensory nerve fibers.
Subjects were asked to place their hands over a table, and keep their eyes closed for the duration of this test. Each filament, starting with the smallest caliber, was tested over the pulp of digits. The filament was applied perpendicularly for 1 to 1.5 s in three trials. Subjects were asked to indicate the area where the filament was felt. We examined the sensory threshold of all fingers in random order. A positive response in at least 2 of the 3 trials marked the sensory threshold. We used the test results of the third digit where sensory nerve conduction study was also done, for data analysis.

(3) *The Purdue Pegboard Test.* We used the Purdue Pegboard Test (Model 32020, Lafayette Instrument Company, IN, USA) to monitor the impact of CTS with and without ES on manual dexterity. The Purdue Pegboard Test is a standardized hand function tool with proven validity and reliability in the functional evaluation of CTS patients. It consisted of 50 holes arranged in two parallel columns. Subjects were instructed to start the test on a verbal cue, while an examiner timed the test with a stopwatch. They had 30 s to fill the holes with pegs, initially with the hand that was intended for CTS surgery and then with the other hand. Each subset was repeated three times to obtain an average. Test scores equaled the number of filled holes.

Interventions

Subjects were randomized to the control or the stimulation group by using the random number generation function in a commercially available software program (Excel, Microsoft Inc.). The control group underwent open carpal tunnel release surgery (CTRS) only. The stimulation group underwent CTRS followed by 1 h of electrical stimulation of the median nerve.

Surgical technique

Operations were performed by a plastic surgeon (D.E.). The surgical procedure was the standard CTRS without epineurotomy or neurolysis of the median nerve (Rosenbaum and Ochoa, 1993). A tourniquet was inflated over the forearm. The surgeon drew a curvilinear mark over the palm to guide the incision. The transverse carpal ligament was divided along the ulnar side of the incision. No

further intervention was employed in the control group. For the stimulation group, two sterile 30 gauge stainless steel wires, insulated except 1 cm at the tip, were placed over the median nerve. One electrode was positioned at the proximal end and the other at the distal end of the incision. To record the CMAP during the post-surgical ES, the surgeon placed two surface electrodes (TECA, Oxford Instruments), one over the motor point on the thenar eminence muscles (G1) and the other over the dorsal aspect of the first metacarpophalangeal joint (G2) (see Fig. 1).

Electrical stimulation

Subjects in the stimulation group were transferred to a neurophysiology laboratory after CTRS. There was an approximately 30 min delay between termination of CTRS and initiation of electrical stimulation. With the patient in the lying position, the operated hand was stabilized in an elevated position. The stimulating electrodes were connected to a Grass (SD9) stimulator: the proximal wire electrode was connected to the cathode and the distal one to the anode. The surface electrodes on the thenar eminence were connected to an EMG machine (NeuroSoft Inc., Virginia). We gradually increased the stimulation intensity to the maximal tolerance limit (4–6 V, 0.1–0.8 ms duration) as a continuous 20 Hz train for 1 h. These intensities were sufficient to induce a fused tetanic contraction but low enough to not induce excessive discomfort. This protocol, including configuration of the stimulus polarities, frequency and duration parameters, was so chosen to approximate that used in our animal studies (Al Majed et al., 2000a,b, 2004; Brushart et al., 2002). The only exception is that supramaximal intensities used in animal studies was not feasible in human subjects. The CMAP of the thenar muscles were also monitored. After the termination of stimulation, electrodes were pulled out and discarded.

Outcomes

To compare the effectiveness of electrical stimulation with control CTRS, the subjects were evaluated twice before the operation (pre-op1 and pre-op2) to ensure reliability of the tests. Subjects were then followed for a year at 3 time points after the CTRS. The follow-up schedule was: (1) post-op1: 3rd month, (2) post-op2: 6th to 8th month, and (3) post-op3: 12th month. The 3rd month was selected for the first assessment based on the assumptions that the most optimal axonal growth rate is 1 mm/day and the distance between the compression site and the thenar muscles is ~70 to 80 mm, depending on the size of the hand. At each post-operative assessment, all the baseline measures were repeated.

Motor unit numbers and muscle function

To ascertain whether the motor unit number in CTS patients had an impact on their muscle function, we also measured muscle bulk and force generating capacity in a separate sample of 8 subjects. Cross sectional area of the mid belly of the median innervated thenar muscles (abductor pollicis brevis, opponent pollicis and superficial head of flexor pollicis brevis) was measured using ultrasound imaging (Acuson Sequoia, Siemens, Germany). Mid belly of the muscles was located at the mid shaft of the 1st metacarpal bone. The medial border of the thenar muscles lies over the 2nd metacarpal bone while the lateral border is defined by the 1st metacarpal bone (see Fig. 3A). Superficial head of the flexor pollicis brevis, deepest of the three median innervated thenar muscles, is at the level of the flexor pollicis longus tendon. The tendon served as a useful landmark because it can be easily discerned by its shape and high echogenicity (see Fig. 3A). The perimeter of these muscles was traced and the cross sectional area calculated using the ultrasound machine bundled software.

Twitch force of the median nerve innervated thenar muscles was recorded using a LCCA-25 load cell (Omega Canada, Laval, Quebec) connected to the thumb via a loop placed around the base of the 1st proximal phalanx. Based on previous studies, the maximum resultant vector of the median innervated thenar muscles is at a 45° angle plane from the palm along which the load cell was aligned. After the hand and forearm were secured to the force platform by inelastic Velcro straps, the median nerve was stimulated supramaximally at the wrist and the twitch tension recorded (see Fig. 3C).

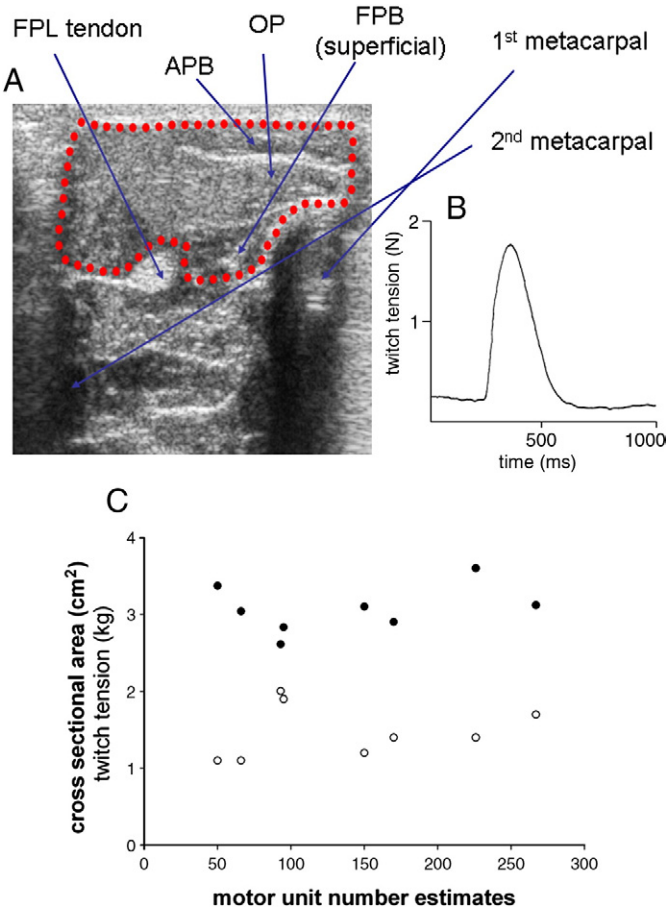


Fig. 3. Muscle bulk and contractile capacity of the median innervated thenar muscles in carpal tunnel syndrome patients. Cross sectional area of the median nerve innervated thenar muscles (APB—abductor pollicis brevis, OP—opponens pollicis, superficial head of the FPB—flexor pollicis brevis) was measured using ultrasound. An example is shown in panel A where the perimeter was outlined by a dotted line. Tendon of the flexor pollicis longus (FPL) muscle is highly echogenic and serves as a useful landmark. The twitch tension of the thenar muscles from the same patient is shown in panel B. As can be seen in panel C, despite the wide range of motor unit numbers in this sample of CTS patients, there was no significant correlations with the cross sectional areas (solid circles) ($r=0.32$, $p=0.43$) or twitch tension (open circles) ($r=0.18$, $p=0.67$).

Statistical analysis

The statistical program SPSS 12.0 for Windows was used in this study. Sample size estimation was done based on published animal data with MUNE being the primary outcome measure (Al Majed et al., 2000b). Assuming a difference in treatment effect size of 26%, standard deviation of 30%, with $\alpha=0.05$ and $\beta=0.20$, to have sufficient power to detect a significant difference, 20 subjects would be required for this study. Test–retest reliability of MUNE, a major outcome measure used in this study, was tested using linear regression analysis. Using Shapiro–Wilk Test of normality, we found that nerve conduction studies, and SWM results were significantly skewed from the Gaussian distribution ($p<0.05$). Additionally, Mauchley's test of sphericity was statistically significant ($p<0.05$) for the Levine's Self-Assessment Questionnaire and Purdue Pegboard

Test scores rendering parametric tests unsuitable. To be conservative and to reduce the chances of type I error, we decided to use non-parametric statistical methods for their analysis. We used Kendall's W and Wilcoxon Signed Ranks test to compare those outcome measures within each group of subjects. To examine whether the preoperative outcome measure values were significantly different between the two groups, the Kruskal–Wallis test was employed. In contrast, the MUNE results were normally distributed and the variance was homogeneous between the treatment and control groups, changes within each group following intervention were therefore analyzed using paired Student's *t* tests. In addition, comparisons of changes between the two groups following intervention were analyzed using univariate general linear model statistics. Linear regression analysis between the MUNE, cross sectional area and twitch force of the thenar muscles was done. The statistical significance was set at $p<0.05$.

Results

Subjects with carpal tunnel syndrome

Twenty five eligible CTS subjects participated in the study, all of whom had surgical decompression of the carpal tunnel under local anesthesia (1% lidocaine). However, 4 subjects (2 males and 2 females) withdrew from the study because of development of other medical conditions or occupational commitments which prevented them to return for follow up. Two of these patients belonged to the control and 2 to the stimulation group. Therefore, the results are from 21 subjects: 8 males and 13 females. The patients were 20 to 86 years old, with a mean (±SD) age of 56±17 years. The breakdown of age and sex and the physical attributes in both groups are shown in Table 1. The subjects were housewives, nurses, medical and laboratory technicians, cooks, manual laborers, and retirees. All had had progressive symptoms for at least 2 years.

Eighteen subjects were right hand dominant. Although they all had bilateral symptoms, it was more severe in their dominant hand that was subsequently operated. Ten patients were assigned to the control group (no electrical stimulation, ES) and 11 patients to the stimulation group (1 h 20 Hz ES). All subjects attended the first post-operative follow-up, whereas 19 of them were available for the second and third post-operative evaluations. Two of the subjects who missed appointments belonged to the control and one to the stimulation group.

Muscle denervation in severe carpal tunnel syndrome

We stimulated the median nerve proximal (Sw) and distal (Sp) to the site of compression at the carpal tunnel and recorded the evoked compound muscle action potential (CMAP) with the recording electrode (G1) placed over the muscles at the thenar eminence (Fig. 1). As shown in Fig. 4, we discriminated and excluded patients with early CTS on the basis of conduction block where CMAPs evoked distal to the compression site closer to the thenar muscles were much larger than the CMAPs evoked proximal to the compression site (Fig. 4B). Only those patients in whom the amplitude of the CMAP evoked above and below the sites of compression was equally reduced, were selected (Fig. 4A).

Table 1
Mean (±SE) of age, gender and handedness of the human patient subjects in control (no electrical stimulation) and stimulation (1 h 20 Hz electrical stimulation) groups.

	Control	Stimulated
Age	61±16 years.	53±18 years.
Gender	7 females: 3 males	6 females: 5 males
Handedness	2 left:8 right	1 left:10 right

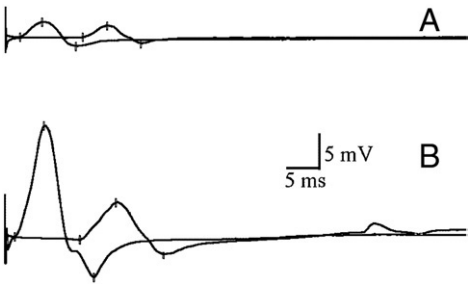


Fig. 4. Discrimination of nerve injury from conduction block in carpal tunnel syndrome patients. Examples of recordings of maximal CMAPs in (A) a patient with marked axonal loss in the median nerve where amplitudes of the CMAPs evoked at the wrist and palm were equally reduced, and (B) another patient with conduction block of the median nerve at the carpal tunnel where the amplitude of the CMAP was reduced at the site proximal to the carpal tunnel as compared to the normal CMAP amplitude evoked by stimulation below the carpal tunnel. The latter patients were excluded from the study.

Using the multiple point stimulation technique for motor unit number estimation (MUNE), Doherty and Brown reported 288±23 (mean±SE) motor units (MU) in the thenar muscles of healthy subjects (Doherty and Brown, 1993). The preoperative MUNE in the selected patients with severe CTS was reduced by ~50% as compared to that in the healthy subjects (Fig. 5A). The estimated number of innervated MUs was the same in 2 preoperative recording sessions and the numbers were also not different in the control and stimulated groups of patients.

The underlying axonal injury seen in these CTS patients was likely long-standing as reflected by the substantially larger single surface recorded motor unit action potential (S-MUAP) amplitudes recorded in the 2 preoperative recording sessions as compared to healthy subjects (Fig. 5B). Amplitudes of the S-MUAP in healthy subjects reported by Doherty and Brown were 0.91±0.11% of the maximum CMAP (Doherty and Brown, 1997). In contrast, for the CTS subjects in

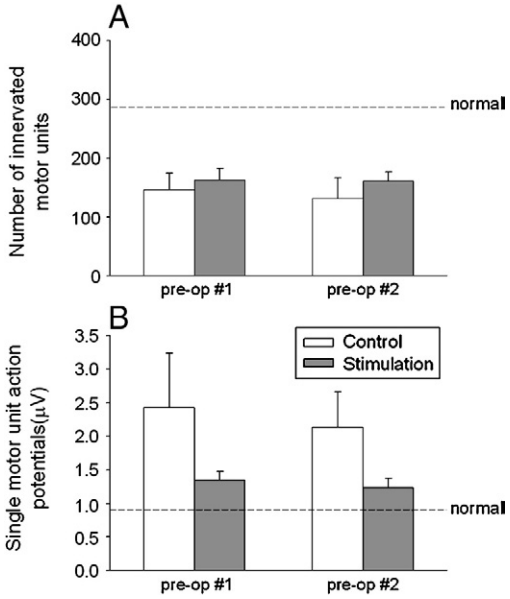


Fig. 5. Reduced numbers of motor units in carpal tunnel syndrome (CTS) patients. (A) The number (mean±SE) of innervated motor units (MUs) that were determined with MUNE in 2 preoperative recording sessions was substantially reduced compared to healthy controls (broken line). MU numbers were reduced in both the control (non-stimulated) and experimental (stimulation) groups of CTS patients preoperatively. (B) The amplitude (mean±SE) of surface recorded motor unit action potentials (S-MUAPs) from the thenar muscles in the same recording sessions. S-MUAPs were larger than in normal subjects (broken line), likely reflecting chronic loss of motor axons in both groups of patients.

this study, amplitude of the S-MUAPs was 1.92 ± 0.44% of maximum CMAP (range 0.06–61%; median ± 95%CI = 0.64 ± 1.06%). Although amplitudes of the S-MUAPs in the control group was substantially larger than the stimulation group, the difference was not statistically significant ($p = 0.22$). This shift of the distribution to larger values indicated that the fewer surviving MUs had had adequate time to sprout and enlarge by reinnervation of denervated muscle fibers.

Brief electrical stimulation accelerates reinnervation of denervated muscle in severe carpal tunnel syndrome

Brief (1 h) ES of surgically repaired rat peripheral nerve accelerated axon regeneration across the repair site without affecting the rate of axon regeneration within the distal nerve stump (Al Majed et al., 2000b; Brushart et al., 2002). We used the same stimulation regime, in this study of CTS patients. MUNE was used to evaluate whether ES immediately after CTRS in severe CTS patients, promotes and/or accelerates reinnervation of denervated thenar muscles. In the control (non-stimulated) group of patients, the numbers of innervated MUs were determined by MUNE at regular intervals up to 12 months after CTRS. There was no significant change in the MUNE even up to a year after surgery, even though there was a trend for the number to increase between 6 and 12 months (Fig. 6A). In contrast, there was already a trend for the MUNE to increase within 3 months in the patients after CTRS and ES (Fig. 6B). By 6–8 months, the number of MUs in the thenar muscles had increased significantly, comparable to the numbers reported in healthy subjects. Hence, in striking contrast to the failure of regenerating nerves after CTRS alone, *all* the regenerating motor axons in the stimulation group had made functional connections with denervated muscle fibers by 6–8 months.

The mean amplitude of the S-MUAPs 3 months after CTRS without ES did not change significantly compared to preoperative baseline (Fig. 6C). In contrast, 3 months after CTRS with ES, there was a significant reduction in the mean S-MUAP amplitude as compared to preoperative values (from 1.35% maximum CMAP to 0.89% maximum CMAP, Mann–Whitney *U* test) (Fig. 6D). The early reduction in the ES group indicated the presence of newly regenerated motor axons had innervated some muscle fibers while they had not in the control non-stimulated group.

Small, newly regenerated MUs contribute little to the amplitude of the maximum CMAP so that the lack of significant change in the CMAP amplitude following CTRS with and without ES was not surprising (Fig. 7). Since the maximum CMAP amplitudes were not normally distributed, they are shown as box and whisker plots where the upper and lower limits of the box represent the 75th and 25th percentiles, respectively, while the upper and lower limits of the whiskers represent the 90th and 10th percentiles, respectively. The transverse line within the box represents the median. Not surprisingly, the maximum CMAP amplitudes recorded preoperatively were smaller than in the healthy controls and they remained so throughout the postoperative follow-up period in both the control and stimulated groups of CTS patients.

Brief electrical stimulation promotes improvements in axonal conduction speeds in severe carpal tunnel syndrome

Demyelination is one of the most common sequelae of compressive neuropathy (O'Brien et al., 1987). In order to determine whether ES also affects remyelination, we measured the conduction speeds of both motor and sensory nerve fibers across the carpal tunnel. The

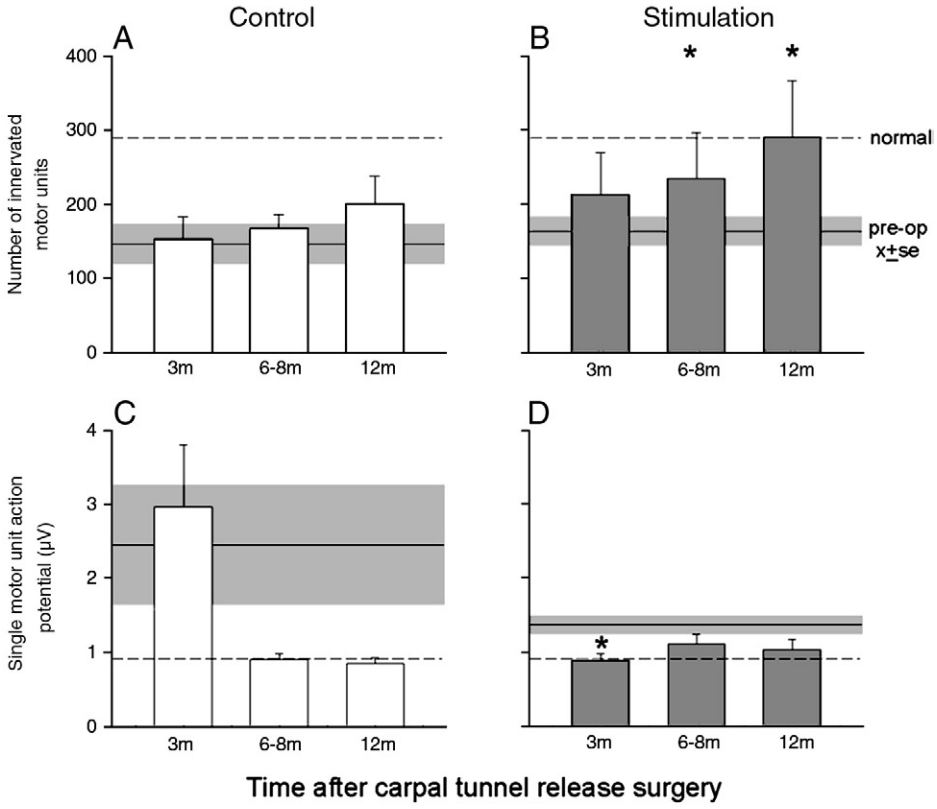


Fig. 6. Brief (1 h) 20 Hz electrical stimulation (ES) of axotomized motoneurons led to the complete reinnervation of the thenar eminence muscles. The mean(±SE) numbers of reinnervated motor units are shown in A and B and surface recorded motor unit action potential (S-MUAP) amplitudes are shown in C and D. MUNE did not increase significantly as a function of time after surgery in the control group but did in the stimulation group of CTS patients where MUNE increased progressively with a significant increase being recorded at 6–8 and 12 months after CTRS when the MUNE reaching the same level as normal healthy subjects. The increase seen in the stimulation group was likely due to new muscle fiber reinnervation as reflected by the presence of small S-MUAPs. Although the amplitudes of the S-MUAPs also declined in the control group, that did not occur until 6 months after surgery.

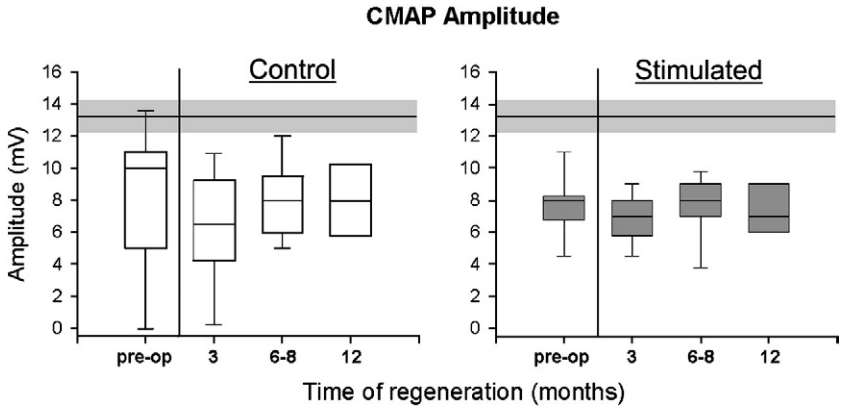


Fig. 7. Brief (1 h) 20 Hz electrical stimulation (ES) of axotomized motoneurons did not change the amplitude of the compound motor action potentials (CMAP) recorded in the thenar eminence muscles after carpal tunnel release surgery (CTRS). The median values of CMAP amplitudes did not change significantly in either (A) the control or (B) the stimulated groups of patients after intervention. The grey band represents data from the healthy control (mean ± SD). The upper and lower limits of the box represent the 75th and 25th percentiles, respectively, while the upper and lower limits of the whiskers represent the 90th and 10th percentiles, respectively. The median is represented by the line within the box.

motor terminal latency in the severe CTS patients was similarly slower than normal in both the control and stimulation groups at baseline (Fig. 8). The latency did not change significantly in the control group in the post-operative period, while, in contrast, significant acceleration in the motor latency occurred early in the stimulation group at 3 months (Fig. 8B). Motor terminal latencies from 3 months onward were the same as that for healthy subjects (Fig. 8B). Similarly, earlier recovery of conduction velocity of the sensory nerve fibers was found in the stimulation group at 3 months when amplitude of the SNAP had not yet changed significantly from pre-operative values (Figs. 9B, D). In contrast, recovery was delayed in the control patient group (Figs. 9A, C). Together, these data buttress the possibility that ES may enhance remyelination in addition to accelerating axon regeneration and muscle reinnervation.

Rapid improvements in behavioral outcomes following CTRS

In order to evaluate the functional outcome of motor and sensory target reinnervation, we chose the Purdue Pegboard Test to gauge hand performance, Semmes Weinstein Monofilaments for pressure sensation and the Levine's CTS Questionnaire for subjective symptoms. Rapid improvements in all these functional outcomes were found regardless of whether the subjects were in the control or stimulation groups (Figs. 10A, B and 11A, B). We compared the test results with those in the opposite untreated hands in order to determine whether the improvements seen in the Purdue Pegboard Test were due to practice. Since there was no change of performance in the non-treated hand, practice effect is an unlikely explanation for the improvements of hand function after CTRS in both the control and stimulation groups (Figs. 10C, D). Rather, a more likely explanation for better hand performance on the Purdue Pegboard Test was rapid recovery in pressure sensitivity at the digit tips after CTRS (Fig. 11A and B). Since smaller, poorly myelinated sensory nerve fibers are less vulnerable to degeneration due to compression (Nishimura et al., 2004), transmission along those nerve fibers can be more readily restored once the compression is alleviated. Lastly, with subjective interpretation of symptom severity on the Levine's CTS Questionnaire, the subjects reported rapid resolution of symptoms with or without stimulation (Figs. 11C, D). Given that pain and tingling sensations experienced by CTS patients are positive symptoms of sensory nerve fiber irritation, ready resolution of these symptoms is commonly observed in patients following conventional CTRS.

Motor unit number does not affect cross sectional area and twitch tension of the thenar muscles in CTS

Because damage to the median nerve in the vast majority of CTS patients is a chronic process, the remaining surviving motor axons usually have ample time to sprout and to reinnervate the muscle fibers. Indeed, previous studies on chronic axonal injury did not find significant decline in muscle force until the motor unit number fell below 90% of the control subjects (McComas et al., 1971). To test that

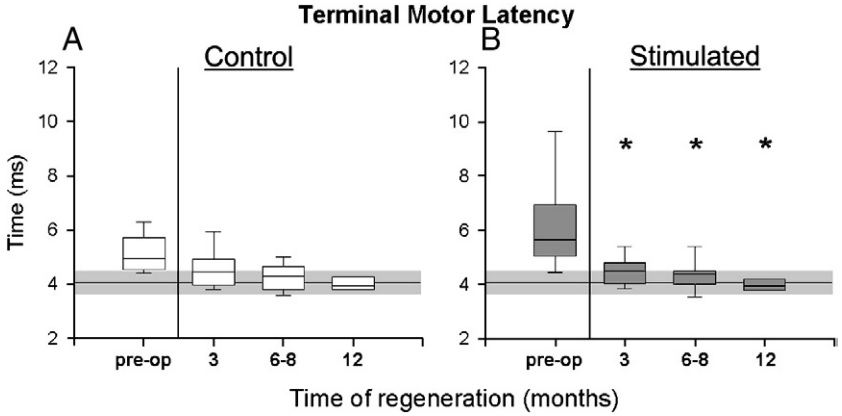


Fig. 8. Brief (1 h) 20 Hz electrical stimulation (ES) of axotomized motoneurons accelerated the reduction in terminal motor latency in the thenar eminence muscles after carpal tunnel release surgery (CTRS). The terminal motor latency declined significantly following CTRS in the stimulation group (B) but not in the control group (A). The grey band represents data from the healthy control (mean ± SD). The upper and lower limits of the box represent the 75th and 25th percentiles, respectively, while the upper and lower limits of the whiskers represent the 90th and 10th percentiles, respectively. The median is represented by the line within the box.

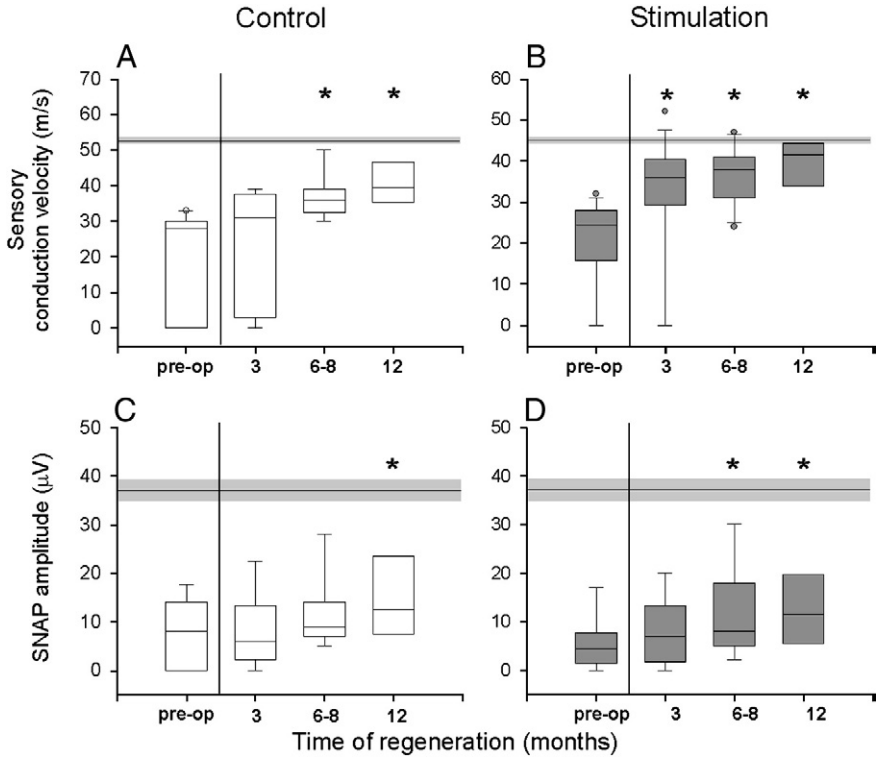


Fig. 9. Brief (1 h) 20 Hz electrical stimulation (ES) of axotomized motoneurons accelerated the increase in sensory nerve conduction velocity and the amplitude of the sensory nerve action potential (SNAP) after carpal tunnel release surgery (CTRS). Both axonal conduction velocity (B) and sensory nerve action potential amplitude (D) improved earlier in the stimulation group compared to the control group (A, C). The grey band represents data from the healthy control (mean ± SD). The upper and lower limits of the box represent the 75th and 25th percentiles, respectively, while the upper and lower limits of the whiskers represent the 90th and 10th percentiles, respectively. The median is represented by the line within the box.

hypothesis in CTS patients, we measured the cross sectional area and twitch tension of the median innervated thenar muscles in a separate sample of 8 CTS patients. Although they had motor unit numbers ranged from 50 to 267, no significant correlations between the motor unit number, cross sectional area and twitch tension were found (see Fig. 3C). These results support our contention that in a chronic axonal loss injury process such as CTS, the extent of motor axonal loss except in the most severe cases does not affect the muscle force and mass.

Discussion

This pilot study serves as proof of principle for positive outcomes of brief post-surgical ES and demonstrated that indeed, brief 1 h low frequency ES immediately following decompression surgery in patients suffering from severe CTS resulted in early and complete reinnervation of the thenar muscles. Surgery alone was not sufficient to cause significant improvement in muscle reinnervation even 1 year after the operation.

The findings are not simply due to resolution of conduction block following carpal tunnel decompression because all patients were screened for conduction block preoperatively and excluded from the study if block was evident. The findings demonstrated for the first time that the brief continuous ES at 20 Hz that accelerates axon outgrowth in animal models of nerve injury in rats (Al Majed et al., 2000b; Brushart et al., 2002, 2005; Geremia et al., 2007) and mice (Ahlborn et al., 2007; English et al., 2007) is also effective in accelerating target reinnervation in the human. Moreover these findings provide direct evidence of accelerated muscle reinnervation to account for the earlier functional recovery of muscle force and reflex discharge demonstrated in rats by Nix and Hopf (1983) and Pockett and Gavin (1985). Importantly the single bout of ES immediately after surgery, by accelerating axon outgrowth, was sufficient to result in target reinnervation 6 months later.

Since the compressive axonal injury that occurs in CTS is a chronic one, the ability for the affected motor axons to grow and regenerate is likely compromised by the delay. Diminished capacity for axonal regeneration was demonstrated in a chronic axotomy animal model where the extent of axon regeneration was reduced by up to 66% when a chronically axotomized tibial nerve was cross-sutured and regrew into a freshly cut common peroneal nerve in the rat hindlimb (Boyd and Gordon., 2002; Fu and Gordon, 1995a). With consideration of the diminished regenerative capacity of chronically injured neurons, our findings of no significant thenar muscle reinnervation even a year after carpal tunnel release without ES is perhaps not surprising. In that light, the striking regenerative capacity of axotomized median motoneurons that were electrically stimulated for 1 h after CTR surgery, was remarkable: the axon regeneration in the group of patients whose median nerve was electrical stimulated, was not only more rapid but *all* the axotomized motoneurons regenerated their axons and the MU number in the reinnervated thenar muscles was the same as that in normal healthy individuals (Fig. 6). These data imply that even chronically injured motor axons retain the ability to regenerate if they are electrically stimulated for just 1 h after surgical repair, a conclusion that is readily testable in an animal model. Death of motoneurons after prolonged axotomy at distal sites is unlikely because motoneurons can survive a year or more after chronic axotomy (Gordon et al., 1991; Vanden Noven et al., 1993).

Animal studies demonstrated that 1 h 20 Hz ES accelerates axonal outgrowth at the site of injury but *not* the rate of axonal regeneration in distal nerve stumps (Brushart et al., 2002; Udina et al., 2008). Given the distance of 70–80 mm from the site of compression in the carpal tunnel to the thenar muscle endplates in CTS patients, and assuming an approximate regeneration rate of 1 mm/day (Sunderland, 1947), the regenerating axons in the distal nerve stumps would be expected to reach the intramuscular nerve sheaths of the partially denervated

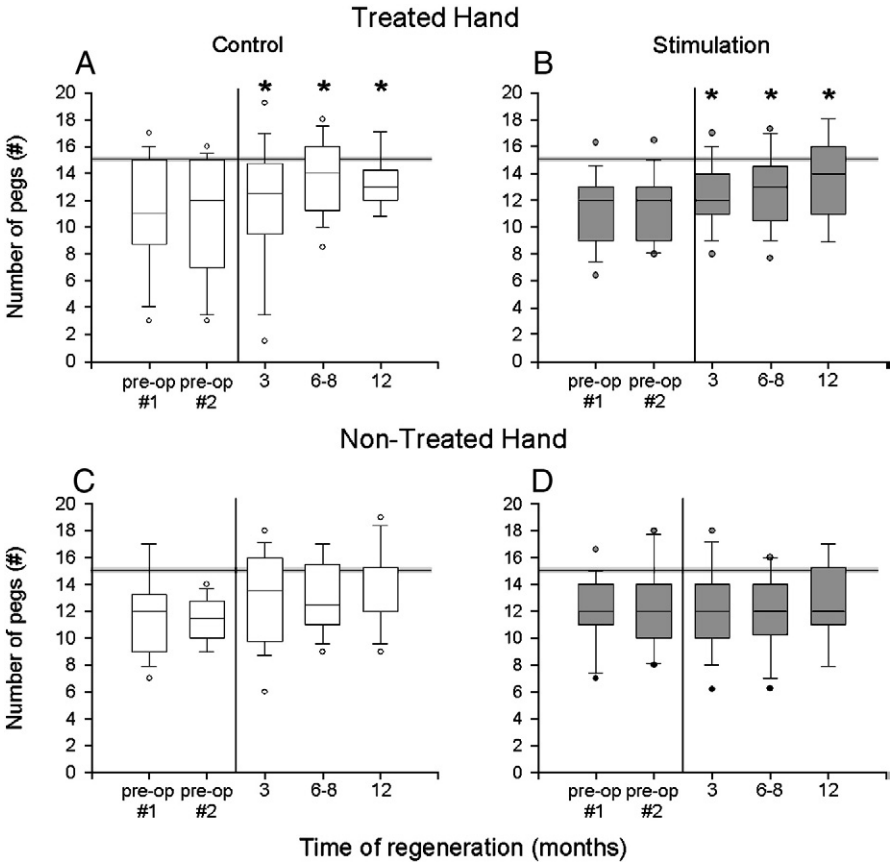


Fig. 10. Hand dexterity performance assessed by the Purdue Pegboard Test improved equally quickly after CTRS in both the control and stimulated groups of patients. The number of pegs placed by the control group (A, C) control and the stimulated group (B, D) increased significantly in the treated but not the non-treated hands. This effect is related to treatment as the non-treated hand did not show any significant improvement (C, D). The grey band represents data from the healthy control (mean ± SE). The upper and lower limits of the box represent the 75th and 25th percentiles, respectively while the upper and lower limits of the whiskers represent the 90th and 10th percentiles, respectively. The median is represented by the line within the box and the outliers are represented by the dots that lie beyond the whiskers.

thenar muscles within 3–4 months. Our finding that the MUNE did not increase significantly even as late as 12 months after CTRS without ES indicates that the progress of axon outgrowth across the site of compression is very slow. In this context, the acceleration of axon outgrowth by ES to achieve the significant muscle reinnervation by 6 months and complete muscle reinnervation by 12 months is considerable.

The motor nerve conduction studies further affirmed the positive impact of stimulations on axon regeneration: the significant improvement in the terminal motor latency of the median nerve occurred earlier in the stimulation group and was detectable as early as 3 months post-CTRS and stimulation (Fig. 8). The fact that the CMAP amplitude did not change in the stimulated group of patients following CTRS and ES is not surprising even though significant axonal regeneration had occurred, the reason being that CMAP amplitude is affected by changes in the amplitude and configuration of the constituent MUAPs (Rashidipour and Chan, 2008). In early reinnervation, MUAPs are usually small, polyphasic and contribute little to increase the CMAP amplitude. That was one of the major reasons that led to the introduction of more direct methods of estimating MU numbers (McComas, 1995).

Similar trends were also found in the sensory nerve conduction studies designed to evaluate regeneration of the large myelinated nerve fibers. Recovery of the conduction velocity and SNAP amplitude occurred earlier, by the 3rd month post-intervention in the stimulated group as opposed to the 6th month in the control group. However, these physiological differences are not likely to be functionally important as large myelinated fibers subserving vibration and proprioception sensations do not play a critical role in most daily activities (Videler et al., 2008). Rather, the ability to perceive touch and pressure subserved by small thinly myelinated nerve fibers is more important for hand function. Since those nerve fibers are less vulnerable to compressive injury, it is not surprising that there was no significant difference in the patterns of recovery in sensory symptom and hand function assessed by the Levine's Questionnaire and Purdue Pegboard Test between the control and stimulated groups of patients. Both groups reported marked symptom improvement within 3 months of surgery. Symptoms including tingling, burning and aching pain due to mechanical nerve irritation and micro-ischemia can all be readily alleviated by CTRS.

The lack of blinding in this human study was unlikely to affect the quantitative tests of axon regeneration and of muscle reinnervation. The validity of the MUNE technique used, the multiple point stimulation method, has been established (Doherty and Brown, 1993; Rashidipour and Chan, 2008) and its test–retest reliability is high (Felice, 1995; Porter et al., 2008). Therefore, despite the relatively small number of subjects and baseline inter-subject variability, the sample size was sufficient to detect the remarkable reinnervation of the denervated thenar muscles by all the injured (axotomized) motoneurons. The outcome measure tools of nerve conduction studies and the MUNE are objective measures that cannot be easily influenced by the subject or the examiner. The Levine's Self-Assessment Questionnaire for CTS was the only subjective outcome measure that had the potential to be biased by patients' knowledge about the treatment. However, in this study both the stimulation and control groups showed a significant improvement in their symptom severity by 3 months.

The molecular basis for the effects seen with post-surgical ES has been investigated in a number of recent studies (Al Majed et al., 2004;

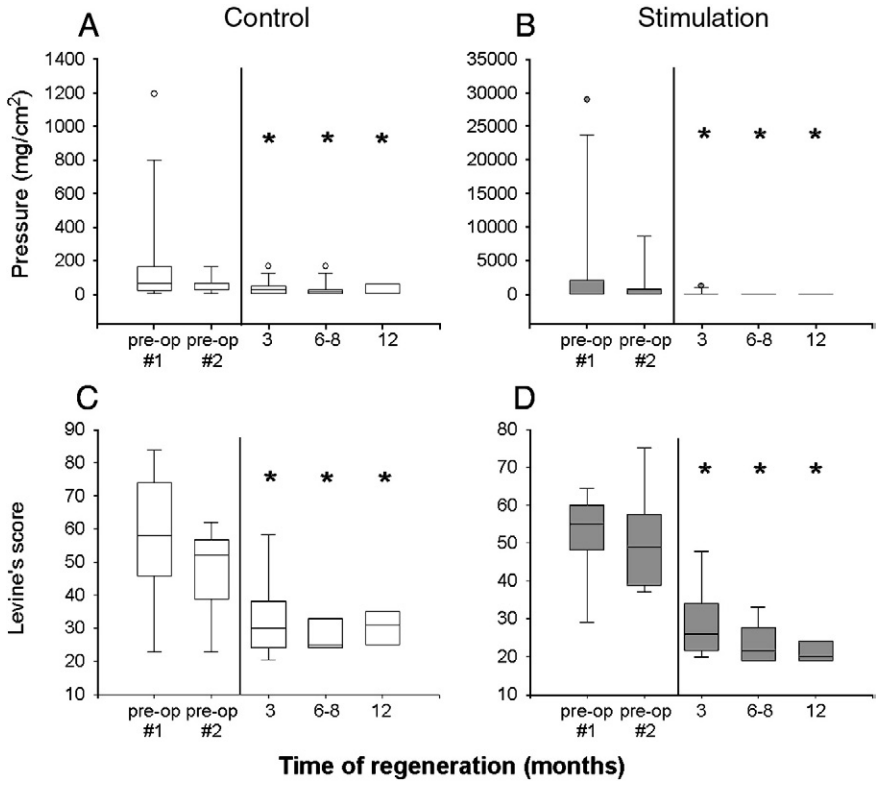


Fig. 11. The Semmes–Weinstein Monofilament Test (A, B) and the Levine's Self-Assessment Questionnaire (C, D) improved equally quickly after CTRS in both the control and stimulated groups of patients. The upper and lower limits of the box represent the 75th and 25th percentiles, respectively while the upper and lower limits of the whiskers represent the 90th and 10th percentiles, respectively. The median is represented by the line within the box and the outliers are represented by the dots that lie beyond the whiskers.

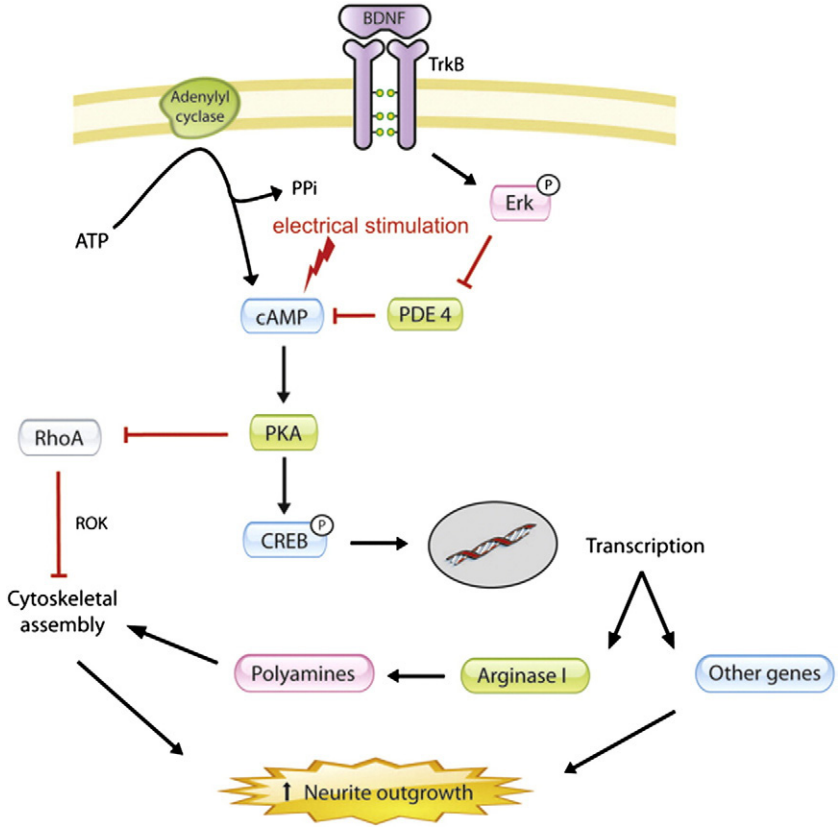


Fig. 12. Molecular mechanisms of enhanced nerve regeneration (modified from Hannila and Filbin, 2008). Electrical stimulation has been shown to upregulate cAMP that promotes nerve regeneration by activating cAMP response element binding (CREB) while inhibiting Rho via protein kinase A (PKA). See text for a detailed description.

Sharma et al., 2010; Udina et al., 2008). A key player that emerges is cyclic AMP (cAMP). Through activation of protein kinase A (PKA) and cAMP response element binding (CREB) protein, transcription of cytoskeletal proteins including actin and tubulin, required to accelerate nerve regeneration is triggered. In addition, cAMP is also instrumental in up-regulating a number of cytokines including IL6 while inhibiting Rho, a key protein in the Ngr/p75NTR pathway that prevents cytoskeletal assembly. Electrical stimulation brings about these changes by upregulating brain derived neurotrophic factor (BDNF) and its trkB receptor at the soma. A summary of these molecular pathways is shown schematically in Fig. 12.

Employing a constellation of outcome measure tools in this study, we have provided proof of principle that, in this randomized control pilot study, 1 h ES of the median nerve after surgical decompression accelerates axonal regeneration to promote complete muscle reinnervation. The procedure of ES immediately after surgery was proven feasible in the clinical setting. Additionally, patients did not develop any complications due to surgery or the stimulation. The present study sets the stage for future human trials of ES in promoting axon regeneration and muscle reinnervation. The increase in the speed of axon regeneration may be particularly crucial for functional recovery after nerve injuries such as cubital tunnel syndrome with entrapment of the ulnar nerve at the elbow or within the Arcade of Struthers at the upper arm where the axotomized neurons must regenerate their axons over much longer distances. Lastly, post-surgical ES may also benefit transected nerve injuries. Lundborg et al. reported motor and sensory recovery in transected median nerve after the proximal and distal nerve stumps were approximated by a silicone chamber but the recovery took 3 years (Lundborg et al., 1994). It is our hope that brief low frequency ES of the proximal nerve stump immediately after surgical repair will expedite the functional outcome of these procedures.

Acknowledgments

We gratefully acknowledge the generous operating grants awarded to TG (CIHR) and KMC (CIHR, WCB Alberta, Glenrose Foundation) and a CIHR strategic group grant that includes Drs Zochodne, Sayed, Midha and Julien from University of Calgary and Dr. Verge from University of Saskatchewan. TG is an AHFMR Senior Investigator.

References

Ahlborn, P., Schachner, M., Irintchev, A., 2007. One hour electrical stimulation accelerates functional recovery after femoral nerve repair. Exp. Neurol. 208, 137–144.
Al Majed, A.A., Brushart, T.M., Gordon, T., 2000a. Electrical stimulation accelerates and increases expression of BDNF and trkB mRNA in regenerating rat femoral motoneurons. Eur. J. Neurosci. 12, 4381–4390.
Al Majed, A.A., Neumann, C.M., Brushart, T.M., Gordon, T., 2000b. Brief electrical stimulation promotes the speed and accuracy of motor axonal regeneration. J. Neurosci. 20, 2602–2608.
Al Majed, A.A., Tam, S.L., Gordon, T., 2004. Electrical stimulation accelerates and enhances expression of regeneration-associated genes in regenerating rat femoral motoneurons. Cell Mol. Neurobiol. 24, 379–402.
Bell-Krotoski, J., Tomancik, E., 1987. The repeatability of testing with Semmes-Weinstein monofilaments. J. Hand Surg. [Am] 12, 155–161.
Boyd, J.G., Gordon, T., 2002. A dose-dependent facilitation and inhibition of peripheral nerve regeneration by brain-derived neurotrophic factor. Eur. J. Neurosci. 15, 613–626.
Brushart, T.M., Hoffman, P.N., Royall, R.M., Murinson, B.B., Witzel, C., Gordon, T., 2002. Electrical stimulation promotes motoneuron regeneration without increasing its speed or conditioning the neuron. J. Neurosci. 22, 6631–6638.
Brushart, T.M., Jari, R., Verge, V., Rohde, C., Gordon, T., 2005. Electrical stimulation restores the specificity of sensory axon regeneration. Exp. Neurol. 194, 221–229.
Doherty, T.J., Brown, W.F., 1993. The estimated numbers and relative sizes of thenar motor units as selected by multiple point stimulation in young and older adults. Muscle Nerve 16, 355–366.
Doherty, T.J., Brown, W.F., 1997. Age related changes in human thenar motor unit twitch contractile properties. J. Appl. Physiol. 82, 93–101.
Doherty, T., Simmons, Z., O'Connell, B., Felice, K.J., Conwit, R., Chan, K.M., Komori, T., Brown, T., Stashuk, D.W., Brown, W.F., 1995. Methods for estimating the numbers of motor units in human muscles. J. Clin. Neurophysiol. 12, 565–584.
Dumitru, D., 1995. Electrodiagnostic medicine. Mosby, St. Louis.
English, A.W., Schwartz, G., Meador, W., Sabatier, M.J., Mulligan, A., 2007. Electrical stimulation promotes peripheral axon regeneration by enhanced neuronal neurotrophin signaling. Dev. Neurosci. 67, 158–172.
Felice, K.J., 1995. Thenar motor unit number estimates using the multiple point stimulation technique: reproducibility studies in ALS patients and normal subjects. Muscle Nerve 18, 1412–1416.
Fu, S.Y., Gordon, T., 1995a. Contributing factors to poor functional recovery after delayed nerve repair: prolonged axotomy. J. Neurosci. 15, 3876–3885.
Fu, S.Y., Gordon, T., 1995b. Contributing factors to poor functional recovery after delayed nerve repair: prolonged denervation. J. Neurosci. 15, 3886–3895.
Fu, S.Y., Gordon, T., 1997. The cellular and molecular basis of peripheral nerve regeneration. Mol. Neurobiol. 14, 67–116.
Geremia, N.M., Gordon, T., Brushart, T.M., Al Majed, A.A., Verge, V.M.K., 2007. Electrical stimulation promotes sensory neuron regeneration and growth-associated gene expression. Exp. Neurol. 205, 347–359.
Gordon, T., Gillespie, J., Orozco, R., Davis, L., 1991. Axotomy-induced changes in rabbit hindlimb nerves and the effects of chronic electrical stimulation. J. Neurosci. 11, 2157–2169.
Gordon, T., Sulaiman, O., Boyd, J.G., 2003. Experimental strategies to promote functional recovery after peripheral nerve injuries. J. Peripher. Nerv. Syst. 8, 236–250.
Gordon, T., Chan, K.M., Sulaiman, O.A., Udina, E., Amirjani, N., Brushart, T.M., 2009. Accelerating axon growth to overcome limitations in functional recovery after peripheral nerve injury. Neurosurgery 65, 238.
Hannila, S.S., Filbin, M.T., 2008. The role of cyclic AMP signaling in promoting axonal regeneration after spinal cord injury. Exp. Neurol. 209, 321–332.
Imai, H., Tajima, T., Natsuma, Y., 1989. Interpretation of cutaneous pressure threshold (Semmes–Weinstein monofilament measurement) following median nerve repair and sensory reeducation in the adult. Microsurgery 10, 142–144.
Kline, D.G., Kim, D.H., 2008. Kline and Hudson's Nerve Injuries : Operative Results for Major Nerve Injuries, Entrapments and Tumors. Elsevier Saunders, Philadelphia, Pa.
Lee, S., Kim, H., Choi, S., Park, Y., Kim, Y., Cho, B., 2003. Clinical usefulness of the two-site Semmes-Weinstein monofilament test for detecting diabetic peripheral neuropathy. J. Korean Med. Sci. 18, 103–107.
Levine, D.W., Simmons, B.P., Koris, M.J., Daltroy, L.H., Hohl, G.G., Fossel, A.H., Katz, 1993. A self-administered questionnaire for the assessment of severity of symptoms and functional status in carpal tunnel syndrome. J. Bone Joint Surg. [Am.] 75, 1585–1592.
Lundborg, G., Rosen, B., Abrahamson, S.O., Dahlin, L., Danielsen, N., 1994. Tubular repair of the median nerve in the human forearm—preliminary findings. J. Hand Surg. [Br] 19, 273–276.
McComas, A.J., 1995. Motor-unit estimation: the beginning. J. Clin. Neurophysiol. 12, 560–564.
McComas, A.J., Sica, R.E., Campbell, M.J., Upton, A.R., 1971. Functional compensation in partially denervated muscles. J. Neurol. Neurosurg. Psychiatry 34, 453–460.
Nishimura, A., Ogura, T., Hase, H., Makinodan, A., Hojo, T., Katsumi, Y., Yagi, K., Mikami, Y., Kubo, T., 2004. A correlative electrophysiologic study of nerve fiber involvement in carpal tunnel syndrome using current perception thresholds. Clin. Neurophysiol. 115, 1921–1924.
Nix, W.A., Hopf, H.C., 1983. Electrical stimulation of regenerating nerve and its effect on motor recovery. Brain Res. 272, 21–25.
O'Brien, J.P., Mackinnon, S.E., MacLean, A.R., Hudson, A.R., Dellon, A.L., 1987. A model of chronic nerve compression in the rat. Ann. Plast. Surg. 19, 430–435.
Padua, L., LoMonaco, M., Gregori, B., Valente, E.M., Padua, R., Tonali, P., 1997. Neurophysiological classification and sensitivity in 500 carpal tunnel syndrome hands. Acta Neurol. Scand. 96, 211–217.
Pockett, S., Gavin, R.M., 1985. Acceleration of peripheral nerve regeneration after crush injury in rat. Neurosci. Lett. 59, 221–224.
Porter, C.L., Alvarez, A., Jones, K.E., Chan, K.M., 2008. Test retest reliability of a modified multiple point stimulation technique for motor unit number estimation. Clin. Neurophysiol. 119, 2287–2290.
Rashidipour, O., Chan, K.M., 2008. Motor unit number estimation in neuromuscular disease. Can J. Neurol. Sci. 35, 153–159.
Rosenbaum, R.B., Ochoa, J.L., 1993. Surgical treatment of carpal tunnel syndrome. In: Rosenbaum, R.B., Ochoa, J.L. (Eds.), Carpal Tunnel Syndrome and Other Disorders of the Median Nerve. Butterworth-Heinemann, Stoneham, pp. 263–283.
Sharma, N., Marzo, S.J., Jones, K.J., Foecking, E.M., 2010. Electrical stimulation and testosterone differentially enhance expression of regeneration-associated genes. Exp. Neurol. 223, 183–191.
Sulaiman, O.A., Gordon, T., 2000. Effects of short- and long-term Schwann cell denervation on peripheral nerve regeneration, myelination, and size. GLIA 32, 234–246.
Sunderland, S., 1947. Rate of regeneration in human peripheral nerves. Arch. Neurol. Psychiatry 58, 1–6.
Sunderland, S., 1978. Nerve and Nerve Injuries. Churchill Livingstone, Edinburgh.
Udina, E., Furey, M., Busch, S., Silver, J., Gordon, T., Fouad, K., 2008. Electrical stimulation of intact peripheral sensory axons in rats promotes outgrowth of their central projections. Exp. Neurol. 210, 238–247.
Vanden Noven, S., Wallace, N., Muccio, D., Turtz, A., Pinter, M.J., 1993. Adult spinal motoneurons remain viable despite prolonged absence of functional synaptic contact with muscle. Exp. Neurol. 123, 147–156.
Videler, A.J., Van Dijk, J.P., Beelen, A., de Visser, M., Nollet, F., van Schaik, I.N., 2008. Motor axon loss is associated with hand dysfunction in Charcot–Marie–Tooth disease 1a. Neurology 71, 1254–1260.
Witzel, C., Rohde, C., Brushart, T.M., 2005. Pathway sampling by regenerating peripheral axons. J. Comp. Neurol. 485, 183–190.
You, S., Petrov, T., Chung, P.H., Gordon, T., 1997. The expression of the low affinity nerve growth factor receptor in long-term denervated Schwann cells. GLIA 20, 87–100.

Experimental Neurology 269 (2015) 142–153

Contents lists available at ScienceDirect

Experimental Neurology

journal homepage: www.elsevier.com/locate/yexnr

Regular Article

Brief electrical stimulation improves nerve regeneration after delayed repair in Sprague Dawley rats

Kate Elzinga [a], Neil Tyreman [b], Adil Ladak [a], Bohdan Savaryn [a], Jaret Olson [a], Tessa Gordon [b,*]

[a] Division of Plastic Surgery, University of Alberta, Edmonton, Alberta, Canada
[b] Center for Neuroscience, Faculty of Medicine and Dentistry, University of Alberta, Edmonton, Alberta, Canada

ARTICLE INFO

Article history:
Received 2 February 2015
Revised 23 March 2015
Accepted 25 March 2015
Available online 2 April 2015

Keywords:
Peripheral nerve regeneration
Brief electrical stimulation
Delayed nerve repair
Chronic neuronal axotomy
Chronic Schwann cell denervation

ABSTRACT

Functional recovery after peripheral nerve injury and surgical repair declines with time and distance because the injured neurons without target contacts (chronic axotomy) progressively lose their regenerative capacity and chronically denervated Schwann cells (SCs) atrophy and fail to support axon regeneration. Findings that brief low frequency electrical stimulation (ES) accelerates axon outgrowth and muscle reinnervation after immediate nerve surgery in rats and human patients suggest that ES might improve regeneration after delayed nerve repair. To test this hypothesis, common peroneal (CP) neurons were chronically axotomized and/or tibial (TIB) SCs and ankle extensor muscles were chronically denervated by transection and ligation in rats. The CP and TIB nerves were cross-sutured after three months and subjected to either sham or one hour 20 Hz ES. Using retrograde tracing, we found that ES significantly increased the numbers of both motor and sensory neurons that regenerated their axons after a three month period of chronic CP axotomy and/or chronic TIB SC denervation. Muscle and motor unit forces recorded to determine the numbers of neurons that reinnervated gastrocnemius muscle demonstrated that ES significantly increased the numbers of motoneurons that reinnervated chronically denervated muscles. We conclude that electrical stimulation of chronically axotomized motor and sensory neurons is effective in accelerating axon outgrowth into chronically denervated nerve stumps and improving target reinnervation after delayed nerve repair. Possible mechanisms for the efficacy of ES in promoting axon regeneration and target reinnervation after delayed nerve repair include the upregulation of neurotrophic factors.

© 2015 Elsevier Inc. All rights reserved.

Introduction

We reported in 2000 that brief low frequency electrical stimulation (ES) accelerates nerve regeneration after immediate nerve repair (Al-Majed et al., 2000b). This finding has been confirmed many times in rodents, several of the studies also demonstrating accelerated target reinnervation and functional return in hindlimb and facial muscles (Ahlborn et al., 2007; Al-Majed et al., 2000a, 2000b; Alrashdan et al., 2010; Asensio-Pinilla et al., 2009; Brushart et al., 2005; Eberhardt et al., 2006; English et al., 2007; Franz et al., 2005; Geremia et al., 2007; Hetzler et al., 2008; Huang et al., 2009, 2010, 2013; Lu et al., 2008; Nix and Hopf, 1983; Sharma et al., 2009, 2010b; Singh et al., 2012). More recently ES was found to accelerate muscle reinnervation in the human hand (Gordon et al., 2010). Axon regeneration across a surgical repair site is normally slow, as neurons require three-four weeks for the regenerating axons to cross the site (Brushart et al., 2002). This staggered axon regeneration across the suture site is accelerated by continuous 20 Hz ES applied for 1 h after the surgical repair; ES does not change the rate of axon regeneration within the distal nerve stump (Brushart et al., 2002). The accelerated axon outgrowth at the suture site is responsible for the observed accelerated target reinnervation and functional return. ES accelerates axon outgrowth in association with raised intracellular cAMP levels (Udina et al., 2008; Udina et al., 2010), accelerated neuronal expression of neurotrophic factors and their receptors followed by accelerated upregulation of regeneration associated genes, that include tubulin, actin and GAP-43 (Al-Majed et al., 2000a, 2004; Geremia et al., 2007). Neuronal production of BDNF is downstream of androgen receptor signaling, the latter being essential for ES-mediated acceleration of axon outgrowth (Thompson et al., 2014). Neurotrophin 4/5 is also essential in the effectiveness of ES in accelerating axon outgrowth (English et al., 2007).

Functional recovery is frequently poor after surgical repair in humans especially after proximal nerve lesions where, at a regeneration rate of 1 mm/day, months and even years pass before target reinnervation is expected (Gordon and Sulaiman, 2013; Sulaiman et al., 2011; Sulaiman and Gordon, 2013). The poor recovery is generally attributed to irreversible atrophy of denervated targets (Hudson and Hunter, 1977; Lundborg, 2004) but, experimental evidence demonstrates that prolonged deprivation of target contact of regenerating nerves (chronic

* Corresponding author at: Neuroscience and Mental Health Institute, Faculty of Medicine and Dentistry, 525 Heritage Medical Research Center, University of Alberta, Edmonton, Alberta T6G 2S2, Canada. Fax: +1 780 492 1617.
E-mail address: tessat.gordon@gmail.com (T. Gordon).

http://dx.doi.org/10.1016/j.expneurol.2015.03.022
0014-4886/© 2015 Elsevier Inc. All rights reserved.

axotomy) and chronic denervation of Schwann cells (SCs) in distal nerve stumps account for the progressive failure of recovery (Fu and Gordon, 1995a, 1995b; Gordon et al., 2011). The transient expression of growth associated genes in neurons and SCs after nerve injury parallel and account for the decline in the regenerative capacity of axotomized neurons and the regenerative support of the SCs, respectively (Boyd and Gordon, 2003; Brushart et al., 2014; Hoke et al., 2002, 2006; Miller et al., 1989; Scheib and Hoke, 2013; Sulaiman and Gordon, 2013; Tetzlaff et al., 1988).

In the present study, we ask whether the same ES paradigm that accelerates nerve regeneration after immediate repair promotes axon regeneration and target reinnervation after delayed nerve repair. We used a rat nerve cross-suture paradigm to determine whether ES promotes axon regeneration 1) of chronically axotomized motor and sensory neurons into freshly denervated nerve stumps, 2) of freshly axotomized neurons through chronically denervated SCs, and 3) into chronically denervated muscles. Finally we asked whether 4) the ES promoted axon regeneration after both chronic axotomy and chronic denervation, namely after delayed nerve repair.

Materials & methods

Animals and surgical methods

The experiments were performed on 132 female Sprague Dawley rats with an initial body weight of 200–250 g. The rats were divided into four groups: 1) acute axotomy of the common peroneal (CP) neurons and acute denervation of the tibial (TIB) nerve (n = 18), 2) chronic axotomy of CP neurons (n = 36), 3) chronic TIB nerve denervation (n = 60), and 4) combined chronic CP neuron axotomy and chronic TIB nerve denervation (n = 18). (Retrograde backlabeling of neurons was carried out in all the groups. In the third group, 24 of the 60 rats were used for motor unit number estimation [MUNE]). Within each group, after cross-suture of the CP proximal nerve stump to the TIB distal stump (CP-TIB nerve cross-suture), the CP nerve in half of the animals (n = 63) was electrically stimulated at 20 Hz for 1 h, while the nerve in the remaining 63 rats received sham electrical stimulation (ES). Within each of these groups, retrograde labeling of the distal TIB nerve was performed at two (n = 9) and four (n = 9) weeks after CP-TIB cross-suture and motor unit (MU) isometric force recordings were made at five months after the cross-suture (n = 9). The study protocol was approved by the animal committee of the University of Alberta Health Sciences Animal Care and Use Committee, Edmonton, Alberta, Canada. The animal care and all operative procedures were performed according to animal care and safety guidelines.

Nerve cross-coaptation (cross-neurorrhaphy)

Under general anesthesia induced by intraperitoneal injection of sodium pentobarbital (45 mg/kg) and aseptic conditions, the skin and muscles overlying the sciatic nerve of the right hindlimb were opened surgically to reveal the sciatic nerve and its CP, TIB and sural nerve branches (Fig. 1A; sural nerve not shown). The epineurial sheaths of the CP and TIB nerves were freed along the parent sciatic nerve by gentle dissection. In the first rat group, the CP and TIB nerves were transected and the proximal CP nerve stump immediately coapted together (Fig. 1A, E). In the remaining groups, either the CP nerve (Fig. 1B) and/or the TIB nerve (Fig. 1C) were transected and the CP and/or TIB proximal and distal nerve stumps each ligated and sutured into the normally innervated quadriceps muscle to prevent regeneration for a period of three months as described previously (Fu and Gordon, 1995a; Fu and Gordon, 1995b; Watson, 1970) (Fig. 1B–D). Under these circumstances the CP neurons were either chronically axotomized, not having the opportunity to remake functional contacts with denervated targets, and/or the distal TIB nerve stump was chronically denervated. The incisions were closed and the rats were allowed to recover under a heat lamp. Three months later, the nerves were exposed. The absence of axon regeneration of either or both the CP and TIB nerves was assured by examining the surgical site carefully and by electrically stimulating the proximal nerve stumps with a sterile pair of electrodes to assess whether there was any muscle movement under microscopic amplification. There being no evidence of reinnervation, no rats were discarded. The nerve stumps were freed and a 1–2 mm portion of the stumps removed to refresh the appropriate nerve stump for cross-coaptation of either the chronically axotomized CP and/or the chronically denervated TIB distal stumps (Fig. 1F–H).

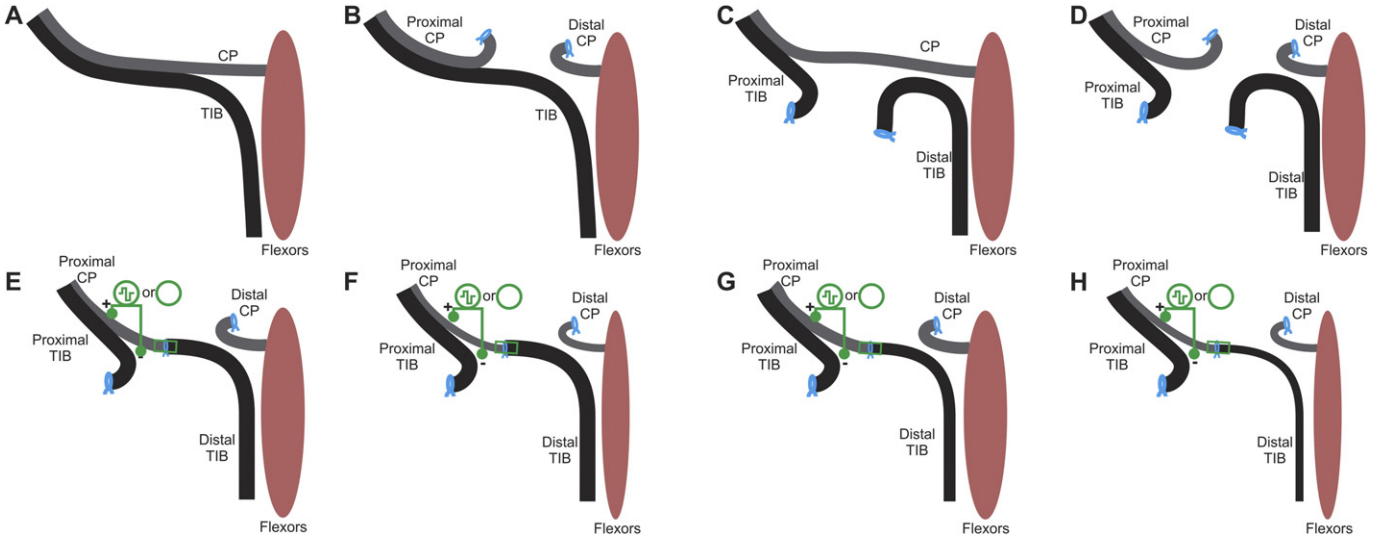


Fig. 1. Diagrammatic illustration of the surgical procedures of chronic axotomy and/or denervation, and of cross-coaptation (cross-suture). Nerve surgeries were performed unilaterally on one or both of the common peroneal (CP) and tibial (TIB) nerves (*A–D*). The CP and/or TIB nerve(s) was/were cut and the proximal CP nerve stump coapted to the distal TIB nerve stump (cross-coaptation) immediately (*E*) and/or either the CP (*B, D*) or TIB nerve stumps (*C, D*) ligated to prevent CP nerve regeneration and reinnervation of denervated targets (chronic axotomy) and/or to sustain the denervation of the Schwann cells in the distal nerve stump (chronic denervation). Three months later, the proximal CP nerve stump whose diameter is reduced following chronic axotomy (Gordon and Stein, 1982), was cross-sutured to the a freshly transected distal TIB nerve stump (*F*), or a freshly transected CP proximal nerve stump was sutured to a chronically denervated distal TIB nerve stump (*G*), or chronically axotomized CP nerve stump was cross-sutured to the chronically denervated TIB nerve stump (*H*). At the time of the cross-suture surgery, the CP nerve proximal to the cross-coaptation site was either electrically stimulated at supramaximal intensity (2× threshold) at 20 Hz for 1 h, or the nerve was subjected to sham stimulation for 1 h (*E–H*).

Chronic axotomy

In order to examine the nerve regeneration of the three month chronically axotomized CP neurons, the proximal CP nerve stump was freed and refreshed, the intact TIB nerve was transected and the proximal CP and distal TIB nerve stumps aligned for cross-suture within a 3 mm-long Silastic nerve cuff (Dow Corning 0.64 mm inner diameter) (Fig. 1F). Under 40× magnification, 9–0 Ethilon (Ethicon, Peterborough, ON, Canada) was sewn through the middle of the tube, the epineurium of the proximal and distal nerve stumps, and then out the middle of the tube. The CP and TIB nerve stumps were drawn together by gently pulling on the suture before tying the suture tied to secure the cross-coaptation (Furey et al., 2007). The freshly transected proximal TIB nerve stump was ligated and sutured to innervated muscle to prevent any regeneration of axons through the distal CP stump that remained ligated and sutured to innervated muscle (Fig. 1F).

Chronic denervation

In order to examine the efficacy of nerve regeneration of freshly axotomized CP neurons through a three month chronically denervated TIB nerve stump, the intact CP nerve was cut to cross-suture the proximal nerve stump to the refreshed TIB distal nerve stump within a 3 mm silastic tube (Fig. 1G). Again, the freshly transected distal CP nerve was ligated and axon regeneration prevented by suturing the stump to innervated muscle. The proximal TIB nerve stump remained ligated and the freshly transected distal CP nerve was ligated and sutured to the innervated muscle to prevent any CP nerve regeneration through the freshly denervated TIB distal nerve stump.

Chronic axotomy and denervation

Chronic axotomy of CP motor and sensory neurons and chronic denervation of distal TIB nerve were induced by cutting both the CP and TIB nerves at the same location and suturing the nerve stumps to innervated muscle to prevent nerve regeneration (Fig. 1D). After three months, the proximal CP nerve stump and the distal TIB nerve stumps were refreshed prior to their cross-union within a 3 mm-long Silastic nerve cuff (Fig. 1H).

Temporary placement of stimulating electrodes for 1 h for electrical or sham stimulation

Stainless steel wires were placed on the CP nerve stump proximal to the site of cross-suture of the proximal CP and distal TIB nerve stumps. The cathode was placed ~10 mm proximal to the suture site for supramaximal continuous electrical stimulation (ES) (100 μs, 3 V) of the proximal CP nerve stump for 1 h (experimental group n = 24) or sham stimulation with the stimulator off (control group n = 24) (Fig. 1E–H). The injury site was kept moist during the one hour period of ES by covering the exposed tissues with saline-moistened gauze. We chose the same low frequency 20 Hz train of electrical pulses that we used previously in several rat and human studies to demonstrate that the ES accelerates axon regeneration (Al-Majed et al., 2000a, 2000b; Brushart et al., 2002; Brushart et al., 2005; Eberhardt et al., 2006; Geremia et al., 2007; Gordon et al., 2010; Singh et al., 2012). Subsequently, the electrodes were removed and the wound was sutured closed. The rats were then allowed to recover under a heat lamp and returned to their cages.

The rats either survived for two or four weeks after which the CP motor and sensory neurons that had regenerated their axons into the TIB distal nerve stump were enumerated after fluorescent dye backlabeling (Fig. 2). A five month period of axon regeneration after CP-TIB cross-suture was allowed for reinnervation and recovery of reinnervated muscles from denervation atrophy before carrying out isometric force recordings from the reinnervated gastrocnemius muscles, as described below and shown in Fig. 3.

Retrograde labeling and counts of neurons that regenerate axons

The distal stump of the TIB nerve was exposed under sterile conditions, transected 10 mm distal to the site of the CP-TIB cross-coaptation, and the tip of the cut TIB nerve was exposed for 1 h to 5% fluororuby dextran tetramethylrhodamine (FR) (Molecular Probes, Eugene, OR, USA) diluted in saline within a silastic well created around the nerve stump (Fig. 2). Thereafter, the dye and the well were carefully removed after ensuring that the nerve stump was visibly stained with the retrograde dye. The incision site was then closed and the rats were allowed to recover consciousness. One week later, under deep pentobarbital anesthesia, the rats were transcardially perfused with 4% paraformaldehyde. The lumbosacral spinal cord and L4–5 dorsal root ganglia (DRG) was dissected, embedded in optimum cutting temperature (OCT) medium, and frozen for cryosectioning in 50 μm sagittal sections (spinal cord) or 20 μm cross-sections (DRG) to visualize and count retrogradely labeled motor and sensory neurons, respectively, under a fluorescent filter (excitation band pass 515–560) (Fig. 2). All the backlabeled motoneurons were counted by visualizing every spinal cord section while the sensory DRG neurons were visualized and counted on every 4th section. Only neurons in which a distinct nucleus could be seen were counted. These numbers were corrected to control for the counting of split nuclei using the method of Abercrombie (Abercrombie, 1946).

Recordings of isometric force of muscles and motor units in vivo

Under deep surgical anesthesia induced by intraperitoneal injection of pentobarbital, the CP nerve was exposed to place bipolar stimulating electrodes of the CP nerve proximal to the CP-TIB cross-coaptation site and to free and tie the tendon of the gastrocnemius muscle with #1 silk thread for attachment to a Grass (FT10) or Kulite (KH102A) force transducer (Fig. 3A). The rat was placed onto a heating pad at 37 °C for recording of isometric maximum twitch and tetanic forces in response to single and repetitive 100 Hz supramaximal (2× threshold) CP nerve stimulation with 100 μs long biphasic stimuli delivered to the CP nerve (Fig. 2B, C). Thereafter, the stimulus voltage was increased from 0 V upwards to recruit single MUs in an all-or-none manner with the contractile force increasing (Fig. 3D) to a maximum of 60% of the maximum muscle twitch force. The number of axotomized CP motoneurons that reinnervated the gastrocnemius muscle was computed by motor unit number estimation (MUNE), namely the division of the maximal muscle twitch force divided by the mean contractile force of the MUs (Fig. 3D), as described in detail previously (Hegedus et al., 2002, 2007; Major et al., 2007).

Statistics

Statistical comparisons were performed using SPSS 14.0 software. Values were expressed as a mean ± standard error (SE). The non-paired student T-test was used for comparisons of two groups or time points. Significance was accepted at 5% ($p < 0.05$).

Results

Electrical stimulation promotes motor and sensory nerve regeneration after immediate nerve repair

Axon outgrowth across a lesion site is normally a relatively slow process with growth cones encountering a disorganized array of denervated Schwann cells (SCs) and extracellular matrix components (Brushart et al., 2002; Witzel et al., 2005). The latter components include chondroitin sulfate that is inhibitory for growth and must be digested before axon growth proceeds through the suture site (Sabatier et al., 2012). Hence, after only two weeks, the number of CP motor and sensory neurons that regenerated their axons into the distal stump of tibial (TIB)

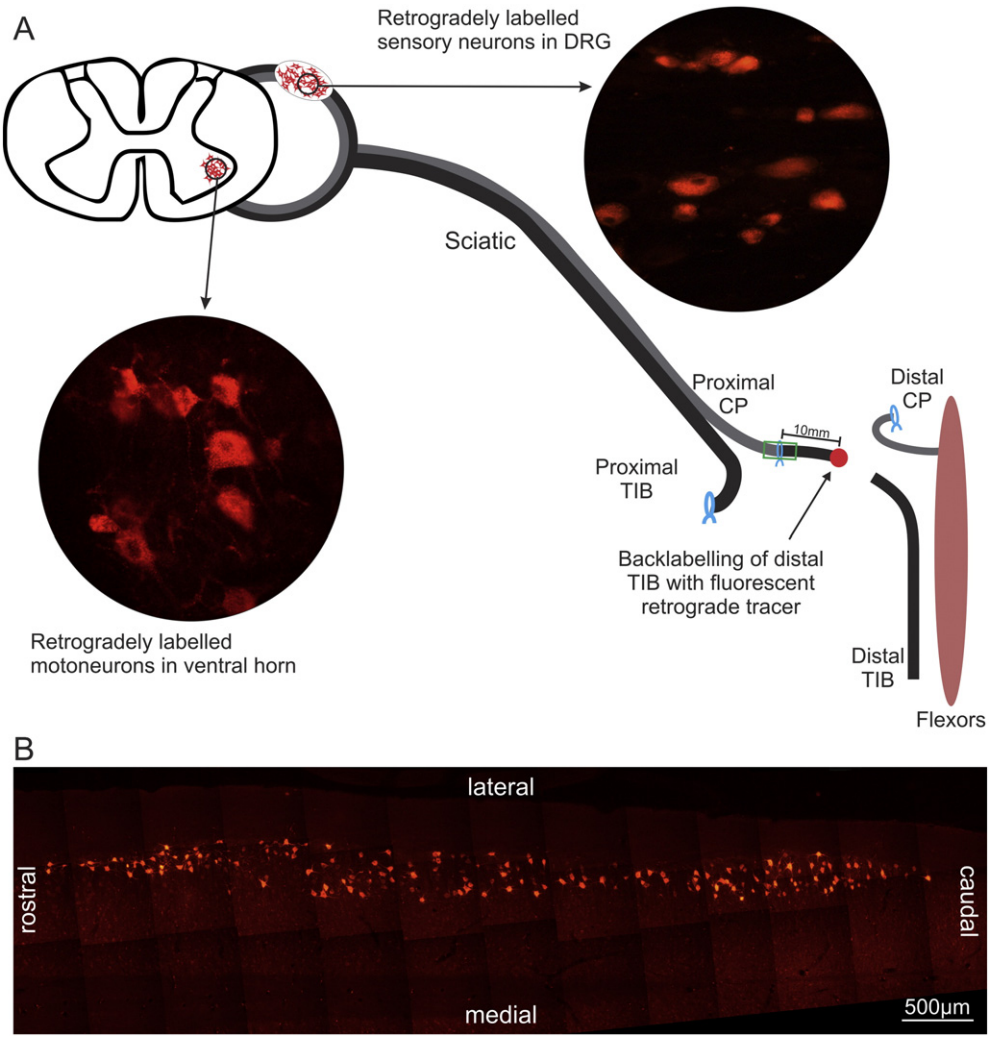


Fig. 2. Backlabeling of common peroneal (CP) motor and sensory neurons that regenerated their axons into the tibial (TIB) distal nerve stump for enumeration of neurons that regenerated their axons 2 and 4 weeks after cross-coaptation. *A.* Under aseptic conditions, the TIB distal nerve stump was cut 10 mm distal to the site of the cross-coaptation for application of 5% fluororuby (FR) diluted in saline within a silastic well. A week later the lumbosacral spinal cord and L4 and L5 dorsal root ganglia (DRGs) were dissected for cutting sagittal spinal cord sections and cross-sections of the DRG to examine and count the neurons containing FR that had regenerated their axons. *B.* An example of a sagittal section through the spinal cord of the CP motoneurons that regenerated their axons 10 mm from the cross-coaptation site. The motoneurons are located in the ventrolateral ventral horn of the spinal cord.

nerve was a fraction of the total number of CP neurons with axons in the intact common peroneal (CP) nerve (Fig. 4), consistent with the staggered axon regeneration described previously (Al-Majed et al., 2000a, 2000b; Boyd and Gordon, 2002). A one hour period of low frequency 20 Hz continuous electrical stimulation (ES) of axotomized CP neurons via electrodes on the proximal CP nerve stump significantly increased the number of motor and sensory CP neurons that regenerated their axons after immediate cross-CP-TIB nerve repair (Fig. 4). This is consistent with previous findings of the effect of ES in promoting axon regeneration after femoral, facial, and sciatic nerve crush injuries and after transection injuries in which the proximal and distal stumps of the transected nerves were opposed for coaptation (Al-Majed et al., 2000a, 2000b; Brushart et al., 2002; Eberhardt et al., 2006; Foecking et al., 2012; Geremia et al., 2007; Hetzler et al., 2008; Huang et al., 2013; Sharma et al., 2010a, 2010b; Singh et al., 2012). In turn, the ES promotes earlier reinnervation of denervated muscle (Gordon et al., 2010; Singh et al., 2012).

Electrical stimulation promotes motor and sensory nerve regeneration after chronic axotomy

Staggered axon regeneration across a suture site of transected nerve stumps (Brushart et al., 2002) was evident in the progressive increase in numbers of both motor and sensory neurons that regenerated their axons into the freshly denervated TIB nerve stump two and four weeks after CP-TIB cross-suture of a three month chronically axotomized CP nerve and a freshly denervated TIB nerve stump (Fig. 5B, C). ES at 20 Hz for 1 h that increased the number of motor and sensory neurons that regenerated their axons after immediate nerve repair (Fig. 4) also significantly increased the numbers of motor and sensory neurons that regenerated their axons over the same 10 mm distance into the freshly denervated TIB stump two and four weeks after the cross-suture repair *and* ES (Fig. 5B). Importantly, the ~1.8 increase in the number of motoneurons regenerating their axons was the same after two (Fig. 5B) and four weeks (Fig. 5C) and was the same increase seen after immediate nerve repair (Fig. 4). The effect of the ES is to promote axon outgrowth and *not* to accelerate the regeneration of the axons through the denervated endoneurial tubes of the distal nerve stump (Brushart et al., 2002).

The same ES paradigm was also effective in promoting sensory axon outgrowth to significantly increase the numbers of DRG neurons that regenerated their axons over the 10 mm distance to the site of retrograde dye application (Fig. 5C). Only ~10% of the DRG CP neurons regenerated their axons with two weeks after the three month period of chronic CP axotomy consistent with the deleterious effect of chronic axotomy on motor nerve regeneration (Fu and Gordon, 1995a). This

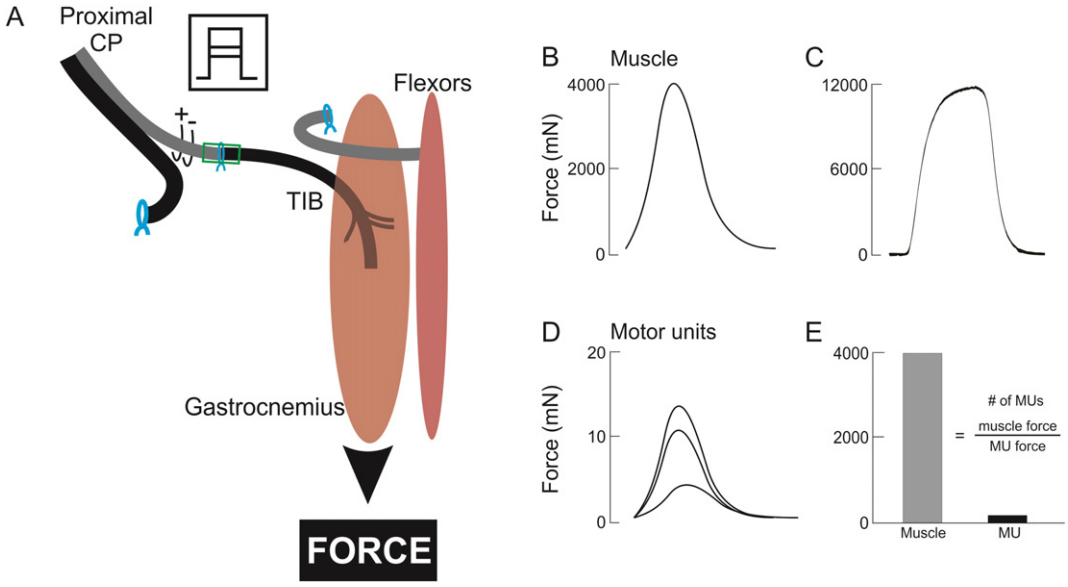


Fig. 3. Recording of isometric twitch and tetanic contractile forces of the reinnervated gastrocnemius muscle, five months after cross-suture of the proximal common peroneal (CP) and distal tibial nerve stumps. *A.* The CP nerve was stimulated proximal to the cross-suture site to evoke isometric twitch (*B*) and tetanic (*C*) forces in response to supramaximal (2× threshold) stimuli. *D.* All-or none increments in muscle force up to a maximum of 60% of the maximal twitch force were recorded in response to progressive increase of stimulus voltage from 0 V upwards with 100 μs biphasic stimuli delivered at 0.5 Hz (*E*). The number of CP motoneurons that reinnervated the gastrocnemius muscle was computed by motor unit estimation (MUNE), the division of the maximal muscle twitch force and mean twitch contractile force of the MUs (*E*).

number of DRG neurons increased ~3-fold at the four week time point of regeneration after surgical repair with the ES increasing the mean number of sensory neurons that regenerated their axons by the same factor of ~1.8 as for the freshly and chronically axotomized motoneurons (Figs. 4B and 5B).

Electrical stimulation promotes motor and sensory nerve regeneration and muscle reinnervation after chronic denervation

Chronic denervation of SCs in the denervated nerve stump is even more deleterious to nerve regeneration than chronic axotomy of the neurons, reducing the capacity of freshly axotomized neurons to regenerate their axons through the stumps to ~5% within six months, the decline being to ~40% within three months (Fu and Gordon, 1995b; Sulaiman and Gordon, 2009, 2000). A pronounced decline in axon regeneration through chronically denervated nerve stumps was evident as low numbers of freshly denervated CP motoneurons regenerating their axons 10 mm into a three month chronically denervated TIB distal nerve stump (Fig. 6B and D). We observed the same pronounced decline in sensory nerve regeneration (Fig. 6E), the effect of chronic denervation of SCs not having been documented before. Interestingly, there was a greater increase in the numbers of freshly axotomized CP neurons, both motor and sensory, that regenerated their axons into the chronically denervated TIB nerve stump after four weeks as compared to two weeks (Fig. 6). The same 1 h 20 Hz ES regime that promoted the ~1.8-fold increase in numbers of both freshly and chronically axotomized CP motor and sensory neurons to regenerate their axons into freshly denervated TIB nerve stump, promoted the same increase in freshly axotomized CP neurons that regenerated their axons into the chronically denervated TIB nerve stump (Fig. 6B-E).

Both the chronic denervation of SCs and the chronic muscle denervation contribute to reduced recovery of muscle after delayed nerve repair (Gordon et al., 2011). In a second group of rats, the freshly cut proximal CP nerve stump was cross-sutured to the three month chronically denervated TIB distal nerve stump as before but a five month period of nerve regeneration and muscle reinnervation was allowed after which muscle reinnervation was evaluated. Isometric twitch and tetanic contractions in the gastrocnemius muscle were evoked by stimulation of the CP nerve proximal to the cross-coaptation site (Fig. 3). The evoked twitch and tetanic contractions of the chronically denervated gastrocnemius muscle were substantially lower than the normally innervated contralateral control muscles, ~10 and 20%, respectively (Fig. 7A, B). While left to right comparisons of muscle contractions are frequently criticized, our studies demonstrated little compensatory increases in the contractile forces and weights in the contralateral control muscles as compared to those measured in a group of unoperated rats of the same body weights (Tam et al., 2001).

The one hour period of 20 Hz ES of the CP nerve proximal to the cross-coaptation with chronically denervated TIB nerve was effective in increasing the contractile twitch and tetanic force outcome measures of axon regeneration (Fig. 7A, B): ES almost doubled the contractile muscle forces of the reinnervated gastrocnemius muscle (Fig. 7A). This increase reflected the two-fold increase in the number of motoneurons that regenerated and reinnervated the gastrocnemius muscle (Fig. 7C) as estimated by the ratio of the maximal muscle twitch force (evoked in response to stimulating all the regenerated motor nerves) and the mean MU twitch force (evoked by all-or-none increments in the voltage of 100 μs stimulus pulses) (Fig. 3D, E). These findings demonstrated the effectiveness of the ES in enhancing regeneration through the chronically denervated SCs and into the chronically denervated muscles.

Electrical stimulation promotes motor and sensory nerve regeneration after delayed nerve repair of injured nerve

We determined whether the ES for 1 h is effective in promoting the regeneration of axons after delayed nerve repair where the neurons suffer the same period of chronic axotomy as the denervated SCs in the distal nerve stump and the denervated muscles suffer chronic denervation. The proximal nerve stump of both the transected CP and TIB nerves were ligated for three months in order to chronically axotomize and denervate the CP neurons and the TIB nerve SCs, respectively. Thereafter, we refreshed the proximal CP and the distal TIB nerve stumps for surgical repair and backlabeled the neurons that regenerated their axons 10 mm into the distal nerve stump (Fig. 8A). Consistent with the findings that the ES promoted axon outgrowth after chronic neuronal axotomy (Fig. 5) as well after chronic SC and muscle denervation

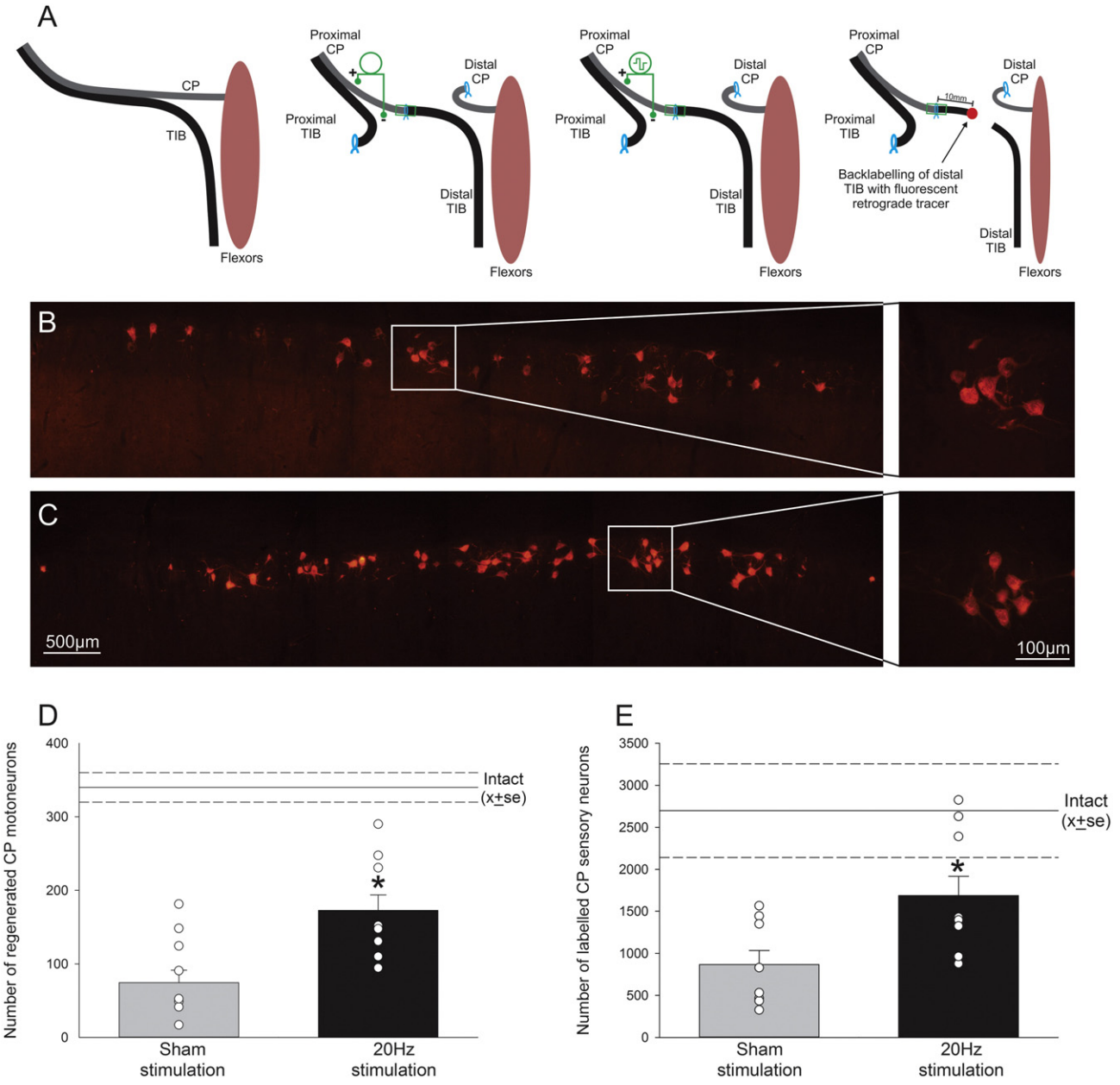


Fig. 4. Electrical stimulation (ES) promotes nerve regeneration after immediate nerve repair. The proximal stump of common peroneal (CP) nerve was cross-sutured to the distal tibial (TIB) nerve stump and either subjected to 20 Hz stimulation or sham 20 Hz ES for 1 h immediately after repair. Neurons were retrogradely labeled 10 mm from the cross-suture site with fluororuby (*A*). Typical sagittal sections of the spinal cord are shown at low and high magnification after sham ES (*B*) or ES (*C*). The ES significantly increased the number of both CP motor (*D*) and sensory (*E*) neurons that regenerated their axons into the distal TIB nerve stump within two weeks. Mean values ± SEs are shown with individual data points. $^{*}p < 0.05$. The means (x) ± SEs of the corresponding motor and sensory neurons that were not transected (intact neurons) prior to application of the retrograde dye, are shown by the horizontal lines, for comparison.

(Fig. 6), ES was also effective in significantly increasing the number of chronically axotomized neurons that regenerated their axons into the chronically denervated nerve stump (Fig. 8). This result demonstrates the efficacy of ES in promoting axon regeneration following delayed repair of a transection nerve injury. Indeed the ES affected the same increase in the number of motor and sensory neurons that regenerated their axons after delayed nerve repair as after immediate nerve suture (cf. Figs. 8 and 4).

Discussion

In a rat model of cross-coaptation of injured nerves, we found that brief low frequency electrical stimulation (ES) is as effective in accelerating nerve regeneration after delayed nerve repair as it is after immediate repair. Continuous 20 Hz ES for 1 h either immediately or after three months of chronic axotomy of hindlimb motor and sensory neurons, was equally effective in accelerating nerve regeneration through fresh or chronically denervated nerve stumps. Our experimental model of chronic axotomy prevented a transected nerve from regenerating and reinnervating denervated targets by ligating the proximal stump (Fu and Gordon, 1995a; Furey et al., 2007). The model of chronic denervation was to ligate the distal stump to prevent regenerating axons from entering into the stump (Fu and Gordon, 1995b). This rat model mimics the conditions of chronic neuron axotomy and chronic distal nerve and target denervation in patients who undergo delayed nerve repair and/or lengthy periods for axons to regenerate axons across inserted natural or artificial nerve grafts (Szynkaruk et al., 2013). The delay of a month or more for axons to

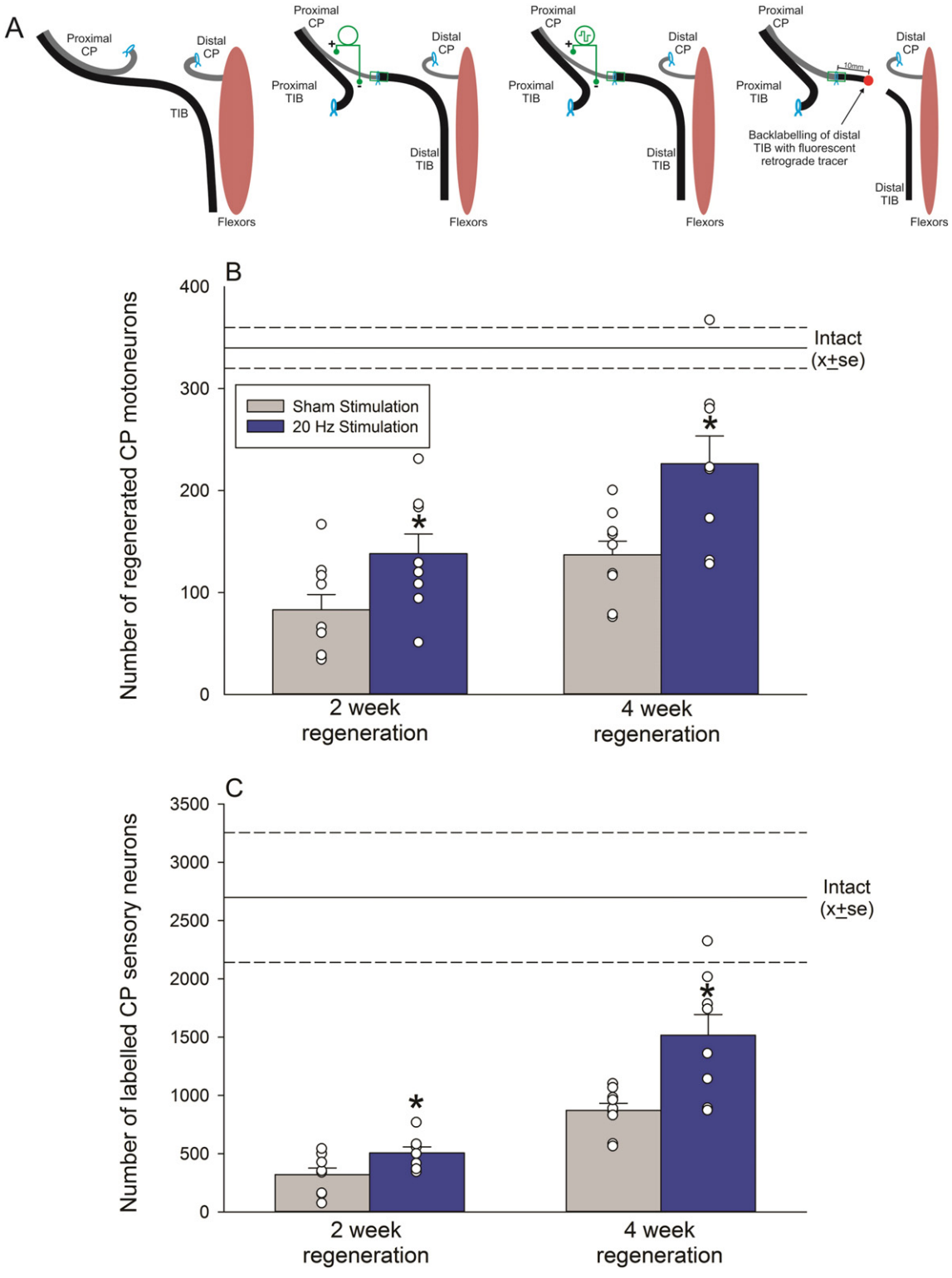


Fig. 5. One hour, 20 Hz electrical stimulation (ES) promotes axonal regeneration of chronically axotomized motor and sensory neurons. Following chronic axotomy of common peroneal (CP) neurons and subsequent cross-coaptation to the CP nerve to freshly cut tibial (TIB) distal nerve stump (*A*). The 20 Hz ES resulted in a significant increase in the number of chronically axotomized motor (B) and sensory (*C*) CP neurons that regenerated their axons into the freshly denervated TIB nerve stump 10 mm from the cross-suture site after two and four weeks. Mean values ± SEs are shown with individual data points. *$p < 0.05$. The means (x) ± SEs of the corresponding motor and sensory neurons that were not transected (intact neurons) prior to application of the retrograde dye, are shown by the horizontal lines, for comparison.

cross the first suture site (Brushart et al., 2002) may however, be considerably shorter across the second suture site because SCs will cross into the second site as the extracellular matrix becomes aligned within two weeks (Witzel et al., 2005).

In the relatively small rat model of chronic axotomy used here, where proximal nerve stump ligation is a good mimic of the lengthy periods of axon growth without target reinnervation (Fu and Gordon, 1995a; Furey et al., 2007), the finding that ES promotes the same degree

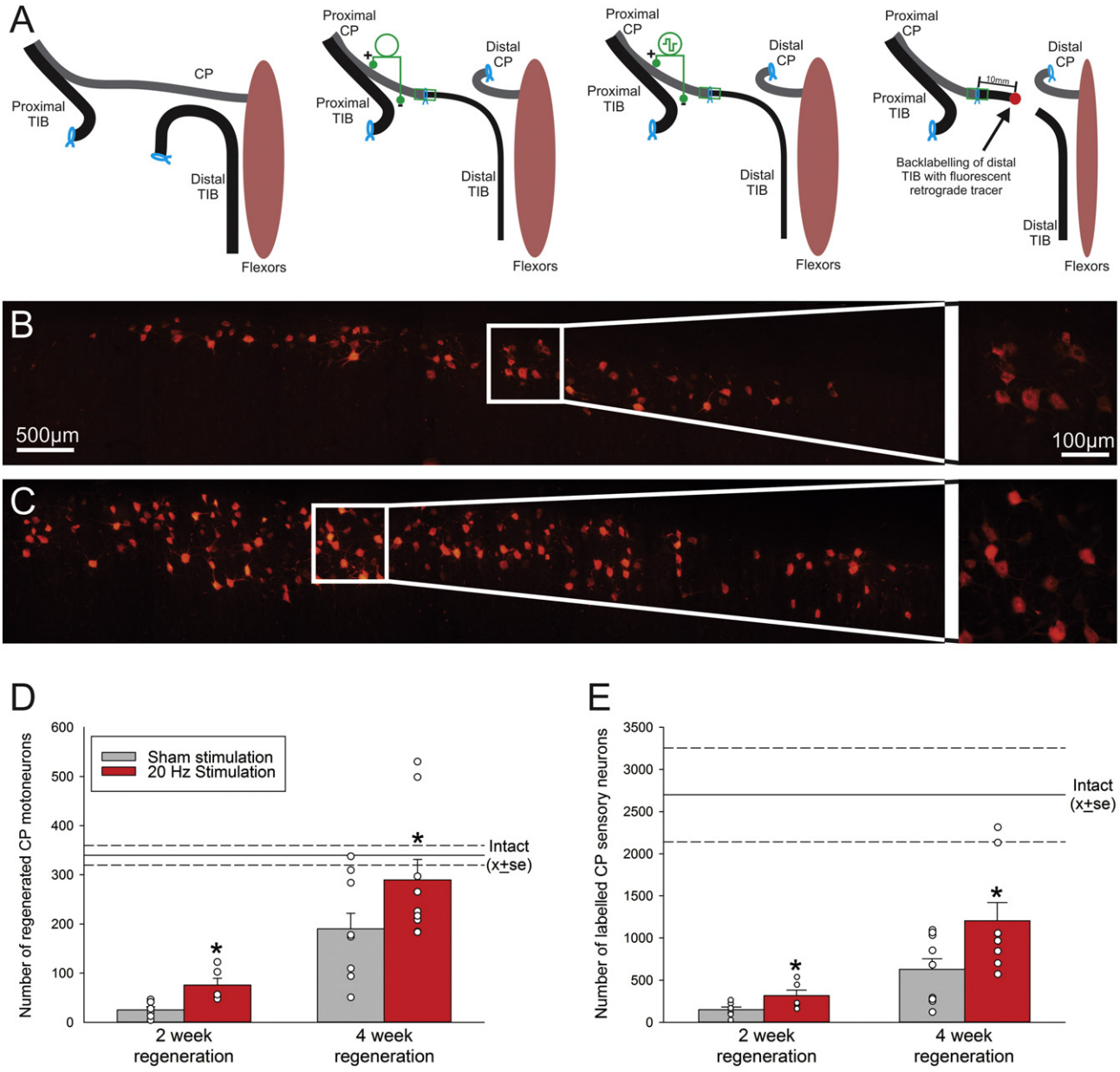


Fig. 6. One hour 20 Hz electrical stimulation (ES) promotes axonal regeneration of freshly axotomized common peroneal (CP) motor and sensory neurons through chronically denervated tibial (TIB) distal nerve stumps. Immediately following cross-coaptation of a freshly transected CP proximal nerve stump to a three month chronically denervated TIB distal nerve stump (*A*). Typical sagittal sections of the spinal cord containing retrogradely labeled motoneurons that regenerated their axons after sham ES (*B*) and ES (*C*) are shown at low and high magnifications. ES resulted in a significant increase in the number of freshly axotomized motor (*D*) and sensory (*E*) neurons that regenerated their axons into the chronically denervated TIB nerve stump at both two and four weeks following repair. Mean values ± SEs are shown with individual data points. *$p < 0.05$. The means (x) ± SEs of the corresponding motor and sensory neurons that were not transected (intact neurons) prior to application of the retrograde dye, are shown by the horizontal lines, for comparison.

of nerve regeneration and muscle reinnervation after delayed nerve repair as after immediate repair is encouraging for translation of ES to the clinic. The cross-coaptation nerve repair model allowed systematic investigation of the ES effect after chronic neuronal axotomy or Schwann cell (SC) denervation, as well after delayed nerve repair which combined both. ES effectively increased the capacities of chronically injured neurons to regenerate axons (Fig. 5) and of the chronically denervated SCs to support regeneration of both freshly and chronically injured neurons (Fig. 8) and of neurons to reinnervate chronically denervated muscle (Figs. 6, 7). These findings corroborate the effect of the same ES paradigm in accelerating muscle reinnervation after human carpal tunnel release surgery that was frequently delayed after symptoms (Gordon et al., 2010). Hence, ES may be beneficial for a broad patient population, including those patients with chronic nerve compression syndromes, delayed presentation or identification of nerve injuries, proximal nerve injuries, and where nerve transfers promote the reinnervation of chronically denervated distal nerve stumps and their target muscles and sense organs (Sulaiman et al., 2011).

Expression of regeneration associated genes in neurons [including tubulin, actin, neurotrophic factors and their receptors (Al-Majed et al., 2004; Bisby and Tetzlaff, 1992)] and in SCs [including several neurotrophic factors such as pleiotrophin, and the p75 receptor (Brushart et al., 2013; Hoke et al., 2006; Mi et al., 2007; You et al., 1997)] declines concomitant with an exponential decline in the regenerative capacity of axotomized neurons and the support of regenerating axons by denervated SCs (Boyd and Gordon, 2002; Fu and Gordon, 1995a; Fu and Gordon, 1995b; Sulaiman and Gordon, 2009.; Sulaiman and Gordon, 2000; You et al., 1997). ES elevates neuronal cAMP after immediate axotomy

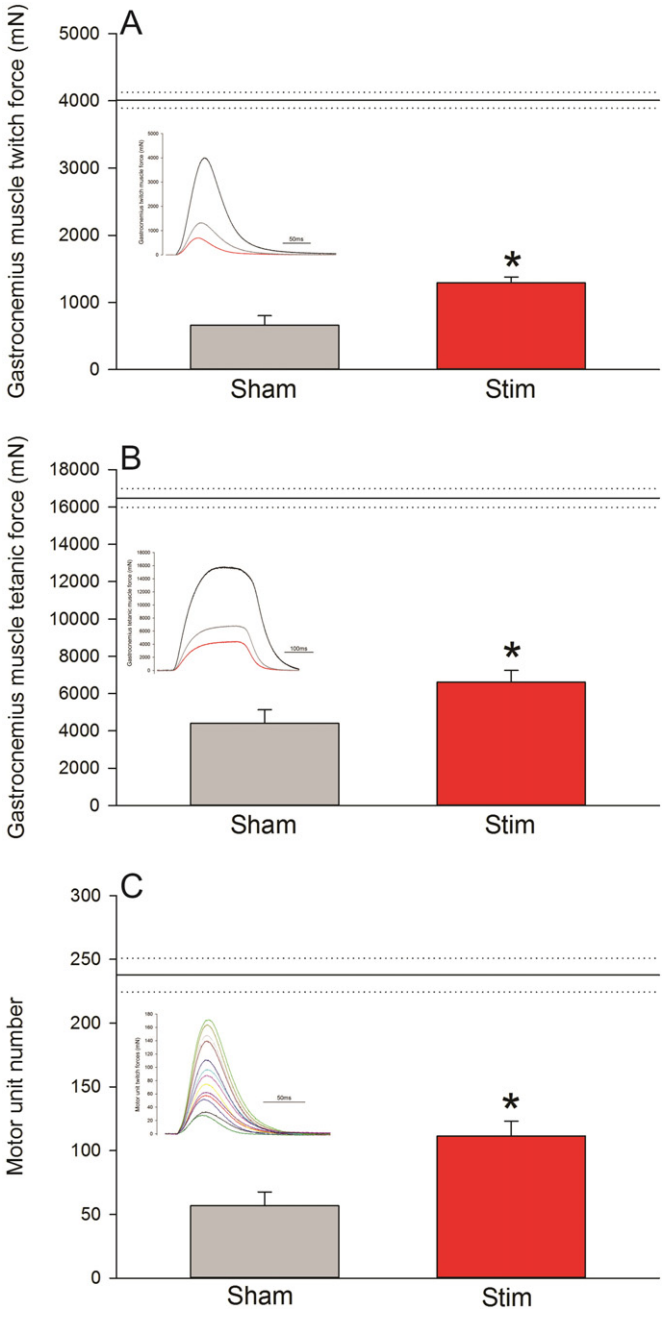


Fig. 7. One hour 20 Hz electrical stimulation (ES) accelerates recovery of muscle contraction and increases the number of regenerating motor axons that reinnervate muscle after reinnervation of a 3 month chronically denervated muscle. Isometric contractile forces of the gastrocnemius muscle and motor units (MUs) in response to single and tetanic stimulation of the CP motoneurons that cross-reinnervate the muscle via the TIB nerve. Mean (± SE) of the maximal twitch (*A*) and tetanic (*B*) contractile forces of gastrocnemius muscles reinnervated five months after CP-TIB nerve cross-suture was significantly higher after one hour 20 Hz ES (Stim) as compared to sham stimulation. There was a corresponding increase in MU numbers (*C*). Shown in the inserts are typical contractions of sham stimulated (red), stimulated (green) and contralateral unoperated (black) muscles. *$p < 0.05$.

(Aglah et al., 2008; Gordon et al., 2009; Udina et al., 2008; Udina et al., 2010), accelerates and increases the upregulation of neurotrophic factors and their receptors in neurons (Al-Majed et al., 2000a, 2000b; Sharma et al., 2010a) and SCs (Huang et al., 2010; Koppes et al., 2014b; Wan et al., 2010). Thereafter, ES accelerates and increases the neuronal expression of cytoskeletal proteins and growth associated proteins that include GAP-43 (Al-Majed et al., 2004).

That ES increases the release of nerve growth factor from SCs *in vivo* in a calcium-dependent manner indicated a possible role of the stimulated SCs in accelerating axon outgrowth especially as ES of the co-culture of sensory neurons and SCs is more effective than on neurons or SCs alone (Koppes et al., 2014a; Koppes et al., 2011; Koppes et al., 2014b). However, ES was effective in promoting axon outgrowth *in vivo* after delayed nerve repair whether or not SCs were chronically denervated (Fig. 5 and 8). SCs that remain chronically denervated for three months as was the case here, fail to express neurotrophic factors so that their response to ES is likely to be muted. Release of mitogens and possible other agents from the stimulated proximal CP nerve stump might be sufficient to promote proliferation of the chronically denervated SCs and their conversion to a growth permissive state with upregulated regeneration associated genes that include the neurotrophic factors.

After chronic axotomy, the refreshment injury of the proximal nerve stump to release the nerve from ligation before the cross-suture surgery, elevates regeneration associated genes but not to the same levels as after a fresh nerve injury (Gordon et al., 2015). The efficacy of ES in elevating the genes likely accounts for the increased regenerative capacity of the chronically axotomized neurons that were subjected to ES (Al-Majed et al., 2000a, 2000b, 2004; Geremia et al., 2007). The regeneration associated genes include BDNF, glial derived neurotrophic factor and NT-4/5, the latter in particular, being critical for the efficacy of ES in promoting nerve regeneration (English et al., 2007).

Neurotrophic factor expression may be sustained by androgens that are released in stimulated neurons, the efficacy of the ES blocked by flutamide blockade of androgen receptors (Thompson et al., 2014; Wood et al., 2012). Androgens released in males and females by daily exercise implemented within three days of nerve injury and repair (Thompson et al., 2014; Wood et al., 2012), promote nerve regeneration, continuous and intermittent exercise regimes being effective in males and females, respectively (Wood et al., 2012). The excellent motor and sensory nerve regeneration that was promoted by ES at the time of delayed nerve repair in the present study suggests that androgen receptors in the chronically axotomized neurons were sufficient to sustain, at least in part, neurotrophic factor expression. In turn, the factors enhance nerve regeneration, irrespective of whether the factors were expressed by SCs (Wilhelm et al., 2012). Hence, even after chronic SC denervation when neurotrophic factors and their receptors have long since been downregulated (Hoke et al., 2002; Hoke et al., 2006; Scheib and Hoke, 2013; You et al., 1997), ES likely promotes nerve regeneration by accelerating the upregulation of BDNF and likely other neurotrophic factors, and sustaining their expression via androgen activation of their receptors. In turn the regeneration associated genes that include the genes for cytoskeletal proteins, would be increased and axon outgrowth accelerated.

The same 1 h 20 Hz ES regime used in this study was used in several other studies to demonstrate accelerated axon regeneration and target reinnervation in rats after immediate nerve repair (Ahlborn et al., 2007; Al-Majed et al., 2000a, 2000b; Alrashdan et al., 2010; Asensio-Pinilla et al., 2009; English et al., 2007; Franz et al., 2008; Geremia et al., 2007; Hetzler et al., 2008; Huang et al., 2009, 2010, 2013; Koppes et al, 2014a, 2014b; Lu et al., 2008; Nix and Hopf, 1983; Sharma et al., 2009, 2010a, 2010b; Singh et al., 2012; Wan et al, 2010) and in humans after delayed release of the carpal tunnel (Gordon et al., 2010). Other ES paradigms have been used. A 20 Hz ES paradigm that commenced a day after a facial nerve crush injury and was repeated daily for 30 minutes, upregulated 1regeneration associated genes and accelerated axon outgrowth and functional return of eye movements (Hetzler et al., 2008; Lal et al., 2008; Sharma et al., 2009; Sharma et al., 2010a, 2010b). Some improvement was also demonstrated after a week of daily 15 minute 2 Hz ES of sciatic nerve commenced immediately after nerve coaptation or coaptation via a 10 mm long silicone tube (Lu et al., 2008; Yeh et al., 2010). It is pertinent to point out that exogenous androgens prolonged expression of BDNF in castrated male rats (Sharma et al., 2010a, 2010b) alongside their effectiveness in potentiating the efficacy of the daily 30 minute

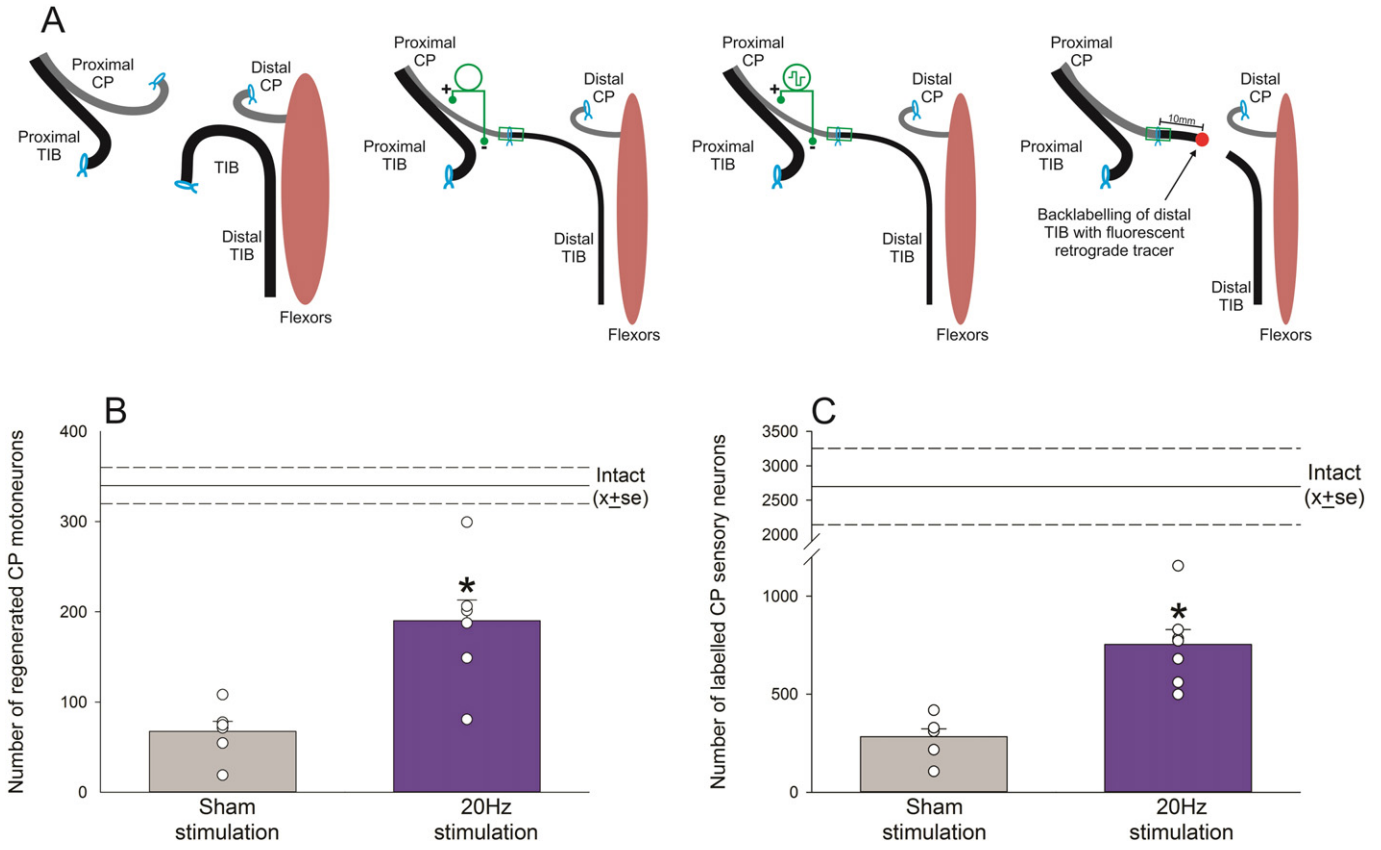


Fig. 8. One hour 20 Hz electrical stimulation (ES) is effective in promoting nerve regeneration after combined chronic neuronal axotomy and chronic Schwann cell denervation. Transected common peroneal (CP) proximal nerve *and* the denervated distal tibial (TIB) nerve stumps were prevented from regenerating for three months before cross-coaptation. Stimulation at 20 Hz for 1 h significantly increased the number of CP motor (*B*) and sensory (*C*) neurons that regenerated their axons 10 mm into the TIB nerve stump, as compared to the number after sham stimulation. Mean values ± SEs are shown with individual data points. *$p < 0.05$. The means (x) ± SEs of the corresponding motor and sensory neurons that were not transected (intact neurons) prior to application of the retrograde dye, are shown by the horizontal lines, for comparison.

20 Hz ES paradigm in promoting nerve regeneration and functional recovery in these rats after facial nerve crush injuries (Hetzler et al., 2008; Lal et al., 2008; Sharma et al., 2009). Accelerated axon growth was also observed two weeks after a five day 1 h period of exercise in rats (Boeltz et al., 2013; Udina et al., 2011a; Udina et al., 2011b). While these ES regimes were effective when the duration of the 20 Hz ES regimen was an hour or less and regardless of whether ES was administered once or repeated on successive days, it is noteworthy that longer periods of ES were ineffective because the trk receptors on sensory neurons are downregulated by ES periods of more than an hour (Geremia et al., 2007).

The only study of the efficacy of ES in accelerating axon regeneration after delayed nerve repair prior to the present study, used a 20 minute period of 20 Hz ES to evaluate nerve regeneration after delayed coaptation of three month ligated proximal and distal sciatic nerve stumps via a 5 mm long hollow nerve conduit (Huang et al., 2013). Using backlabeling to count neurons that had regenerated their axons during a four week period, ES was shown to promote small but significant increases of ~10% and ~3% in the proportions of axotomized motor and sensory neurons, respectively, that had regenerated their axons. These are small compared with the much higher proportions of 51% and 27% of the total number of CP motor and sensory neurons in this study that had regenerated their axons in the same four week period of axon regeneration after three months delayed coaptation of the CP proximal stump and TIB distal nerve stump and a full one hour period of 20 Hz ES (Fig. 8). Explanations for the relatively small effect of the 20 minute period of 20 Hz ES in promoting regeneration after delayed sciatic nerve repair include the insertion of the 5 mm hollow artificial conduit repair between proximal and distal nerve sciatic stumps and, perhaps more important, the shorter duration of ES period in the Huang study. An additional factor was the two coaptation sites required to insert the conduit in Huang's study. The short ES duration may also impact negatively on regeneration of chronically injured neurons through two coaptation sites, a possibility that is imminently testable.

In summary, brief 20 Hz ES promotes nerve regeneration after delayed nerve repair. Deleterious effects of prolonged neuronal axotomy and SC denervation in the distal nerve stumps after nerve injuries that are sustained far from their denervated targets, result in poor if any functional recovery. The efficacy of ES to promote functional recovery has immediate clinical relevance especially in light of the positive findings reported in a proof of principle study of the efficacy of ES is promoting nerve regeneration and target muscle reinnervation after carpal tunnel release surgery (Gordon et al., 2010).

Conflict of interest

The authors declare no competing financial interests. All coauthors have seen and agree with the contents of the manuscript, believe that it represents honest work, and meet the ICMJE requirements for authorship. This manuscript is not under review at any other publication.

References

Abercrombie, M., 1946. Estimation of nuclear population from microtome sections. Anat. Rec. 94, 239–247.
Aglah, C., Gordon, T., Posse De Chaves, E.I., 2008. cAMP promotes neurite outgrowth and extension through protein kinase A but independently of Erk activation in cultured rat motoneurons. Neuropharmacology 55, 8–17.
Ahlborn, P., Schachner, M., Irintchev, A., 2007. One hour electrical stimulation accelerates functional recovery after femoral nerve repair. Exp. Neurol. 208, 137–144.
Al-Majed, A.A., Brushart, T.M., Gordon, T., 2000a. Electrical stimulation accelerates and increases expression of BDNF and trkB mRNA in regenerating rat femoral motoneurons. Eur. J. Neurosci. 12, 4381–4390.

Al-Majed, A.A., Neumann, C.M., Brushart, T.M., Gordon, T., 2000b. Brief electrical stimulation promotes the speed and accuracy of motor axonal regeneration. J. Neurosci. 20, 2602–2608.
Al-Majed, A.A., Tam, S.L., Gordon, T., 2004. Electrical stimulation accelerates and enhances expression of regeneration-associated genes in regenerating rat femoral motoneurons. Cell. Mol. Neurobiol. 24, 379–402.
Alrashdan, M.S., Park, J.C., Sung, M.A., Yoo, S.B., Jahng, J.W., Lee, T.H., Kim, S.J., Lee, J.H., 2010. Thirty minutes of low intensity electrical stimulation promotes nerve regeneration after sciatic nerve crush injury in a rat model. Acta Neurol. Belg. 110, 168–179.
Asensio-Pinilla, E., Udina, E., Jaramillo, J., Navarro, X., 2009. Electrical stimulation combined with exercise increase axonal regeneration after peripheral nerve injury. Exp. Neurol. 219, 258–265.
Bisby, M.A., Tetzlaff, W., 1992. Changes in cytoskeletal protein synthesis following axon injury and during axon regeneration. Mol. Neurobiol. 6, 107–123.
Boeltz, T., Ireland, M., Mathis, K., Nicolini, J., Poplavski, K., Rose, S.J., Wilson, E., English, A.W., 2013. Effects of treadmill training on functional recovery following peripheral nerve injury in rats. J. Neurophysiol. 109, 2645–2657.
Boyd, J.G., Gordon, T., 2002. A dose-dependent facilitation and inhibition of peripheral nerve regeneration by brain-derived neurotrophic factor. Eur. J. Neurosci. 15, 613–626.
Boyd, J.G., Gordon, T., 2003. Neurotrophic factors and their receptors in axonal regeneration and functional recovery after peripheral nerve injury. Mol. Neurobiol. 27, 277–324.
Brushart, T.M., Hoffman, P.N., Royall, R.M., Murinson, B.B., Witzel, C., Gordon, T., 2002. Electrical stimulation promotes motoneuron regeneration without increasing its speed or conditioning the neuron. J. Neurosci. 22, 6631–6638.
Brushart, T.M., Jari, R., Verge, V., Rohde, C., Gordon, T., 2005. Electrical stimulation restores the specificity of sensory axon regeneration. Exp. Neurol. 194, 221–229.
Brushart, T.M., Aspalter, M., Griffin, J.W., Redett, R., Hameed, H., Zhou, C., Wright, M., Vyas, A., Hoke, A., 2013. Schwann cell phenotype is regulated by axon modality and central-peripheral location, and persists in vitro. Exp. Neurol. 247C, 272–281.
Eberhardt, K.A., Irintchev, A., Al-Majed, A.A., Simova, O., Brushart, T.M., Gordon, T., Schachner, M., 2006. BDNF/TrkB signaling regulates HNK-1 carbohydrate expression in regenerating motor nerves and promotes functional recovery after peripheral nerve repair. Exp. Neurol. 198, 500–510.
English, A.W., Schwartz, G., Meador, W., Sabatier, M.J., Mulligan, A., 2007. Electrical stimulation promotes peripheral axon regeneration by enhanced neuronal neurotrophin signaling. Dev. Neurobiol. 67, 158–172.
Foecking, E.M., Fargo, K.N., Coughlin, L.M., Kim, J.T., Marzo, S.J., Jones, K.J., 2012. Single session of brief electrical stimulation immediately following crush injury enhances functional recovery of rat facial nerve. J. Rehabil. Res. Dev. 49, 451–458.
Franz, C.K., Rutishauser, U., Rafuse, V.F., 2005. Polysialylated neural cell adhesion molecule is necessary for selective targeting of regenerating motor neurons. J. Neurosci. 25, 2081–2091.
Franz, C.K., Rutishauser, U., Rafuse, V.F., 2008. Intrinsic neuronal properties control selective targeting of regenerating motoneurons. Brain 131, 1492–1505.
Fu, S.Y., Gordon, T., 1995a. Contributing factors to poor functional recovery after delayed nerve repair: prolonged axotomy. J. Neurosci. 15, 3876–3885.
Fu, S.Y., Gordon, T., 1995b. Contributing factors to poor functional recovery after delayed nerve repair: prolonged denervation. J. Neurosci. 15, 3886–3895.
Furey, M.J., Midha, R., Xu, Q.G., Belkas, J., Gordon, T., 2007. Prolonged target deprivation reduces the capacity of injured motoneurons to regenerate. Neurosurgery 60, 723–732.
Geremia, N.M., Gordon, T., Brushart, T.M., Al-Majed, A.A., Verge, V.M., 2007. Electrical stimulation promotes sensory neuron regeneration and growth-associated gene expression. Exp. Neurol. 205, 347–359.
Gordon, T., Stein, R.B., 1982. Time course and extent of recovery in reinnervated motor units of cat triceps surae muscles. J. Physiol. Lond. 323, 307–323.
Gordon, T., Sulaiman, O.A.R., 2013. In: Kettenmann, H., Ransom, B.R. (Eds.), Nerve Regeneration In The Peripheral Nervous System. Neuroglia Oxford University Press, pp. 701–714.
Gordon, T., Udina, E., Verge, V.M., de Chaves, E.I., 2009. Brief electrical stimulation accelerates axon regeneration in the peripheral nervous system and promotes sensory axon regeneration in the central nervous system. Mot. Control. 13, 412–441.
Gordon, T., Amirjani, N., Edwards, D.C., Chan, K.M., 2010. Brief post-surgical electrical stimulation accelerates axon regeneration and muscle reinnervation without affecting the functional measures in carpal tunnel syndrome patients. Exp. Neurol. 223, 192–202.
Gordon, T., Tyreman, N., Raji, M.A., 2011. The basis for diminished functional recovery after delayed peripheral nerve repair. J. Neurosci. 31, 5325–5334.
Gordon, T., You, S., Cassar, S.L., Tetzlaff, W., 2015. Reduced expression of regeneration associated genes in chronically axotomized facial motoneurons. Exp. Neurol. 264, 26–32.
Hegedus, J., Yu, J.S.C., Bathini, V., Gordon, T., 2002. Muscle fiber type distribution in patients with ALS and in a transgenic mouse model of familial ALS. Soc Neurosci 32nd Annual Meeting. 27, p. 888.7 (Ref Type: Abstract).
Hegedus, J., Putman, C.T., Gordon, T., 2007. Time course of preferential motor unit loss in the SOD1(G93A) mouse model of amyotrophic lateral sclerosis. Neurobiol. Dis. 28, 154–164.
Hetzler, L.E., Sharma, N., Tanzer, L., Wurster, R.D., Leonetti, J., Marzo, S.J., Jones, K.J., Foecking, E.M., 2008. Accelerating functional recovery after rat facial nerve injury: effects of gonadal steroids and electrical stimulation. Otolaryngol. Head Neck Surg. 139, 62–67.
Hoke, A., Gordon, T., Zochodne, D.W., Sulaiman, O.A.R., 2002. A decline in glial cell-line-derived neurotrophic factor expression is associated with impaired regeneration after long-term Schwann cell denervation. Exp. Neurol. 173, 77–85.
Hoke, A., Redett, R., Hameed, H., Jari, R., Zhou, C., Li, Z.B., Griffin, J.W., Brushart, T.M., 2006. Schwann cells express motor and sensory phenotypes that regulate axon regeneration. J. Neurosci. 26, 9646–9655.
Huang, J., Hu, X., Lu, L., Ye, Z., Wang, Y., Luo, Z., 2009. Electrical stimulation accelerates motor functional recovery in autograft-repaired 10 mm femoral nerve gap in rats. J. Neurotrauma 26,185–1813.
Huang, J., Ye, Z., Hu, X., Lu, L., Luo, Z., 2010. Electrical stimulation induces calcium-dependent release of NGF from cultured Schwann cells. GLIA 58, 622–631.
Huang, J., Zhang, Y., Lu, L., Hu, X., Luo, Z., 2013. Electrical stimulation accelerates nerve regeneration and functional recovery in delayed peripheral nerve injury in rats. Eur. J. Neurosci.
Hudson, A.R., Hunter, D., 1977. Timing of peripheral nerve repair: important local neuropathological factors. Clin. Neurosurg. 24, 391–405.
Koppes, A.N., Seggio, A.M., Thompson, D.M., 2011. Neurite outgrowth is significantly increased by the simultaneous presentation of Schwann cells and moderate exogenous electric fields. J. Neural Eng. 8, 046023.
Koppes, A.N., Nordberg, A.L., Paolillo, G.M., Goodsell, N.M., Darwish, H.A., Zhang, L., Thompson, D.M., 2014a. Electrical stimulation of Schwann cells promotes sustained increases in neurite outgrowth. Tissue Eng. A 20, 494–506.
Koppes, A.N., Zaccor, N.W., Rivet, C.J., Williams, L.A., Piselli, J.M., Gilbert, R.J., Thompson, D.M., 2014b. Neurite outgrowth on electrospun PLLA fibers is enhanced by exogenous electrical stimulation. J. Neural Eng. 11, 046002.
Lal, D., Hetzler, L.T., Sharma, N., Wurster, R.D., Marzo, S.J., Jones, K.J., Foecking, E.M., 2008. Electrical stimulation facilitates rat facial nerve recovery from a crush injury. Otolaryngol. Head Neck Surg. 139, 68–73.
Lu, M.C., Ho, C.Y., Hsu, S.F., Lee, H.C., Lin, J.H., Yao, C.H., Chen, Y.S., 2008. Effects of electrical stimulation at different frequencies on regeneration of transected peripheral nerve. Neurorehabil. Neural Repair 22, 367–373.
Lundborg, G., 2004. Nerve Injury And Repair. Churchill Livingstone, New York.
Major, L.A., Hegedus, J., Weber, D.J., Gordon, T., Jones, K.E., 2007. Method for counting motor units in mice and validation using a mathematical model. J. Neurophysiol. 97, 1846–1856.
Mi, R., Chen, W., Hoke, A., 2007. Pleiotrophin is a neurotrophic factor for spinal motor neurons. Proc. Natl. Acad. Sci. U. S. A. 104, 4664–4669.
Miller, F.D., Tetzlaff, W., Bisby, M.A., Fawcett, J.W., Milner, R.J., 1989. Rapid induction of the major embryonic alpha-tubulin mRNA, T alpha 1, during nerve regeneration in adult rats. J. Neurosci. 9, 1452–1463.
Nix, W.A., Hopf, H.C., 1983. Electrical stimulation of regenerating nerve and its effect on motor recovery. Brain Res. 272, 21–25.
Sabatier, M.J., To, B.N., Rose, S., Nicolini, J., English, A.W., 2012. Chondroitinase ABC reduces time to muscle reinnervation and improves functional recovery after sciatic nerve transection in rats. J. Neurophysiol. 107, 747–757.
Scheib, J., Hoke, A., 2013. Advances in peripheral nerve regeneration. Nat. Rev. Neurol. 9, 668–676.
Sharma, N., Coughlin, L., Porter, R.G., Tanzer, L., Wurster, R.D., Marzo, S.J., Jones, K.J., Foecking, E.M., 2009. Effects of electrical stimulation and gonadal steroids on rat facial nerve regenerative properties. Restor. Neurol. Neurosci. 27, 633–644.
Sharma, N., Marzo, S.J., Jones, K.J., Foecking, E.M., 2010a. Electrical stimulation and testosterone differentially enhance expression of regeneration-associated genes. Exp. Neurol. 223, 183–191.
Sharma, N., Moeller, C.W., Marzo, S.J., Jones, K.J., Foecking, E.M., 2010b. Combinatorial treatments enhance recovery following facial nerve crush. Laryngoscope 120, 1523–1530.
Singh, B., Xu, Q.G., Franz, C.K., Zhang, R., Dalton, C., Gordon, T., Verge, V.M., Midha, R., Zochodne, D.W., 2012. Accelerated axon outgrowth, guidance, and target reinnervation across nerve transection gaps following a brief electrical stimulation paradigm. J. Neurosurg. 116, 498–512.
Sulaiman, O.A.R., Gordon, T., 2000. Effects of short- and long-term Schwann cell denervation on peripheral nerve regeneration, myelination, and size. GLIA 32, 234–246.
Sulaiman, O.A., Gordon, T., 2009. Role of chronic Schwann cell denervation in poor functional recovery after nerve injuries and experimental strategies to combat it. Neurosurgery 65, A105–A114.
Sulaiman, W., Gordon, T., 2013. Neurobiology of peripheral nerve injury, regeneration, and functional recovery: from bench top research to bedside application. Ochsner. J. 13, 100–108.
Sulaiman, O.A.R., Midha, R., Gordon, T., 2011. In: Winn, H.R. (Ed.), Athophysiology Of Surgical Nerve Disorders. Yeomans Neurological Surgery Saunders, Philadelphia.
Szynkaruk, M., Kemp, S.W., Wood, M.D., Gordon, T., Borschel, G.H., 2013. Experimental and clinical evidence for use of decellularized nerve allografts in peripheral nerve gap reconstruction. Tissue Eng. B Rev. 19, 83–96.
Tam, S.L., Archibald, V., Tyreman, N., Jassar, B., Gordon, T., 2001. Increased neuromuscular activity reduces sprouting in partially denervated muscles. J. Neurosci. 21, 654–667.
Tetzlaff, W., Bisby, M.A., Kreutzberg, G.W., 1988. Changes in cytoskeletal proteins in the rat facial nucleus following axotomy. J. Neurosci. 8, 3181–3189.
Thompson, N.J., Sengelaub, D.R., English, A.W., 2014. Enhancement of peripheral nerve regeneration due to treadmill training and electrical stimulation is dependent on androgen receptor signaling. Dev. Neurobiol. 74, 531–540.
Udina, E., Furey, M., Busch, S., Silver, J., Gordon, T., Fouad, K., 2008. Electrical stimulation of intact peripheral sensory axons in rats promotes outgrowth of their central projections. Exp. Neurol. 210, 238–247.
Udina, E., Ladak, A., Furey, M., Brushart, T., Tyreman, N., Gordon, T., 2010. Rolipram-induced elevation of cAMP or chondroitinase ABC breakdown of inhibitory proteoglycans in the extracellular matrix promotes peripheral nerve regeneration. Exp. Neurol. 223, 143–152.
Udina, E., Cobianchi, S., Allodi, I., Navarro, X., 2011a. Effects of activity-dependent strategies on regeneration and plasticity after peripheral nerve injuries. Ann. Anat. 193, 347–353.

Udina, E., Puigdemasa, A., Navarro, X., 2011b. Passive and active exercise improve regeneration and muscle reinnervation after peripheral nerve injury in the rat. Muscle Nerve 43, 500–509.
Wan, L.D., Xia, R., Ding, W.L., 2010. Electrical stimulation enhanced remyelination of injured sciatic nerves by increasing neurotrophins. Neuroscience 169, 1029–1038.
Watson, W.E., 1970. Some metabolic responses of axotomized neurones to contact between their axons and denervated muscle. J. Physiol. Lond. 210, 321–343.
Wilhelm, J.C., Xu, M., Cucoranu, D., Chmielewski, S., Holmes, T., Lau, K.S., Bassell, G.J., English, A.W., 2012. Cooperative roles of BDNF expression in neurons and Schwann cells are modulated by exercise to facilitate nerve regeneration. J. Neurosci. 32, 5002–5009.
Witzel, C., Rohde, C., Brushart, T.M., 2005. Pathway sampling by regenerating peripheral axons. J. Comp. Neurol. 485, 183–190.
Wood, K., Wilhelm, J.C., Sabatier, M.J., Liu, K., Gu, J., English, A.W., 2012. Sex differences in the effectiveness of treadmill training in enhancing axon regeneration in injured peripheral nerves. Dev. Neurobiol. 72, 688–698.
Yeh, C.C., Lin, Y.C., Tsai, F.J., Huang, C.Y., Yao, C.H., Chen, Y.S., 2010. Timing of applying electrical stimulation is an important factor deciding the success rate and maturity of regenerating rat sciatic nerves. Neurorehabil. Neural Repair 24, 730–735.
You, S., Petrov, T., Chung, P.H., Gordon, T., 1997. The expression of the low affinity nerve growth factor receptor in long-term denervated Schwann cells. GLIA 20, 87–100.

Available online at www.sciencedirect.com
ScienceDirect
Experimental Neurology 210 (2008) 238–247
Experimental Neurology
www.elsevier.com/locate/yexnr

Electrical stimulation of intact peripheral sensory axons in rats promotes outgrowth of their central projections

Esther Udina [a], Matthew Furey [a], Sarah Busch [c], Jerry Silver [c], Tessa Gordon [a,*], Karim Fouad [b]

[a] *Division of Physical Medicine and Rehabilitation, Faculty of Medicine and Dentistry, University of Alberta, Edmonton, Alberta, Canada T6G 2S2*
[b] *Faculty of Rehabilitation Medicine, Division of Neurosciences, University of Alberta, Edmonton, Alberta, Canada T6G 2S2*
[c] *Case Western Reserve University School of Medicine, Department of Neurosciences, 2109 Adelbert Road E-658, Cleveland, Ohio 44106, USA*

Received 12 September 2007; revised 30 October 2007; accepted 2 November 2007
Available online 22 November 2007

Abstract

A lesion of a peripheral nerve before a second injury (conditioning lesion, CL), enhances peripheral and central regeneration of dorsal root ganglion (DRG) axons. This effect is mediated by elevated neuronal cAMP. Here we wanted to investigate whether electrical stimulation (ES) of an intact nerve, which has been shown to accelerate peripheral axon outgrowth, is also effective in promoting axon regeneration of injured DRG axons *in vitro* and of the central DRG axons *in vivo* and, whether this effect is mediated by elevation of cAMP. For the *in vitro* assay, the intact sciatic nerve of adult rats was stimulated at 20 Hz for 1 h, 7 days before harvest and primary culture of DRG neurons on a growth permissive substrate. In the *in vivo* study, the central axons of the lumbosacral DRGs were cut in the Th8 dorsal column, and the sciatic nerve was either cut or left intact, and subjected to 1 h ES at 20 Hz or 200 Hz. *In vitro*, ES increased neurite outgrowth 4-fold as compared to non-stimulated DRG neurons. *In vivo*, ES at 20 Hz significantly increased axon outgrowth into the central lesion site as compared to the Sham control. The 20 Hz ES was as effective as the CL in increasing axon outgrowth into the lesion site but not in promoting axonal elongation even though 20 Hz ES increased intracellular cAMP levels in DRG neurons as effectively as the CL. Thus elevation of cAMP may account for the central axonal outgrowth after ES and a CL.
© 2007 Elsevier Inc. All rights reserved.

Keywords: Electrical stimulation; Axonal regeneration; Conditioning lesion; DRG; Neurite outgrowth; Spinal cord; cAMP; Peripheral nerve; Rat

Introduction

Injured axons in the central nervous system (CNS) fail to regenerate (Schwab and Bartholdi, 1996; Silver and Miller, 2004) in contrast to those in the peripheral nervous system (PNS) (Fu and Gordon, 1997). This disparity is illustrated by the capacity of injured peripheral but not central axons of dorsal root ganglion (DRG) sensory neurons to regenerate. Axonal injury in the PNS but not the CNS, leads to pronounced expression of growth associated genes (Broude et al., 1997; Schreyer and Skene, 1993). Moreover, the injured CNS has an abundance of inhibitory molecules such as myelin associated proteins (Filbin, 2003) and proteoglycans at the glial scar (Busch and Silver, 2007) that are an impediment to axonal regeneration.

Experimental strategies to promote axonal regeneration in the CNS include attempts to create a growth permissive environment (Fouad and Pearson, 2004; Houle et al., 2006), and/or altering the neuronal response to inhibitory molecules (Domeniconi and Filbin, 2005). For example, the neuronal regenerative response has been altered by elevating intraneuronal cAMP levels pharmacologically or by a conditioning lesion (CL) of DRG sensory neurons (Neumann et al., 2002; Qiu et al., 2002; Cai et al., 1999; Dergham et al., 2002; Lehmann et al., 1999). The CL, a lesion of a peripheral axons before a second injury, enhances peripheral (McQuarrie and Grafstein, 1973; McQuarrie et al., 1977) and central (Neumann and Woolf, 1999; Richardson and Issa, 1984) axonal regeneration. Recently, a relatively noninvasive 1 h period of electrical stimulation (ES) proximal to a site of transection and surgical repair of a pheripheral nerve has also been shown to accelerate axonal outgrowth across the injury site (Al-Majed et al., 2000b; Brushart et al., 2002). This effect has been related to an up-

* Corresponding author. 525HMRC, Center for Neurosciences, University Alberta, Edmonton, Alberta, Canada T6G 2S2.
E-mail address: tessa.gordon@ualberta.ca (T. Gordon).

0014-4886/$ - see front matter © 2007 Elsevier Inc. All rights reserved.
doi:10.1016/j.expneurol.2007.11.007

regulation of regeneration associated genes (Al-Majed et al., 2000a, 2004). In this study, we asked whether ES of the intact sciatic nerve also promotes regeneration of DRG axons in the CNS after a dorsal column lesion. First, we determined the effects of ES on neurite growth in an *in vitro* preparation of DRG neurons, and second, we examined and compared the effects of sciatic ES and a CL on the regeneration of central axons of DRG sensory neurons in an *in vivo* model of spinal cord injury. In order to test a clinically relevant scenario, we applied ES immediately following the central lesion of DRG axons rather than a week before. This was despite the fact that a CL of the DRG neurons at the same time as the central lesion is not as effective as a CL 7 days before (Neumann and Woolf, 1999). We found that ES enhanced neurite and axonal outgrowth *in vitro* and *in vivo* and that this effect was associated with increased intracellular cAMP levels in the DRG sensory neurons. ES was not as effective as a CL in promoting elongation of the regenerating axons further into the lesion site but the advantage of ES over a CL is its clinical feasibility because ES can be applied to an intact nerve and conditions the neuron without cutting its axon.

Materials and methods

Experiments were performed on adult female Sprague Dawley rats (200–220 g), and approved by local authorities according to the Canadian Council for Animal Care guidelines. All surgeries were performed under Ketamine (Vetalar, Bioniche, Belleville, Ontario) and Xylacine (Rompun, Bayer, Toronto, Ontario) anesthesia.

In vivo ES 1d or 7d prior to DRG neuron culture

In anesthetized rats ($n=3$), the sciatic nerve was exposed and 1 h ES (20 Hz, 0.02 ms) was applied to the intact nerve using a Grass SD-9 stimulator (Quincy, MA) as the period of 1 h ES was the most effective for promoting DRG peripheral axon outgrowth (Geremia et al., 2007). Electrodes were built from Teflon insulated stainless steel wires (Cooner Wire, Chatsworth, CA, USA). The cathode was looped around the sciatic nerve and the anode was placed distally. The stimulus intensity was adjusted to 2X the motor threshold required for eliciting contraction in the gastrocnemius muscle (~3 to 5 V). This stimulus intensity excites both afferent and efferent large myelinated nerve fibers (grouped as A fibers) which have a similar threshold for electrical activation (Kimura, 1983). It is unlikely that unmyelinated axons (grouped as C fibers) were recruited with this stimulation protocol since the threshold for stimulation of these C fibers is 15X higher than sensory A fibers (Valero-Cabre and Navarro, 2002). The pulse duration of 0.02 ms was chosen to recruit large sensory myelinated fibers (Aα, Aβ), the small Aδ and unmyelinated C fibers requiring longer duration (of at least 0.1 ms and 1 ms respectively) and higher voltage pulses for threshold stimulation (Harper and Lawson, 1984).

One day (1d) or 7 days (7d) after ES, rats were euthanized and the right (ES) and the left (control, Con-1d, Con-7d) L4, L5 and L6 DRGs were removed and dissociated as described previously (Steinmetz et al., 2005). Briefly, DRGs were incubated in collagenase/dispase in Hanks buffered saline solution (HBSS; Invitrogen, Gaithersburg, MD) and then mechanically dissociated. The cells (1000 per well) were plated on glass coverslips within the well that were coated with poly-L-lysine, nitrocellulose and 5 μg/ml laminin (Biomedical technologies, Stoughton, MA). The cells were incubated for 24 h and then fixed in 4% paraformaldehyde, blocked with 5% normal goat antiserum (Invitrogen) and incubated overnight in anti-β-tubulin-type III (1:400, Sigma), followed by a secondary antibody. In a Leitz (Wetzlar, Germany) fluorescence microscope, pictures of ~125 neurons for each condition were taken at 25X and the length of the longest neurite for each neuron was measured using Metamorph imaging software (Universal Imaging Corporation, Downingtown, PA).

In vivo ES of sciatic nerve and section of central axons of DRG neurons

Following a hemi-laminectomy at thoracic spinal level 8 (Th8), a lesion of the dorsal funiculus was performed using micro-scissors. This ablated, amongst others, ascending sensory axons including those with axons in the sciatic nerve (Fig. 1). The surgeon was blind to the designation of the rats in the different groups.

Following the spinal lesion the sciatic nerve was exposed and, in the control group of rats no further treatment was applied (Sham; $n=7$). As shown figuratively in Fig. 1, the sciatic nerve was transected and the proximal stump was sutured to underlying muscle tissue to prevent axonal regeneration in the CL group ($n=7$; ①CL). In the 20 Hz ES group ($n=6$; ②20 Hz), ES was applied as described above (1 h supramaximal ES at 20 Hz). To test if variation in the frequency of ES could affect the results, the third experimental group received ES at 200 Hz ($n=7$; ③200 Hz) but with the same overall number of pulses (72,000 pulses/h in an intermittent firing of 200 Hz for 25 ms every 250 ms). Postoperative pain relief was supplied by buprenorphine (0.05 mg/kg Buprenex; Reckitt Benckiser, Slough, UK).

Fourteen weeks after the spinal cord lesion, DRG sensory nerve fibers were labeled with cholera toxin B (CTB) as previously described (Oudega et al., 1994). Briefly, the right sciatic nerve was dissected, crushed with a fine tipped forceps and 1% CTB in distilled water (List Biological laboratories Inc., Campbell Cawas) was injected with a Hamilton syringe at the site of the nerve crush (Fig. 1). One week later, rats were anesthetized and intracardially perfused with saline solution followed by 4% paraformaldehyde in 0.1 M PBS. A piece of spinal cord including the segments T7–T9 was frozen for histological analysis.

Immunohistochemistry

Using a cryostat (CM 3000, Leica, Germany), 25 μm sagittal sections of the spinal cord tissue were cut and serially mounted. CTB was visualized by immunohistochemistry (Oudega et al., 1994). Slides were incubated with 5% normal rabbit serum

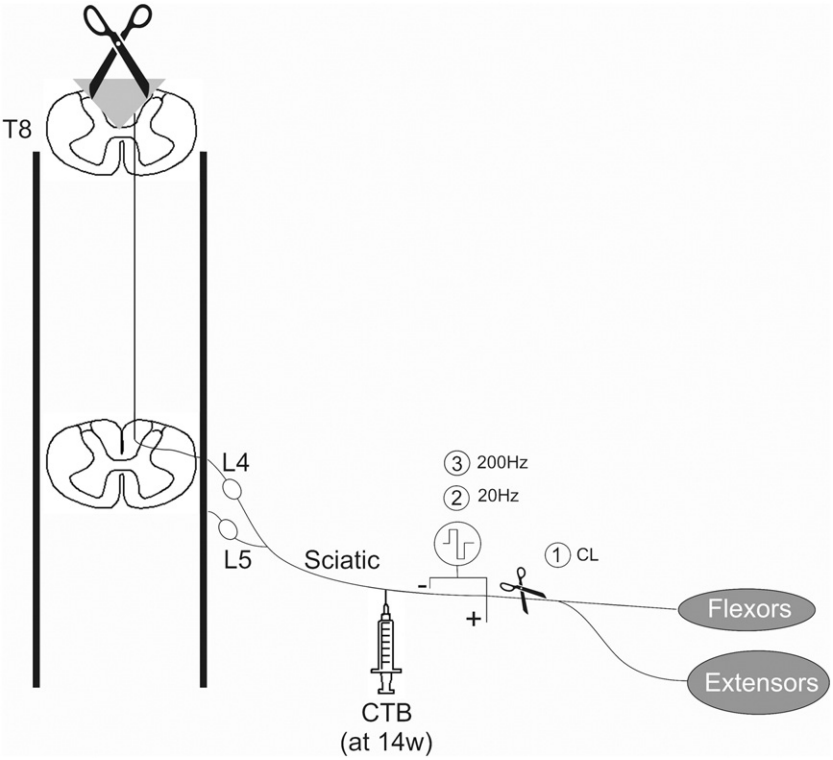


Fig. 1. The *in vivo* model of axonal regeneration of central DRG axons after a T8 level transection of the dorsal columns in the CNS is illustrated. The peripheral axons of the sensory neurons in the L4, L5 and L6 dorsal root ganglia (DRG) were subjected to Sham surgery in the control group of rats and, in 3 experimental rat groups, to a conditioning lesion (CL) by cutting the sciatic nerve (1) or electrically stimulating the sciatic nerve supramaximally (ES) for 1 h at 20 Hz (2) or 200 Hz (3). Central sensory axons of the DRG neurons were anterogradely labeled with cholera toxin B (CTB) solution injected into the sciatic nerve proximal to the site of either the CL or the ES, 14 weeks after the CNS and PNS surgical interventions.

(NRS), then in 1:8000 anti-CTB for 2 nights at 4 °C followed with a secondary antibody, and afterwards incubated with an Avidin–biotin–peroxidase complex in TBS. Slides were treated with DAB solution (Vector DAB kit, SK4100, Vector laboratories) for 2 min. The reaction was stopped by extensive washing in water.

Histological analysis

Using a digital camera mounted on a Leica microscope, consecutive pictures were taken at 200× magnification and composed using digital image software (Adobe Photoshop CS, Adobe Systems Inc. U.S.A.). The distance the axons were able to regenerate was calculated with Image Pro Plus (Media Cybernetics) software. We measured the distance between the caudal border of the lesion, defined by phase contrast, and the tip of all the traced axons that grew into the lesion site. The number of regenerated axons in each group was counted every 100 μm and the progressive reduction in the count number (C_x) with distance (x to infinity) was expressed by the cumulative sum of the number of regenerated axons (N_x) in 100 μm steps.

$$C_x = \sum_x^{\infty} N_x$$

This count number was then expressed as a percentage of all the labeled axons caudal to the lesion site.

Reconstructions of regenerated/sprouted axons from one representative rat of each group were created at 40X using a camera Lucida. The borders of the lesion were delimited in the drawings and were represented in a final picture as the shaded area (Fig. 3).

Measurement of intracellular cAMP

In a separate experiment, we measured intracellular levels of cAMP 24 h after cutting (CLct, $n=15$) or stimulating the sciatic nerve at 20 Hz ($n=6$) or 200 Hz ($n=8$). In the control group the rats received no lesion or treatment (Cont, $n=18$). For comparison, an additional control group of rats was included in which the dorsal column was transected as described above (Sham group, $n=6$). In order to assess if a CL by *cutting* the nerve is as effective at increasing cAMP levels as a CL by *crushing* the nerve, we added another experimental group ($n=6$) where the CL was performed by crushing (CLcr) instead of cutting (CLct) the sciatic nerve. The L4, L5 and L6 DRGs were removed and dissociated 24 h after the surgery as described above for the DRG neuron cultures, and immediately frozen in liquid nitrogen.

The DRGs were homogenized in 20X of their volume of 0.1 M HCl with a mechanical frosted glass pestle and centrifuged at 600×g for 10 min. The supernatant was diluted in 0.1 M HCl (1:6) and then analyzed following the manufacturer's instructions in a Direct cAMP low pH

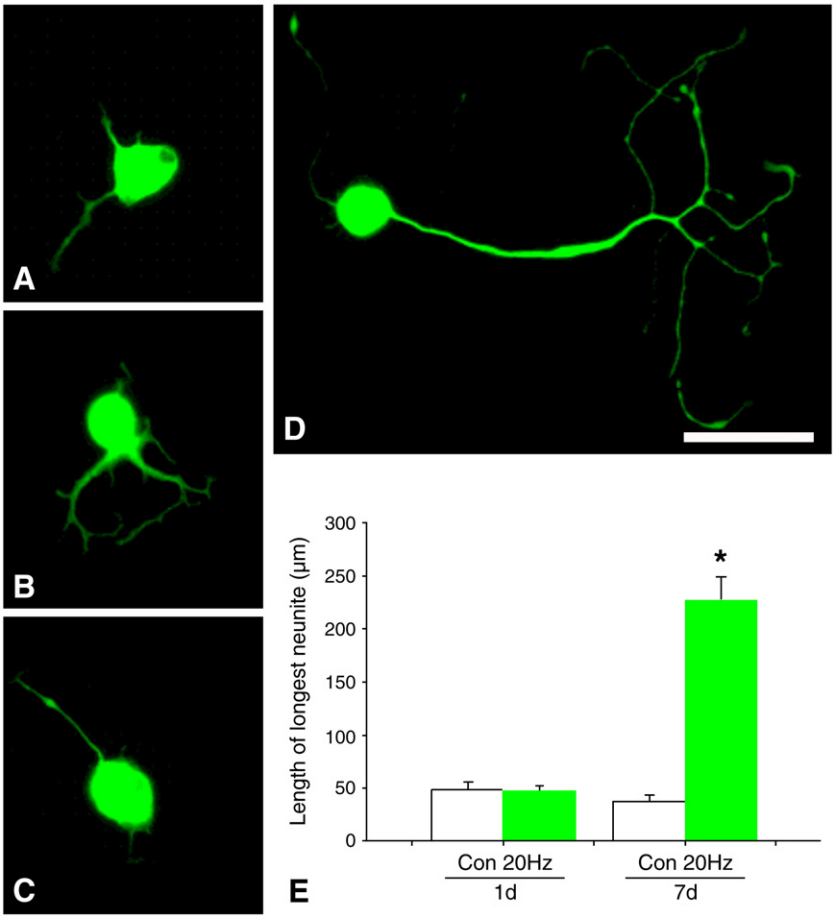


Fig. 2. Conditioning DRG sensory neurons by *in vivo* ES of the sciatic nerve promotes neurite outgrowth on a laminin substrate *in vitro*. The length of the longest neurites was not visually different in typical examples of a left non-stimulated DRG sensory neuron (A) that was harvested simultaneously with a right stimulated DRG neuron 1d after ES (B) and cultured for 24 h on a substrate of 5 μg/ml laminin. Similarly, the length of the longest neurite was not different for the neurite of non-stimulated left DRG neuron harvested 7d after ES of the contralateral right side (C). In contrast, the length of the longest neurite in DRG neurons that were harvested 7d after ES (D) was obviously much longer. Mean ± SE of the lengths of the longest neurite (in μm) are compared for the stimulated and control DRG neurons that were harvested 1d and 7d after ES (E). The neurons are immunostained with β-tubulin III. The calibration bar = 50 μm. *Statistical significance was tested for using ANOVA and accepted when $p < 0.05$.

Enzyme immunoassay Kit (Assay Designs, Ann Arbor, USA).

Statistics

Statistical comparisons were performed using SPSS 14.0 software. Comparisons between different groups were performed using one-way analysis of variance (ANOVA), and statistical significance was accepted at p values <0.05. Mean values were expressed as mean ± standard error (SE).

Results

ES promotes neurite outgrowth in vitro

The capacity of dissociated adult rat DRG sensory neurons to grow neurites when plated on a permissive substrate (Lindsay, 1988) can be accelerated if a CL has been applied previously (Smith and Skene, 1997). Here we wanted to determine if ES of the intact sciatic nerve can mimic this CL effect.

One or 7d after ES of the right sciatic nerve, DRGs were harvested and the sensory neurons whose axons projected into the left non-stimulated and right stimulated sciatic nerves were plated for 24 h on a laminin substrate. After 24 h, the neurite pattern varied from unipolar to multipolar as previously described (Figs. 2A–D) (Lindsay, 1988). When DRG neurons were plated 1d after 20 Hz ES for 1 h, their neurites were not visibly longer than those from non-stimulated neurons (cf. Fig. 2B vs A). In contrast, there was a 4-fold increase in the average length of the longest neurite in the DRG neurons stimulated 7d before the harvesting when compared to the control (cf. Fig. 2D vs C) or the 1d ES groups (Fig. 2E).

ES promotes axonal outgrowth of sensory fibers in the spinal cord in vivo

CTB-labeled sensory fibers were visualized 14 weeks after the transection of the dorsal columns. Caudal to the lesion, we observed axons that had retracted from the border of the lesion and formed retraction bulbs in all the experimental and control

groups of rats (cf. photomicrograph A and B in Fig. 3). Camera Lucida reconstructions caudal to and within the lesion site from spinal cords of a rat after sham sciatic nerve surgery showed that only few axons sprouted into the lesion site and these axons did not proceed very far (Fig. 3A). In contrast, the CL of the sciatic nerve, performed just after the spinal cord lesion, promoted the growth of axons through the lesion site (Fig. 3B) up to a maximum distance of 2400 μm. In 33% of the animals in the CL group, axons regenerated further than 2000 μm through the lesion site. Application of 20 Hz ES after spinal cord injury also stimulated axons to enter the lesion (Fig. 3B), although the ES was less effective than a CL: after 20 Hz ES, the regenerating axons did not grow further than 1500 μm from the lesion border and through the lesion site. In contrast, after 200 Hz ES, axons did not grow much farther than after sham surgery (Figs. 3C, D).

Distance of axonal outgrowth of severed sensory fibers in the spinal cord

The mean (±SE) number of CTB-labeled axons in each group was not statistically different, being 181±26 for the Sham group, 161±19 for the CL group, 194±20 for the 20 Hz groups and 203±26 for the 200 Hz group. In the Sham control group, the cumulative percentage of all the labeled axons caudal to the lesion site over a distance of just 100 μm was 23% and rapidly

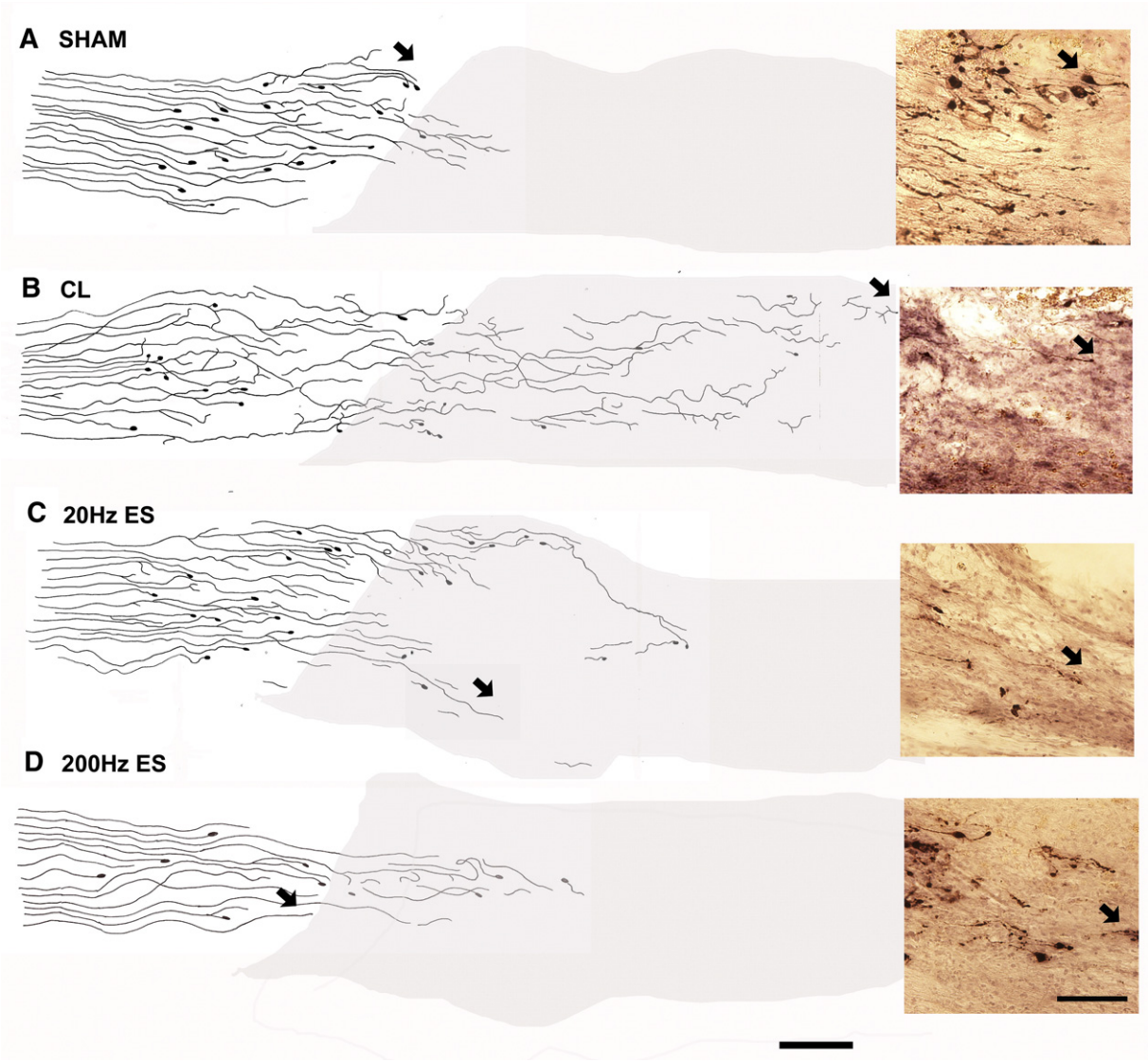


Fig. 3. Camera Lucida drawings of spinal cord sagittal sections and cholera toxin B-labeled DRG sensory axons. Axons are shown proximal to the lesion as well as within the lesion site of T8 from representative rats from the control (A), the CL (B), the 20 Hz ES (C), and the 200 Hz ES (D) groups, 14 weeks after surgery. The shaded area illustrates the outline of the lesion with the axons caudal to the lesion on the left side of the figures. The black arrows mark the CTB-stained axons in the photomicrograph of the right side and the corresponding drawn axon in the drawing at the left side. A. After sham sciatic nerve surgery, there was extensive axon retraction before the lesion and axon outgrowth into the lesion site was severely restricted. B. After a CL, there were fewer retraction bulbs with considerable axon outgrowth that proceeded well into the lesion site. (C) After 20 Hz ES, there were many retraction bulbs but the axon outgrowth exceeded that after Sham surgery. One of the axons that grew further into the lesion is shown in the photomicrograph. (D) After 200 Hz ES, there was little axon outgrowth into the lesion site. Some axons and retraction bulbs are shown at the pre-lesion site in the photomicrograph. Calibration bar is 250 μm in the drawing, and 90 μm in the photomicrograph.

decreased within a distance of 1000 μm into the lesion (Fig. 4A). After a CL there was a significant increase in axon outgrowth (42%) over the same distance of 100 μm into the lesion site. There was also a large and significant increase in the number of regenerating axons that advanced through and into the lesion site as far as 2000 μm (Fig. 4A). ES at 20 Hz for 1 h also significantly increased axonal outgrowth and elongation of the axons into the lesion site but the distance was not as great as the CL; significantly more axons grew after 20 Hz ES as compared to the Sham control, the axons growing as far as 800 μm past the caudal border of the lesion, as compared to the Sham control (Fig. 4B). In contrast to the CL, the percentage of axons that advanced further than 800 μm into the lesion site was not significantly increased when compared to the Sham group (Figs. 4A, B). In the 200 Hz ES group there was a trend, albeit not statistically significant, to increase axon outgrowth but not the distance of axon regeneration as compared to the Sham surgery (Fig. 4C).

The effects of CL, 20 Hz and 200 Hz ES are compared directly in Fig. 4D where the standard errors are not included with the mean values for ease of comparison of the experimental and control groups. The significant effect of 20 Hz ES in promoting axon outgrowth did not translate to more regenerating axons further into the lesion as compared to the CL. Only the CL significantly increased the elongation of axons within the lesion.

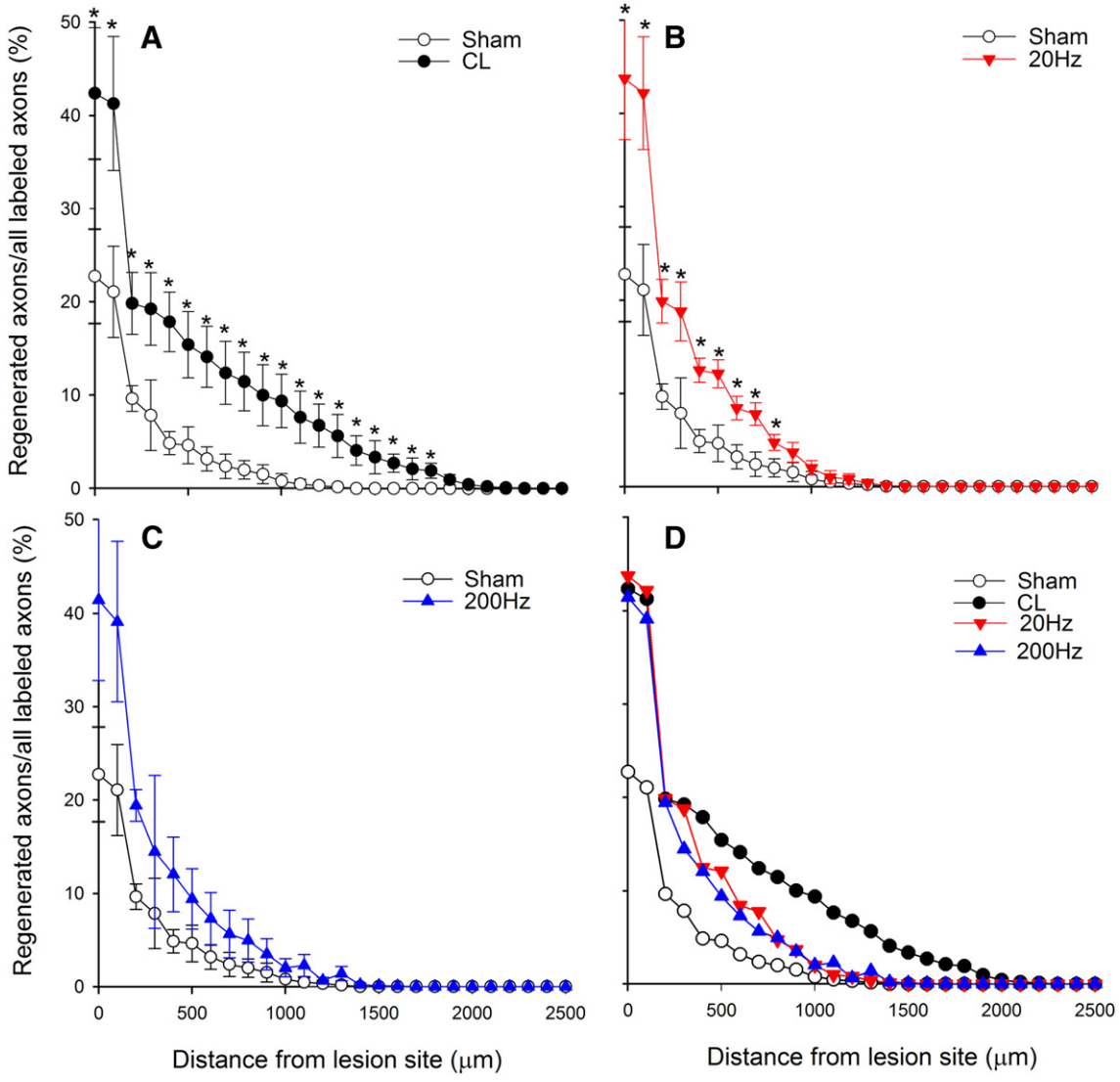


Fig. 4. ES promotes axonal outgrowth into the lesion site but not regeneration over long distances, in contrast to the CL that promotes elongation of regenerating axons into the lesion site. The cumulative sum of the number of regenerated axons that advanced into the lesion site expressed as a percentage of all the labeled axons proximal to the lesion in A) the Sham control group compared to the CL group, B) the 20 Hz ES group compared to the Sham group, C) the 200 Hz Es group compared to the Sham group and C) the 3 experimental groups and the Sham control group. The small percentage outgrowth of axons over a distance of 100 μm in the Sham group was significantly increased after a CL, that also increased the number of axons that regenerated over distances of up to 1800 μm (A). The percentage outgrowth was also significantly elevated after 20 Hz and slightly after 200 Hz without any significant increases beyond 800 μm (cf. B and C). The contrasting effects of the CL in promoting axon elongation with the effect of ES in promoting axon outgrowth are illustrated in the comparisons in (D). *Statistical significance vs Sham when $p<0.05$.

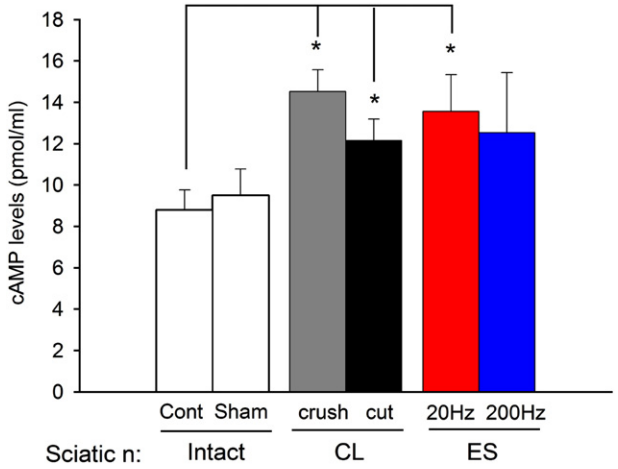


Fig. 5. 20 Hz ES of the intact sciatic nerve significantly increased intracellular levels of cAMP in the DRG neurons to the same levels as a CL by crushing or cutting the sciatic nerve. Intracellular levels of cAMP from right L4, L5 and L6 DRG homogenates were measured for the rats in which the sciatic nerve was intact or sham operated. In the latter rats, the central DRG axons were cut in the CNS at T8. The levels of cAMP were measured in homogenates of L4, L5 and L6 DRG's 24 h after either a crush or a cut CL, and after 20 Hz or 200 Hz ES for 1 h. *Statistical significance vs C when $p<0.05$.

ES increases cAMP levels in DRG neurons

The effects of CL on enhancing central sensory axonal regeneration have been related to the levels of intracellular cAMP in the DRG neurons (Neumann et al., 2002; Qiu et al., 2002). We therefore examined whether ES and/or CL elevates intracellular cAMP levels in conjunction with increasing axon outgrowth. The mean level of cAMP in DRGs of the unoperated rats was 8.8±0.97 pmol/ml (Fig. 5). Following a spinal lesion (24 h), the mean cAMP level was 9.5±1.3 pmol/ml in the Sham treated group, not significantly higher than in the control unoperated group. The CL of the peripheral axons by cutting (CLct) or by crushing (CLcr) led to a significant rise in cAMP levels (12.2±0.97 and 14.5±1.05 pmol/ml respectively). ES of the peripheral nerve at 20 Hz also led to a significant increase of cAMP levels (13.6±1.76 pmol/ml) when compared to the untreated rats. An increase in cAMP levels after ES at 200 Hz to 12.5±2.9 pmol/ml was not statistically significant when compared to the control unoperated group. Increased levels of cAMP in the DRG neurons after a CL have been previously reported in P18 rats (Qiu et al., 2002). To assess if a CL by cutting the nerve was less effective than crushing the nerve we also measured cAMP levels 24 h after crushing the sciatic nerve. The increase of cAMP levels in this group (CLcr) was the highest measured in our study.

Discussion

In this study we demonstrated that a single ES session of an intact peripheral nerve for 1 h enhances neurite outgrowth of DRG neurons *in vitro*, outgrowth of the central sensory axons into the lesion site *in vivo*, and elevates intracellular cAMP levels in the DRG neurons. ES has been shown to promote axonal outgrowth in the PNS (Al-Majed et al., 2000b; Brushart et al., 2002; Nix and Hopf, 1983) but, in contrast to the CL, did not accelerate the rate of axonal regeneration (Bisby and Pollock, 1983; Jacob and McQuarrie, 1993; McQuarrie and Grafstein, 1973). Our findings here indicate that ES acts similarly to promote sensory axon outgrowth in the CNS, but that it does not promote the elongation of these axons into the lesion site as far as the CL does. The finding that 20 Hz ES however, is as effective as the CL in increasing cAMP levels, suggests that the elevation in cAMP may account for the axonal outgrowth across the lesion site but would account less for long distance regeneration in the CNS after a CL. Accordingly, 200 Hz ES that also slightly increased cAMP levels, showed a tendency to increase the axonal outgrowth into the lesion site. To ultimately demonstrate the link between ES, intracellular cAMP levels and axon regeneration loss-of-function experiments by blocking or reducing cAMP elevation have to be performed.

Analysis of ES effectiveness in promoting neurite outgrowth *in vitro* demonstrated that ES, similar to a CL, needs to precede the harvesting of the DRGs for a period of time to promote neurite outgrowth. ES for a period of 1 h was ineffective if delivered 1d prior to harvesting of the DRGs but 4X as effective in promoting outgrowth if the ES preceded the DRG culture by 7d (Fig. 2). This is akin to the maximal effect of a CL 7d prior to DRG culture in promoting neurite outgrowth (Smith and Skene, 1997). Thus our results suggest that, comparable to the CL effect (Smith and Skene, 1997), enhanced neurite outgrowth may require time for gene transcription to precede the harvesting of the cells. This is supported by findings of ES-induced up-regulation of regeneration associated genes such as brain-derived neurotrophic factor (BDNF), its trkB receptor, tubulin and actin (Al-Majed et al., 2000a).

Consistent with the *in vitro* findings, ES *in vivo* promoted axon outgrowth in the CNS (as far as 800 μm into the lesion site) but did not promote axonal regeneration over longer distances (Figs. 3 and 4). The latter may explain why the same ES did not apparently promote regeneration of lesioned rubrospinal tract neurons because the putative axon outgrowth was not analyzed (Harvey et al., 2005). It is also possible that different neurons respond differently to ES. For example, we reported that for DRG neurons the higher frequency of ES (200 Hz) was not more effective than the lower frequency (20 Hz). In contrast, a higher stimulus frequency could be more effective in enhancing outgrowth of descending axons, which is supported by a related experiment where ES at 330 Hz for 2 h daily over 2–3 weeks applied to the intact corticospinal tract improved compensatory sprouting of its axons after the lesion of the contralateral tract (Brus et al., 2006).

In our study we selectively stimulated large diameter myelinated axons (Harper and Lawson, 1984; Valero-Cabre and Navarro, 2002). It has been reported that CTB labeling of small C fibers is preferentially increased after peripheral nerve injuries (Tong et al., 1999; Bao et al., 2002; Hughes et al., 2003; Shehab et al., 2003) and there are both unmyelinating as well as myelinated axons in the dorsal columns (Langford and Coggeshall, 1981). This may result in the underestimation of

the extent to which ES promotes axon outgrowth as compared to the CL because ES does not injure the peripheral nerves as does the CL 14 weeks before tracing. This is unlikely however, as we found no significant differences in the number of labeled axons distal to the spinal lesion in any of the 2 experimental and control groups of rats. Two possibilities to explain the equal number of traced axons are that first, a peripheral nerve crush was performed immediately before the CTB injection in all the groups and second, the CTB injection was performed 14 weeks after the CL of the peripheral nerve — a much later time point than the studies that reported the increased C fiber tracing.

Our findings that ES in association with elevated cAMP, was effective in promoting axon outgrowth into the lesion site but not in promoting further elongation through the site substantiate the findings of Han et al. (2004): elevated cAMP failed to promote the elongation of central branches of DRG axons into a segment of peripheral nerve transplanted into the transected dorsal columns (Han et al., 2004). A CL in contrast, significantly increased both outgrowth and the number of axons that regenerated further than 800 μm into the lesion site. These differences between the effects of ES and the CL in the CNS are similar to the differences found in the PNS: ES promoted only the onset of axonal growth (Al-Majed et al., 2000b; Brushart et al., 2002) without increasing the overall rate of axonal regeneration (Brushart et al., 2002) whilst a CL increased the rate of regeneration (Bisby and Pollock, 1983; Jacob and McQuarrie, 1993; McQuarrie and Grafstein, 1973).

The axon outgrowth observed in the ES and the CL groups correlated with an increase in the intracellular levels of cAMP in DRG neurons (cf. Figs. 4 vs 5). A CL-induced elevation of cAMP in DRG neurons has been reported previously (Qiu et al., 2002), but we report here for the first time that 20 Hz ES for 1 h also increased cAMP levels to the same levels. Although there were no changes in cAMP levels after a transection of the dorsal columns (Sham group) when compared to a control unoperated group, a decline in cAMP levels has been reported after a lesion of the corticospinal tract, where cut axons failed to grow (Pearse et al., 2004). The reduced cAMP could explain why this neuronal population fails to grow axons in the CNS spontaneously after a corticospinal tract lesion in mice, in contrast to the DRG neurons that do (Inman and Steward, 2003). Accordingly, in the Sham group, we observed very limited axonal growth into the lesion site (~20%) over the same 100 μm distance in which ~40% axons grew after ES or a CL. Similar findings were reported for the same lesion in rats by Neumann et al. (2002) and Qiu et al. (2002), but not by others (Bradbury et al., 1999; Neumann and Woolf, 1999).

Several studies have linked the CL effect in the CNS to increased levels of cAMP in the DRG neurons (Neumann et al., 2002; Qiu et al., 2002; Wu et al., 2007). For example, injection of cAMP in DRG neurons mimicked a CL in promoting regeneration of transected central DRG sensory axons (Neumann et al., 2002; Qiu et al., 2002). However, these studies did not perform a direct comparison between the two treatments. Injection of cAMP alone could have been less effective in enhancing sensory axonal regeneration than a CL. This possibility is supported by the failure of Wu et al. (2007) to match the CL effect in *in vivo* and *in vitro* studies by cAMP injection in the DRG and by findings that the rate of axonal regeneration in the optic nerve was enhanced by a CL (McQuarrie and Grafstein, 1981) but not by cAMP injection (McQuarrie and Grafstein, 1983). It was also reported that increased cAMP levels failed to promote axonal elongation into a segment of a peripheral nerve that was transplanted into the spinal cord at the site of dorsal column transaction. Finally, some studies (Han et al., 2004; McQuarrie et al., 1977) but not others (Kilmer and Carlsen, 1987) found that cAMP administration did not increase the rate of axonal regeneration in the PNS either.

The finding that a significant increase in cAMP in DRG neurons by ES did not mimic the CL effect in promoting axonal regeneration within the CNS lesion site suggests that the CL effect could be mediated in part, by other mechanisms. These may include the contribution of non-neuronal cells in light of previous findings that an inflammatory reaction induced by injection of inflammatory agents promoted axonal regeneration within the CNS that was comparable to the effect of the CL (Lu and Richardson, 1991; Steinmetz et al., 2005). A recently identified molecule, oncomodulin, that is released by macrophages, stimulates outgrowth of DRG sensory axons (Yin et al., 2006a) and therefore may be implicated in the CL effect. Indeed, administration of cAMP does not mimic the effects of oncomodulin, but further enhances the neurite outgrowth promoted by oncomodulin (Yin et al., 2006b).

In conclusion, ES of an intact peripheral nerve for 1 h at 20 Hz promotes sensory neurite outgrowth *in vitro* and in the spinal cord *in vivo*. Our findings are important because ES contrasts with the CL in being a feasible clinical approach in which ES of intact nerves can promote axon outgrowth. ES has been shown to accelerate PNS nerve regeneration in humans after carpal tunnel release surgery (Gordon et al., 2007) and is also a potentially feasible clinical tool to promote axonal regeneration in the injured CNS.

Acknowledgments

We would like to thank N. Tyreman and R. Vavrek for their helpful technical support and Dr X. Navarro for his helpful editorial suggestions. The work was supported by an operating grant to TG from the Canadian Institutes of Health Research. EU was a recipient of a research fellowship from the Spanish Ministry of Education and Sciences. JS is funded by the NINDS/NS25713.

References

Al-Majed, A.A., Brushart, T.M., Gordon, T., 2000a. Electrical stimulation accelerates and increases expression of BDNF and trkB mRNA in regenerating rat femoral motoneurons. Eur. J. Neurosci. 12, 4381–4390.

Al-Majed, A.A., Neumann, C.M., Brushart, T.M., Gordon, T., 2000b. Brief electrical stimulation promotes the speed and accuracy of motor axonal regeneration. J. Neurosci. 20, 2602–2608.

Al-Majed, A.A., Tam, S.L., Gordon, T., 2004. Electrical stimulation accelerates and enhances expression of regeneration-associated genes in regenerating rat femoral motoneurons. Cell. Mol. Neurobiol. 24, 379–402.

Bao, L., Wang, H.F., Cai, H.J., Tong, Y.G., Jin, S.X., Lu, Y.J., Grant, G., Hökfelt, T., Zhang, X., 2002. Peripheral axotomy induces only very limited sprouting of coarse myelinated afferents into inner lamina II of rat spinal cord. Eur. J. Neurosci. 16, 175–185.

Bisby, M.A., Pollock, B., 1983. Increased regeneration rate in peripheral nerve axons following double lesions: enhancement of the conditioning lesion phenomenon. J. Neurobiol. 14, 467–472.

Bradbury, E.J., Khemani, S., Von, R., King, Priestley, J.V., McMahon, S.B., 1999. NT-3 promotes growth of lesioned adult rat sensory axons ascending in the dorsal columns of the spinal cord. Eur. J. Neurosci. 11, 3873–3883.

Broude, E., McAtee, M., Kelley, M.S., Bregman, B.S., 1997. c-Jun expression in adult rat dorsal root ganglion neurons: differential response after central or peripheral axotomy. Exp. Neurol. 148, 367–377.

Brus, M., Carmel, J.B., Raz, D.J., Martin, J.H., 2006. Electrical stimulation of the corticospinal tract promotes growth of spared axons after partial injury. Abstract Society for Neurosciencies, Atlanta. 646.10/U9.

Brushart, T.M., Hoffman, P.N., Royall, R.M., Murinson, B.B., Witzel, C., Gordon, T., 2002. Electrical stimulation promotes motoneuron regeneration without increasing its speed or conditioning the neuron. J. Neurosci. 22, 6631–6638.

Busch, S.A., Silver, J., 2007. The role of extracellular matrix in CNS regeneration. Curr. Opin. Neurobiol. 17, 120–127.

Cai, D., Shen, Y., De, B.M., Tang, S., Filbin, M.T., 1999. Prior exposure to neurotrophins blocks inhibition of axonal regeneration by MAG and myelin via a cAMP-dependent mechanism. Neuron 22, 89–101.

Dergham, P., Ellezam, B., Essagian, C., Avedissian, H., Lubell, W.D., McKerracher, L., 2002. Rho signaling pathway targeted to promote spinal cord repair. J. Neurosci. 22, 6570–6577.

Domeniconi, M., Filbin, M.T., 2005. Overcoming inhibitors in myelin to promote axonal regeneration. J. Neurol. Sci. 233, 43–47.

Filbin, M.T., 2003. Myelin-associated inhibitors of axonal regeneration in the adult mammalian CNS. Nat. Rev., Neurosci. 4, 703–713.

Fouad, K., Pearson, K., 2004. Restoring walking after spinal cord injury. Prog. Neurobiol. 73, 107–126.

Fu, S.Y., Gordon, T., 1997. The cellular and molecular basis of peripheral nerve regeneration. Mol. Neurobiol. 14, 67–116.

Geremia, N.M., Gordon, T., Brushart, T.M., Al-Majed, A.A., Verge, V.M., 2007. Electrical stimulation promotes sensory neuron regeneration and growth-associated gene expression. Exp. Neurol. 205, 347–359.

Gordon, T., Brushart, T.M., Amirjani, N., Chan, K.M., 2007. The potential of electrical stimulation to promote functional recovery after peripheral nerve injury: comparisons between rats and humans. Acta Neurochir. Suppl. 100, 3–11.

Han, P.J., Shukla, S., Subramanian, P.S., Hoffman, P.N., 2004. Cyclic AMP elevates tubulin expression without increasing intrinsic axon growth capacity. Exp. Neurol. 189, 293–302.

Harper, A.A., Lawson, S.N., 1984. Conduction velocity is related to morphological cell type in rat dorsal root ganglion neurones. J. Physiol. 359, 31–46.

Harvey, P.J., Grochmal, J., Tetzlaff, W., Gordon, T., Bennett, D.J., 2005. An investigation into the potential for activity-dependent regeneration of the rubrospinal tract after spinal cord injury. Eur. J. Neurosci. 22, 3025–3035.

Houle, J.D., Tom, V.J., Mayes, D., Wagoner, G., Phillips, N., Silver, J., 2006. Combining an autologous peripheral nervous system "bridge" and matrix modification by chondroitinase allows robust, functional regeneration beyond a hemisection lesion of the adult rat spinal cord. J. Neurosci. 26, 7405–7415.

Hughes, D.I., Scott, D.T., Todd, A.J., Riddell, J.S., 2003. Lack of evidence for sprouting of Abeta afferents into the superficial laminas of the spinal cord dorsal horn after nerve section. J. Neurosci. 22, 9491–9499.

Inman, D.M., Steward, O., 2003. Ascending sensory, but not other long-tract axons, regenerate into the connective tissue matrix that forms at the site of a spinal cord injury in mice. J. Comp. Neurol. 462, 431–449.

Jacob, J.M., McQuarrie, I.G., 1993. Acceleration of axonal outgrowth in rat sciatic nerve at one week after axotomy. J. Neurobiol. 24, 356–367.

Kilmer, S.L., Carlsen, R.C., 1987. Chronic infusion of agents that increase cyclic AMP concentration enhances the regeneration of mammalian peripheral nerves *in vivo*. Exp. Neurol. 95, 357–367.

Kimura, J., 1983. Nerve conduction studies. In: Kimura, J. (Ed.), Electrodiagnosis in Diseases of Nerve and Muscle. FA Davies Company, United States of America, pp. 59–80.

Langford, L.A., Coggeshall, R.E., 1981. Unmyelinated axons in the posterior funiculi. Science 211, 176–177.

Lehmann, M., Fournier, A., Selles-Navarro, I., Dergham, P., Sebok, A., Leclerc, N., Tigyi, G., McKerracher, L., 1999. Inactivation of Rho signaling pathway promotes CNS axon regeneration. J. Neurosci. 19, 7537–7547.

Lindsay, R.M., 1988. Nerve growth factors (NGF, BDNF) enhance axonal regeneration but are not required for survival of adult sensory neurons. J. Neurosci. 8, 2394–2405.

Lu, X., Richardson, P.M., 1991. Inflammation near the nerve cell body enhances axonal regeneration. J. Neurosci. 11, 972–978.

McQuarrie, I.G., Grafstein, B., 1973. Axon outgrowth enhanced by a previous nerve injury. Arch. Neurol. 29, 53–55.

McQuarrie, I.G., Grafstein, B., 1981. Effect of a conditioning lesion on optic nerve regeneration in goldfish. Brain Res. 216, 253–264.

McQuarrie, I.G., Grafstein, B., 1983. Effect of acetoxycycloheximide and dibutyryladenosine cyclic 3′:5′-monophosphate on axonal regeneration in the goldfish optic nerve. Brain Res. 279, 377–381.

McQuarrie, I.G., Grafstein, B., Gershon, M.D., 1977. Axonal regeneration in the rat sciatic nerve: effect of a conditioning lesion and of dbcAMP. Brain Res. 132, 443–453.

Neumann, S., Woolf, C.J., 1999. Regeneration of dorsal column fibers into and beyond the lesion site following adult spinal cord injury. Neuron 23, 83–91.

Neumann, S., Bradke, F., Tessier-Lavigne, M., Basbaum, A.I., 2002. Regeneration of sensory axons within the injured spinal cord induced by intraganglionic cAMP elevation. Neuron 34, 885–893.

Nix, W.A., Hopf, H.C., 1983. Electrical stimulation of regenerating nerve and its effect on motor recovery. Brain Res. 272, 21–25.

Oudega, M., Varon, S., Hagg, T., 1994. Distribution of corticospinal motor neurons in the postnatal rat: quantitative evidence for massive collateral elimination and modest cell death. J. Comp. Neurol. 347, 115–126.

Pearse, D.D., Pereira, F.C., Marcillo, A.E., Bates, M.L., Berrocal, Y.A., Filbin, M.T., Bunge, M.B., 2004. cAMP and Schwann cells promote axonal growth and functional recovery after spinal cord injury. Nat. Med. 10, 610–616.

Qiu, J., Cai, D., Dai, H., McAtee, M., Hoffman, P.N., Bregman, B.S., Filbin, M. T., 2002. Spinal axon regeneration induced by elevation of cyclic AMP. Neuron 34, 895–903.

Richardson, P.M., Issa, V.M., 1984. Peripheral injury enhances central regeneration of primary sensory neurones. Nature 309, 791–793.

Schreyer, D.J., Skene, J.H., 1993. Injury-associated induction of GAP-43 expression displays axon branch specificity in rat dorsal root ganglion neurons. J. Neurobiol. 24, 959–970.

Schwab, M.E., Bartholdi, D., 1996. Degeneration and regeneration of axons in the lesioned spinal cord. Physiol. Rev. 76, 319–370.

Shehab, S.A., Spike, R.C., Todd, A.J., 2003. Evidence against cholera toxin B subunit as a reliable tracer for sprouting of primary afferents following peripheral nerve injury. Brain Res. 964, 218–227.

Silver, J., Miller, J.H., 2004. Regeneration beyond the glial scar. Nat. Rev., Neurosci. 5, 146–156.

Smith, D.S., Skene, J.H., 1997. A transcription-dependent switch controls competence of adult neurons for distinct modes of axon growth. J. Neurosci. 17, 646–658.

Steinmetz, M.P., Horn, K.P., Tom, V.J., Miller, J.H., Busch, S.A., Nair, D., Silver, D.J., Silver, J., 2005. Chronic enhancement of the intrinsic growth

capacity of sensory neurons combined with the degradation of inhibitory proteoglycans allows functional regeneration of sensory axons through the dorsal root entry zone in the mammalian spinal cord. J. Neurosci. 25, 8066–8076.

Tong, Y.G., Wand, H.F., Ju, G., Grant, G., Höffelt, T., Zhang, X., 1999. Increased uptake and transport of cholera toxin B-subunit in dorsal root ganglion neurons after peripheral axotomy: possible implications for sensory sprouting. J. Comp. Neurol. 404, 143–158.

Valero-Cabre, A., Navarro, X., 2002. Changes in crossed spinal reflexes after peripheral nerve injury and repair. J. Neurophysiol. 87, 1763–1771.

Wu, D., Zhang, Y., Bo, X., Huang, W., Xiao, F., Zhang, X., Miao, T., Magoulas, C., Subang, M.C., Richardson, P.M., 2007. Actions of neuropoietic cytokines and cyclic AMP in regenerative conditioning of rat primary sensory neurons. Exp. Neurol. 204, 66–76.

Yin, Y., Henzl, M.T., Lorber, B., Nakazawa, T., Thomas, T.T., Jiang, F., Langer, R., Benowitz, L.I., 2006a. Oncomodulin is a macrophage-derived signal for axon regeneration in retinal ganglion cells. Nat. Neurosci. 9, 843–852.

Yin, Y., Lorber, B., Nakazawa, T., Jiang, F., Benowitz, L.I., 2006b. Oncomodulin is a novel growth factor for CNS and PNS neurons. Abstract Society for Neurosciencies, Atlanta, Georgia, USA. 522.5/C24.

The Journal of Neuroscience, January 15, 2001, 21(2):654–667

Increased Neuromuscular Activity Reduces Sprouting in Partially Denervated Muscles

Siu Lin Tam, Vey Archibald, Balvinder Jassar, Neil Tyreman, and Tessa Gordon

Department of Pharmacology, Division of Neuroscience, University of Alberta, Edmonton, Canada T6G 2S2

The effects of increasing neural activity on sprouting remain unclear and controversial. In a rat model of partial denervation of skeletal muscles, we investigated the effect of neuromuscular activity on sprouting. Rat hindlimb muscles were partially denervated by avulsion of either L4 or L5 spinal root. Immediately after partial denervation, the rats were divided into three groups: (1) normal caged activity, (2) running exercise on wheels, 8 hr daily, and (3) functional electrical stimulation (FES) of sciatic nerves, 20 Hz for 8 hr daily. At 1 month, muscle unit (MU) enlargement was quantitated electrophysiologically and histochemically. MU twitch force was increased by four- to fivefold by partial denervation in extensively denervated tibialis anterior (TA) and medial gastrocnemius (MG) and by approximately twofold in moderately denervated plantaris (PL) and soleus (SOL). For the extensively denervated TA and MG muscles, MU enlargement, measured electrophysiologically, declined significantly after an average of 1757 $\pm$ 310 m/d running exercise and daily FES for 1 month. The detrimental effects on MU enlargement were much less but significant in the moderately denervated PL and did not reach statistical significance in the moderately denervated SOL muscle. Histochemical evaluation of sprouting showed a reduction in the number of sprouts in the extensively denervated TA muscle, but not the moderately denervated PL and SOL muscles, by increased neuromuscular activity. Thus, increased neuromuscular activity is detrimental primarily in muscles that are extensively denervated, and the MUs are smaller than under conditions in which the muscles experience normal physiological levels of activation.

Key words: sprouting; motor unit; motoneuron disease; neuromuscular activity; partial denervation; poliomyelitis



ELSEVIER

Neurobiology of Disease

www.elsevier.com/locate/ynbdi
Neurobiology of Disease 28 (2007) 154–164

Time course of preferential motor unit loss in the SOD1^{G93A} mouse model of amyotrophic lateral sclerosis

J. Hegedus,[a] C.T. Putman,[a,c] and T. Gordon[a,b,*]

[a]*Centre for Neuroscience, University of Alberta, Edmonton, AB, Canada T6G 2S2*
[b]*Division of Physical Medicine and Rehabilitation, University of Alberta, Edmonton, AB, Canada T6G 2S2*
[c]*Biochemistry Laboratory, Faculty of Physical Education, University of Alberta, Edmonton, AB, Canada T6G 2S2*

Received 12 April 2007; revised 28 June 2007; accepted 1 July 2007
Available online 10 July 2007

Electromyographical analyses of pre-symptomatic motor unit loss in the SOD1^{G93A} transgenic mouse model of amyotrophic lateral sclerosis (ALS) have yielded contradictory findings as to the onset and time course. We recorded hindlimb muscle and motor unit isometric forces to determine motor unit number and size throughout the life span of the mice. Motor unit numbers in fast-twitch tibialis anterior, extensor digitorum longus and medial gastrocnemius muscles declined from 40 days of age, 50 days before reported overt symptoms and motoneuron loss. Motor unit numbers fell after overt symptoms in the slow-twitch soleus muscle. Muscle forces declined in parallel with motor unit numbers, indicating little or no functional compensation by sprouting. Early muscle-specific decline was due to selective preferential vulnerability of large, fast motor units, innervated by large motoneurons. Large motoneurons are hence the most vulnerable in ALS with die-back occurring prior to overt symptoms. We conclude that size of motoneurons, their axons, and their motor unit size are important determinants of motoneuron susceptibility in ALS.
© 2007 Elsevier Inc. All rights reserved.

Keywords: ALS; Motor unit; Muscle force; Motoneuron; Mouse; Compensation

Introduction

The neurodegenerative disease amyotrophic lateral sclerosis (ALS) is characterized by progressive death of motoneurons and consequent skeletal muscle denervation, manifesting as weakness and eventually paralysis. Approximately 10% of ALS cases are familial (fALS), and of these, 20% have been linked to mutations of the superoxide dismutase (SOD) gene (Rosen, 1993). In the most widely used model of fALS, human mutant cytosolic Cu/Zn SOD1 with a glycine to alanine conversion at the 93rd codon is over-expressed in transgenic mice (SOD1^{G93A} mice) (Gurney et al., 1994).

In the SOD1^{G93A} mouse, the earliest signs of pathology at 30–37 days of age include aggregation of mutant SOD1 proteins in muscle (Turner et al., 2003) and motoneurons (Johnston et al., 2000), and vacuole formation in motoneurons and their axons (Chiu et al., 1995). Yet the ALS-like disease with initial symptoms including of fine tremors and weakness, develop in the hindlimbs only at ~90 days of age, followed by severe hindlimb paralysis at ~120 days of age (Gurney et al., 1994). Although critical motoneuron loss from the lumbar spinal cord occurred coincident with the onset of symptoms (Chiu et al., 1995), there was already anatomical evidence of axon die-back with preferential involvement of the largest axons. We hypothesized that the early pathology seen in the hindlimb muscles and peripheral nerves of the SOD1^{G93A} mouse would result in early functional motor unit loss, in line with evidence of muscle denervation at 60 days of age (Hegedus et al., 2006; Pun et al., 2006).

Early denervation of fast-twitch muscles was reported by Caroni and colleagues (Frey et al., 2000; Pun et al., 2006). Yet functional measurements of the number of functional motor units that may support this anatomical measurement did not provide consistent data. These measurements have to date used electromyography (EMG). Kennel et al. (1996) reported the earliest significant decrement in whole compound muscle action potential (CMAP) and loss of motor units in the gastrocnemius muscle of SOD1^{G93A} mice at 47 days of age. These authors used needle EMG to demonstrate that this loss continued in a linear manner until end-stage disease. Yet with the same method of EMG recording from the same muscle, Azzouz et al. (1997) reported a biphasic decline of the CMAP and motor unit number, with a small, slow decline between 60 and 100 days of age. The only study to include slow-twitch muscles used surface EMG electrodes to record from all of the hindlimb muscles simultaneously; Shefner and colleagues found that CMAP begins to rapidly decline at

* Corresponding author. Division of Physical Medicine and Rehabilitation/Centre for Neuroscience, 525 Heritage Medical Research Centre, Faculty of Medicine, University of Alberta, Edmonton, AB, Canada T6G 2S2. Fax: +1 780 492 1617.
E-mail address: tessa.gordon@ualberta.ca (T. Gordon).
Available online on ScienceDirect (www.sciencedirect.com).

0969-9961/$ - see front matter © 2007 Elsevier Inc. All rights reserved.
doi:10.1016/j.nbd.2007.07.003

~60 days of age, concomitant with a loss of functional motor units (Shefner et al., 1999, 2001). In light of this contradictory data, it is important to establish the time course of motor unit loss in ALS. Moreover, the observations that sprouting from the motoneurons which innervate the largest type IIB muscle fibers may be defective in normal (De Winter et al., 2006) and in SOD1^{G93A} transgenic mice (Frey et al., 2000; Pun et al., 2006) indicate that the normal capacity of remaining intact motor units to enlarge by sprouting (Gordon and Pattullo, 1993; Rafuse et al., 1992; Tam and Gordon, 2003) may not be evident in the SOD1^{G93A} mouse. Anatomical evidence in rats (Pun et al., 2006) and electrophysiological evidence from human ALS studies (Dengler et al., 1990) also indicated that the less forceful, slower motor units may preferentially survive in ALS.

In the current study in which we record whole muscle and motor unit isometric contractile forces from both fast- and slow-twitch muscles in the SOD1^{G93A} mouse model of ALS, we explore the time course of loss of functional motor units, the extent to which motor unit enlargement can maintain whole muscle contractile forces, and the question of whether there is preferential loss of functional motor units from fast- as compared to slow-twitch muscles. We measured isometric contractile force of the muscle and their component motor units in order to count motor units from four morphologically distinct hindlimb muscles throughout the life span of SOD1^{G93A} mice. The muscles include three fast-twitch muscles, the medial gastrocnemius (MG), tibialis anterior (TA) and extensor digitorum longus (EDL), and one slow-twitch muscle – the soleus (SOL).

We found a significant decline in both whole muscle contractile force and the number of functional motor units from fast- but not slow-twitch muscles at 40 days of age, 50 days prior to the reported onset of overt symptoms. There were no deficits in whole muscle contractile force or decline in motor unit numbers in the slow-twitch SOL muscle until 90 days of age, coincident with symptom onset. The loss of motor units from the fast-twitch hindlimb muscles was initially quick and then reached a plateau in the symptomatic phase of the disease. Despite the reported capacity for some effective axonal sprouting, the contractile force of the fast-twitch muscles declined in parallel with the reduction in number of motor units, indicating that the sprouting capacity was either very limited or absent. Our findings established that muscle fiber type composition rather than function determines preferential vulnerability of motor units and that functional enlargement of motor units does not effectively compensate for progressive loss of intact motor units.

Materials and methods

Mice

Transgenic mice used in this study were obtained from Jackson Laboratories, USA. The transgenic mice expressed a high copy number of the human SOD gene with a glycine to alanine base pair mutation at the 93rd codon of the cytosolic Cu/Zn superoxide dismutase (SOD1) gene (SOD1^{G93A}; B6JSL-TgN (SOD1-G93A)) or a high copy number of normal human SOD1 gene (SOD1^{WT}; B6JSL-TgN (SOD1)). The transgenic male SOD1^{G93A} and SOD1^{WT} mice were bred to non-transgenic B6JSL hybrid females. The resulting progeny was identified using standard PCR protocol for the human SOD1 (Rosen, 1993) performed on ear biopsy samples taken at the time of weaning (approximately 21 days of age). The mice were identified using ear punches, and kept in standard animal housing with free access to food and standard rodent chow. The University of Alberta Health Sciences Laboratory Animal Ethics committee approved all experimental procedures, which were in accordance with the Canadian Council for Animal Care.

To avoid ambiguity associated with reported gender-related differences in mean survival time of SOD1^{G93A} mice (Veldink et al., 2003), we used only male mice in the present study. The male SOD1^{G93A} mice became symptomatic at approximately 90 days of age. Symptoms include fine shaking, tremors and spasticity in the hind-legs (Chiu et al., 1995). Complete paralysis of the hindlimbs occurs within 30 to 40 days after the onset of the symptoms. The SOD1^{WT} mice have not been reported to develop ALS-like disease (Gurney et al., 1994).

Four morphologically distinct hindlimb muscles were examined: the mixed fast-twitch tibialis anterior (TA), extensor digitorum longus (EDL) and medial gastrocnemius (MG) muscles, and the slow-twitch soleus (SOL). We enumerated motor units and recorded maximal isometric contractile forces from an average of 6 (n = 4–11) male SOD1^{G93A} mouse muscles at each of 40, 50, 60, 70, 80, 90,100, 110, and 120 days of age. A total of 57 SOD1^{G93A} transgenic mice and 37 wild type control mice were used in this study.

Electrophysiological studies

Surgery

Mice were anaesthetized with an intraperitoneal (i.p.) injection of a cocktail made up of ketamine (100 mg/mL), Atravet (10 mg/mL) and 0.9% sodium chloride, at a dosage of 17.5 mL/kg body weight. At regular time intervals, additional anaesthetic was administered i.p. to maintain anaesthesia. The body temperature of the mice was maintained using a heat lamp. The TA, EDL, MG and SOL muscle tendons were isolated and individually attached with 4.0 silk to a strain gauge (Kulite model KH-102) to record the isometric force produced by each muscle in response to stimulation of the sciatic nerve (Fig. 1A). Two silver wire electrodes were placed alongside the sciatic nerve. A controlled stimulation was applied to the nerve to evoke and record unitary and maximal isometric twitch and tetanic isometric contractions from each muscle. The electrodes were sutured in place to prevent dislocation during stimulation. Hindlimbs of the anaesthetized mice were immobilized by clamping the knees and the ankles, while being careful not to interfere with the blood supply to the muscles.

Recordings

Evoked isometric forces were amplified and visualized on an oscilloscope and digitized using Axoscope (Version 8.0, Axon Instruments, USA). Muscle length was adjusted for maximal isometric twitch force in response to stimulation of the sciatic nerve. Whole muscle twitch and tetanic forces were recorded in response to single and repetitive suprathreshold (twice threshold amplitude) stimulation of the sciatic nerve at 0.5 and 100 Hz, respectively. The tetani lasted for 210 ms and the maximum tetanic force was measured. An example of force recordings from a 60-day control mouse TA muscle is shown in Fig. 1B.

To estimate the number of motor units in the hindlimb muscles of the mice, we used a modified version of the mechanical motor unit number estimation (MUNE) that was first described by

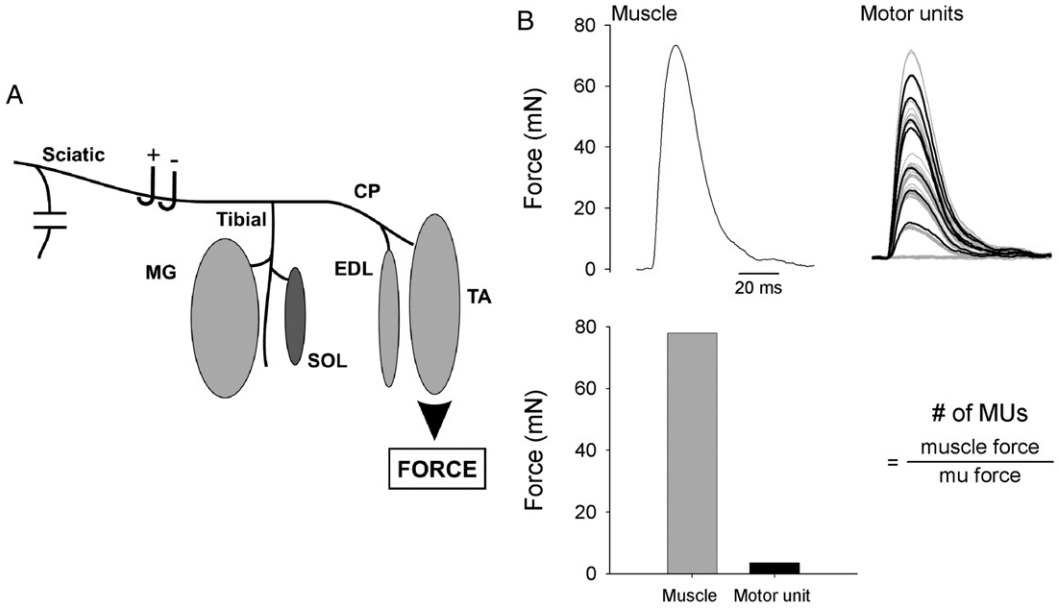


Fig. 1. Schematic illustrating the procedure of recording of whole muscle and motor unit isometric contractile forces from the hindlimb muscles of mice. (A) Tendons of the MG, SOL, EDL and TA muscles were exposed and individually attached to the force transducer in order to record the contractile force generated by stimulating the sciatic nerve through silver wire electrodes. (B) The sciatic nerve was supramaximally stimulated to elicit maximal isometric twitch- and tetanic-contractile forces in each of the hindlimb muscles. Twitch force from a $SOD1^{WT}$ TA muscle is shown. The stimulus voltage was then reduced so that no force was elicited. The voltage was then slowly increased, resulting in the incremental increases in the whole muscle isometric force. Each increment in whole muscle force was assumed to be the force associated with the addition of one motor unit. A computer randomly selected 8 to 15 increments, which were averaged to yield the mean motor unit force. Motor unit number was calculated by dividing the mean motor unit force into the whole muscle twitch.

McComas et al. (1971) for EMG measurements of single motor units. The validity of this new method, the ITS-MUNE method of counting motor units, is described by Major et al. (2007). The mechanical MUNE method which records up to 10 incremental steps in the M-wave, makes the important assumption that each distinguishable incremental increase represents the recruitment of an additional motor unit. However, the method fails to account for the alternation of motor units, namely that motor units can be recruited in numerous combinations by stimulation of a motor nerve (Galea et al., 1991). Alternation results in overestimation of motor unit numbers and increases progressively with the number of motor units recruited (Stein and Yang, 1990). In this study, we used the ITS-MUNE method to overcome the problem of alternation by not counting the incremental increases in muscle twitch force but instead, calculating the average of 8 to 15 randomly chosen motor unit forces associated with incremental force increases at different stimulus amplitudes (Major et al., 2007) (Fig. 1B).

Beginning at a stimulus voltage of 100 μs duration that was below the threshold for recruitment of motor units, we applied a manually controlled graded 0 to 10 V electrical stimuli to the sciatic nerve at a frequency of 0.5 Hz.. At each stimulus intensity, the few motor units with thresholds very close to that voltage were variably recruited (due to alternation); the stimulus voltage was held constant for several pulses so that the change in isometric twitch force resulting from the intermittent firing of motor units with similar thresholds could be recorded. Thus, every possible combination of motor unit addition was recorded. The voltage was manually raised until the voltage required to elicit the maximal isometric twitch force was reached. Even though the motor units added in multiple combinations at each of the stimulus intensities, we can still assume that each distinguishable "all-or-none" change in the isometric force is the addition of individual motor units, as in the incremental method of McComas et al. (1971). However, in contrast with the incremental method, we did not count the number of incremental steps to yield motor unit number, as we know that we have intermittent firing and associated alternation.

We calculated the force associated with 8 to 15 random increments in whole muscle force chosen by the computer from various stimulus voltage intensities. Average motor unit force was obtained by overlaying the digitized forces in MATLAB and template subtraction of the forces to give the individual motor unit twitch forces. As motor units were chosen at random, a representative sample of motor unit forces was obtained. In addition, if the threshold of the chosen motor units is different enough, we can assume that they are not the result of alternation (Major et al., 2007). The average motor unit force was divided into the maximal isometric twitch force to give an estimate of the number of motor units, as previously described (McComas, 1995) (Fig. 1B).

Myosin heavy chain (MHC) determination

We used electrophoresis to quantitatively determine the MHC-isoform content of TA, EDL, MG and SOL muscles, as previously described (Gallo et al., 2004; Hamalainen and Pette, 1993; Martins et al., 2006; Putman et al., 2003). In brief, muscles were homogenized in a buffer containing 100 mM $Na_4P_2O_7$ (pH 8.5), 5 mM EGTA, 5 mM $MgCl_2$, 0.3 M KCl, 10 mM DTT and 5 mg/mL of Complete™ protease inhibitor cocktail (Roche Diagnostics, Indianapolis, IN, USA) and stirred for 30 min on ice. Homogenates were then cleared by centrifugation (12,000×*g* at 4 °C), diluted 1:1 with glycerol and stored at −20 °C. Prior to dilution in Laemmli lysis buffer and boiling for 5 min, the protein concentration of the samples was determined (Lowry et al., 1951). Following the dilution, 1 μg of total protein was loaded

into each lane of a 4% polyacrylamide stacking gel that also contained glycerol. Under a constant voltage of 275 V, the samples were separated under denaturing conditions on a 7% polyacrylamide separating gel that also contained glycerol, for 24 h at 8 °C (Hoefer SE600; Amersham Biosciences). Gels were subsequently silver stained (Oakley et al., 1980) and evaluated in triplicate by densitometry (Syngene) (Hamalainen and Pette, 1993; Martins et al., 2006).

Statistics

Data are presented as means ± standard errors (SE). Statistical significance between experimental and control groups was assessed using a Student's *t*-test (SPSS, Version 8.0). Differences were considered statistical significant at $p < 0.05$. Power calculations were completed to confirm sufficient power and/or sample size using PC-Size (STATOOLS, Version 2.13, 1986).

Results

Comparison of SOD1^{WT} and non-transgenic control mice

SOD1^{WT} transgenic mice, which express normal human SOD1, do not develop symptoms of weakness or paralysis during the life span of the SOD1^{G93A} or even at 1 year of age (Chiu et al., 1995; Gurney et al., 1994). We measured contractile isometric force and determined the number of motor units in the hindlimbs of both SOD1^{WT} and control, non-transgenic mice. The whole muscle contractile twitch force (Fig. 2A), and the number of motor units (Fig. 2B) were the same for all the hindlimb muscles when the SOD1^{WT} and age-matched non-transgenic mice were compared at 120 days of age. Hence, we assumed that the contractile force and motor unit numbers for the SOD1^{WT} and age-matched non-transgenic mice do not differ at any time point throughout the life span of the SOD1^{G93A} mouse. Therefore, we combined our data from SOD1^{WT} mice and non-transgenic mice as the control group (CON) with an average of 6 mice at 40, 80, and 120 days of age.

Phenotypic composition of fast- and slow-twitch hindlimb muscles

In order to establish the muscle fiber type composition in the mixed fast-twitch MG, TA, and EDL muscles, and in the slow-twitch SOL of the SOD1^{WT} mouse, gel electrophoresis was used to separate and quantify the various MHC isoforms (i.e., MHC-I, MHC-Iia, MHC-IId/x and MHC-IIb). This method has previously been shown to accurately reflect the corresponding fiber type proportions in rodent skeletal muscles (i.e., type-I, -IIA, -IID/X and -IIB fibers) (Putman et al., 1993).

All three fast-twitch muscles contained very high proportions of type II MHC's with 10% or less being MHC-I (Fig. 3). The 3 fast-twitch muscles differed, however, in the relative proportions of the three fast MHC-isoforms (i.e., MHC-IIa, MHC-IId/x and MHC-IIb) with the TA muscle containing comparatively high levels of MHC-IId/x. The proportion of MHC-IId/x was ~32% in the TA muscle, as compared to ~15–20% within the MG and EDL muscles; the proportion of MHC-IIb was significantly lower in the TA (Fig. 3C). The slow-twitch SOL comprised ~44% MHC-I and ~29% MHC-IIa. Thus 71% of all fibers were either slow-oxidative or fast-oxidative; the remaining were much smaller proportions of IID/X and IIB (Fig. 3F). The muscle

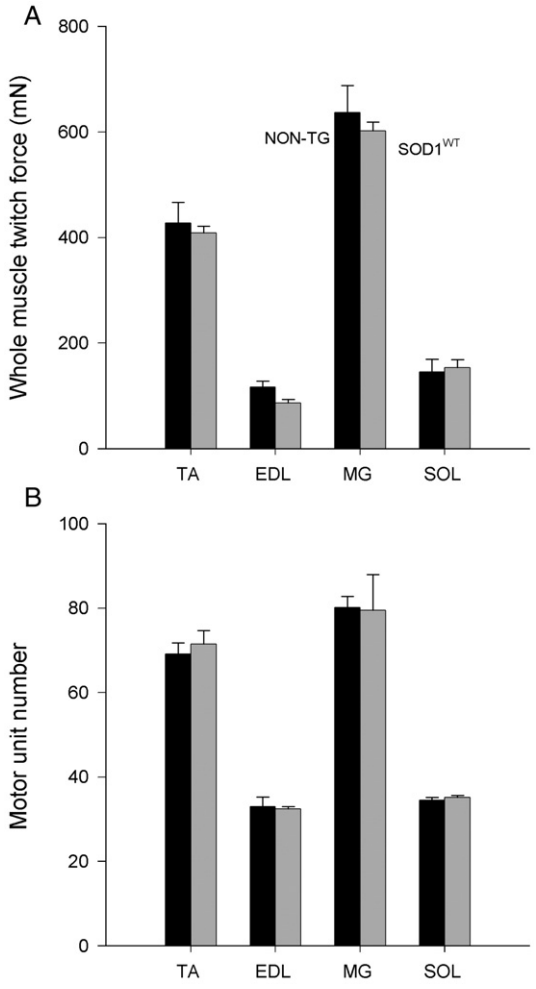


Fig. 2. Comparison of the whole muscle twitch force (A) and calculated motor unit numbers (B) in the hindlimb muscles of 120-day-old non-transgenic wild-type (black bars) and SOD1^{WT} (grey bars). There were no significant differences in either whole muscle twitch force or motor unit number between the non-transgenic and SOD1^{WT} in any of the four muscles studied. Data is reported as means ± SEM. Significant difference: $*p < 0.05$, $**p < 0.01$.

fiber type observed in all the CON mice muscles agrees well with previously published mouse data (Agbulut et al., 2003; Hamalainen and Pette, 1993; Harrison et al., 2003).

Selective muscle susceptibility in pre-symptomatic SOD1^{G93A} mice

We first compared the muscle forces developed by the fast-twitch EDL and the slow SOL, which differ considerably in their fiber type compositions and in their functions, the EDL being a physiological flexor, whilst the SOL muscle is a physiological extensor. At the age of 80 days when normal numbers of motoneurons were reported in the SOD1^{G93A} mouse, the tetanic force developed by the SOD1^{G93A} mouse EDL muscle was already significantly decreased as compared to the control mouse EDL at 80 days of age (Fig. 4A). The mean tetanic force declined by approximately half (45%) in the EDL while mean force developed by the SOL muscles in the SOD1^{G93A} mice was not significantly different from the muscles of the age-matched

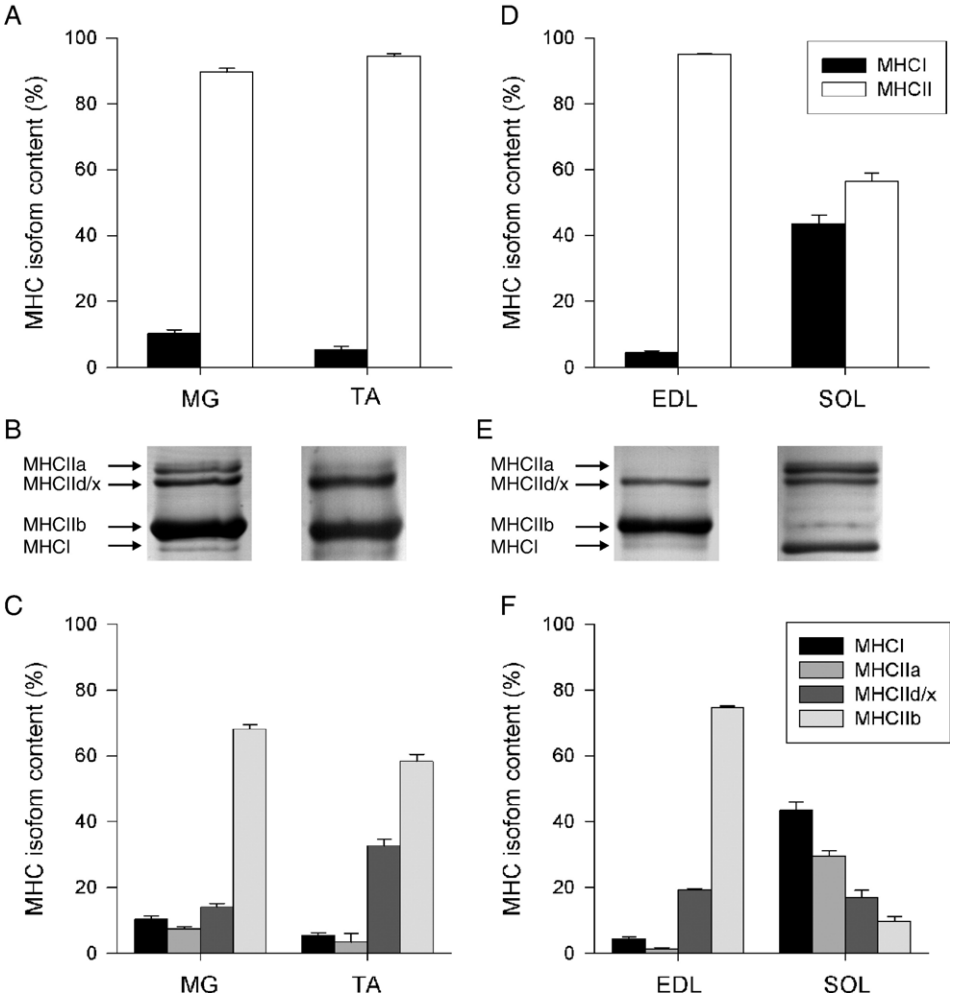


Fig. 3. MHC isoforms composition in hindlimb muscles of 80-day-old SOD1^{WT} mice. (A,D) The MG, TA and EDL muscles expressed predominantly fast MHC-II isoforms. In contrast, the SOL muscle had a much higher proportion of slow MHC-I. (B,E) Representative SDS–PAGE gels showing the MHC isoforms. (C) Proportions of the MHC-isoforms in the MG and TA muscles and in the (F) EDL and SOL muscles of the SOD1^{WT} mice. Data is presented as mean ± SE.

control mice (Fig. 4A). This is the first report of a selective susceptibility of fast-twitch whole muscle contractile force, as compared to slow-twitch muscle contractile force before the onset of overt symptoms in the SOD1^{G93A} mouse.

To further investigate the selective neuromuscular deficit in the fast-twitch EDL but not within the largely slow-twitch SOL of the pre-symptomatic SOD1^{G93A} mouse, we next determined the number of intact motor units in these muscles. Motor unit force was measured by incremental stimulation of the sciatic nerve to evoke all-or-none increments in twitch force (see Materials and methods and Fig. 1). A mean motor unit force was obtained from 8 to 15 motor units, allowing us to calculate the number of functional motor units. At 80 days of age, the number of EDL motor units declined by 48% in the SOD1^{G93A} mice, as compared to control mice. In contrast, there was no significant loss of motor units in the SOL muscle at the same age (Fig. 4B).

The magnitude of the decline in the mean tetanic force produced by the EDL muscle in the SOD1^{G93A} mice was the same as the decline in the number of functional motor units in the EDL muscle (Fig. 4). This parallel decline in whole muscle force and motor unit number indicated that there was little or no functional enlargement of the remaining motor units in the EDL muscles.

Selective motor unit loss at earliest signs of disease pathology

As expected from the normal number of motor units in the 80-day-old SOD1^{G93A} SOL muscle (Fig. 4), the number of motor units in the 40-day-old SOD1^{G93A} SOL muscle was not significantly different from the number of motor units in the control SOL (Fig. 5A). In contrast, the number of motor units in the fast-twitch MG muscle was significantly reduced by ~22% as compared to control mice at 40 days of age (Fig. 5B). There was also a trend for the number of motor units to decrease in the fast-twitch EDL and TA muscles (Fig. 5). This early loss at 40 days of age, occurs before other investigators reported denervation with electromyographic (Azzouz et al., 1997; Kennel et al., 1996; Shefner et al., 2001) or immunohistochemical methods (Frey et al., 2000). This early and selective pattern of motor unit loss from the fast-twitch muscles indicates the increased susceptibility of the larger motoneurons, which innervate the fast type IIB and IID/X muscle fibers. Motoneurons that innervate the type I and IIA

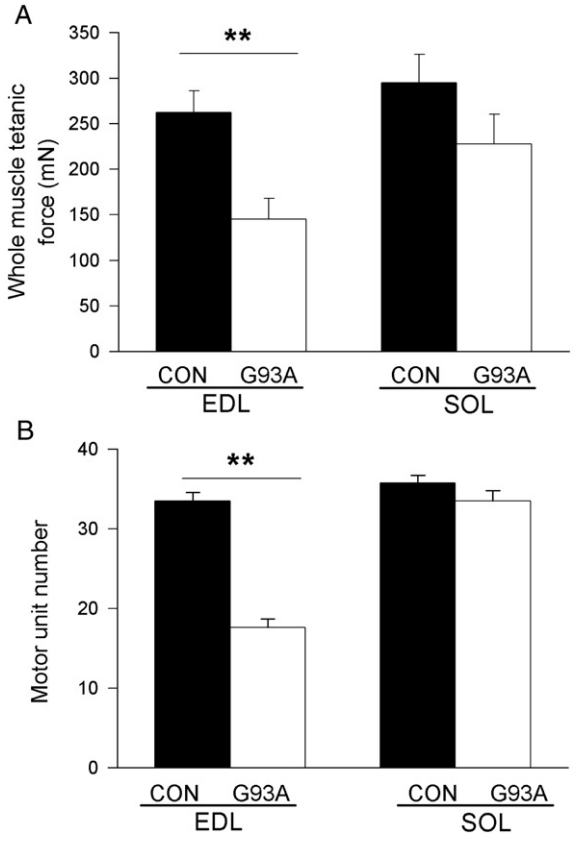


Fig. 4. Whole muscle isometric tetanic forces and the number of intact motor units in the SOD1^{G93A} mouse EDL and SOL muscles at 80 days of age. (A) The whole muscle tetanic contractile force developed by the 2 muscles indicates that there was a significant decline in the twitch force generated by the EDL, but not the SOL, in the SOD1^{G93A} mouse as compared to control mouse muscles. The tetanic force produced by the SOD1^{G93A} mouse was approximately half of the control EDL muscle values. (B) The number of motor units in the EDL muscle also declined to half of the number in the control EDL muscle. Statistical symbols as per Fig. 2.

muscle fibers, as in the SOL, are smaller and appear to be less susceptible in pre-symptomatic SOD1^{G93A} mice.

Muscle phenotype dictates susceptibility to motor unit loss

To determine whether muscle fiber type proportions dictate motor unit susceptibility from 40 days of age when we first detected a significant decline in the number of motor units (Fig. 5) and across the life span of the SOD1^{G93A} mouse, we determined the number of motor units in the TA, MG, EDL and SOL muscles at 10 day intervals from 40 to 120 days of age in the SOD1^{G93A} mice.

In the slow-twitch SOL muscle, there was no pre-symptomatic loss of motor units in the SOD1^{G93A} mice as compared to age-matched controls (Figs. 4–6). At 90 days of age, coincident with the onset of detected hindlimb weakness in the SOD1^{G93A} mouse, there was a significant decline of ~20% in the number of motor units in the SOL muscle. The decline in numbers of motor units in the SOL muscle continued until 100 days of age (Fig. 6A), by which time the mice were spastic and trembled (Chiu et al., 1995). From 100 to 120 days of age, the number of motor units remained constant at ~20 motor units, which is approximately 60% of the motor units in the control mouse SOL (Fig. 6C). In contrast, the number of motor units in the EDL declined exponentially, with a sharp initial drop in motor unit numbers that was already evident at 40 days of age (Fig. 6A). The sharp decline of motor units in the EDL muscle continued until 90 days of age, when the number of motor units reached a plateau of ~15 motor units, or ~40% of the motor units in the control EDL muscle. There was no decline in the number of EDL motor units following the onset of symptoms of weakness and tremors in the SOD1^{G93A} mouse at 90 days of age.

Similar to the EDL, the MG and TA muscles also contained low proportions of the slow muscle fibers and exhibited early and exponential declines in the number of motor units (Fig. 6B). The sharpest decline in motor unit numbers occurred in the TA muscle between 40 and 50 days of age. After 50 days of age, the decline in TA motor units proceeded in a more gradual manner, until the motor unit numbers reached an initial plateau at 70 days of age. Thereafter, there was a second sharp drop in the number of TA motor units between 80 and 100 days of age, around the time of

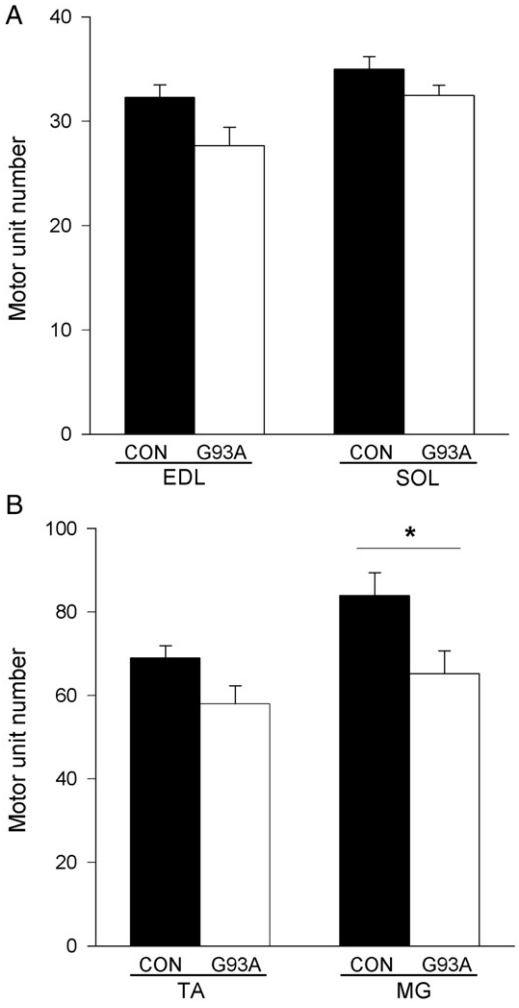


Fig. 5. The number of intact motor units in pre-symptomatic 40-day-old SOD1^{G93A} and age-matched control (CON) mice. (A) As compared to controls, the number of motor units in the EDL, but not SOL muscle, tended to be lower in the SOD1^{G93A} mouse at 40 days of age. (B) The number of intact motor units was significantly decreased in the SOD1^{G93A} mouse MG, but and tended toward being lower in the TA muscles, as compared to controls. Statistical symbols as per Fig. 2.

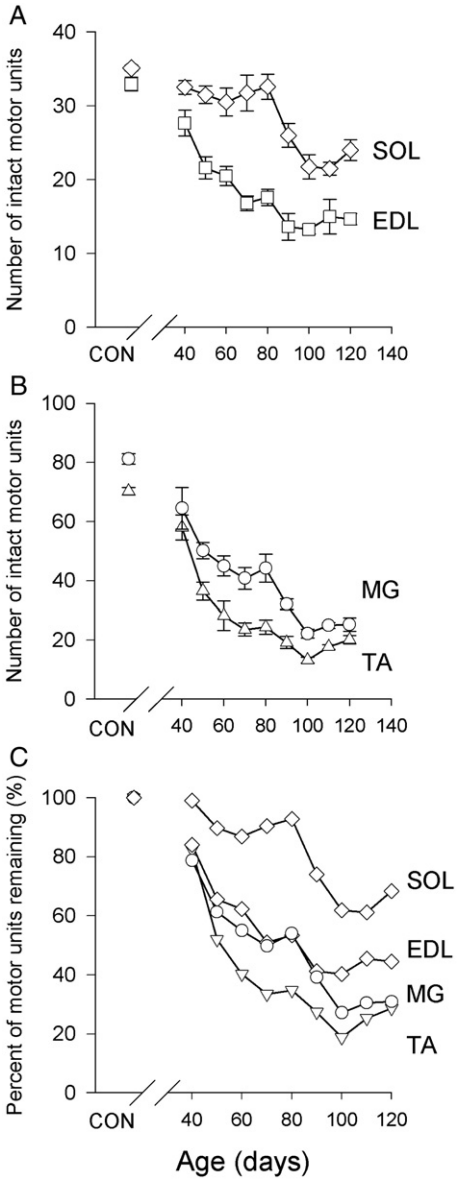


Fig. 6. The time course of motor unit loss in the SOD1^{G93A} mice, from 40 to 120 days of age. The number of motor units in the control mice did not change throughout the life span of the SOD1^{G93A} mouse, and control values are presented as averages of 3 time-points, 40, 80 and 120 days of age. (A) There was no loss of motor units from the SOL muscle until 90 days of age, coincident with the reported onset of symptoms. In the EDL, there was an exponential loss, with an initial steep decline of motor units. (B) Motor units are also exponentially lost from the TA and MG muscles, with a slight biphasic effect. Motor units are lost quickly from 40 to 60 days of age, and again from 80 to 100 days of age. (C) The percent of motor units remaining, as compared to control muscles. In all 4 hindlimb muscles, the initial decline in motor unit numbers is very steep, but the number of motor units reaches a plateau in the symptomatic stage of disease, with no motor units being lost after 100 days of age.

symptom-onset. There was no decline in the number of motor units in the TA after 100 days of age in the SOD1^{G93A}; ~20 motor units remained in TA muscles until 120 days of age. The MG muscle had, respectively, lower and higher proportions of type IID/X and IIB muscle fibers compared to the TA and did not exhibit as great an exponential decline of motor units as the TA muscle. The decline in MG motor units was biphasic, as in the TA muscle, with an initial decline from 40 to 60 days of age and a second significant phase of decline from 80 to 100 days of age. This second phase was followed by a plateau in the number of motor units, from 100 to 120 days of age, wherein only ~25 motor units remained in the MG muscle.

In all four of the hindlimb muscles studied, there was no significant motor unit loss from 100 to 120 days of age (Fig. 6C), regardless of muscle fiber type composition or muscle function. As compared to the number of motor units in control mice, ~70%, 45%, 30% and 30% of motor units remained in the SOL, EDL, MG and TA, respectively, at 120 days of age. The high percentage of surviving motor units at 120 days of age in the SOL is due to the greater proportions of slow type-I and -IIA fibers. This correspondence of surviving motor units to the proportion of slower MHC-I and MHC-IIa isoforms provides further support for the hypothesis that there is a preferential loss of motoneurons innervating the fast-twitch muscle fibers.

Contractile force declines in parallel with motor unit numbers

As shown in Fig. 4, the loss of motor units in the 80-day-old SOD1^{G93A} mouse EDL muscle resulted in a corresponding decrease in the force producing capacity of this fast-twitch muscle. This correspondence between motor unit loss and decline in force producing capability indicates that there is no functional compensation for the loss of motor units in the EDL muscle at 80 days of age. It is possible that this uncompensated neuromuscular deficit in the EDL muscle is not detectable in behavioural tests because the EDL produces only a fraction of the force produced by the antagonistic MG and the agonist TA muscles.

Therefore, we wanted to determine whether there was any evidence of functional compensation in the fast-twitch MG and TA muscles during the life span of the SOD1^{G93A} mouse. We recorded muscle tetanic forces from the MG and TA throughout the life span of the mouse and compared the magnitude and time-course of the fall in contractile force to the decline in motor unit numbers. In both the MG and TA muscles, the contractile muscle forces decreased with age in the SOD1^{G93A} mice as compared to age matched control mice, in which the tetanic forces remained constant (Figs. 7A,B). In the SOD1^{G93A} mouse at 40 days of age, there was already a significant decline in the force generating capacity of the fast-twitch TA and MG muscles. In both muscles the decline in tetanic force was exponential, with a sharp initial drop that plateaus at ~100 days of age (Figs. 7A,B).

In the fast-twitch TA and MG muscles, the motor unit numbers fell in proportion to the decline in tetanic force (Figs. 7C,D). Had there been compensatory axonal sprouting, we would have seen sustained twitch and tetanic isometric forces, despite a decline in motor unit numbers, a 5-fold increase in motor unit size normally compensating for loss of up to 85% of the motor units (Gordon and Pattullo, 1993). The parallel decline demonstrates that there is little or no functional compensatory enlargement of the remaining motor units in the SOD1^{G93A} mice in the fast-twitch muscles studied.

Discussion

The major finding of the present study was an early and selective decline in the number of motor units in fast-twitch hindlimb muscles, but not slow-twitch muscles, which was already

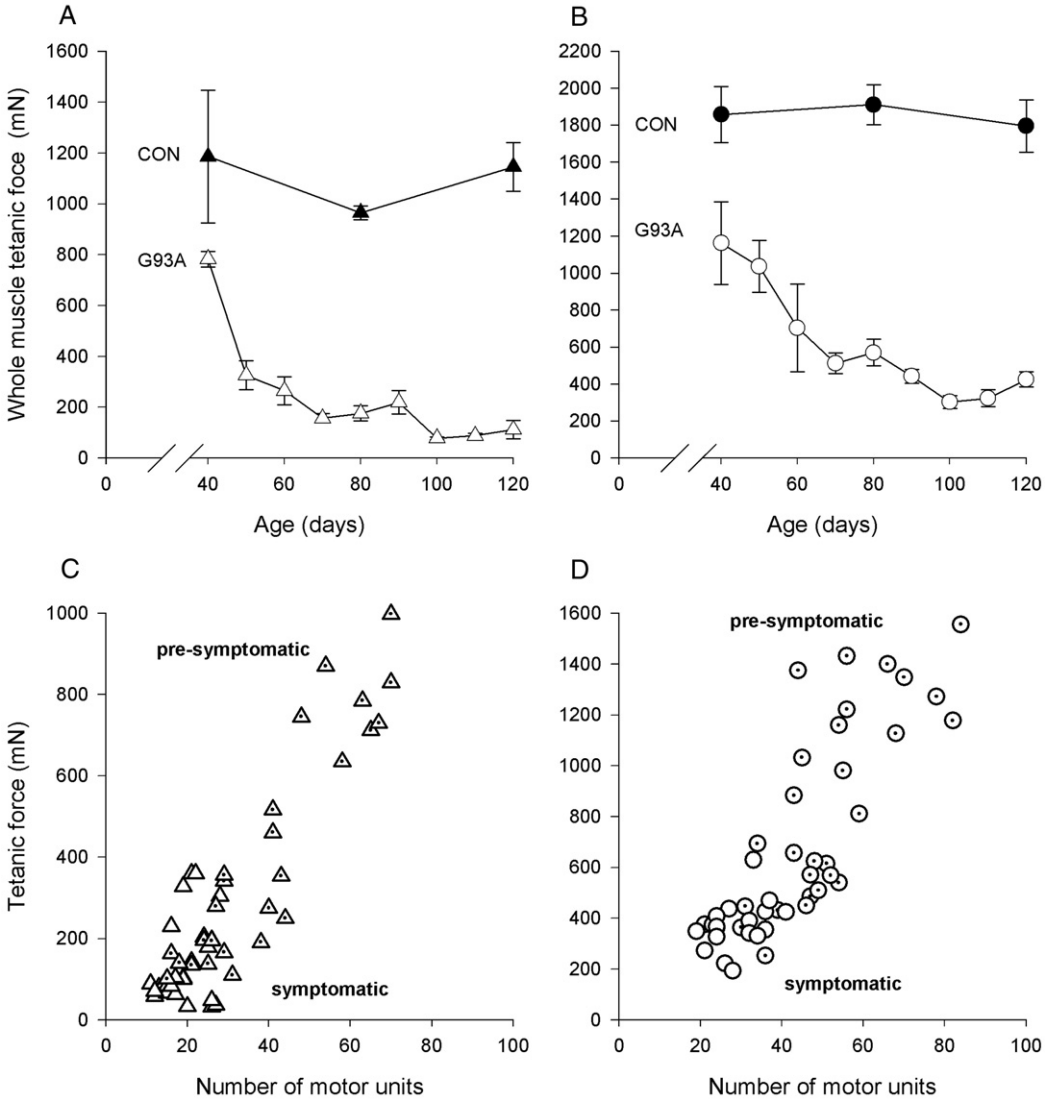


Fig. 7. The whole muscle isometric tetanic forces produced by the MG and TA muscles in SOD1^{G93A} as compared to control mice. Tetanic force was measured at 10-day intervals from 40 to 120 days of age in the SOD1^{G93A} mice. (A) The tetanic contractile force generated by the control TA muscle stayed constant throughout the life span of the SOD1^{G93A} mouse. In the SOD1^{G93A} mice, the tetanic force declined exponentially in the TA muscle. (B) The same exponential decline was seen in the tetanic force produced by the SOD1^{G93A} mouse MG muscle, as compared to the unchanging tetanic force produced by the control mouse MG. Data in A and B are reported as mean ± SEM. (C and D) In the TA and MG muscles of the SOD1^{G93A} mouse, the tetanic force generating capacity and the number of motor units declined in parallel (symbols with dots are pre-symptomatic mouse values, open symbols are symptomatic mouse values). (C) The tetanic force is plotted against the number of motor units remaining in the TA muscle.

evident at 40 days of age, a full 50 days before the onset of symptoms in the SOD1^{G93A} mouse model of ALS. This preferential loss of fast-twitch motor units was dictated by muscle fiber type proportions and not by muscle function. Furthermore, we report the novel finding that the loss of motor units continued with increasing age and paralleled reductions in whole muscle force. The only previous study to compare whole muscle contractile forces of a fast- and slow-muscles in the SOD1^{G93A} mouse found a significant decline in the whole muscle tetanic force at 120 days for the EDL, but not the SOL muscle (Derave et al., 2003).

Our findings of selective motor unit vulnerability support immunohistochemical evidence indicating that denervation proceeds in a muscle-specific manner, with the denervation of type IIB muscle fibers before slower, type I, IIA and IID/X fibers in the triceps surae (Frey et al., 2000) and TA muscles of the SOD1^{G93A} mouse (Hegedus et al., 2006; Pun et al., 2006). Longitudinal visualization of single motor units in SOD1^{G93A} mice also revealed that some axons were maintained, and that these were selectively able to compensate for the loss of other degenerating axons (Schaefer et al., 2005). Although they did not draw parallels between slow and fast-motor units, the results of Schaefer et al. (2005) showed a greater number of innervated endplates in the slow-twitch SOL muscles, as compared to the fast-twitch EDL muscle.

With accumulating anatomical evidence for a die-back process in the SOD1 mouse (Fischer et al., 2004a), it has become increasingly important to reconcile electrophysiological studies that had reported contrasting rates of motor unit loss in pre-symptomatic SOD1^{G93A} mice. Our present findings resolve the apparent differences in the

time course of motor unit loss reported by the EMG studies (Azzouz et al., 1997; Kennel et al., 1996; Shefner et al., 1999; Shefner et al., 2001). Although our data agree with those of Kennel et al. (1996) which showed that the motor unit loss from the gastrocnemius muscle was already significant at 47 days of age, the authors did not characterize the time course of motor unit loss and we are unable to compare our data with theirs. In contrast, Azzouz et al. (1997) reported that there was a dramatic decline in the number of motor units in the MG muscle only after 100 days of age. Based on those data, they suggested that motor unit loss was coincident with motoneuron death in the lumbar spinal cord in symptomatic SOD1^{G93A} mice. We evaluated and detected a biphasic decline in MG motor units earlier than any of the previous studies (40 days of age). The motor unit number declined dramatically between birth and ~60 days in all the fast-twitch muscles that we studied, including the MG, TA and EDL after which the number reached a plateau prior to a second and later fall in numbers to the second lower plateau in parallel with the decline in motor unit number in the slow-twitch soleus muscle (Fig. 6). The plateau of motor unit numbers in the asymptomatic phase of the disease before 90 days of age coincided with the age of the SOD1^{G93A} mice at which Azzouz et al. (1997) began their EMG studies of motor unit numbers of MG muscle in the same mouse. The plateau reached by the motor units in fast-twitch muscles may explain why these authors did not detect the first of two dramatic declines in motor unit number during the life span of the SOD1^{G93A} mouse.

The biphasic decline in motor unit numbers that we observed in the fast-twitch muscles of the SOD1^{G93A} mouse mirrors the disease progression in ALS patients, where the fastest rate of motor unit loss is within the first year of disease diagnosis, after which the loss becomes more gradual (Dantes and McComas, 1991). The selective vulnerability of motor units innervating fast-twitch muscles in the SOD1^{G93A} mice also corroborates with findings in human patients of a higher susceptibility of the motor units with larger twitch forces (Dengler et al., 1990). Using two different methods to enumerate motor units from functional EMG recordings in SOD1^{G93A} mice, Shefner et al. (2002) consistently estimated the number of motor units in all the extensor and flexor muscles of the lower hindlimb. They reported an exponential loss of motor units, that was significant by ~60 days of age when they began their examination (Shefner et al., 1999; Shefner et al., 2002). However, they studied both fast- and slow-twitch muscles simultaneously, and neither the biphasic motor unit loss in the MG and TA muscles nor the preferential loss of the fastest motor units could be detected. In order to observe the selective vulnerability of motor units, fast-twitch muscles had to be studied in isolation, and contrasted with slow-twitch SOL muscles as we have done here.

Our second major finding was that this selective vulnerability of the motor units innervating fast-twitch muscles was maintained throughout the life span of the SOD1^{G93A} mouse (Fig. 6). In the fast-twitch muscles, there was an exponential decline in motor units, with a significant loss detected in the MG muscle at 40 days of age. In the slow-twitch SOL muscle, there was no significant decline in the number of motor units until 90 days of age. The decline in motor unit numbers reached a plateau in all of the muscles we studied at ~100 days of age. In the SOL muscle, ~70% of the motor units remained at end-stage disease, corresponding to the proportion of muscle fibers that express the slower MHC-I and MHC-IIa isoforms (~70%). This correspondence between muscle fiber type proportions and motor unit loss is supporting evidence for the selective vulnerability of motor units innervating the fast-twitch muscles. Moreover, the decline in motor unit numbers in the slow-twitch muscles that occurred after 80 days of age, coincided with the phase of the second decline in motor unit numbers in the fast-twitch muscles. Since the motor units containing the type IIB muscle fibers were lost first, with evidence of some sprouting capacity of nerves to the type I and IIA muscle fibers (Frey et al., 2000; Pun et al., 2006), the progressive loss of the type IID/X and IIA muscle fibers during the symptomatic phase of the disease is quite consistent with the loss of extensor tone in the hindlimbs and the reduced numbers of motor units detected by others as well as with findings of enlarged motor units at the late stage of disease in the mice (Schaefer et al., 2005).

Selective loss of functional motor units may be linked to the characteristics that distinguish motoneurons innervating muscle fibers expressing slow type MHC-I isoform from those expressing fast type MHC-II isoforms. According to the Henneman size principle, motoneurons that innervate fast motor units are those with the largest innervation ratios, soma sizes and axon calibers (Gordon et al., 2004; Henneman and Mendell, 1981). Smaller motoneurons, which are recruited first under physiological conditions, innervate the smallest and slowest motor units. It has been shown that axons are susceptible in a caliber-specific order, with the largest caliber axons being the most susceptible to loss in mouse models of ALS (Bendotti et al., 2001; Fischer et al., 2004b; Kong and Xu, 1998) and in human patients (Feinberg et al., 1999). Interestingly, when axons are converted to smaller calibers by experimentally inducing peripheral nerve injury and axon regeneration, they become less susceptible (Kong and Xu, 1999). Here, we provide further supporting evidence that motor unit type, and the associated differences in innervation ratio, axon caliber and soma size appear to have a role in specific vulnerability of motoneurons. Hence, larger soma size and axon diameter appear to be important determinants of differential motoneuron susceptibility and our results corroborate the hypothesis that implicates soma size and metabolic demands in the preferential susceptibility of motoneurons (Shaw and Eggett, 2000).

Our third major finding was that motor unit loss was paralleled by a decline in the force generating capacity of the hindlimb muscles in the SOD1^{G93A} mouse. At 80 days of age, there was no evidence of functional compensation for the selective motor unit loss in the EDL muscle (Fig. 4). When we compared the decline in motor unit numbers to the drop in force generating capacity in the MG and TA muscles throughout the life span of the SOD1^{G93A} mouse, we also found no evidence of functional compensation (Fig. 7). Previous immunohistochemical work showed that the motoneurons innervating muscle fibers expressing slow MHC isoforms exhibit a compensatory sprouting response (Frey et al., 2000; Pun et al., 2006). Using transgenic mice that express both green fluorescent protein and mutant SOD1^{G93A}, Schaefer et al. (2005) also showed a robust compensatory sprouting response in axons that were preferentially spared. Our results suggest that this sprouting process is ineffective and few, if any, functional connections are formed as a result of compensatory axonal sprouting. Work by Shefner et al. (2001) that showed a proportional decline in CMAP and motor unit numbers is also indicative of a lack of compensatory motor unit enlargement.

Despite the early and significant fast-twitch muscle deficits, commonly employed behavioural tests have failed to reliably detect these early neuromuscular deficits in the hindlimbs of the SOD1^{G93A} mice (Weydt et al., 2003). Recently, a novel gait analysis technique performed on a similar mouse model of ALS

revealed behavioural deficits in pre-symptomatic mice (Wooley et al., 2005). In the SOD1^{G93A} mouse, an early deficit was also uncovered when the mice were made to exercise; 56-day-old SOD1^{G93A} mice were only able to run at a speed of 12 m/min, but mice with a delayed disease onset could run at speeds of 16 m/min (Veldink et al., 2003). We have shown that by 56 days of age, half the motor units innervating the TA muscle have already been lost, resulting in significant deficits in the force produced by the TA muscle (Fig. 6). Given that the TA muscle is proportionally activated with increases in treadmill speeds (Roy et al., 1991), TA muscle deficits should become increasingly apparent with faster running speeds. Novel functional tests that measure changes in stance and locomotion need to be implemented to fully assess neuromuscular function in the SOD1^{G93A} mouse.

In conclusion, we show that clinically detectable muscle deficits are present at the time of earliest pathological dysfunction in the SOD1^{G93A} mouse model of fALS. Our findings provide convincing evidence that motor unit loss and associated muscle function precedes motoneuron death in accordance with the "die-back" hypothesis (Fischer et al., 2004b), in accord with indications from EMG studies and in agreement with anatomical studies. Moreover, our time-course of preferential motor unit loss reconciles previous contradictory reports of pre-symptomatic motor unit loss in the SOD1^{G93A} mouse model of ALS and supports the available anatomical evidence that has suggested that motoneurons that innervate the slower muscle fibers are more resilient in the SOD1^{G93A} mice (Frey et al., 2000; Schaefer et al., 2005). Further study is required to examine the mechanisms underlying this preferential motor unit loss. Here, we have shown that the largest motoneurons with the biggest axon calibers are the most vulnerable to cell death, implicating size as contributing factor for selective vulnerability. These large motoneurons also have the largest innervation ratios (Gordon et al., 2004), and the smallest complement of oxidative enzymes (Ishihara et al., 1995), suggesting that the activity and antioxidant capability of the small motoneurons play an important role in the survival of functional motor units, at least in the pre-symptomatic phase of disease. Our data do not support compensatory motor unit expansion in any of the hindlimb muscles studied. The parallel decline in motor unit numbers and whole muscle contractile force did not detect the motor unit expansion that would be expected for the motor units containing type I and IIA muscle fibers where axonal sprouting does occur (Pun et al., 2006). Despite mice appearing asymptomatic, deficits in whole muscle contractile force were detected in the fast-twitch muscles as early as 40 days of age, highlighting the need for more sensitive behavioural tests that can detect subtle muscle deficits in the hindlimbs.

Acknowledgments

Operating grants from CIHR/NRP, NSERC and AHFMR supported this work. JH received graduate studentships from AHFMR and NSERC. Kelvin Jones and Doug Weber were instrumental in developing the MATLAB program for motor unit number estimation. CT Putman is an AHFMR Senior Scholar. T Gordon is an AHFMR Senior Scientist.

References

Agbulut, O., Noirez, P., Beaumont, F., Butler-Browne, G., 2003. Myosin heavy chain isoforms in postnatal muscle development of mice. Biol. Cell 95, 399–406.

Azzouz, M., Leclerc, N., Gurney, M., Warter, J.M., Poindron, P., Borg, J., 1997. Progressive motor neuron impairment in an animal model of familial amyotrophic lateral sclerosis. Muscle Nerve 20, 45–51.

Bendotti, C., Calvaresi, N., Chiveri, L., Prelle, A., Moggio, M., Braga, M., Silani, V., De Biasi, S., 2001. Early vacuolization and mitochondrial damage in motor neurons of FALS mice are not associated with apoptosis or with changes in cytochrome oxidase histochemical reactivity. J. Neurol. Sci. 191, 25–33.

Chiu, A.Y., Zhai, P., Dal Canto, M.C., Peters, T.M., Kwon, Y.W., Prattis, S.M., Gurney, M.E., 1995. Age-dependent penetrance of disease in a transgenic mouse model of familial amyotrophic lateral sclerosis. Mol. Cell. Neurosci. 6, 349–362.

Dantes, M., McComas, A., 1991. The extent and time course of motoneuron involvement in amyotrophic lateral sclerosis. Muscle Nerve 14, 416–421.

Dengler, R., Konstanzer, A., Kuther, G., Hesse, S., Wolf, W., Struppler, A., 1990. Amyotrophic lateral sclerosis: macro-EMG and twitch forces of single motor units. Muscle Nerve 13, 545–550.

Derave, W., Van Den, B.L., Lemmens, G., Eijnde, B.O., Robberecht, W., Hespel, P., 2003. Skeletal muscle properties in a transgenic mouse model for amyotrophic lateral sclerosis: effects of creatine treatment. Neurobiol. Dis. 13, 264–272.

De Winter, F., Vo, T., Stam, F.J., Wisman, L.A., Bar, P.R., Niclou, S.P., vanMuiswinkel, F.L., Verhaagen, J., 2006. The expression of the chemorepellent Semaphorin 3A is selectively induced in terminal Schwann cells of a subset of neuromuscular synapses that display limited anatomical plasticity and enhanced vulnerability in motor neuron disease. Mol. Cell. Neurosci. 32, 102–117.

Feinberg, D.M., Preston, D.C., Shefner, J.M., Logigian, E.L., 1999. Amplitude-dependent slowing of conduction in amyotrophic lateral sclerosis and polyneuropathy. Muscle Nerve 22, 937–940.

Fischer, D., He, Z., Benowitz, L.I., 2004a. Counteracting the Nogo receptor enhances optic nerve regeneration if retinal ganglion cells are in an active growth state. J. Neurosci. 24, 1646–1651.

Fischer, L.R., Culver, D.G., Tennant, P., Davis, A.A., Wang, M., Castellano-Sanchez, A., Khan, J., Polak, M.A., Glass, J.D., 2004b. Amyotrophic lateral sclerosis is a distal axonopathy: evidence in mice and man. Exp. Neurol. 185, 232–240.

Frey, D., Schneider, C., Xu, L., Borg, J., Spooren, W., Caroni, P., 2000. Early and selective loss of neuromuscular synapse subtypes with low sprouting competence in motoneuron diseases. J. Neurosci. 20, 2534–2542.

Galea, V., de, B.H., Cavasin, R., McComas, A.J., 1991. The numbers and relative sizes of motor units estimated by computer. Muscle Nerve 14, 1123–1130.

Gallo, M., Gordon, T., Tyreman, N., Shu, Y., Putman, C.T., 2004. Reliability of isolated isometric function measures in rat muscles composed of different fibre types. Exp. Physiol. 89, 583–592.

Gordon, T., Pattullo, M.C., 1993. Plasticity of muscle fiber and motor unit types. Exerc. Sport Sci. Rev. 21, 331–362.

Gordon, T., Thomas, C.K., Munson, J.B., Stein, R.B., 2004. The resilience of the size principle in the organization of motor unit properties in normal and reinnervated adult skeletal muscles. Can. J. Physiol. Pharmacol. 82, 645–661.

Gurney, M.E., Pu, H., Chiu, A.Y., Dal Canto, M.C., Polchow, C.Y., Alexander, D.D., Caliendo, J., Hentati, A., Kwon, Y.W., Deng, H.X., 1994. Motor neuron degeneration in mice that express a human Cu,Zn superoxide dismutase mutation. Science 264, 1772–1775.

Hamalainen, N., Pette, D., 1993. The histochemical profiles of fast fiber types IIB, IID, and IIA in skeletal muscles of mouse, rat, and rabbit. J. Histochem. Cytochem. 41, 733–743.

Harrison, B.C., Allen, D.L., Girten, B., Stodieck, L.S., Kostenuik, P.J., Bateman, T.A., Morony, S., Lacey, D., Leinwand, L.A., 2003. Skeletal muscle adaptations to microgravity exposure in the mouse. J. Appl. Physiol. 95, 2462–2470.

Hegedus, J., Putman, C.T., Gordon, T., 2006. Activity-dependent conversion saves motor units (MUs) in a transgenic mouse model of amyotrophic lateral sclerosis (ALS). Neurosci. Soc. 31, 823.10.

Henneman, E., Mendell, L.M., 1981. Functional organization of the motoneurone pool and its inputs. In: Brooks, V.B. (Ed.), Handbook of Physiology. Sect. I. Vol. II. The Nervous System: motor control Part I. American Physiology Society, Washington, DC, pp. 345–442.

Ishihara, A., Roy, R.R., Edgerton, V.R., 1995. Succinate dehydrogenase activity and soma size of motoneurons innervating different portions of the rat tibialis anterior. Neuroscience 68, 813–822.

Johnston, J.A., Dalton, M.J., Gurney, M.E., Kopito, R.R., 2000. Formation of high molecular weight complexes of mutant Cu,Zn-superoxide dismutase in a mouse model for familial amyotrophic lateral sclerosis. Proc. Natl. Acad. Sci. U. S. A. 97, 12571–12576.

Kennel, P.F., Finiels, F., Revah, F., Mallet, J., 1996. Neuromuscular function impairment is not caused by motor neurone loss in FALS mice: an electromyographic study. NeuroReport 7, 1427–1431.

Kong, J., Xu, Z., 1998. Massive mitochondrial degeneration in motor neurons triggers the onset of amyotrophic lateral sclerosis in mice expressing a mutant SOD1. J. Neurosci. 18, 3241–3250.

Kong, J., Xu, Z., 1999. Peripheral axotomy slows motoneuron degeneration in a transgenic mouse line expressing mutant $SOD1^{G93A}$. J. Comp. Neurol. 412, 373–380.

Lowry, O.H., Rosebrough, N.J., Farr, A.L., Randall, R.J., 1951. Protein measurement with the Folin phenol reagent. J. Biol. Chem. 193, 265–275.

Major, L.A., Hegedus, J., Weber, D.J., Gordon, T., Jones, K.E., 2007. Method for counting motor units in mice and validation using a mathematical model. J. Neurophysiol. 97, 1846–1856.

Martins, K.J., Gordon, T., Pette, D., Dixon, W.T., Foxcroft, G.R., Maclean, I.M., Putman, C.T., 2006. Effect of satellite cell ablation on low-frequency-stimulated fast-to-slow fibre-type transitions in rat skeletal muscle. J. Physiol. 572, 281–294.

McComas, A.J., 1995. Motor-unit estimation: the beginning. J. Clin. Neurophysiol. 12, 560–564.

McComas, A.J., Fawcett, P.R., Campbell, M.J., Sica, R.E., 1971. Electrophysiological estimation of the number of motor units within a human muscle. J. Neurol. Neurosurg. Psychiatry 34, 121–131.

Oakley, B.R., Kirsch, D.R., Morris, N.R., 1980. A simplified ultrasensitive silver stain for detecting proteins in polyacrylamide gels. Anal. Biochem. 105, 361–363.

Pun, S., Santos, A.F., Saxena, S., Xu, L., Caroni, P., 2006. Selective vulnerability and pruning of phasic motoneuron axons in motoneuron disease alleviated by CNTF. Nat. Neurosci. 9, 408–419.

Putman, C.T., Spriet, L.L., Hultman, E., Lindinger, M.I., Lands, L.C., McKelvie, R.S., Cederblad, G., Jones, N.L., Heigenhauser, G.J., 1993. Pyruvate dehydrogenase activity and acetyl group accumulation during exercise after different diets. Am. J. Physiol. 265, E752–E760.

Putman, C.T., Kiricsi, M., Pearcey, J., Maclean, I.M., Bamford, J.A., Murdoch, G.K., Dixon, W.T., Pette, D., 2003. AMPK activation increases uncoupling protein-3 expression and mitochondrial enzyme activities in rat muscle without fibre type transitions. J. Physiol. 551, 169–178.

Rafuse, V.F., Gordon, T., Orozco, R., 1992. Proportional enlargement of motor units after partial denervation of cat triceps surae muscles. J. Neurophysiol. 68, 1261–1275.

Rosen, D.R., 1993. Mutations in Cu/Zn superoxide dismutase gene are associated with familial amyotrophic lateral sclerosis. Nature 364, 362.

Roy, R.R., Baldwin, K.M., Edgerton, V.R., 1991. The plasticity of skeletal muscle: effects of neuromuscular activity. Exerc. Sport Sci. Rev. 19, 269–312.

Schaefer, A.M., Sanes, J.R., Lichtman, J.W., 2005. A compensatory subpopulation of motor neurons in a mouse model of amyotrophic lateral sclerosis. J. Comp. Neurol. 490, 209–219.

Shaw, P.J., Eggett, C.J., 2000. Molecular factors underlying selective vulnerability of motor neurons to neurodegeneration in amyotrophic lateral sclerosis. J. Neurol. 247 (Suppl. 1), I17–I27.

Shefner, J.M., Reaume, A.G., Flood, D.G., Scott, R.W., Kowall, N.W., Ferrante, R.J., Siwek, D.F., Upton-Rice, M., Brown Jr., R.H., 1999. Mice lacking cytosolic copper/zinc superoxide dismutase display a distinctive motor axonopathy. Neurology 53, 1239–1246.

Shefner, J.M., Brown Jr., R.H., Cole, D., Chaturvedi, P., Schoenfeld, D., Pastuszak, K., Matthews, R., Upton-Rice, M., Cudkowicz, M.E., 2001. Effect of neurophilin ligands on motor units in mice with SOD1 ALS mutations. Neurology 57, 1857–1861.

Shefner, J.M., Cudkowicz, M.E., Brown Jr., R.H., 2002. Comparison of incremental with multipoint MUNE methods in transgenic ALS mice. Muscle Nerve 25, 39–42.

Stein, R.B., Yang, J.F., 1990. Methods for estimating the number of motor units in human muscles. Ann. Neurol. 28, 487–495.

Tam, S.L., Gordon, T., 2003. Mechanisms controlling axonal sprouting at neuromuscular junction. J. Neurocytol. Invited Review 32, 961–974.

Turner, B.J., Lopes, E.C., Cheema, S.S., 2003. Neuromuscular accumulation of mutant superoxide dismutase 1 aggregates in a transgenic mouse model of familial amyotrophic lateral sclerosis. Neurosci. Lett. 350, 132–136.

Veldink, J.H., Bar, P.R., Joosten, E.A., Otten, M., Wokke, J.H., van den Berg, L.H., 2003. Sexual differences in onset of disease and response to exercise in a transgenic model of ALS. Neuromuscul. Disord. 13, 737–743.

Weydt, P., Hong, S.Y., Kliot, M., Moller, T., 2003. Assessing disease onset and progression in the SOD1 mouse model of ALS. NeuroReport 14, 1051–1054.

Wooley, C.M., Sher, R.B., Kale, A., Frankel, W.N., Cox, G.A., Seburn, K.L., 2005. Gait analysis detects early changes in transgenic SOD1(G93A) mice. Muscle Nerve 32, 43–50.

J Physiol 586.14 (2008) pp 3337–3351

Preferential motor unit loss in the SOD1^{G93A} transgenic mouse model of amyotrophic lateral sclerosis

J. Hegedus[1], C. T. Putman[1,2], N. Tyreman[1] and T. Gordon[1,3]

[1] *Centre for Neuroscience and* [3] *Division of Physical Medicine and Rehabilitation, Faculty of Medicine, University of Alberta, Edmonton, AB, Canada, T6G 2S2*

[2] *Biochemistry Laboratory, Faculty of Physical Education and Recreation, University of Alberta, Edmonton, AB, Canada, T6G 2S2*

The present study investigated motor unit (MU) loss in a murine model of familial amyotrophic lateral sclerosis (ALS). The fast-twitch tibialis anterior (TA) and medial gastrocnemius (MG) muscles of transgenic SOD1^{G93A} and SOD1^{WT} mice were studied during the presymptomatic phase of disease progression at 60 days of age. Whole muscle maximum isometric twitch and tetanic forces were 80% lower ($P < 0.01$) in the TA muscles of SOD1^{G93A} compared to SOD1^{WT} mice. Enumeration of total MU numbers within TA muscles showed a 60% reduction ($P < 0.01$) within SOD1^{G93A} mice (38 ± 7) compared with SOD1^{WT} controls (95 ± 12); this was attributed to a lower proportion of the most forceful fast-fatigable (FF) MU in SOD1^{G93A} mice, as seen by a significant ($P < 0.01$) leftward shift in the cumulative frequency histogram of single MU forces. Similar patterns of MU loss and corresponding decreases in isometric twitch force were observed in the MG. Immunocytochemical analyses of the entire cross-sectional area (CSA) of serial sections of TA muscles stained with anti-neural cell adhesion molecule (NCAM) and various monoclonal antibodies for myosin heavy chain (MHC) isoforms showed respective 65% ($P < 0.01$) and 28% ($P < 0.05$) decreases in the number of innervated IIB and IID/X muscle fibres in SOD1^{G93A}, which paralleled the 60% decrease ($P < 0.01$) in the force generating capacity of individual fibres. The loss of fast MUs was partially compensated by activity-dependent fast-to-slower fibre type transitions, as determined by increases ($P < 0.04$) in the CSA and proportion of IIA fibres (from 4% to 14%) and IID/X fibres (from 31% to 39%), and decreases ($P < 0.001$) in the CSA and proportion of type IIB fibres (from 65% to 44%). We conclude that preferential loss of IIB fibres is incomplete at 60 days of age, and is consistent with a selective albeit gradual loss of FF MUs that is not fully compensated by sprouting of the remaining motoneurons that innervate type IIA or IID/X muscle fibres. Our findings indicate that disease progression in fast-twitch muscles of SOD1^{G93A} mice involves parallel processes: (1) gradual selective motor axon die-back of the FF motor units that contain large type IIB muscle fibres, and of fatigue-intermediate motor units that innervate type IID/X muscle fibres, and (2) activity-dependent conversion of motor units to those innervated by smaller motor axons innervating type IIA fatigue-resistant muscle fibres.

(Received 14 December 2007; accepted after revision 7 May 2008; first published online 15 May 2008)

Corresponding author T. Gordon: Division of Physical Medicine and Rehabilitation/ Centre for Neuroscience, 525 Heritage Medical Research Centre, Faculty of Medicine, University of Alberta, Edmonton, AB, Canada T6G 2S2.
Email: tessa.gordon@ualberta.ca

Adaptive and maladaptive motor axonal sprouting in aging and motoneuron disease

Tessa Gordon, Janka Hegedus and Siu Lin Tam

Centre of Neuroscience, Division of Physical Medicine and Rehabilitation, Faculty of Medicine and Dentistry, University of Alberta, Edmonton, Canada

Motor unit (MU) enlargement by sprouting is an important compensatory mechanism for loss of functional MUs during normal aging and neuromuscular disease. Perisynaptic Schwann cells at neuromuscular junctions extend processes that bridge between denervated and reinnervated endplates, and guide axonal sprouts to reinnervate the denervated endplates. In a rat model of partial denervation, high levels of daily neuromuscular activity have been shown to inhibit the outgrowth of sprouts by preventing Schwann cell bridging. In this review, we consider (1) the relative roles of increasing levels of oxidative stress and neuromuscular activity to the destabilization of neuromuscular junctions with age and disease, and (2) how a progressive increase in the neuromuscular activity of declining numbers of functional MUs contributes to the progressive failure of adaptive sprouting and, in turn, to the progressive muscle weakness in the motoneuron diseases of post-polio syndrome and amyotrophic lateral sclerosis. We conclude that there is a time-related progression of MU loss, adaptive sprouting followed by maladaptive sprouting, and continuing recession of terminals during normal aging. The progression is accelerated in motoneuron disease, progressing more rapidly in the post-polio syndrome after prolonged denervation and extremely rapidly in ALS.
[Neurol Res 2004; **26**: 174–185]

Keywords: Axonal sprouting; ALS; poliomyelitis; post-polio syndrome; partial denervation; Schwann cells

Neurosurg Focus 26 (2):E3, 2009

The role of neurotrophic factors in nerve regeneration

Tessa Gordon, Ph.D.

Centre for Neuroscience, Division of Physical Medicine and Rehabilitation, Faculty of Medicine and Dentistry, University of Alberta, Edmonton, Alberta, Canada

This review considers the 2 sources of neurotrophic factors in the peripheral nervous system (PNS), the neurons and the nonneuronal cells in the denervated distal nerve stumps, and their role in axon regeneration. Morphological assessment of regenerative success in response to administration of exogenous growth factors after nerve injury and repair has indicated a role of the endogenous neurotrophic factors from Schwann cells in the distal nerve stump. However, the increased number of axons may reflect more neurons regenerating their axons and/or increased numbers of axon sprouts from the same number of neurons. Using fluorescent dyes to count neurons that regenerated their axons across a suture site and into distal nerve stumps, brain-derived neurotrophic factor (BDNF) and glial cell–derived neurotrophic factor (GDNF) were found not to increase the number of neurons that regenerated their axons after immediate nerve repair. Nevertheless, the factors did reverse the deleterious effect of delayed nerve repair, indicating that the axons that regenerate into the distal nerve stump normally have access to sufficient levels of endogenous neurotrophic factors to sustain their regeneration, while neurons that do not have access to these factors require exogenous factors to sustain axon regeneration. Neurons upregulate neurotrophic factors after axotomy. The upregulation is normally slow, beginning after 7 days and occurring in association with a protracted period of axonal regeneration in which axons grow out from the proximal nerve stump across a suture site over a period of 1 month in rodents. This staggered axon regeneration across the suture site is accelerated by a 1-hour period of low-frequency electrical stimulation that simultaneously accelerates the expression of BDNF and its trkB receptor in the neurons. Elevation of the level of BDNF after 2 days to > 3 times that found in unstimulated neurons was accompanied by elevation of the level of cAMP and followed by accelerated upregulation of growth-associated genes, tubulin, actin, and GAP-43 and downregulation of neurofilament protein. Elevation of cAMP levels via rolipram inhibition of phosphodiesterase 4 mimicked the effect of the low-frequency electrical stimulation. In conclusion, the enhanced upregulation of neurotrophic factors in the electrically stimulated axotomized neurons accelerates axon outgrowth into the distal nerve stumps where endogenous sources of growth factors in the Schwann cells support the regeneration of the axons toward the denervated targets. The findings provide strong support for endogenous neurotrophic factors of axotomized neurons and of denervated Schwann cells playing a critical role in supporting axon regeneration in the PNS.
(DOI: 10.3171/FOC.2009.26.2.E3)

Key Words • axon regeneration • cAMP • electrical stimulation • neurotrophic factors • rolipram and accelerated axon regeneration

EJN European Journal of Neuroscience

FENS Federation of European Neuroscience Societies

European Journal of Neuroscience, pp. 1–15, 2015 doi:10.1111/ejn.13005

20.

Strategies to promote peripheral nerve regeneration: electrical stimulation and/or exercise

Tessa Gordon[1] and Arthur W. English[2]

[1]Division of Plastic Reconstructive Surgery, Department of Surgery, 06.9706 Peter Gilgan Centre for Research and Learning, The Hospital for Sick Children, Toronto, ON M4G 1X8, Canada

[2]Department of Cell Biology, Emory University School of Medicine, Atlanta, GA, USA

Keywords: electrical stimulation, exercise and nerve regeneration, exercise or electrical stimulation, nerve stimulation, peripheral nerve regeneration

Abstract

Enhancing the regeneration of axons is often considered to be a therapeutic target for improving functional recovery after peripheral nerve injury. In this review, the evidence for the efficacy of electrical stimulation (ES), daily exercise and their combination in promoting nerve regeneration after peripheral nerve injuries in both animal models and in human patients is explored. The rationale, effectiveness and molecular basis of ES and exercise in accelerating axon outgrowth are reviewed. In comparing the effects of ES and exercise in enhancing axon regeneration, increased neural activity, neurotrophins and androgens are considered to be common requirements. Similarly, there are sex-specific requirements for exercise to enhance axon regeneration in the periphery and for sustaining synaptic inputs onto injured motoneurons. ES promotes nerve regeneration after delayed nerve repair in humans and rats. The effectiveness of exercise is less clear. Although ES, but not exercise, results in a significant misdirection of regenerating motor axons to reinnervate different muscle targets, the loss of neuromuscular specificity encountered has only a very small impact on resulting functional recovery. Both ES and exercise are promising experimental treatments for peripheral nerve injury that seem to be ready to be translated to clinical use.

European Journal of Neuroscience, Vol. 15, pp. 613–626, 2002 *© Federation of European Neuroscience Societies*

A dose-dependent facilitation and inhibition of peripheral nerve regeneration by brain-derived neurotrophic factor

J. G. Boyd and T. Gordon
University Centre for Neuroscience, Faculty of Medicine and Dentistry, University of Alberta, Edmonton, AB, Canada T6G 2S2

Keywords: BDNF, motoneuron, p75, retrograde tracers, Sprague–Dawley, trkB

Abstract

The time-dependent decline in the ability of motoneurons to regenerate their axons after axotomy is one of the principle contributing factors to poor functional recovery after peripheral nerve injury. A decline in neurotrophic support may be partially responsible for this effect. The up-regulation of BDNF after injury, both in denervated Schwann cells and in axotomized motoneurons, suggests its importance in motor axonal regeneration. In adult female Sprague–Dawley rats, we counted the number of freshly injured or chronically axotomized tibial motoneurons that had regenerated their axons 1 month after surgical suture to a freshly denervated common peroneal distal nerve stump. Motor axonal regeneration was evaluated by applying fluorescent retrograde neurotracers to the common peroneal nerve 20 mm distal to the injury site and counting the number of fluorescently labelled motoneurons in the T_{11}–L_1 region of the spinal cord. We report that low doses of BDNF (0.5–2 μg/day for 28 days) had no detectable effect on axonal regeneration after immediate nerve repair, but promoted axonal regeneration of motoneurons whose regenerative capacity was reduced by chronic axotomy 2 months prior to nerve resuture, completely reversing the negative effects of delayed nerve repair. In contrast, high doses of BDNF (12–20 μg/day for 28 days) significantly inhibited motor axonal regeneration, after both immediate nerve repair and nerve repair after chronic axotomy. The inhibitory actions of high dose BDNF could be reversed by functional blockade of p75 receptors, thus implicating these receptors as mediators of the inhibitory effects of high dose exogenous BDNF.

ACADEMIC PRESS

Available online at www.sciencedirect.com

SCIENCE DIRECT®

Experimental Neurology

Experimental Neurology 183 (2003) 610–619

www.elsevier.com/locate/yexnr

Glial cell line-derived neurotrophic factor and brain-derived neurotrophic factor sustain the axonal regeneration of chronically axotomized motoneurons in vivo

J.G. Boyd[a] and T. Gordon[b,*]

[a] *Queen's University, Department of Anatomy and Cell Biology, Kingston, ON, Canada*
[b] *University Centre for Neuroscience, University of Alberta, Edmonton, AB, Canada*

Received 9 July 2002; revised 22 January 2003; accepted 24 February 2003

Abstract

In contrast to injuries in the central nervous system, injured peripheral neurons will regenerate their axons. However, axotomized motoneurons progressively lose their ability to regenerate their axons, following peripheral nerve injury often resulting in very poor recovery of motor function. A decline in neurotrophic support may be partially responsible for this effect. The initial upregulation of glial cell line-derived neurotrophic factor (GDNF) and brain-derived neurotrophic factor (BDNF) by Schwann cells of the distal nerve stump after nerve injury has led to the speculation that they are important for motor axonal regeneration. However, few experiments directly measure the effects of exogenous BDNF or GDNF on motor axonal regeneration. This study provided the first direct and quantitative evidence that long-term continuous treatment with exogenous GDNF significantly increased the number of motoneurons which regenerate their axons, completely reversing the negative effects of chronic axotomy. The beneficial effect of GDNF was not dose-dependent. A combination of exogenous GDNF and BDNF on motor axonal regeneration was significantly greater than either factor alone, and this effect was most pronounced following long-term continuous treatment. The ability of GDNF, either alone or in combination with BDNF, to increase the number of motoneurons that regenerated their axons correlated well with an increase in axon sprouting within the distal nerve stump. Thus long-term continuous treatment with neurotrophic factors, such as GDNF and BDNF, can be used as a viable treatment to sustain motor axon regeneration.
© 2003 Elsevier Science (USA). All rights reserved.

Introduction

One of the major contributing factors to the poor functional recovery observed following peripheral nerve injury is the progressive decline in the capacity of motoneurons to regenerate their axons, particularly during the prolonged period in which motoneurons remain axotomized prior to reinnervating denervated muscle targets (Fu and Gordon, 1995, 1997). Neurotrophic factors that are expressed after nerve injury are important for neuronal survival, and may also be important for axonal regeneration (Meyer et al., 1992; Sendtner et al., 1992; Koliatsos et al., 1993; Kobayashi et al., 1996; Novikov et al., 1997; Naveilhan et al., 1997). However, neurotrophic factor expression after injury is generally transient, and the failure to maintain the expression of neurotrophic factors over an extended period of time may partially account for the poor axonal regeneration of chronically axotomized motoneurons. Thus exogenous application of these neurotrophic factors may be able to sustain motor axonal regeneration after peripheral nerve injury.

We have recently examined the role of brain-derived neurotrophic factor (BDNF) and its receptors in motor axonal regeneration (Boyd and Gordon, 2001; 2002). BDNF mediates its effects via two classes of receptors: a member of the tropomyosin receptor kinase (trk) family of receptors, trkB, and a member of the tumor necrosis factor family of receptors, the p75 neurotrophin receptor (p75NTR; Friedman and Greene, 1999; Yano and Chao, 2000). Although

* Corresponding author. University Centre for Neuroscience, 513 Heritage Medical Research Centre, University of Alberta, Edmonton, AB, Canada T6G 2S2. Fax: +780-492-1617.

E-mail address: tessa.gordon@ualberta.ca (T. Gordon).

0014-4886/03/$ – see front matter © 2003 Elsevier Science (USA). All rights reserved.
doi:10.1016/S0014-4886(03)00183-3

low doses of exogenous BDNF completely reverse the negative effects of chronic axotomy, progressively higher doses potently inhibit axonal regeneration (Boyd and Gordon, 2002). The facilitatory and inhibitory effects of BDNF are attributed to its binding to trkB and p75NTR, respectively. A differential role for trkB and p75NTR in motor axonal regeneration is supported by several lines of experimental evidence. First, the inhibitory effects of high-dose BDNF can be eliminated by preventing BDNF binding to p75NTR with function blocking antibodies (Boyd and Gordon, 2002). Second, there is decreased axonal regeneration in trkB heterozygous mutant mice, and increased axonal regeneration in p75NTR hypomorphic mice (Boyd and Gordon, 2001). The strong dose-dependent effects of exogenous BDNF may limit its effectiveness as a therapeutic strategy to promote motor axonal regeneration.

Glial cell line-derived neurotrophic factor (GDNF) is another candidate trophic factor for motoneurons during axonal regeneration. GDNF belongs to a subfamily within the transforming growth factor-β superfamily, together with neurturin, persephin, and artemin (Lin et al., 1993; Kotzbauer et al., 1996; Creedon et al., 1997). In contrast to BDNF, which binds to two distinct classes of receptors, GDNF mediates its effects via a single receptor complex composed of a ligand-binding glycosylphosphatidyl inositol membrane-linked receptor subunit, termed GDNF-family receptor α-1 (GFRα-1), and a signal-transducing tyrosine kinase subunit, Ret (reviewed in Saarma and Sariola, 1999). The expression of GDNF in the denervated distal nerve stump and its receptors in axotomized motoneurons after injury are consistent with a functional role for GDNF in motor axonal regeneration. Specifically, the GDNF receptor subunits are upregulated in axotomized motoneurons (Tsujino et al., 1999; Burazin and Gundlack, 1998; Naveilhan et al., 1997). GDNF is rapidly upregulated in denervated Schwann cells after sciatic nerve injury (Naveilhan et al., 1997; Hoke et al., 2002), and is retrogradely transported by motoneurons (Yan et al., 1995).

There is considerable evidence demonstrating that GDNF is a potent survival factor for axotomized neonatal and adult motoneurons (Henderson et al., 1994; Yan et al., 1995; Oppenheim et al., 1995; Li et al., 1995; Vejsada et al., 1998; Yuan et al., 2000). In addition, overexpression of GDNF in developing muscle causes hyperinnervation of motor endplates during development (Nguyen et al., 1998) and adenoviral gene transfection of axotomized neonatal motoneurons with GDNF increases the numbers of myelinated axons in the distal nerve stump of the facial nerve after a crush injury. This increased number of myelinated axons is associated with significantly improved whisker function compared to nontransfected controls (Baumgartner and Shine, 1998). However, a direct role for GDNF in increasing the number of axotomized motoneurons that regenerate their axons remains to be established. In the present study, we will test whether exogenous GDNF, either alone or in combination with exogenous BDNF, will mediate only positive effects on motor axonal regeneration under conditions of both acute and chronic axotomy.

Materials and methods

Nerve repair and pump implantation

All animal procedures were conducted in accordance with the Canadian guidelines for animal experimentation, and a local animal welfare committee. The details of the surgical procedures and pump implantation have been described elsewhere (Boyd and Gordon, 2002). Briefly, under sodium pentobarbitol anesthesia (45 mg/kg), the right sciatic nerve was exposed and the main branches were dissected in adult female Sprague–Dawley rats (200–225 g). The tibial (TIB) nerve was transected 5 mm distal to its bifurcation from the common peroneal (CP) and sural nerves with fine microsurgical scissors (Fig. 1A, sural not shown for simplicity). The TIB nerve stump was cross-sutured to the distal stump of a cut CP nerve either immediately, or following a 2-month period of chronic axotomy (Fig. 1B). To prevent regeneration during the period in which motoneurons remained chronically axotomized, the proximal stump of the TIB nerve was ligated and sutured to the innervated biceps femoris muscle (Fu and Gordon, 1995). Nerve stumps were sutured together in a 5-mm silastic cuff (Dow Corning, 0.64 mm ID, 1.19 mm OD) with a single 8-O suture (Fig. 1*B*; Ethicon, Peterborough, ON) and attached to an Alzet 2ML4 (Alza Corp., Palo Alto, CA) mini-osmotic pump via a 4-cm-long silastic catheter. The pump and drug delivery catheter were anchored subdurally, and the skin was closed with 4-O silk. The osmotic pump and drug delivery hardware have been previously shown not to be detrimental to motor axonal regeneration (Boyd and Gordon, 2002).

Delivery of exogenous GDNF and BDNF via Alzet mini osmotic pumps

GDNF (kindly provided by Amgen Pharmaceuticals) was diluted in saline (0.9% NaCl) and administered via Alzet 28-day mini-osmotic pumps (Model 2ML4) in doses of 0.1, 1, and 10 μg/day at a continual flow rate of 2.5 μl/h. For delivery of combined BDNF and GDNF, the neurotrophic factors were diluted in saline to provide a daily dose of 0.1 μg/day GDNF and 2 μg/day BDNF for a period of 28 days following delayed nerve repair after a 2-month period of chronic axotomy. To determine the duration of treatment required to promote regeneration of chronically axotomized motoneurons, combined BDNF and GDNF solutions were loaded into 7-day mini-osmotic pumps (Alzet Model 2001) and the pumps were removed 1, 4, and 7 days after nerve repair. In control rats, the pumps were loaded with saline alone ($n = 10$). Although there have been previous reports that high doses of exogenous GDNF can prevent normal

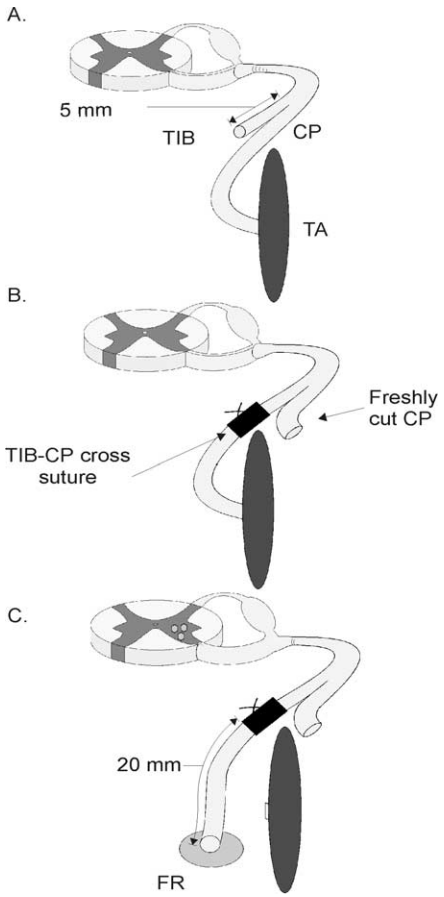


Fig. 1. Schematic representation of surgical procedures. (A) The tibial (TIB) nerve was dissected and transected 5 mm distal to the trifurcation from the common peroneal (CP) and sural (not shown) branches of the sciatic nerve. For rats in which axonal regenerative capacity was reduced by chronic axotomy, the proximal TIB stump was sutured to surrounding innervated muscle to prevent regeneration for a 2-month period of chronic axotomy. (B) Either immediately following transection or after a 2-month period of chronic axotomy, the proximal TIB nerve stump was cross-sutured to a freshly denervated CP distal nerve stump within a 5-mm silastic nerve cuff. Seven- or 28-day miniosmotic pumps were connected to the nerve cuff via a silastic catheter (not shown) and implanted under the skin of the back. (C) Axotomized TIB motoneurons which have regenerated their axons a distance of 20 mm are labeled with fluororuby (FR).

weight gain in experimental animals (Giehl et al., 1998; Vejsada et al., 1998) no such detrimental effects were observed in any of the experimental animals at any of the GDNF doses tested (data not shown).

Retrograde labeling of TIB motoneurons

Following the 28-day period of axonal regeneration, the right CP nerve was transected 20 mm distal to the TIB-CP surgical repair line for application of fluororuby (dextran tetramethylrhodamine; Molecular Probes, D-1817, Eugene, OR). Fluororuby is effectively endocytosed and retrogradely transported (Schmued and Fallon, 1986), and reliably and consistently labels TIB motoneurons (Boyd and Gordon, 2002). Back-labeling was performed by placing the tip of the cut CP nerve above a small weighing paper with fluororuby for 2 h and then irrigating the nerve. The skin was closed using 4-O silk (Ethicon) and the animals were allowed to recover for 6 days to allow for consistent retrograde transport of the dyes to all motoneuronal cell bodies (Sagot et al., 1998).

Animal perfusion and tissue preparation

The rats were deeply anesthetized with sodium pentobarbitol (90 mg/kg ip) for transcardial perfusion of 300 ml saline followed by 500 ml ice-cold paraformaldehyde (4% paraformaldehyde in 0.1 M phosphate buffer). The T11-L1 spinal segments which include the entire TIB motoneuronal pool (Swett et al., 1986) were removed. Following overnight postfixation and cryoprotection in a 4% paraformaldehyde, 30% sucrose, the cords were frozen in liquid nitrogen and stored at −70°C.

Enumeration of TIB motoneurons

Longitudinal 50-μm sections were cut on a cryostat (Leica, Jung CM 3000) and mounted serially on glass slides. Each section was viewed under a Leitz-Diaplan fluorescent microscope (Fig. 1D, excitation bandpass 515–560). Only motoneurons in which a distinct nucleus could be seen were counted. These numbers were corrected to control for the counting of split nuclei using the method of Abercrombie (1946).

Preparation of nerves for electron microscopy

During the retrograde back-labeling surgery, a small (~3 mm) section of CP nerve distal to the site of dye application was dissected and removed prior to application of the dye. These nerve pieces were fixed in glutaraldehyde (3% in 0.1 M phosphate buffer), stained with OsO_4 (3% solution in 0.1 M phosphate buffer), dehydrated in ascending alcohols, and embedded in araldite. Ultrathin sections were cut using a glass blade and examined using a transmitting electron microscope. Black and white photographs were taken of representative sections through the distal nerve stump. A minimum of three animals were examined per group.

Statistics

Differences between groups were detected using independent *T* tests. Statistical significance was accepted at the level of $P < 0.05$. Values are presented as the mean ± SE. To determine whether the combined effects of exogenous BDNF and GDNF had a significantly stronger effect on motor axonal regeneration than the sum of the effects of BDNF alone plus GDNF alone, the "bootstrap" method of random resampling was used (Effron, 1979). This method has been previously described to evaluated the combined

effects of BDNF and GDNF on motoneuronal survival (Vejsada et al., 1998). Briefly, prior to statistical analysis, the mean number of TIB motoneurons which regenerated their axons in saline control animals was subtracted from the number of TIB motoneurons which regenerated their axons in the BDNF alone, GDNF alone, or combined BDNF and GDNF experimental groups. This subtraction was performed to remove the population of TIB motoneurons which would regenerate their axons in absence of any treatment and would thus be represented twice in the sum. The numbers were then divided into two groups, the mathematical sum of BDNF alone and GDNF alone (Group A), and the experimentally observed sum of combined BDNF and GDNF treatment (Group B). Fifty pairs consisting of $n = 5$ values from group A and $n = 5$ values from group B were constructed by random resampling the cell counts; repetition of individual values was allowed during this sampling procedure. Statistical significance between group A and group B was determined with the nonparametric Mann–Whitney *U* test (SPSS, Version 10.0.7), the probability distribution of all 50 *P* values obtained was plotted, and the median and mean *P* values are reported.

Results

GDNF does not promote motor axonal regeneration after immediate nerve repair

As shown in Fig. 2A, the mean (± SE) number of TIB motoneurons that regenerate their axons a distance of 20 mm into a freshly denervated CP distal nerve stump following immediate nerve repair and 28 days continuous saline infusion is 410 ± 28. This is almost half the number of motoneurons previously demonstrated to be in the intact TIB motoneuron pool (Boyd and Gordon, 2002). The ~55% of TIB motoneurons which regenerate their axons a distance of 20 mm in a 4-week period of time is consistent with our previous findings (Boyd and Gordon, 2002), most likely due to previous findings that it takes at least twice as long (8–10 weeks) for all femoral motor axons to successfully cross the injury site and regenerate a comparable distance into a distal nerve stump after immediate nerve repair (Al-Majed et al., 2000).

To examine the effects of exogenous GDNF on motor axonal regeneration, we counted the number of fluororuby labeled motoneurons which regenerated a distance of 20 mm into a freshly cut distal CP nerve stump in 4 weeks after immediate nerve repair. Continuous local application of exogenous GDNF for the 4-week period of axonal regeneration, at low doses of 0.1 μg/day which approximate the dose that was previously reported to promote sensory fiber regeneration after sciatic nerve injury in adult mice (Naveilhan et al., 1997), had no detectable effect on the number of TIB motoneurons which regenerated axons following immediate nerve repair compared to the saline control

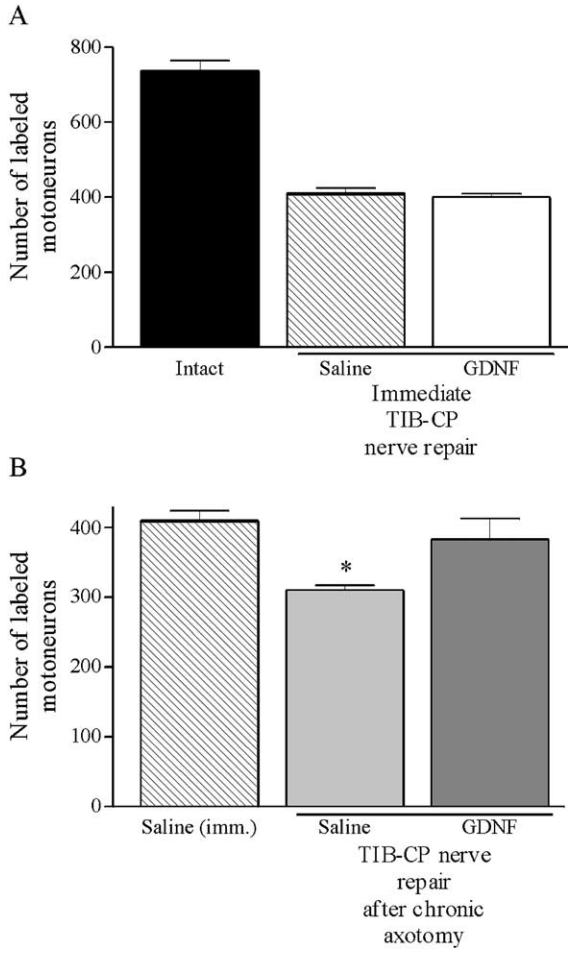


Fig. 2. Effects of exogenous GDNF on motor axonal regeneration after immediate nerve repair and nerve repair after chronic axotomy. (A) Compared to saline controls (hatched bar, $n = 6$), 0.1 μg/day exogenous GDNF (white bar, $n = 5$) had no significant effect on the number of motoneurons which regenerated their axons after immediate nerve repair. The number of contralateral intact tibial motoneurons is shown for comparison (black bar, from Boyd and Gordon, 2002). (B) Compared to immediate nerve repair (hatched bar, $n = 6$ from (A)), a 2-month period of chronic axotomy significantly reduces the number of TIB motoneurons which regenerate their axons (light gray bar, $n = 4$). A dose of 0.1 μg/day exogenous GDNF (dark gray bar, $n = 4$) completely reverses the negative effects of chronic axotomy. $^*P < 0.05$.

(Fig.2A). This is consistent with the previous findings showing that exogenous BDNF had no beneficial effect on motor axonal regeneration after immediate nerve repair (Boyd and Gordon, 2002). Thus, in contrast to short periods of continuous electrical stimulation which increases the number of motor axons that cross the injury site into the distal nerve stump (Al-Majed et al., 2000), the neurotrophic factors GDNF and BDNF do not significantly accelerate regeneration.

The number of TIB motoneurons which regenerated their axons after a period of 2-month chronic axotomy prior to delayed nerve repair to a freshly denervated CP distal nerve stump was significantly reduced compared to immediate nerve repair (Fig. 2B). The low number of chronically

axotomized motoneurons which regenerated their axons reflects a reduction to 75% of the regenerative capacity after immediate nerve repair. This reduction is comparable to the findings of a 66% reduction in the number of reinnervated motor units after the same 2-month period of chronic axotomy (Fu and Gordon, 1995). These data demonstrate that chronic axotomy reduces the capacity of TIB motoneurons to regenerate their axons, thereby extending the conclusions made by Fu and Gordon (1995) that chronic axotomy reduces the number of motoneurons which regenerate axons and reinnervate the denervated tibialis anterior muscle and confirming our previous findings (Boyd and Gordon, 2002). Since motoneurons rarely die after injuries that occur long distances from their cell bodies (Boyd and Gordon, 2002; Fu and Gordon, 1995), this reduction in the number of chronically axotomized TIB motoneurons that regenerated their axons most likely reflects a reduced regenerative capacity, and not axotomy-induced cell death.

Continuous exogenous GDNF delivered to the site of nerve injury and repair, at a dose of 0.1 μg/day, significantly increased the number of 2-month chronically axotomized TIB motoneurons which regenerated their axons into a freshly denervated CP distal nerve stump compared to the saline controls (Fig. 2B). The number of 2-month chronically axotomized TIB motoneurons which regenerated their axons after GDNF treatment was not significantly different from the number of motoneurons which regenerated their axons after immediate nerve repair. Thus, like low doses of exogenous BDNF (Boyd and Gordon, 2002), exogenous GDNF completely reversed the negative effects of chronic axotomy on motor axonal regeneration.

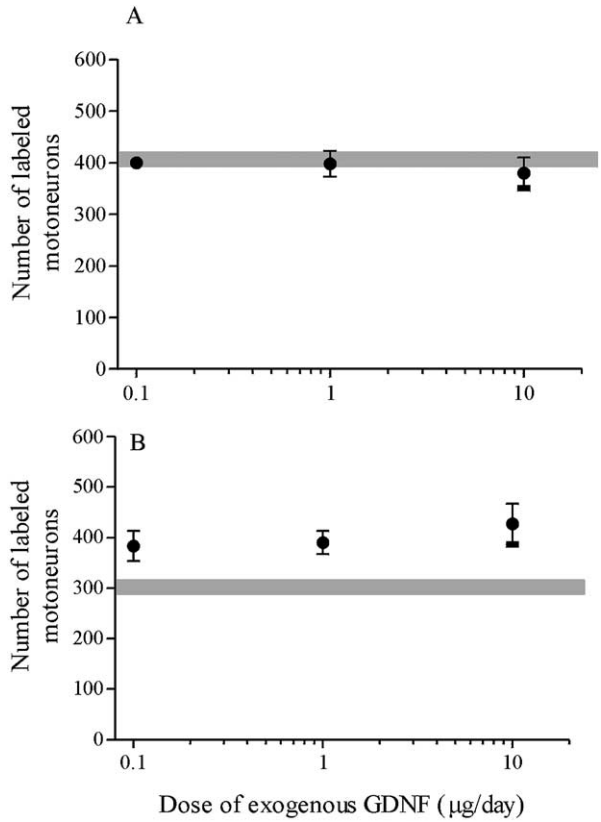


Fig. 3. GDNF shows only monophasic effects on motor axonal regeneration. (A) Exogenous GDNF does not promote motor axonal regeneration after immediate nerve repair at any of the doses tested. (B) In contrast to BDNF (Boyd and Gordon, 2002), exogenous GDNF shows only facilitatory effects on motor axonal regeneration. Gray bars represent saline control (±SE). Each data point represents the mean (±SE) of four to five animals per group. *$P < 0.05$.

Exogenous GDNF does not show dose-dependent effects on motor axonal regeneration

To explore the possibility that the dose of GDNF (0.1 μg/day) was too low to increase motor axonal regeneration after immediate nerve repair, the dose was increased to 1 and 10 μg/day. As shown in Fig. 3A, compared to saline control animals, exogenous GDNF was not able to promote TIB motor axonal regeneration after immediate nerve repair at any of the doses tested. Similarly, to explore possible dose-dependent effects of exogenous GDNF on motor axonal regeneration after a period of 2-month chronic axotomy, the range of doses tested was expanded to include 1 and 10 μg/day. Surprisingly, the initial dose of 0.1 μg/day appears to be saturating, as it is as effective at reversing the negative effects of chronic axotomy as 1 and 10 μg/day (Fig. 3B). The lack of an observable dose-dependent effect on motor axonal regeneration for exogenous GDNF is in marked contrast the dramatic dose-dependent biphasic facilitatory and inhibitory effects of exogenous BDNF through a similar range of doses (Boyd and Gordon, 2002).

GDNF and BDNF show possible synergistic effects in promoting motor axonal regeneration

It has been previously reported that GDNF and BDNF can act together either synergistically in promoting the survival of axotomized neonatal motoneurons (Vejsada et al., 1998), or additively in promoting differentiation of embryonic motoneurons in vitro (Zurn et al., 1996). To determine the combined effects of GDNF and BDNF on TIB motor axonal regeneration in vivo, we administered the effective doses of 0.1 μg/day GDNF and 2 μg/day BDNF to 2-month chronically axotomized TIB motoneurons for 28 days. The combined GDNF and BDNF treatment substantially promoted axonal regeneration of chronically axotomized TIB motoneurons (Fig. 4). This particularly strong effect of combined GDNF and BDNF treatment could possibly be due to synergistic interactions between the two neurotrophic factors, as this effect was significantly greater than the mathematical sum of beneficial effects of the two individual treatments (median of P distribution = 0.032, mean of P distribution = 0.048).

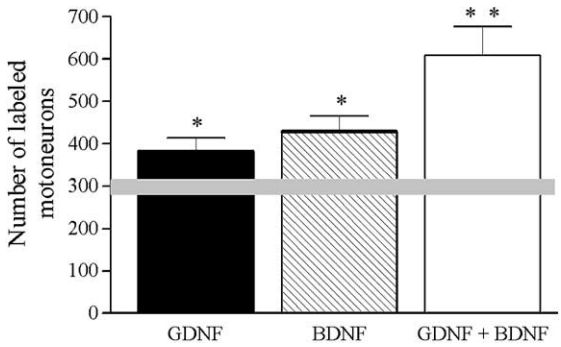


Fig. 4. Possible synergistic effects of exogenous GDNF and BDNF on motor axonal regeneration. The number of chronically axotomized motoneurons which regenerated their axons in the presence of combined exogenous BDNF (2 μg/day) and GDNF (0.1 μg/day) was significantly greater than the arithmetic sum of the beneficial effects of each individual factor (see text for details). Horizontal bar represents mean (±SE) number of motoneurons which regenerated axons in saline treated control animals. *Significance compared to saline controls; **significance compared to individual neurotrophic factor treatments.

BDNF and GDNF increase axonal sprouting

To determine whether the ability of GDNF, BDNF, and/or combined treatments to promote axonal regeneration of chronically axotomized motoneurons is correlated with morphological changes in the regenerating axons in the distal nerve stump, we removed a small portion of the nerve stump at the time of retrograde back-labeling of regenerated TIB motoneurons. Thus the segment includes only axons that have regenerated a distance of 20 mm from the site of initial nerve injury and repair. Tissue sections were evaluated using a transmitting electron microscope, and representative sections are shown in Fig. 5.

In intact nerves, a single Schwann cell is normally associated with only one axon (Fig. 5A); however, after nerve injury, a parent axon usually gives rise to three to five daughter axons and together they are called a regenerating unit (reviewed in Fu and Gordon, 1997). Schwann cells and their corresponding sprouting daughter axons in the regenerating unit are clearly visible in saline-treated control animals, as shown in the representative transmitting electron micrograph (Fig. 5B). In GDNF-treated animals, there is an increase in the number of axons that accompany a single Schwann cell (Fig. 5C). Moreover, there is a profound and significant increase in the number of small regenerating axons accompanying a single Schwann cell in combined GDNF- and BDNF-treated animals (Figs. 5D and E). The number of axonal sprouts per endoneurial sheath in combined GDNF- and BDNF-treated animals was significantly greater than that in GDNF alone (Fig. 5E). Thus, there is a strong agreement between the ability of both GDNF alone, and in combination with BDNF, to promote motor axonal regeneration and increase the number of regenerating axons accompanying Schwann cells in the distal nerve stumps.

Beneficial effects of GDNF and BDNF are dependent on the duration of treatment

There have been conflicting reports with regard to whether chronic administrations of neurotrophic factors are necessary to elicit significant biological effects (Vejsada et al., 1998), or if similar long-term biological effects can be elicited after a single dose (Chai et al., 1999; Koliatsos et

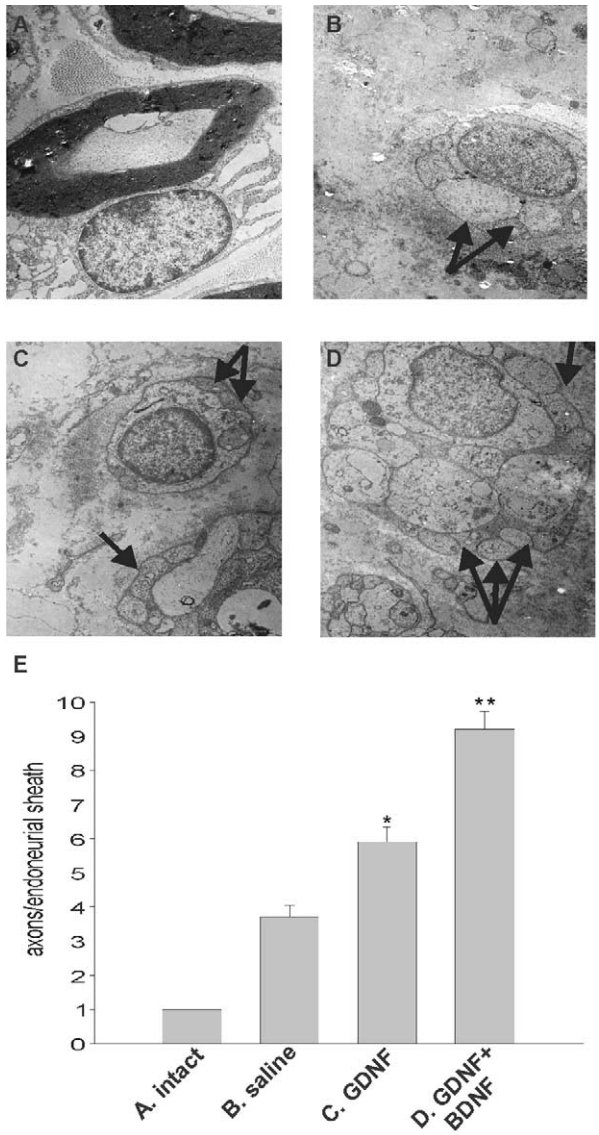


Fig. 5. GDNF and BDNF promote regenerative sprouting after 28 days after peripheral nerve injury. (A–D) Transmitting electron micrographs of Schwann cells and their axons in an intact nerve (A), and a typical regenerating unit consisting of a Schwann cell and four daughter axons in saline controls (B). The number of axon sprouts/Schwann cell is increased following exogenous GDNF treatment (C), and dramatically increased following combined GDNF/BDNF treatment (D). (E) Summary histogram of the number of axons/endoneurial sheath for each treatment. Each bar represents the mean (±SE) of at least three animals per group in which five representative fields of the distal nerve stump were counted. *$P < 0.05$ compared to saline controls; **$P < 0.05$ compared to GDNF treatment alone.

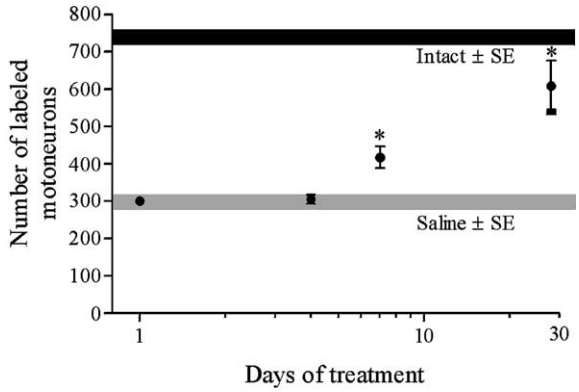


Fig. 6. Maximum beneficial effect of exogenous GDNF and BDNF requires sustained administration. Compared to saline controls (light gray horizontal reference line), a beneficial effect of combined GDNF and BDNF on the number of chronically axotomized motoneurons which regenerated their axons was apparent after 7 days, but not 1 or 3 days of treatment. Each data point represents the mean (±SE) for four to five animals per group. $*P < 0.05$. For comparison, the number of intact TIB motoneurons is shown (black horizontal reference line, from Boyd and Gordon, 2002).

al., 1996). To evaluate whether the substantial beneficial effects of combined GDNF and BDNF treatment on the axonal regeneration of chronically axotomized TIB motoneurons are dependent on the duration of treatment, we performed the TIB-CP cross suture as described above for the long-term treated animals, but 7-day, instead of 28-day mini-osmotic pumps were used. These pumps were removed from their subcutaneous position 1, 4, and 7 days after nerve repair without trauma to the site of nerve injury and repair. All animals were examined 28 days after nerve repair. As shown in Fig. 6, there was no detectable effect of 1 or 4 days combined GDNF and BDNF treatment. A significant beneficial effect on motor axonal regeneration by exogenous application of GDNF and BDNF was detected only after 7 days treatment. However, the full 28-day combined GDNF and BDNF treatment was required for maximal beneficial effect. Thus in contrast to other studies which demonstrated that the biological effects of exogenous neurotrophic factors outlast the duration of treatment (Chai et al., 1999; Kobayashi et al., 1996), we demonstrated that continuous treatment with exogenous GDNF and BDNF is required for maximal benefit.

Discussion

This study uses a direct and quantitative assay to compare and contrast the effects of GDNF to BDNF in its ability to promote motor axonal regeneration, either alone or in combination. Similar to what was reported for BDNF, GDNF does not improve motor axonal regeneration after immediate nerve repair, suggesting that it does not accelerate regeneration across the injury site, yet GDNF completely reverses the negative effects of chronic axotomy on the number of motoneurons which regenerated their axons. However, in contrast to the effects previously reported for exogenous BDNF (Boyd and Gordon, 2002), GDNF does not show any inhibitory effects on motor axonal regeneration after either immediate nerve repair, or nerve repair after chronic axotomy. Furthermore, the combined effects of GDNF and BDNF on promoting motor axonal regeneration after chronic axotomy are possibly synergistic in nature, and this potent beneficial effect strongly depends on the duration of treatment. The beneficial effects of these GDNF and BDNF on motor axonal regeneration correlated well with their ability to increase axonal sprouting.

Exogenous neurotrophic factors sustain, not accelerate, motor axonal regeneration

In response to nerve injury, there are many changes which occur in both motoneurons, as well as in Schwann cells of the regenerative environment of the distal nerve stump, which has been denoted as a transition from a mature "transmitting" to a "regenerating" phenotype (Fu and Gordon, 1997). In particular, motoneurons downregulate enzymes associated with neurotransmission, such as ChAT (Yan et al., 1995; Friedman et al., 1995; Tuszynski et al., 1996; Kishino et al., 1997), and acetylcholinesterase (Fernandes et al., 1997; Kishino et al., 1997). In close temporal correlation with the decline in ChAT and AChE is an upregulation of regeneration associated genes, such as actin, GAP-43, and Tα1-tubulin (Miller et al., 1989; Tetzlaff et al., 1991), as well as neurotrophic factors and their receptors (reviewed in Fu and Gordon, 1997). In addition, denervated Schwann cells become a rich source of neurotrophic factors, such as BDNF and GDNF (Meyer et al., 1992; Funakoshi et al., 1993; Naveilhan et al., 1997; Trupp et al., 1997; Hoke et al., 2002), and create a permissive growth environment for regenerating axons. Importantly, however, upregulation of neurotrophic factor receptors in axotomized motoneurons is generally transient, and as time progresses, levels of neurotrophic factors and their receptors return to basal levels regardless of whether successful regeneration has occurred. Specifically, although the functional receptors for BDNF (trkB and p75NTR) and GDNF (GFRα-1 and Ret) are upregulated in motoneurons within 7 days of axotomy, this receptor mRNA returns to basal levels 6 weeks later (Hammarberg et al., 2000). Thus it appears that immediately after injury, motoneurons are at their peak regenerative capacity, but there is a time-limited and narrow window of opportunity for axonal regeneration to occur. It is possible that the immediate, but transient, nature of the ability of motoneurons to successfully regenerate their axons may explain why exogenous neurotrophic factors, such as GDNF and BDNF, cannot accelerate motor axonal regeneration after immediate nerve repair but significantly improve the poor motor axonal regeneration observed after chronic axotomy (Boyd and Gordon, 2002, Figs. 2, 3). In

other words, saturating levels of endogenous trophic support may be present after immediate nerve repair, but exogenous GDNF and BDNF may be required to sustain the regeneration of chronically axotomized motoneurons over extended periods of time.

GDNF and BDNF exert distinct effects on motor axonal regeneration

We have also demonstrated that in vivo, GDNF is much more potent than BDNF in promoting motor axonal regeneration after chronic axotomy. Using the same experimental paradigm, exogenous BDNF was without significant effect on motor axonal regeneration at a dose of 0.1 μg/day (Boyd and Gordon, 2002), whereas the same dose of GDNF exerted a maximal beneficial effect in reversing the negative effects of chronic axotomy in the present study (Fig. 3). This is consistent with previous findings that GDNF is significantly more potent than BDNF in promoting motoneuronal survival, both of developing chick motoneurons (Oppenheim et al., 1995), and of neonatal motoneurons following sciatic nerve injury (Vejsada et al., 1998). The monophasic dose–response curve for GDNF on motor axonal regeneration (Fig. 3) is in marked contrast to the biphasic dose–response effects demonstrated for BDNF, where low doses (1–4 μg/day) promote, but higher doses ($>$4 μg/day) potently inhibit, motor axonal regeneration (Boyd and Gordon, 2002). Since GDNF and BDNF belong to distinct families of neurotrophic factors, the lack of a biphasic dose-dependent response elicited by exogenous GDNF is consistent with the idea that the inhibitory effects of high-dose BDNF are mediated by binding to p75NTR (since GDNF does not bind to p75NTR), and biphasic effects on motor axonal regeneration are not an inherent property that can be generalized to all neurotrophic factors

We have also provided evidence suggesting that GDNF and BDNF have synergistic positive effects on motor axonal regeneration after chronic axotomy (Fig. 5). This is in agreement with the combination of a GDNF and BDNF supporting significantly more neonatal motoneurons after axotomy than either factor alone (Vejsada et al., 1998), and consistent with shared intracellular pathways induced by both GDNF and BDNF signaling. For example, both GDNF (Creedon et al., 1997; Hinas et al., 1997) and BDNF (Atwal et al., 2000; Dolcet et al., 1999; Yano and Chao, 2000) can activate Ras-MAP and PI3 kinase pathways. It has been recently demonstrated that GDNF and BDNF activated similar pathways to promote the survival of embryonic motoneurons (Dolcet et al., 1999; Soler et al., 1999). At the cell membrane, GDNF binding to GFR-α1 and Ret induces tyrosine phosphorylation of Ret, and subsequent phosphorylation of MEK and Akt, indicative of MAP kinase and PI3 kinase activity, respectively (Soler et al., 1999). Likewise, BDNF binding to trkB also induces trkB phosphorylation, and downstream phosphorylation of MEK and Akt (Atwal et al., 2000; Dolcet et al., 1999). Pharmacological blockade of the PI3 kinase, but not the MAP kinase, pathway prevented the survival promoting effects of both GDNF (Dolcet et al., 1999) and BDNF (Soler et al., 1999). Thus there is both molecular and functional overlap of signaling pathways induced by both GDNF and BDNF stimulation which may explain the large beneficial effect of combined GDNF and BDNF treatment on promoting motor axonal regeneration.

Continuous exogenous neurotrophic factor treatment is required for maximal beneficial effect

There have been conflicting reports concerning the duration of neurotrophic factor treatment required to elicit long-term effects in injured neurons. For instance, a single dose of BDNF was as effective as continuous treatment for the 6-week period following ventral root avulsion in maintaining motoneuronal survival (Chai et al., 1999). Similarly, the effect of BDNF in preventing axotomy-induced atrophy in rubrospinal neurons lasted up to 2 weeks following cessation of treatment (Kobayashi et al., 1996). In contrast, although a single dose of either BDNF or GDNF provided transient protection, continuous neurotrophic factor delivery was required to promote the long-term survival of axotomized neonatal motoneurons (Vejsada et al., 1998). Our findings are consistent with the latter study. We did not observe any significant benefit from the combined GDNF and BDNF treatment on the axonal regeneration of chronically axotomized motoneurons until after 7 days continuous treatment (Fig. 6). Furthermore, maximum positive effect was elicited only when the combined treatment was given for the entire 28-day period of regeneration. One possible explanation for the delay in the ability of motoneurons to respond to exogenous application of neurotrophic factors is based on the fact that endocytosis and retrograde transport of GDNF and BDNF are receptor-mediated (Curtis et al., 1998; Oppenheim et al., 1995). Although the receptor mRNA required for GDNF and BDNF endocytosis and retrograde transport of GDNF and BDNF are upregulated early in axotomized motoneurons ($<$3 days), considerable delays may arise as a result of the long distance over which receptor proteins need to be anterogradely transported from the cell bodies in the ventral horn of the spinal cord to the site of nerve transection and exogenous application, or endogenous presence of neurotrophic factors. Thus, regenerating axons may not have the receptors present on their growth cones, and not be able to respond to local neurotrophic factor infusion, until several days after axotomy. This mechanism would resolve the apparent contradiction between the above studies concerning the duration of neurotrophin treatment. The experiments which demonstrated long-lasting effects of neurotrophic factors after a single dose were applied in very close proximity to the cell bodies (Chai et al., 1999; Kobayashi et al., 1996); thus it might be assumed that the neurons would be able to respond almost immediately to exogenous neurotrophic factor appli-

cation. However, in our experiments (Fig. 6) and others (Vejsada et al., 1998) which have shown that continuous neurotrophic factor treatment is required to elicit beneficial effects, exogenous neurotrophic factors were applied peripherally to cut axons which may not be able to respond immediately to their local delivery.

Conclusions

In summary, these results demonstrate that the poor motor axonal regeneration observed after chronic axotomy can be reversed by exogenous application of continuous neurotrophic factors. Thus, it is possible that the poor functional recovery observed clinically as a result of traumatic peripheral nerve injury may be improved by promoting axonal regeneration of chronically axotomized motoneurons using long-term administration of low doses of neurotrophic factors, such as GDNF and BDNF, to sustain their regeneration over long periods of time.

Acknowledgments

This research was supported by a grant from the Rick Hansen Foundation/Canadian Neurotrauma Initiative. J.G.B. was supported by a Rick Hansen/Alberta Paraplegic Association studentship. T.G. is an Alberta Heritage Foundation for Medical Research Senior Scientist. We thank Amgen Pharmaceuticals and Regeneron Pharmaceuticals for generous provision of the GDNF and BDNF, respectively. We also thank Mr. Neil Tyreman for technical assistance, and Dr. Ming Chen for assistance with electron microscopy.

References

Abercrombie, M., 1946. Estimation of nuclear population from microtome sections. Anat. Rec. 94, 239–247.

Al-Majed, A.A., Neumann, C.M., Brushart, T.M., Gordon, T., 2000. Brief electrical stimulation promotes the speed and accuracy of motor axonal regeneration. J. Neurosci. 20, 2602–2608.

Atwal, J.K., Massie, B., Miller, F.D., Kaplan, D.R., 2000. The TrkB-Shc site signals neuronal survival and local axon growth via MEK and P13-kinase. Neuron 27, 265–277.

Baumgartner, B.J., Shine, H.D., 1998. Permanent rescue of lesioned neonatal motoneurons and enhanced axonal regeneration by adenovirus-mediated expression of glial cell-line-derived neurotrophic factor. J. Neurosci. Res. 15, 766–777.

Boyd, J.G., Gordon, T., 2001. The neurotrophin receptors, trkB and p75, differentially regulate motor axonal regeneration. J. Neurobiol. 49, 314–325.

Boyd, J.G., Gordon, T., 2002. Dose-dependent facilitation and inhibition of peripheral nerve regeneration by exogenous brain-derived neurotrophic factor. Eur. J. Neurosci. 15, 613–626.

Burazin, T.C., Gundlach, A.L., 1998. Up-regulation of GDNFR-alpha and c-ret mRNA in facial motor neurons following facial nerve injury in the rat. Brain Res. Mol. Brain Res. 55, 331–336.

Chai, H., Wu, W., So, K.F., Prevette, D.M., Oppenheim, R.W., 1999. Long-term effects of a single dose of brain-derived neurotrophic factor on motoneuron survival following spinal root avulsion in the adult rat. Neurosci. Lett. 274, 147–150.

Creedon, D.J., Tansey, M.G., Baloh, R.H., Osborne, P.A., Lampe, P.A., Fahrner, T.J., Heuckeroth, R.O., Milbrandt, J., Johnson Jr., E.M., 1997. Neurturin shares receptors and signal transduction pathways with glial cell line-derived neurotrophic factor in sympathetic neurons. PNAS 94, 7018–7023.

Curtis, R., Tonra, J.R., Stark, J.L., Adryan, K.M., Park, J.S., Cliffer, K.D., Lindsay, R.M., DiStefano, P.S., 1998. Neuronal injury increases retrograde axonal transport of the neurotrophins to spinal sensory neurons and motor neurons via multiple receptor mechanisms. Mol. Cell Neurosci. 12, 105–118.

Dolcet, X., Egea, J., Soler, R.M., Martin-Zanca, D., Comella, J.X., 1999. Activation of phosphatidylinositol 3-kinase, but not extracellular-regulated kinases, is necessary to mediate brain-derived neurotrophic factor-induced motoneuron survival. J. Neurochem. 73, 521–531.

Effron, B., 1979. Bootstrap methods: another look at the Jacknife. Ann. Stat. 7, 1–26.

Fernandes, K.J., Kobayashi, N.R., Jasmin, B.J., Tetzlaff, W., 1998. Acetylcholinesterase gene expression in axotomized rat facial motoneurons is differentially regulated by neurotrophins: correlation with trkB and trkC mRNA levels and isoforms. J. Neurosci. 18, 9936–9947.

Friedman, B., Kleinfeld, D., Ip, N.Y., Verge, V.M.K., Moulton, R., Boland, P., Zlotchenko, E., Lindsay, R.R., Liu, L., 1995. Neurotrophic influence on injured spinal motoneurons. J. Neurosci. 15, 1044–1056.

Friedman, W.J., Greene, L.A., 1999. Neurotrophin signaling via Trks and p75. Exp. Cell Res. 253, 131–142.

Fu, S.Y., Gordon, T., 1995. Contributing factors to poor functional recovery after delayed nerve repair: prolonged axotomy. J. Neurosci. 15, 3876–3885.

Fu, S.Y., Gordon, T., 1997. The cellular and molecular basis of peripheral nerve regeneration. Mol. Neurobiol. 14, 67–116.

Funakoshi, H., Frisen, J., Barbany, G., Timmusk, T., Zacrisson, O., Verge, V., Persson, H., 1993. Differential expression of mRNAs for neurotrophins and their receptors after axotomy of the sciatic nerve. J. Cell Biol. 123, 455–465.

Giehl, K.M., Schutte, A., Mestres, P., Yan, Q., 1998. The survival-promoting effect of glial cell line-derived neurotrophic factor on axotomized corticospinal neurons *in vivo* is mediated by an endogenous brain-derived neurotrophic factor mechanism. J. Neurosci. 18, 7351–7360.

Hammarberg, H., Piehl, F., Risling, M., Cullheim, S., 2000. Differential regulation of trophic factor receptor mRNAs in spinal motoneurons after sciatic nerve transection and ventral root avulsion in the rat. J. Comp. Neurol. 426, 587–601.

Henderson, C.E., Phillips, H.S., Pollock, R.A., Davies, A.M., Lemeulle, C., Armanini, M., Simpson, L.C., Moffet, B., Vandlen, R.A., Koliatsos, V.E., Rosenthal, A., 1994. GDNF: a potent survival factor for motoneurons present in peripheral nerve and muscle. Science 266, 1062–1064.

Hiwas, T., Kondo, K., Hishiki, T., Koshizawa, S., Umezawa, K., Nakagawara, A., 1997. GDNF-induced neurite formation was stimulated by protein kinase inhibitors and suppressed by Ras inhibitors. Neurosci. Lett. 238, 115–118.

Hoke, A., Gordon, T., Zochodne, D.W., Sulaiman, O.A., 2002. A decline in glial cell-line-derived neurotrophic factor expression is associated with impaired regeneration after long-term Schwann cell denervation. Exp. Neurol. 173, 77–85.

Kishino, A., Ishige, Y., Tatsuno, T., Nakayama, C., Noguchi, H., 1997. BDNF prevents and reverses adult rat motor neuron degeneration and induces axonal outgrowth. Exp. Neurol. 144, 273–286.

Kobayashi, N.R., Fan, D.-P., Giehl, K.M., Bedard, A.M., Wiegand, S.J., Tetzlaff, W., 1997. BDNF and NT-4/5 prevent atrophy of rat rubrospinal neurons after cervical axotomy, stimulate GAP-43 and Tα1-

tubulin mRNA expression, and promote axonal regeneration. J. Neurosci. 17, 9583–9595.
Koliatsos, V.E., Clatterbuck, R.E., Winslow, J.W., Cayouette, M.H., Price, D.L., 1993. Evidence that brain-derived neurotrophic factor is a trophic factor for motor neurons in vivo. Neuron 10, 359–367.
Kotzbauer, P.T., Lampe, P.A., Heuckeroth, R.O., Golden, J.P., Creedon, D.J., Johnson, E.M., Milbrandt, J., 1996. Neurturin, a relative of glial-cell-line-derived neurotrophic factor. Nature 384, 467–470.
Li, L., Wu, W., Lin, L.F., Lei, M., Oppenheim, R.W., Houenou, L.J., 1995. Rescue of adult mouse motoneurons from injury-induced cell death by glial cell line-derived neurotrophic factor. PNAS. 92, 9771–9775.
Lin, L.F., Doherty, D.H., Lile, J.D., Bektesh, S., Collins, F., 1993. GDNF: a glial cell line-derived neurotrophic factor for midbrain dopaminergic neurons. Science 260, 1130–1132.
Meyer, M., Tatsuoka, I., Wetmore, C., Olson, L., Thoenen, H., 1992. Enhanced synthesis of brain derived neurotrophic factor in the lesioned peripheral nerve: different mechanisms are responsible for the regulation of BDNF and NGF mRNA. J. Cell Biol. 119, 45–54.
Miller, F.D., Tetzlaff, W., Bisby, M.A., Fawcett, J.W., Milner, R.J., 1989. Rapid induction of the major embryonic alpha-tubulin mRNA, T alpha 1, during nerve regeneration in adult rats. J. Neurosci. 9, 1452–1463.
Naveilhan, P., ElShamy, W.M., Ernfors, P., 1997. Differential regulation of mRNAs for GDNF and its receptors Ret and GDNFR alpha after sciatic nerve lesion in the mouse. Eur. J. Neurosci. 9, 1450–1460.
Nguyen, Q.T., Parsadanian, A.S., Snider, W.D., Lichtman, J.W., 1998. Hyperinnervation of neuromuscular junctions caused by GDNF overexpression in muscle. Science 279, 1725–1729.
Novikov, L., Novikova, L., Kellerth, J.O., 1997. Brain-derived neurotrophic factor promotes axonal regeneration and long-term survival of adult rat spinal motoneurons in vivo. Neurosci. 79, 765–774.
Oppenheim, R.W., Houenou, L.J., Johnson, J.E., Lin, L.F., Li, L., Lo, A.C., Newsome, A.L., Prevette, D.M., Wang, S., 1995. Developing motor neurons rescued from programmed and axotomy-induced cell death by GDNF. Nature 373, 344–346.
Saarma, M., Sariola, H., 1999. Other neurotrophic factors: glial cell line-derived neurotrophic factor (GDNF). Microsc. Res. Tech. 45, 292–302.
Sagot, Y., Rosse, T., Vejsada, R., Perrelet, D., Kato, A.C., 1998. Differential effects of neurotrophic factors on motoneuron retrograde labeling in a murine model of motoneuron disease. J. Neurosci. 18, 1132–1141.
Schmued, L.C., Fallon, J.H., 1986. Fluoro-Gold: a new fluorescent retrograde axonal tracer with numerous unique properties. Brain Res. 377, 147–154.
Segal, R.A., Greenberg, M.E., 1996. Intracellular signaling pathways activated by neurotrophic factors. Annu. Rev. Neurosci. 19, 463–489.
Sendtner, M., Holtmann, B., Kolbeck, R., Thoenen, H., Barde, Y.-A., 1992. Brain-derived neurotrophic factor prevents the death of motoneurons in newborn rats after nerve section. Nature 360, 757–759.
Soler, R.M., Dolcet, X., Encinas, M., Egea, J., Bayascas, J.R., Comella, J.X., 1999. Receptors of the glial cell line-derived neurotrophic factor family of neurotrophic factors signal cell survival through the phosphatidylinositol 3-kinase pathway in spinal cord motoneurons. J. Neurosci. 19, 9160–9169.
Swett, J.E., Wikholm, R.P., Blanks, R.H., Swett, A.L., Conley, L.C., 1986. Motoneurons of the rat sciatic nerve. Exp. Neurol. 93, 227–252.
Tetzlaff, W., Alexander, S.W., Miller, F.D., Bisby, M.A., 1991. Response of facial and rubrospinal neurons to axotomy: changes in mRNA expression for cytoskeletal proteins and GAP-43. J. Neurosci. 11, 2528–2544.
Trupp, M., Belluardo, N., Funakoshi, H., Ibanez, C.F., 1997. Complementary and overlapping expression of glial cell line-derived neurotrophic factor (GDNF), c-ret proto-oncogene, and GDNF receptor-alpha indicates multiple mechanisms of trophic actions in the adult rat CNS. J. Neurosci. 17, 3554–3567.
Tsujino, H., Mansur, K., Kiryu-Seo, S., Namikawa, K., Kitahara, T., Tanabe, K., Ochi, T., Kiyama, H., 1999. Discordant expression of c-Ret and glial cell line-derived neurotrophic factor receptor alpha-1 mRNAs in response to motor nerve injury in neonate rats. Brain Res. Mol. Brain Res. 70, 298–303.
Tuszynski, M.H., Mafong, E., Meyer, S., 1996. Central infusions of brain-derived neurotrophic factor and neurotrophin-4/5, but not nerve growth factor and neurotrophin-3, prevent loss of the cholinergic phenotype in injured adult motor neurons. Neuroscience 71, 761–771.
Vejsada, R., Tseng, J.L., Lindsay, R.M., Acheson, A., Aebischer, P., Kato, A.C., 1998. Synergistic but transient rescue effects of BDNF and GDNF on axotomized neonatal motoneurons. Neuroscience 84, 129–139.
Yan, Q., Matheson, C., Lopez, O.T., 1995. *In vivo* neurotrophic effects of GDNF on neonatal and adult facial motor neurons. Nature 373, 341–344.
Yano, H., Chao, M.V., 2000. Neurotrophin receptor structure and interactions. Pharm. Acta Helv. 74, 253–260.
Yuan, Q., Wu, W., So, K.F., Cheung, A.L., Prevette, D.M., Oppenheim, R.W., 2000. Effects of neurotrophic factors on motoneuron survival following axonal injury in newborn rats. NeuroReport 11, 2237–2241.
Zurn, A.D., Winkel, L., Menoud, A., Djabali, K., Aebischer, P., 1996. Combined effects of GDNF, BDNF and CNTF on motoneuron differentiation in vito. J. Neurosci. Res. 44, 133–141.

GLIA 32:234–246 (2000)

Effects of Short- and Long-Term Schwann Cell Denervation on Peripheral Nerve Regeneration, Myelination, and Size

OLAWALE A.R. SULAIMAN AND TESSA GORDON*
Department of Pharmacology, Division of Neuroscience, University of Alberta, Edmonton, Alberta, Canada

KEY WORDS PNS injury and regeneration; chronic denervation; distal nerve stump; Schwann cells; PNS myelination; nerve fiber diameters; retrograde labeling; poor functional recovery

ABSTRACT Poor functional recovery after peripheral nerve injury has been generally attributed to inability of denervated muscles to accept reinnervation and recover from denervation atrophy. However, deterioration of the Schwann cell environment may play a more vital role. This study was undertaken to evaluate the effects of chronic denervation on the capacity of Schwann cells in the distal nerve stump to support axonal regeneration and to remyelinate regenerated axons. We used a delayed cross-suture anastomosis technique in which the common peroneal (CP) nerve in the rat was denervated for 0–24 weeks before cross-suture of the freshly axotomized tibial (TIB) and chronically denervated CP nerve stumps. Motor neurons were backlabeled with either fluoro-ruby or fluorogold 12 months later, to identify and count TIB motor neurons that regenerated axons into chronically denervated CP nerve stumps. Number, size, and myelination of regenerated sensory and motor axons were determined using light and electron microscopy. We found that short-term denervation of ≤4weeks did not affect axonal regeneration but more prolonged denervation profoundly reduced the numbers of backlabeled motor neurons and axons in the distal nerve stump. Yet, atrophic Schwann cells retained their capacity to remyelinate regenerated axons. In fact, the axons were larger and well myelinated by long-term chronically denervated Schwann cells. These findings demonstrate a progressive inability of chronically denervated Schwann cells to support axonal regeneration and yet a sustained capacity to remyelinate the axons which do regenerate. Thus, axonal interaction can effectively switch the nonmyelinating phenotype of atrophic Schwann cells back into the myelinating phenotype. *GLIA 32: 234–246, 2000.* © 2000 Wiley-Liss, Inc.

The Neurotrophin Receptors, trkB and p75, Differentially Regulate Motor Axonal Regeneration

J. G. Boyd, T. Gordon

University Centre for Neuroscience, Faculty of Medicine and Dentistry, University of Alberta, 523 Heritage Medical Research Centre, Edmonton, AB T6G 2S2, Canada

Received 4 June 2001; accepted 7 August 2001

ABSTRACT: **Neurotrophic factors that support neuronal survival are implicated in axonal regeneration after injury. Specifically, a strong role for BDNF in motor axonal regeneration has been suggested based on its pattern of expression after injury, as well as the expression of its receptors, trkB and p75. Despite considerable *in vitro* evidence, which demonstrate specific and distinct physiological responses elicited following trkB and p75 activation, relatively little is known about the function of these receptors *in vivo*. To investigate the roles of the trkB and p75 receptors in motor axonal regeneration, we have used a tibial (TIB)- common peroneal (CP) cross suture paradigm in p75 homozygous (−/−) knockout mice, trkB heterozygous (+/−) knockout mice, as well as in their wild-type controls. Contralateral intact TIB motoneurons, and axotomized TIB motoneurons that regenerated their axons 10 mm into the CP distal nerve stump were identified by fluorescent retrograde tracers and counted in the T11-L1 spinal segments. Regeneration was evaluated 2, 3, 4, 6, and 8 weeks after nerve repair. Compared to wild-type animals, there are significantly fewer intact TIB motoneurons in p75 (−/−), but not trkB (+/−) mice. The number of motoneurons that regenerated their axons was significantly increased in the p75 (−/−) knockout mice, but significantly attenuated in the trkB (+/−) mice compared to wild-type controls. These results suggest that p75 is important for motoneuronal survival during development, but p75 expression after injury serves to inhibit motor axonal regeneration. In addition, full expression of trkB is critical for complete axonal regeneration to proceed.** © 2001 John Wiley & Sons, Inc. J Neurobiol 49: 314–325, 2001

Keywords: **BDNF; trkB; p75; axonal regeneration; motoneuron; retrograde labeling; staggered regeneration**



Experimental Neurology 264 (2015) 26–32

Contents lists available at ScienceDirect

Experimental Neurology

journal homepage: www.elsevier.com/locate/yexnr

Regular Article

Reduced expression of regeneration associated genes in chronically axotomized facial motoneurons

T. Gordon *, S. You, S.L. Cassar, W. Tetzlaff **

Department of Neuroscience, University of Alberta, Edmonton, AB T6G 2S2, Canada
ICORD (International Collaboration on Repair Discoveries), Canada
Department Zoology, University of British Columbia, Vancouver, V5Z 1M9, BC, Canada
Department Surgery, University of British Columbia, Vancouver, BC, Canada

ARTICLE INFO

Article history:
Received 18 July 2014
Revised 15 September 2014
Accepted 29 October 2014
Available online 9 November 2014

Keywords:
Regeneration associated genes
Axotomy
Motoneuron
GAP-43
Tubulin
Actin
Neurofilament

ABSTRACT

Chronically axotomized motoneurons progressively fail to regenerate their axons. Since axonal regeneration is associated with the increased expression of tubulin, actin and GAP-43, we examined whether the regenerative failure is due to failure of chronically axotomized motoneurons to express and sustain the expression of these regeneration associated genes (RAGs). Chronically axotomized facial motoneurons were subjected to a second axotomy to mimic the clinical surgical procedure of refreshing the proximal nerve stump prior to nerve repair. Expression of α1-tubulin, actin and GAP-43 was analyzed in axotomized motoneurons using *in situ* hybridization followed by autoradiography and silver grain quantification. The expression of these RAGs by acutely axotomized motoneurons declined over several months. The chronically injured motoneurons responded to a refreshment axotomy with a re-increase in RAG expression. However, this response to a refreshment axotomy of chronically injured facial motoneurons was less than that seen in acutely axotomized facial motoneurons. These data demonstrate that the neuronal RAG expression can be induced by injury-related signals and does not require acute deprivation of target derived factors. The transient expression is consistent with a transient inflammatory response to the injury. We conclude that transient RAG expression in chronically axotomized motoneurons and the weak response of the chronically axotomized motoneurons to a refreshment axotomy provides a plausible explanation for the progressive decline in regenerative capacity of chronically axotomized motoneurons.
Crown Copyright © 2014 Published by Elsevier Inc. All rights reserved.

Introduction

Functional recovery after chronic nerve injury is generally poor. This has generally been attributed to deterioration of the peripheral growth environment as well as irreversible atrophy of the denervated targets (Gutmann, 1948); for review see Fu and Gordon, 1997). During axon regeneration especially over long distances, many neurons remain without targets, a state of chronic axotomy (Fu and Gordon, 1997). In experiments in which chronically axotomized lumbar motoneurons were encouraged to regenerate axons into the permissive environment of a freshly denervated nerve stump, a progressive deterioration in the neurons' capacity to regenerate axons demonstrated that prolonged axotomy reduces regenerative capacity of injured neurons (Fu and Gordon, 1995a, 1997). Axotomized motoneurons undergo characteristic changes in gene expression which has been considered to be a switch from "transmitting" to "growth" (Fu and Gordon, 1997; Gordon, 1983). These changes include increased expression of immediate early genes such as c-jun (Arthur-Farraj et al., 2012; Herdegen et al., 1997), neurotrophic factors and their receptors (Al-Majed et al., 2000) cytoskeletal proteins, tubulin and actin (Al-Majed et al., 2004; Bisby and Tetzlaff, 1992), as well as growth associated proteins, most prominently GAP-43 (Skene, 1989) and CAP-23 (for review see Boyd and Gordon, 2003; Caroni, 1997; Fu and Gordon, 1997). In addition, genes associated with neurotransmission are down-regulated including choline-acetyltransferase and acetylcholinesterase (Fernandes et al., 1998; Flumerfelt and Lewis, 1975; Tetzlaff and Kreutzberg, 1984). Collectively the genes of the cytoskeletal proteins, tubulin, actin, and GAP-43 that are upregulated after injury, are frequently referred to as regeneration associated genes (RAGs) (Fu and Gordon, 1997).

The rate of axonal growth correlates directly with the rate of transport of tubulin and actin in slow component b (SCb) of axonal transport during both development and nerve regeneration in the adult (Hoffman and Lasek, 1980). The upregulation of tubulin and actin concurrent with a downregulation of neurofilament expression has been suggested to increase the fraction of tubulin and actin which is transported with the SCb component to the growing axons (Tetzlaff et al., 1996). The

* Correspondence to: T. Gordon, Department of Surgery, Division of Plastic Reconstructive Surgery, 5549A, The Hospital for Sick Children, 555 University Ave, Toronto, ON M5G 1X8, Canada. Fax: +1 416 813 6637, +1 647 678 1314 (cell).
** Correspondence to: W. Tetzlaff, ICORD (International Collaboration on Repair Discoveries), Blusson Spinal Cord Center, 818 W. 10th Avenue, Vancouver, V5Z 1M9, Canada.
E-mail addresses: tessat.gordon@gmail.com (T. Gordon), tetzlaff@icord.org (W. Tetzlaff).

http://dx.doi.org/10.1016/j.expneurol.2014.10.022
0014-4886/Crown Copyright © 2014 Published by Elsevier Inc. All rights reserved.

protein kinase C substrates GAP-43 and CAP-23, are concentrated in the axonal growth cone and regulate the actin based cytoskeletal motility via PI(4,5)P(2) modulation (Frey et al., 2000; Laux et al., 2000). GAP-43 is required for the stimulation of axonal growth on neuronal cell adhesion molecules such as N-CAM (Meiri et al., 1998). The transgenic overexpression of GAP-43 and CAP-23 induces terminal axonal sprouting at neuromuscular endplates (Aigner et al., 1995) and regeneration of the central axons of sensory neurons (Bomze et al., 2001). Hence, RAGs are required for a vigorous regeneration response. This is supported by studies in which electrical stimulation accelerates axon outgrowth *and* accelerates and enhances the expression of neurotrophic factors and their receptors, followed by acceleration and enhancement of RAGs (Al-Majed et al., 2000; Geremia et al., 2007; Gordon et al., 2009). Their expression is an important component of the molecular response of neurons to axotomy referred to as the 'cell body response" (Abe and Cavalli, 2008; Gordon, 1983; Gordon et al., 2009; Grafstein, 1975; Michaelevski et al., 2010; Rishal and Fainzilber, 2010).

Neuronal expression of RAGs has only been studied after acute injury and axonal regeneration after nerve crush with the exception of a study of GAP-43 expression in chronically axotomized dorsal root ganglion neurons (Bisby, 1988). In the latter study GAP-43 expression was found to be elevated after axotomy and sustained over the 6 months period of study. We report here that, in motoneurons, neither the expression of GAP-43 mRNA nor that of cytoskeletal tubulin and actin mRNA is sustained with time after axotomy. In addition, we undertook the present study to determine whether the poor regenerative capacity of chronically axotomized motoneurons is due to their failure to re-express or sustain the expression of these genes when the proximal nerve stump is subjected to a refreshment injury prior to suture of proximal and distal nerve stumps to encourage nerve regeneration. We studied axotomized facial motoneurons and demonstrated that the chronically axotomized facial motoneurons fail to fully re-express the mRNA for the tubulin, actin and GAP-43 after a refreshment injury.

Materials and methods

Surgical procedures

Sprague–Dawley male rats (Charles River) weighing 200–300 g were used for this study and all surgeries were done under deep anesthesia with intraperitoneal injection of a combination of chloral hydrate (150 mg/kg) plus sodium pentobarbital (30 mg/kg). The experimental procedures were in agreement with the guidelines of the Canadian Council for Animal Care and approved by the local animal care committees.

Design A [Chronic time course of expression of regeneration associated genes (RAGs)]

Facial motoneurons were axotomized 3–5 mm distal to the stylomastoid foramen and a 5–8 mm long segment of the facial nerve was resected to prevent reconnection with the distal stump. The rats were allowed to survive 6 or 11 months for *chronic axotomy* of the facial motoneurons and killed by an overdose of sodium pentobarbital (50 mg/kg) followed by transcardial perfusion with 4% paraformaldehyde.

Design B (Chronically axotomized motoneurons respond to a second axotomy)

In order to determine whether chronically axotomized motoneurons respond to a second axotomy (refreshment cut), we cut both the left and right facial nerves 3–5 mm distal to the stylomastoid foramen and resected 5–8 mm on each side to prevent regeneration. We allowed these rats to survive for 6 or 11 months (*chronic axotomy*). Thereafter the neuroma which had formed at the proximal stump of the facial nerve was resected on the right side (*chronic axotomy with refreshment axotomy*) while the left side was left untouched (*chronic axotomy*). Seven days later the rats were killed by an overdose of chloral hydrate followed by perfusion with 4% paraformaldehyde (for histological details, see Fernandes et al., 1999).

Design C (Response of chronically injured motoneuron to refreshment axotomy versus acute axotomy)

To determine whether chronically axotomized motoneurons respond to a refreshment cut in a similar manner and magnitude as to an acute axotomy, we compared the expression of RAGs in chronically axotomized and refreshed vs. acutely axotomized motoneurons in the same animals. We resected the left facial nerve 5 mm distal to its exit at the stylomastoid foramen (as above) and, 6–11 months later, we performed a resection of the neuroma on this left side (*refreshment axotomy after chronic axotomy*). At the same time of the second surgery, the contralateral right facial nerve, which was not previously injured, was resected (*acute axotomy*). Hence, this design allowed us to determine whether the response after refreshment cut is of the same magnitude as after acute axotomy.

In situ hybridization (ISH)

ISH was performed according a modified protocol by Miller et al. (1987) which has been described in extensive detail previously (Tetzlaff et al., 1991). For GAP-43, total α- and ß-tubulins, and actin, cDNA probes were used which were kindly provided by Dr. Pate Skene (GAP-43) (Basi et al., 1987) and Dr. N. Cowan (Mα1-tubulin and Mß2-tubulin) (Lewis and Schmalbruch, 1995) and the neurofilament-M probe was kindly provided by Dr. J.P. Julien (Julien et al., 1986). Both total α- and ß-tubulin cDNAs contain coding regions which are conserved among all other members of the α- or ß-tubulin family, thus they reveal total α- or ß-tubulin mRNA levels, respectively. In addition, for GAP-43, a 50-mer (5′GCATCGGTAGTAGCAGAGCCATCTCCCTCCTTCT TCTCCACACCATCAGCAA-3′) complementary to bases 270-220 (Basi et al., 1987) was used. No homologies were found in BLASTN database searches (Altschul et al., 1990). These oligo-probes were end-labeled using deoxynucleotide terminal transferase and ^{35}S-ATP according to a standard protocol (Ausubel et al., 1987). One hundred and seven cpm/ml of this probe was applied to the proteinase K treated, postfixed, and dehydrated sections (see above) using a hybridization cocktail that contained formamide (50%), 4x sodium chloride sodium citrate (SSC), dextran sulfate (0.1 g/ml), sarcosyl (1%), salmon sperm DNA (250 μg/ml) yeast tRNA (500 μg/ml), DDT (50 mM) and phosphate buffer (0.02 M, pH 7.2). After overnight hybridization at 43°C, the sections were washed four times in 1x SSC for 15 min at 55°C, rinsed in distilled water, dried, dipped in Kodak NTB2 emulsion, and exposed for 2 (T-α1) or 7 days (GAP-43) respectively.

In control experiments we determined that the concentration of the oligonucleotide probes used and the duration of hybridization of >14 h were saturating. We also confirmed in northern blots of RNA from facial nuclei, that the probes recognized a single band of expected size under identical hybridization conditions (Tetzlaff et al., 1991); equivalent data were obtained for the oligonucleotide probes (not shown). RNAse digestions and competitions with cold probe were performed as further specificity controls. These resulted in background signals only (not shown). Since hybridizations with sense probes shows that a sequence of similar GC content (typically around 50% for our probes) gives no signal, but still does not rule out cross-hybridizations, we refrained from using them. We obtained the same results using cDNA probes several hundred base pairs long as with the oligonucleotide probes. Single stranded oligonucleotide probes, however, revealed stronger signals overall and thus required 4–6 times shorter radioautographic exposure times.

Quantification of in situ hybridization and statistics

Darkfield pictures of the silver grains in the facial motoneurons were visualized. The motoneurons were stained for 20 s in diluted cresyl

violet (less than 0.01%) and blotted dry. Sections were briefly dipped in toluene and coverslipped in DePeX (BDH). Only labeled neurons with a visible nucleolus were measured. Details of this procedure are given in Fernandes et al. (1999) and Tetzlaff et al. (1991). In brief, the fraction of the cross-sectional area of the cytoplasm which was occupied by grains was multiplied by the volume of the cytoplasm. Thus, the signal was expressed as "counts per neuron" which takes into account the changes in soma size (shrinkage) typically seen in chronically injured facial motoneurons (Tetzlaff and Kreutzberg, 1984). Twenty five to 50 neurons per probe were measured and the mean counts per neuron from the double lesioned side were expressed as a percentage of the equivalent mean value from the contralateral (single lesioned or intact) side. Thus, each point in the graphs shows the percentage of contralateral [$\pm$ the standard error of the mean (SEM)] based on 50 to 100 facial motoneurons in an individual animal. Student's *t*-test was applied to the mean soma size data to detect significant changes between experimental and contralateral neurons. To detect significant differences in the mean ISH signals (percentage of contralateral), the non-parametric Wilcoxon–Mann–Whitney test was used. The criterion for significance was $p < 0.05$.

Results

Expression of regeneration associated genes (RAGs) declines in chronically axotomized motoneurons

A comparison of the tubulin and GAP-43 mRNA expression in facial motoneurons was made between chronically axotomized motoneurons (11 months axotomy) and chronically axotomized motoneurons that were acutely axotomized after the same 11 month period of chronic axotomy (11 months + 7 days) (Fig. 1). Although the facial motoneurons from the acute and chronic groups stemmed from different animal groups [B and C (see Methods)], the comparison of tubulin and GAP-43 mRNA expression in the soma of the motoneurons illustrates that the expression of the RAGs was not maintained in the motoneurons after chronic axotomy (cf. Fig. 1A,C, for 11 months chronic axotomy vs. Fig. 3A,C for a single acute axotomy). After 11 months of chronic axotomy, the facial motoneurons atrophied to 56.2% (cross-sectional area, $p < 0.001$) of the 7 day acutely axotomized motoneurons. The expression of GAP-43 was retained in a small subpopulation of the chronically axotomized motoneurons (see Fig. 1C).

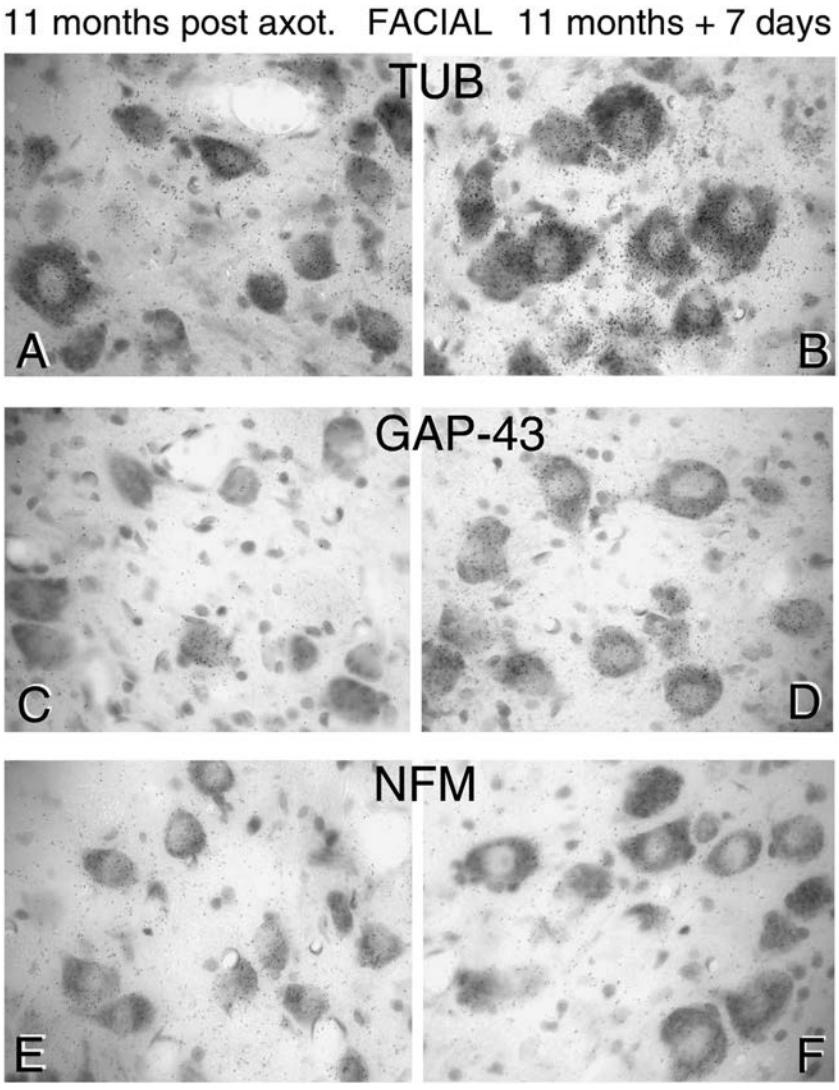


Fig. 1. Downregulation of α-tubulin mRNA and GAP-43 mRNA in chronically axotomized facial motoneurons (A, C) was reversed by a 7 day refreshment injury (B, D) whilst the downregulation of neurofilament-M (NFM) mRNA in chronically axotomized facial motoneurons (E) was exacerbated by the refreshment axotomy (F). *In situ* hybridization for α-tubulin mRNA (A, B), GAP-43 mRNA (C, D), and NFM mRNA (E, F) in 11 month chronically axotomized facial motoneurons (A, C, E) and the response of the chronically injured motoneurons to a refreshment axotomy at 7 days (B, D, F). Note the increase in soma size concurrent with upregulation of α-tubulin and GAP-43 as well as the downregulation of NFM in response to a refreshment injury (B, D, F).

Chronically axotomized neurons re-express RAGs when subjected to a refreshment axotomy

Using experimental design B to mimic the clinical refreshment cut performed on the proximal nerve stump prior to suture, facial motoneurons responded to a second axotomy (refreshment axotomy) 7 months (Fig. 3), and even 11 months after the first axotomy (Fig. 1). The chronically axotomized facial motoneurons that had undergone massive atrophy within the period of 11 months of chronic axotomy (Fig. 1A, C, E) dramatically recovered in size concurrent with the upregulation of tubulin, GAP-43 and actin (Fig. 3B, D, F). In addition, we noticed a pronounced glial response on the chronically axotomized and refreshed neurons (Fig. 1B,D). The expression of neurofilament-M (NFM) which was low 11 months post-axotomy, declined further after a 7 day refreshment injury (Fig. 1E,F).

The relative increases in gene expression of α-tubulin and GAP-43 of the chronically axotomized facial motoneurons in response to a refreshment axotomy (Fig. 2) are comparable to the 3–4 fold increases in α- and β-tubulin expression and the 10–20 fold increase in GAP-43 that we had previously demonstrated in acutely axotomized facial motoneurons (Tetzlaff et al., 1991). Interestingly, NFM mRNA in chronically axotomized motoneurons (Fig. 1E) was further downregulated by the refreshment axotomy to ~40% of the level of the chronically denervated motoneurons (data not shown). Hence, the chronically axotomized facial motoneurons show the same qualitative response to a second axotomy as intact motoneurons which respond to a naive injury. However this response was elicited in grossly atrophic motoneurons whose atrophy was reversed by the refreshment injury and the response started from a lower level of mRNA expression of the RAGs.

RAG expression after refreshment axotomy fails to reach the levels after acute injury

Using experimental design C (see Methods), the magnitude of RAG expression in chronically axotomized facial motoneurons responding to a refreshment axotomy (7 months + 7 days) was compared directly with the expression in naive acutely axotomized contralateral facial motoneurons (7 days) (Figs. 3 and 4). The lesser increase in expression of α-tubulin, actin and GAP-43 in chronically axotomized motoneurons responding to a refreshment axotomy (7 months + 7 days; Fig. 3B, D, F) compared with a greater increased expression of the same proteins in naïve acutely axotomized motoneurons (Fig. 3A, C, E). The expression in chronically axotomized motoneurons as a percentage of the expression after acute axotomy was ~20–60% in 3 rats, demonstrating the significantly smaller response of the chronically axotomized facial motoneurons to a refreshment injury (Fig. 4).

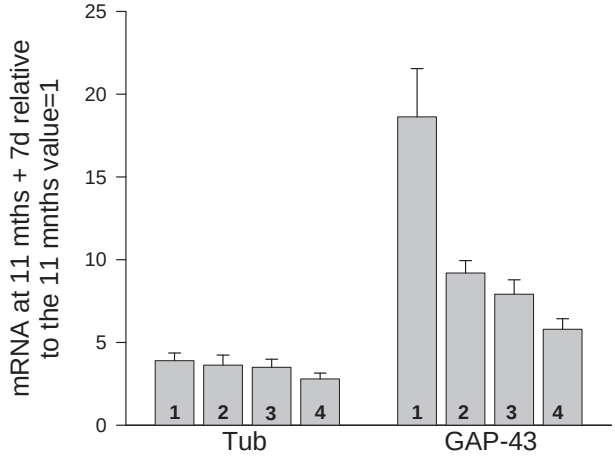


Fig. 2. A refreshment injury promotes the re-increase in expression of α-tubulin and GAP-43 in chronically axotomized facial motoneurons. In 4 rats, the *in situ* hybridization (ISH) signals/neuron (mean ± SEM of 50–100 motoneurons/rat) in the chronically axotomized *and* refreshed facial motoneurons (11 months + 7 days) were expressed as a ratio of the ISH signals/neuron in the chronically axotomized motoneurons (11 months) on the contralateral side. The expression in chronically axotomized motoneurons is set to equal unity. The increase in the expression of tubulin and GAP-43 above 1 was significant ($p < 0.05$) and it was as high as previously reported in acutely axotomized facial motoneurons (Tetzlaff et al., 1991).

Discussion

In the present study we demonstrated that the expression of regeneration associated genes (RAGs) by acutely axotomized facial motoneurons declines over several months. We further show that chronically injured motoneurons respond to a second axotomy which mimics a refreshment nerve section as it is performed in the clinical setting prior to nerve suture. The increase in the RAGs in response to a refreshment axotomy of chronically injured motoneurons was significantly less that that seen in acutely axotomized motoneurons.

Expression of RAGs is initiated by axotomy but requires additional factors to be sustained

This study confirms the upregulation of actin, tubulin and GAP-43 in facial motoneurons in response to acute axotomy that was shown in previous studies in several neuronal models (Bisby and Tetzlaff, 1992; Fernandes and Tetzlaff, 2000; Hoffman, 1989; Hoffman and Cleveland, 1988; Tetzlaff et al., 1991; Tetzlaff et al., 1988). The molecular signals responsible for these changes in expression of RAGs are incompletely understood. They are conceptualized as being of positive nature arising directly from the injury site, and of a negative nature deriving from the deprivation of the target. The *positive* injury related signals may include neurotrophic factors such as leukemia inhibitory factor (LIF) and cytokines (IL-6) released at the site of injury (Bolin et al., 1995; Sun and Zigmond, 1996; Zigmond, 2011, 2012). The dual leucine zipper kinase (DLK) has been identified as a key mediator of the positive retrograde injury signals, responsible for the activation of jun kinase (phosphorylating c-jun) and the retrograde transport of the transcription factor, p-STAT3 (Rishal and Fainzilber, 2010, 2014; Shin et al., 2012). Importin β1 is synthesized locally in response to the injury and forms a heterodimer with importin α1 to generate a complex with the high affinity nuclear localization signal (NLS) binding sites on a vimentin backbone (Hanz et al., 2003). This complex which includes transcription factors such as STAT3, is transported retrogradely to the nucleus via dynein interaction with microtubules (Ben-Yaakov et al., 2012).

A prominent negative signal in sensory and sympathetic neurons appears to be nerve growth factor (NGF). NGF application reverses some axotomy-induced neuropeptide changes in these neurons, and the treatment with NGF antiserum induces some of them (Verge et al., 1992, 1995). In motoneurons, disruption of nerve–muscle contacts may deprive the neurons of neurotrophic factors (Oppenheim, 1996; Thoenen et al., 1993) or alternatively, deprives the soma of the molecular signals from active neuromuscular junctions that sustain the transmitting phenotype (Gordon, 1983; Gordon et al., 2009). Our findings here demonstrate that the expression of RAGs is initiated by axotomy but that it is not sustained, indicating that negative signals are not sufficient to sustain their expression and that the positive signals probably required to sustain their expression, are transient.

The *negative* injury molecular signals are thought of as the deprivation of axotomized motoneurons of target derived neurotrophic factors such as brain derived neurotrophic factor (BDNF) and neurotrophin-4/5 (NT-4/5). This view is based on the expression of neurotrophic factors by the muscle (Funakoshi et al., 1993; Funakoshi 1995) and on the ability of these factors to maintain transmitter-related enzymes that include choline acetyl transferase (ChAT) (Friedman et al., 1995) and acetylcholine esterase (AChE) (Fernandes et al., 1998). However application of

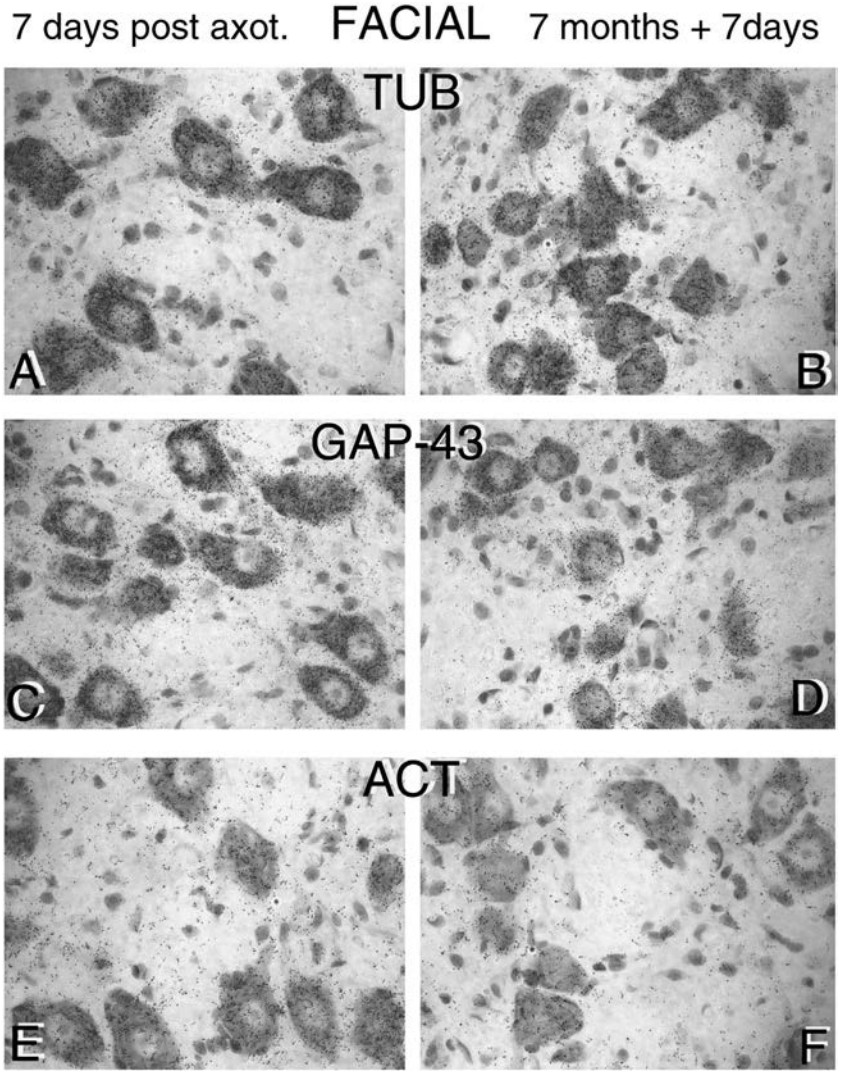


Fig. 3. Reduced *in situ* hybridization (ISH) signals of α-tubulin (A,B), GAP-43 (C,D) and actin (E,F) in chronically axotomized facial motoneurons were increased again by a refreshment axotomy but they were *not* increased to former levels. The typical ISH signals in chronically axotomized facial motoneurons responding to a refreshment axotomy (7 months + 7 days; B, D, F) are compared to the response of naïve acutely axotomized contralateral motoneurons (7 days post axotomy; A, C, E). Note that the lesser ISH signals for tubulin, GAP-43 and actin mRNA in the chronically axotomized and refreshed motoneurons (B, D, F) as compared to the signals after acute naïve axotomy (A, C, E).

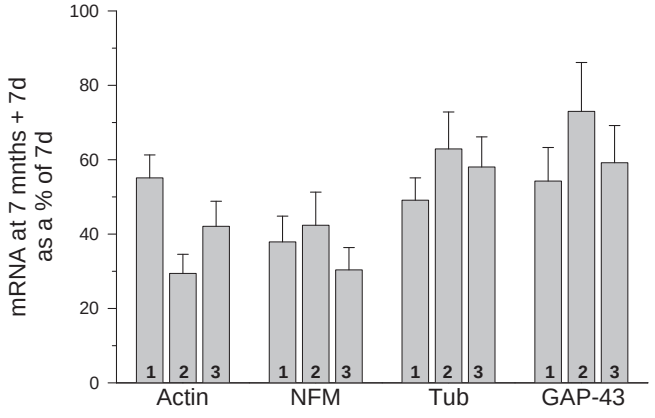


Fig. 4. The elevated expression of regeneration associated genes in response to a refreshment injury was reduced in the chronically axotomized motoneurons. The mean (+ SEM) expression of 50–100 motoneurons/rat of actin, neurofilament, α-tubulin and GAP-43 mRNA in chronically axotomized facial motoneurons (7 months + 7 days) in response to a refreshment axotomy in 3 rats is expressed as a percentage of the mean (+ SEM of 50–100 motoneurons/rat) values of the mRNA levels of the same proteins in the acutely axotomized contralateral motoneurons (7 days).

BDNF or NT-4/5 to the proximal stump of axotomized motoneurons does not reverse the axotomy-induced increase in tubulin, actin or GAP-43 expression, that in fact, are further enhanced (Fernandes and Tetzlaff, 2000). Interestingly, facial and spinal motoneurons transiently express BDNF after acute axotomy (Kobayashi et al., 1996; Al-Majed et al., 2000a). Indeed axotomized motoneurons upregulate several neurotrophic factors including BDNF and NT-4/5 that may be accelerated and boosted by brief low electrical stimulation of the transected nerve (Al-Majed et al., 2000a). The upregulation is followed in time by the upregulation of α-tubulin, actin and GAP-43 (Al-Majed et al, 2004). This regimen of a single 1 hour stimulation at 20 Hz in spinal motoneurons accelerates axon outgrowth and in turn, reinnervation of targets in both rats and humans (Al-Majed et al., 2000b; Brushart et al., 2002; Gordon et al., 2010). NT4/5 was demonstrated to be a critical neurotrophic factor in accelerating axon outgrowth in mice (English et al., 2007). The increased expression of some of the RAGs was sustained by administration of androgens in concert with accelerated outgrowth and regeneration rate of facial motoneurons (Sharma et al., 2010). Neuronal neurotrophic factors including BDNF and NT4/5 are therefore endogenous modifiers of RAG expression and of the regenerative capacity in axotomized motoneurons.

Some axotomy signals operate in the absence of target

Our finding that chronically axotomized motoneurons upregulate RAGs in response to a second axotomy is strong support for the involvement of the positive injury-related signals. Even when RAG expression in chronically axotomized motoneurons had fallen to below the normal levels of the contralateral intact motoneurons, re-induction of this expression occurred due to the refreshment axotomy. This re-induction is clearly independent of negative signals associated with the loss of target derived factors. We cannot rule out that the latter factors may contribute to RAG expression after an acute axotomy but their absence in the case of the response to the refreshment axotomy makes it unlikely. We are confident that the response to the second axotomy was not associated with target derived signals because the low level of neurofilament expression in the chronically axotomized facial motoneurons clearly indicates effective chronic disconnection from the target. Also, the atrophy of the chronically axotomized motoneurons was a reliable indicator of chronic target deprivation. The atrophy of chronically axotomized facial motoneurons was more pronounced than in hindlimb motoneurons (McPhail et al., 2004). The precise reason for this difference is unknown but it is conceivable that differences in the availability of trophic factors may play a role. Trophic support may come from the glial environment of the proximal stump which has been shown to produce trophic factors (Funakoshi et al., 1993; Meyer et al., 1992). Among other factors, BDNF as well as glial derived neurotrophic factor (GDNF) may be derived from the reactive Schwann cells in the neuroma and ciliary neurotrophic factor (CNTF) from intact myelinating Schwann cells (Hammarberg et al., 1996; Meyer et al., 1992; Richardson, 1994; Terenghi, 1999; Boyd and Gordon, 2003). The longer 45–50 mm proximal stump of the sciatic nerve may be a larger source of trophic factors compared to the 12–15 mm long stump of the facial nerve.

Weak RAG expression correlates with poor regenerative capacity of chronically axotomized motoneurons

Despite the capacity of the chronically axotomized facial motoneurons to respond to a refreshment axotomy, we show that the level of RAG expression is either lower than after acute axotomy. The upregulation of RAGs reaches only about half the levels reached after acute axotomy, based on data derived from experimental design C in which we directly compared RAG expression in response to a refreshment axotomy versus an acute injury.

The ability to express RAGs closely correlates with the neuronal capacity for axonal regeneration. Axotomized rubrospinal neurons regenerate successfully into peripheral nerve transplants only if RAG expression is induced by the axotomy. Both, regeneration and RAG expression are only observed after cervical but not after thoracic spinal cord hemisection (Fernandes et al., 1999a). Application of BDNF to axotomized rubrospinal neurons induces and sustains the expression of RAGs and thereby stimulates successful regeneration into peripheral nerve transplants even after thoracic axotomy (Kobayashi et al., 1997). Similar BDNF application one year after chronic cervical axotomy reversed the atrophy of rubrospinal neurons and reinstated their RAG expression and axonal regeneration mode (Kwon et al., 2002). In the light of the strong correlation of RAG expression and regeneration, the transient expression of RAGs and the weaker response to refreshment axotomy explains, at least in part, the progressive failure of chronically axotomized motoneurons to regenerate their axons (Fu and Gordon, 1995a). It is unlikely that high expression of merely actin, tubulin or GAP-43 is sufficient to support a strong regenerative response, as shown with isolated overexpression of GAP-43 or c-jun in Purkinje cells (Carulli et al., 2002). Rather a coordinated and sustained expression with other growth associated proteins, e.g. CAP-23 (Widmer and Caroni, 1990), microtubule associated proteins (Fawcett, 1994; Nothias et al., 1995) and/or cell adhesion molecules (Anderson et al., 1998; Chaisuksunt et al., 2000) as well as transcription and key signaling molecules (for review see Patodia and Raivich, 2012) is part of a network of RAGs contributing to a robust regenerative response (van Kesteren et al., 2011). Indeed, this was first shown by the combined transgenic overexpression of GAP-43 or CAP-23, but not either of the two alone, enhancing the regenerative capacity of the central axon of dorsal root ganglion cells (Bomze et al., 2001). Hence, failure to re-initiate or to maintain high levels of RAG expression is most likely one reason for the poor regenerative success we observed after chronic nerve injury.

In addition to chronic axotomy, progressive deterioration of the distal nerve stumps and Schwann cell atrophy in addition to the atrophy of chronically denervated muscles are important factors which significantly reduce the success of axonal regeneration after those nerve injuries which incur long delays between the injury and reinnervation of denervated targets (Fu and Gordon, 1995a, 1995b, 1997; Gordon et al., 2011). Nevertheless, by experimentally isolating the effects of chronic axotomy and denervation, it is apparent that chronic axotomy itself reduces regenerative capacity.

Acknowledgments

This work was funded by grants from the Canadian Institute of Medical Research of Canada to W.T. (10689) and to T.G. (12072). Our thanks to Neil Tyreman for his technical assistance.

References

Abe, N., Cavalli, V., 2008. Nerve injury signaling. Curr. Opin. Neurobiol. 18, 276–283.
Aigner, L., Arber, A., Kapfhammer, J.P., Laux, T., Schneider, C., Botteri, F., Brenner, H.R., Caroni, P., 1995. Overexpression of the neural growth-associated protein GAP-43 induces nerve sprouting in the adult nervous system of transgenic mice. Cell 83, 269–278.
Al-Majed, A.A., Brushart, T.M., Gordon, T., 2000. Electrical stimulation accelerates and increases expression of BDNF and trkB mRNA in regenerating rat femoral motoneurons. Eur. J. Neurosci. 12, 4381–4390.
Al-Majed, A.A., Tam, S.L., Gordon, T., 2004. Electrical stimulation accelerates and enhances expression of regeneration-associated genes in regenerating rat femoral motoneurons. Cell. Mol. Neurobiol. 24, 379–402.
Altschul, S.F., Gish, W., Miller, W., Myers, E.W., Lipman, D.J., 1990. Basic alignment search tool. J. Mol. Biol. 215, 403–410.
Anderson, P.N., Campbell, G., Zhang, Y., Lieberman, A.R., 1998. Cellular and molecular correlates of the regeneration of adult mammalian CNS axons into peripheral nerve grafts. Prog. Brain Res. 117, 211–232.
Arthur-Farraj, P.J., Latouche, M., Wilton, D.K., Quintes, S., Chabrol, E., Banerjee, A., Woodhoo, A., Jenkins, B., Rahman, M., Turmaine, M., Wicher, G.K., Mitter, R., Greensmith, L., Behrens, A., Raivich, G., Mirsky, R., Jessen, K.R., 2012. c-Jun reprograms Schwann cells of injured nerves to generate a repair cell essential for regeneration. Neuron 75, 633–647.
Ausubel, F.M., Brent, T., Kingston, R.E., Moore, D.D., Seidman, J.G., Smith, K.A., Struhl, K., 1987. Current Protocols in Molecular Biology. Wiley Interscience, New York.
Basi, G.S., Jacobson, R.D., Virag, I., Schilling, J., Skene, J.H., 1987. Primary structure and transcriptional regulation of GAP-43, a protein associated with nerve growth. Cell 49, 785–791.
Ben-Yaakov, K., Dagan, S.Y., Segal-Ruder, Y., Shalem, O., Vuppalanchi, D., Willis, D.E., Yudin, D., Rishal, I., Rother, F., Bader, M., Blesch, A., Pilpel, Y., Twiss, J.L., Fainzilber, M., 2012. Axonal transcription factors signal retrogradely in lesioned peripheral nerve. EMBO J. 31, 1350–1363.
Bisby, M.A., 1988. Dependence of GAP43 (B50, F1) transport on axonal regeneration in rat dorsal root ganglion neurons. Brain Res. 458, 157–161.
Bisby, M.A., Tetzlaff, W., 1992. Changes in cytoskeletal protein synthesis following axon injury and during axon regeneration. Mol. Neurobiol. 6, 107–123.
Bolin, L.M., Verity, A.N., Silver, J.E., Shooter, E.M., Abrams, J.S., 1995. Interleukin-6 production by Schwann cells and induction in sciatic nerve injury. J. Neurochem. 64, 850–858.
Bomze, H.M., Bulsara, K.R., Iskandar, B.J., Caroni, P., Skene, J.H., 2001. Spinal axon regeneration evoked by replacing two growth cone proteins in adult neurons. Nat. Neurosci. 4, 38–43.
Boyd, J.G., Gordon, T., 2003. Neurotrophic factors and their receptors in axonal regeneration and functional recovery after peripheral nerve injury. Mol. Neurobiol. 27, 277–324.
Brushart, T.M., Hoffman, P.N., Royall, R.M., Murinson, B.B., Witzel, C., Gordon, T., 2002. Electrical stimulation promotes motoneuron regeneration without increasing its speed or conditioning the neuron. J. Neurosci. 22, 6631–6638.
Caroni, P., 1997. Intrinsic neuronal determinants that promote axonal sprouting and elongation. BioEssays 19, 767–775.
Carulli, D., Buffo, A., Botta, C., Altruda, F., Strata, P., 2002. Regenerative and survival capabilities of Purkinje cells overexpressing c-Jun. Eur. J. Neurosci. 16, 105–118.

Chaisuksunt, V., Zhang, Y., Anderson, P.N., Campbell, G., Vaudano, E., Schachner, M., Lieberman, A.R., 2000. Axonal regeneration from CNS neurons in the cerebellum and brainstem of adult rats: correlation with the patterns of expression and distribution of messenger RNAs for L1, CHL1, c-jun and growth-associated protein-43. Neuroscience 100, 87–108.
English, A.W., Schwartz, G., Meador, W., Sabatier, M.J., Mulligan, A., 2007. Electrical stimulation promotes peripheral axonal regeneration by enhancing neuronal neurotrophin signaling. Dev. Neurobiol. 67, 158–172.
Fawcett, J., 1994. Astrocytes and axon regeneration in the central nervous system. J. Neurol. 242, S25–S28.
Fernandes, K.J., Tetzlaff, W.G., 2000. Gene expression in axotomized neurons: identifying the intrinsic determinants of axonal growth. In: Murray, M. (Ed.), Ingoglia, N.A. Axonal Regeneration in the Central Nervous System, Marcel Dekker New York, pp. 219–266.
Fernandes, K.J., Kobayashi, N.R., Jasmin, B.J., Tetzlaff, W., 1998. Acetylcholinesterase gene expression in axotomized rat facial motoneurons is differentially regulated by neurotrophins: correlation with trkB and trkC mRNA levels and isoforms. J. Neurosci. 18, 9936–9947.
Fernandes, K.J., Fan, D.P., Tsui, B.J., Cassar, S.L., Tetzlaff, W., 1999. Influence of the axotomy to cell body distance in rat rubrospinal and spinal motoneurons: differential regulation of GAP-43, tubulins, and neurofilament-M. J. Comp. Neurol. 414, 495–510.
Flumerfelt, B.A., Lewis, P.R., 1975. Cholinesterase activity in the hypoglossal nucleus of the rat and the changes produced by axotomy: a light and electron microscopic study. J. Anat. 119, 309–331.
Frey, D., Schneider, C., Xu, L., Borg, J., Spooren, W., Caroni, P., 2000. Early and selective loss of neuromuscular synapse subtypes with low sprouting competence in motoneuron diseases. J. Neurosci. 20, 2534–2542.
Friedman, B., Kleinfeld, D., Ip, N.Y., Verge, V.M., Moulton, R., Boland, P., Zlotchenko, E., Lindsay, R.M., Liu, L., 1995. BDNF and NT-4/5 exert neurotrophic infleunces on injured adult spinal motor neurons. J. Neurosci. 15, 1044–1056.
Funakoshi, H., Frisen, J., Barbany, G., Timmusk, T., Zachrisson, O., Verge, V.M., Persson, H., 1993. Differential expression of mRNAs for neurotrophins and their receptors after axotomy of the sciatic nerve. J. Cell Biol. 123, 455–465.
Funakoshi, J., Belluardo, N., Arenas, E., Yamamoto, Y., Casabona, A., Persson, H., Ibanez, C.F., 1995. Muscle-derived neurotrophin-4 as an activity-dependent trophic signal for adult motor neurons. Science 268, 1495–1499.
Fu, S.Y., Gordon, T., 1995a. Contributing factors to poor functional recovery after delayed nerve repair: prolonged axotomy. J. Neurosci. 15, 3876–3885.
Fu, S.Y., Gordon, T., 1995b. Contributing factors to poor functional recovery after delayed nerve repair: prolonged denervation. J. Neurosci. 15, 3886–3895.
Fu, S.Y., Gordon, T., 1997. The cellular and molecular basis of peripheral nerve regeneration. Mol. Neurobiol. 14, 67–116.
Geremia, N.M., Gordon, T., Brushart, T.M., Al-Majed, A.A., Verge, V.M., 2007. Electrical stimulation promotes sensory neuron regeneration and growth-associated gene expression. Exp. Neurol. 205, 347–359.
Gordon, T., Amirjani, N., Edwards, D.C., Chan, K.M., 2010. Brief post-surgical electrical stimulation accelerates axon regeneration and muscle reinnervation without affecting the functional measures in carpal tunnel syndrome patients. Exp. Neurol. 223, 192–202.
Gordon, T., 1983. Dependence of peripheral nerves on their target organs. In: O'Brien, R., Vrbova, G., Burnstock, G. (Eds.), Somatic and Autonomic Nerve–Muscle Interactions. Elsevier, Amsterdam, pp. 289–316.
Gordon, T., Udina, E., Verge, V.M., de Chaves, E.I., 2009. Brief electrical stimulation accelerates axon regeneration in the peripheral nervous system and promotes sensory axon regeneration in the central nervous system. Mot. Control. 13, 412–441.
Gordon, T., Tyreman, N., Raji, M.A., 2011. The basis for diminished functional recovery after delayed peripheral nerve repair. J. Neurosci. 31, 5325–5334.
Grafstein, B., 1975. The nerve cell body response to axotomy. Exp. Neurol. 48, 32–51.
Gutmann, E., 1948. Effect of delay of innervation on recovery of muscle after nerve lesions. J. Neurophysiol. 11, 279–294.
Hammarberg, H., Piehl, F., Cullheim, S., Fjell, J., Hokfelt, T., Fried, K., 1996. GDNF mRNA in Schwann cells and DRG satellite cells after chronic sciatic nerve injury. NeuroReport 7, 857–860.
Hanz, S., Perlson, E., Willis, D., Zheng, J.Q., Massarwa, R., Huerta, J.J., Koltzenburg, M., Kohler, M., van-Minnen, J., Twiss, J.L., Fainzilber, M., 2003. Axoplasmic importins enable retrograde injury signaling in lesioned nerve. Neuron 40, 1095–1104.
Herdegen, T., Skene, P., Bahr, M., 1997. The c-Jun transcription factor—bipotential mediator of neuronal death, survival and regeneration. Trends Neurosci. 20, 227–231.
Hoffman, P.N., Lasek, R.J., 1980. Axonal transport of the cytoskeleton in regenerating motor neurons: constancy and change. Brain Res. 202, 317–333.
Hoffman, P.N., 1989. Expression of GAP-43, a rapidly transported growth-associated protein, and class II beta tubulin, a slowly transposrted cytoskeletal protein, are coordinated in regenerating neurons. J. Neurosci. 9, 893–897.
Hoffman, P.N., Cleveland, D.W., 1988. Neurofilament and tubulin expression recapitulates the developmental program during axonal regeneration: induction of a specific beta-tubulin isotype. Proc. Natl. Acad. Sci. U. S. A. 85, 4530–4533.
Julien, J.P., Meyer, D., Flavell, D., Hurst, J., Grosveld, F., 1986. Cloning and developmental expression of the murine neurofilament gene family. Brain Res. 387, 243–250.
Kobayashi, N.R., Bedard, A.M., Hincke, M.T., Tetzlaff, W., 1996. Increased expression of BDNF and trkB mRNA in rat facial motoneurons after axotomy. Eur. J. Neurosci. 8, 1018–1029.
Kobayashi, N.R., Fan, D.P., Giehl, K.M., Bedard, A.M., Wiegand, S.J., Tetzlaff, W., 1997. BDNF and NT-4/5 prevent atrophy of rat rubrospinal neurons after cervical axotomy, stimulate GAP-43 and Talpha1-tubulin mRNA expression, and promote axonal regeneration. J. Neurosci. 17, 9583–9595.
Kwon, B.K., Liu, J., Messerer, C., Kobayashi, N.R., McGraw, J., Oschipok, L., Tetzlaff, W., 2002. Survival and regeneration of rubrospinal neurons 1 year after spinal cord injury. Proc. Natl. Acad. Sci. U. S. A. 99, 3246–3251.
Laux, T., Fukami, K., Thelen, M., Golub, T., Frey, D., Caroni, P., 2000. GAP43, MARCKS, and CAP23 modulate PI(4,5)P(2) at plasmalemmal rafts, and regulate cell cortex actin dynamics through a common mechanism. J. Cell Biol. 149, 1455–1472.
Lewis, D.M., Schmalbruch, H., 1995. Effects of age on aneural regeneration of soleus muscle in rat. J. Physiol. Lond. 488 (Pt 2), 483–492.
McPhail, L.T., Fernandes, K.J., Chan, C.C., Vanderluit, J.L., Tetzlaff, W., 2004. Axonal reinjury reveals the survival and re-expression of regeneration-associated genes in chronically axotomized adult mouse motoneurons. Exp. Neurol. 188, 331–340.
Meiri, K.F., Saffell, J.L., Walsh, F.S., Doherty, P., 1998. Neurite outgrowth stimulated by neural cell adhesion molecules requires growth-associated protein-43 (GAP-43) function and is associated with GAP-43 phosphorylation in growth cones. J. Neurosci. 18, 10429–10437.
Meyer, M., Matsuoka, I., Wetmore, C., Olson, L., Thoenen, H., 1992. Enhanced synthesis of brain-derived neurotrophic factor in the lesioned peripheral nerve: different mechanisms are responsible for the regulation of BDNF and NGF mRNA. J. Cell Biol. 119, 45–54.
Michaelevski, I., Segal-Ruder, Y., Rozenbaum, M., Medzihradszky, K.F., Shalem, O., Coppola, G., Horn-Saban, S., Ben-Yaakov, K., Dagan, S.Y., Rishal, I., Geschwind, D.H., Pilpel, Y., Burlingame, A.L., Fainzilber, M., 2010. Signaling to transcription networks in the neuronal retrograde injury response. Sci. Signal. 3, ra53.
Miller, F.D., Naus, C.C., Higgins, G.A., Bloom, F.E., Milner, R.J., 1987. Developmentally regulated at brain mRNAs: molecule and anatomical characterization. J. Neurosci. 7, 2433–2444.
Nothias, F., Boyne, L., Murray, M., Tessler, A., Fischer, I., 1995. The expression and distribution of tau proteins and messenger RNA in rat dorsal root ganglion neurons during development and regeneration. Neuroscience 66, 707–719.
Oppenheim, R.W., 1996. Neurotrophic survival molecules for motoneurons: an embarrassment of riches. Neuron 17, 195–197.
Patodia, S., Raivich, G., 2012. Downstream effector molecules in successful peripheral nerve regeneration. Cell Tissue Res. 349, 15–26.
Richardson, P.M., 1994. Ciliary neurotrophic factor: a review. Pharmacol. Ther. 63, 187–198.
Rishal, I., Fainzilber, M., 2010. Retrograde signaling in axonal regeneration. Exp. Neurol. 223, 5–10.
Rishal, I., Fainzilber, M., 2014. Axon-soma communication in neuronal injury. Nat. Rev. Neurosci. 15, 32–42.
Sharma, N., Marzo, S.J., Jones, K.J., Foecking, E.M., 2010. Electrical stimulation and testosterone differentially enhance expression of regeneration-associated genes. Exp. Neurol. 223, 183–191.
Shin, J.E., Cho, Y., Beirowski, B., Milbrandt, J., Cavalli, V., DiAntonio, A., 2012. Dual leucine zipper kinase is required for retrograde injury signaling and axonal regeneration. Neuron 74, 1015–1022.
Skene, J.H., 1989. Axonal growth-associated proteins. Annu. Rev. Neurosci. 12, 127–156.
Sun, Y., Zigmond, R.E., 1996. Leukaemia inhibitory factor induced in the sciatic nerve after axotomy is involved in the induction of galanin in sensory neurons. Eur. J. Neurosci. 8, 2213–2220.
Terenghi, G., 1999. Peripheral nerve regeneration and neurotrophic factors. J. Anat. 194 (Pt1), 1–14.
Tetzlaff, W., Kreutzberg, G.W., 1984. Enzyme changes in the rat facial nucleus following a conditioning lesion. Exp. Neurol. 85, 547–564.
Tetzlaff, W., Bisby, M.A., Kreutzberg, G.W., 1988. Changes in cytoskeletal proteins in the rat facial nucleus following axotomy. J. Neurosci. 8, 3181–3189.
Tetzlaff, W., Alexander, S.W., Miller, F.D., Bisby, M.A., 1991. Response of facial and rubrospinal neurons to axotomy: changes in mRNA expression for cytoskeletal proteins and GAP-43. J. Neurosci. 11, 2528–2544.
Tetzlaff, W., Leonard, C., Krekoski, C.A., Parhad, I.M., Bisby, M.A., 1996. Reductions in motoneuronal neurofilament synthesis by successive axotomies: a possible explanation for the conditioning lesion effect on axon regeneration. Exp. Neurol. 139, 95–106.
Thoenen, H., Hughes, R.A., Sendtner, M., 1993. Towards a comprehensive understanding of the trophic support of motoneurons. C.R. Acad. Sci. III 316, 1158–1163.
van Kesteren, R.E., Mason, M.R., Macgillavry, H.D., Smit, A.B., Verhaagen, J., 2011. A gene network perspective on axonal regeneration. Front. Mol. Neurosci. 4, 46.
Verge, V.M., Merlio, J.P., Grondin, J., Ernfors, P., Persson, H., Riopelle, R.J., Hokfelt, T., Richardson, P.M., 1992. Colocalization of NGF binding sites, trk mRNA, and low-affinity NGF receptor mRNA in primary sensory neurons: responses to injury and infusion of NGF. J. Neurosci. 12, 4011–4022.
Verge, V.M., Richardson, P.M., Wiesenfeld-Hallin, Z., Hokfelt, T., 1995. Differential influence of nerve growth factor on neuropeptide expression n vivo: a novel role in peptide suppression in adult sensor neurons. J. Neurosci. 15, 2081–2096.
Widmer, F., Caroni, P., 1990. Identification, localization, and primary structure of CAP-23, a particle-bound cytosolic protein of early development. J. Cell Biol. 111, 3035–3047.
Zigmond, R.E., 2011. gp130 cytokines are positive signals triggering changes in gene expression and axon outgrowth in peripheral neurons following injury. Front. Mol. Neurosci. 4, 62.
Zigmond, R.E., 2012. Cytokines that promote nerve regeneration. Exp. Neurol. 238, 101–106.

Experimental Neurology **173,** 77–85 (2002)
doi:10.1006/exnr.2001.7826, available online at http://www.idealibrary.com on IDEAL®

A Decline in Glial Cell-Line-Derived Neurotrophic Factor Expression Is Associated with Impaired Regeneration after Long-Term Schwann Cell Denervation

A. Höke,*,†,[1] T. Gordon,‡ D. W. Zochodne,† and O. A. R. Sulaiman‡

**Department of Neurology, Johns Hopkins University, Baltimore, Maryland 21287; ‡Department of Neuroscience, University of Alberta, Edmonton, Alberta T6G 2M7, Canada; and †Department of Clinical Neurosciences, University of Calgary, Calgary, Alberta T2N 1N4, Canada*

Received May 29, 2001; accepted September 14, 2001

In the peripheral nervous system, regeneration of motor and sensory axons into chronically denervated distal nerve segments is impaired compared to regeneration into acutely denervated nerves. In order to find possible causes for this phenomenon we examined the changes in the expression pattern of the glial cell-line-derived neurotrophic factor (GDNF) family of growth factors and their receptors in chronically denervated rat sciatic nerves as a function of time with or without regeneration. Among the GDNF family of growth factors, only GDNF mRNA expression was rapidly upregulated in Schwann cells as early as 48 h after denervation. This upregulation peaked at 1 week and then declined to minimal levels by 6 months of denervation. The changes in the protein expression paralleled the changes in the expression of the GDNF mRNA. The mRNAs for receptors GFRα-1 and GFRα-2 were upregulated only after maximal GDNF upregulation and remained elevated as late as 6 months. There were no significant changes in the expression of GFRα-3 or the tyrosine kinase coreceptor, RET. When we examined the expression of GDNF in a delayed regeneration paradigm, there was no upregulation in the distal chronically denervated tibial nerve even when the freshly axotomized peroneal branch of the sciatic nerve was sutured to the distal tibial nerve. This study suggests that one of the reasons for impaired regeneration into chronically denervated peripheral nerves may be the inability of Schwann cells to maintain important trophic support for both motor and sensory neurons. © 2002 Elsevier Science

Key Words: **long-term denervation; GDNF; regeneration; distal nerve stump; Schwann cells.**

INTRODUCTION

Although peripheral nerves regenerate after nerve injury, functional recovery in human patients is generally poor, even when nerves are surgically repaired immediately (44). This compromised recovery is exacerbated by delayed nerve repair when the distal nerve segment is left denervated for a prolonged period of time (43, 44, 54). This was recognized as early as the 1940s with the experience in World War II injuries, but detailed studies as to the causes of this delayed regeneration were not carried out until very recently. Little is known about the causes of changes that occur morphologically in nerves that remain denervated for prolonged periods of time. We know that there are significant changes in the Schwann cells and in the extracellular matrix (ECM): atrophy of the distal denervated segment of an injured nerve, decrease in number and atrophy of Schwann cells, breakdown of the basement membrane, and change in the composition of the basement membrane. These changes were recognized early on (45, 46) and had been reconfirmed with more recent studies in both humans (47) and experimental animal models (16, 35, 50).

Using a model of chronic denervation and delayed cross reinnervation of the tibial and peroneal branches of the sciatic nerve, Gordon and co-workers showed that it is both the duration of axotomy and denervation that dictate the eventual success of a delayed repair (12, 13, 42). Using a similar model, Hall and co-workers showed that endoneurial Schwann cell proliferation, levels of expression of c-erbB receptors by Schwann cells, and the degree to which axons regenerated into the distal nerve stumps all decreased as the duration of prior denervation was increased (26). Similarly, Gordon and co-workers showed that expression of regeneration-associated molecules, especially the neurotrophin receptor p75NTR, decreased with prolonged denervation (56). These studies are just begin-

[1] To whom correspondence should be addressed at Department of Neurology, Johns Hopkins University, Path 509, 600 North Wolfe Street, Baltimore, MD 21287. Fax: (410) 614-1008. E-mail: ahoke@mail.jhmi.edu.

0014-4886/02 $35.00
© 2002 Elsevier Science
All rights reserved.

ning to elucidate the molecular changes that occur in Schwann cells with prolonged denervation.

Other families of trophic factors are certain to be involved in this lack of regenerative support by chronically denervated Schwann cells. GDNF belongs to a growing family of neurotrophic factors that are distantly related to the tumor necrosis factor-β (TGF-β) family of neurotrophic factors. Initially, it was isolated based on its neurotrophism of dopaminergic basal ganglia neurons (28), but later was shown to be a potent neurotrophin for motor neurons (22), as well as a subset of sensory and autonomic neurons (3). GDNF is retrogradely transported to motor neurons (55) and sensory neurons (31), and it is upregulated in the Schwann cells of the sciatic nerve after injury (21, 23, 32). What is unknown is whether this early upregulation of GDNF after nerve injury is maintained in chronic denervation.

Using a chronic denervation model of peripheral nerve injury in the present study we show that the initial upregulation of GDNF mRNA was not maintained by denervated Schwann cells. The mRNA for GDNF became almost undetectable as the duration of denervation was prolonged. The long-term denervated Schwann cells were also unable to upregulate the expression of GDNF mRNA even when they were challenged with freshly axotomized nerves in a delayed regeneration paradigm. The changes in the GDNF protein level paralleled the changes in the GDNF mRNA level. There were no significant changes in the mRNA levels of other members of the GDNF family of growth factors. The mRNAs for receptors GFRα-1 and GFRα-2 were upregulated only after maximal GDNF upregulation and remained elevated as late as 6 months. There was no significant upregulation in the expression of GFRα-3 or the tyrosine kinase coreceptor RET in the distal denervated nerves.

MATERIALS AND METHODS

Animal Surgery

All experimental protocols involving animals were reviewed and approved by the University of Calgary and University of Alberta animal care committees following the Canadian Council of Animal Care guidelines. Adult male Sprague–Dawley rats (200–300 g) were used to create a model of chronic denervation. Briefly, a unilateral sciatic nerve transection was done at the midthigh level, 1 cm above the sciatic trifurcation, using aseptic surgical techniques under anesthesia (65 mg/kg pentobarbital ip). The distal end of the proximal sciatic nerve was trimmed approximately 3 mm and sutured to a nearby muscle in order to prevent regeneration into the cut distal segment. Sham-operated contralateral sciatic nerves that were exposed but not injured were used as controls. In delayed coaptation experiments a previously described model of regeneration into long-term denervated nerve stumps was used (13, 42). Adult male Sprague–Dawley rats also received a unilateral transection of the tibial branch of the sciatic nerve. The proximal end of the tibial nerve was prevented from regeneration into the distal segment by deflecting it cranially and then suturing it to a nearby innervated muscle. After 1 month (short-term) or 6 months (long-term) of denervation, a fresh transection of the peroneal branch of the sciatic nerve was done and the proximal end of this branch was resutured into the distal end of the previously denervated tibial nerve. Five to 15 animals were used in each group at each time point in the study.

mRNA and Protein Studies

At 48 h, 1 week, 1 month, 3 months, and 6 months, a 1-cm segment of the sciatic nerve immediately distal to the transection and a segment from the corresponding contralateral side were harvested for mRNA and protein studies. Similarly in regeneration studies, a 1-cm segment of the tibial nerve immediately distal to the resuture site containing the presumed regenerating peroneal nerve axons and a segment from the comparable contralateral side were harvested on dry ice. Total RNA was isolated with TRIzol reagent (Life Technologies, Burlington, Ontario, Canada) (8) and reverse-transcribed using random hexamer primers. Semiquantitative multiplex PCR was done using the "primer-dropping" technique (53) with primers for the gene of interest and an internal control, GAPDH, in the same reaction tube. Primer sequences for GDNF, Neurturin (NTN), Persephin (PSP), Artemin (ART), GFRα-1, GFRα-2, GFRα-3, and RET were designed from mRNA sequences deposited in GenBank and were described previously (23). Primer sequences for GAPDH were published previously (53). These primer pairs were optimized to remain in the linear phase of the PCR at the cycle numbers used. PCR cycle parameters were as published (23). PCR products were electrophoresed in a 2% agarose gel and bands were visualized with ethidium bromide. Image analysis was done using NIH Image for Macintosh (Version 1.6.1, http://rsb.info.nih.gov/nih-image/). The density of the band for the gene of interest was normalized by the density of the band of the GAPDH and compared to that of the sham-operated side. Statistical analysis was done using a 3-factor split-plot analysis of variance corrected for multiple comparisons (the critical α level was set at $P = 0.005$) in the Statview program for Macintosh (version 5.0.1, SAS Institute Inc.). Appropriate controls including omission of the reverse-transcriptase enzyme were used to exclude genomic DNA amplification.

Fresh frozen distal nerves were homogenized and solubilized in RIPA buffer with protease inhibitors (5)

for the determination of GDNF protein content GDNF protein content was measured using standard ELISA techniques with anti-GDNF antibody (Santa Cruz Biotechnologies, Santa Cruz, CA) and normalized to the amount of total protein in the samples. Recombinant human GDNF (a gift from Amgen Inc., Thousand Oaks, CA) was used to create the standard curve in the ELISAs. Measurements were done in triplicate.

Immunohistochemistry

For immunohistochemical studies the animals were anesthetised and perfused with 4% paraformaldehyde through the heart. The distal sciatic nerves were harvested and postfixed with 4% paraformaldehyde at 4°C for another 4–8 h. The tissue was cryoprotected in 15% sucrose and then in 30% sucrose and cross-sectioned at 7 μm using a cryostat. Standard immunofluorescent staining was done using the anti-GDNF antibody (Santa Cruz Biotechnologies).

RESULTS

Changes with Chronic Denervation

GDNF mRNA was expressed at very low levels in the sham-operated control sciatic nerves. However, there was a significant upregulation of GDNF mRNA in the distal segment of transected sciatic nerves, as early as 48 h (Fig. 1). This upregulation of GDNF mRNA was not sustained with chronic denervation beyond 3 months and GDNF mRNA levels declined to baseline by 6 months (Fig. 1). In contrast to GDNF, the mRNA for NTN, PSP, and ART was easily detectable in the sham-operated sciatic nerves but there were no statistically significant changes with chronic denervation (Fig. 1).

The changes in GDNF protein level in the denervated sciatic nerve paralleled the changes in the mRNA levels (Figs. 2 and 3). Using ELISA we showed that the GDNF content of a sham-operated sciatic nerve was 0.17 ng per 1 mg/ml of total protein. At 1 month, the GDNF protein content in the denervated sciatic nerve was upregulated by almost three-fold to 0.53 ng per 1 mg/ml of total protein. However, by 6 months the levels in the denervated sciatic nerve were back to baseline at 0.18 ng per 1 mg/ml of total protein. The level of GDNF protein at 1 month of denervation was statistically significantly different from the sham-operated or 6-month-denervated sciatic nerves (Fig. 2). Similarly, the upregulation in protein content could be observed with indirect immunohistochemistry (Fig. 3). Taken together, these findings showed that the Schwann cells of the sciatic nerve respond to denervation or loss of axonal contact by upregulating their expression of GDNF but not the other family members, NTN, PSP, and ART. Moreover, they are unable to maintain the GDNF upregulation as the duration of denervation is prolonged.

The mRNA levels of the receptors for the GDNF family of growth factors, GFRα-1 and GFRα-2, showed a relative delayed upregulation after denervation (Fig. 4). These two receptors have the ability to bind to GDNF and signal through the RET tyrosine kinase (1). In contrast there were no significant changes in the mRNA levels of GFRα-3, which does not bind to GDNF (data not shown). RET mRNA levels were not upregulated throughout the course of the study (Fig. 4).

Effects of Delayed Regeneration

In order to test the hypothesis that prolonged denervation results in irreversible changes in Schwann cells that hamper delayed regenerative efforts, we used a delayed coaptation model of sciatic nerve injury (13). We chose an early time point (1 month) when regeneration is still robust with delayed coaptation (42, 56) and a late time point (6 months) when regeneration is impaired in order to examine the changes in gene expression. Freshly cut peroneal nerve stumps were sutured to previously denervated tibial nerve stumps and the nerve distal to the suture site was collected after 11 days when we expected to see a large upregulation of GDNF expression, associated with regeneration of peroneal axons into the stump. The GDNF mRNA levels of the distal nerve 11 days after early coaptation (i.e., cross-suture of the proximal nerve stump of the peroneal nerve to the distal stump of the 1-month-denervated tibial nerve) were similar to the GDNF upregulation after the initial denervation (Fig. 5). The presence of regenerating axons did not induce any further increase in GDNF mRNA expression at 11 days after coaptation. In contrast, the GDNF mRNA levels 11 days after late coaptation (i.e., a peroneal–tibial nerve cross-suture 6 months after chronic denervation of the tibial nerve) were very low and similar to the levels seen in chronically denervated sciatic nerves (Fig. 5). Similar results were obtained when the tissue collection was done 21 days after coaptation (data not shown). This showed that the Schwann cells of the distal tibial nerve that were denervated for a prolonged period of time were unable to upregulate GDNF mRNA levels when they were challenged with the regenerating axons of the freshly transected peroneal nerve.

DISCUSSION

The factors responsible for impaired regeneration in the peripheral nervous system after prolonged denervation are unknown. In this study we showed that changes in the Schwann cell expression of GDNF correlate well with the impaired outcome of motor nerve regeneration that has been demonstrated in our prior studies (13, 42). There was an initial upregulation of

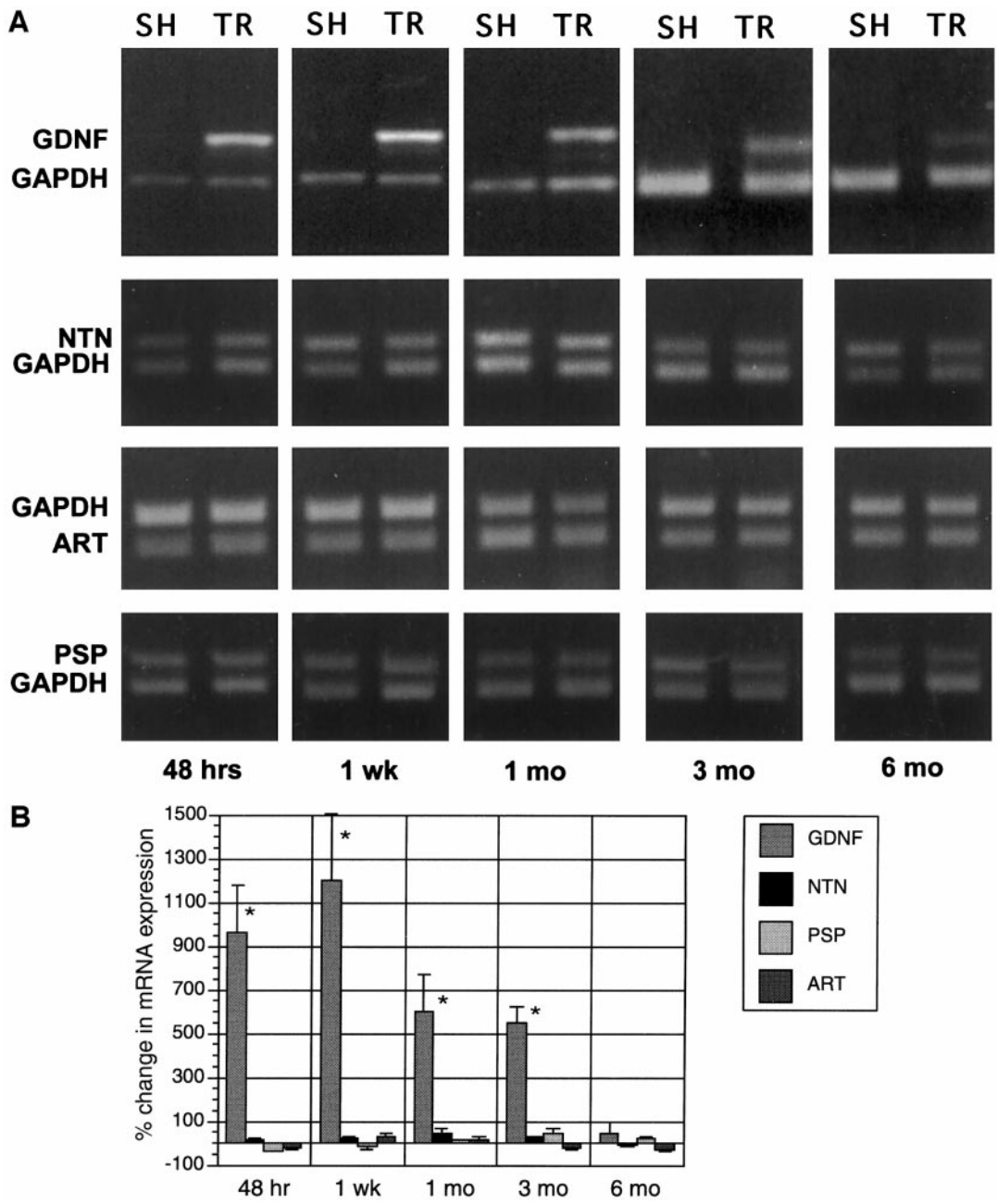


FIG. 1. Changes in the GDNF, NTN, PSP, and ART mRNA levels in denervated sciatic nerve as measured by semiquantitative multiplex PCR using GAPDH as an internal control. (A) At all time points the level of GDNF mRNA is almost undetectable in the sham-operated animals. In transected sciatic nerves the GDNF mRNA is upregulated as early as 48 h and it returns to baseline levels by 6 months. In contrast, there are no significant changes in the levels of expression of NTN, PSP, and ART as measured by semiquantitative multiplex RT-PCR. (SH, sham-operated control side; TR, transected sciatic nerve). (B) GDNF, NTN, PSP, and ART mRNA levels expressed as the percentage change in transected versus sham-operated nerves. The GDNF mRNA levels are upregulated rapidly but decline as the duration of denervation is increased. There is no significant change in the expression of NTN, PSP, and ART. (Means are the average of three samples done in triplicate and error bars are SEM; *statistically significant at $P < 0.005$.)

GDNF mRNA and protein in the regenerative milieu of the denervated distal nerve stump but this was not sustained as the duration of denervation was increased. In addition, the long-term chronically denervated Schwann cells had lost their ability to upregulate GDNF in response to freshly transected axons in the delayed coaptation paradigm.

We believe that these changes in GDNF expression may have an important impact on the success of motor nerve regeneration. GDNF is the most potent neuro-

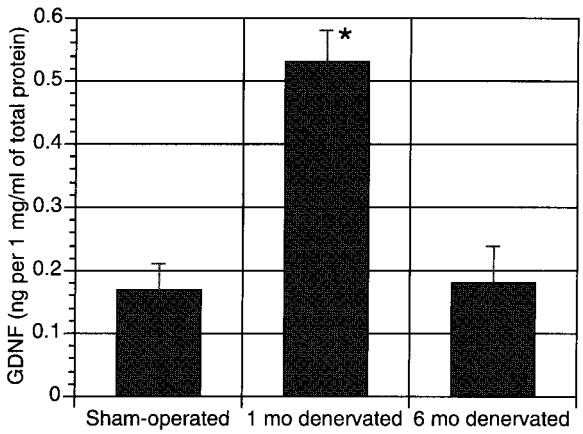


FIG. 2. GDNF content in the denervated and sham-operated nerves by ELISA. GDNF content of a sham-operated sciatic nerve was 0.17 ng per 1 mg/ml of total protein. At 1 month, the GDNF protein content in the denervated sciatic nerve was upregulated by almost threefold to 0.53 ng per 1 mg/ml of total protein. However, by 6 months the levels in the denervated sciatic nerve were back to baseline at 0.18 ng per 1 mg/ml of total protein. (Means are the average of three samples done in duplicate and error bars are SEM; *statistically significant at $P < 0.005$.)

trophic factor for motor neurons and rescues motor neurons from death in many different paradigms (22, 27, 33, 34, 48, 55, 57). Spinal motor neurons also express GDNF receptors RET and GFRα-1 and upregulate them after axotomy (32). In addition to these changes in the spinal motor neurons with injury, there are changes in the expression of GDNF and its receptors in the Schwann cells of a denervated nerve. Similar to our findings, GDNF and one of its receptors, GFRα-1, is upregulated in the distal segment of a transected mouse sciatic nerve (32). The long-term course of these changes was not investigated in that study. It is postulated that following axotomy, the GFRα-1 and GDNF are secreted and taken up by the regenerating axons that express the coreceptor, RET tyrosine kinase. The trimolecular complex of GDNF and its receptors is likely required for the biological action of GDNF (1). Although there are reports of RET-independent signaling pathways for GDNF action through the GFRα-1 alone (37, 49), the significance of RET-independent signaling pathways in denervated Schwann cells is unknown. In our chronic denervation model we observed delayed upregulation of GFRα-1 and to a lesser extent GFRα-2. It is possible that there may be an autocrine action of GDNF on the Schwann cells as seen in a spontaneously immortalized Schwann cell line *in vitro* (51). When the expression of GDNF decreases with prolonged denervation, the Schwann cells may upregulate their expression of the receptors that may be important for the autocrine action.

The Schwann cells of the nerve stump distal to the site of injury are essential for successful axonal regeneration and reinnervation of denervated target (18, 19). Immediately after nerve injury, Schwann cells enter a proliferative phase and undergo changes in gene expression that reflect their phenotypic changes (17). Regeneration-associated molecules like p75NTR, neuregulins and their receptors c-erbB2, c-erbB3, and c-erbB4, glial fibrillary acidic protein, neural-cell adhesion molecule, and growth-associated protein (GAP-43) are upregulated in Schwann cells soon after

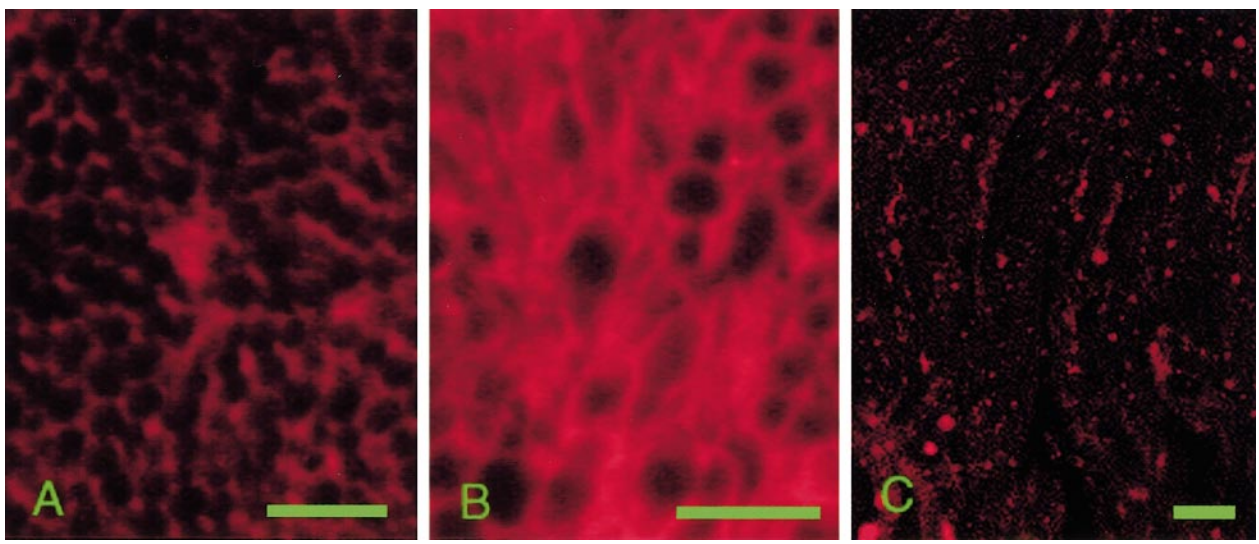


FIG. 3. Immunohistochemistry for GDNF in cross section of sham-operated and transected sciatic nerves. (A) In sham-operated sciatic nerves there is minimal GDNF immunoreactivity in structures that surround axonal profiles (presumably these areas correspond to Schwann cell cytoplasm). (B) In the distal segment of a sciatic nerve 1 week after transection there is more abundant GDNF immunoreactivity (notice the degenerating axon profiles as areas lacking GDNF immunoreactivity). (C) After 6 months of denervation there is minimal background staining for GDNF. The scale bars correspond to 50 μm.

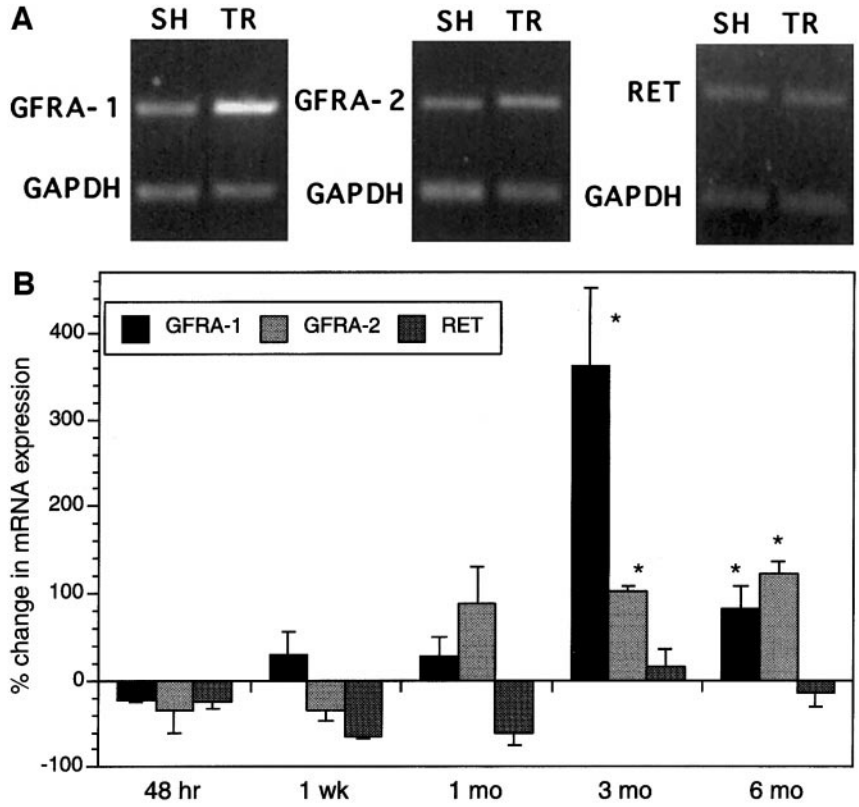


FIG. 4. Changes in the GFRα-1, GFRα-2, and RET mRNA levels with chronic denervation. (A) At 3 months of denervation, GFRα-1 and GFRα-2 levels are upregulated in the distal segment of the sciatic nerve but there is no upregulation in RET mRNA as measured by semiquantitative multiplex PCR using GAPDH as an internal control (SH, sham-operated control side; TR, transected sciatic nerve). (B) Measurement of GFRα-1, GFRα-2, and RET mRNA levels expressed as the percentage change in transected versus sham-operated nerves shows a delayed upregulation that is most significant for GFRα-1. (Means are the average of three samples done in triplicate and error bars are SEM; *statistically significant at $P < 0.005$.)

denervation (4, 6, 9, 20, 26, 36, 40, 41, 56). The distal nerve stump assumes the role of a "temporary target" for neurons by upregulating the expression of neurotrophins that are normally target-derived ((15, 29, 32, 38, 52) reviewed in (11)).

The trophic environment created by the Schwann cells of the distal nerve stump is not, however, sustained indefinitely as the upregulated regeneration-associated molecules, p75 and c-erbB receptors, are downregulated with chronic denervation (14, 26, 56). In the present study, we demonstrate the rapid upregulation of GDNF after nerve injury and its subsequent progressive downregulation as Schwann cells remained denervated for a prolonged period of time. Chronically denervated Schwann cells were unable to upregulate the expression of GDNF even when they were challenged with freshly transected axons which were presumably in an optimum intrinsic growth state. Our studies indicate that a known potent neurotrophic factor may be unavailable for growing axons at levels that will sustain their regeneration through chronically denervated nerve segments. This is yet another indication that chronically denervated Schwann cells lose their ability to supply regeneration-related molecules.

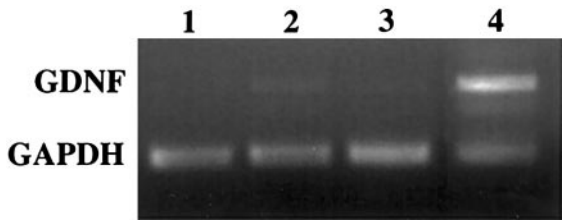


FIG. 5. Changes in the GDNF mRNA levels in the denervated tibial nerve with early and delayed coaptation. In sham-operated control sciatic nerve (lane 1) and in 6 month-denervated nerve with no coaptation (lane 2) there is minimal GDNF expression. There is no upregulation of GDNF expression at 11 days of delayed coaptation after 6 months of denervation (lane 3) but the GDNF is upregulated at 11 days of early coaptation following only 1 month of denervation (lane 4).

In contrast to GDNF, we did not observe significant changes in the expression levels of other members of this family of growth factors. Similar to GDNF, Neurturin, Artemin, and Persephin can support the survival of many neuronal types including motor neurons, do-

paminergic neurons, sensory neurons, and autonomic ganglion neurons (2, 24, 30). However, their main roles in development and regeneration may differ from their *in vitro* activity. Neurturin is important in the development of the parasympathetic (25, 39) and sympathetic nervous systems (10). Since autonomic nerves of the vasa nervorum comprise only a small portion of fibers in the sciatic nerve, we may not have the sensitivity to detect a change in only a small fraction of denervated Schwann cells.

Our findings of downregulation of GDNF in chronically denervated distal nerves may have implications for peripheral nerve regeneration after trauma in humans. In contrast to open trauma with nerve injury, nerve repair is not done immediately following closed trauma, and a conservative nonsurgical approach is taken (7). Closed injuries may not be associated with physical separation of the nerve trunk and surgical exploration is initiated only after a delay, if recovery has not ensued. Unfortunately, this approach may be counterproductive, as the denervated distal stump is not suited to support regeneration. Future animal studies are warranted to determine whether administration of GDNF will improve motor nerve regeneration after prolonged periods of denervation, as has been demonstrated after chronic axotomy (unpublished observations). Since systemic administration of GDNF may have unwanted gastrointestinal side effects, modes of local delivery will need to be developed. In initial animal studies these may include the use of miniosmotic pumps filled with GDNF or transplantation of stem cells or engineered cells that secrete large quantities of GDNF.

One possible caveat of our findings is the fact that the nerves used in our study are mixed nerves with motor and sensory axons. It is possible that these observations may be more relevant to only one subpopulation of axons and not the other. However, subpopulations of both motor neurons and sensory neurons do express the appropriate receptors and do respond to the neurotrophic effects of GDNF. Planned future experiments in which we will be delivering exogenous GDNF to chronically denervated nerves with delayed coaptation will help answer this question of whether GDNF is able to improve regeneration of one or both populations of motor and sensory axons. GDNF is probably one of the many factors that may play an important role in the successful regeneration of the injured axons. Additionally, more studies will be needed to dissect out how these different and often interrelated factors could be manipulated to arrive at a successful regeneration.

ACKNOWLEDGMENTS

This work was supported by a grant from the Alberta Heritage Foundation of Medical Research (AHFMR), Canadian Institute of Health Research (formerly Medical Research Council of Canada), and Spinal Cord Foundation (USA). A. Hoke was an AHFMR Clinical Research Fellow. O. A. R. Sulaiman is supported by a fellowship from the Medical Research Council of Canada/Canadian Neurotrauma Partnership Fellowship and by an incentive award and a research allowance from the AHFMR. This article partially fulfills the requirement for the Ph.D. thesis of O.A.R.S. T. Gordon and D. W. Zochodne were supported by AHFMR as a Senior Scientist and Senior Scholar, respectively.

REFERENCES

1. Airaksinen, M. S., A. Titievsky, and M. Saarma. 1999. GDNF family neurotrophic factor signaling: Four masters, one servant? *Mol. Cell. Neurosci.* **13:** 313–325.
2. Baloh, R. H., M. G. Tansey, P. A. Lampe, T. J. Fahrner, H. Enomoto, K. S. Simburger, M. L. Leitner, T. Araki, E. M. Johnson, Jr., and J. Milbrandt. 1998. Artemin, a novel member of the GDNF ligand family, supports peripheral and central neurons and signals through the GFRalpha3-RET receptor complex. *Neuron* **21:** 1291–1302.
3. Buj-Bello, A., V. L. Buchman, A. Horton, A. Rosenthal, and A. M. Davies. 1995. GDNF is an age-specific survival factor for sensory and autonomic neurons. *Neuron* **15:** 821–828.
4. Bunge, R. P. 1987. Tissue culture observations relevant to the study of axon–Schwann cell interactions during peripheral nerve development and repair. *J. Exp. Biol.* **132:** 21–34.
5. Canning, D. R., A. Hoke, C. J. Malemud, and J. Silver. 1996. A potent inhibitor of neurite outgrowth that predominates in the extracellular matrix of reactive astrocytes. *Int. J. Dev. Neurosci.* **14:** 153–175.
6. Carroll, S. L., M. L. Miller, P. W. Frohnert, S. S. Kim, and J. A. Corbett. 1997. Expression of neuregulins and their putative receptors, ErbB2 and ErbB3, is induced during Wallerian degeneration. *J. Neurosci.* **17:** 1642–1659.
7. Chaudhry, V., and A. J. Belzberg. 1997. Peripheral nerve injury. In *Current Therapy in Neurologic Disease* (R. T. Johnson and J. W. Griffin, Eds.), pp. 230–238. Mosby, St. Louis.
8. Chomczynski, P., and N. Sacchi. 1987. Single-step method of RNA isolation by acid guanidinium thiocyanate–phenol–chloroform extraction. *Anal. Biochem.* **162:** 156–159.
9. Daniloff, J. K., G. Levi, M. Grumet, F. Rieger, and G. M. Edelman. 1986. Altered expression of neuronal cell adhesion molecules induced by nerve injury and repair. *J. Cell Biol.* **103:** 929–945.
10. Forgie, A., E. Doxakis, A. Buj-Bello, S. Wyatt, and A. M. Davies. 1999. Differences and developmental changes in the responsiveness of PNS neurons to GDNF and neurturin. *Mol. Cell. Neurosci.* **13:** 430–440.
11. Frostick, S. P., Q. Yin, and G. J. Kemp. 1998. Schwann cells, neurotrophic factors, and peripheral nerve regeneration. *Microsurgery* **18:** 397–405.
12. Fu, S. Y., and T. Gordon. 1995. Contributing factors to poor functional recovery after delayed nerve repair: Prolonged axotomy. *J. Neurosci.* **15:** 3876–3885.
13. Fu, S. Y., and T. Gordon. 1995. Contributing factors to poor functional recovery after delayed nerve repair: Prolonged denervation. *J. Neurosci.* **15:** 3886–3895.
14. Fu, S. Y., and T. Gordon. 1997. The cellular and molecular basis of peripheral nerve regeneration. *Mol. Neurobiol.* **14:** 67–116.
15. Funakoshi, H., J. Frisen, G. Barbany, T. Timmusk, O. Zachrisson, and V. M. Verge. and H. Persson. 1993. Differential expression of mRNAs for neurotrophins and their receptors after axotomy of the sciatic nerve. *J. Cell Biol.* **123:** 455–465.

16. Giannini, C., and P. J. Dyck. 1990. The fate of Schwann cell basement membranes in permanently transected nerves. *J. Neuropathol. Exp. Neurol.* **49:** 550–563.
17. Griffin, J. W., and P. N. Hoffman. 1993. Degeneration and regeneration in the peripheral nervous system. In *Peripheral Neuropathy* (P. J. Dyck, *et al.*, Eds.), pp. 361–376. Saunders, Philadelphia.
18. Hall, S. M. 1986. The effect of inhibiting Schwann cell mitosis on the re-innervation of acellular autografts in the peripheral nervous system of the mouse. *Neuropathol. Appl. Neurobiol.* **12:** 401–414.
19. Hall, S. M. 1986. Regeneration in cellular and acellular autografts in the peripheral nervous system. *Neuropathol. Appl. Neurobiol.* **12:** 27–46.
20. Hall, S. M., A. P. Kent, R. Curtis, and D. Robertson. 1992. Electron microscopic immunocytochemistry of GAP-43 within proximal and chronically denervated distal stumps of transected peripheral nerve. *J. Neurocytol.* **21:** 820–831.
21. Hammarberg, H., F. Piehl, S. Cullheim, J. Fjell, T. Hokfelt, and K. Fried. 1996. GDNF mRNA in Schwann cells and DRG satellite cells after chronic sciatic nerve injury. *NeuroReport* **7:** 857–860.
22. Henderson, C. E., H. S. Phillips, R. A. Pollock, A. M. Davies, C. Lemeulle, M. Armanini, L. Simmons, B. Moffet, R. A. Vandlen, L. C. Simpson, *et al.* 1994. GDNF: A potent survival factor for motoneurons present in peripheral nerve and muscle [See comments] [Published erratum appears in *Science* 1995, Feb 10; **267**(5199):777]. *Science* **266:** 1062–1064.
23. Hoke, A., C. Cheng, and D. W. Zochodne. 2000. Expression of glial cell line-derived neurotrophic factor family of growth factors in peripheral nerve injury in rats. *NeuroReport* **11:** 1651–1654.
24. Kotzbauer, P. T., P. A. Lampe, R. O. Heuckeroth, J. P. Golden, D. J. Creedon, E. M. Johnson, Jr., and J. Milbrandt. 1996. Neurturin, a relative of glial-cell-line-derived neurotrophic factor. *Nature* **384:** 467–470.
25. Laurikainen, A., J. O. Hiltunen, J. Thomas-Crusells, S. Vanhatalo, U. Arumae, M. S. Airaksinen, E. Klinge, and M. Saarma. 2000. Neurturin is a neurotrophic factor for penile parasympathetic neurons in adult rat. *J. Neurobiol.* **43:** 198–205.
26. Li, H., G. Terenghi, and S. M. Hall. 1997. Effects of delayed re-innervation on the expression of c-erbB receptors by chronically denervated rat Schwann cells in vivo. *Glia* **20:** 333–347.
27. Li, L., W. Wu, L. F. Lin, M. Lei, R. W. Oppenheim, and L. J. Houenou. 1995. Rescue of adult mouse motoneurons from injury-induced cell death by glial cell line-derived neurotrophic factor. *Proc. Natl. Acad. Sci. USA* **92:** 9771–9775.
28. Lin, L. F., D. H. Doherty, J. D. Lile, S. Bektesh, and F. Collins. 1993. GDNF: A glial cell line-derived neurotrophic factor for midbrain dopaminergic neurons [See comments]. *Science* **260:** 1130–1132.
29. Meyer, M., I. Matsuoka, C. Wetmore, L. Olson, and H. Thoenen. 1992. Enhanced synthesis of brain-derived neurotrophic factor in the lesioned peripheral nerve: Different mechanisms are responsible for the regulation of BDNF and NGF mRNA. *J. Cell Biol.* **119:** 45–54.
30. Milbrandt, J., F. J. De Sauvage, T. J. Fahrner, R. H. Baloh, M. L. Leitner, M. G. Tansey, P. A. Lampe, R. O. Heuckeroth, P. T. Kotzbauer, K. S. Simburger, J. P. Golden, J. A. Davies, R. Vejsada, A. C. Kato, M. Hynes, D. Sherman, M. Nishimura, L. C. Wang, R. Vandlen, B. Moffat, R. D. Klein, K. Poulsen, C. Gray, A. Garces, E. M. Johnson, Jr., *et al.* 1998. Persephin, a novel neurotrophic factor related to GDNF and neurturin. *Neuron* **20:** 245–253.
31. Molliver, D. C., D. E. Wright, M. L. Leitner, A. S. Parsadanian, K. Doster, D. Wen, Q. Yan, and W. D. Snider. 1997. IB4-binding DRG neurons switch from NGF to GDNF dependence in early postnatal life. *Neuron* **19:** 849–861.
32. Naveilhan, P., W. M. ElShamy, and P. Ernfors. 1997. Differential regulation of mRNAs for GDNF and its receptors Ret and GDNFR alpha after sciatic nerve lesion in the mouse. *Eur. J. Neurosci.* **9:** 1450–1460.
33. Oppenheim, R. W., L. J. Houenou, J. E. Johnson, L. F. Lin, L. Li, A. C. Lo, A. L. Newsome, D. M. Prevette, and S. Wang. 1995. Developing motor neurons rescued from programmed and axotomy-induced cell death by GDNF [See comments]. *Nature* **373:** 344–346.
34. Oppenheim, R. W., L. J. Houenou, A. S. Parsadanian, D. Prevette, W. D. Snider, and L. Shen. 2000. Glial cell line-derived neurotrophic factor and developing mammalian motoneurons: Regulation of programmed cell death among motoneuron subtypes. *J. Neurosci.* **20:** 5001–5011.
35. Pellegrino, R. G., and P. S. Spencer. 1985. Schwann cell mitosis in response to regenerating peripheral axons in vivo. *Brain Res.* **341:** 16–25.
36. Plantinga, L. C., J. Verhaagen, P. M. Edwards, E. M. Hol, P. R. Bar, and W. H. Gispen. 1993. The expression of B-50/GAP-43 in Schwann cells is upregulated in degenerating peripheral nerve stumps following nerve injury. *Brain Res.* **602:** 69–76.
37. Poteryaev, D., A. Titievsky, Y. F. Sun, J. Thomas-Crusells, M. Lindahl, M. Billaud, U. Arumae, and M. Saarma. 1999. GDNF triggers a novel ret-independent Src kinase family-coupled signaling via a GPI-linked GDNF receptor alpha1. *FEBS Lett.* **463:** 63–66.
38. Raivich, G., and G. W. Kreutzberg. 1987. Expression of growth factor receptors in injured nervous tissue. I. Axotomy leads to a shift in the cellular distribution of specific beta-nerve growth factor binding in the injured and regenerating PNS. *J. Neurocytol.* **16:** 689–700.
39. Rossi, J., K. Luukko, D. Poteryaev, A. Laurikainen, Y. F. Sun, T. Laakso, S. Eerikainen, R. Tuominen, M. Lakso, H. Rauvala, U. Arumae, M. Pasternack, M. Saarma, and M. S. Airaksinen. 1999. Retarded growth and deficits in the enteric and parasympathetic nervous system in mice lacking GFR alpha2, a functional neurturin receptor. *Neuron* **22:** 243–252.
40. Schachner, M., I. Sommer, and C. Lagenaur. 1984. Expression of glial antigens C1 and M1 in the peripheral nervous system during development and regeneration. *Brain Res.* **316:** 165–178.
41. Scherer, S. S., Y. T. Xu, D. Roling, L. Wrabetz, M. L. Feltri, and J. Kamholz. 1994. Expression of growth-associated protein-43 kD in Schwann cells is regulated by axon–Schwann cell interactions and cAMP. *J. Neurosci. Res.* **38:** 575–589.
42. Sulaiman, O. A., and T. Gordon. 2000. Effects of short- and long-term Schwann cell denervation on peripheral nerve regeneration, myelination, and size. *Glia* **32:** 234–246.
43. Sunderland, S. 1952. Factors influencing the course of regeneration and quality of recovery after nerve suture. *Brain* **75:** 19–54.
44. Sunderland, S. 1978. *Nerves and Nerve Injuries*. Livingstone, Edinburgh.
45. Sunderland, S., and K. C. Bradley. 1950. Denervation atrophy of the distal stump of a severed nerve. *J. Comp. Neurol.* **93:** 401–409.
46. Sunderland, S., and K. C. Bradley. 1950. Endoneurial tube shrinkage in the distal segment of a severed nerve. *J. Comp. Neurol.* **93:** 411–420.
47. Terenghi, G., J. S. Calder, R. Birch, and S. M. Hall. 1998. A morphological study of Schwann cells and axonal regeneration

in chronically transected human peripheral nerves. *J. Hand Surg.* **23:** 583–587.

48. Trupp, M., M. Ryden, H. Jornvall, H. Funakoshi, T. Timmusk, E. Arenas, and C. F. Ibanez. 1995. Peripheral expression and biological activities of GDNF, a new neurotrophic factor for avian and mammalian peripheral neurons. *J. Cell Biol.* **130:** 137–148.
49. Trupp, M., R. Scott, S. R. Whittemore, and C. F. Ibanez. 1999. Ret-dependent and -independent mechanisms of glial cell line-derived neurotrophic factor signaling in neuronal cells. *J. Biol. Chem.* **274:** 20885–20894.
50. Vuorinen, V., J. Shronen, and M. Roytta. 1995. Axonal regeneration into chronically denervated distal stump. 1. Electron microscope studies. *Acta Neuropathol.* **89:** 209–218.
51. Watabe, K., T. Fukuda, J. Tanaka, H. Honda, K. Toyohara, and O. Sakai. 1995. Spontaneously immortalized adult mouse Schwann cells secrete autocrine and paracrine growth-promoting activities. *J. Neurosci. Res.* **41:** 279–290.
52. Windebank, A. J., and J. F. Poduslo. 1986. Neuronal growth factors produced by adult peripheral nerve after injury. *Brain Res.* **385:** 197–200.
53. Wong, H., W. D. Anderson, T. Cheng, and K. T. Riabowol. 1994. Monitoring mRNA expression by polymerase chain reaction: The "primer-dropping" method. *Anal. Biochem.* **223:** 251–258.
54. Woodhall, B., and G. W. Beebe. 1956. *Peripheral Nerve Regeneration: A Follow-Up Study of 3,656 World War II Injuries.* U.S. Government Printing Office, Washington, DC.
55. Yan, Q., C. Matheson, and O. T. Lopez. 1995. In vivo neurotrophic effects of GDNF on neonatal and adult facial motor neurons [See comments]. *Nature* **373:** 341–344.
56. You, S., T. Petrov, P. H. Chung, and T. Gordon. 1997. The expression of the low affinity nerve growth factor receptor in long-term denervated Schwann cells. *Glia* **20:** 87–100.
57. Zurn, A. D., E. E. Baetge, J. P. Hammang, S. A. Tan, and P. Aebischer. 1994. Glial cell line-derived neurotrophic factor (GDNF), a new neurotrophic factor for motoneurones. *NeuroReport* **6:** 113–118.

GLIA 20:87–100 (1997)

The Expression of the Low Affinity Nerve Growth Factor Receptor in Long-Term Denervated Schwann Cells

SIJUN YOU, THEODOR PETROV, PHILIP H. CHUNG, AND TESSA GORDON*
Department of Pharmacology and Division of Neuroscience, University of Alberta, Edmonton, Alberta, Canada T6G 2S2

KEY WORDS p75 mRNA; S100 protein; regeneration; immunocytochemistry; in situ hybridization; ultrastructure

ABSTRACT Schwann cells in the distal stump of injured peripheral nerves synthesize the low affinity nerve growth factor receptor (p75). In this study we used short-term (1 week) and long-term (1–12 months) transected distal sciatic nerves of rats to determine the variations of p75 expression by using immunocytochemistry and in situ hybridization.

Semi-quantitative analysis revealed that the synthesis of the protein product of the p75 gene is rapidly enhanced to reach a peak within the 1 month after denervation. After that it gradually decreased and was barely detectable 6 months following denervation. Double immunocytochemistry for p75 and the S100 protein revealed that p75 immunoreactivity is confined to the Schwann cells. Quantitative analysis of our in situ hybridization experiments revealed that the upregulation of the p75 mRNA parallels the enhanced synthesis of the corresponding protein and reaches a peak within 1 month, which is maintained until the second month after the transection and declines thereafter to reach background levels at 4 months. The electron microscopic observations reveal that the increase in the number of nuclei in the distal stump belong to severely atrophied Schwann cells and fibroblasts.

Since the presence of p75 in the Schwann cells is necessary for reinnervation, our results indicate that, based on the expression of p75, the Schwann cells will provide a most suitable environment for the regenerating axons up to the first month. At later stages the ability of the Schwann cells to synthesize p75 and cell adhesion proteins such as N-CAM and GAP 43 decreases which may be one of the factors that contribute to poor functional recovery if the regenerating axons reach the distal stump after long periods of time. *GLIA 20:87–100, 1997.* © 1997 Wiley-Liss, Inc.



Experimental Neurology 254 (2014) 99–108

Contents lists available at ScienceDirect

Experimental Neurology

journal homepage: www.elsevier.com/locate/yexnr

Commentary

Neurotrophic factor expression in denervated motor and sensory Schwann cells: Relevance to specificity of peripheral nerve regeneration

Tessa Gordon*

Department of Surgery, Division of Plastic Reconstructive Surgery 5549A, The Hospital for Sick Children, 555 University Ave, Toronto, ON M5G 1X8, Canada

ARTICLE INFO

Article history:
Received 5 November 2013
Revised 9 January 2014
Accepted 11 January 2014
Available online 24 January 2014

Following peripheral nerve injury, the cell body of the injured neurons undergoes morphological and molecular changes referred to as the cell body response (Grafstein, 1975), the axon reaction (Lieberman, 1971) and/or the cell body reaction (Titmus and Faber, 1990). The neuron is referred to as axotomized after disruption of the axon and before the regenerating axon remakes functional connections with denervated target organs (Fu and Gordon, 1997). The cell body response includes the upregulation of regeneration associated genes (RAGs) such as the cytoskeletal proteins tubulin and actin, and the downregulation of genes that transcribe the proteins responsible for the normal functioning of the adult neuron such as choline acetyltransferase, the rate limiting synthetic enzyme in the synthesis of acetylcholine in motoneurons (Fu and Gordon, 1997; Zigmond, 2012). The altered gene expression in motor, sensory and sympathetic neurons may be regarded as a switch from the state of chemical transmission to that of nerve growth and regeneration (Gordon, 1983; Grafstein and McQuarrie, 1978; Zigmond, 2012). The changes have also been referred to as dedifferentiation to the less mature form of the developing neuron that has the capacity for axon growth and formation of functional contacts with targets (Gordon, 1983).

The axons that are disconnected from the neuronal cell body after nerve injury undergo progressive fragmentation with separation and disintegration of their myelin sheath (Coleman, 2005; Fu and Gordon, 1997; Gaudet et al., 2011; Lubinska, 1977; Zigmond, 2012). The denervated Schwann cells (SCs) that normally form the myelin sheaths of the myelinated large axons or surround clusters of unmyelinated smaller nerves, also undergo fundamental changes in gene expression. These too may be regarded as preliminary to their dedifferentiation to a less mature SC that supports axon outgrowth, regeneration and target reinnervation (Arthur-Farraj et al., 2012; Jessen and Mirsky, 2005, 2008). The regeneration associated genes that are expressed by denervated SCs of peripheral nerves include the upregulation of several neurotrophic factors (Boyd and Gordon, 2003; Fu and Gordon, 1997). The apparent selective upregulation of different neurotrophic factors in adult denervated SCs in motor and sensory nerve pathways is the subject of a seminal paper published in 2006 (Hoke et al., 2006) and a more recent paper by the same authors that elaborates on the first (Brushart et al., 2013). In these two studies the investigators used several surgical paradigms to isolate the SCs that previously provided myelin to motor or sensory axons. The studies describe differences in expression of eleven neurotrophic factors in denervated SCs from adult nerves where they formerly myelinated either motor or sensory axons. The underlying assumption was that these factors may play a role in the preferential reinnervation of motor and sensory pathways by motor and sensory axons, respectively (Al-Majed et al., 2000a; Brushart, 1988, 1993; Brushart et al., 2002, 2005, 2013; Franz et al., 2008; Geremia et al., 2007; Hoke et al., 2006; Mears et al., 2003).

Before providing a commentary specific to these studies, a brief review is given of 1) the glial cells of the nervous system, 2) the developmental lineage of SCs and 3) the conversion of SC phenotype back to that of the immature SC after nerve injury. This review is provided as the context in which to consider the reported differences and the time course of expression of neurotrophic factors in denervated SCs of motor and sensory nerve pathways. Of particular interest is whether these differences in neurotrophic factor expression provide insight into the process of axon regeneration and specifically, the selective reinnervation of appropriate distal nerve pathways by regenerating axons of motoneurons and dorsal root ganglion (DRG) sensory neurons (Al-Majed et al., 2000a; Brushart, 1988, 1993; Brushart et al., 2002, 2013).

Glial cells of the nervous system

Glial cells are essential components of the central and peripheral nervous systems. They include the astrocytes and oligodendrocytes of the central nervous system (CNS) and the myelinating Schwann cells and the non-myelinating Remak SCs of the peripheral nervous system (PNS). Schwann cells comprise ~48% of the endoneurial cell population, a substantial portion of the remaining cells being the fibroblasts of the connective tissue matrices (Schubert and Friede, 1981). Each SC forms a myelin sheath around an axon of >1μm diameter and each Remak cell surrounds several unmyelinated axons that are each <1μm in diameter (Griffin and Thompson, 2008; Salzer, 2012). The myelin insulates the axons at the internodes between the ~1μm nodes of Ranvier where sodium channels propagate action potentials from one node to another; delayed rectifier potassium channels at the juxtaparanodes are thought to be responsible for the repolarization event that equilibrates the membrane potential after it has been depolarized

* Fax: +1 416 813 6637.
E-mail address: tessa.gordon@gmail.com.

0014-4886/$ – see front matter © 2014 Elsevier Inc. All rights reserved.
http://dx.doi.org/10.1016/j.expneurol.2014.01.012

(Buttermore et al., 2013; Salzer et al., 2008; Thaxton and Bhat, 2009; Zhang et al., 2012). The juxtaparanodes are the transition between the paranodes where internodal myelin sheath edges are anchored to the axons, and the nodes of Ranvier. Saltatory conduction of action potentials from one node to the next accelerates their axonal propagation several fold: conduction velocity of myelinated axons is proportional to the diameter of the axons (Huxley and Stampfli, 1949) whilst the slower conduction velocity of the unmyelinated axons varies with the square root of the axon diameter (Waxman and Bennett, 1972). Immature SCs are likely to have an equivalent developmental potential but their fate is determined by which axons the cells randomly associate with during development. Those immature SCs that associate with single large-diameter (~1 μm) axons will follow the myelination program whilst those that associate with the smaller axons will not, the molecular basis being poorly understood at present (Jessen and Mirsky, 2005; Mirsky et al., 2008).

Oligodendrocytes of the CNS contrast with the SCs of the PNS in their mode of myelination of the axons and their inability to support axon regeneration. Oligodendrocytes are post-mitotic; remyelination occurs by endogenous proliferating progenitor cells (Almad et al., 2011; Blakemore and Keirstead, 1999). Each oligodendrocyte provides the myelin sheath to a number of axons: the number of axons myelinated by each cell varies from >30 and >10 for types I and II oligodendrocytes that supply small caliber axons and between ~5 and 1–2 for types III and IV (Berry et al., 1995; Hildebrand et al., 1993; Ibrahim et al., 1995). The length of the internodes between the myelin sheaths are longest for the type IV and shortest for those of type I and II oligodendrocytes. Unlike the SCs, the oligodendrocyte cell body does not encircle the axons with the myelin sheath but rather maintains contact with the sheath via thin cytoplasmic bridges (Bunge et al., 1962; Hirano et al., 1968). The failure of these glial cells to support axon regeneration relates to their synthesis of growth inhibitory molecules, Nogo-A, oligodendrocyte myelin glycoprotein (OMgp), and myelin associated protein (MAG) that are enriched in CNS myelin sheaths and that interact with the same receptor, NgR1, leading to growth cone collapse (Fenrich and Gordon, 2004).

The interdependence of Schwann cells and their axons during development

Bidirectional dialog between axons and SCs is fundamental to the formation of myelin during development, its maintenance during adult life, and remyelination of regenerating axons after injury. During embryonic development, the axonal signals are critical for SC migration, survival and proliferation to ensure that the number of SCs and the axons with which they are associated are matched (Jessen and Mirsky, 2005). SCs in turn, provide crucial trophic support for immature neurons and the development of their axon properties, especially through myelination. SCs originate from neural crest-derived SC precursors directed by the key regulator, the transmembrane type neuronal isoform III of neuregulin (NRG1) (Dong et al., 1995; Falls, 2003; Wang et al., 2001; Winseck and Oppenheim, 2006) as well as the Notch proteins (Woodhoo et al., 2009) (Fig. 1). The evidence for Notch signaling in SC development is incomplete in contrast to that for NRG1 on the membrane of motor and sensory neurons that binds to erbB2/3 receptors on glial cells (Birchmeier, 2009; Birchmeier and Nave, 2008; Taveggia et al., 2005). NRG1 plays a central role in the neuron-SC interdependence: the survival of SC precursors is dependent on NRG1 without which embryonic nerve trunks become essentially devoid of SC precursors unless they are rescued by NRG1 application (Garratt et al., 2000; Winseck and Oppenheim, 2006; Winseck et al., 2002). Survival of embryonic neurons is, in turn, dependent on their contact with the immature SCs, possibly through signaling via the intracellular domain of NRG1 (Britsch et al., 2001; Wolpowitz et al., 2000).

The emergence of several molecular markers allowed the rapid elucidation of the developmental stages of SCs and their axons. These markers include the transcription factor, Y (sex determining region Y) box 10 (SOX10), that is expressed by neurons and their axons during three irreversible stages of SC development from the migrating neural crest cells to the SC precursor cells, and to the immature SCs (Fig. 1). The number of developing SCs is controlled by the balance of the expression of SOX10 as the key factor driving the genesis of SCs from trunk neural crest cells, gliogenesis, and the expression of NRG-1 (Britsch et al., 2001; Jessen and Mirsky, 2005; Mirsky et al., 2008; Paratore et al., 2001). NRG-1 via the Erb2/3 receptors, inhibits neurogenesis (Shah et al., 1994). NRG-1 also mediates embryonic SC proliferation and survival, depending on the axon transmembrane isoform III of NRG1 for their paracrine support and survival during cell division and the survival of the axons with which the SCs are closely associated (Morrissey et al., 1995). The embryonic SCs from the neural crest cell stage of development through to the SC precursor and immature SC stages, express the cell adhesion molecule L1 and the p75 neurotrophic receptor ($p75^{NTR}$) (Fig. 1). The second stage SC precursor cells, like the neurons, express and rely on several neurotrophic factors. These include neurotrophin-3 (NT-3), fibroblast growth factor (FGF), insulin-like growth factor-1 (IGF-1), platelet-derived growth factor (PDGF), and endothelin that provide paracrine support for the second stage SC precursor cells and autocrine support of the third stage of immature SCs (Jessen and Mirsky, 2005, 2008). The basal lamina is elaborated around the immature SCs that each encircle several axons and the immature SCs express S100β, GFAP and the glycolipid antigen, 04, proteins that are either not expressed or expressed only at very low levels by SC precursors in the preceding stage of development before birth (Fig. 1). These proteins are commonly used to identify denervated SCs in the adult (Jessen and Mirsky, 2005, 2008). Myelin associated genes, including *protein 0* (P_0), *peripheral myelin protein 22* (*PMP 22*), *proteolipid protein* (*PLP*), *myelin associated glycoprotein* (*MAG*), and *galactocerobroside* (*GalC*), are expressed at low levels in the SC precursor cells and the immature SCs in the second and third stages of SC differentiation, prior to their differentiation into myelinating SCs (Fig. 1) and non-myelinating SCs (not shown). O4 and S100 are expressed in immature SCs and, because they are expressed in both the myelinating and non-myelinating SCs after the reversible postnatal transition, they are shown in a second box below the cells in Fig. 1.

The reversible stages of SC development occur after birth in rodents when immature SCs are organized in SC-axon families. In the process of radial axonal sorting, the SC precursor cells extend processes into axon bundles (Fig. 1), selecting and extracting large caliber axons of >1 μm diameter (in the mouse), to establish a one SC-to-one axon relationship at the pre-myelinating stage of the myelinated axons (Feltri et al., 2002; Jessen and Mirsky, 2005, 2008; Mirsky et al., 2008; Pereira et al., 2012). The small axons left behind remain engulfed by a SC but will not be myelinated and form the Remak bundles. The myelination process relies first, on SOX10 activating octomer-binding transcription factor-6 (Oct-6) and both transcription factors inducing Krox-20. Krox-20 in turn, promotes the exit of immature SCs from the cell cycle and their resistance to apoptosis as their transition to the mature myelinated SC stage proceeds (Fig. 1) (Crawford et al., 2008; Parkinson et al., 2003, 2004; Topilko et al., 1994). Secondly the myelination process relies on the activation of cAMP that, in turn, switches the NRG1 action on SCs from promoting their mitosis to promoting their myelination (Arthur-Farraj et al., 2011). Myelin genes including P_0, *MAG*, and *Gal-C*, are upregulated and the molecular markers of the immature SCs, including *c-Jun*, *growth associated protein-43* (*GAP-43*), *and* $p75^{NTR}$, are downregulated (Feltri et al., 2002; Jessen and Mirsky, 2005, 2008; Mirsky et al., 2008). Non-myelinating SCs retain their expression of $p75^{NTR}$, L1, GFAP, and GAP-43 (not shown).

Schwann cells after denervation and reinnervation: restoring the undifferentiated state and reversal by axon contact

Following a nerve injury that separates axons from the cell bodies of their motor and sensory neurons, the axons and their myelin sheaths

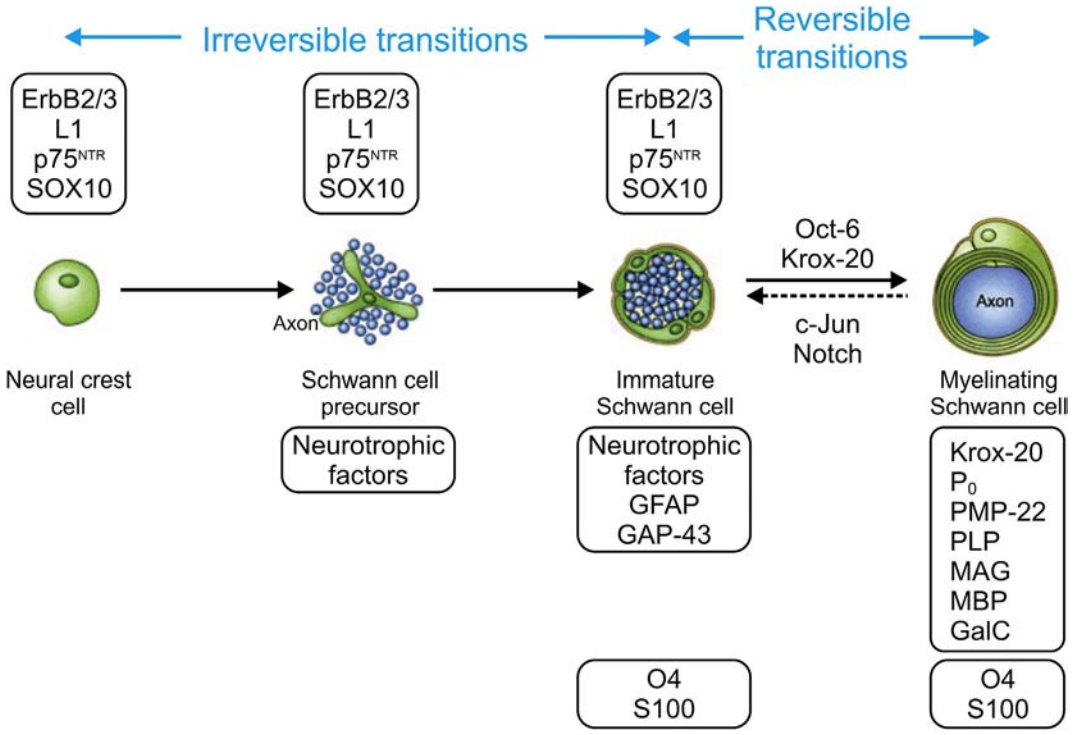


Fig. 1. Stages of Schwann cell development from neural crest cell through to the myelinated Schwann cell. The transcription factor SOX10, drives gliogenesis and expression of neuregulin-1 that in turn, binds to ErbB2/3 receptors on the neural crest cells, halting neurogenesis, and allowing differentiation into Schwann cell precursors and immature Schwann cells to proceed. As shown in the boxes above the neural crest and Schwann cells, the p75 neurotrophic factor, $p75^{NTF}$, the cell adhesion L1 molecule, neuregulin (not shown) and ErbB/3 receptors are expressed with SOX10 throughout the three irreversible stages of Schwann cell development during embryonic life. Neural crest cells that migrate through surrounding extracellular matrix, cease to proliferate before proceeding to the second and third stages of embryonic development (in rodents) where the Schwann cell precursor and the immature Schwann cells (green) lie in intimate contact with axons (blue). SC precursor cells depend on the axon transmembrane isoform III of neuregulin (NRG1) for their paracrine support and survival during cell division. As shown in the boxes below the cells and their associated axons, the Schwann cell precursor cells begin to synthesize neurotrophic factors before the transition to the immature Schwann cell takes place in the presence of a basal lamina. The immature Schwann cells begin to express neurotrophic factors and several markers that include GFAP and GAP-43. These markers are retained with $p75^{NTF}$ in the non-myelinating cells (not shown) as development proceeds reversibly after birth, to the mature state of myelinating and non-myelinating (not shown) Schwann cells. The immature Schwann cells begin to express lipid antigen,O4, and S100 that are shown in a separate box because these are retained in *both* myelinating and non-myelinating Schwann cells of the large and small (<1 um) axons, respectively, after their transition. The immature Schwann cells, driven by Krox-20 with cAMP, withdraw from the cell cycle, downregulate c-Jun and Notch transcription factors, and switch the NRG1 effect from cell division to myelination in their transition to the myelinating Schwann cell that upregulates myelin associated genes that transcribe proteins and glycoproteins as myelination proceeds. This step from the immature to the myelinating SC, unlike the preceding embryonic stages, is reversible after nerve injury and denervation of Schwann cells. The myelin sheath disintegrates and the upregulation of c-Jun and Notch allow the cells to re-enter the cell cycle and dedifferentiate toward the phenotype of the immature Schwann cell that supports axonal growth. (For interpretation of the references to color in this figure legend, the reader is referred to the web version of this article.)
Adapted from figures in reviews of Jessen and Mirsky (2005) and Mirsky et al. (2008).

disintegrate to leave SCs denervated in the distal nerve stump. The denervated SCs re-enter the cell cycle, inactivate myelin associated genes, and proceed to dedifferentiate under the control of upregulated c-Jun and Notch, to the SC phenotype of the immature SC beyond which the differentiation process does not proceed (Fig. 1) (De and Hunt, 1994; Parkinson et al., 2008; Shy et al., 1996). In the conditional c-jun knockout transgenic mouse, the processes of degradation of the myelin sheath, inactivation of the myelin associated genes, and the normal upregulation of the growth associated genes of the dedifferentiated SC precursor cell, are all delayed (Arthur-Farraj et al., 2012). The dedifferentiated denervated SCs transcribe cell-adhesion molecules, including L1, neural cell adhesion molecule (N-CAM), and n-cadherin, the $p75^{NTR}$ receptor for neurotrophins, and several neurotrophic factors. The factors include hepatocyte growth factor (HGF), brain derived neurotrophic factor (BDNF), vascular endothelial growth factor (VEGF), nerve growth factor (NGF), insulin-like growth factors 1 and 2 (IGF-1, IGF-2), glial derived neurotrophic factor (GDNF) and pleiotrophin (PTN) (Boyd and Gordon, 2003; Brushart et al., 2013; Hoke et al., 2006).

The dedifferentiation of the denervated SC is akin to the switch of axotomized neurons after nerve injury from the transmitting to a growth mode in conjunction with expression of c-Jun (Fu and Gordon, 1997; Herdegen et al., 1994; Jenkins and Hunt, 1991). The stereotypic cell body response of the axotomized neurons returns the neurons to an earlier dedifferentiated state with alterations that include loss of synaptic contacts and upregulation of several neurotrophic factors (Funakoshi et al., 1993; Gordon, 2009; Gordon et al., 2009; Lieberman, 1971; Verge et al., 1996). The extent of dedifferentiation of the neurons is not to an early embryonic form but rather to the state of an 'immature' neuron (Fu and Gordon, 1997; Grafstein and McQuarrie, 1978; Zigmond, 2011). This resembles the dedifferentiation of the mature SCs to the immature form and not beyond into earlier embryonic forms although denervated adult SCs have been seen to generate melanocytes, a property of SC precursors (Arthur-Farraj et al., 2012; Mirsky et al., 2008).

Denervated SCs lose the differentiated morphology of the mature SC. They adopt the form of elongated cells with long parallel processes along the walls of the endoneurium as the Bands of Büngner that guide regenerating axons across the injury site and through the distal nerve stumps (Fenrich and Gordon, 2004; Fu and Gordon, 1997). In the process of Wallerian degeneration as myelin breaks down in a poorly understood manner, the dedifferentiated SCs take the active role in phagocytosis of the axon and myelin debris during the first days. Thereafter, macrophages penetrate the permeated nerve blood barrier and predominate in the phagocytosis that proceeds over weeks in the rat (Avellino et al., 2004; Brushart, 2011; Gaudet et al., 2011; Rotshenker, 2011; Stoll and Muller, 1999; Stoll et al., 1989).

Close axon-SC contact during nerve regeneration re-initiates the SC differentiation program with withdrawal of the SCs from the cell cycle,

downregulation of the regeneration associated genes of the denervated SC, and upregulation of myelin associated genes as myelination proceeds (Arthur-Farraj et al., 2012). Axon outgrowth across the injury site is a slow process as dedifferentiated SCs migrate into and across the injury site through disrupted extracellular matrix with axons following on closely (Brushart et al., 2002; Chen et al., 2005). The regenerating axons 'wander' and 'stagger' across the suture site in an asynchronous manner as a result of the asynchronous and frequent abortive outgrowth of axons and the misalignment of SCs in the fragmented extracellular matrix (Witzel et al., 2005). When the regenerating axons enter the endoneurial tubes of the distal nerve stumps they elongate between the inner surface of the basal lamina and the SCs in the Bands of Büngner (Brushart, 2011; Fu and Gordon, 1997; Haftek and Thomas, 1968). The basal lamina allows regenerating axons and their accompanying SCs to cross into distal nerve stump or into natural or artificial nerve conduits (Hall, 1986; Pfister et al., 2011; Szynkaruk et al., 2013), but regeneration does not proceed if SC proliferation is prevented with mitomycin C (Hall, 1986). The axon-SC contact initiates a second proliferation phase before the SC differentiation program is initiated and myelination proceeds (Arthur-Farraj et al., 2012; Pellegrino and Spencer, 1985), the extent of myelination being directly proportional to the size of the parent axons, a process also controlled by NRG1 (Devor and Govrin-Lippmann, 1979; Hall, 1986; Michailov et al., 2004). Evidence that pharmacological block of the nicotinic acetylcholine and purinergic receptors on the SC membranes reduces the number of neurons that regenerate through the suture site and into the distal nerve stump, is consistent with a role of acetylcholine and ATP, released from the growth cones, in the collapse of the cytoplasmic processes of the denervated SCs (Vrbova et al., 2009). This process is analogous to the withdrawal of the processes of perisynaptic Schwann cells at the neuromuscular junction in response to acetylcholine release (Georgiou et al., 1999; Jahromi et al., 1992; Son and Thompson, 1995; Son et al., 1996; Vrbova et al., 2009).

Specificity of motor and sensory nerve regeneration: sensory and motor SC phenotypic differences?

Preferential reinnervation of motor and sensory pathways by regenerating nerves

Brushart demonstrated 20 and 25 years ago, that, after femoral nerve transection and surgical repair, the axotomized motoneurons initially regenerated their axons in a random fashion into the 'appropriate' motor nerve branch to quadriceps muscle and 'inappropriately' into the saphenous sensory pathway. Yet, six weeks later, significantly more motoneurons regenerated their axons into the 'appropriate' motor pathway, a process that he termed preferential motor reinnervation (Fig. 2) (Brushart, 1988, 1993). The clinical problem associated with misdirection of regenerating nerves remains one of the most vexing issues of functional recovery in the patients who suffer injuries that result in degeneration of the disconnected distal nerve stump and require surgical repair (Brushart, 2011). The promise of some remaining capacity of regenerating neurons to select appropriate pathways is therefore, of considerable importance. The apparent specificity demonstrated for motor axons has, in more recent years, been extended to sensory neurons that too appear to be able, again only to some degree, to select the appropriate sensory pathways (Brushart et al., 2005; Geremia et al., 2007; Hoke et al., 2006; Mears et al., 2003). The temporal course of this sensory specificity was not followed as it was for motor specificity but the preferential sensory reinnervation is likely to develop gradually in the same way that preferential motor reinnervation does (Al-Majed et al., 2000b; Brushart et al., 2002). The question of the basis for this specificity with preferential reinnervation of appropriate motor and sensory pathways has occupied Brushart's attention ever since its first discovery in 1988 (Brushart, 1988).

Sensory and motor SC phenotypic differences

The SCs that are in close association with axons during development and during adult nerve regeneration are the obvious cellular choice to determine whether there are phenotypic differences in motor and sensory pathways that may explain the preferential regeneration of motor and sensory axons. The L2 carbohydrate moiety, HNK-1, associated with several neural recognition molecules, was identified as a candidate because it is expressed selectively on SCs and the basement membrane of motor axons in the mouse (Schachner, 1990). The HNK-1 expression remains for 2–3 weeks after the onset of Wallerian degeneration. Following nerve injury and regeneration, the expression of HNK-1 in motor pathways was enhanced by motor but not sensory axons (Martini and Schachner, 1988; Martini et al., 1994). These findings were promising. Later experiments demonstrated that accelerated reinnervation of motor pathways after brief (1h) low frequency electrical stimulation was temporally associated with enhanced HNK-1 expression and that this effect of the stimulation was not seen in the motor nerves of heterozygous BDNF or homozygous trkB knockout transgenic mice (Eberhardt et al., 2006). Brushart and colleagues pointed out that these findings, although consistent with some involvement of the HNK-1 epitope in preferential motor reinnervation, failed to establish a causal link (Brushart et al., 2013; Hoke et al., 2006). As a result, the role of the carbohydrate HNK-1 moiety still remains uncertain.

Brushart and colleagues redirected their attention to investigating whether there were phenotypic differences in expression of any of several neurotrophic factors, including PTN, in the SCs of motor and sensory pathways (Brushart et al., 2013; Hoke et al., 2006). The precise rationale was not explicitly stated in either paper but the experimental evidence obtained in Hoke's laboratory, for a novel and motor nerve specific neurotrophic factor, PTN (Mi et al., 2007), was the most likely reason. Focused cDNA microarrays were used to determine the expression of several neurotrophic factors in SCs in the denervated sciatic nerve of rats, but only the expression of PTN was presented (Mi et al., 2007). The striking upregulation of PTN discovered in denervated sciatic distal nerve stumps, was the impetus to explore whether the factor had a neurotrophic role in survival and/or a neurotropic role in promoting axon outgrowth and regeneration *in vitro* and *in vivo* experiments (Mi et al., 2007). Indeed the PTN was found to have both neurotrophic and neurotropic effects on motoneurons. That motor axons from a spinal cord explant grew toward a point source of PTN whilst sensory axons from dorsal root ganglion neurons did not, provided enticing evidence that the neurotropic effect of PTN is 'motor' specific (Mi et al., 2007). PTN also promoted the regeneration of axons in vivo across a 15 mm long silicone tube that was filled with HK-293 cells transfected with PTN but not when the tubes were filled with the vector or saline (Mi et al., 2007). This evidence likely provided the impetus to determine whether such specific expression of one or more neurotrophic factor in denervated 'motor' SCs underlies the preferential motor reinnervation of axotomized motoneurons. This relatively novel idea extended the evidence of PTN expression in skeletal muscles during development (Peng et al., 1995) to the possibility of selective expression of PTN in motor SCs that might account for preferential motor reinnervation. The evidence of sensory selective neurotrophic factors that was obtained in elegant *in vitro* experiments of Tucker et al. (2001), was likely the basis for the choice of neurotrophic factors other than PTN for differential expression in 'sensory' SCs in the later experiments of Hoke and Brushart (Brushart et al., 2013; Hoke et al., 2006). In the experiments of Tucker et al. (2001) in which neurons containing green fluorescent protein were cultured and their neurite outgrowth visualized in real time, neurites emanating from sensory neurons and not motoneurons, grew toward chromatographic beads that were soaked in NGF, BDNF, NT-3, or neurotrophin 4/5 (NT4/5) as well as combinations of these factors.

In the first study of Hoke and colleagues of whether there are 'motor' and 'sensory' specific SCs that can be identified by their expression of

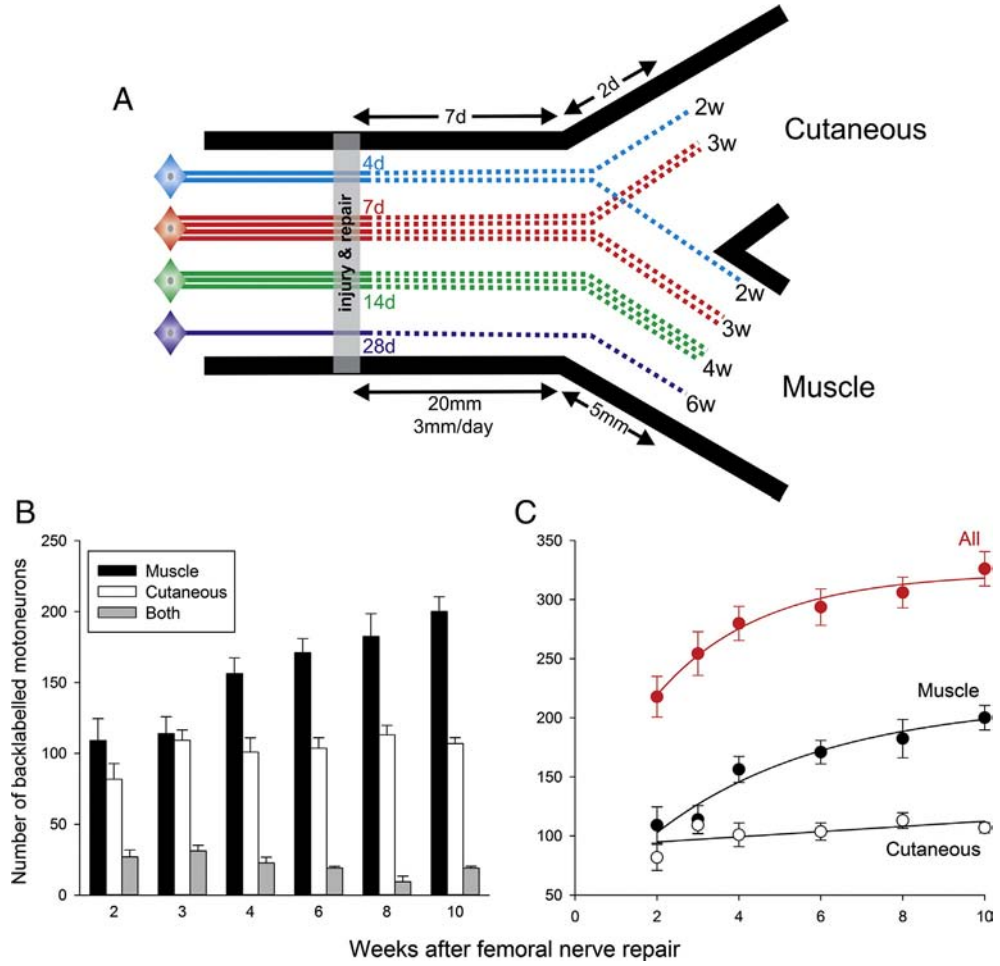


Fig. 2. Time course of motoneurons to regenerate their axons after femoral nerve transection and surgical repair. The asynchronous regeneration of motor axons across the suture line is shown diagrammatically in A. The representation of the number of motoneurons that regenerate their axons across the suture site is derived from data obtained by backlabeling femoral motoneurons with retrograde dyes, 1.5 mm from the site of the femoral nerve transection and microsurgical repair. Adapted from Brushart et al. (2002). The representation of the proportions of motoneurons whose axons regenerate randomly into the appropriate muscle and inappropriate cutaneous nerve branches within 2 and 3 weeks is derived from enumeration of the motoneurons that regenerated their axons over a distance of 20 mm before entering the appropriate muscle branch (mu), the inappropriate cutaneous sensory branch (cu) or both branches (b), after application of two retrograde dyes to the motor and sensory nerve branches (adapted from Al-Majed et al., 2000b). The number of backlabeled motoneurons that regenerated their axons is plotted as a function of time as histograms in B and as a graph in C. Note that the plot labeled 'All' includes not only those motoneurons that regenerated their axons into the appropriate muscle branch and inappropriately into the cutaneous branch, but also the small proportion of motoneurons that regenerated their axons into both branches. The relatively small number of regenerating axons that emerge from the proximal nerve stump within the first week after femoral nerve surgical repair, is shown to grow randomly into appropriate 'muscle' and inappropriate 'cutaneous sensory' endoneurial tubes, a smaller proportion sending collaterals into both tubes (A) because the counts of the neurons that were backlabeled from the axons that had regenerated at a rate of 3 mm/day into the 'motor' and 'sensory' branches were equal 2 and 3 weeks after the nerve repair (B,C). The axons that grow out from the proximal nerve stump and cross the suture site at 14 days, are, by extrapolation, those motor axons that regenerate specifically into the appropriate motor branch by 4 weeks. The regeneration of axons from the remaining axotomized motoneurons is extrapolated diagrammatically in A and the evidence of their gradual increase to a peak between 8 and 10 weeks whilst the number motoneurons with axons in the inappropriate sensory branch does not change over time is shown in the histogram in B and the graphs in C. (For interpretation of the references to color in this figure, the reader is referred to the web version of this article.)

neurotrophic factors, total RNA was extracted from ventral roots (motor) and from the saphenous sensory nerve at three time points in the course of a one month period of denervation (Hoke et al., 2006). RT-PCR analysis was performed to examine the expression of the eleven chosen neurotrophic factors as the first step taken to first, address the question of whether indeed there is selective expression of PTN in the denervated SCs of motor pathways and to second, extend this investigation to addressing whether the other neurotrophic factors demonstrate phenotypic expression in the denervated motor SCs of ventral roots, and in denervated sensory SCs in denervated saphenous nerve (Hoke et al., 2006). Expression of the eleven chosen neurotrophic factors was examined in intact and denervated motor and sensory pathways. These were BDNF, NGF, and NT-3, GDNF, insulin-growth factors I and II (IGF-I and IGF-II), ciliary neurotrophic factor (CNTF), vascular epithelium growth factor (VEGF) and basic fibroblast growth factor (FGF-2), hepatocyte growth factor (HGF) and pleiotrophin (PTN). Findings of dramatic elevation (>10 fold) of PTN mRNA in the 15 day denervated ventral root but not in denervated cutaneous nerves (Figs. 3B,C) (Hoke et al., 2006) provided more support that, indeed PTN is a 'motor' specific factor that promotes motor nerve regeneration toward its source *in vitro* and *in vivo* (Mi et al., 2007). The RT-PCR analyses also identified the sensory specific expression of several neurotrophic factors in the denervated sensory cutaneous nerve, specifically finding elevations of >10-fold in the mRNAs of HGF, VEGF, BDNF, and IGF-1 at 15 and 30 days after denervation of the cutaneous nerve (cf. Figs. 3A and C) (Brushart et al., 2013; Hoke et al., 2006). The elevation of GDNF mRNA in dorsal and ventral roots was in contrast, very similar (Figs. 3A and C). The findings of elevated levels of the neurotrophins BDNF and NGF were consistent with the earlier findings of chemotaxis of sensory neurites toward a source of these factors (Tucker et al., 2001). Upregulation of neurotrophins and GDNF in denervated SCs of the sciatic had been demonstrated before (Funakoshi et al., 1993; Heumann et al., 1987a, 1987b;

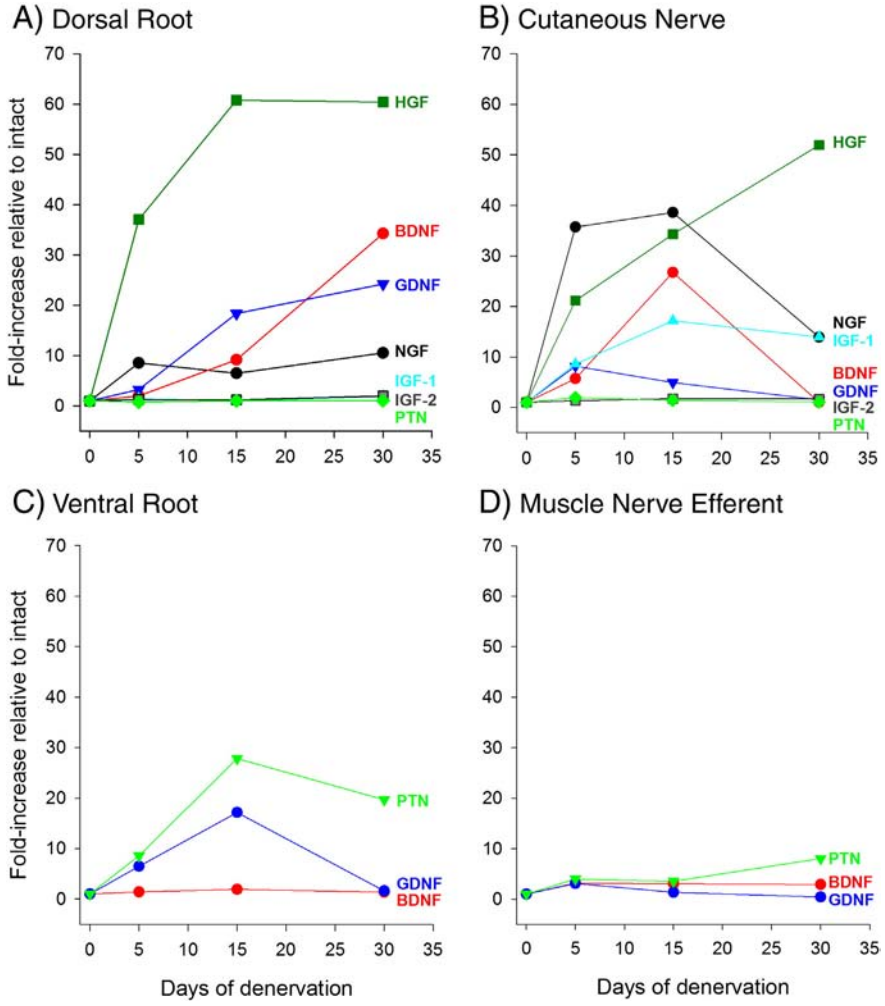


Fig. 3. Expression patterns of growth factor genes to proximal and distal regions of cutaneous and muscle branches of the femoral nerve as a function of time after denervation. Gene expression is plotted as a function of time after denervation as the fold-increase in mRNA relative to intact levels in order to follow the extent and time course of the upregulation of the genes after Schwann cell denervation. The mRNA data were normalized to the housekeeping gene of glyceraldehyde 3-phosphate dehydrogenase (GAPDH).
Data are replotted from Brushart et al. (2013) and Hoke et al. (2006).

Meyer et al., 1992) but the specific question of whether these and other trophic factors were differentially expressed in denervated 'motor' and 'sensory' nerve pathways had not been addressed until the studies of Hoke and Brushart. The latter studies answered the question of whether there is differential 'motor' and 'sensory' SC expression of the neurotrophic factors with their findings of relatively clear differences in the phenotypic expression of neurotrophic factors in denervated motor and sensory SCs (Brushart et al., 2013; Hoke et al., 2006). These differences were in line with the chemotactic effect of the neurotrophins for sensory axons and of PTN for motor axons (Mi et al., 2007; Tucker et al., 2001). However, in the same way that the specific HNK1 expression by motor SCs was *associated with* rather than causally linked to preferential motor reinnervation under several experimental conditions, the differential expression of the neurotrophic factors discovered in the denervated motor and sensory SCs was correlated with preferential motor and sensory reinnervation without direct evidence of causality.

It was the imaginative experiments that directed either motor or sensory axons into denervated nerve grafts of either a ventral root or the saphenous nerve which contained 'motor' or 'sensory' specific denervated SCs, respectively, that provided more enlightening and promising evidence for a role of the SC motor or sensory phenotypic expression of neurotrophic factors in preferential motor or sensory regeneration (Hoke et al., 2006). These experiments demonstrated that the ventral root grafts that contained 'motor' SCs supported the regeneration of motor axons significantly better than the saphenous nerve grafts that contained 'sensory' SCs. Similarly, the grafts containing 'sensory' SCs supported the regeneration of sensory neurons significantly better than the grafts that contained the 'motor' SCs. An important cross-reinnervation experiment was also conducted in the studies reported in 2006: regenerating sensory axons were directed to inappropriately reinnervate a ventral root autograft and the SC phenotype examined after a month (Hoke et al., 2006). The 'motor' SCs retained their 'motor' phenotype with sustained high levels of PTN as well as with an interesting 8-fold increase in GDNF mRNA levels (Fig. 9 in Hoke et al., 2006). Yet, a striking 'conversion' of the 'motor' SCs to the sensory phenotype was seen with a strong elevation of BDNF mRNA. These findings demonstrate that inappropriately reinnervated 'motor' SCs adopt a mixed 'sensory–motor' phenotype with respect to their expression of neurotrophic factors. This experiment provides some insights into why motoneurons that regenerate their axons into inappropriate pathways containing 'sensory' SCs, remain in these pathways prior to the later preferential motor reinnervation of appropriate 'motor' pathways but axons of motoneurons that regenerate their axons later (Al-Majed et al., 2000b) (Fig. 2A). As an aside, the careful surgical experimental designs were exquisite with the care taken to match the size of the nerve grafts to the proximal stump of the cut motor or sensory branches of the femoral nerve. The same care was taken to ensure that the number of axons in the saphenous sensory and the quadriceps branches of the femoral nerve were equal in the

experiments in which preferential motor reinnervation was first demonstrated (Brushart, 1993).

The third study from the Hoke and Brushart laboratories expanded on the delineation of sensory and motor SCs by comparisons of their neurotrophic factor expression at the anatomical levels of the spinal roots and the peripheral nerves (Brushart et al., 2013). This delineation was again achieved with considerable surgical skill in an inventive (and exhaustive) analysis of denervated sensory and motor SCs. The skills were brought to bear on the surgical isolation of denervated motor SCs in ventral roots and in the femoral nerve and in the isolation of denervated sensory SCs in dorsal roots, the saphenous cutaneous nerve, the unmyelinated saphenous cutaneous (after capsaicin treatment) and the quadriceps muscle nerve afferents. These extended analyses of the expression of the same eleven neurotrophic factors that were investigated in the 2006 study, revealed relatively small differences in the proximo-distal axis for the denervated SCs in the sensory pathways, there still be a small decline from the dorsal root level to the level of the peripheral nerve (Figs. 3A and B) (Brushart et al., 2013). The same proximo-distal trend was evident for PTN expression In denervated motor SCs as well as for the marginally higher GDNF expression in the motor as compared to the sensory SCs (Figs. 3C and D). The translation of GDNF mRNA to protein was robust retaining the proximo-distal distribution of the GDNF in the SCs (Brushart et al., 2013). As in the earlier 2006 study, the evidence for PTN as a 'motor' neurotrophic factor was convincing despite the lesser expression of PTN in the denervated 'motor' SCs as compared to the more robust upregulation of the more 'sensory' specific factors of HGF, BDNF, and NGF in sensory pathways (Figs. 3A and B). Overall though, the study was disappointing in that it too failed to prove causality between either preferential motor reinnervation and the demonstrated preferential expression of PTN in the denervated 'motor' SCs, or the preferential sensory reinnervation and the demonstrated preferential expression of HGF, BDNF, VEGF and to a lesser extent, IGF-1 and IGF-2 in denervated 'sensory' SCs. This was so despite the better delineation of the motor and sensory pathways than in the earlier study (Brushart et al., 2013; Hoke et al., 2006).

A nagging question regarding both the 2006 and 2013 studies is why the eleven neurotrophic factors were chosen to address the question of whether there are phenotypic differences in the SCs of motor and sensory nerves (Brushart et al., 2013; Hoke et al., 2006). Whilst there is evidence of neurotrophic effects of all the chosen factors, including that for VEGF, IGF1 and 2, HGF and PTN (Barres and Barde, 2000; Jin et al., 2002; Knusel et al., 1990; Mi et al., 2007; Neufeld et al., 1999), the rationale for the choice that was made to study these factors was not given in the published papers. The neurotrophic factors are well known to regulate the survival of many neuronal populations in vertebrates, especially from *in vitro* studies but their function in nerve growth *in vivo* is less clear despite many published studies (Bibel and Barde 2000; Gordon, 2009; Zigmond, 2012). The definitive experiments documenting the neurotropic effects of PTN and of the neurotrophins on PNS nerve growth are relatively scarce (Mi et al., 2007; Tucker et al., 2001).

Why is preferential reinnervation of appropriate endoneurial tubes preceded by random reinnervation?

The delineation of 'motor' and 'sensory' denervated SCs that sustain their phenotypic expression of neurotrophic factors for weeks in vivo and in vitro, could provide an experimental or clinical means of distinguishing the endoneurial tubes of motor and sensory nerves in mixed nerves, at least for short periods in addition to the more classical histochemical method of identifying motor axons in nerve cross-sections by their presence of actylcholinesterase in the axons (Gruber and Zenker, 1973). However, the delineation does not necessarily provide insight into the mechanism by which the initial random process of axon regeneration into appropriate and inappropriate sensory and motor pathways is followed by subsequent specification of those pathways to accept the regeneration of only the appropriate nerves — the preferential motor or sensory reinnervation by regenerating axons of motoneurons and sensory neurons, respectively.

Dedifferentiation of denervated SCs from the mature myelinating form to the immature SC incurs the re-expression of neurotrophic factors during the re-entry into the cell cycle (Mirsky et al., 2008), The differential expression of 'sensory' and 'motor' neurotrophic factors in the denervated 'sensory' and 'motor' SCs is retained through several cycles *in vivo* and *in vitro* (Brushart et al., 2013; Hoke et al., 2006). An important consideration then, is whether the time course of the upregulation of the neurotrophic factors in the denervated SCs can explain why regenerating axons randomly reinnervate appropriate and inappropriate denervated pathways initially before demonstrating preferential reinnervation of the appropriate pathways. This consideration requires that the time course of regeneration be considered in detail (Fig. 2). Staggered regeneration at the site of nerve transection and surgical repair results in the slow progression of regenerating axons into the distal nerve stumps and through the stumps to the denervated targets. As illustrated in Fig. 2A, the axotomized motoneurons that regenerate axons into the distal nerve stump and are backlabeled at the site of entry, progressively increase in number over a period of a month (Brushart et al., 2002). Once the regenerating axons enter the distal nerve stump in the rat model of femoral nerve transection and surgical repair, they regenerate at a rate of ~3 mm/day through the endoneurial tubes of the femoral nerve that progress into the sensory and motor nerve branches. The motoneurons that regenerate their axons into the 'appropriate' motor and 'inappropriate' sensory nerves can be recognized and counted after application of the dyes to the two branches (Fig. 2A).

As diagramed in Fig. 2A, the axotomized motoneurons whose regenerating axons cross the surgical site within the first week after nerve transection and surgical repair, regenerate randomly into and through the endoneurial tubes containing appropriate denervated 'motor' SCs and inappropriate denervated 'sensory' SCs to reinnervate the muscle and cutaneous nerve branches within 3 weeks. At this time point, ~200 femoral motoneurons randomly reinnervated the appropriate motor and inappropriate sensory branches of the femoral nerve (Figs. 2B,C) as illustrated by the dotted red lines in Fig. 2A. In contrast, the motoneurons that regenerated their axons across the suture line and into the distal nerve stump within 14 days, and by extrapolation, into the femoral nerve branches by 4 weeks, preferentially reinnervated the appropriate muscle pathway (Fig. 2). It must be noted that the number of motoneurons that regenerate their axons progressively increases with *all* the motoneurons regenerating their axons across the suture site within a month (Brushart et al., 2002), and these axons growing appropriately into the muscle branches because they are backlabeled only from this muscle branch after 4 weeks (Fig. 2A). Indeed the progressive increase in the number of motoneurons that regenerate into the appropriate muscle branch increases progressively with time whist those motoneurons that regenerate into the inappropriate cutaneous nerve branch, and which send their axons into both branches, do not increase or decrease significantly in numbers (Fig. 2) (Al-Majed et al., 2000b). Hence those motoneurons whose axons enter both branches do not display the pruning in these adult rats in contrast to the more obvious pruning that was described in younger rats in the earlier study of Brushart (Al-Majed et al., 2000b; Brushart, 1993).

From the extrapolation, it is apparent that the appropriate and inappropriate distal nerve pathways that the regenerating axons enter at the site of nerve transection and surgical repair, are not specified until ~15 days after denervation of the distal nerve stumps. It is at this time point that the selective expression of the neurotrophic factors in the denervated 'motor' and 'sensory' SCs is evident with the elevations in the expression of the growth factors being evident and in many cases, peaking at 15 days after nerve injury and repair and coinciding with the time when regenerating motor axons selectively enter into the appropriate denervated distal nerve stumps (cf. Figs. 2 and 3). The

expression of GDNF and BDNF, in particular, increases further in the dorsal root but not the in the cutaneous nerve, with HGF showing a progressive increase in the cutaneous nerve (Figs. 3A,B). The specified 'motor' SCs lead regenerating axons back to the appropriate denervated quadriceps muscle target for reinnervation. The coincidence of the time frames of the emergence of differential motor reinnervation with the peak expression of 'motor' specific factors in the denervated motor pathways is striking. It is also certainly provocative with the correlations being quite consistent with the denervated 'motor' and 'sensory' SCs exerting a neurotropic effect of promoting the appropriate regeneration of motor and not sensory nerve fibers into the pathway containing the 'motor' SCs after the initial period of random reinnervation. Also relevant to this argument is that the brief 1 hour low frequency electrical stimulation that accelerates axon outgrowth and in turn, results in accelerated regeneration through the nerve pathways (Al-Majed et al., 2000b; Brushart et al., 2002), accelerates upregulation of BDNF and trkB receptors in the motoneurons (Al-Majed et al., 2000a). Moreover, the same stimulation paradigm upregulates BDNF and NGF in Schwann cells in vitro (Huang et al., 2010; Wan et al., 2010) With the same arguments used above, it is possible that the earlier upregulation of neurotrophic factors plays a central role in the earlier manifestation of preferential motor reinnervation with outgrowing axons being attracted to appropriate pathways that contain SCs that express the appropriate neurotrophic factors. One caveat is that, in addition, the known effect of neurotrophic factors of promoting sprouting of outgrowing neurites in vitro or axons in vivo (Klimaschewski et al., 2013) could increase the branching of regenerating axons with the possible negative effect of increasing the chances of regenerating axons entering inappropriate pathways. This possibility cannot be excluded without further analysis of numbers of regenerating axons in the distal nerve stumps. The findings that the numbers of motoneurons sending their axons into both motor and sensory nerve branches were not increased after brief electrical stimulation (Al-Majed et al., 2000b) makes this explanation unlikely.

The experiments that demonstrated 'motor' SCs acquiring a mixed motor–sensory SC profile (see Fig. 9 in Hoke et al., 2006) a month after their reinnervation by inappropriate sensory axons, provide insights into why the random reinnervation of inappropriate pathways remains (Al-Majed et al., 2000b) (Fig. 2A). The regenerating motor axons that enter a pathway that contains 'motor' SCs are supported and remyelinated by these SCs. These SCs, whilst retaining some 'motor' phenotype with high levels of both PTN and GDNF, begin to express high levels of BDNF mRNA, more typical of the 'sensory' SC (Hoke et al., 2006). These 'semi-converted' 'motor–sensory' SCs myelinate and sustain the regenerated axons, that in turn, do not appear to 'die-back' but remain in their inappropriate endoneurial tubes.

The extrapolations made from the time course of regeneration and from the emergence of the 'motor' phenotype of the SCs in the appropriate motor pathways also may explain why the preferential reinnervation of appropriate motor pathways only becomes evident after a delay, the delay corresponding with the time course of upregulation of the neurotrophic factors. It now behooves the Hoke and Brushart's laboratories to perform definitive experiments to prove that these 'sensory' and 'motor' specific SC phenotypes are not only consistent with observed preferential reinnervation of appropriate nerve pathways by sensory and motor regenerating axons but, that these phenotypes are *critical and responsible for* the relatively late promotion of the appropriate reinnervation of the pathways that contain these appropriate neurotrophic phenotypes. In the first instance, experiments that use siRNA for example to knockdown the expression of motor or sensory specific neurotrophic factors may begin to uncover the mechanism by which motor and sensory regenerating axons show some preferential reinnervation of appropriate distal nerve stumps leading to reinnervation of appropriate denervated targets. Experimental systems such as the in vitro model of adult mammalian nerve repair that has been developed by Brushart and colleagues, will allow controlled manipulation of the nerve grafts and their expression of genes in a controlled environment (Vyas et al., 2010). Whilst the description of the in vitro model has not yet included target tissue, this inclusion is likely to be considered in the future.

References

Almad, A., Sahinkaya, F.R., McTigue, D.M., 2011. Oligodendrocyte fate after spinal cord injury. Neurotherapeutics 8, 262–273.

Al-Majed, A.A., Brushart, T.M., Gordon, T., 2000a. Electrical stimulation accelerates and increases expression of BDNF and trkB mRNA in regenerating rat femoral motoneurons. Eur. J. Neurosci. 12, 4381–4390.

Al-Majed, A.A., Neumann, C.M., Brushart, T.M., Gordon, T., 2000b. Brief electrical stimulation promotes the speed and accuracy of motor axonal regeneration. J. Neurosci. 20, 2602–2608.

Arthur-Farraj, P., Wanek, K., Hantke, J., Davis, C.M., Jayakar, A., Parkinson, D.B., Mirsky, R., Jessen, K.R., 2011. Mouse Schwann cells need both NRG1 and cyclic AMP to myelinate. GLIA 59, 720–733.

Arthur-Farraj, P.J., Latouche, M., Wilton, D.K., Quintes, S., Chabrol, E., Banerjee, A., Woodhoo, A., Jenkins, B., Rahman, M., Turmaine, M., Wicher, G.K., Mitter, R., Greensmith, L., Behrens, A., Raivich, G., Mirsky, R., Jessen, K.R., 2012. c-Jun reprograms Schwann cells of injured nerves to generate a repair cell essential for regeneration. Neuron 75, 633–647.

Avellino, A.M., Dailey, A.T., Harlan, J.M., Sharar, S.R., Winn, R.K., McNutt, L.D., Kliot, M., 2004. Blocking of up-regulated ICAM-1 does not prevent macrophage infiltration during Wallerian degeneration of peripheral nerve. Exp. Neurol. 187, 430–444.

Barres, B.A., Barde, Y., 2000. Neuronal and glial cell biology. Curr. Opin. Neurobiol. 10, 642–648.

Berry, M., Ibrahim, M., Carlile, J., Ruge, F., Duncan, A., Butt, A.M., 1995. Axon–glial relationships in the anterior medullary velum of the adult rat. J. Neurocytol. 24, 965–983.

Bibel, M., Barde, Y.A., 2000. Neurotrophins: key regulators of cell fate and cell shape in the vertebrate nervous system. Genes Dev 14, 2919–2937.

Birchmeier, C., 2009. ErbB receptors and the development of the nervous system. Exp. Cell Res. 315, 611–618.

Birchmeier, C., Nave, K.A., 2008. Neuregulin-1, a key axonal signal that drives Schwann cell growth and differentiation. GLIA 56, 1491–1497.

Blakemore, W.F., Keirstead, H.S., 1999. The origin of remyelinating cells in the central nervous system. J. Neuroimmunol. 98, 69–76.

Boyd, J.G., Gordon, T., 2003. Neurotrophic factors and their receptors in axonal regeneration and functional recovery after peripheral nerve injury. Mol. Neurobiol. 27, 277–324.

Britsch, S., Goerich, D.E., Riethmacher, D., Peirano, R.I., Rossner, M., Nave, K.A., Birchmeier, C., Wegner, M., 2001. The transcription factor Sox10 is a key regulator of peripheral glial development. Genes Dev. 15, 66–78.

Brushart, T.M., 1988. Preferential reinnervation of motor nerves by regenerating motor axons. J. Neurosci. 8, 1026–1031.

Brushart, T.M., 1993. Motor axons preferentially reinnervate motor pathways. J. Neurosci. 13, 2730–2738.

Brushart, T.M., 2011. Nerve Repair. Oxford University Press, USA.

Brushart, T.M., Hoffman, P.N., Royall, R.M., Murinson, B.B., Witzel, C., Gordon, T., 2002. Electrical stimulation promotes motoneuron regeneration without increasing its speed or conditioning the neuron. J. Neurosci. 22, 6631–6638.

Brushart, T.M., Jari, R., Verge, V., Rohde, C., Gordon, T., 2005. Electrical stimulation restores the specificity of sensory axon regeneration. Exp. Neurol. 194, 221–229.

Brushart, T.M., Aspalter, M., Griffin, J.W., Redett, R., Hameed, H., Zhou, C., Wright, M., Vyas, A., Hoke, A., 2013. Schwann cell phenotype is regulated by axon modality and central–peripheral location, and persists in vitro. Exp. Neurol. 247, 272–281.

Bunge, M.B., Bunge, R.P., PAPPAS, G.D., 1962. Electron microscopic demonstration of connections between glia and myelin sheaths in the developing mammalian central nervous system. J. Cell Biol. 12, 448–453.

Buttermore, E.D., Thaxton, C.L., Bhat, M.A., 2013. Organization and maintenance of molecular domains in myelinated axons. J. Neurosci. Res. 91, 603–622.

Chen, Y.Y., McDonald, D., Cheng, C., Magnowski, B., Durand, J., Zochodne, D.W., 2005. Axon and Schwann cell partnership during nerve regrowth. J. Neuropathol. Exp. Neurol. 64, 613–622.

Coleman, M., 2005. Axon degeneration mechanisms: commonality amid diversity. Nat. Rev. Neurosci. 6, 889–898.

Crawford, A.T., Desai, D., Gokina, P., Basak, S., Kim, H.A., 2008. E-cadherin expression in postnatal Schwann cells is regulated by the cAMP-dependent protein kinase a pathway. GLIA 56, 1637–1647.

De, F.C., Hunt, S.P., 1994. The differential control of c-jun expression in regenerating sensory neurons and their associated glial cells. J. Neurosci. 14, 2911–2923.

Devor, M., Govrin-Lippmann, R., 1979. Maturation of axonal sprouts after nerve crush. Exp. Neurol. 64, 260–270.

Dong, Z., Brennan, A., Liu, N., Yarden, Y., Lefkowitz, G., Mirsky, R., Jessen, K.R., 1995. Neu differentiation factor is a neuron-glia signal and regulates survival, proliferation, and maturation of rat Schwann cell precursors. Neuron 15, 585–596.

Eberhardt, K.A., Irintchev, A., Al-Majed, A.A., Simova, O., Brushart, T.M., Gordon, T., Schachner, M., 2006. BDNF/TrkB signaling regulates HNK-1 carbohydrate expression in regenerating motor nerves and promotes functional recovery after peripheral nerve repair. Exp. Neurol. 198, 500–510.

Falls, D.L., 2003. Neuregulins and the neuromuscular system: 10 years of answers and questions. J. Neurocytol. 32, 619–647.

Feltri, M.L., Graus, P.D., Previtali, S.C., Nodari, A., Migliavacca, B., Cassetti, A., Littlewood-Evans, A., Reichardt, L.F., Messing, A., Quattrini, A., Mueller, U., Wrabetz, L., 2002.

Conditional disruption of beta 1 integrin in Schwann cells impedes interactions with axons. J. Cell Biol. 156, 199–209.
Fenrich, K., Gordon, T., 2004. Canadian Association of Neuroscience review: axonal regeneration in the peripheral and central nervous systems—current issues and advances. Can. J. Neurol. Sci. 31, 142–156.
Franz, C.K., Rutishauser, U., Rafuse, V.F., 2008. Intrinsic neuronal properties control selective targeting of regenerating motoneurons. Brain 131, 1492–1505.
Fu, S.Y., Gordon, T., 1997. The cellular and molecular basis of peripheral nerve regeneration. Mol. Neurobiol. 14, 67–116.
Funakoshi, H., Frisen, J., Barbany, G., Timmusk, T., Zachrisson, O., Verge, V.M., Persson, H., 1993. Differential expression of mRNAs for neurotrophins and their receptors after axotomy of the sciatic nerve. J. Cell Biol. 123, 455–465.
Garratt, A.N., Britsch, S., Birchmeier, C., 2000. Neuregulin, a factor with many functions in the life of a Schwann cell. Bioessays 22, 987–996.
Gaudet, A.D., Popovich, P.G., Ramer, M.S., 2011. Wallerian degeneration: gaining perspective on inflammatory events after peripheral nerve injury. J. Neuroinflammation 8, 110.
Georgiou, J., Robitaille, R., Charlton, M.P., 1999. Muscarinic control of cytoskeleton in perisynaptic glia. J. Neurosci. 19, 3836–3846.
Geremia, N.M., Gordon, T., Brushart, T.M., Al-Majed, A.A., Verge, V.M., 2007. Electrical stimulation promotes sensory neuron regeneration and growth-associated gene expression. Exp. Neurol. 205, 347–359.
Gordon, T., 1983. Dependence of peripheral nerves on their target organs. In: Burnstock, G., O'Brien, R., Vrbova, G. (Eds.), Somatic and Autonomic Nerve–Muscle Interactions. Elsevier, Amsterdam, pp. 289–316.
Gordon, T., 2009. The role of neurotrophic factors in nerve regeneration. Neurosurg. Focus 26 (E3), 1–10.
Gordon, T., Udina, E., Verge, V.M., de Chaves, E.I., 2009. Brief electrical stimulation accelerates axon regeneration in the peripheral nervous system and promotes sensory axon regeneration in the central nervous system. Motor Control 13, 412–441.
Grafstein, B., 1975. The nerve cell body response to axotomy. Exp. Neurol. 48, 32–51.
Grafstein, B., McQuarrie, I.G., 1978. Role of the nerve cell body in axonal regeneration. In: Cotman, C.W. (Ed.), Neuronal Plasticity. Raven, New York, pp. 155–196.
Griffin, J.W., Thompson, W.J., 2008. Biology and pathology of nonmyelinating Schwann cells. GLIA 56, 1518–1531.
Gruber, H., Zenker, W., 1973. Acetylcholinesterase: histochemical differentiation between motor and sensory nerve fibres. Brain Res. 51, 207–214.
Haftek, J., Thomas, P.K., 1968. Electron-microscope observations on the effects of localized crush injuries on the connective tissues of peripheral nerve. J. Anat. 103, 233–243.
Hall, S.M., 1986. The effect of inhibiting Schwann cell mitosis on the re-innervation of acellular autografts in the peripheral nervous system of the mouse. Neuropathol. Appl. Neurobiol. 12, 401–414.
Herdegen, T., Gass, P., Brecht, S., Neiss, W.F., Schmid, W., 1994. The transcription factor CREB is not phosphorylated at serine 133 in axotomized neurons: implications for the expression of AP-1 proteins. Brain Res. Mol. Brain Res. 26, 259–270.
Heumann, R., Korsching, S., Bandtlow, C., Thoenen, H., 1987a. Changes of nerve growth factor synthesis in nonneuronal cells in response to sciatic nerve transection. J. Cell Biol. 104, 1623–1631.
Heumann, R., Lindholm, D., Bandtlow, C., Meyer, M., Radeke, M.J., Misko, T.P., Shooter, E., Thoenen, H., 1987b. Differential regulation of mRNA encoding nerve growth factor and its receptor in rat sciatic nerve during development, degeneration, and regeneration: role of macrophages. Proc. Natl. Acad. Sci. U. S. A. 84, 8735–8739.
Hildebrand, C., Remahl, S., Persson, H., Bjartmar, C., 1993. Myelinated nerve fibres in the CNS. Prog. Neurobiol. 40, 319–384.
Hirano, A., Levine, S., Zimmerman, H.M., 1968. Remyelination in the central nervous system after cyanide intoxication. J. Neuropathol. Exp. Neurol. 27, 234–245.
Hoke, A., Redett, R., Hameed, H., Jari, R., Zhou, C., Li, Z.B., Griffin, J.W., Brushart, T.M., 2006. Schwann cells express motor and sensory phenotypes that regulate axon regeneration. J. Neurosci. 26, 9646–9655.
Huang, J., Ye, Z., Hu, X., Lu, L., Luo, Z., 2010. Electrical stimulation induces calcium-dependent release of NGF from cultured Schwann cells. GLIA 58, 622–631.
Huxley, A.F., Stampfli, R., 1949. Evidence for saltatory conduction in peripheral myelinated nerve fibres. J. Physiol. 108, 315–339.
Ibrahim, M., Butt, A.M., Berry, M., 1995. Relationship between myelin sheath diameter and internodal length in axons of the anterior medullary velum of the adult rat. J. Neurol. Sci. 133, 119–127.
Jahromi, B.S., Robitaille, R., Charlton, M.P., 1992. Transmitter release increases intracellular calcium in perisynaptic Schwann cells in situ. Neuron 8, 1069–1077.
Jenkins, R., Hunt, S.P., 1991. Long-term increase in the levels of c-jun mRNA and jun protein-like immunoreactivity in motor and sensory neurons following axon damage. Neurosci. Lett. 129, 107–110.
Jessen, K.R., Mirsky, R., 2005. The origin and development of glial cells in peripheral nerves. Nat. Rev. Neurosci. 6, 671–682.
Jessen, K.R., Mirsky, R., 2008. Negative regulation of myelination: relevance for development, injury, and demyelinating disease. GLIA 56, 1552–1565.
Jin, K., Zhu, Y., Sun, Y., Mao, X.O., Xie, L., Greenberg, D.A., 2002. Vascular endothelial growth factor (VEGF) stimulates neurogenesis in vitro and in vivo. Proc. Natl. Acad. Sci. U. S. A. 99, 11946–11950.
Klimaschewski, L., Hausott, B., Angelov, D.N., 2013. The pros and cons of growth factors and cytokines in peripheral axon regeneration. Int. Rev. Neurobiol. 108, 137–171.
Knusel, B., Michel, P.P., Schwaber, J.S., Hefti, F., 1990. Selective and nonselective stimulation of central cholinergic and dopaminergic development in vitro by nerve growth factor, basic fibroblast growth factor, epidermal growth factor, insulin and the insulin-like growth factors I and II. J. Neurosci. 10, 558–570.
Lieberman, A.R., 1971. The axon reaction: a review of the principal features of perikaryal responses to axon injury. Int. Rev. Neurobiol. 14, 49–124.
Lubinska, L., 1977. Early course of Wallerian degeneration in myelinated fibres of the rat phrenic nerve. Brain Res. 130, 47–63.
Martini, R., Schachner, M., 1988. Immunoelectron microscopic localization of neural cell adhesion molecule (L1, N-CAM, and myelin-associated glycoprotein) in regenerating adult mouse sciatic nerve. J. Cell Biol. 106, 1735–1746.
Martini, R., Schachner, M., Brushart, T.M., 1994. The L2/HNK-1 carbohydrate is preferentially expressed by previously motor axon-associated Schwann cells in reinnervated peripheral nerves. J. Neurosci. 14, 7180–7191.
Mears, S., Schachner, M., Brushart, T.M., 2003. Antibodies to myelin-associated glycoprotein accelerate preferential motor reinnervation. J. Peripher. Nerv. Syst. 8, 91–99.
Meyer, M., Matsuoka, I., Wetmore, C., Olson, L., Thoenen, H., 1992. Enhanced synthesis of brain-derived neurotrophic factor in the lesioned peripheral nerve: different mechanisms are responsible for the regulation of BDNF and NGF mRNA. J. Cell Biol. 119, 45–54.
Mi, R., Chen, W., Hoke, A., 2007. Pleiotrophin is a neurotrophic factor for spinal motor neurons. Proc. Natl. Acad. Sci. U. S. A. 104, 4664–4669.
Michailov, G.V., Sereda, M.W., Brinkmann, B.G., Fischer, T.M., Haug, B., Birchmeier, C., Role, L., Lai, C., Schwab, M.H., Nave, K.A., 2004. Axonal neuregulin-1 regulates myelin sheath thickness. Science 304, 700–703.
Mirsky, R., Woodhoo, A., Parkinson, D.B., Arthur-Farraj, P., Bhaskaran, A., Jessen, K.R., 2008. Novel signals controlling embryonic Schwann cell development, myelination and de-differentiation. J. Peripher. Nerv. Syst. 13, 122–135.
Morrissey, T.K., Levi, A.D., Nuijens, A., Sliwkowski, M.X., Bunge, R.P., 1995. Axon-induced mitogenesis of human Schwann cells involves heregulin and p185erbB2. Proc. Natl. Acad. Sci. U. S. A. 92, 1431–1435.
Neufeld, G., Cohen, T., Gengrinovitch, S., Poltorak, Z., 1999. Vascular endothelial growth factor (VEGF) and its receptors. FASEB J. 13, 9–22.
Paratore, C., Goerich, D.E., Suter, U., Wegner, M., Sommer, L., 2001. Survival and glial fate acquisition of neural crest cells are regulated by an interplay between the transcription factor Sox10 and extrinsic combinatorial signaling. Development 128, 3949–3961.
Parkinson, D.B., Dickinson, S., Bhaskaran, A., Kinsella, M.T., Brophy, P.J., Sherman, D.L., Sharghi-Namini, S., Duran Alonso, M.B., Mirsky, R., Jessen, K.R., 2003. Regulation of the myelin gene periaxin provides evidence for Krox-20-independent myelin-related signalling in Schwann cells. Mol. Cell. Neurosci. 23, 13–27.
Parkinson, D.B., Bhaskaran, A., Droggiti, A., Dickinson, S., D'Antonio, M., Mirsky, R., Jessen, K.R., 2004. Krox-20 inhibits Jun-NH2-terminal kinase/c-Jun to control Schwann cell proliferation and death. J. Cell Biol. 164, 385–394.
Parkinson, D.B., Bhaskaran, A., Arthur-Farraj, P., Noon, L.A., Woodhoo, A., Lloyd, A.C., Feltri, M.L., Wrabetz, L., Behrens, A., Mirsky, R., Jessen, K.R., 2008. c-Jun is a negative regulator of myelination. J. Cell Biol. 181, 625–637.
Pellegrino, R.G., Spencer, P.S., 1985. Schwann cell mitosis in response to regenerating peripheral axons in vivo. Brain Res. 341, 16–25.
Peng, H.B., Ali, A.A., Dai, Z., Daggett, D.F., Raulo, E., Rauvala, H., 1995. The role of heparin-binding growth-associated molecule (HB-GAM) in the postsynaptic induction in cultured muscle cells. J. Neurosci. 15, 3027–3038.
Pereira, J.A., Lebrun-Julien, F., Suter, U., 2012. Molecular mechanisms regulating myelination in the peripheral nervous system. Trends Neurosci. 35, 123–134.
Pfister, B.J., Gordon, T., Loverde, J.R., Kochar, A.S., Mackinnon, S.E., Cullen, D.K., 2011. Biomedical engineering strategies for peripheral nerve repair: surgical applications, state of the art, and future challenges. Crit. Rev. Biomed. Eng. 39, 81–124.
Rotshenker, S., 2011. Wallerian degeneration: the innate-immune response to traumatic nerve injury. J. Neuroinflammation 8, 109.
Salzer, J.L., 2012. Axonal regulation of Schwann cell ensheathment and myelination. J. Peripher. Nerv. Syst. 17 (Suppl. 3), 14–19.
Salzer, J.L., Brophy, P.J., Peles, E., 2008. Molecular domains of myelinated axons in the peripheral nervous system. GLIA 56, 1532–1540.
Schachner, M., 1990. Functional implications of glial cell recognition molecules. Semin. Neurosci. 2, 497–507.
Schubert, T., Friede, R.L., 1981. The role of endoneurial fibroblasts in myelin degradation. J. Neuropathol. Exp. Neurol. 40, 134–154.
Shah, N.M., Marchionni, M.A., Isaacs, I., Stroobant, P., Anderson, D.J., 1994. Glial growth factor restricts mammalian neural crest stem cells to a glial fate. Cell 77, 349–360.
Shy, M.E., Shi, Y., Wrabetz, L., Kamholz, J., Scherer, S.S., 1996. Axon–Schwann cell interactions regulate the expression of c-jun in Schwann cells. J. Neurosci. Res. 43, 511–525.
Son, Y.J., Thompson, W.J., 1995. Schwann cell processes guide regeneration of peripheral axons. Neuron 14, 125–132.
Son, Y.J., Trachtenberg, J.T., Thompson, W.J., 1996. Schwann cells induce and guide sprouting and reinnervation of neuromuscular junctions. Trends Neurosci. 19, 280–285.
Stoll, G., Muller, H.W., 1999. Nerve injury, axonal degeneration and neural regeneration: basic insights. Brain Pathol. 9, 313–325.
Stoll, G., Griffin, J.W., Li, C.Y., Trapp, B.D., 1989. Wallerian degeneration in the peripheral nervous system: participation of both Schwann cells and macrophages in myelin degradation. J. Neurocytol. 18, 671–683.
Szynkaruk, M., Kemp, S.W., Wood, M.D., Gordon, T., Borschel, G.H., 2013. Experimental and clinical evidence for use of decellularized nerve allografts in peripheral nerve gap reconstruction. Tissue Eng. Part B Rev. 19, 83–96.
Taveggia, C., Zanazzi, G., Petrylak, A., Yano, H., Rosenbluth, J., Einheber, S., Xu, X., Esper, R.M., Loeb, J.A., Shrager, P., Chao, M.V., Falls, D.L., Role, L., Salzer, J.L., 2005. Neuregulin-1 type III determines the ensheathment fate of axons. Neuron 47, 681–694.
Thaxton, C., Bhat, M.A., 2009. Myelination and regional domain differentiation of the axon. Results Probl. Cell Differ. 48, 1–28.
Titmus, M.J., Faber, D.S., 1990. Axotomy-induced alterations in the electrophysiological characteristics of neurons. Prog. Neurobiol. 35, 1–51.
Topilko, P., Schneider-Maunoury, S., Levi, G., Baron-Van, E.A., Chennoufi, A.B., Seitanidou, T., Babinet, C., Charnay, P., 1994. Krox-20 controls myelination in the peripheral nervous system. Nature 371, 796–799.

Tucker, K.L., Meyer, M., Barde, Y.A., 2001. Neurotrophins are required for nerve growth during development. Nat. Neurosci. 4, 29–37.
Verge, V.M., Gratto, K.A., Karchewski, L.A., Richardson, P.M., 1996. Neurotrophins and nerve injury in the adult. Philos. Trans. R. Soc. Lond. B Biol. Sci. 351, 423–430.
Vrbova, G., Mehra, N., Shanmuganathan, H., Tyreman, N., Schachner, M., Gordon, T., 2009. Chemical communication between regenerating motor axons and Schwann cells in the growth pathway. Eur. J. Neurosci. 30, 366–375.
Vyas, A., Li, Z., Aspalter, M., Feiner, J., Hoke, A., Zhou, C., O'Daly, A., Abdullah, M., Rohde, C., Brushart, T.M., 2010. An in vitro model of adult mammalian nerve repair. Exp. Neurol. 223, 112–118.
Wan, L.D., Xia, R., Ding, W.L., 2010. Electrical stimulation enhanced remyelination of injured sciatic nerves by increasing neurotrophins. Neurosciences 169, 1029–1038.
Wang, J.Y., Miller, S.J., Falls, D.L., 2001. The N-terminal region of neuregulin isoforms determines the accumulation of cell surface and released neuregulin ectodomain. J. Biol. Chem. 276, 2841–2851.
Waxman, S.G., Bennett, M.V., 1972. Relative conduction velocities of small myelinated and non-myelinated fibres in the central nervous system. Nat. New Biol. 238, 217–219.
Winseck, A.K., Oppenheim, R.W., 2006. An in vivo analysis of Schwann cell programmed cell death in embryonic mice: the role of axons, glial growth factor, and the pro-apoptotic gene Bax. Eur. J. Neurosci. 24, 2105–2117.
Winseck, A.K., Caldero, J., Ciutat, D., Prevette, D., Scott, S.A., Wang, G., Esquerda, J.E., Oppenheim, R.W., 2002. In vivo analysis of Schwann cell programmed cell death in the embryonic chick: regulation by axons and glial growth factor. J. Neurosci. 22, 4509–4521.
Witzel, C., Rohde, C., Brushart, T.M., 2005. Pathway sampling by regenerating peripheral axons. J. Comp. Neurol. 485, 183–190.
Wolpowitz, D., Mason, T.B., Dietrich, P., Mendelsohn, M., Talmage, D.A., Role, L.W., 2000. Cysteine-rich domain isoforms of the neuregulin-1 gene are required for maintenance of peripheral synapses. Neuron 25, 79–91.
Woodhoo, A., Alonso, M.B., Droggiti, A., Turmaine, M., D'Antonio, M., Parkinson, D.B., Wilton, D.K., Al-Shawi, R., Simons, P., Shen, J., Guillemot, F., Radtke, F., Meijer, D., Feltri, M.L., Wrabetz, L., Mirsky, R., Jessen, K.R., 2009. Notch controls embryonic Schwann cell differentiation, postnatal myelination and adult plasticity. Nat. Neurosci. 12, 839–847.
Zhang, Y., Bekku, Y., Dzhashiashvili, Y., Armenti, S., Meng, X., Sasaki, Y., Milbrandt, J., Salzer, J.L., 2012. Assembly and maintenance of nodes of Ranvier rely on distinct sources of proteins and targeting mechanisms. Neuron 73, 92–107.
Zigmond, R.E., 2011. gp130 Cytokines are positive signals triggering changes in gene expression and axon outgrowth in peripheral neurons following injury. Front. Mol. Neurosci. 4, 62.
Zigmond, R.E., 2012. Cytokines that promote nerve regeneration. Exp. Neurol. 238, 101–106.

Experimental Neurology 223 (2010) 192–202

Contents lists available at ScienceDirect

Experimental Neurology

journal homepage: www.elsevier.com/locate/yexnr

Brief post-surgical electrical stimulation accelerates axon regeneration and muscle reinnervation without affecting the functional measures in carpal tunnel syndrome patients

Tessa Gordon, Nasim Amirjani, David C. Edwards, K. Ming Chan *

Division of Physical Medicine and Rehabilitation/Center for Neuroscience, University of Alberta, 525 Heritage Medical Research Centre, Edmonton, Alberta, Canada T6G 2S2

ARTICLE INFO

Article history:
Received 1 April 2009
Revised 23 September 2009
Accepted 25 September 2009
Available online 1 October 2009

Keywords:
Electrical stimulation
Motor unit numbers
Peripheral nerve injury
Reinnervation
Motor evoked potential
Sensory evoked potential
Hand muscles
Human
Behavior

ABSTRACT

Electrical stimulation (ES) of injured peripheral nerves accelerates axonal regeneration in laboratory animals. However, clinical applicability of this intervention has never been investigated in human subjects. The aim of this pilot study was to determine the effect of ES on axonal regeneration after surgery in patients with median nerve compression in the carpal tunnel causing marked motor axonal loss. A randomized control trial was conducted to provide proof of principle for ES-induced acceleration of axon regeneration in human patients. Carpel tunnel release surgery (CTRS) was performed and in the stimulation group of patients, stainless steel electrode wires placed alongside the median nerve proximal to the surgical decompression site for immediate 1 h 20 Hz bipolar ES. Subjects were followed for a year at regular intervals. Axonal regeneration was quantified using motor unit number estimation (MUNE) and sensory and motor nerve conduction studies. Purdue Pegboard Test, Semmes Weinstein Monofilaments, and Levine's Self-Assessment Questionnaire were used to assess functional recovery. The stimulation group had significant axonal regeneration 6–8 months after the CTRS when the MUNE increased to 290 ± 140 (mean $\pm$ SD) motor units (MU) from 150 ± 62 MU at baseline ($p<0.05$). In comparison, MUNE did not significantly improve in the control group ($p>0.2$). Terminal motor latency significantly accelerated in the stimulation group but not the control group ($p>0.1$). Sensory nerve conduction values significantly improved in the stimulation group earlier than the controls. Other outcome measures showed a significant improvement in both patient groups. We conclude that brief low frequency ES accelerates axonal regeneration and target reinnervation in humans.

© 2009 Elsevier Inc. All rights reserved.

Introduction

It is well known that, in man, functional recovery after peripheral nerve injuries is frequently poor despite the regenerative capacity of injured neurons and the permissive growth environment provided by the Schwann cells in the distal nerve stumps (Fu and Gordon., 1997; Gordon et al., 2003, 2009; Kline and Kim, 2008). Although poor functional recovery especially after proximal nerve injuries has generally been attributed to irreversible denervation atrophy of targets (Kline and Kim, 2008; Sunderland, 1978), progressive decline in the capacities of the neurons and Schwann cells to regenerate and support regeneration are now recognized for decline to ~5% in numbers of neurons that regenerate over time and distance (Fu and Gordon, 1995a,b; Sulaiman and Gordon, 2000; You et al., 1997).

Axon outgrowth is another factor that delays axon regeneration with a surprisingly long period of ~1 month required for all motoneurons to regenerate their axons across a surgical repair site in rats (Brushart et al., 2002). This "staggered axonal regeneration" with wandering of axons within the poorly organized extracellular matrix of the suture site into which Schwann cells migrate, culminates in many weeks for all neurons to regenerate their axons within the distal nerve stumps (Al Majed et al., 2000a; Witzel et al., 2005). Given the sluggish movement of Schwann cells in humans, the delayed outgrowth at the suture site may be even longer (Wood and Bunge, personal communication).

A 1-h period of low frequency electrical stimulation (ES) of surgically repaired rat hindlimb nerves accelerates axon outgrowth to promote regeneration of all motor axons within 3 rather than 8–10 weeks and with similar effect on sensory nerve regeneration (Al Majed et al., 2000b; Brushart et al., 2002, 2005; Geremia et al., 2007). Similar effects of ES in mice have been reported (Ahlborn et al., 2007; English et al., 2007). The important unanswered question that remains is whether this acceleration translates into earlier target reinnervation. More rapid recovery of muscle contractile force and evoked withdrawal reflexes after ES of crushed nerves are consistent with the accelerating ES effect on axon outgrowth but these outcome measures failed to distinguish whether ES promotes early axon regeneration of more neurons or it promotes sprouting and in turn,

* Corresponding author. Fax: +1 780 492 1617.
E-mail address: ming.chan@ualberta.ca (K.M. Chan).

0014-4886/$ – see front matter © 2009 Elsevier Inc. All rights reserved.
doi:10.1016/j.expneurol.2009.09.020

earlier muscle force recovery through reinnervation (Nix and Hopf, 1983; Pockett and Gavin, 1985).

In this study, we asked whether ES accelerates nerve regeneration and target reinnervation in a human model of median nerve crush injury, carpal tunnel syndrome (CTS). In selected patients with clear evidence of at least 50% axonal loss, motor unit number estimation (MUNE) was used to evaluate how many axons reinnervated target thenar muscles over time, electrophysiological recordings to evaluate time course of regeneration of sensory as well as motor axons, and behavioral measures to evaluate functional outcomes. A randomized controlled pilot study was carried out to provide proof of principle that electrical stimulation accelerates axon regeneration and promotes more rapid reinnervation of denervated targets by the regenerating axons.

Materials and methods

This was a randomized controlled clinical trial that complied with the guidelines of and was approved by the Human Research Ethics Board at the University of Alberta. All subjects gave their informed consent.

Participants

Patients with carpal tunnel syndrome (CTS) were recruited from a university hospital electromyography clinic. The inclusion criterion used in this study was the presence of at least one of the following constellation of symptoms: (1) numbness and tingling in the median nerve distribution, (2) precipitation of these symptoms by repetitive hand activities and relieved by resting, rubbing, and shaking the hand, (3) nocturnal awakening by such sensory symptoms and (4) weakness of thumb abduction and thenar muscle atrophy. Subsequently, the presence of median nerve compression was confirmed by electrophysiological studies. Conventionally, confirmation of the diagnosis of CTS and classification of its severity are commonly based on nerve conduction results (Padua et al., 1997). Based on those criteria, patients with moderate and severe CTS who had not responded to conservative treatments were recruited for this study. Patients with electrophysiological evidence of conduction block across the carpal tunnel were excluded because in those cases, changes in MUNE cannot be meaningfully interpreted. Other exclusion criteria were presence of other neurological conditions and previous carpal tunnel release surgery (CTRS). We evaluated these factors through interviews and clinical examination. When indicated, further electrophysiological studies and investigations were carried out. The ulnar and superficial radial nerves were evaluated through clinical examination and electrophysiological studies to rule out other peripheral neuropathies which may have contributed to the hand symptoms.

Conventional nerve conduction study

All sensory and motor nerve conduction studies were performed on patients using a Viking Select EMG machine (Nicolet Biomedical, Minneapolis). Sensory and motor nerve conduction studies of the median nerve were done using standard techniques (Dumitru, 1995).

Median sensory nerve conduction study

The hand was cleansed with rubbing alcohol and the skin temperature was maintained at 32–34 °C with an infrared heatlamp. Disposable silver/silver chloride surface strip electrodes (Nicolet VIASYS Healthcare), measuring 1×2.5 cm, were used. The recording electrode was placed on the proximal interphalangeal joint (G1) and the reference electrode on the distal interphalangeal joint of the third digit (G2) (Fig. 1). A ground electrode (Gd) was placed on the dorsum of the hand. The median nerve was stimulated in mid palm and also just proximal to the distal wrist crease at Sw and Sp. The transcarpal sensory conduction velocity and the negative peak amplitude of the sensory nerve action potential (SNAP) were measured.

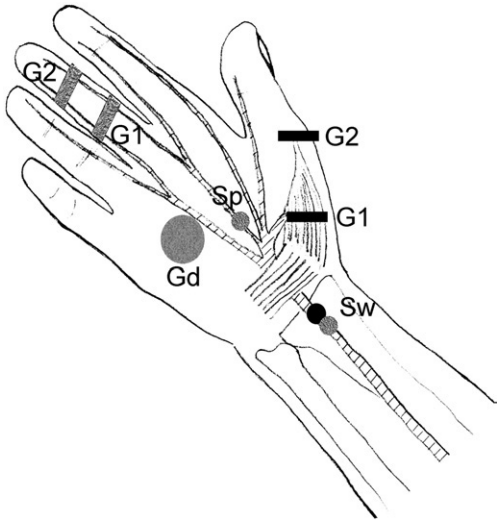


Fig. 1. Experimental setup for the nerve conduction studies. G1 is the recording electrode, G2 the reference electrode. Gd is the ground electrode placed on the dorsum of the hand. The sensory nerves were stimulated at the wrist (Sw) and at the palm (Sp). The stimulating and recording electrodes used for the motor conduction study are shown in solid black color while those used for the sensory conduction study are shown in stippled grey color. Detailed descriptions of the methods are given in the text.

Median motor nerve conduction study

A disposable recording surface strip electrode was placed over the motor point on the thenar eminence muscles with a reference electrode placed over the dorsal aspect of the first metacarpophalangeal joint (Fig. 1). The median nerve was stimulated at supramaximal intensity at the wrist (Sw) (8 cm proximal to the recording electrode) and also at the elbow. The negative peak amplitude of the maximal compound muscle action potential, terminal motor latency and conduction velocity in the forearm were measured. The median nerve was also stimulated at the palm (Sp). Those patients with evidence of conduction block across the carpal tunnel were excluded from the study.

Motor unit number estimation (MUNE)

MUNE was performed on all patients using the multiple point stimulation technique to determine the number of motoneurons that regenerate their axons and innervate thenar muscles (Doherty et al., 1995). This was done using proprietary software on an Advantage EMG machine (Neurosoft, Virginia).

Recording

Disposable, self-adhesive surface electrodes over the thenar muscles of the thumb were used to detect the maximum compound muscle action potential (CMAP) and surface-detected motor unit action potential (S-MUAP) (Fig. 2). Placement of the electrodes was the same as that used for motor nerve conduction study. A 3×3 cm metal plate was positioned on the back of the hand as a ground. The bandpass filter was set at 5–2000 Hz.

Stimulation

Electrical stimulation of the nerve was performed with a hand-held constant-current bipolar surface bar stimulator. The maximum CMAP of the median nerve was evoked by stimulating the median nerve at the wrist at 10 % above the maximal intensity with a stimulus duration of 0.01 ms (Fig. 2B). The course of the median nerve was mapped from the elbow to the axilla by advancing the bar

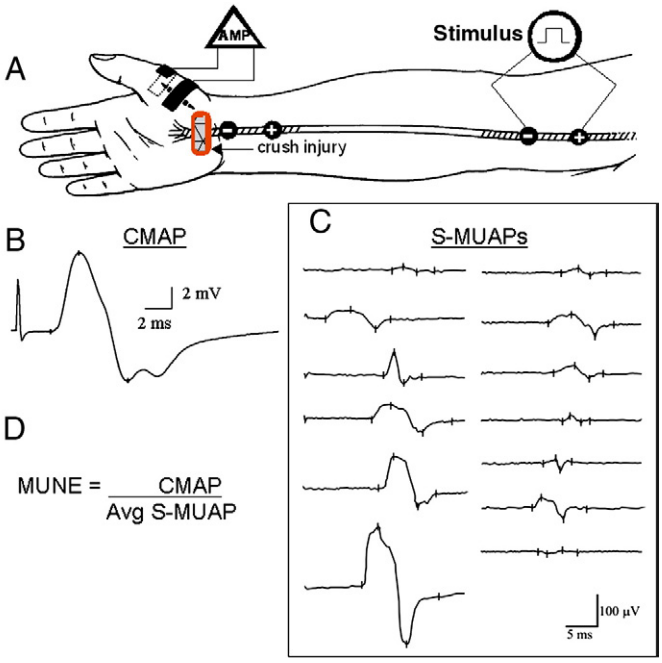


Fig. 2. The experimental setup for motor unit number estimation. (A) Placement of the recording and reference electrodes depicted are identical to those used for the motor conduction study in Fig. 1. Shaded stretches of the median nerve are the superficial portions at the wrist and between the elbow and axilla used for multiple point stimulation. (B) The maximal compound motor action potential (CMAP) was recorded in response to maximal electrical stimulation of the median nerve. (C) A collection of 13 surface recorded motor unit action potentials (S-MUAPs) was activated by stimulation of the median nerve along the arm with finely graded, low intensity threshold stimulation. (D) A motor unit number estimation (MUNE) was then calculated by dividing the CMAP by the average S-MUAP.

stimulator over the medial aspect of the arm at 1–2 cm intervals (Fig. 2A). Because the median and ulnar nerves are in close proximity in the upper arm, it was necessary to avoid co-stimulation of the ulnar nerve while mapping the course of the median nerve. Co-activation of the ulnar nerve was recognized by (1) an initial positive deflection of the CMAP, (2) abduction of the fifth digit, and (3) the radiation of an electrical sensation into the fourth and fifth digits. In earlier experiments, we also co-recorded from the hypothenar eminence and found that when the above conditions were avoided, there was no detectable action potential generated by the hypothenar muscles.

Using the same recording electrodes, S-MUAPs with the lowest stimulus thresholds were elicited by stimulating the median nerve at multiple sites where the nerve is more superficially located at the wrist and between the elbow and the axilla (Fig. 2C). Stimulation was performed at 1 Hz with gradually increasing intensity until the first reproducible, "all-or-none" S-MUAP was evoked. To increase the yield, the next higher threshold S-MUAP could sometimes be obtained through template subtraction. By this means, up to a maximum of 3 S-MUAPs were acquired at each site and a total of 13 to 20 S-MUAPs was stored in computer memory. The mean peak-to-peak amplitude of this sample of S-MUAPs was calculated using "datapoint-by-datapoint" summation. All S-MAUPs were temporally aligned at the same onset latency before they were averaged. The motor unit number estimate was obtained using the following equation:

$$\frac{\text{Peak–to–peak amplitude of the maximum CMAP}}{\text{Peak–to–peak amplitude of the average S–MUAP}}$$

Behavioral measures

(1) *Levine's Self-Assessment Questionnaire for CTS.* To assess the subjective symptoms, patients were asked to complete the Levine's Self-Assessment Questionnaire for CTS symptom severity before and at intervals after the surgery (Levine et al., 1993). This questionnaire consisted of two parts: (1) symptom severity scale comprised of 11 items scored on a Likert scale inquiring about pain, paraesthesia, numbness, weakness, nocturnal symptoms and overall functional status, and (2) functional status scale comprised of 8 questions regarding activities of daily life commonly affected by CTS. The symptom severity scores ranged from 1 to 5 with 1 representing no symptoms and 5, very severe symptoms. The functional status scores also ranged from 1: no difficulty to do a task, to 5: inability to do a task. The patients were asked to rate the severity of the symptoms on the hand that was to be operated on.

(2) *Semmes Weinstein Monofilaments (SWM).* As sensory complaints are prominent in CTS, we used a test kit of 20 SWM (Sammons Preston Rolyan, Canada) to assess the impact of the CTS with and without electrical stimulation (ES) treatments on hand sensation. This tool, which examines the sensation threshold, has proven reliability (Bell-Krotoski and Tomancik, 1987) and is utilized in the clinical evaluation of peripheral nerve diseases such as diabetic neuropathy (Imai et al., 1989; Lee et al., 2003). Since pressure sensation involves primarily small, unmyelinated or poorly myelinated nerve fibers, this test complements the convention sensory nerve conduction study well because the latter only evaluates large myelinated sensory nerve fibers.
Subjects were asked to place their hands over a table, and keep their eyes closed for the duration of this test. Each filament, starting with the smallest caliber, was tested over the pulp of digits. The filament was applied perpendicularly for 1 to 1.5 s in three trials. Subjects were asked to indicate the area where the filament was felt. We examined the sensory threshold of all fingers in random order. A positive response in at least 2 of the 3 trials marked the sensory threshold. We used the test results of the third digit where sensory nerve conduction study was also done, for data analysis.

(3) *The Purdue Pegboard Test.* We used the Purdue Pegboard Test (Model 32020, Lafayette Instrument Company, IN, USA) to monitor the impact of CTS with and without ES on manual dexterity. The Purdue Pegboard Test is a standardized hand function tool with proven validity and reliability in the functional evaluation of CTS patients. It consisted of 50 holes arranged in two parallel columns. Subjects were instructed to start the test on a verbal cue, while an examiner timed the test with a stopwatch. They had 30 s to fill the holes with pegs, initially with the hand that was intended for CTS surgery and then with the other hand. Each subset was repeated three times to obtain an average. Test scores equaled the number of filled holes.

Interventions

Subjects were randomized to the control or the stimulation group by using the random number generation function in a commercially available software program (Excel, Microsoft Inc.). The control group underwent open carpal tunnel release surgery (CTRS) only. The stimulation group underwent CTRS followed by 1 h of electrical stimulation of the median nerve.

Surgical technique

Operations were performed by a plastic surgeon (D.E.). The surgical procedure was the standard CTRS without epineurotomy or neurolysis of the median nerve (Rosenbaum and Ochoa, 1993). A tourniquet was inflated over the forearm. The surgeon drew a curvilinear mark over the palm to guide the incision. The transverse carpal ligament was divided along the ulnar side of the incision. No

further intervention was employed in the control group. For the stimulation group, two sterile 30 gauge stainless steel wires, insulated except 1 cm at the tip, were placed over the median nerve. One electrode was positioned at the proximal end and the other at the distal end of the incision. To record the CMAP during the post-surgical ES, the surgeon placed two surface electrodes (TECA, Oxford Instruments), one over the motor point on the thenar eminence muscles (G1) and the other over the dorsal aspect of the first metacarpophalangeal joint (G2) (see Fig. 1).

Electrical stimulation

Subjects in the stimulation group were transferred to a neurophysiology laboratory after CTRS. There was an approximately 30 min delay between termination of CTRS and initiation of electrical stimulation. With the patient in the lying position, the operated hand was stabilized in an elevated position. The stimulating electrodes were connected to a Grass (SD9) stimulator: the proximal wire electrode was connected to the cathode and the distal one to the anode. The surface electrodes on the thenar eminence were connected to an EMG machine (NeuroSoft Inc., Virginia). We gradually increased the stimulation intensity to the maximal tolerance limit (4–6 V, 0.1–0.8 ms duration) as a continuous 20 Hz train for 1 h. These intensities were sufficient to induce a fused tetanic contraction but low enough to not induce excessive discomfort. This protocol, including configuration of the stimulus polarities, frequency and duration parameters, was so chosen to approximate that used in our animal studies (Al Majed et al., 2000a,b, 2004; Brushart et al., 2002). The only exception is that supramaximal intensities used in animal studies was not feasible in human subjects. The CMAP of the thenar muscles were also monitored. After the termination of stimulation, electrodes were pulled out and discarded.

Outcomes

To compare the effectiveness of electrical stimulation with control CTRS, the subjects were evaluated twice before the operation (pre-op1 and pre-op2) to ensure reliability of the tests. Subjects were then followed for a year at 3 time points after the CTRS. The follow-up schedule was: (1) post-op1: 3rd month, (2) post-op2: 6th to 8th month, and (3) post-op3: 12th month. The 3rd month was selected for the first assessment based on the assumptions that the most optimal axonal growth rate is 1 mm/day and the distance between the compression site and the thenar muscles is ~70 to 80 mm, depending on the size of the hand. At each post-operative assessment, all the baseline measures were repeated.

Motor unit numbers and muscle function

To ascertain whether the motor unit number in CTS patients had an impact on their muscle function, we also measured muscle bulk and force generating capacity in a separate sample of 8 subjects. Cross sectional area of the mid belly of the median innervated thenar muscles (abductor pollicis brevis, opponent pollicis and superficial head of flexor pollicis brevis) was measured using ultrasound imaging (Acuson Sequoia, Siemens, Germany). Mid belly of the muscles was located at the mid shaft of the 1st metacarpal bone. The medial border of the thenar muscles lies over the 2nd metacarpal bone while the lateral border is defined by the 1st metacarpal bone (see Fig. 3A). Superficial head of the flexor pollicis brevis, deepest of the three median innervated thenar muscles, is at the level of the flexor pollicis longus tendon. The tendon served as a useful landmark because it can be easily discerned by its shape and high echogenicity (see Fig. 3A). The perimeter of these muscles was traced and the cross sectional area calculated using the ultrasound machine bundled software.

Twitch force of the median nerve innervated thenar muscles was recorded using a LCCA-25 load cell (Omega Canada, Laval, Quebec) connected to the thumb via a loop placed around the base of the 1st proximal phalanx. Based on previous studies, the maximum resultant vector of the median innervated thenar muscles is at a 45° angle plane from the palm along which the load cell was aligned. After the hand and forearm were secured to the force platform by inelastic Velcro straps, the median nerve was stimulated supramaximally at the wrist and the twitch tension recorded (see Fig. 3C).

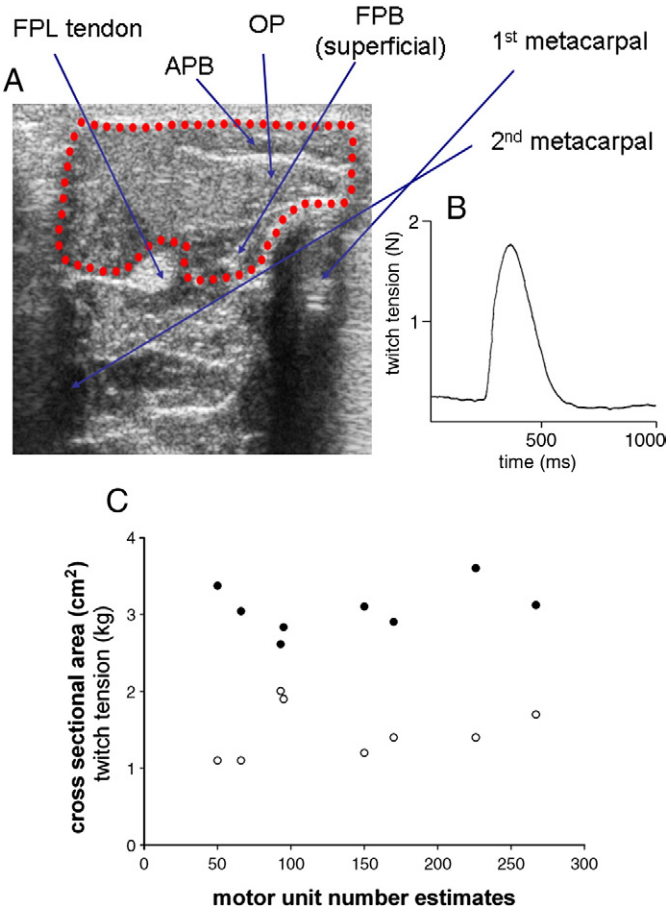


Fig. 3. Muscle bulk and contractile capacity of the median innervated thenar muscles in carpal tunnel syndrome patients. Cross sectional area of the median nerve innervated thenar muscles (APB—abductor pollicis brevis, OP—opponens pollicis, superficial head of the FPB—flexor pollicis brevis) was measured using ultrasound. An example is shown in panel A where the perimeter was outlined by a dotted line. Tendon of the flexor pollicis longus (FPL) muscle is highly echogenic and serves as a useful landmark. The twitch tension of the thenar muscles from the same patient is shown in panel B. As can be seen in panel C, despite the wide range of motor unit numbers in this sample of CTS patients, there was no significant correlations with the cross sectional areas (solid circles) ($r=0.32$, $p=0.43$) or twitch tension (open circles) ($r=0.18$, $p=0.67$).

Statistical analysis

The statistical program SPSS 12.0 for Windows was used in this study. Sample size estimation was done based on published animal data with MUNE being the primary outcome measure (Al Majed et al., 2000b). Assuming a difference in treatment effect size of 26%, standard deviation of 30%, with $\alpha=0.05$ and $\beta=0.20$, to have sufficient power to detect a significant difference, 20 subjects would be required for this study. Test–retest reliability of MUNE, a major outcome measure used in this study, was tested using linear regression analysis. Using Shapiro–Wilk Test of normality, we found that nerve conduction studies, and SWM results were significantly skewed from the Gaussian distribution ($p<0.05$). Additionally, Mauchley's test of sphericity was statistically significant ($p<0.05$) for the Levine's Self-Assessment Questionnaire and Purdue Pegboard

Test scores rendering parametric tests unsuitable. To be conservative and to reduce the chances of type I error, we decided to use non-parametric statistical methods for their analysis. We used Kendall's W and Wilcoxon Signed Ranks test to compare those outcome measures within each group of subjects. To examine whether the preoperative outcome measure values were significantly different between the two groups, the Kruskal–Wallis test was employed. In contrast, the MUNE results were normally distributed and the variance was homogeneous between the treatment and control groups, changes within each group following intervention were therefore analyzed using paired Student's *t* tests. In addition, comparisons of changes between the two groups following intervention were analyzed using univariate general linear model statistics. Linear regression analysis between the MUNE, cross sectional area and twitch force of the thenar muscles was done. The statistical significance was set at $p<0.05$.

Results

Subjects with carpal tunnel syndrome

Twenty five eligible CTS subjects participated in the study, all of whom had surgical decompression of the carpal tunnel under local anesthesia (1% lidocaine). However, 4 subjects (2 males and 2 females) withdrew from the study because of development of other medical conditions or occupational commitments which prevented them to return for follow up. Two of these patients belonged to the control and 2 to the stimulation group. Therefore, the results are from 21 subjects: 8 males and 13 females. The patients were 20 to 86 years old, with a mean (±SD) age of 56±17 years. The breakdown of age and sex and the physical attributes in both groups are shown in Table 1. The subjects were housewives, nurses, medical and laboratory technicians, cooks, manual laborers, and retirees. All had had progressive symptoms for at least 2 years.

Eighteen subjects were right hand dominant. Although they all had bilateral symptoms, it was more severe in their dominant hand that was subsequently operated. Ten patients were assigned to the control group (no electrical stimulation, ES) and 11 patients to the stimulation group (1 h 20 Hz ES). All subjects attended the first post-operative follow-up, whereas 19 of them were available for the second and third post-operative evaluations. Two of the subjects who missed appointments belonged to the control and one to the stimulation group.

Muscle denervation in severe carpal tunnel syndrome

We stimulated the median nerve proximal (Sw) and distal (Sp) to the site of compression at the carpal tunnel and recorded the evoked compound muscle action potential (CMAP) with the recording electrode (G1) placed over the muscles at the thenar eminence (Fig. 1). As shown in Fig. 4, we discriminated and excluded patients with early CTS on the basis of conduction block where CMAPs evoked distal to the compression site closer to the thenar muscles were much larger than the CMAPs evoked proximal to the compression site (Fig. 4B). Only those patients in whom the amplitude of the CMAP evoked above and below the sites of compression was equally reduced, were selected (Fig. 4A).

Table 1
Mean (±SE) of age, gender and handedness of the human patient subjects in control (no electrical stimulation) and stimulation (1 h 20 Hz electrical stimulation) groups.

	Control	Stimulated
Age	61±16 years.	53±18 years.
Gender	7 females: 3 males	6 females: 5 males
Handedness	2 left:8 right	1 left:10 right

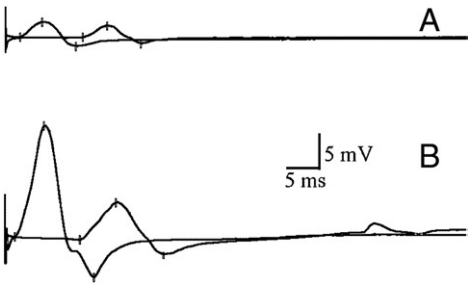


Fig. 4. Discrimination of nerve injury from conduction block in carpal tunnel syndrome patients. Examples of recordings of maximal CMAPs in (A) a patient with marked axonal loss in the median nerve where amplitudes of the CMAPs evoked at the wrist and palm were equally reduced, and (B) another patient with conduction block of the median nerve at the carpal tunnel where the amplitude of the CMAP was reduced at the site proximal to the carpal tunnel as compared to the normal CMAP amplitude evoked by stimulation below the carpal tunnel. The latter patients were excluded from the study.

Using the multiple point stimulation technique for motor unit number estimation (MUNE), Doherty and Brown reported 288±23 (mean±SE) motor units (MU) in the thenar muscles of healthy subjects (Doherty and Brown, 1993). The preoperative MUNE in the selected patients with severe CTS was reduced by ~50% as compared to that in the healthy subjects (Fig. 5A). The estimated number of innervated MUs was the same in 2 preoperative recording sessions and the numbers were also not different in the control and stimulated groups of patients.

The underlying axonal injury seen in these CTS patients was likely long-standing as reflected by the substantially larger single surface recorded motor unit action potential (S-MUAP) amplitudes recorded in the 2 preoperative recording sessions as compared to healthy subjects (Fig. 5B). Amplitudes of the S-MUAP in healthy subjects reported by Doherty and Brown were 0.91±0.11% of the maximum CMAP (Doherty and Brown, 1997). In contrast, for the CTS subjects in

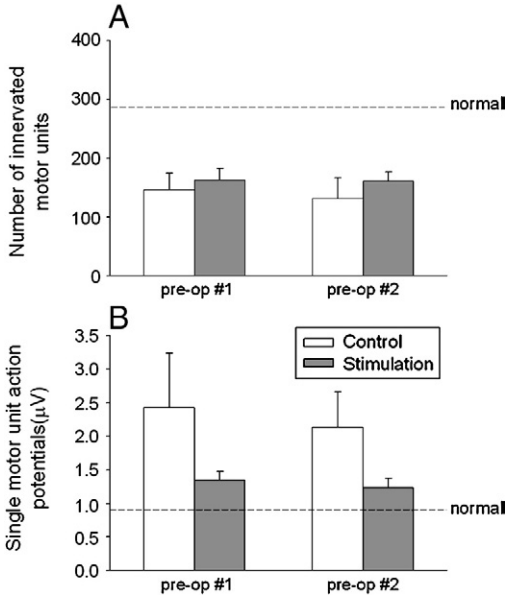


Fig. 5. Reduced numbers of motor units in carpal tunnel syndrome (CTS) patients. (A) The number (mean±SE) of innervated motor units (MUs) that were determined with MUNE in 2 preoperative recording sessions was substantially reduced compared to healthy controls (broken line). MU numbers were reduced in both the control (non-stimulated) and experimental (stimulation) groups of CTS patients preoperatively. (B) The amplitude (mean±SE) of surface recorded motor unit action potentials (S-MUAPs) from the thenar muscles in the same recording sessions. S-MUAPs were larger than in normal subjects (broken line), likely reflecting chronic loss of motor axons in both groups of patients.

this study, amplitude of the S-MUAPs was 1.92 ± 0.44% of maximum CMAP (range 0.06–61%; median ± 95%CI = 0.64 ± 1.06%). Although amplitudes of the S-MUAPs in the control group was substantially larger than the stimulation group, the difference was not statistically significant ($p = 0.22$). This shift of the distribution to larger values indicated that the fewer surviving MUs had had adequate time to sprout and enlarge by reinnervation of denervated muscle fibers.

Brief electrical stimulation accelerates reinnervation of denervated muscle in severe carpal tunnel syndrome

Brief (1 h) ES of surgically repaired rat peripheral nerve accelerated axon regeneration across the repair site without affecting the rate of axon regeneration within the distal nerve stump (Al Majed et al., 2000b; Brushart et al., 2002). We used the same stimulation regime, in this study of CTS patients. MUNE was used to evaluate whether ES immediately after CTRS in severe CTS patients, promotes and/or accelerates reinnervation of denervated thenar muscles. In the control (non-stimulated) group of patients, the numbers of innervated MUs were determined by MUNE at regular intervals up to 12 months after CTRS. There was no significant change in the MUNE even up to a year after surgery, even though there was a trend for the number to increase between 6 and 12 months (Fig. 6A). In contrast, there was already a trend for the MUNE to increase within 3 months in the patients after CTRS and ES (Fig. 6B). By 6–8 months, the number of MUs in the thenar muscles had increased significantly, comparable to the numbers reported in healthy subjects. Hence, in striking contrast to the failure of regenerating nerves after CTRS alone, *all* the regenerating motor axons in the stimulation group had made functional connections with denervated muscle fibers by 6–8 months.

The mean amplitude of the S-MUAPs 3 months after CTRS without ES did not change significantly compared to preoperative baseline (Fig. 6C). In contrast, 3 months after CTRS with ES, there was a significant reduction in the mean S-MUAP amplitude as compared to preoperative values (from 1.35% maximum CMAP to 0.89% maximum CMAP, Mann–Whitney *U* test) (Fig. 6D). The early reduction in the ES group indicated the presence of newly regenerated motor axons had innervated some muscle fibers while they had not in the control non-stimulated group.

Small, newly regenerated MUs contribute little to the amplitude of the maximum CMAP so that the lack of significant change in the CMAP amplitude following CTRS with and without ES was not surprising (Fig. 7). Since the maximum CMAP amplitudes were not normally distributed, they are shown as box and whisker plots where the upper and lower limits of the box represent the 75th and 25th percentiles, respectively, while the upper and lower limits of the whiskers represent the 90th and 10th percentiles, respectively. The transverse line within the box represents the median. Not surprisingly, the maximum CMAP amplitudes recorded preoperatively were smaller than in the healthy controls and they remained so throughout the postoperative follow-up period in both the control and stimulated groups of CTS patients.

Brief electrical stimulation promotes improvements in axonal conduction speeds in severe carpal tunnel syndrome

Demyelination is one of the most common sequelae of compressive neuropathy (O'Brien et al., 1987). In order to determine whether ES also affects remyelination, we measured the conduction speeds of both motor and sensory nerve fibers across the carpal tunnel. The

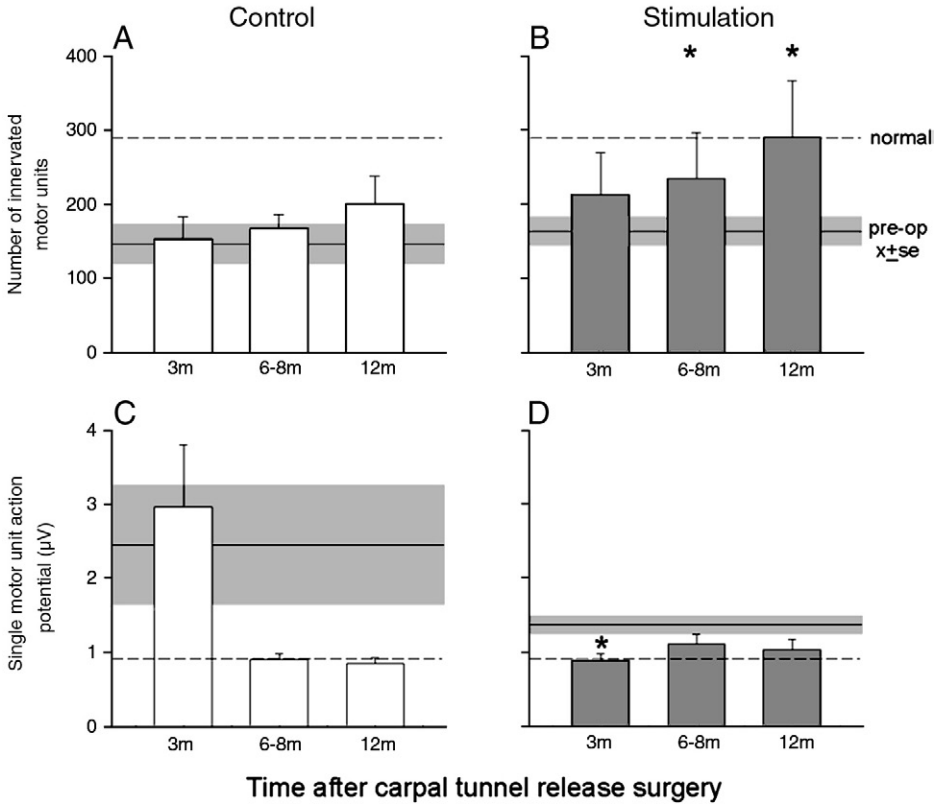


Fig. 6. Brief (1 h) 20 Hz electrical stimulation (ES) of axotomized motoneurons led to the complete reinnervation of the thenar eminence muscles. The mean(±SE) numbers of reinnervated motor units are shown in A and B and surface recorded motor unit action potential (S-MUAP) amplitudes are shown in C and D. MUNE did not increase significantly as a function of time after surgery in the control group but did in the stimulation group of CTS patients where MUNE increased progressively with a significant increase being recorded at 6–8 and 12 months after CTRS when the MUNE reaching the same level as normal healthy subjects. The increase seen in the stimulation group was likely due to new muscle fiber reinnervation as reflected by the presence of small S-MUAPs. Although the amplitudes of the S-MUAPs also declined in the control group, that did not occur until 6 months after surgery.

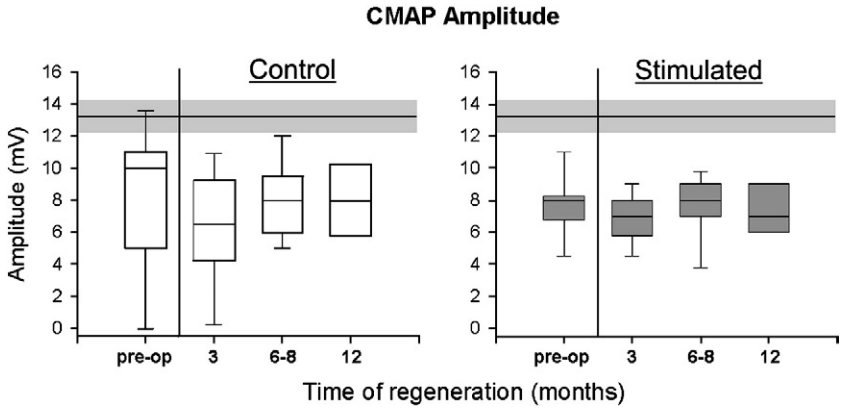


Fig. 7. Brief (1 h) 20 Hz electrical stimulation (ES) of axotomized motoneurons did not change the amplitude of the compound motor action potentials (CMAP) recorded in the thenar eminence muscles after carpal tunnel release surgery (CTRS). The median values of CMAP amplitudes did not change significantly in either (A) the control or (B) the stimulated groups of patients after intervention. The grey band represents data from the healthy control (mean ± SD). The upper and lower limits of the box represent the 75th and 25th percentiles, respectively, while the upper and lower limits of the whiskers represent the 90th and 10th percentiles, respectively. The median is represented by the line within the box.

motor terminal latency in the severe CTS patients was similarly slower than normal in both the control and stimulation groups at baseline (Fig. 8). The latency did not change significantly in the control group in the post-operative period, while, in contrast, significant acceleration in the motor latency occurred early in the stimulation group at 3 months (Fig. 8B). Motor terminal latencies from 3 months onward were the same as that for healthy subjects (Fig. 8B). Similarly, earlier recovery of conduction velocity of the sensory nerve fibers was found in the stimulation group at 3 months when amplitude of the SNAP had not yet changed significantly from pre-operative values (Figs. 9B, D). In contrast, recovery was delayed in the control patient group (Figs. 9A, C). Together, these data buttress the possibility that ES may enhance remyelination in addition to accelerating axon regeneration and muscle reinnervation.

Rapid improvements in behavioral outcomes following CTRS

In order to evaluate the functional outcome of motor and sensory target reinnervation, we chose the Purdue Pegboard Test to gauge hand performance, Semmes Weinstein Monofilaments for pressure sensation and the Levine's CTS Questionnaire for subjective symptoms. Rapid improvements in all these functional outcomes were found regardless of whether the subjects were in the control or stimulation groups (Figs. 10A, B and 11A, B). We compared the test results with those in the opposite untreated hands in order to determine whether the improvements seen in the Purdue Pegboard Test were due to practice. Since there was no change of performance in the non-treated hand, practice effect is an unlikely explanation for the improvements of hand function after CTRS in both the control and stimulation groups (Figs. 10C, D). Rather, a more likely explanation for better hand performance on the Purdue Pegboard Test was rapid recovery in pressure sensitivity at the digit tips after CTRS (Fig. 11A and B). Since smaller, poorly myelinated sensory nerve fibers are less vulnerable to degeneration due to compression (Nishimura et al., 2004), transmission along those nerve fibers can be more readily restored once the compression is alleviated. Lastly, with subjective interpretation of symptom severity on the Levine's CTS Questionnaire, the subjects reported rapid resolution of symptoms with or without stimulation (Figs. 11C, D). Given that pain and tingling sensations experienced by CTS patients are positive symptoms of sensory nerve fiber irritation, ready resolution of these symptoms is commonly observed in patients following conventional CTRS.

Motor unit number does not affect cross sectional area and twitch tension of the thenar muscles in CTS

Because damage to the median nerve in the vast majority of CTS patients is a chronic process, the remaining surviving motor axons usually have ample time to sprout and to reinnervate the muscle fibers. Indeed, previous studies on chronic axonal injury did not find significant decline in muscle force until the motor unit number fell below 90% of the control subjects (McComas et al., 1971). To test that

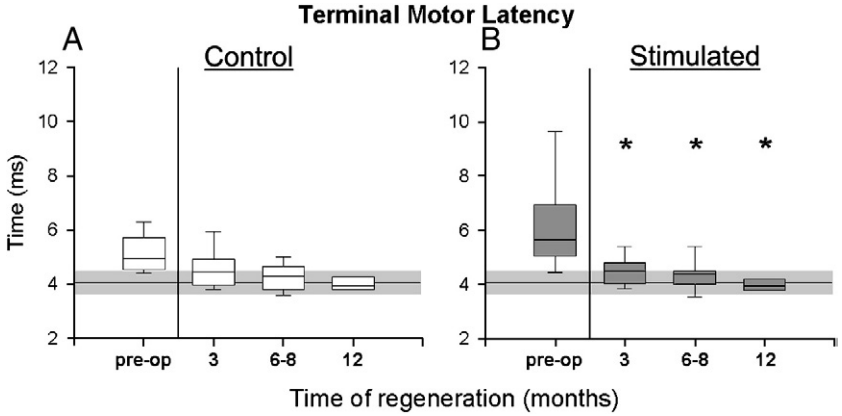


Fig. 8. Brief (1 h) 20 Hz electrical stimulation (ES) of axotomized motoneurons accelerated the reduction in terminal motor latency in the thenar eminence muscles after carpal tunnel release surgery (CTRS). The terminal motor latency declined significantly following CTRS in the stimulation group (B) but not in the control group (A). The grey band represents data from the healthy control (mean ± SD). The upper and lower limits of the box represent the 75th and 25th percentiles, respectively, while the upper and lower limits of the whiskers represent the 90th and 10th percentiles, respectively. The median is represented by the line within the box.

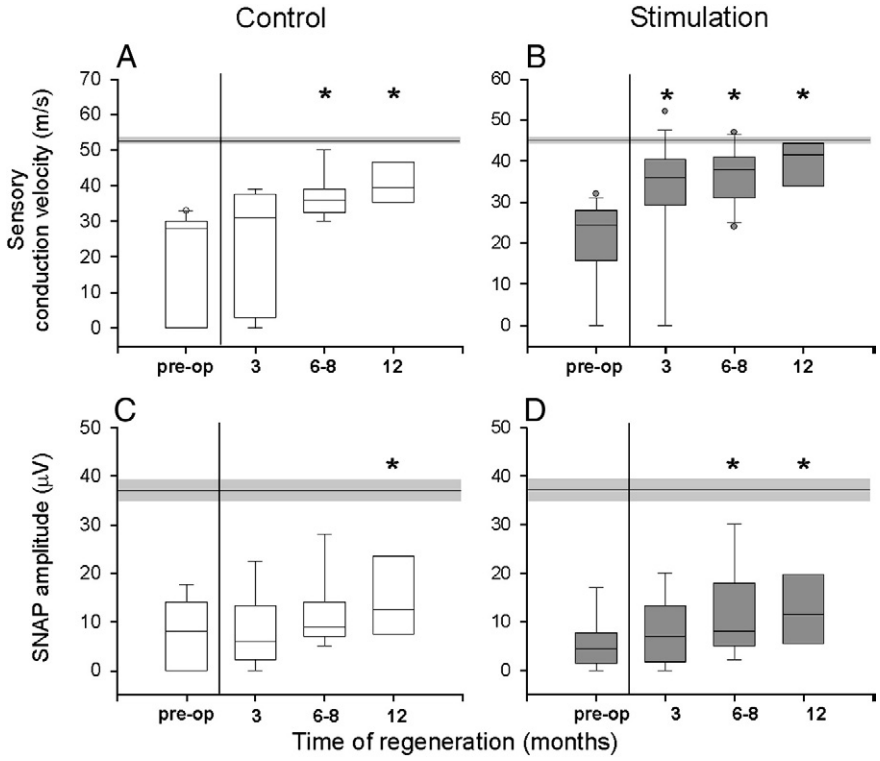


Fig. 9. Brief (1 h) 20 Hz electrical stimulation (ES) of axotomized motoneurons accelerated the increase in sensory nerve conduction velocity and the amplitude of the sensory nerve action potential (SNAP) after carpal tunnel release surgery (CTRS). Both axonal conduction velocity (B) and sensory nerve action potential amplitude (D) improved earlier in the stimulation group compared to the control group (A, C). The grey band represents data from the healthy control (mean ± SD). The upper and lower limits of the box represent the 75th and 25th percentiles, respectively, while the upper and lower limits of the whiskers represent the 90th and 10th percentiles, respectively. The median is represented by the line within the box.

hypothesis in CTS patients, we measured the cross sectional area and twitch tension of the median innervated thenar muscles in a separate sample of 8 CTS patients. Although they had motor unit numbers ranged from 50 to 267, no significant correlations between the motor unit number, cross sectional area and twitch tension were found (see Fig. 3C). These results support our contention that in a chronic axonal loss injury process such as CTS, the extent of motor axonal loss except in the most severe cases does not affect the muscle force and mass.

Discussion

This pilot study serves as proof of principle for positive outcomes of brief post-surgical ES and demonstrated that indeed, brief 1 h low frequency ES immediately following decompression surgery in patients suffering from severe CTS resulted in early and complete reinnervation of the thenar muscles. Surgery alone was not sufficient to cause significant improvement in muscle reinnervation even 1 year after the operation.

The findings are not simply due to resolution of conduction block following carpal tunnel decompression because all patients were screened for conduction block preoperatively and excluded from the study if block was evident. The findings demonstrated for the first time that the brief continuous ES at 20 Hz that accelerates axon outgrowth in animal models of nerve injury in rats (Al Majed et al., 2000b; Brushart et al., 2002, 2005; Geremia et al., 2007) and mice (Ahlborn et al., 2007; English et al., 2007) is also effective in accelerating target reinnervation in the human. Moreover these findings provide direct evidence of accelerated muscle reinnervation to account for the earlier functional recovery of muscle force and reflex discharge demonstrated in rats by Nix and Hopf (1983) and Pockett and Gavin (1985). Importantly the single bout of ES immediately after surgery, by accelerating axon outgrowth, was sufficient to result in target reinnervation 6 months later.

Since the compressive axonal injury that occurs in CTS is a chronic one, the ability for the affected motor axons to grow and regenerate is likely compromised by the delay. Diminished capacity for axonal regeneration was demonstrated in a chronic axotomy animal model where the extent of axon regeneration was reduced by up to 66% when a chronically axotomized tibial nerve was cross-sutured and regrew into a freshly cut common peroneal nerve in the rat hindlimb (Boyd and Gordon., 2002; Fu and Gordon, 1995a). With consideration of the diminished regenerative capacity of chronically injured neurons, our findings of no significant thenar muscle reinnervation even a year after carpal tunnel release without ES is perhaps not surprising. In that light, the striking regenerative capacity of axotomized median motoneurons that were electrically stimulated for 1 h after CTR surgery, was remarkable: the axon regeneration in the group of patients whose median nerve was electrical stimulated, was not only more rapid but *all* the axotomized motoneurons regenerated their axons and the MU number in the reinnervated thenar muscles was the same as that in normal healthy individuals (Fig. 6). These data imply that even chronically injured motor axons retain the ability to regenerate if they are electrically stimulated for just 1 h after surgical repair, a conclusion that is readily testable in an animal model. Death of motoneurons after prolonged axotomy at distal sites is unlikely because motoneurons can survive a year or more after chronic axotomy (Gordon et al., 1991; Vanden Noven et al., 1993).

Animal studies demonstrated that 1 h 20 Hz ES accelerates axonal outgrowth at the site of injury but *not* the rate of axonal regeneration in distal nerve stumps (Brushart et al., 2002; Udina et al., 2008). Given the distance of 70–80 mm from the site of compression in the carpal tunnel to the thenar muscle endplates in CTS patients, and assuming an approximate regeneration rate of 1 mm/day (Sunderland, 1947), the regenerating axons in the distal nerve stumps would be expected to reach the intramuscular nerve sheaths of the partially denervated

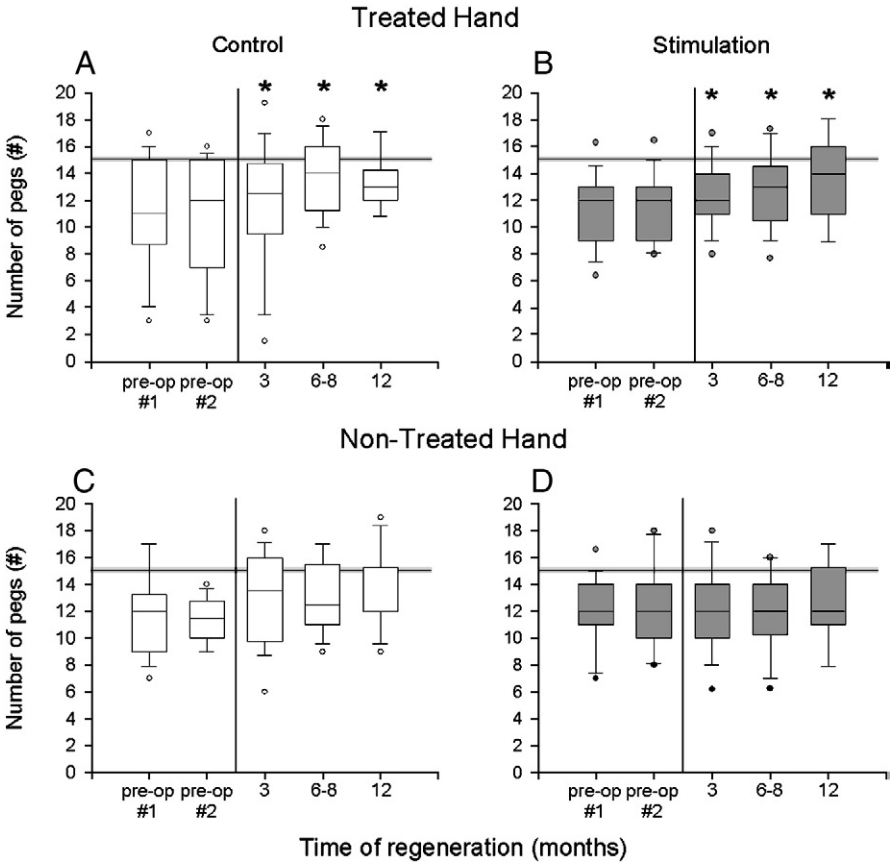


Fig. 10. Hand dexterity performance assessed by the Purdue Pegboard Test improved equally quickly after CTRS in both the control and stimulated groups of patients. The number of pegs placed by the control group (A, C) control and the stimulated group (B, D) increased significantly in the treated but not the non-treated hands. This effect is related to treatment as the non-treated hand did not show any significant improvement (C, D). The grey band represents data from the healthy control (mean ± SE). The upper and lower limits of the box represent the 75th and 25th percentiles, respectively while the upper and lower limits of the whiskers represent the 90th and 10th percentiles, respectively. The median is represented by the line within the box and the outliers are represented by the dots that lie beyond the whiskers.

thenar muscles within 3–4 months. Our finding that the MUNE did not increase significantly even as late as 12 months after CTRS without ES indicates that the progress of axon outgrowth across the site of compression is very slow. In this context, the acceleration of axon outgrowth by ES to achieve the significant muscle reinnervation by 6 months and complete muscle reinnervation by 12 months is considerable.

The motor nerve conduction studies further affirmed the positive impact of stimulations on axon regeneration: the significant improvement in the terminal motor latency of the median nerve occurred earlier in the stimulation group and was detectable as early as 3 months post-CTRS and stimulation (Fig. 8). The fact that the CMAP amplitude did not change in the stimulated group of patients following CTRS and ES is not surprising even though significant axonal regeneration had occurred, the reason being that CMAP amplitude is affected by changes in the amplitude and configuration of the constituent MUAPs (Rashidipour and Chan, 2008). In early reinnervation, MUAPs are usually small, polyphasic and contribute little to increase the CMAP amplitude. That was one of the major reasons that led to the introduction of more direct methods of estimating MU numbers (McComas, 1995).

Similar trends were also found in the sensory nerve conduction studies designed to evaluate regeneration of the large myelinated nerve fibers. Recovery of the conduction velocity and SNAP amplitude occurred earlier, by the 3rd month post-intervention in the stimulated group as opposed to the 6th month in the control group. However, these physiological differences are not likely to be functionally important as large myelinated fibers subserving vibration and proprioception sensations do not play a critical role in most daily activities (Videler et al., 2008). Rather, the ability to perceive touch and pressure subserved by small thinly myelinated nerve fibers is more important for hand function. Since those nerve fibers are less vulnerable to compressive injury, it is not surprising that there was no significant difference in the patterns of recovery in sensory symptom and hand function assessed by the Levine's Questionnaire and Purdue Pegboard Test between the control and stimulated groups of patients. Both groups reported marked symptom improvement within 3 months of surgery. Symptoms including tingling, burning and aching pain due to mechanical nerve irritation and micro-ischemia can all be readily alleviated by CTRS.

The lack of blinding in this human study was unlikely to affect the quantitative tests of axon regeneration and of muscle reinnervation. The validity of the MUNE technique used, the multiple point stimulation method, has been established (Doherty and Brown, 1993; Rashidipour and Chan, 2008) and its test–retest reliability is high (Felice, 1995; Porter et al., 2008). Therefore, despite the relatively small number of subjects and baseline inter-subject variability, the sample size was sufficient to detect the remarkable reinnervation of the denervated thenar muscles by all the injured (axotomized) motoneurons. The outcome measure tools of nerve conduction studies and the MUNE are objective measures that cannot be easily influenced by the subject or the examiner. The Levine's Self-Assessment Questionnaire for CTS was the only subjective outcome measure that had the potential to be biased by patients' knowledge about the treatment. However, in this study both the stimulation and control groups showed a significant improvement in their symptom severity by 3 months.

The molecular basis for the effects seen with post-surgical ES has been investigated in a number of recent studies (Al Majed et al., 2004;

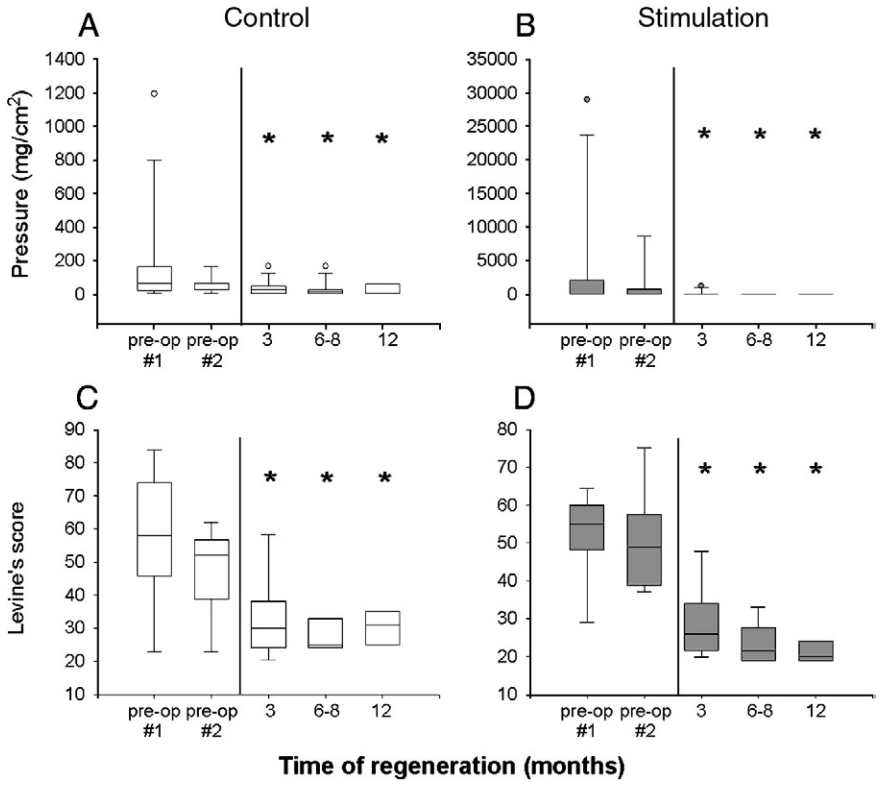


Fig. 11. The Semmes–Weinstein Monofilament Test (A, B) and the Levine's Self-Assessment Questionnaire (C, D) improved equally quickly after CTRS in both the control and stimulated groups of patients. The upper and lower limits of the box represent the 75th and 25th percentiles, respectively while the upper and lower limits of the whiskers represent the 90th and 10th percentiles, respectively. The median is represented by the line within the box and the outliers are represented by the dots that lie beyond the whiskers.

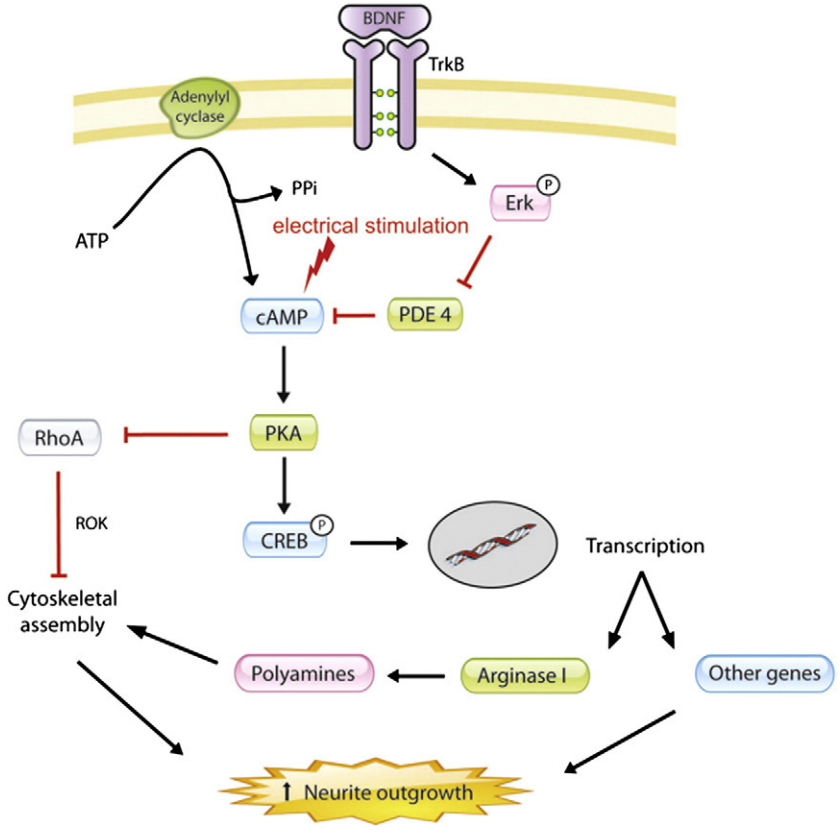


Fig. 12. Molecular mechanisms of enhanced nerve regeneration (modified from Hannila and Filbin, 2008). Electrical stimulation has been shown to upregulate cAMP that promotes nerve regeneration by activating cAMP response element binding (CREB) while inhibiting Rho via protein kinase A (PKA). See text for a detailed description.

Sharma et al., 2010; Udina et al., 2008). A key player that emerges is cyclic AMP (cAMP). Through activation of protein kinase A (PKA) and cAMP response element binding (CREB) protein, transcription of cytoskeletal proteins including actin and tubulin, required to accelerate nerve regeneration is triggered. In addition, cAMP is also instrumental in up-regulating a number of cytokines including IL6 while inhibiting Rho, a key protein in the Ngr/p75NTR pathway that prevents cytoskeletal assembly. Electrical stimulation brings about these changes by upregulating brain derived neurotrophic factor (BDNF) and its trkB receptor at the soma. A summary of these molecular pathways is shown schematically in Fig. 12.

Employing a constellation of outcome measure tools in this study, we have provided proof of principle that, in this randomized control pilot study, 1 h ES of the median nerve after surgical decompression accelerates axonal regeneration to promote complete muscle reinnervation. The procedure of ES immediately after surgery was proven feasible in the clinical setting. Additionally, patients did not develop any complications due to surgery or the stimulation. The present study sets the stage for future human trials of ES in promoting axon regeneration and muscle reinnervation. The increase in the speed of axon regeneration may be particularly crucial for functional recovery after nerve injuries such as cubital tunnel syndrome with entrapment of the ulnar nerve at the elbow or within the Arcade of Struthers at the upper arm where the axotomized neurons must regenerate their axons over much longer distances. Lastly, post-surgical ES may also benefit transected nerve injuries. Lundborg et al. reported motor and sensory recovery in transected median nerve after the proximal and distal nerve stumps were approximated by a silicone chamber but the recovery took 3 years (Lundborg et al., 1994). It is our hope that brief low frequency ES of the proximal nerve stump immediately after surgical repair will expedite the functional outcome of these procedures.

Acknowledgments

We gratefully acknowledge the generous operating grants awarded to TG (CIHR) and KMC (CIHR, WCB Alberta, Glenrose Foundation) and a CIHR strategic group grant that includes Drs Zochodne, Sayed, Midha and Julien from University of Calgary and Dr. Verge from University of Saskatchewan. TG is an AHFMR Senior Investigator.

References

Ahlborn, P., Schachner, M., Irintchev, A., 2007. One hour electrical stimulation accelerates functional recovery after femoral nerve repair. Exp. Neurol. 208, 137–144.
Al Majed, A.A., Brushart, T.M., Gordon, T., 2000a. Electrical stimulation accelerates and increases expression of BDNF and trkB mRNA in regenerating rat femoral motoneurons. Eur. J. Neurosci. 12, 4381–4390.
Al Majed, A.A., Neumann, C.M., Brushart, T.M., Gordon, T., 2000b. Brief electrical stimulation promotes the speed and accuracy of motor axonal regeneration. J. Neurosci. 20, 2602–2608.
Al Majed, A.A., Tam, S.L., Gordon, T., 2004. Electrical stimulation accelerates and enhances expression of regeneration-associated genes in regenerating rat femoral motoneurons. Cell Mol. Neurobiol. 24, 379–402.
Bell-Krotoski, J., Tomancik, E., 1987. The repeatability of testing with Semmes-Weinstein monofilaments. J. Hand Surg. [Am] 12, 155–161.
Boyd, J.G., Gordon, T., 2002. A dose-dependent facilitation and inhibition of peripheral nerve regeneration by brain-derived neurotrophic factor. Eur. J. Neurosci. 15, 613–626.
Brushart, T.M., Hoffman, P.N., Royall, R.M., Murinson, B.B., Witzel, C., Gordon, T., 2002. Electrical stimulation promotes motoneuron regeneration without increasing its speed or conditioning the neuron. J. Neurosci. 22, 6631–6638.
Brushart, T.M., Jari, R., Verge, V., Rohde, C., Gordon, T., 2005. Electrical stimulation restores the specificity of sensory axon regeneration. Exp. Neurol. 194, 221–229.
Doherty, T.J., Brown, W.F., 1993. The estimated numbers and relative sizes of thenar motor units as selected by multiple point stimulation in young and older adults. Muscle Nerve 16, 355–366.
Doherty, T.J., Brown, W.F., 1997. Age related changes in human thenar motor unit twitch contractile properties. J. Appl. Physiol. 82, 93–101.
Doherty, T., Simmons, Z., O'Connell, B., Felice, K.J., Conwit, R., Chan, K.M., Komori, T., Brown, T., Stashuk, D.W., Brown, W.F., 1995. Methods for estimating the numbers of motor units in human muscles. J. Clin. Neurophysiol. 12, 565–584.
Dumitru, D., 1995. Electrodiagnostic medicine. Mosby, St. Louis.
English, A.W., Schwartz, G., Meador, W., Sabatier, M.J., Mulligan, A., 2007. Electrical stimulation promotes peripheral axon regeneration by enhanced neuronal neurotrophin signaling. Dev. Neurosci. 67, 158–172.
Felice, K.J., 1995. Thenar motor unit number estimates using the multiple point stimulation technique: reproducibility studies in ALS patients and normal subjects. Muscle Nerve 18, 1412–1416.
Fu, S.Y., Gordon, T., 1995a. Contributing factors to poor functional recovery after delayed nerve repair: prolonged axotomy. J. Neurosci. 15, 3876–3885.
Fu, S.Y., Gordon, T., 1995b. Contributing factors to poor functional recovery after delayed nerve repair: prolonged denervation. J. Neurosci. 15, 3886–3895.
Fu, S.Y., Gordon, T., 1997. The cellular and molecular basis of peripheral nerve regeneration. Mol. Neurobiol. 14, 67–116.
Geremia, N.M., Gordon, T., Brushart, T.M., Al Majed, A.A., Verge, V.M.K., 2007. Electrical stimulation promotes sensory neuron regeneration and growth-associated gene expression. Exp. Neurol. 205, 347–359.
Gordon, T., Gillespie, J., Orozco, R., Davis, L., 1991. Axotomy-induced changes in rabbit hindlimb nerves and the effects of chronic electrical stimulation. J. Neurosci. 11, 2157–2169.
Gordon, T., Sulaiman, O., Boyd, J.G., 2003. Experimental strategies to promote functional recovery after peripheral nerve injuries. J. Peripher. Nerv. Syst. 8, 236–250.
Gordon, T., Chan, K.M., Sulaiman, O.A., Udina, E., Amirjani, N., Brushart, T.M., 2009. Accelerating axon growth to overcome limitations in functional recovery after peripheral nerve injury. Neurosurgery 65, 238.
Hannila, S.S., Filbin, M.T., 2008. The role of cyclic AMP signaling in promoting axonal regeneration after spinal cord injury. Exp. Neurol. 209, 321–332.
Imai, H., Tajima, T., Natsuma, Y., 1989. Interpretation of cutaneous pressure threshold (Semmes–Weinstein monofilament measurement) following median nerve repair and sensory reeducation in the adult. Microsurgery 10, 142–144.
Kline, D.G., Kim, D.H., 2008. Kline and Hudson's Nerve Injuries : Operative Results for Major Nerve Injuries, Entrapments and Tumors. Elsevier Saunders, Philadelphia, Pa.
Lee, S., Kim, H., Choi, S., Park, Y., Kim, Y., Cho, B., 2003. Clinical usefulness of the two-site Semmes-Weinstein monofilament test for detecting diabetic peripheral neuropathy. J. Korean Med. Sci. 18, 103–107.
Levine, D.W., Simmons, B.P., Koris, M.J., Daltroy, L.H., Hohl, G.G., Fossel, A.H., Katz, 1993. A self-administered questionnaire for the assessment of severity of symptoms and functional status in carpal tunnel syndrome. J. Bone Joint Surg. [Am.] 75, 1585–1592.
Lundborg, G., Rosen, B., Abrahamson, S.O., Dahlin, L., Danielsen, N., 1994. Tubular repair of the median nerve in the human forearm—preliminary findings. J. Hand Surg. [Br] 19, 273–276.
McComas, A.J., 1995. Motor-unit estimation: the beginning. J. Clin. Neurophysiol. 12, 560–564.
McComas, A.J., Sica, R.E., Campbell, M.J., Upton, A.R., 1971. Functional compensation in partially denervated muscles. J. Neurol. Neurosurg. Psychiatry 34, 453–460.
Nishimura, A., Ogura, T., Hase, H., Makinodan, A., Hojo, T., Katsumi, Y., Yagi, K., Mikami, Y., Kubo, T., 2004. A correlative electrophysiologic study of nerve fiber involvement in carpal tunnel syndrome using current perception thresholds. Clin. Neurophysiol. 115, 1921–1924.
Nix, W.A., Hopf, H.C., 1983. Electrical stimulation of regenerating nerve and its effect on motor recovery. Brain Res. 272, 21–25.
O'Brien, J.P., Mackinnon, S.E., MacLean, A.R., Hudson, A.R., Dellon, A.L., 1987. A model of chronic nerve compression in the rat. Ann. Plast. Surg. 19, 430–435.
Padua, L., LoMonaco, M., Gregori, B., Valente, E.M., Padua, R., Tonali, P., 1997. Neurophysiological classification and sensitivity in 500 carpal tunnel syndrome hands. Acta Neurol. Scand. 96, 211–217.
Pockett, S., Gavin, R.M., 1985. Acceleration of peripheral nerve regeneration after crush injury in rat. Neurosci. Lett. 59, 221–224.
Porter, C.L., Alvarez, A., Jones, K.E., Chan, K.M., 2008. Test retest reliability of a modified multiple point stimulation technique for motor unit number estimation. Clin. Neurophysiol. 119, 2287–2290.
Rashidipour, O., Chan, K.M., 2008. Motor unit number estimation in neuromuscular disease. Can J. Neurol. Sci. 35, 153–159.
Rosenbaum, R.B., Ochoa, J.L., 1993. Surgical treatment of carpal tunnel syndrome. In: Rosenbaum, R.B., Ochoa, J.L. (Eds.), Carpal Tunnel Syndrome and Other Disorders of the Median Nerve. Butterworth-Heinemann, Stoneham, pp. 263–283.
Sharma, N., Marzo, S.J., Jones, K.J., Foecking, E.M., 2010. Electrical stimulation and testosterone differentially enhance expression of regeneration-associated genes. Exp. Neurol. 223, 183–191.
Sulaiman, O.A., Gordon, T., 2000. Effects of short- and long-term Schwann cell denervation on peripheral nerve regeneration, myelination, and size. GLIA 32, 234–246.
Sunderland, S., 1947. Rate of regeneration in human peripheral nerves. Arch. Neurol. Psychiatry 58, 1–6.
Sunderland, S., 1978. Nerve and Nerve Injuries. Churchill Livingstone, Edinburgh.
Udina, E., Furey, M., Busch, S., Silver, J., Gordon, T., Fouad, K., 2008. Electrical stimulation of intact peripheral sensory axons in rats promotes outgrowth of their central projections. Exp. Neurol. 210, 238–247.
Vanden Noven, S., Wallace, N., Muccio, D., Turtz, A., Pinter, M.J., 1993. Adult spinal motoneurons remain viable despite prolonged absence of functional synaptic contact with muscle. Exp. Neurol. 123, 147–156.
Videler, A.J., Van Dijk, J.P., Beelen, A., de Visser, M., Nollet, F., van Schaik, I.N., 2008. Motor axon loss is associated with hand dysfunction in Charcot–Marie–Tooth disease 1a. Neurology 71, 1254–1260.
Witzel, C., Rohde, C., Brushart, T.M., 2005. Pathway sampling by regenerating peripheral axons. J. Comp. Neurol. 485, 183–190.
You, S., Petrov, T., Chung, P.H., Gordon, T., 1997. The expression of the low affinity nerve growth factor receptor in long-term denervated Schwann cells. GLIA 20, 87–100.

Experimental Neurology 223 (2010) 143–152

Contents lists available at ScienceDirect

Experimental Neurology

journal homepage: www.elsevier.com/locate/yexnr

Rolipram-induced elevation of cAMP or chondroitinase ABC breakdown of inhibitory proteoglycans in the extracellular matrix promotes peripheral nerve regeneration

E. Udina [a,b], A. Ladak [c], M. Furey [a], T. Brushart [d], N. Tyreman [a], T. Gordon [a,*]

[a] Division of Physical Medicine and Rehabilitation, Faculty of Medicine and Dentistry, Center for Neurosciences, University of Alberta, Edmonton, Alberta, Canada T6G 2S2
[b] Institut Neurosciences, Department Cell Biology, Physiology and Immunology and Centro Investigación Biomédica en Red Enfermedades Neurodegenerativas (CIBERNED), Universitat Autonoma de Barcelona, Barcelona 08913, Spain
[c] Division of Plastic Surgery, University of Alberta, Edmonton, Alberta, Canada T6G 2S2
[d] Departments of Orthopedics and Neurology, John Hopkins School of Medicine, Baltimore, MD 21287, USA

ARTICLE INFO

Article history:
Received 3 April 2009
Revised 25 August 2009
Accepted 26 August 2009
Available online 4 September 2009

Keywords:
cAMP
Chondroitinase ABC
Axon regeneration
Axon outgrowth
Staggered regeneration
Motoneurons
DRG neurons

ABSTRACT

The inhibitory growth environment of myelin and extracellular matrix proteoglycans in the central nervous system may be overcome by elevating neuronal cAMP or degrading inhibitory proteoglycans with chondroitinase ABC (ChABC). In this study, we asked whether similar mechanisms operate in peripheral nerve regeneration where effective Wallerian degeneration removes myelin and extracellular proteoglycans slowly. We repaired transected common peroneal (CP) nerve in rats and either elevated cAMP in the axotomized neurons by subcutaneous rolipram, a specific inhibitor of phosphodiesterase IV, and/or promoted degradation of proteoglycans in the distal nerve stump by local ChABC administration. Rolipram treatment significantly increased the number of motoneurons that regenerated axons across the repair site at 1 and 2 weeks, and increased the number of sensory neurons that regenerated axons across the repair site at 2 weeks. Local application of ChABC had a similar effect to rolipram treatment in promoting motor axon regeneration, the effect being no greater when rolipram and ChABC were administered simultaneously. We conclude that blocking inhibitors of axon regeneration by elevating cAMP or degrading proteoglycans in the distal nerve stump promotes peripheral axon regeneration after surgical repair of a transected nerve. It is likely that elevated cAMP is sufficient to encourage axon outgrowth despite the inhibitory growth environment such that simultaneous enzymatic proteoglycan degradation does not promote more axon regeneration than either elevated cAMP or proteoglycan degradation alone.

Crown Copyright © 2009 Published by Elsevier Inc. All right reserved.

Introduction

Axons in the peripheral (PNS) but not the central nervous system (CNS) regenerate after injury (Fu and Gordon, 1995a,b, 1997). Nevertheless there is only a short window of opportunity for effective PNS regeneration to occur, whereby regenerative success of injured nerves progressively decreases after prolonged axotomy and Schwann cell denervation (Fu and Gordon, 1995a,b; Gordon et al., 2003; Sulaiman and Gordon, 2000). Axon outgrowth from the proximal stump of transected and surgically repaired nerves is a slow process (Brushart et al., 2002) and this lengthy period when regenerating axons wander in the suture site of surgically repaired peripheral nerves (Cajal, 1928; Witzel et al., 2005) accounts, at least in part, for the delays of several weeks for all regenerating axons to cross a repair site (Brushart et al., 2002). Chondroitin sulfate proteoglycans (CSPGs) of the extracellular matrix and myelin-associated inhibitors, both potent inhibitors of neuronal regeneration in the CNS (Mueller, 1999; Sandvig et al., 2004; Tang, 2003), are also present in the peripheral nerve. These molecules are up-regulated after nerve injury, show neurite-inhibitory activity (Braunewell et al., 1995; Shen et al., 1998; Zuo et al., 1998), and may play a role in delayed axon outgrowth following peripheral nerve injury. The prolonged time course of weeks for effective removal of myelin debris by macrophages and Schwann cells (Avellino et al., 1995; Fansa and Keilhoff, 2003; George and Griffin, 1994; Stoll et al., 1989) and for degradation of glycoproteins of the extracellular matrix (Hughes et al., 2002) may account for the staggered outgrowth of axons from the proximal stump of an injured nerve (Al-Majed et al., 2000; Gordon et al., 2003).

Injured nerves in the CNS may be stimulated to regenerate their axons despite the inhibitory environment by interfering with signaling pathways that are activated by inhibitory myelin associated molecules (Cai et al., 1999; Dergham et al., 2002; Lehmann et al., 1999; Neumann and Woolf, 1999; Neumann et al., 2002; Qiu et al., 2002). The inhibition can be overcome by increasing neuronal cAMP levels *in vivo* (Cai et al., 1999; Dergham et al., 2002; Lehmann et al., 1999; Neumann and Woolf, 1999; Neumann et al., 2002; Qiu et al., 2002) and *in vitro* (Cai et al., 1999) and by selectively cleaving

* Corresponding author. Faculty of Medicine, Division of Physical Medicine and Rehabilitation/Centre for Neuroscience, 525 Heritage Medical Research Centre, University of Alberta, Edmonton, AB, Canada T6G 2S2. Fax: +1 780 492 1617.
E-mail address: tessa.gordon@ualberta.ca (T. Gordon).

0014-4886/$ – see front matter. Crown Copyright © 2009 Published by Elsevier Inc. All right reserved.
doi:10.1016/j.expneurol.2009.08.026

glycosaminoglycan (GAG) side chains from the protein core of proteoglycans with chondroitinase ABC (ChABC) (Fawcett and Asher, 1999). However, applying these pharmacological approaches to PNS regeneration has generated conflicting data. Some have reported that cAMP does promote axon outgrowth (Gershenbaum and Roisen, 1980; Kilmer and Carlsen, 1987; Pichichero et al., 1973) while others have failed to demonstrate increased axon outgrowth (Black and Lasek, 1979; Han et al., 2004; McQuarrie et al., 1977). The use of ChABC in the PNS has been shown to accelerate axon outgrowth into distal nerve stumps and acellular nerve grafts in rats (Krekoski et al., 2001; Zuo et al., 2002). Analyses of the distance of regenerating axons of *thy-1 TFP-H* transgenic mice demonstrated longer axon profiles in nerve grafts from wild-type littermates with ChABC, which specifically degrades CSPGs but not other proteoglycans such as heparin sulfate proteoglycans (Groves et al., 2005).

Using retrograde labeling techniques, we aim to further investigate whether elevation of cAMP or removal of GAG side chains from inhibitory proteoglycans in axotomized motor and sensory neurons in the peripheral nerve promotes PNS regeneration. We also question whether a combinational strategy of rolipram and ChABC that has proven to be effective in CNS regeneration (Fouad et al., 2005; Houle et al., 2006; Tropea et al., 2003) is also effective in the PNS.

Material and methods

All experiments were performed on adult female Sprague–Dawley rats (200–220 g) and approved by local authorities (Health Sciences Laboratory Animal Services, University of Alberta) according to the Canadian Council for Animal Care guidelines.

Surgery: nerve repair and delivery of rolipram and/or chondroitinase ABC (ChABC)

All surgeries were performed under Ketamine (Vetalar, Bioniche, Bellville, Ontario) and Xylazine (Rompun, Bayer, Toronto, Ontario) intraperitoneal anesthesia at doses of 0.6 and 0.4 mg/kg, respectively. Eye lubricant (Duratears Naturale, Alcon, Ontario) was used to prevent corneal damage during surgery.

Using aseptic technique, the right CP nerve was exposed distal to the sciatic notch and transected 10 mm proximal to its entrance into the flexor muscle group including the tibialis anterior muscle (Fig. 1A). Silicone silastic guides (Helix Medical, Inc., Carpinteria, CA) of 0.76 mm interior diameter and 3 mm length were implanted, and the proximal and distal CP nerve stumps were approximated within the nerve guide using 9-0 Ethicon nylon suture (Ethicon, Inc. ,Somerville, NJ) as described in Furey et al. (2007). An Alzet mini-osmotic pump (Durect Corporation, Cupertino, CA) was then implanted subcutaneously on the back of the rat to release its content of either rolipram or saline systemically. The Alzet pump (model 2ML2) was filled with the appropriate solution for 24 h and incubated at 37 °C prior to implantation. The pump delivered either rolipram (Nikulina et al., 2004) diluted in 1:1 saline/dimethyl sulfoxide (DMSO) (rolipram group, $n=26$) or vehicle solution (1:1 saline/DMSO; control group, $n=22$), both delivered at a rate of 0.4 μmol/kg/h continuously over 7, 14 or 21 days. The surgical wound was sutured closed and the rats were monitored and kept warm until they recovered from the anesthetic.

Chondroitinase ABC application

In two groups of rats, the CP nerve was exposed and transected under surgical anesthesia 10 mm proximal to the entrance of the nerve into the flexor muscle group of the hindlimb. In the first group of animals, 8 mm of the cut end of the distal stump was dipped into a vaseline well containing 20 U/ml protease free ChABC (Seikagaku, Japan) in 1% protease free bovine serum albumin for 1 h. The nerve ends were then repaired using a silicone silastic guide. An Alzet miniosmotic pump was then placed on the back of the animal and a vehicle solution of 1:1 saline/DMSO was delivered systemically over 2 weeks at a delivery rate of 5 μl/ml (ChABC group $n=9$). In the second group of rats, the ChABC was again applied to the distal nerve stump as described, and an Alzet pump implanted on the back of the rat was filled with rolipram solution for systemic delivery over a 2-week period at the same rate as for the vehicle solution group (Roli + ChABC group, $n=8$). The skin was closed after surgery and the rats were warmed and monitored during recovery from the anesthetic.

Surgical application of retrograde dyes

A second sterile surgery was carried out under surgical anesthesia at 7–21 days following the CP nerve section and repair, and for the systemic delivery of saline/DMSO vehicle or rolipram, and/or local application of ChABC to the CP nerve suture site. Fluororuby (Dextran, tetramethylrodamine, Invitrogen, Molecular Probes, Eugene, OR) was either injected 3 mm distal to the site of the nerve repair or applied directly to the proximal stump of the cut CP nerve 10 mm distal to the repair site (Figs. 1B, C). For the microinjection, the CP nerve was crushed just distal to the cuff (3 mm distal to the suture site) and the dye was injected via a micropipette that was attached to a picospritzer (Intercel Picospritzer III) (Brushart et al., 2002). For the application of the dye to the proximal stump of the CP nerve cut 10 mm distal to the suture site, the stump was dipped into a 5% fluororuby solution contained within a vaseline well for 1 h. Following the dye exposure, excess dye was carefully rinsed off before suturing the skin and allowing the rats to wake. In control experiments, we injected the dye 3 mm distal to the suture site immediately after nerve repair rather than after 7, 14, and 21 days. This was done to ensure that the injected dye was confined to the injection site within the distal nerve stump and did not penetrate to the axons in the proximal nerve stump.

Tissue removal and analysis of the backlabeled neurons

Rats were deeply anesthetized 5–6 days after backlabeling of the neurons and transcardially perfused with 200 ml saline followed by 500 ml of 4% paraformaldehyde at pH 7.4. After perfusion, the spinal cord was dissected and spinal cord segments T11 to L2 (containing the CP motoneuron pool) and L4 and L5 dorsal root ganglia (DRGs) (containing most of the cell bodies of the CP sensory nerves) were harvested and post-fixed with 30% sucrose in 4% paraformaldehyde solution overnight. The tissue was then frozen in liquid nitrogen after been embedded in OCT Tissue-Tek Liquid (Sakura, Japan).

Frozen tissues were sectioned in a cryostat (Jung 3000). Longitudinal spinal cord sections were cut at 50 μm thickness and DRG cross-sections were cut at 25 μm thickness. The fluorescent bodies of the labeled motor and sensory neurons of the CP nerve were visualized and counted at 40× magnification under fluorescent microscopy at barrier filters of 580 nm (Fig. 2). The number of neurons counted was corrected according to the thickness of the sections and the diameter of the neuron cell bodies (30 and 15 μm for motor and DRG neurons, respectively) by the method of Abercrombie and Johnson (1946). The correction factor in our samples was 0.635 for motoneuron counts in the spinal cord sections and 0.574 for the DRG sensory neurons.

Morphological analysis of nerve sections

In a third set of rats, surgery was performed to administer rolipram ($n=9$) or vehicle solution ($n=9$) immediately after CP nerve transection and repair via an Alzet miniosmotic pump for periods of 4 or 14 days. The surgeries were the same as described for the previous sets of rats. A segment of the CP nerve 3 mm distal to the suture site was removed at 4- and 14-day time points. The nerve pieces were fixed with gluteraldehyde (3% in 0.1 M phosphate buffer),

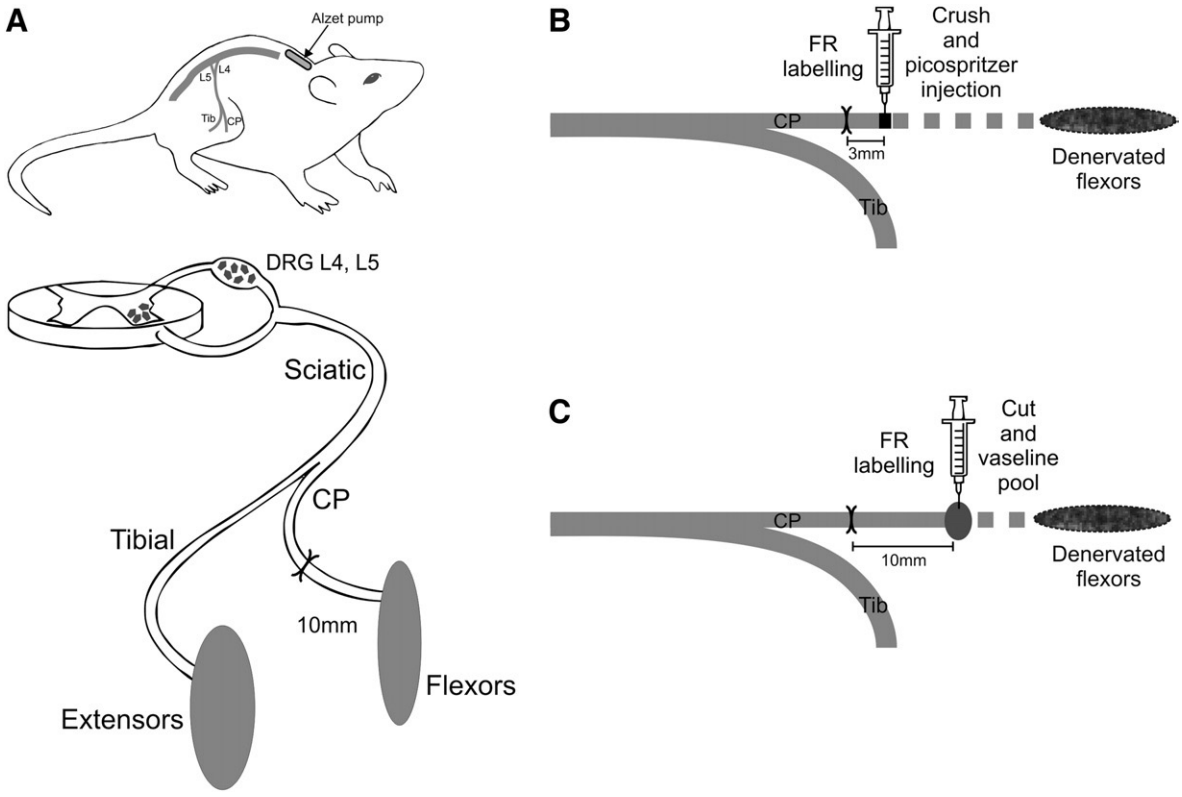


Fig. 1. The *in vivo* model of peripheral nerve regeneration in the common peroneal (CP) nerve in the rat. (A) The CP nerve was exposed, transected 10 mm proximal to the nerve entry into the flexor group of muscles that includes the tibialis anterior muscle, and repaired by tubulization. The Alzet osmotic pump was implanted subcutaneously at the back of the rats after the nerve surgery. (B) After 7 or 14 days, the nerve was re-exposed, crushed 3 mm distal to the suture site and fluroruby was injected into the nerve via a micropipette that was attached to a picospritzer. (C) After 14 or 21 days, the nerve was re-exposed, cut 10 mm distal to the suture site and the proximal stump was dipped for 1 h in a solution with fluororuby contained in a vaseline pool. Details are provided in the text.

stained with osmium tetroxide (3% solution in 0.1 M phosphate buffer), dehydrated in ascending alcohols, and embedded in araldite. Sections of 2 μm thickness were stained with methylene blue and observed under the light microscope with a 100× oil-objective lens. In both groups, the number of myelinated fibers with normal appearance and the number of myelinated fibers undergoing Wallerian degeneration were counted to obtain a percentage of degenerative versus intact fibers in the nerve (Ceballos et al., 2003). The number of phagocytic cells present in the cross-section area was also counted.

Degradation of proteoglycans by ChABC

To guarantee that the ChABC application was successful in degrading the proteoglycans of the extracellular matrix, immunohistochemistry was performed to determine the success of the ChABC in degrading CSPG. CP nerve cross-sections were immunolabeled using a CSPG-neoepitope antibody that binds to new epitopes created on the CSPG core protein after its lysis by chABC (adapted from García-Alías et al., 2008). The distal nerve stumps were treated with the same concentration of chABC used in the studies of axon regeneration in four rats. One day after application of chABC to the distal CP nerve stump, a length of 10 mm of nerve was fixed with 4% paraformaldhyde and then preserved in 30% sucrose. The nerves were frozen in isopentane and cryosectioned at 30 μm. Cryosections were cut from the nerve segments 0–4 and 4–8 mm distal to the suture site. The nerve sections were blocked in PBS with 0.3% Triton × and 5% FCS for 1 h, then incubated overnight at 4°C with Proteoglycan Delta Di0S (1B5) anti-mouse (Seikagakubb, 1:5000), incubated for 1 h at room temperature

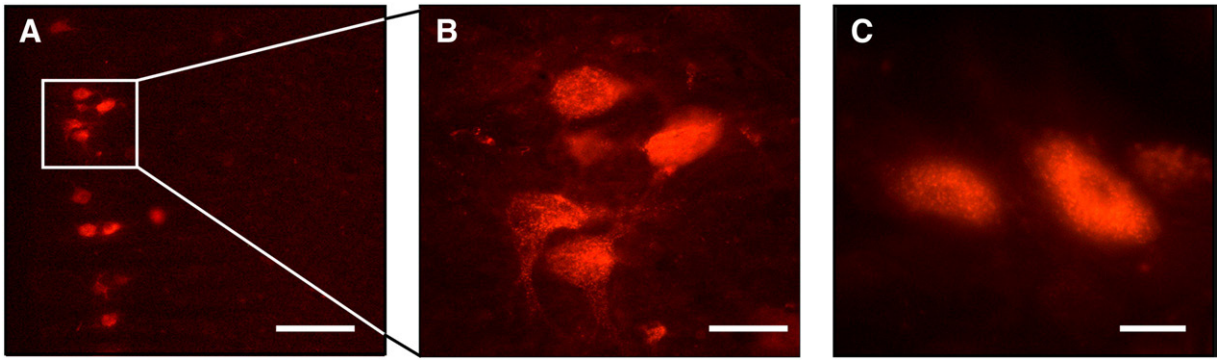


Fig. 2. Visualization of motor and sensory neurons backlabeled with fluororuby. (A, B) An example of a column of common peroneal motoneurons in 50-μm-thick longitudinal sections of the spinal cord at the lumbar level. The neurons are visualized at low and higher magnification to illustrate the laterally located motoneuron column in the ventral horn and the morphology of the motoneurons, respectively. (B) Sensory neurons in 25 μm thick cross-sections of the L5 dorsal root ganglion. The scale bars are (A) 200 μm, (B) 50 μm and (C) 20 μm.

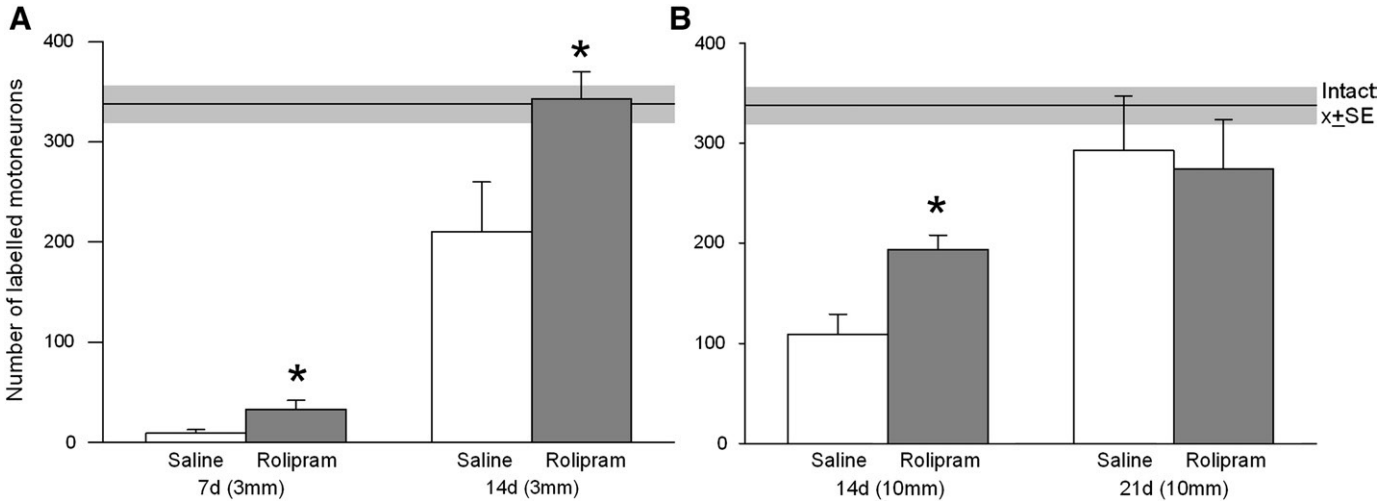


Fig. 3. Subcutaneous rolipram administration accelerates the onset of motor regeneration after transection and repair of the CP nerve. (A)Mean number (±SE) of motoneurons backlabeled 3 mm distal to the suture site at 7 and 14 days in the vehicle (saline; white bars) and the rolipram (grey bars) treated groups. (B)Mean number (±SE) of motoneurons backlabeled 10 mm distal to the suture site at 14 and 21 days in the vehicle- and the rolipram-treated groups. Rolipram increased the number of motoneurons that regenerated axons across the suture site and into the distal nerve stump at 7 and 14 days with all motoneurons regenerating their axons 10 mm from the suture site by 21 days. The numbers of motoneurons that regenerated axons 21 days after saline and rolipram administration were not statistically different from the numbers of contralateral motoneurons that supply axons to the contralateral intact CP nerve. The dashed lines show the SE of the mean number of intact CP motoneurons. *Statistical significance vs. vehicle when $p<0.05$.

with biotinylated goat anti-mouse secondary antibody (1:200), and then anti-goat Cyanine-2 (1:200, Jackson Immunoresearch) for 1 h. Samples were washed three times with PBS after each step.

Measurement of cAMP levels in DRG neurons and spinal cord homogenates

In the rats with the distal nerve stump removed 4 days after nerve transection and repair for morphological analysis (described above), the right L4 and L5 DRGs were removed and immediately frozen in liquid nitrogen. The segment of the spinal cord where L4 and L5 roots enter was also removed, and the left and right sides were separated and frozen in liquid nitrogen. The tissues were homogenized in 0.1 N hydrochloric acid (HCl) and cAMP levels were measured with a cAMP immunoassay kit (R&D Systems Inc., MN).

Statistics

Statistical comparisons were performed using SPSS 14.0 software. Comparisons between two groups were performed using an independent *t*-test, whereas comparison between four groups were performed using one-way analysis of variance (ANOVA), and statistical significance was accepted at p values of <0.05 (*) and <0.01 (**). Values are expressed as means ± SE.

Results

Rolipram delivery accelerates motor and sensory nerve regeneration

In order to increase cellular levels of cAMP pharmacologically in rat motor and sensory neurons, we infused rolipram systemically at a rate of 0.4 μmol/kg/h (Nikulina et al., 2004) to inhibit PDE IV, the most common isoform of phosphodiesterase in neural tissue (Jin et al., 1999). One week after transecting and repairing the nerve, a thin regenerative cord connecting the proximal and the distal stumps was observed through the silicone guide. After 2–3 weeks, there was more connective tissue surrounding the guide and the distal stump was obviously thicker and pearly.

Elevation of cAMP by rolipram has been shown to increase neurite outgrowth of DRG neurons on a non-permissive substrate *in vitro* (Cai et al., 1999) and of motoneurons on a permissive substrate *in vitro* (Aglah et al., 2008) but it remains to be determined whether cAMP plays a definitive role in peripheral nerve regeneration *in vivo*. We asked whether rolipram delivery to regenerating axons promotes axon outgrowth across a surgical repair site and into the distal nerve stump. Rolipram was delivered systemically for 7, 14 and 21 days, after which the motor and sensory neurons that had regenerated their axons across the suture site and into the distal nerve stump were backlabeled with fluororuby either 3 or 10 mm distal to the surgical site (Fig. 1). When the fluorescent dye was applied at a distance of 3 mm from the suture site immediately after nerve repair, the counts of labeled motoneurons in the spinal cord or sensory neurons in the DRGs were zero. This control experiment demonstrated that the injected retrograde dye was confined within the distal nerve stump. Hence counts of labeled neurons days after nerve transection and repair represented only those neurons whose axons had regenerated across the suture site to the site of dye application. At 7 days after nerve repair, only a few motoneurons were backlabeled with fluororuby 3 mm distal to the repair site. In the vehicle saline-treated

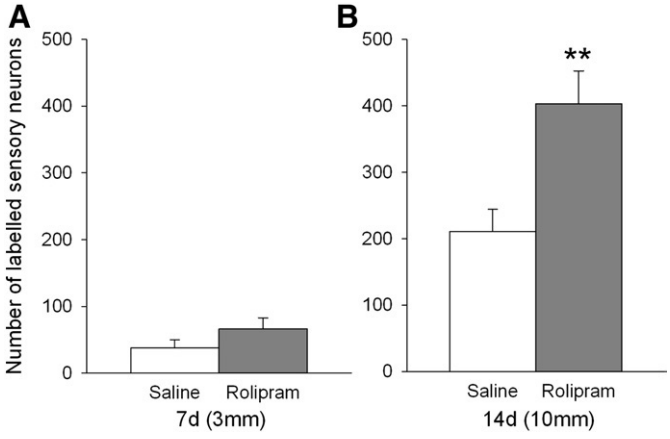


Fig. 4. Rolipram administration significantly increased the number of sensory neurons regenerating axons across the repair site at 14 days following nerve transection and repair ($p<0.01$). (A)Mean number (±SE) of the DRG sensory neurons backlabeled 3 mm distal to the suture site at 7 days in the vehicle (saline; white bars) and the rolipram (grey bars) treated groups. (B)Mean (±SE) number of DRG sensory neurons backlabeled 10 mm distal to the suture site at 14 days in the vehicle- and the rolipram-treated groups.

group, a mean (±SE) of 9.1±3.2 motoneurons were backlabeled in the ventral horn of the right spinal cord (Fig. 3A) whereas with rolipram treatment, the mean (±SE) number of motoneurons was 32.8±9.3, a significant 3.6-fold increase compared to the vehicle group. There were no backlabeled motoneurons in the spinal cord in 2 of 9 animals in the vehicle group and in 1 of 10 animals in the rolipram group. In other words, there were no motoneurons which regenerated their axons across the surgical site at that time point in ~22% and 10% of the vehicle- and rolipram-treated rats, respectively. One week later, at 14 days after nerve repair and either vehicle or rolipram treatment, all motoneurons had regenerated their axons to 3 mm distal to the suture site in the rolipram-treated group with the mean (±SE) number of 343.5±27.1, falling within one SE of the mean number of intact CP motoneurons on the contralateral side of the spinal cord (Fig. 3A). In contrast, the mean (±SE) number of motoneurons in the vehicle-treated group (210.9±50.6) was significantly lower. Hence, systemic rolipram administration significantly increased the number of motoneurons that regenerated axons across the surgical repair site.

When motor axon regeneration through the distal nerve stump was assessed by backlabeling motoneurons 10 mm distal to the suture site at 14 days following transection and repair of the CP nerve, the mean number (±SE) of motoneurons that regenerated their axons through the distal nerve stump was significantly higher in the rolipram group (193.6±14.3) as compared to the vehicle-treated group (109.1±20.3), a ~2-fold increase (Fig. 3B). All motoneurons, in both the control and rolipram group, had regenerated their axons by 21d, with mean (±SE) numbers of motoneurons not being significantly different from the number of intact motoneurons in the contralateral intact motoneuron pool (Fig. 3B). These data are quite consistent with the view that rolipram accelerates axon outgrowth across the suture site and has little or no effect in accelerating the rate of regeneration through the distal nerve stump.

As expected in a nerve that has ~3 times more sensory than motor fibers (Lozeron et al., 2004; Swett et al., 1986), the sensory neuron count in the DRGs were 3× higher than the motoneuron count in the vehicle-treated group at each of the different time points after CP nerve transection and repair. There was a positive trend for rolipram treatment to increase the number of DRG neurons that regenerated axons across the suture site at 7 days (66.3±16.8) but the increase was not significant compared to the vehicle-treated group (38.3±11.8) (Fig. 4A). At 2 weeks and 10 mm distal to the suture site, the number of DRG neurons that regenerated their axons in the rolipram group was significantly higher than in the vehicle-treated group (403.3±49.4 and 210.9±33.6 respectively) (Fig. 4B), demonstrating a ~2-fold increase in the number of sensory neurons regenerating axons into the distal nerve stump with rolipram treatment. Thus, rolipram was equally effective in promoting both motor and sensory axon outgrowth across a surgical repair site into the distal nerve stump.

Clear signs of Wallerian degeneration were evident at 4 days after suture of the stumps of the cut nerve as seen in the micrographs of the distal nerve stump after suture of proximal and distal nerve stumps (Figs. 5A, C). At this time point, most of the fibers (67±7%) showed

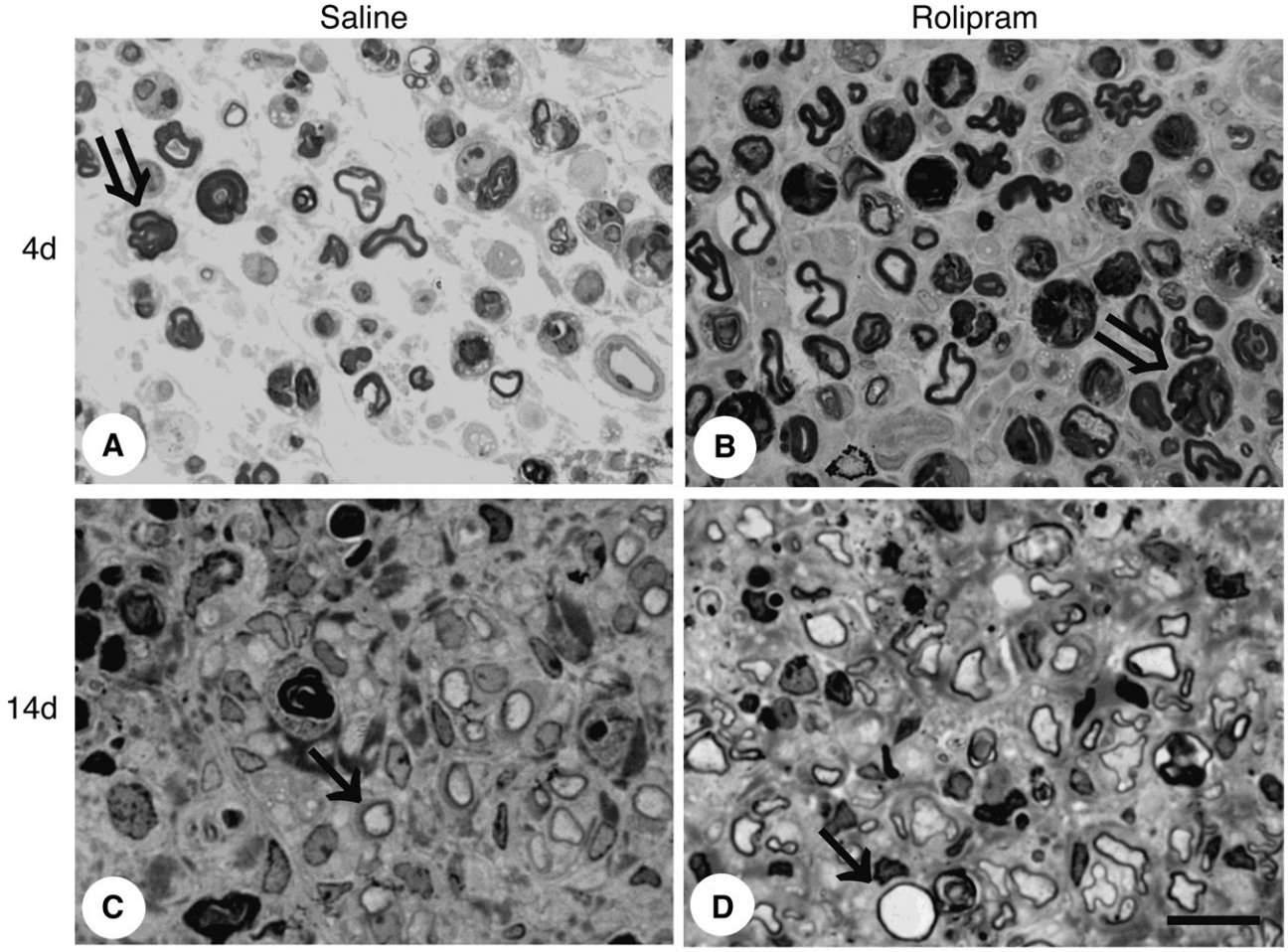


Fig. 5. Cross-sections of distal nerves 3 mm distal to the suture site 4d (A, B) and 14d (C, D) after saline (vehicle) (A, C) and rolipram (B, D) treatment. Quantifications of proportions of nerve fibers that had undergone Wallerian degeneration at 4d and of regenerating axons were made, as detailed in the text. Regenerating axons with thinly myelinated sheaths are visible within the distal nerve stumps after CP nerve transection and surgical repair, especially from the rolipram-treated group, at this early time point of axon regeneration. Calibration bar = 10 μ. Examples of degenerating axons and the regenerating axons are shown by the symbols ⇒ and →, respectively.

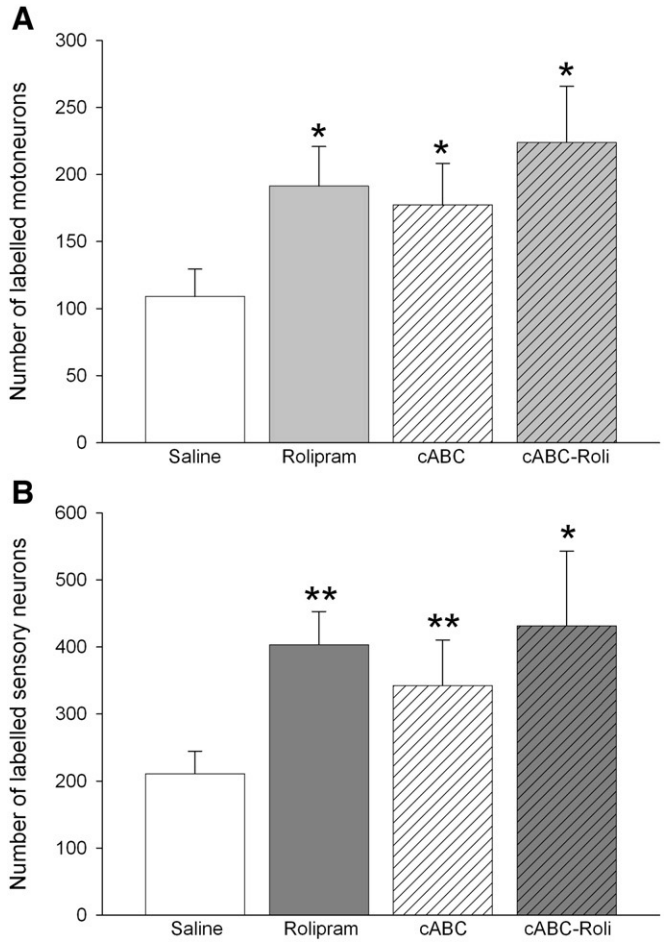


Fig. 6. Rolipram and ChABC significantly increased the number of motor and sensory neurons that regenerated their axons across the CP nerve transection and repair site. Combination therapy with both agents did not result in an additive effect above each agent alone. The mean (± SE) number of motoneurons (A) and DRG sensory neurons (B) that were backlabeled 10 mm distal to the suture site 14d after the injury in the vehicle-treated group (white bar), the rolipram group (grey bar), the ChABC group (white stripped bar) and the group that received both rolipram treatment and ChABC application (ChABC + Roli, grey-stripped bar). Rolipram or ChABC significantly increased the number of motoneurons and sensory neurons that regenerated their axons 10 mm into the distal nerve stump at 14 days, and the combination of the two treatments had similar effects to each of the two treatments applied separately. Statistical significance vs. vehicle at $*p<0.05$ and $**p<0.01$.

signs of degeneration in the saline-treated group (Fig. 5A). Some phagocytic cells could be observed in the distal nerve stumps of saline-treated rats with mean (±SE) total numbers of 21±7. Rolipram treatment did not alter the proportion of degenerating nerve fibers compared to visually intact fibers (67%±12) nor the number of phagocytic cells (31±9) at 4 days when compared to the vehicle-treated group. These findings provide evidence that elevated cAMP levels by rolipram administration are unlikely to affect the rate of Wallerian degeneration. At 14 days after transection and repair of the CP nerve, myelinated axons were observed in four of the five animals in the vehicle-treated group 3 mm distal to the suture site, the mean (±SE) number of axons being 98±116. Axons were thinly myelinated and demonstrated the typical morphology of regenerating fibers (Fig. 5B). In contrast, all the animals in the rolipram-treated group showed myelinated regenerating fibers at 14d (Fig. 5D), their numbers being significantly higher at 765±340, an ~8-fold increase. These findings are in agreement with our observations that rolipram treatment increased the number of backlabeled axons that cross the suture site at 7 and 14 days. The relative increase in myelinated fibers seen in the distal nerve stump with rolipram treatment at 14 days was 8-fold as compared to the 2-fold increase in the number of sensory and motor neurons extending axons across the suture site and into the distal nerve stump at 14 days (Figs. 3B and 4B). This demonstrates that rolipram promotes the outgrowth of multiple axon sprouts across the a surgical repair site in addition to accelerating the *number* of motoneurons that regenerate their axons across the suture site and into the distal nerve stump. These effects are the same as those of low frequency electrical stimulation (Brushart et al., 2002; Franz et al., 2008).

Chondroitinase ABC degrades proteoglycans in vivo and promotes peripheral nerve regeneration

ChABC degrades CSPGs present in the endoneurial tissues of the peripheral nerve after nerve injury (Krekoski et al., 2001; Zuo et al., 2002). This degradation occurs without compromising the basal lamina scaffold and does not disturb laminin content. The fact that ChABC injected 2 mm distal to the injury site in peripheral nerve accelerates detection of immunoreactive regenerating axons at the site of nerve transection repair, but not after crush injury, strongly

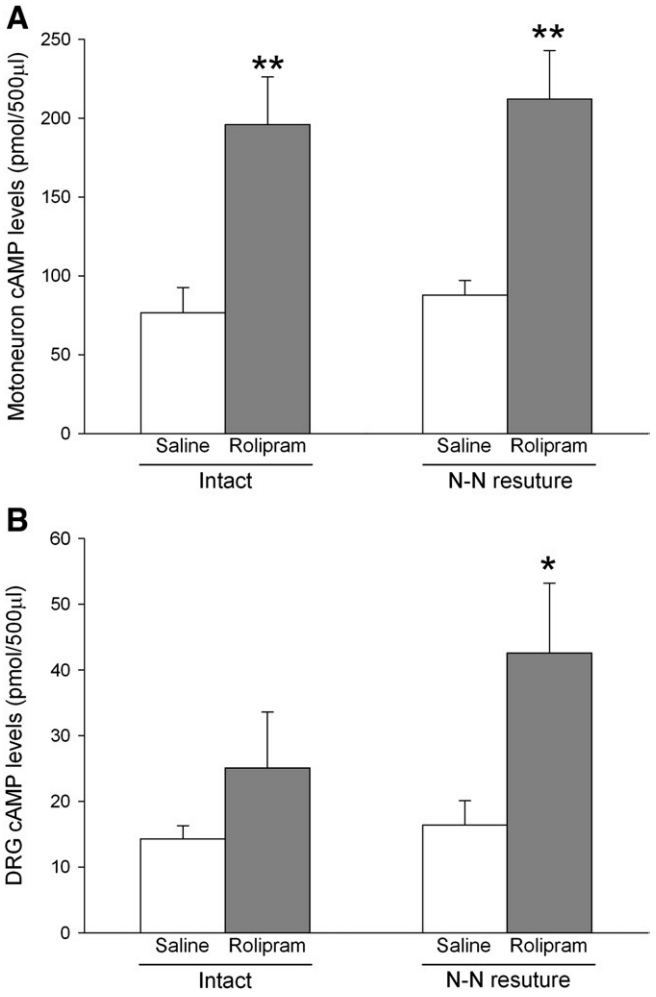


Fig. 7. Rolipram significantly increased intracellular levels of cAMP in axotomized motor (A) and sensory (B) neurons. Intracellular levels of cAMP from L4 to L5 DRG homogenates and from hemisected T12 to L1 spinal cord segments containing the CP motoneurons from the left intact hindlimb were measured. The neurons were axotomized by cutting and resuturing the right CP nerve (N-N resuture) and the neurons on the contralateral side served as intact controls. Assays were performed 4 days after surgery and treatment with either saline (white bar) or rolipram (grey bar). Rolipram significantly increased cAMP levels in both intact and axotomized motoneurons but only in the axotomized DRG sensory neurons. Mean (±SE) values of cAMP concentrations are plotted in the histograms. Statistical significance: $*p<0.05$ or $**p<0.01$.

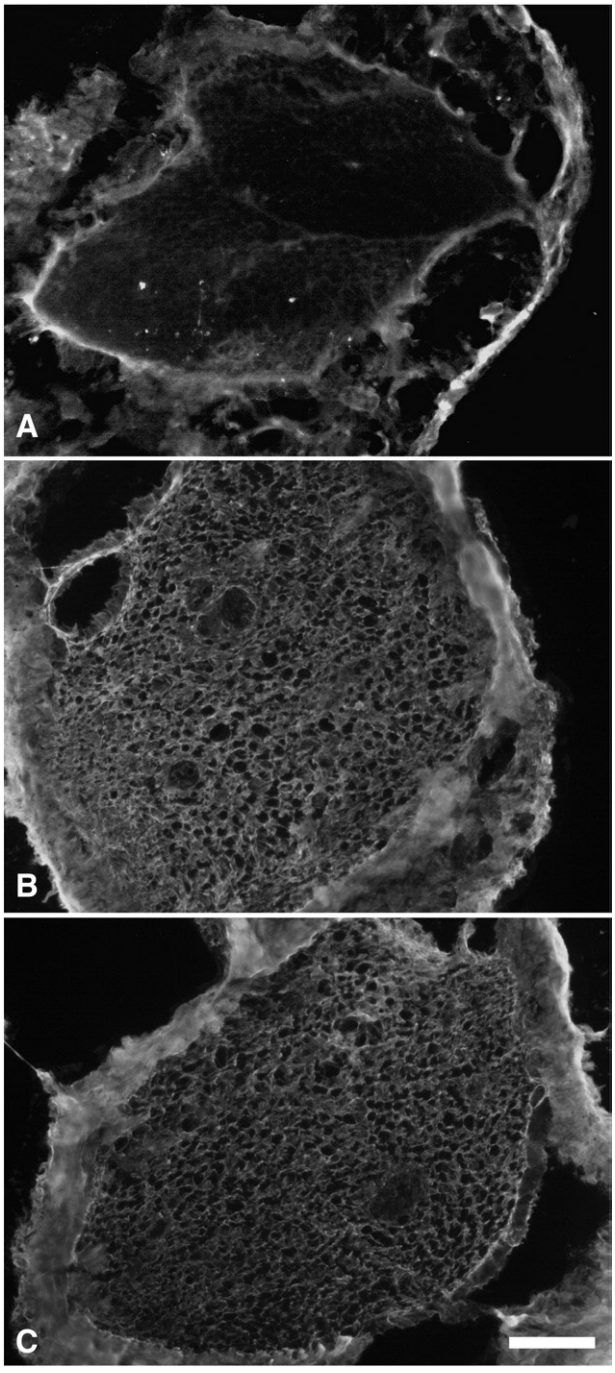


Fig. 8. Cross-sections of an intact CP nerve (A) or CP nerves which had been treated with application of chABC for 1 h and visualized 1 day later, 4 mm (B) or 8 mm distal (C) to the suture site. Sections were immunolabeled against 4S and 6S chondroitin and dermatan sulfate, degradation products of the proteolgycans. Immunoreactivity was only detectable in the treated nerves (compare A with B and C) both close, 4 mm (B) and 8 mm distal (C) to the suture site, corroborating that chABC is effective in degrading proteoglycans along the treated nerve. Calibration bar = 0.1 mm.

indicates that the bacterial enzyme accelerates axon outgrowth rather than rate of regeneration within the nerve stumps (Krekoski et al., 2001; Zuo et al., 2002). We treated the distal CP nerve stump with 20 U/ml of ChABC, the same dose that was shown to be effective in promoting motor axonal regeneration in the mouse (English, 2005; Groves et al., 2005) and in degrading CSPGs in the rat sciatic nerve (Krekoski et al., 2001; Zuo et al., 2002).

In order to evaluate the success of the *in vivo* chABC application in degrading the proteoglycans in the CP distal nerve stump, we immunolabeled 4S and 6S chondroitin and dermatan sulphate, new epitopes created on the CSPG core protein after its lysis by chABC. In comparison with there being no immunoreactivity in the intact nerve (Fig. 6A), immunoreactivity that was localized around the nerve fibers in the extracellular space was detected both close to the suture site (Fig. 6B) and 4–8 mm distal to the site (Fig. 6C). This verified that the *in vivo* application of ChABC did successfully degrade proteoglycans of the extracellular matrix.

Treatment with ChABC significantly increased the number of motoneurons that regenerated their axons through the distal nerve stump at 14 days post-nerve repair as compared with the vehicle saline control (Fig. 7A). This effect was similar to the effect of rolipram administration over the same period of time. Hence, ChABC and rolipram, delivered separately, were equally effective in significantly increasing the number of motoneurons that regenerated their axons 10 mm into the distal CP nerve stump (Fig. 7A). When a combination of one time local ChABC application to the CP nerve and continuous systemic delivery of rolipram over 14 days was performed, the increase in the number of motoneurons regenerating their axons was the same as with the application of each agent alone, there being no additive effect when combining rolipram with ChABC (Fig. 7A).

Similar to that observed in motoneurons, ChABC was equally effective in promoting sensory axon regeneration as treatment with rolipram (Fig. 7B). Treatment with ChABC significantly increased the number of DRG sensory neurons that regenerated their axons across the surgical repair site (342.3 ± 68.0) when compared to the vehicle treatment group (210.9 ± 33.6) at 10 mm distal to the repair site. As observed in the motoneurons, combination therapy of local ChABC and systemic rolipram was not additive in effect. Possible reasons for this are considered in the discussion.

cAMP levels in DRG neurons after systemic rolipram administration

In order to verify that systemic rolipram administration was effective in raising neuronal cAMP levels, we prepared another group of rats where the CP nerve was transected and surgically repaired with either saline solution or rolipram delivered systemically via a mini-osmotic pump over 4 days. After 4 days, we harvested the lumbar portion of the spinal cord containing the axotomized CP motoneurons (T12 to L1) and the L4 and L5 DRGs supplying the right hindlimb. The corresponding tissues supplying the left hindlimb with intact CP nerve were harvested. Rolipram significantly increased cAMP levels in the right hemisected portion of the spinal cord containing the axotomized CP motoneurons (212.2 ± 30.7 pmol/ml) when compared to the saline group (87.8 ± 30.7 pmol/ml) (Fig. 8A). The same increase with systemic rolipram treatment was observed in the left hemisected cord containing the intact motoneurons compared to the saline control. In the right axotomized DRG sensory neurons, there was a similar significant increase in cAMP but the trend to increase cAMP in the left intact DRG sensory neurons did not reach statistical significance (Fig. 8B).

Discussion

Local inhibitors of regeneration in the distal nerve stump of a transected nerve are a temporal impediment to regeneration in the PNS before Wallerian degeneration rapidly degrades proteoglycans in the extracellular matrix (Hughes et al., 2002) and clears myelin debris (Fu and Gordon, 1997). However, the onset of Wallerian degeneration is slowed by the delayed entry of macrophages into the distal nerve stump (Bruck, 1997). We provide evidence here that overcoming the inhibitory effects of myelin by rolipram-mediated elevation of cAMP, or the inhibitory effects of proteoglycans through their degradation by ChABC, accelerates the onset of axon regeneration by promoting motor and sensory axon outgrowth across a surgical repair site.

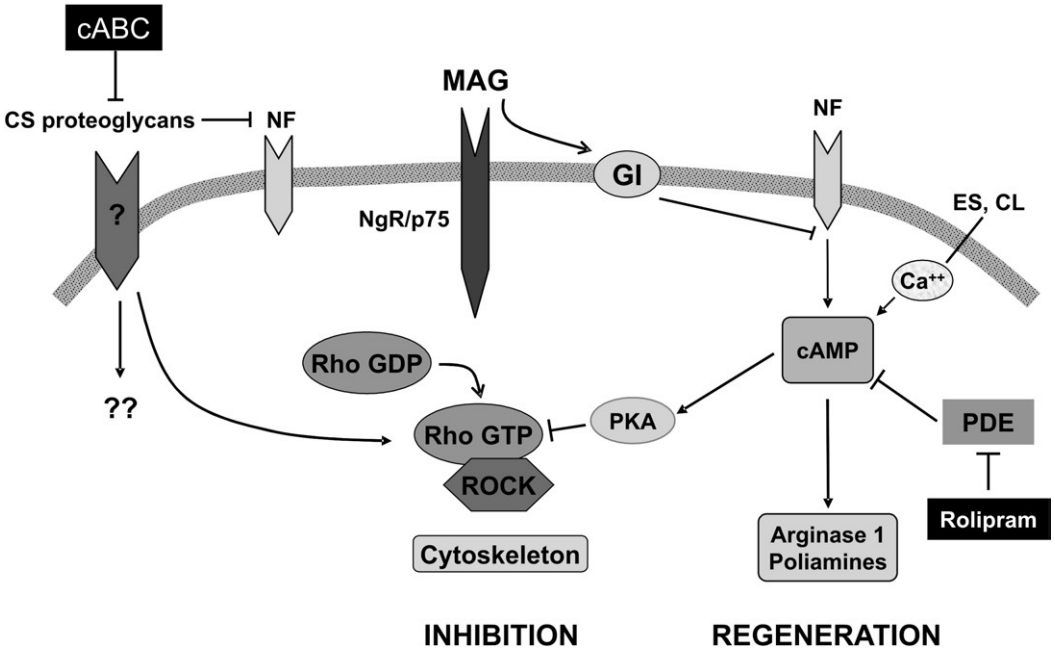


Fig. 9. Schematic representation of the cross-talk between the inhibitory and regenerative pathways in neurons. Increased cAMP levels by neurotrophic factors (NF), electrical stimulation (ES), a conditioning lesion (CL) or by administration of an inhibitor of phosphodiesterase (PDE) such as rolipram, activate the pro-regenerative pathway and block the pro-inhibitory pathway through phosphokinase A (PKA). Degradation of chondroitin sulfate proteoglycans by local application of chondroitinase ABC (cABC) blocks the inhibitory effects on regeneration induced by proteoglycans (Grados-Munro and Fournier, 2003; Mueller, 1999; Sandvig et al., 2004; Tang, 2003).

Rolipram delivered at the same concentration reported to be effective in CNS axon regeneration (Nikulina et al., 2004) accelerated motor and sensory axon outgrowth across a surgical site of peripheral nerve repair. Rolipram administration resulted in a ~3.6-fold increase in the number of motoneurons whose axons had crossed the suture site at 1 week while resulting in a lesser ~2-fold increase in number of motoneurons that regenerated their axons through the distal nerve stump at 2 weeks. The temporal attenuation of effect provides convincing evidence that the primary effect of rolipram is to promote axon outgrowth across a suture site rather than to increase the rate of axon regeneration, similar to that seen with a 1-h period of low frequency electrical stimulation of motor and sensory neurons just after surgical repair of a transected peripheral nerve (Brushart et al., 2002, 2005; Geremia et al., 2007). Accordingly, studies have reported that increased cAMP levels do not enhance the rate of elongation of peripheral motor (Black and Lasek, 1979) and sensory axons (Han et al., 2004; McQuarrie et al., 1977).

The effect of the rolipram in rats essentially mimicked the effectiveness of electrical stimulation in accelerating axon outgrowth in both the PNS and CNS whilst not affecting the rate of axonal extension within the distal nerve stumps (Brushart et al., 2002, 2005; Geremia et al., 2007, Udina et al., 2008). The accelerated axon outgrowth following electrical stimulation has also been linked to increased neuronal cAMP levels (Ming et al., 2001; Udina et al., 2008) and thus rolipram and low frequency electrical stimulation may promote axon outgrowth along similar pathways. It is possible that a more sustained increase in cellular cAMP achieved by continuous rolipram administration accounts for a higher percentage of motoneurons that regenerated their axons across the suture site at 2 weeks in the rolipram-treated rats as compared to the application of electrical stimulation for 1 h just after nerve repair.

Although effects of systemically delivered rolipram at the site of nerve transection and repair could enhance proliferation of Schwann cells (Levi et al., 1995; Raff et al., 1978) and has been reported to accelerate Wallerian degeneration (Gershenbaum and Roisen, 1980), this is unlikely to have made significant contributions to the accelerated outgrowth that was seen at 7 and 14 days after nerve repair and rolipram treatment. Our findings of clear signs of Wallerian degeneration, including the presence of phagocytes and axons undergoing Wallerian degeneration in the distal CP nerve stump, was the same whether or not rolipram was administered.

Rolipram induced elevation of cAMP in axotomized neurons most likely overcomes inhibition from myelin debris and inhibitory CSPGs initially encountered by regenerating axons at the distal nerve stump (Shen et al., 1998). In the PNS, probably the main myelin associated inhibitor protein is MAG (myelin associated glycoprotein; Shen et al., 1998), whilst NogoR1 (the receptor of Nogo) is not present in regenerating peripheral axons. In fact, recent findings suggest that NogoR1 plays an important role in macrophage recruitment during Wallerian degeneration and would not adversely affect axon regeneration (David et al., 2008). Thus rolipram induced elevation of cAMP in axotomized neurons most likely overcomes inhibition from MAG contained in myelin debris initially encountered by regenerating axons at the distal nerve stump (Shen et al., 1998). However, even in the absence of inhibitory molecules, rolipram-induced elevation of cAMP in motoneurons *in vitro* promotes the outgrowth and elongation of neurites (Aglah et al., 2008). These recent findings support the view that the effectiveness of rolipram in promoting axon outgrowth *in vivo* is mediated at the neuronal cell body level rather than at the local site of axonal injury. Whilst cAMP promotes Schwann cell division, the same extent of Wallerian degeneration in the rolipram and saline control groups supports the view that the primary effect of rolipram is at the neuronal cell body.

Our finding that proteoglycan breakdown by localized application of ChABC was equally effective in accelerating motor and sensory axon regeneration as rolipram administration provides evidence that rolipram and ChABC mediate their growth promoting effects at different locations. In contrast to cAMP, less is known about the mechanism(s) through which proteoglycans inhibit axon regeneration (Sandvig et al., 2004). CSPGs are abundant and rapidly accumulate after injury in endoneurial tissue (Braunewell et al., 1995). In the PNS, degradation of CSPGs does not seem to play a major role in nerve crush lesions but accelerates the regeneration of axons across a suture site after repair of a transected nerve (Krekoski et al., 2001; Zuo et al., 2002) and improves motor functional recovery (Graham et al., 2007). In agreement with previous studies (English,

2005; Groves et al., 2005), we report that local application of ChABC increases the number of motor and sensory neurons that regenerate their axons through the distal nerve stump. Zuo et al. (2002) attributed the effects of ChABC to the increased ability of regenerating axons to access the basal laminae of the distal nerve stump, which is left intact. Additionally, ChABC degrades CSPGs without displacing laminin in the extracellular matrix which further promotes axon outgrowth into the distal nerve stump (Bixby and Harris, 1991). CSPG degradation with ChABC treatment was effective in our study consistent with previous reports of immunohistochemical evidence of efficient degradation of CSPGs with ChABC treatment (Zuo et al., 2002). Additionally, we performed a single treatment with ChABC at the time of nerve transection and repair, which would have degraded the CPSGs present in the distal nerve stump. However, ChABC has a relatively short half-life and thus our treatment method would have had limited impact on *de novo* CSPG formation in the distal nerve stump. However, the purpose of our experiment was to degrade CSPGs present in the distal nerve stump immediately after nerve transection and repair, thereby limiting the normal delay in degradation which occurs with the progression of Wallerian degeneration.

Although rolipram and ChABC each promote axon outgrowth following nerve injury and repair, the combination of rolipram and ChABC treatments did not result in an additive promotion of axon regeneration. Possible mechanisms to explain this are (i) rolipram-induced elevation in neuronal cAMP is sufficient to overcome the inhibitory growth environment such that simultaneous enzymatic proteoglycan degradation by ChABC does not impact the outgrowth of regenerating axons; (ii) the individual effects of rolipram and ChABC result in maximum axonal regeneration such that a combination of the two agents would not result in further improvement; and (iii) both rolipram and ChABC act at different points in the same signaling pathway. The first mechanism seems unlikely because if it was true, the individual effect on axonal regeneration of ChABC would have been less than that of rolipram, which was not observed in our data. The second mechanism is plausible, whereby individual effects on axonal regeneration were similar between the two treatment groups individually and in combination, suggesting that a maximum level of regeneration had been reached. In this explanation, both agents act through different mechanisms, rolipram at the neuronal cell body and ChABC at the local site of nerve injury (Groves et al., 2005; Zuo et al., 2002) to produce the same outcome. The third mechanism is also possible, whereby up-regulation of cAMP by rolipram and proteoglycan degradation by ChABC both inactivate the inhibitory Rho/ROCK pathway, thereby promoting axon outgrowth via cytoskelatal formation and organization (Fig. 9). Thus, the combination of rolipram and ChABC would produce the same end effect on the inhibitory pathway as each of the agents individually.

In summary, we have demonstrated that administration of rolipram, a PDEIV specific inhibitor, immediately following peripheral nerve transection and repair was effective in increasing the number of motor and sensory neurons that regenerated axons across the repair site. Our findings are consistent with this effect being mediated through up-regulation of cAMP at the level of the neuronal cell body. Specific breakdown of CSPGs with ChABC was also shown to increase the number of motor and sensory neurons that regenerated axons across the repair site. The findings that simultaneous rolipram and ChABC did not have additive effects demonstrate that either elevation of cAMP or degradation of CSPGs alone is sufficient to overcome inhibitory environmental factors and accelerate axon outgrowth.

Acknowledgments

This work was supported by Canadian Institute for Health Research (CHIR) (T.G.) and by the National Institute of Health (T.M.B.). E.U. was recipient of a postdoctoral fellowship from the Spanish ministry of Sciences. The authors thank Guillermo García-Alías for helpful support with the immunohistochemistry.

References

Abercrombie, M., Johnson, M.L., 1946. Quantitative histology of Wallerian degeneration: I. Nuclear population in rabbit sciatic nerve. J. Anat. 80, 37–50.
Aglah, C., Gordon, T., Posse de Chaves, E.I., 2008. cAMP promotes neurite outgrowth and extension through protein kinase A but independently of Erk activation in cultured rat motoneurons. Neuropharmacology 55, 8–17.
Al-Majed, A.A., Neumann, C.M., Brushart, T.M., Gordon, T., 2000. Brief electrical stimulation promotes the speed and accuracy of motor axonal regeneration. J. Neurosci. 20, 2602–2608.
Avellino, A.M., Hart, D., Dailey, A.T., MacKinnon, M., Ellegala, D., Kliot, M., 1995. Differential macrophage responses in the peripheral and central nervous system during wallerian degeneration of axons. Exp. Neurol. 136, 183–198.
Bixby, J.L., Harris, W.A., 1991. Molecular mechanisms of axon growth and guidance. Annu. Rev. Cell Biol. 7, 117–159.
Black, M.M., Lasek, R.J., 1979. Slowing of the rate of axonal regeneration during growth and maturation. Exp. Neurol. 63, 108–119.
Braunewell, K.H., Pesheva, P., McCarthy, J.B., Furcht, L.T., Schmitz, B., Schachner, M., 1995. Functional involvement of sciatic nerve-derived versican- and decorin-like molecules and other chondroitin sulphate proteoglycans in ECM-mediated cell adhesion and neurite outgrowth. Eur. J. Neurosci. 7, 805–814.
Bruck, W., 1997. The role of macrophages in Wallerian degeneration. Brain Pathol. 7, 741–752.
Brushart, T.M., Hoffman, P.N., Royall, R.M., Murinson, B.B., Witzel, C., Gordon, T., 2002. Electrical stimulation promotes motoneuron regeneration without increasing its speed or conditioning the neuron. J. Neurosci. 22, 6631–6638.
Brushart, T.M., Jari, R., Verge, V., Rohde, C., Gordon, T., 2005. Electrical stimulation restores the specificity of sensory axon regeneration. Exp. Neurol. 194, 221–229.
Cai, D., Shen, Y., De Bellard, M., Tang, S., Filbin, M.T., 1999. Prior exposure to neurotrophins blocks inhibition of axonal regeneration by MAG and myelin via a cAMP-dependent mechanism. Neuron 22, 89–101.
Cajal, S., 1928. Degeneration and Regeneration of the Nervous System. Oxford University Press.
Ceballos, D., Lago, N., Verdu, E., Penkowa, M., Carrasco, J., Navarro, X., Palmiter, R.D., Hidalgo, J., 2003. Role of metallothioneins in peripheral nerve function and regeneration. Cell. Mol. Life Sci. 60, 1209–1216.
David, S., Fry, E.J., Lopez-Vales, R., 2008. Novel roles for Nogo receptor in inflammation and disease. Trends Neurosci. 31, 221–226.
Dergham, P., Ellezam, B., Essagian, C., Avedissian, H., Lubell, W.D., McKerracher, L., 2002. Rho signaling pathway targeted to promote spinal cord repair. J. Neurosci. 22, 6570–6577.
English, A.W., 2005. Enhancing axon regeneration in peripheral nerves also increases functionally inappropriate reinnervation of targets. J. Comp. Neurol. 490, 427–441.
Fansa, H., Keilhoff, G., 2003. Factors influencing nerve regeneration. Handchir. Mikrochir. Plast. Chir. 35, 72–82.
Fawcett, J.W., Asher, R.A., 1999. The glial scar and central nervous system repair. Brain Res. Bull. 49, 377–391.
Fouad, K., Schnell, L., Bunge, M.B., Schwab, M.E., Liebscher, T., Pearse, D.D., 2005. Combining Schwann cell bridges and olfactory-ensheathing glia grafts with chondroitinase promotes locomotor recovery after complete transection of the spinal cord. J. Neurosci. 25, 1169–1178.
Franz, C.K., Rutishauser, U., Rafuse, V.F., 2008. Intrinsic neuronal properties control selective targeting of regenerating motoneurons. Brain 131, 1492–1505.
Fu, S.Y., Gordon, T., 1995a. Contributing factors to poor functional recovery after delayed nerve repair: prolonged axotomy. J. Neurosci. 15, 3876–3885.
Fu, S.Y., Gordon, T., 1995b. Contributing factors to poor functional recovery after delayed nerve repair: prolonged denervation. J. Neurosci. 15, 3886–3895.
Fu, S.Y., Gordon, T., 1997. The cellular and molecular basis of peripheral nerve regeneration. Mol. Neurobiol. 14, 67–116.
Furey, M.J., Midha, R., Xu, Q.G., Belkas, J., Gordon, T., 2007. Prolonged target deprivation reduces the capacity of injured motoneurons to regenerate. Neurosurgery 60, 723–732 discussion 732–723.
García-Alías, G., Lin, R., Akrimi, S.F., Story, D., Bradbury, E.J., Fawcett, J, 2008. Therapeutic time window for the application of chondroitinase ABC after spinal cord injury. Exp. Neurol. 210, 331–338.
George, R., Griffin, J.W., 1994. Delayed macrophage responses and myelin clearance during Wallerian degeneration in the central nervous system: the dorsal radiculotomy model. Exp. Neurol. 129, 225–236.
Geremia, N.M., Gordon, T., Brushart, T.M., Al-Majed, A.A., Verge, V.M., 2007. Electrical stimulation promotes sensory neuron regeneration and growth-associated gene expression. Exp. Neurol. 205, 347–359.
Gershenbaum, M.R., Roisen, F.J., 1980. The effects of dibutyryl cyclic adenosine monophosphate on the degeneration and regeneration of crush-lesioned rat sciatic nerves. Neuroscience 5, 1565–1580.
Gordon, T., Sulaiman, O., Boyd, J.G., 2003. Experimental strategies to promote functional recovery after peripheral nerve injuries. J. Peripher. Nerv. Syst. 8, 236–250.
Grados-Munro, E.M., Fournier, A.E., 2003. Myelin-associated inhibitors of axon regeneration. J. Neurosci. Res. 74, 479–485.
Graham, J.B., Neubauer, D., Xue, Q.S., Muir, D., 2007. Chondroitinase applied to peripheral nerve repair averts retrograde axonal regeneration. Exp. Neurol. 203, 185–195.

Groves, M.L., McKeon, R., Werner, E., Nagarsheth, M., Meador, W., English, A.W., 2005. Axon regeneration in peripheral nerves is enhanced by proteoglycan degradation. Exp. Neurol. 195, 278–292.
Han, P.J., Shukla, S., Subramanian, P.S., Hoffman, P.N., 2004. Cyclic AMP elevates tubulin expression without increasing intrinsic axon growth capacity. Exp. Neurol. 189, 293–302.
Houle, J.D., Tom, V.J., Mayes, D., Wagoner, G., Phillips, N., Silver, J., 2006. Combining an autologous peripheral nervous system "bridge" and matrix modification by chondroitinase allows robust, functional regeneration beyond a hemisection lesion of the adult rat spinal cord. J. Neurosci. 26, 7405–7415.
Hughes, P.M., Wells, G.M., Perry, V.H., Brown, M.C., Miller, K.M., 2002. Comparison of matrix metalloproteinase expression during Wallerian degeneration in the central and peripheral nervous systems. Neuroscience 113, 273–287.
Jin, S.L., Richard, F.J., Kuo, W.P., D'Ercole, A.J., Conti, M., 1999. Impaired growth and fertility of cAMP-specific phosphodiesterase PDE4D-deficient mice. Proc. Natl. Acad. Sci. U. S. A. 96, 11998–12003.
Kilmer, S.L., Carlsen, R.C., 1987. Chronic infusion of agents that increase cyclic AMP concentration enhances the regeneration of mammalian peripheral nerves in vivo. Exp. Neurol. 95, 357–367.
Krekoski, C.A., Neubauer, D., Zuo, J., Muir, D., 2001. Axonal regeneration into acellular nerve grafts is enhanced by degradation of chondroitin sulfate proteoglycan. J. Neurosci. 21, 6206–6213.
Lehmann, M., Fournier, A., Selles-Navarro, I., Dergham, P., Sebok, A., Leclerc, N., Tigyi, G., McKerracher, L., 1999. Inactivation of Rho signaling pathway promotes CNS axon regeneration. J. Neurosci. 19, 7537–7547.
Levi, A.D., Bunge, R.P., Lofgren, J.A., Meima, L., Hefti, F., Nikolics, K., Sliwkowski, M.X., 1995. The influence of heregulins on human Schwann cell proliferation. J. Neurosci. 15, 1329–1340.
Lozeron, P., Krarup, C., Schmalbruch, H., 2004. Regeneration of unmyelinated and myelinated sensory nerve fibres studied by a retrograde tracer method. J. Neurosci. Methods 138, 225–232.
McQuarrie, I.G., Grafstein, B., Gershon, M.D., 1977. Axonal regeneration in the rat sciatic nerve: effect of a conditioning lesion and of dbcAMP. Brain Res. 132, 443–453.
Ming, G., Henley, J., Tessier-Lavigne, M., Song, H., Poo, M., 2001. Electrical activity modulates growth cone guidance by diffusible factors. Neuron 29, 441–452.
Mueller, B.K., 1999. Growth cone guidance: first steps towards a deeper understanding. Annu. Rev. Neurosci. 22, 351–388.
Neumann, S., Bradke, F., Tessier-Lavigne, M., Basbaum, A.I., 2002. Regeneration of sensory axons within the injured spinal cord induced by intraganglionic cAMP elevation. Neuron 34, 885–893.
Neumann, S., Woolf, C.J., 1999. Regeneration of dorsal column fibers into and beyond the lesion site following adult spinal cord injury. Neuron 23, 83–91.
Nikulina, E., Tidwell, J.L., Dai, H.N., Bregman, B.S., Filbin, M.T., 2004. The phosphodiesterase inhibitor rolipram delivered after a spinal cord lesion promotes axonal regeneration and functional recovery. Proc. Natl. Acad. Sci. U. S. A. 101, 8786–8790.
Pichichero, M., Beer, B., Clody, D.E., 1973. Effects of dibutyryl cyclic AMP on restoration of function of damaged sciatic nerve in rats. Science 182, 724–725.
Qiu, J., Cai, D., Dai, H., McAtee, M., Hoffman, P.N., Bregman, B.S., Filbin, M.T., 2002. Spinal axon regeneration induced by elevation of cyclic AMP. Neuron 34, 895–903.
Raff, M.C., Hornby-Smith, A., Brockes, J.P., 1978. Cyclic AMP as a mitogenic signal for cultured rat Schwann cells. Nature 273, 672–673.
Sandvig, A., Berry, M., Barrett, L.B., Butt, A., Logan, A., 2004. Myelin-, reactive glia-, and scar-derived CNS axon growth inhibitors: expression, receptor signaling, and correlation with axon regeneration. Glia 46, 225–251.
Shen, Y.J., DeBellard, M.E., Salzer, J.L., Roder, J., Filbin, M.T., 1998. Myelin-associated glycoprotein in myelin and expressed by Schwann cells inhibits axonal regeneration and branching. Mol. Cell. Neurosci. 12, 79–91.
Stoll, G., Griffin, J.W., Li, C.Y., Trapp, B.D., 1989. Wallerian degeneration in the peripheral nervous system: participation of both Schwann cells and macrophages in myelin degradation. J. Neurocytol. 18, 671–683.
Sulaiman, O.A., Gordon, T., 2000. Effects of short- and long-term Schwann cell denervation on peripheral nerve regeneration, myelination, and size. Glia 32, 234–246.
Swett, J.E., Wikholm, R.P., Blanks, R.H., Swett, A.L., Conley, L.C., 1986. Motoneurons of the rat sciatic nerve. Exp. Neurol. 93, 227–252.
Tang, B.L., 2003. Inhibitors of neuronal regeneration: mediators and signaling mechanisms. Neurochem. Int. 42, 189–203.
Tropea, D., Caleo, M., Maffei, L., 2003. Synergistic effects of brain-derived neurotrophic factor and chondroitinase ABC on retinal fiber sprouting after denervation of the superior colliculus in adult rats. J. Neurosci. 23, 7034–7044.
Udina, E., Furey, M., Busch, S., Silver, J., Gordon, T., Fouad, K., 2008. Electrical stimulation of intact peripheral sensory axons in rats promotes outgrowth of their central projections. Exp. Neurol. 210, 238–247.
Witzel, C., Rohde, C., Brushart, T.M., 2005. Pathway sampling by regenerating peripheral axons. J. Comp. Neurol. 485, 183–190.
Zuo, J., Hernandez, Y.J., Muir, D., 1998. Chondroitin sulfate proteoglycan with neurite-inhibiting activity is up-regulated following peripheral nerve injury. J. Neurobiol. 34, 41–54.
Zuo, J., Neubauer, D., Graham, J., Krekoski, C.A., Ferguson, T.A., Muir, D., 2002. Regeneration of axons after nerve transection repair is enhanced by degradation of chondroitin sulfate proteoglycan. Exp. Neurol. 176, 221–228.

Experimental Neurology **175,** 127–137 (2002)
doi:10.1006/exnr.2002.7878, available online at http://www.idealibrary.com on IDEAL®

FK506 Increases Peripheral Nerve Regeneration after Chronic Axotomy but Not after Chronic Schwann Cell Denervation

Olawale A. R. Sulaiman,* Jan Voda,† Bruce G. Gold,†‡ and Tessa Gordon*

**Department of Pharmacology, Division of Neuroscience, University of Alberta, Edmonton, Alberta T6G 2S2 Canada; and †Center for Research in Occupational and Environmental Toxicology and ‡Department of Cell and Developmental Biology, Oregon Health & Science University, Portland, Oregon 97201*

Received May 21, 2001; accepted December 19, 2001

Poor functional recovery after peripheral nerve injury is attributable, at least in part, to chronic motoneuron axotomy and chronic Schwann cell (SC) denervation. While FK506 has been shown to accelerate the rate of nerve regeneration following a sciatic nerve crush or immediate nerve repair, for clinical application, it is important to determine whether the drug is effective after chronic nerve injuries. Two models were employed in the same adult rats using cross-sutures: chronic axotomy and chronic denervation of SCs. For chronic axotomy, a chronically (2 months) injured proximal tibial (TIB) was sutured to a freshly cut common peroneal (CP) nerve. For chronic denervation, a chronically (2 months) injured distal CP nerve was sutured to a freshly cut TIB nerve. Rats were given subcutaneous injections of FK506 or saline (5 mg/kg/day) for 3 weeks. In the chronic axotomy model, FK506 doubled the number of regenerated motoneurons identified by retrograde labeling (from 205 to 414 TIB motoneurons) and increased the numbers of myelinated axons (from 57 to 93 per 1000 μm^2) and their myelin sheath thicknesses (from 0.42 to 0.78 μm) in the distal nerve stump. In contrast, after chronic denervation, FK506 did not improve the reduced capacity of SCs to support axonal regeneration. Taken together, the results suggest that FK506 acts directly on the neuron (as opposed to the denervated distal nerve stump) to accelerate and promote axonal regeneration of neurons whose regenerative capacity is significantly reduced by chronic axotomy. © 2002 Elsevier Science (USA)

Key Words: **sciatic nerve; PNS injury and regeneration; functional recovery; chronic denervation; motoneurons; PNS myelination; rate of axonal regeneration; retrograde labeling.**

INTRODUCTION

Despite the capacity of Schwann cells of the peripheral nervous system to support axonal regeneration, clinical experience has shown that functional recovery is often poor even after microsurgical repair. This is especially true for injuries that sever large nerve trunks or after delayed nerve repair. After injuries to large nerve trunks, motoneurons are required to regenerate over long distance, which they do at a very slow rate (13). We have previously shown that the long delays incurred by the slow rate of regeneration of injured neurons (over the required distances between the nerve lesion sites and the denervated targets) (1) detrimentally affect the regenerative capacity of motoneurons, which remain without targets during a prolonged period of regeneration (chronic axotomy; 11), and (2) lead to deterioration of the growth-permissive Schwann cell environment of the distal nerve stumps (chronic denervation; 12, 37). Thus, injured motoneurons remain chronically axotomized and the Schwann cells of the distal nerve stumps remain chronically denervated as a result of their delayed reinnervation. Likewise, delayed nerve repair leads to chronic motoneuron axotomy and chronic Schwann cell denervation. Prolongation of chronic motoneuron axotomy progressively reduces their capacity to regenerate axons to 33% after a 4- to 6-month chronic axotomy, as compared with when motoneurons were not subjected to chronic axotomy (11). Similarly, chronic denervation of the distal nerve stumps beyond 1 month dramatically reduces the number of freshly axotomized motoneurons that regenerate their axons (12, 37). In both cases, a slow rate of axonal regeneration constitutes a major deterrent to functional recovery after peripheral nerve injury.

The immunophilin ligand FK506 is a potent immunosuppressant used extensively in preventing rejection after organ transplantation (20, 34, 35), an effect mediated via binding to the FK506 binding protein-12 (FKBP-12). Binding of FK506 to the FKBP-12 results in the formation of the FK506/FKBP-12 complex which inhibits T cell proliferation through its inhibition of calcium and calmodulin-dependent protein phosphatase, calcineurin (5, 25, 45). This prevents the dephosphorylation of NF-AT by calcineurin required for acti-

0014-4886/02 $35.00
© 2002 Elsevier Science (USA)
All rights reserved.

vation of IL-2 gene transcription. Suppression of IL-2 production is followed by reduction of T cell proliferation and immunosuppression.

In addition to its immunosuppressive effects, FK506 has been shown to enhance neurite outgrowth *in vitro* (7, 14, 27) and to accelerate the rate of nerve regeneration following a sciatic nerve crush or immediate nerve repair (8, 14–17, 22, 24, 43). This effect on nerve regeneration does not appear to involve FKBP-12 but instead involves FK506-binding protein-52 (FKBP-52), a chaperone component of mature steroid receptor complexes (14). For clinical application, however, it is important to determine whether the drug is effective after chronic nerve injuries.

In the present study, we examined the effectiveness of FK506 in (1) increasing the number of motoneurons that regenerate axons and (2) accelerating the rate of regeneration after delayed nerve repair. Two conditions of delayed nerve repair (chronic axotomy and chronic denervation) were examined using cross-anastomosis *in vivo* methods. This surgical procedure has been routinely used in our laboratory to systematically investigate how chronic axotomy and chronic denervation affect the regenerative capacity of motoneurons. Prolonged axotomy is induced by cutting the tibial (TIB) nerve and preventing regeneration for specific periods of time prior to cross-suturing the proximal TIB nerve stump to the distal stump of a freshly cut common peroneal (CP) nerve. This procedure directs regenerating axons from the chronically axotomized motoneurons to the freshly denervated flexor muscles. In contrast, chronic denervation is induced by cutting the CP nerve and ligating both proximal and distal stumps to innervated muscles, thereby subjecting the distal stump to chronic denervation for specific periods of time prior to cross-suturing the proximal stump of the freshly cut TIB nerve into the chronically denervated CP distal stump. Our findings demonstrate the effectiveness of the same dose of FK506 (5 mg/kg) used previously for nerve crush and immediate nerve repair to increase the number of neurons that regenerate and to increase their rate of regeneration after chronic axotomy but not after chronic denervation. The results have been presented in abstract form (39, 42).

MATERIALS AND METHODS

Animals and Drug Administration

Twenty female Sprague–Dawley rats (5 per group) were used in this study. Beginning after the nerve repair, animals received daily subcutaneous injection of FK506 (5 mg/kg) or saline for 21 days.

Surgical Procedures

All animal procedures were conducted in accordance with the Canadian guidelines for animal experimentation and a local animal welfare committee. Rats used in the experiments were maintained in a standard animal facility with 12-h on–off light conditions. They were allowed to acclimatize to the new environment prior to surgical proceedings, housed in flat-bottomed beta chip-lined cages, and allowed *ad libitum* standard rat chow and water. No special treatments such as a need for analgesia or antibiotics were warranted as a result of daily FK506 injections. Also, throughout the duration of the experiments, none of the rats exhibited signs of autophagia.

Chronic axotomy. Deep anesthesia was induced with sodium pentobarbitol anesthesia (30 mg/kg i.p.) in adult female Sprague–Dawley rats weighing between 200 and 225 g and, using aseptic precautions, their right sciatic nerves were exposed to dissect the TIB and CP branches. The TIB nerve was transected 5 mm distal to the trifurcation of the sciatic nerve (Fig. 1A) and its proximal stump was ligated and sutured to the innervated biceps femoris muscle to prevent regeneration, thereby subjecting TIB motoneurons to chronic axotomy (11). Two months later, rats were reanesthetized, the chronically axotomized TIB proximal nerve stump was sutured to the distal stump of a freshly cut ipsilateral CP nerve inside a 5-mm silastic cuff (Dow Corning; 0.64 mm I.D., 1.19 mm O.D.) with a single 8-0 suture (Ethicon, Peterborough, Ontario, Canada), and the first injection of FK506 (experimental group) or saline (control group) was administered.

Chronic denervation. The TIB and CP nerve branches of the sciatic nerve were also used in subjecting Schwann cells of the distal nerve stumps to chronic denervation. Adult female Sprague–Dawley rats were also used for these surgeries, which were performed under aseptic conditions and deep anesthesia induced by sodium phenobarbital (30 mg/kg i.p.). The right CP nerves of 12 rats were cut and regeneration was prevented by ligating both proximal and distal stumps to adjacent innervated muscles (Fig. 1A). In this way, regeneration of axons from the proximal stump into the distal nerve stump was prevented so that the target muscle and the distal nerve sheath were both denervated. Denervation of the distal nerve sheath was prolonged for periods of 2 months after which cross-suture of the proximal stump of freshly cut ipsilateral TIB nerve and the distal denervated stump of CP was performed, also using a silastic cuff (Fig. 1B). This was to facilitate regeneration of the axons of freshly axotomized and regenerating TIB motoneurons through the chronically denervated distal nerve sheaths. Animals were allowed to recover and kept for a period of 21 days during which they received daily subcutaneous injections of 5 mg/kg rat weight FK506 (experimental) or saline (control).

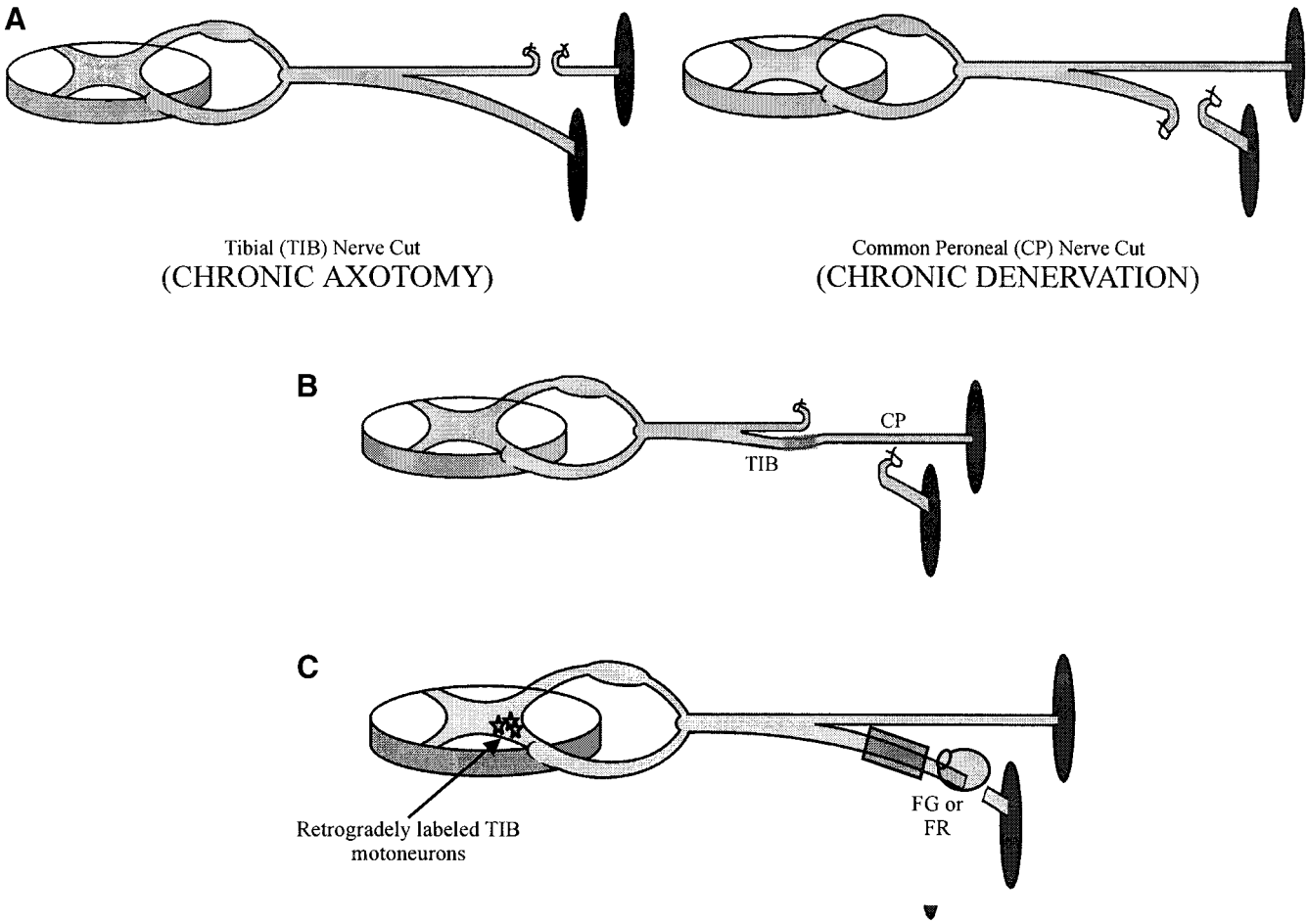


FIG. 1. (A) The TIB nerve was cut and regeneration of the proximal stump was prevented for 2 months (chronic axotomy) or the CP nerve was cut and reinnervation of its distal nerve stump was prevented (chronic denervation). (B) Two months later, the proximal stump of the TIB nerve that was chronically axotomized was sutured to a freshly cut ipsilateral CP + subcutaneous injection of 5 mg/kg/day of FK506 (experimental group) or saline (control group) (old TIB–fresh CP cross-suture) or the proximal stump of a freshly cut TIB nerve was sutured to the ipsilateral CP nerve that was chronically denervated + subcutaneous injection of 5 mg/kg/day of FK506 (experimental group) or saline (control group) (fresh TIB–old CP cross-suture). (C) Three weeks following TIB–CP cross-suture and daily injection of FK506 or saline, either one of retrogradely transported fluorescent dyes (FG or FR) was used to backlabel the TIB motoneurons which regenerated axons.

Retrograde Axonal Tracer Application

Three weeks following TIB–CP cross-suture and daily injection of FK506 or saline, the CP nerve was cut at a distance of 25 mm from the TIB–CP suture site for application of one of the retrogradely transported fluorescent dyes, fluorogold (FG) or fluororuby (FR), for 1 or 2 h, respectively. Backlabeling with FG was done by exposing the tip of the cut CP nerve to 4% FG in 0.1 M cacodylic acid for 1 h (32) in a vaseline well, after which it was extensively irrigated and reflected to a distant portion of the wound. Backlabeling with FR was done by placing the tip of the cut CP nerve on a 1-cm^2 weighing paper (Fisher Scientific Co., Springfield, NJ) with FR crystals for 2 h and then irrigating the nerve and placing it in the opposite corner of the wound to prevent backlabeling of non-TIB motoneurons by diffusion of tracers. The choice of dye was alternated between animals to control for possible differences in retrograde uptake and transport of the dyes. The skin was then sutured and the animals were allowed to recover. Five days later, rats were transcardially perfused with saline and then 4% paraformaldehyde in 0.1 M phosphate-buffered saline. The L4–L6 spinal segment was removed and left in 30% sucrose paraformaldehyde solution overnight. Longitudinal 50-μm cryostat sections of the spinal cord were cut and examined under a fluorescent microscope. FR-labeled motoneurons were visualized with a Rhodamine filter (580 nM), while the FG-labeled motoneurons fluoresced blue under UV light with a 430-nM filter. Each longitudinal section was examined and all labeled motoneurons were counted (see Fig. 2).

Motoneuron Counting

Using a freezing microtome (Jung CM 3000), each lumbar spinal segment was sectioned into 50-μm lon-

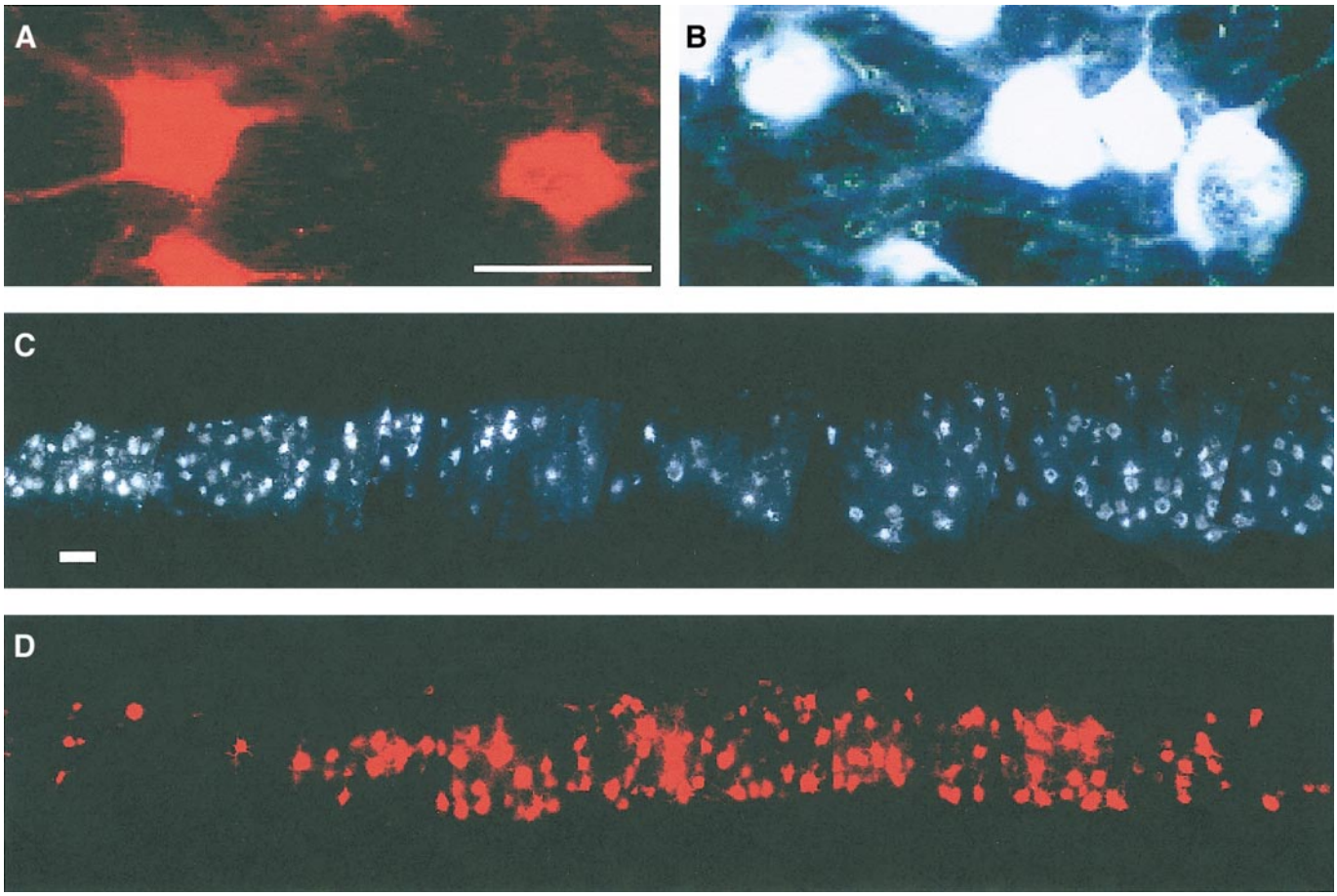


FIG. 2. Photomicrographs of motoneurons backlabeled with fluororuby (A) or fluorogold (B) as viewed under a fluorescent microscope. The locations and distribution of motoneurons backlabeled with either FR (C) or FG (D) in the lumbar spinal cord are also illustrated. Both fluorescent dyes were able to backlabel the somas and dendrites of regenerated TIB motoneurons. Scale bar for A and B is 30 μm, and C and D are visualized under 16X magnification.

gitudinal sections, as previously described (37). The 50-μm sections were serially mounted on glass slides, allowed to dry, and coverslipped. All TIB motoneurons in each spinal cord section that regenerated their axons into the distal CP nerve stumps were retrogradely labeled by the applied fluorescent dyes and could be identified and counted at 20–40X magnification under UV fluorescence. Cells labeled with FR could be easily identified by their red fluorescence and those labeled with FG had blue fluorescence (Fig. 2). Only TIB motoneurons in which there was a distinct nucleus and those that could be visualized only under the UV fluorescent filter specific for the dye with which they were labeled were counted; multiple counting of split neurons was corrected for by the method of Abercrombie and Johnson (1).

Histology and Morphometry

Nerve histology was concluded as previously described (43). Briefly, prior to the application of fluorescent dyes, 3-mm pieces of nerves were excised and fixed by immersion in gluteraldehyde (3% in 0.1 M phosphate buffer), stained with osmium tetroxide (3% solution in 0.1 M phosphate buffer), dehydrated in ascending alcohols, and embedded in araldite. Semithin sections (0.5 μm) were stained with toluidine blue. Myelinated and nonmyelinated axons in the entire nerve were counted under a 63X oil immersion lens (final magnification 790X) with the aid of a 100-unit micrometer reticle (10-mm divisions) using a Leitz Laborlux S light microscope. For determination of myelin sheath thicknesses, the inner and outer perimeters were traced on photographic prints (three fields per nerve; final magnification, 2000X) using a SummaSketch III (Summagraphics, Seymour, CT) digitizing tablet and BIOQUANT Classic 95 software (R&M Biometrics, Nashville, TN). Myelin sheath thicknesses were calculated from these data using the following formula: fiber perimeter − axon perimeter/2.

Statistical Analysis

A one-way analysis of variance (ANOVA) and Student's *t* test were used to compare the mean number of TIB motoneurons that regenerated axons and the re-

spective number of regenerated myelinated and unmyelinated axons and to compare myelin sheath thicknesses in the chronic axotomy and chronic denervation groups. Statistical significance was accepted at the 5% level ($P < 0.05$).

RESULTS

Daily injections of the rats in the experimental groups with FK506 for 3 weeks did not have any apparent generalized secondary effects on their health. Likewise, we encountered no problems of infections or unexpected deaths during the duration of injection, indicating that the immunosuppressive effects of FK506 were tolerated by the animals at this dosage and for the relatively short exposure period.

TIB Motoneuronal Regeneration after 2-Month Chronic TIB Motoneuron Axotomy

Retrograde fluorescent labeling, which labels only neurons that regenerate their axons up to the point of application of the applied fluorescent dyes, was used to identify and count the number of 2-month chronically axotomized TIB motoneurons that regenerated their axons into freshly cut distal CP nerve stumps in the experimental and control rats with daily injections of FK506 and saline, respectively. The two chosen fluorescent dyes, FG and FR, brightly label both the somas and the dendrites of the 2-month chronically axotomized TIB motoneurons that regenerated their axons into the freshly cut CP distal nerve stumps (Fig. 2).

The control group in our experiments, which received daily injections of an equal volume of saline, demonstrate a reduced number of TIB motoneurons that regenerated their axons after a 2-month chronic axotomy [205 ± 27 (mean ± SE)], which is only 24% of the total number of TIB motoneurons in the intact TIB nerve. This represents a 76% decrease in the numbers of 2-month chronically axotomized motor neurons that regenerate axons into the distal nerve stump compared to the reported 66% decline in numbers of motoneurons that reinnervated muscles (11). However, the duration of regeneration in these two experiments differed: tibial motor axonal regeneration was estimated after at least 16 weeks in our previous experiments (in which there was 66% reduction), whereas in the present experiments, this was done after only 3 weeks to minimize the duration of injections of FK506. In addition, we noted that it takes more than 6 weeks (up to 12 weeks) for all TIB motoneurons to regenerate their axons after immediate nerve repair (38) and 8–10 weeks for all femoral motoneurons to regenerate their axons across the surgical site (2). Thus, examination of an earlier (3-week) time point enabled us to maximize the ability to observe a discernable effect of the drug on nerve regeneration.

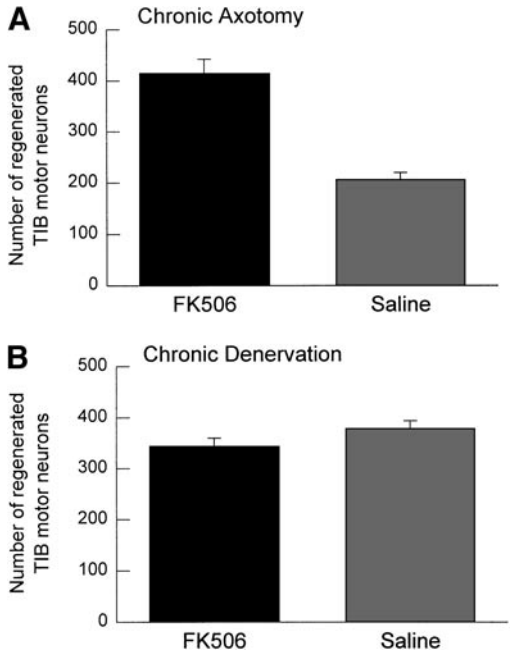


FIG. 3. (A) Numbers (mean + SE) of 2-month chronically axotomized TIB motoneurons which regenerated axons into freshly cut distal CP nerve stumps were compared when animals received daily subcutaneous injections of FK506 (black bars) or saline (gray bars) (5 mg/kg rat weight). Note the significant increase in the number of regenerated TIB motoneurons with FK506 treatments. (B) Numbers (mean + SE) of freshly axotomized TIB motoneurons which regenerated into 2-month chronically denervated CP distal nerve stumps compared under conditions, as in A. FK506 did not exert any effect on the number of TIB motoneurons that regenerated axons. Statistical analysis by one-way analysis of variance and Student *t* test.

Only 205 ± 27 TIB motoneurons regenerated their axons after 2-month chronic axotomy and cross-suture to freshly cut distal CP nerve stump in animals which received daily subcutaneous injections of equal volume of saline (control group). In contrast, in animals that received daily injections of FK506, 414 ± 62 TIB motoneurons regenerated their axons (Fig. 3A). This represents a significant increase, almost doubling the number of TIB motoneurons that regenerated axons, compared to the control group, after only 3 weeks regeneration period and treatment with FK506. Furthermore, the data indicate that 50% of all TIB motoneurons regenerated after FK506 treatment, which is significantly higher than the 34% that regenerated even after 4 weeks of regeneration time (4). Our findings that about half of the TIB motoneurons regenerated into the distal CP nerve stumps after only 3 weeks is impressive when one considers that, assuming a progressive increase in the number of TIB motoneurons that regenerate axons after 2-month axotomy, only 25% of all TIB motoneurons would normally be expected to regenerate after 3 weeks of regeneration. Therefore, FK506 very markedly increased the number of 2-month chronically axotomized TIB motoneurons

that regenerated their axons into freshly cut distal CP nerve stumps after a very short duration (3 weeks) of regeneration.

The total number of myelinated and nonmyelinated axons that regenerated into distal CP nerve stumps in the FK506-treated animals was double the total number of axons that regenerated in the saline-treated animals: mean values (± SE) increased from 33 ± 6 per 1000 μm^2 in saline-treated animals to 76 ± 12 per 1000 μm^2 in FK506-treated animals (Figs. 6B and 6C). This doubling of axon number mirrored the doubling of the number of motoneurons that regenerated axons (Fig. 6). Hence, there is direct correlation between the effects of FK506 on increasing the number of TIB motoneurons which regenerated axons and the total number of regenerated axons.

The number of myelinated axons was also estimated as an indication of the effect of FK506 on the rate of axonal regeneration; axons whose reinnervation of the distal nerve stump is accelerated should induce the myelinating phenotype of Schwann cells earlier than the later-arriving axons and would, consequently, exhibit more extensive myelination. In parallel with its effect of increasing the total number of regenerated axons (Figs. 6B and 6C), FK506 significantly increased the number of myelinated axons to 93 ± 10 per 1000 μm^2 compared to 57 ± 10 per 1000 μm^2 in the control group (see Figs. 4 and 6C). Not only were there more myelinated axons, but the individual axons exhibited thicker myelin sheaths (Fig. 4); mean myelin sheath thicknesses were significantly increased from 0.42 ± 0.006 μm ($n = 403$) in saline-treated animals to 0.78 ± 0.010 μm ($n = 419$) in FK506-treated animals. Taken together, FK506 increased the rate of regeneration (increased number of mature, myelinated axons) and promoted the growth (increased total number of regenerated axons) of regenerating axons in the distal CP nerve stump.

TIB Motoneuronal Regeneration after 2-Month Chronic Schwann Cell Denervation

In a second group of rats, retrograde neuroanatomical tracers and nerve histomorphometry were used to estimate the effects of FK506 on the capacity of freshly axotomized TIB motoneurons to regenerate axons into 2-month chronically denervated Schwann cells of the distal CP nerve stump (see Materials and Methods). In contrast to its effect of increasing regenerative capacity of 2-month chronically axotomized TIB motoneurons, FK506 did not significantly change the number of TIB motoneurons that regenerated axons into the 2-month chronically denervated distal CP nerve stumps; mean values were 344 ± 33 and 378 ± 33 per 1000 μm^2 in FK506-treated and saline-treated animals, respectively (Fig. 3B). There were no apparent differences in the total number of regenerated axons and number of myelinated axons in the control and experimental groups (Fig. 5B), albeit this was not quantitated. Nevertheless, given the direct correlation between the numbers of back-labeled TIB motoneurons and the total number of regenerating axons observed in the chronic axotomy model, this finding is consistent with the lack of any difference in the number of retrogradely labeled TIB motoneurons.

DISCUSSION

This study is the first to demonstrate, using a direct and quantitative neuroanatomical assay, that daily subcutaneous injections of 5 mg/kg FK506 after TIB–CP cross-suture (i) is able to reverse the detrimental effect of 2-month chronic axotomy on the capacity of TIB motoneurons to regenerate axons, but (ii) cannot reverse the effect of 2-month chronic denervation on the capacity of Schwann cells of the distal nerve stump to support axonal regeneration. FK506 increased (a) the number of TIB motoneurons that regenerated axons and the total number of regenerated axons in the distal CP nerve stump (thus promoting growth) and (b) the rate of axonal regeneration as measured by the increased number of mature, myelinated axons.

The present findings extend the initial demonstrations that FK506 increases axonal regeneration of freshly axotomized peripheral neurons (8, 16, 17, 22, 24, 43) by showing that it is also effective in improving axonal regeneration after delayed nerve repair, during which motoneurons are chronically axotomized (present study). Thus, FK506 not only increases the rate of axonal regeneration (17, 43), but also promotes regeneration of neurons whose regenerative capacity is significantly reduced by chronic axotomy, as may occur after injuries to large nerve trunks and delayed nerve repair. We suggest that the lack of effect in the chronic denervation injury model is due to an inability of the drug to improve the reduced capacity of 2-month chronically denervated Schwann cells to support TIB axonal regeneration.

Functional recovery after peripheral nerve injury is often disappointing regardless of the capacity of the glial cells of the distal stumps of injured nerves, the Schwann cells, to provide a growth-permissive environment. Clinical experience has established that functional recovery is particularly poor for injuries which sever large nerve trunks such as brachial and lumbar plexus injuries (13, 29, 31, 40). This is because regenerating axons have to travel over long distances to reinnervate denervated targets, which they do at very slow rate (1–3 mm/day). The slow rate of regeneration may require many months before regenerating axons might be expected to reach denervated targets, during which the motoneurons are chronically axotomized and the growth-supportive environment of the distal nerve stumps is lost (13). Hence, faster rates of

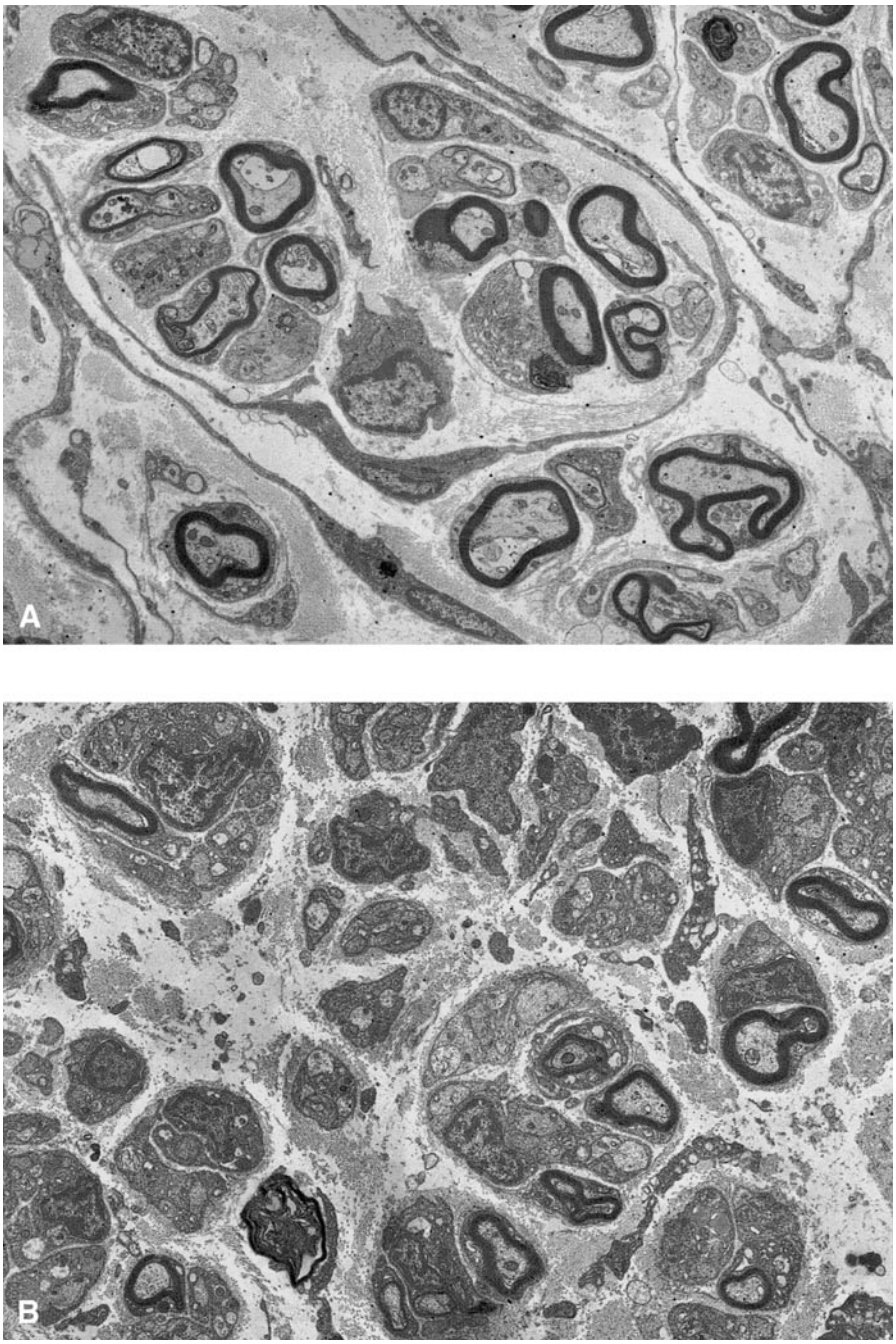


FIG. 4. Light micrographs of TIB nerve fibers which reinnervated the distal CP nerve stumps when animals were treated with either FK506 (A) or saline (B) in the chronic axotomy group. Note that TIB axons from animals which received daily injections of FK506 appear larger and are ensheathed by thicker myelin. This shows that regenerated TIB axons in the FK506-treated animals are in a more advanced state of regeneration than TIB axons from the saline-treated animals. Magnification 2700X.

regeneration are required to eliminate the detrimental effects of chronic axotomy on neurons and to achieve timely reinnervation of the distal nerve stumps, while the Schwann cells are still capable of supporting axonal regeneration.

In the present study, we report that FK506 increases both the rate and the extent of axonal regeneration of chronically injured neurons after delayed nerve repair. Although direct estimation (using retrograde labeling) of the number of regenerated neurons after 2-month chronic axotomy in FK506- and saline-treated animals was restricted to motoneurons in our study, we showed that FK506 also increased the total number of regenerated axons in the distal CP nerve stumps. This effect of

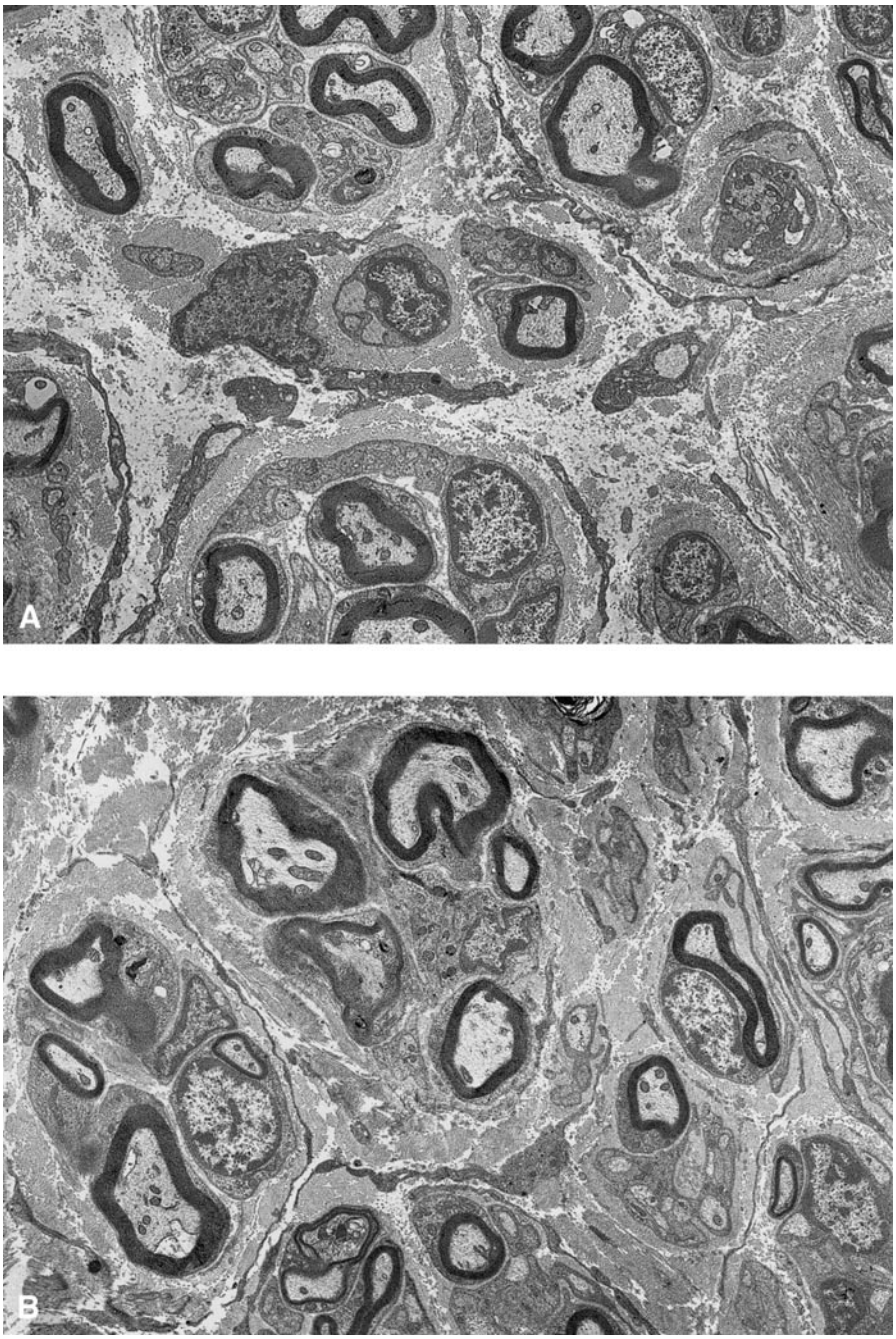


FIG. 5. Light micrographs of TIB nerve fibers which reinnervated the 2-month chronically denervated distal CP nerve stumps with (A) or without (B) FK506 treatment. There is no difference in the thickness of myelin sheaths around the regenerated TIB axons in both groups. Magnification 2700X.

increasing the number of regenerated axons paralleled the increase in the number of 2-month chronically axotomized motoneurons that regenerated axons with FK506 treatment. Therefore, the effect of FK506 on motoneuronal regeneration may extend to sensory neurons also since there is a proportionate increase in the total number of axons (both motor and sensory) which reinnervated the distal CP nerve stumps (although an increase in axonal sprouting cannot be ruled out).

The ubiquitous distribution of the immunophilins in the nervous system (36) suggests that their ligands, including FK506, may play significant roles in the nervous system. Accordingly, it was found that systemic administration of FK506 improved functional recovery following a nerve crush or immediate nerve repair by accelerating the rate of axonal regeneration (8, 16, 17, 22, 24, 43). FK506 has also been shown to exert neuroprotective/neuroregenerative effects (for review, see

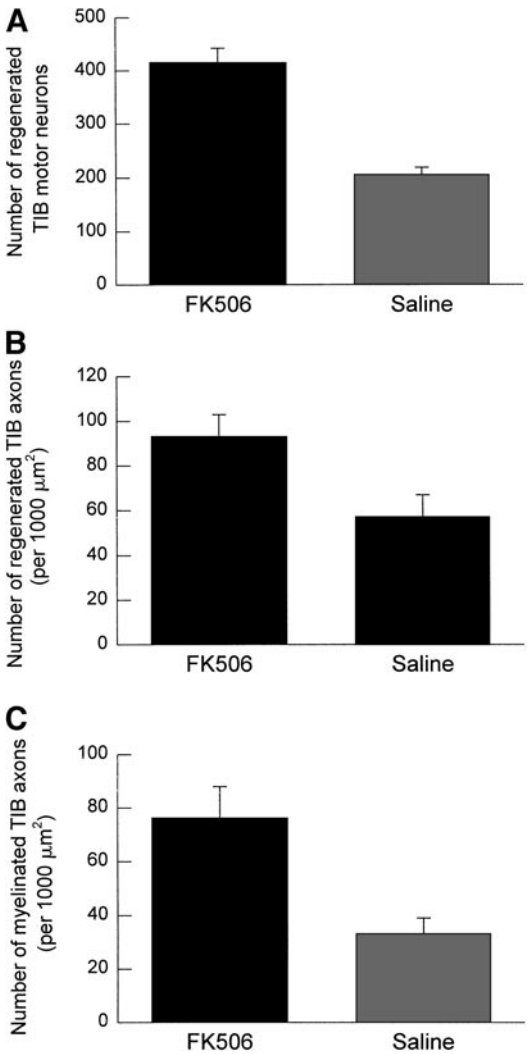


FIG. 6. Numbers (mean + SE) of (A) 2-month chronically axotomized TIB motoneurons that regenerated axons, (B) all regenerated axons, and (C) myelinated axons in the FK506-treated animals compared to saline-treated animals. FK506 increased the capacity of chronically axotomized motoneurons to regenerate axons (A) and increased both the extent (B) and the rate (C) of axonal regeneration.

19) following ischemic insults (9, 33), in spinal cord injuries (3, 30, 44), and in models of degenerative diseases (6, 23). However, none of these studies specifically investigated whether FK506 could exert its effects of improving functional recovery after delayed nerve repair, which is of clinical significance since immediate nerve repairs are nothing but exceptions in clinical practice. Our study was designed to specifically address this question using an outcome measure that is very direct and quantitative.

The fact that we observed a positive effect of FK506 in promoting motoneuronal regeneration and accelerating axonal regeneration only after the chronic axotomy injury model strongly suggests that the effect of FK506 is mediated via the neuron itself (at the level of the neuronal cell body and/or the proximal axon). This hypothesis is consistent with studies showing that FK506 promotes neurite outgrowth in PC12 cells, sensory ganglia, and hippocampal neurons *in vitro* (27) and with the upregulation of FKBP-12 mRNA in axotomized motoneurons (26, 28); while a different immunophilin (FKBP-52) appears to mediate the neurotrophic effect of FK506 (14), it too undergoes fast axonal transport (B. G. Gold, unpublished observation). Growth-associated genes such as tubulin, actin, and GAP-43 are upregulated in the motoneurons after axotomy; however, their expressions are lost if motoneurons remain axotomized for a long time (41). The expression of GAP-43, a protein which is essential for growth cone formation and axonal elongation, is increased by FK506 following either spinal cord (30) or peripheral nerve (18) injuries. Therefore, the positive effect of FK506 on motoneurons may be mediated by maintaining (after crush injury or immediate nerve repair) or reinducing the upregulation of growth-associated genes (after chronic axotomy). Whether FK506 induces the upregulation of these genes directly or indirectly through intermediate mediators remains to be elucidated, although both have been proposed.

In sum, the present study clearly demonstrates that FK506 is effective in promoting peripheral nerve regeneration after chronic injury with delayed nerve repair. Although more mechanistic studies are warranted, the results of our study suggest that application of FK506 as an adjunct treatment after peripheral nerve injury and repair could be an effective way to improve functional recovery after peripheral nerve injuries. Recently, application of FK506 has been shown to speed functional recovery in two successful hand transplantations (10, 21) but more standardized clinical trials are required to further assess the efficacy of FK506 in promoting nerve regeneration after injuries in humans.

ACKNOWLEDGMENTS

This work was supported by CIHR of Canada and The Spinal Cord Research Foundation of the Paralyzed Veterans of America. FK506 was generously provided by Fujisawa Pharmaceutical Co., Ltd., Osaka, Japan. O. A. R. Sulaiman is supported by a fellowship from the CIHR/Canadian Neurotrauma Partnership Fellowship and by an incentive award and a research allowance from the AHFMR. This paper partially fulfills the requirement for the Ph.D. thesis of O.A.R.S. T. Gordon is an AHFMR Senior scientist. We thank Mr. Gordon Boyd for his assistance with the graphic designs and Mr. Dan Austin for his assistance with preparation of the micrographs.

REFERENCES

1. Abercombie, M., and J. L. Johnson. 1946. A quantitative histology of Wallerian degeneration: Nuclear population in rabbit sciatic nerve. *J. Anat.* **80:** 37–50.
2. Al-Majed, A. A., C. M. Neumann, T. M. Brushart, and T. Gordon. 2000. Brief electrical stimulation promotes the speed and

accuracy of motor axonal regeneration. *J. Neurosci.* **20:** 2602–2608.

3. Bavetta, S., P. J. Hamlyn, G. Burnstock, A. R. Lieberman, and P. N. Anderson. 1999. The effects of FK506 on dorsal column axons following spinal cord injury in adult rats: Neuroprotection and local regeneration. *Exp. Neurol.* **158:** 382–393.
4. Boyd, J. G., and T. Gordon. 2002. The dose-dependent fascilitation and inhibition of peripheral nerve regeneration by exogenous brain derived neurotrophic factor. *Eur. J. Neurosci.*, in press.
5. Clipstone, N. A., and G. R. Crabtree. 1993. Calcineurin is a key signaling enzyme in T lymphocyte activation and the target of immunosuppressive drugs cyclosporin and FK506. In *Immunosuppressive and Antiinflammatory Drugs* (A. C. Allison, K. J. Lafferty, and H. Fliri, Eds.), pp. 20–30. New York Acad. Sci., New York.
6. Constantini, L., P. Chaturvedi, D. Armistead, P. McCaffrey, T. Deacon, and O. Isaacson. 1998. A novel immunophilin ligand: Distinct branching effects on dopaminergic neurons in culture and neurotrophic actions after oral administration in an animal model of Parkinson's disease. *Neurobiol. Dis.* **5:** 97–106.
7. Constantini, L., and O. Isaacson. 2000. Immunophilin ligands and GDNF enhance neurite branching or elongation from developing dopamine neurons in culture. *Exp. Neurol.* **164:** 60–70.
8. Doolabh, V. B., and S. E. Mackinnon. 1999. FK506 accelerates functional recovery following nerve grafting in a rat model. *Plast. Reconstr. Surg.* **103:** 1928–1936.
9. Drake, M., H. Friberg, F. Boris-Moller, K. Sakata, and T. Wieloch. 1996. The immunosuppressant FK506 ameliorates ischemic damage in the rat brain. *Acta Physiol. Scand.* **158:** 155–159.
10. Dubernard J.-M., E. Owen, G. Herzberg, M. Lanzetta, X. Martin, H. Kapila, M. Dawahra, and N. S. Hakim. 1999. Human hand allograft: Report on first 6 months. *Lancet* **353:** 1315–1320.
11. Fu, S., and T. Gordon. 1995. Contributing factors to poor functional recovery after delayed nerve repair: Prolonged axotomy. *J. Neurosci.* **15:** 3876–3885.
12. Fu, S., and T. Gordon. 1995. Contributing factors to poor functional recovery after delayed nerve repair: Prolonged muscle denervation. *J. Neurosci.* **15:** 3886–3895.
13. Fu, S., and T. Gordon. 1997. The cellular and molecular basis of peripheral nerve regeneration. *Mol. Neurobiol.* **14:** 67–116.
14. Gold, B. G., V. Densmore, W. Shou, M. M. Matzuk, and H. S. Gordon. 1999. Immunophilin FK506 binding protein 52 (not FK506 binding protein 12) mediates the neurotrophic action of FK506. *J. Pharmacol. Exp. Therap.* **289:** 1202–1210.
15. Gold, B. G., H. S. Gordon, and M. S. Wang. 1999. Efficacy of delayed or discontinous FK506 administration on nerve regeneration in the rat sciatic nerve crush model: Lack of evidence for a conditioning lesion-like-effect. *Neurosci. Lett.* **267:** 33–36.
16. Gold, B. G., K. Katoh, and T. Storm-Dickerson. 1995. The immunosuppressant FK506 increases the rate of axonal regeneration in rat sciatic nerve. *J. Neurosci.* **15:** 7509–7516.
17. Gold, B. G., T. Storm-Dickerson, and D. R. Austin. 1994. The immunosuppressant drug FK506 increases functional recovery and nerve regeneration following peripheral nerve injury. *Restor. Neurol. Neurosci.* **6:** 287–296.
18. Gold, B. G., J. Y. Yew, and M. Zeleny-Pooley. 1998. The immunosuppressant drug FK506 increases GAP-43 mRNA levels in axotomized sensory neurons. *Neurosci. Lett.* **241:** 25–28.
19. Gold, B. G. 2000. Neuroimmunophilin ligands: Evaluation of their therapeutic potential for the treatment of neurological disorders. *Exp. Opin. Invest. Drugs* **9:** 2331–2342.
20. Hoffman, A. L., L. Makowka, B. Banner, X. Cai, D. V. Cramer, A. Pascualone, S. Todo, and T. E., Starzl. 1990. The use of FK-506 for small intestine allo-transplantation: Inhibition of acute rejection and prevention of fatal graft-versus-host disease. *Transplantation* **49:** 483–490
21. Jones, J. W., S. A. Gruber, J. H. Barker, and W. C. Breidenbach. 2000. Successful hand transplantation: One year follow-up. *N. Engl. J. Med.* **343:** 468–473.
22. Jost, S. C., V. B. Doolabh, S. E. Mackinnon, M. Lee, and D. Hunter. 2000. Acceleration of peripheral nerve regeneration following FK506 administration. *Restor. Neurol. Neurosci.* **17:** 39–44.
23. Kitamura, Y., Y. Itano, T. Kubo, and Y. Nomura. 1994. Suppressive effect of FK506, a novel immunosuppressant, against MPTP-induced dopamine depletion in the striatum of young C57BL/6 mice. *J. Neuroimmunol.* **50:** 221–224.
24. Lee, M., V. B. Doolabh, S. E. Mackinnon, and S. Jost. 2000. FK506 promotes functional recovery in crushed rat sciatic nerve. *Muscle Nerve* **23:** 633–640.
25. Liu, J., J. D. Farmer, W. S. Lane, J. Friedman, I. Weissman, and S. L. Schreiber. 1991. Calcineurin is a common target of cyclophilin-cyclosporin A and FKBP-FK506 complexes. *Cell* **66:** 807–815.
26. Lyons, W. E., J. P. Steiner, T. M. Dawson, and S. H. Snyder. 1992. Increased expression of FK506 binding protein during peripheral nerve regeneration. *Soc. Neurosci.* **18:** 604.
27. Lyons, W. E., E. B. George, T. M. Dawson, J. P. Steiner, and S. H. Snyder. 1994. Immunosuppressant FK506 promotes neurite outgrowth in cultures of PC12 cells and sensory ganglia. *Proc. Natl. Acad. Sci. USA* **91:** 3191–3195.
28. Lyons, W. E., J. P. Steiner, S. H. Snyder, and T. M. Dawson. 1995. Neuronal regeneration enhances the expression of the immunophilin FKBP-12. *J. Neurosci.* **15:** 2985–2994.
29. MacKinnon, S. E. 1989. New directions in peripheral nerve surgery. *Ann. Plast Surg.* **22:** 257–272.
30. Madsen, J. R., P. Macdonald, N. Irwin, D. E. Goldberg, G. L. Yao, K. F. Meiri, I. J. Rimm, P. E. Steig, and L. I. Benowitz. 1998. Tacrolimus (FK506) increases neuronal expression of GAP-43 and improves functional recovery after spinal cord injury in rats. *Exp. Neurol.* **154:** 673–683.
31. Millesi, H. 1990. Progress in peripheral nerve reconstruction. *World J. Surg.* **14:** 733–747.
32. Schmued, L. C., and L. Heimer. 1990. Iontophoretic injection of fluoro-gold and other fluorescent tracers. *J. Histochem. Cytochem.* **38:** 721–723.
33. Sharkey, J., and S. P. Butcher. 1994. Immunophilins mediate the neuroprotective effects of FK506 in focal cerebral ischemia. *Nature* **371:** 336–338.
34. Starzl, T. E., L. Makowka, and S. Todo. 1987. FK506: A potential breakthrough in immunosuppression. *Transplant. Proc.* **19:** S3–S104.
35. Starzl, T. E., S. Todo, J. Fung, A. J. Demetris, R. Venkataramman, and A. Jain. 1989. FK506 for liver, kidney, and pancreas transplantation. *Lancet* **2:** 1000–1004.
36. Steiner, J. P., T. M. Dawson, M. Fotuhi, C. E. Glatt, A. M. M. Snowman, N. Cohen, and S. H. Snyder. 1992. High brain densities of the immunophilin FKBP colocalized with calcineurin. *Nature* **358:** 584–587.
37. Sulaiman, O. A. R., and T. Gordon. 2000. Effects of short- and long-term Schwann cell denervation on peripheral nerve regeneration, myelination and size. *Glia* **32:** 234–246.
38. Sulaiman, O. A. R., and T. Gordon. 2002. Transforming growth factor-β and forskolin attenuate the adverse effects of long-term Schwann cell denervation on peripheral nerve regeneration in vivo. *Glia* **37:** 206–218.

39. Sulaiman, O. A. R, J. Voda, B. G. Gold, and T. Gordon. 2000. FK506 increases motor nerve regeneration after chronic axotomy but not after chronic Schwann cell denervation. *Soc. Neurosci.* **26:** 704.

40. Sunderland, S., and K. C. Bradley. 1950. Denervation atrophy of the distal stump of a severed nerve. *J. Comp. Neurol.* **93:** 401–409.

41. Tetzlaff, W., S. W. Alexander, F. D. Miller, and M. A. Bisby. 1991. Response of facial and rubrospinal neurons to axotomy: Changes in mRNA expression for cytoskeletal proteins and GAP-43. *J. Neurosci.* **11:** 2528–2544.

42. Voda, J., O. A. R. Sulaiman, T. Gordon, and B. G. Gold. 2001. FK506 increases nerve regeneration following chronic axotomy but not chronic denervation. *Am. Soc. Peripheral Nerve Meeting, San Diego, California.*

43. Wang, M.-S., M. Zeleny-Pooley, and B. G. Gold. 1997. Comparative dose-dependent study of FK506 and cyclosporin A on the rate of axonal regeneration in the rat sciatic nerve. *J. Pharmacol. Exp. Therap.* **282:** 1084–1093.

44. Wang, M.-S., and B. G. Gold. 1999. FK506 increases the regeneration of spinal cord axons in a predegenerated peripheral nerve autograft. *J. Spinal Cord Med.* **22:** 287–296.

45. Weiderrecht G., E. Lam, S. Hung, M. Martin, and N. Sigal. 1993. The mechanism of action of FK506 and cyclosporin A. *Ann. N. Y. Acad. Sci.* **696:** 9–19.

J. Physiol. (1982), **323**, *pp.* 307–323
With 8 text-figures
Printed in Great Britain

TIME COURSE AND EXTENT OF RECOVERY IN REINNERVATED MOTOR UNITS OF CAT TRICEPS SURAE MUSCLES

BY TESSA GORDON* AND R. B. STEIN

From the Department of Physiology, University of Alberta, Edmonton, Canada T6G 2H7

(*Received 16 April 1981*)

SUMMARY

1. Nerve and muscle properties were studied in single motor units of triceps surae muscles in the cat using chronic recording techniques and intramuscular microstimulation. Recordings were made before and at intervals up to 18 months after a nerve was sectioned and sutured either to its distal stump (nerve–nerve suture) or to a muscle directly (nerve–muscle suture). Thus, each nerve and muscle served as its own control for recovery after reinnervation.

2. Following a delay all muscles recovered their preoperative tension after nerve–nerve suture with a single exponential having a time constant of 1–2 months. Only half the muscles recovered their preoperative tensions after nerve–muscle sutures. Muscles which did not recover fully also had a slower time course of recovery.

3. The estimated number of motor units did not increase significantly later than 2 months after nerve section and suture. Further recovery of muscle tension is due to increased unit tension, rather than increasing numbers of reinnervated motor units. Unit tension recovered completely in all muscles, but did not become enlarged, even when muscles apparently remained partially denervated.

4. The latency of compound nerve potentials often recovered completely, although the amplitude of the potential remained depressed. Single motor axonal potentials recovered to control levels after reinnervation of muscle with a time constant similar to that for the recovery of motor unit tension. Therefore, two distinct populations of motor axons contribute to the compound potential: reinnervating axons whose size recovers fully, and disconnected axons which remain atrophic. Incomplete recovery of the compound potential amplitude mainly results from a failure of all axons to remake peripheral connexions.

5. Thus, formation of functional nerve–muscle connexions completely reverses the effects of axotomy on nerve and muscle. Reinnervated motor units recovered their preoperative size, whether or not much of the muscle remained denervated.

* Present address and address for correspondence: Department of Pharmacology, University of Alberta, Edmonton, Alberta, Canada T6G 2H7.

Downloaded from J Physiol (jp.physoc.org) at University of Alberta on June 10, 2009

REVIEW / SYNTHÈSE

The resilience of the size principle in the organization of motor unit properties in normal and reinnervated adult skeletal muscles[1]

Tessa Gordon, Christine K. Thomas, John B. Munson, and Richard B. Stein

Can. J. Physiol. Pharmacol. Downloaded from www.nrcresearchpress.com by University of Toronto on 05/16/16
For personal use only.

Abstract: Henneman's size principle relates the input and output properties of motoneurons and their muscle fibers to size and is the basis for size-ordered activation or recruitment of motor units during movement. After nerve injury and surgical repair, the relationship between motoneuron size and the number and size of the muscle fibers that the motoneuron reinnervates is initially lost but returns with time, irrespective of whether the muscles are self- or cross-reinnervated by the regenerated axons. Although the return of the size relationships was initially attributed to the recovery of the cross-sectional area of the reinnervated muscle fibers and their force per fiber, direct enumeration of the innervation ratio and the number of muscle fibers per motoneuron demonstrated that a size-dependent branching of axons accounts for the size relationships in normal muscle, as suggested by Henneman and his colleagues. This same size-dependent branching accounts for the rematching of motoneuron size and muscle unit size in reinnervated muscles. Experiments were carried out to determine whether the daily amount of neuromuscular activation of motor units accounts for the size-dependent organization and reorganization of motor unit properties. The normal size-dependent matching of motoneurons and their muscle units with respect to the numbers of muscle fibers per motoneuron was unaltered by synchronous activation of all of the motor units with the same daily activity. Hence, the restored size relationships and rematching of motoneuron and muscle unit properties after nerve injuries and muscle reinnervation sustain the normal gradation of muscle force during movement by size-ordered recruitment of motor units and the process of rate coding of action potentials. Dynamic modulation of size of muscle fibers and their contractile speed and endurance by neuromuscular activity allows for neuromuscular adaptation in the context of the sustained organization of the neuromuscular system according to the size principle.

Key words: motor unit size, motor unit recruitment, innervation ratio, reinnervation.

Résumé : Le principe de taille de Henneman stipule que le recrutement et l'activation des motoneurones et des fibres musculaires qu'ils innervent se fait en fonction de leur taille pendant le mouvement. Suite à un dommage neuronal et à sa réparation chirurgicale, la relation entre la taille d'un motoneurone et le nombre et la taille des fibres musculaires qu'il réinnerve est initialement perdue mais est rétablie en fonction du temps, peu importe si les muscles sont auto- ou trans-innervés par les axones régénérés. Quoique le rétablissement de la relation de taille ait été initialement attribué à la récupération de la zone de la trans-section des fibres musculaires réinnervées et à leur force par fibre, l'énumération directe du rapport d'innervation, soit le nombre de fibres musculaires par motoneurone, a démontré que le branchement des axones dépendant de la taille est responsable des relations de taille dans le muscle normal, selon Henneman et ses collègues. Des expériences ont été entreprises afin de déterminer si la somme quotidienne d'activation neuromusculaire d'unités motrices peut expliquer l'organisation et la réorganisation des unités motrices en fonction de la taille.

Received 2 February 2004. Accepted 8 July 2004. Published on the NRC Research Press Web site at http://cjpp.nrc.ca on 22 October 2004.

T. Gordon[2]. Division of Physical Therapy and Rehabilitation, Center for Neuroscience, 525 Heritage Medical Research Center, Faculty of Medicine, University of Alberta, Edmonton, AB T6G 2S2, Canada.
C.K. Thomas. The Miami Project to Cure Paralysis, University of Miami School of Medicine, Miami, FL 33136, USA.
J.B. Munson. Professor Emeritus, Department of Neuroscience, University of Florida College of Medicine, Gainesville, FL 32610-0244, USA.
R.B. Stein. Department of Physiology, Center for Neuroscience, 513A Heritage Medical Research Center, Faculty of Medicine, University of Alberta, Edmonton, AB T6G 2S2, Canada.

[1]This paper is one of a selection of papers published in this Special Issue, entitled Nerve, muscle, and beyond: the R.B. Stein Symposium.

[2]Corresponding author (email: tessa.gordon@ualberta.ca).

 doi: 10.1139/Y04-081 © 2004 NRC Canada

JOURNAL OF NEUROPHYSIOLOGY
Vol. 67, No. 5, May 1992. *Printed in U.S.A.*

34.

Innervation Ratio is an Important Determinant of Force in Normal and Reinnervated Rat Tibialis Anterior Muscles

JOANNE E. TÖTÖSY DE ZEPETNEK, HOR V. ZUNG, SERAP ERDEBIL, AND TESSA GORDON
Department of Pharmacology, Division of Neuroscience, Heritage Medical Research Center, University of Alberta, Edmonton, Alberta T6G 2S2, Canada

SUMMARY AND CONCLUSIONS

1. The technique of glycogen depletion and periodic acid-Schiff (PAS) staining, which identifies glycogen-free muscle fibers, was used to directly count the number (N) and measure the cross-sectional area (CSA) of muscle fibers in single motor units (MUs) from normal and reinnervated tibialis anterior (TA) muscles. Indirect estimates, derived from the proportions of muscle fiber types to MU types, were also made, and force per unit area (or specific force, SF) was calculated. Previous results using direct and indirect approaches have been contradictory. To shed more light on this issue, the relative contributions of N, mean fiber area (A), and SF to muscle-unit force were determined by the use of both methods.

2. TA muscles were examined in experimental rats 3.5–10 mo after cutting and resuturing the common peroneal nerve in one hindlimb and in muscles in age-matched control rats. Ventral roots were dissected to isolate and characterize single MUs according to contraction speed, sag, and fatigability. One unit per muscle was selected for repetitive tetanic stimulation designed to deplete muscle fiber glycogen stores. Muscles were removed for identification of the unit with the PAS reaction and histochemical fiber typing by the use of modified standard techniques.

3. In the total population of MUs sampled, isometric tetanic force ranged from 5 to 441 mN in normal muscles and from 5 to 498 mN in reinnervated muscles, and the mean values were not significantly different. In the smaller sample of glycogen-depleted units from normal muscle, for a force range of 14–217 mN, N varied from 57 to 202, and A varied from 1,135 ± 45 to 6,706 ± 172 (SE) μm^2. Within each unit the variation in fiber area is broad. After reinnervation, for a force range of 30–278 mN, N varied from 70 to 374, and A varied from 1,694 ± 81 to 5,425 ± 93 μm^2. Mean fiber number was 153 ± 18 in reinnervated muscle, which is significantly higher ($P < 0.01$) than the normal value of 121 ± 9.

4. The contribution of N and A to MU tetanic force was assessed by plotting each factor as a function of force on a log-log scale. N accounts for 39% and A for 49% of the variation in force in normal muscle. The contributions are changed after reinnervation where N, accounting for 65% of force, appears to compensate for the reduced range in A, which accounts for only 19% of the variation in force. The final 12 and 14% in normal and reinnervated muscle, respectively, is accounted for by SF, obtained by dividing MU force by total unit CSA. The mean SF values from normal and reinnervated units were 2.35 ± 0.14 and 2.49 ± 0.15 kg/cm^2, respectively.

5. Indirect estimates of N (termed innervation ratio or IR) agreed reasonably well with direct fiber counts for all unit types with the exception of the underestimation in normal fatigue intermediate (FI) units. These results contrast with previous indirect estimates in demonstrating that there are differences in IR among unit types that correspond to the rank order of tetanic force.

6. It is concluded that the number of muscle fibers per motoneuron (N), and therefore the number of terminal nerve branches, is a significant factor in the control of muscle-unit force. Because force varies both with N and with electrophysiological parameters of motor nerve size in normal and reinnervated muscles, our results suggest that size-related neuronal branching is an important contributing factor in the establishment of the wide range of MU force during development and its reestablishment during muscle reinnervation in the adult.

0022-3077/92 $2.00 Copyright © 1992 The American Physiological Society

JOURNAL OF NEUROPHYSIOLOGY
Vol. 68, No. 4, October 1992. *Printed in U.S.A.*

Proportional Enlargement of Motor Units After Partial Denervation of Cat Triceps Surae Muscles

VICTOR F. RAFUSE, TESSA GORDON, AND ROBERTO OROZCO
Department of Pharmacology and Division of Neuroscience, University of Alberta, Edmonton, Alberta T6G 2H7, Canada

SUMMARY AND CONCLUSIONS

1. To determine the capacity of motoneurons to increase their motor unit (MU) size by collateral sprouting and to assess this capacity in relation to the size of the motor nerve, we partially denervated soleus, lateral gastrocnemius (LG), and medial gastrocnemius (MG) muscles in adult and neonatal cats. Isometric force and extracellular nerve potentials were recorded from ≥7% of the remaining MUs, 2.5–18 mo later. S_1 or L_7 roots were sectioned unilaterally and the number of remaining MUs was quantified by use of charge and force measurements.

2. The mean unit force increased inversely with MU number in partially denervated muscles, but the increase was less than predicted for extensive denervations (≥90%). The same enlargement of MU size occurred whether muscles were partially denervated in neonatal or adult animals.

3. The force distribution of MUs in partially denervated muscles was similar to normal but was shifted to larger force values in direct proportion to the extent of partial denervation (PD). All MUs increased in size by the same factor to preserve the normal force distribution.

4. Normal size relationships among force, contractile speed, and axon potential amplitude were observed for MUs in partially denervated muscles. Because changes in muscle fiber size could not account for the increase in unit force, these data show that increase in MU size, with respect to unit force and innervation ratio (muscle fibers per motoneuron), is proportional to the size of the motor nerve.

5. Enlargement of MU size in partially denervated muscles did not have a retrograde effect on nerve fiber caliber because axon potential amplitude and conduction velocity were not changed after PD.

6. Under conditions of extensive PD (>85%), regenerated nerves from the cut spinal root reinnervated the gastrocnemius muscles. It is likely that nerves supplied muscle fibers that were not innervated by sprouts from nerves in the uncut root as well as displacing sprouts from terminals in extensively enlarged MUs.

7. We conclude that all motoneurons within a motor pool compensate for partial nerve injuries by collateral sprouting and that enlargement of MU size is a function of motor nerve size, consistent with Henneman's size principle.

0022-3077/92 $2.00 Copyright © 1992 The American Physiological Society

36.

Size of myelinated nerve fibres is not increased by expansion of the peripheral field in cats

Tessa Gordon and Victor F. Rafuse*

Department of Pharmacology, Division of Neuroscience, University of Alberta, Edmonton, Alberta, Canada T6G 2H7 and **Department of Anatomy and Neurobiology, Sir Charles Tupper Building, Dalhousie University, Halifax, Canada B3H 4H7*

(Received 10 July 2000; accepted after revision 20 December 2000)

1. This study tests the hypothesis that target size regulates the size of myelinated sensory and motor fibres in peripheral nerves. Cat medial gastrocnemius (MG) muscles were partially denervated and the size of the remaining nerve fibres that sprouted was examined 6.4 ± 0.9 months later to determine whether nerve fibre size increased with target size.

2. Electrophysiological and morphometric analyses were used to quantify myelinated nerve fibre size. Charge measurements from dorsal and ventral roots were used to electrophysiologically quantify the relative number of cut nerve fibres and the average size of the remaining intact sensory and motor nerve fibres. Medial gastrocnemius muscle and motor unit forces provided indirect measurements of the increase in target size. Conduction velocities and amplitude of unitary action potentials of motor nerve fibres innervating single motor units were also measured after partial denervation.

3. Electrophysiological measurements of nerve fibre size and morphometric measurements of outer fibre perimeters and fibre areas concurred and demonstrated that myelinated nerve fibres supplying partially denervated MG muscles did not increase in size in parallel with the increase in the target size.

4. Thus, unlike non-myelinated nerve fibres, the size of myelinated nerve fibres does not increase as target size increases. Retrograde control of size in non-myelinated but not in myelinated nerve fibres demonstrates differences in plasticity of neurons in the somatic and autonomic nervous systems.

Fast-to-Slow Conversion Following Chronic Low-Frequency Activation of Medial Gastrocnemius Muscle in Cats. I. Muscle and Motor Unit Properties

T. GORDON, N. TYREMAN, V. F. RAFUSE, AND J. B. MUNSON
Department of Pharmacology, Division of Neuroscience, University of Alberta, Edmonton T6G 2S2, Canada

Gordon, T., N. Tyreman, V. F. Rafuse, and J. B. Munson. Fast-to-slow conversion following chronic low-frequency activation of medial gastrocnemius muscle in cats. I. Muscle and motor unit properties. *J. Neurophysiol.* 77: 2585–2604, 1997. This study of cat medial gastrocnemius (MG) muscle and motor unit (MU) properties tests the hypothesis that the normal ranges of MU contractile force, endurance, and speed are directly associated with the amount of neuromuscular activity normally experienced by each MU. We synchronously activated all MUs in the MG muscle with the same activity (20 Hz in a 50% duty cycle) and asked whether conversion of whole muscle contractile properties is associated with loss of the normal heterogeneity in MU properties. Chronically implanted cuff electrodes on the nerve to MG muscle were used for 24-h/day stimulation and for monitoring progressive changes in contractile force, endurance, and speed by periodic recording of maximal isometric twitch and tetanic contractions under halothane anesthesia. Chronic low-frequency stimulation slowed muscle contractions and made them weaker, and increased muscle endurance. The most rapid and least variable response to stimulation was a decline in force output of the muscle and constituent MUs. Fatigue resistance increased more slowly, whereas the increase in time to peak force varied most widely between animals and occurred with a longer time course than either force or endurance. Changes in contractile force, endurance, and speed of the whole MG muscle accurately reflected changes in the properties of the constituent MUs both in extent and time course. Normally there is a 100-fold range in tetanic force and a 10-fold range in fatigue indexes and twitch time to peak force. After chronic stimulation, the range in these properties was significantly reduced and, even in MU samples from single animals, the range was shown to correspond with the slow (type S) MUs of the normal MG. In no case was the range reduced to less than the type S range. The same results were obtained when the same chronic stimulation pattern of 20 Hz/50% duty cycle was imposed on paralyzed muscles after hemisection and unilateral deafferentation. The findings that the properties of MUs still varied within the normal range of type S MUs and were still heterogeneous despite a decline in the variance in any one property indicate that the neuromuscular activity can account only in part for the wide range of muscle properties. It is concluded that the normal range of properties within MU types reflects an intrinsic regulation of properties in the multinucleated muscle fibers.

0022-3077/97 $5.00 Copyright © 1997 The American Physiological Society

Fast-to-Slow Conversion Following Chronic Low-Frequency Activation of Medial Gastrocnemius Muscle in Cats. II. Motoneuron Properties

JOHN B. MUNSON, ROBERT C. FOEHRING, LORNE M. MENDELL, AND TESSA GORDON
Department of Neuroscience, University of Florida College of Medicine, Gainesville, Florida 32610-0244

Munson, John B., Robert C. Foehring, Lorne M. Mendell, and Tessa Gordon. Fast-to-slow conversion following chronic low-frequency activation of medial gastrocnemius muscle in cats. II. Motoneuron properties. *J. Neurophysiol.* 77: 2605–2615, 1997. Chronic stimulation (for 2–3 mo) of the medial gastrocnemius (MG) muscle nerve by indwelling electrodes renders the normally heterogeneous MG muscle mechanically and histochemically slow (type SO). We tested the hypothesis that motoneurons of MG muscle thus made type SO by chronic stimulation would also convert to slow phenotype. Properties of all single muscle units became homogeneously type SO (slowly contracting, nonfatiguing, nonsagging contraction during tetanic activation). Motoneuron electrical properties were also modified in the direction of type S, fatigue-resistant motor units. Two separate populations were identified (on the basis of afterhyperpolarization, rheobase, and input resistance) that likely correspond to motoneurons that had been fast (type F) or type S before stimulation. Type F motoneurons, although modified by chronic stimulation, were not converted to the type S phenotype, despite apparent complete conversion of their muscle units to the slow oxidative type (type SO). Muscle units of the former type F motor units were faster and/or more powerful than those of the former type S motor units, indicating some intrinsic regulation of motor unit properties. Experiments in which chronic stimulation was applied to the MG nerve cross-regenerated into skin yielded changes in motoneuron properties similar to those above, suggesting that muscle was not essential for the effects observed. Modulation of group Ia excitatory postsynaptic potential (EPSP) amplitude during high-frequency trains, which in normal MG motoneurons can be either positive or negative, was negative in 48 of 49 chronically stimulated motoneurons. Negative modulation is characteristic of EPSPs in motoneurons of most fatigue-resistant motor units. The general hypothesis of a periphery-to-motoneuron retrograde mechanism was supported, although the degree of control exerted by the periphery may vary: natural type SO muscle appears especially competent to modify motoneuron properties. We speculate that activity-dependent regulation of the neurotrophin-(NT) 4/5 in muscle plays an important role in controlling muscle and motoneuron properties.

0022-3077/97 $5.00 Copyright © 1997 The American Physiological Society

J. Physiol. (1986), **372**, *pp.* 485–500
With 7 text-figures
Printed in Great Britain

REINNERVATION OF THE LATERAL GASTROCNEMIUS AND SOLEUS MUSCLES IN THE RAT BY THEIR COMMON NERVE

BY M. JEAN GILLESPIE*, TESSA GORDON AND PETER R. MURPHY†
From the Departments of Pharmacology and Physiology, University of Alberta, Edmonton, Alberta, Canada, T6G 2H7

(*Received 12 March 1985*)

SUMMARY

1. To determine whether there is any specificity of regenerating nerves for their original muscles, the common lateral gastrocnemius soleus nerve (l.g.s.) innervating the fast-twitch lateral gastrocnemius (l.g.) and slow-twitch soleus muscles was sectioned in the hind limb of twenty adult rats. The proximal nerve stump was sutured to the dorsal surface of the l.g. muscle and 4–14 months later, the contractile properties of the reinnervated l.g. and soleus muscles and their single motor units were studied by dissection and stimulation of the ventral root filaments. Contractile properties of normal contralateral muscles were examined for comparison and motor units were isolated in l.g. and soleus muscles for study in a group of untreated animals.

2. Measurement of time and rate parameters of maximal twitch and tetanic contractions showed that the rate of development of force increased significantly in reinnervated soleus muscles and approached the speed of l.g. muscles but rate of relaxation did not change appreciably. In reinnervated l.g. muscles, contraction speed was similar to normal l.g. muscles but relaxation rate declined toward the rates of relaxation in control soleus muscles.

3. After reinnervation by the common l.g.s. nerve, the proportion of slow motor units in l.g. increased from 10 to 31 % and decreased in soleus from 80 to 31 %. The relative proportions of fast and slow motor units in each muscle were the same as the proportions of fast and slow units in the normal l.g. and soleus muscles combined.

4. It was concluded that fast and slow muscles do not show any preference for their former nerves and that the change in the force profile of the reinnervated muscles is indicative of the relative proportions of fast and slow motor units: fast units dominate the contraction phase and slow units the relaxation phase of twitch and tetanic contractions of the muscle.

* Present address: Department of Occupational Therapy, University of Alberta, Edmonton, Alberta, Canada, T6G 2H7.
† Present address: Anatomy Department, University of Newcastle upon Tyne, Newcastle, NE2 4AA.

Journal of Neurology, Neurosurgery, and Psychiatry 1987;**50**:259–268

Patterns of reinnervation and motor unit recruitment in human hand muscles after complete ulnar and median nerve section and resuture

CHRISTINE K THOMAS, RICHARD B STEIN, TESSA GORDON,*
ROBERT G LEE,‡ M GEORGE ELLEKER†

From the Departments of Physiology, Pharmacology and Medicine,† University of Alberta, Edmonton, and Department of Clinical Neurosciences,‡ University of Calgary, Calgary, Canada*

SUMMARY Following complete ulnar or above-elbow median nerve sections, there was no significant correlation between motor unit size (twitch amplitude) and recruitment threshold, as assessed by spike triggered averaging. This absence of orderly recruitment was attributed to misdirection of motor axons during regeneration. Following median nerve section at wrist level, where the reinnervated muscles have more synergistic actions, orderly recruitment by size appeared to be re-established. Thus, the size principle of motor unit recruitment can be re-established after nerve section in humans, if motor axons innervate their original muscles or ones with closely synergistic functions.



J Physiol 588.15 (2010) pp 2745–2768

The Journal of Physiology

Sprouting capacity of lumbar motoneurons in normal and hemisected spinal cords of the rat

T. Gordon[1] and N. Tyreman[2]

[1] *Senior Scientist, Department of Surgery, Division of Plastic Surgery 5549A The Hospital for Sick Children, 555 University Ave, Toronto, ON M5G 1X8,*
[2] *Division of Physical Therapy and Rehabilitation, Division of Neuroscience, Faculty of Medicine and Dentistry, 525 Heritage Medical Research Centre, University of Alberta, Edmonton, Alberta, Canada T5R 2S2*

Nerve sprouting to reinnervate partially denervated muscles is important in several disease and injury states. To examine the effectiveness of sprouting of active and inactive motor units (MUs) and the basis for a limit to sprouting, one of three rat lumbar spinal roots was cut under normal conditions and when the spinal cord was hemisected at T12. Muscle and MU isometric contractile forces were recorded and muscle fibres in glycogen-depleted single muscle units enumerated 23 to 380 days after surgery. Enlargement of intact MUs by sprouting was effective in compensating for up to 80% loss of innervation. For injuries that removed >70–80% of the intact MUs, muscle contractile force and weight dropped sharply. For partial denervation of <70%, all MUs increased contractile force by the same factor in both normally active muscles and muscles whose activity was reduced by T12 hemisection. Direct measurements of MU size by counting glycogen-depleted muscle fibres in physiologically and histochemically defined muscle units, provided direct evidence for a limit in MU size, whether or not the activity of the muscles was reduced by spinal cord hemisection. Analysis of spatial distribution of muscle fibres within the outer boundaries of the muscle unit demonstrated a progressive increase in fibres within the territory to the limit of sprouting when most of the muscle unit fibres were adjacent to each other. We conclude that the upper limit of MU enlargement may be explained by the reinnervation of denervated muscle fibres by axon sprouts within the spatial territory of the muscle unit, formerly distributed in a mosaic pattern.

(Resubmitted 24 March 2010; accepted after revision 28 May 2010; first published online 2 June 2010)
Corresponding author T. Gordon: Department of Surgery, Division of Plastic Surgery, The Hospital for Sick Children, Ave, Toronto, Ontario M5G 1X8. Email: tessa.gordon@ualberta.ca

Abbreviations ALS, amyotrophic lateral sclerosis; FG, fast glycolytic; Fint, fatigue intermediate; FOG, fast oxidative glycolytic; MU, motor unit; SO, slow oxidative; TA, tibialis anterior.

© 2010 The Authors. Journal compilation © 2010 The Physiological Society

DOI: 10.1113/jphysiol.2010.190389

ABSTRACT: Chronic denervation syndromes such as the post-polio syndrome are associated with progressive muscle weakness and fatigue after motoneuron death. Neither the etiology nor the management of these syndromes is clear. To address this issue, we partially denervated rat hindlimb muscles for 1 or 12 months and examined whether chronically enlarged motor units (MUs) become destabilized with time and further destabilized by daily running on exercise wheels. MU enlargement, measured electrophysiologically and morphologically was significantly reduced at 12 months in extensively denervated muscles, and to a lesser extent in moderately denervated muscles, as compared to the findings at 1 month. A 1-month period of running exercise further reduced the size of the chronically enlarged MUs in the extensively denervated muscles. We have therefore (1) successfully established a rat model of time-related MU size reduction, in which destabilization of chronically enlarged MUs results in loss of axonal terminals, and (2) demonstrated that nonphysiological activity has small but significant effects of further destabilizing the chronically enlarged MUs.
© 2002 Wiley Periodicals, Inc. *Muscle Nerve* **25:** 359–369, 2002

EFFECT OF EXERCISE ON STABILITY OF CHRONICALLY ENLARGED MOTOR UNITS

SIU LIN TAM, MSc, VEY ARCHIBALD, MSc, NEIL TYREMAN, BSc, and T. GORDON, PhD

Department of Pharmacology, Division of Neuroscience, Faculty of Medicine, University of Alberta, 525 Heritage Medical Research Center, Edmonton, Alberta T6G 2S2 Canada

Accepted 5 November 2001

Neuromuscular Activity Impairs Axonal Sprouting in Partially Denervated Muscles by Inhibiting Bridge Formation of Perisynaptic Schwann Cells

S. L. Tam, T. Gordon

Centre of Neuroscience, Division of Physical Medicine and Rehabilitation, Faculty of Medicine and Dentistry, University of Alberta, Edmonton, Canada T6G 2S2

Received 21 February 2003; accepted 20 May 2003

ABSTRACT: **Following partial denervation of rat hindlimb muscle, terminal Schwann cells extend processes from denervated endplates to induce and guide sprouting from the remaining intact axons. Increased neuromuscular activity significantly reduces motor unit enlargement and sprouting during the acute phase of sprouting. These findings led to the hypothesis that increased neuromuscular activity perturbs formation of Schwann cell bridges and thereby reduces sprouting. Adult rat tibialis anterior (TA) muscles were extensively denervated by avulsion of L4 spinal root and were immediately subjected to normal caged activity or running exercise (8 h daily) for 3, 7, 14, 21, and 28 days. Combined silver/cholinesterase histochemical staining revealed that the progressive reinnervation of denervated endplates by sprouts over a 1 month period in the extensively partially denervated TA muscles was completely abolished by increased neuromuscular activity. Immunohistochemical staining and triple immunofluorescence revealed that the increased neuromuscular activity did not perturb the production of Schwann cell processes, but prevented bridging between Schwann cell processes at innervated and denervated endplates. Our findings suggest that failure of Schwann cell processes to bridge between endplates accounts, at least in part, for the inhibitory effect of increased neuromuscular activity on sprouting.** © 2003 Wiley Periodicals, Inc. J Neurobiol 57: 221–234, 2003

Keywords: **physiological running exercise; partial denervation; axonal sprouting; perisynaptic Schwann cells**

Motor Unit Numbers and Contractile Properties after Spinal Cord Injury

Jaynie F. Yang, PhD,*§ Richard B. Stein, DPhil,*§ Jack Jhamandas, MD, PhD,†§ and Tessa Gordon, PhD‡§

The number of motor units in the thenar muscle group was estimated in 11 patients with cervical spinal cord injuries. The surface electromyogram and twitch force, in response to maximal stimulation of the median nerve was divided by the average surface electromyogram and twitch of single units. The average single unit size was obtained by intramuscular microstimulation of motor nerve branches and by graded whole nerve stimulation, which provided three independent estimates, two based on the electromyogram and one based on force. The motor unit estimates from the patients covered a wide range. Some had essentially normal motor units both in numbers and contractile properties, while others had varying reductions in numbers of units. Those patients who showed a large reduction in motor unit numbers also had greatly enlarged units, which produced an average of up to sixfold the normal force. These enlarged units summed to produce maximal compound action potentials and twitches that were sometimes indistinguishable from normal. Magnetic resonance imaging scans of the cervical spine obtained from some patients provided independent evidence that patients with low motor unit counts had sustained direct injury to the anterior aspect of the spinal cord at the relevant segmental levels. Some patients showed a normal number of motor units long after the injury. No evidence of transneuronal degeneration could be demonstrated in the thenar group in these patients with the current techniques.

Yang JF, Stein RB, Jhamandas J, Gordon T. Motor unit numbers and contractile properties after spinal cord injury. Ann Neurol 1990;28:496–502

RESEARCH ARTICLE

Nerve Cross-Bridging to Enhance Nerve Regeneration in a Rat Model of Delayed Nerve Repair

Tessa Gordon*☯, Michael Hendry☯, Christine A. Lafontaine☯, Holliday Cartar☯, Jennifer J. Zhang☯, Gregory H. Borschel☯

Department of Surgery, Hospital for Sick Children, University of Toronto, Toronto, Ontario, Canada

☯ These authors contributed equally to this work.
* tessat.gordon@gmail.com

Abstract

There are currently no available options to promote nerve regeneration through chronically denervated distal nerve stumps. Here we used a rat model of delayed nerve repair asking of prior insertion of side-to-side cross-bridges between a donor tibial (TIB) nerve and a recipient denervated common peroneal (CP) nerve stump ameliorates poor nerve regeneration. First, numbers of retrogradely-labelled TIB neurons that grew axons into the nerve stump within three months, increased with the size of the perineurial windows opened in the TIB and CP nerves. Equal numbers of donor TIB axons regenerated into CP stumps either side of the cross-bridges, not being affected by target neurotrophic effects, or by removing the perineurium to insert 5-9 cross-bridges. Second, CP nerve stumps were coapted three months after inserting 0-9 cross-bridges and the number of 1) CP neurons that regenerated their axons within three months or 2) CP motor nerves that reinnervated the extensor digitorum longus (EDL) muscle within five months was determined by counting and motor unit number estimation (MUNE), respectively. We found that three but not more cross-bridges promoted the regeneration of axons and reinnervation of EDL muscle by *all* the CP motoneurons as compared to only 33% regenerating their axons when no cross-bridges were inserted. The same 3-fold increase in sensory nerve regeneration was found. In conclusion, side-to-side cross-bridges ameliorate poor regeneration after delayed nerve repair possibly by sustaining the growth-permissive state of denervated nerve stumps. Such autografts may be used in human repair surgery to improve outcomes after unavoidable delays.

OPEN ACCESS

Citation: Gordon T, Hendry M, Lafontaine CA, Cartar H, Zhang JJ, Borschel GH (2015) Nerve Cross-Bridging to Enhance Nerve Regeneration in a Rat Model of Delayed Nerve Repair. PLoS ONE 10(5): e0127397. doi:10.1371/journal.pone.0127397

Academic Editor: William D Phillips, University of Sydney, AUSTRALIA

Received: February 12, 2015

Accepted: April 14, 2015

Published: May 27, 2015

Copyright: © 2015 Gordon et al. This is an open access article distributed under the terms of the Creative Commons Attribution License, which permits unrestricted use, distribution, and reproduction in any medium, provided the original author and source are credited.

Data Availability Statement: All relevant data are within the paper.

Funding: This work was supported by Canadian Institutes of Health Research #253172.

Competing Interests: The authors have declared that no competing interests exist.

Introduction

Despite optimal management, recovery of function after peripheral nerve injury and surgical repair is rarely complete; indeed, it is frequently poor [1,2]. Whilst this is usually attributed to fat replacement of atrophic denervated muscles [2], the progressive failure of nerve regeneration over time and distance is accounted for by a progressive decline in the regenerative capacity of the injured neurons and the diminished regenerative support by the chronically

denervated Schwann cells within the denervated nerve stumps [3–9]. The declining regenerative capacity is accompanied by a corresponding decline in the expression of growth-associated genes [3–9].

Chronically denervated muscles contract more forcefully after delayed nerve repair when a prior surgery was carried out to direct sensory nerves into the denervated muscle [10]. The explanation given for the findings was that the sensory nerves 'protected' the muscles [10]. Axon-mediated "Schwann cell protection" was indicated as a contributing factor [11]. We recently re-examined this issue with the surgical procedure of two end-to-side neurorrhaphies which does not require the sacrifice of any nerve. The surgical technique is to place nerve autografts at right angles between a donor intact nerve and a recipient denervated nerve stump with the autografts each connected in an end-to-side manner [12]. Viterbo and colleagues pioneered the technique with electrophysiological and histological evidence that axons passed through the autografts [13]. They did not, however, examine how many axons passed through, their destination(s), nor the outcomes of the procedure. The technique, referred to as side-to-side cross-bridging by Ladak et al [12], is an extension of the more widely used end-to-side nerve coaptation (end-to-side neurorrhaphy) of a recipient denervated distal nerve stump into the side of a donor intact nerve, with and without a perineurial window [14–21]. Retrograde tracing used in the later study of Ladak et al revealed that ~50 tibial motoneurons sent their axons across three cross-bridges into a recipient denervated common peroneal (CP) distal nerve stump. The tibial axons 'protected' chronically denervated Schwann cells because the number of motoneurons that regenerated their axons after delayed coaptation of the proximal and distal CP nerve stumps was increased 1.7-fold [12].

There remain many unanswered and important questions. These are addressed in the current study: 1) Does the size of perineurial windows cut into a donor nerve and a recipient denervated nerve stump impact on the number of neurons that grow axons through side-to-side cross-bridges? 2) Do donor axons that enter the denervated distal nerve stump through side-to-side cross-bridges, continue to grow either proximal and/or distal to the cross-bridges, possibly influenced by a neurotrophic effect of the denervated targets? 3) Do both motor *and* sensory neurons contribute their axons through the side-to-side cross-bridges? 4) Does the number of cross-bridges dictate how many neurons participate in growing axons through the cross-bridges? and 5) Will optimum placement of side-to-side cross-bridges improve the regeneration of motor nerves and/or sensory nerves after delayed nerve repair? In light of there being no reliable medical or surgical options to oppose poor functional recovery when nerves regenerate through chronically denervated Schwann cells, our objective is to promote nerve regeneration and muscle reinnervation after delayed repair by 'protecting' chronically denervated nerve stumps with axons from a nearby donor nerve.

Materials and Methods

Animals

All experiments were carried out on adult female Sprague Dawley rats (250-270g; n = 110). Of these, 26 rats were *Thy*-1-GFP transgenic rats that were developed in our laboratory. Green fluorescent protein (GFP) is expressed in neural cells under the Thy-1 promoter but is not expressed in muscle or connective tissue [22–24].

Surgery

Sterile surgery was carried out under inhalational anesthetic (2% Isofluorane in 98% oxygen; Halocarbon Laboratories, River Edge, NJ) and using an operating microscope (Leitz, Willowdale, ON). The rats were administered subcutaneous Metacam (0.3 mL/100 g body weight;

Boehringer Ingelheim Vetmedica Inc., St. Joseph, MO) for relief of post-operative pain. A warming pad was placed under the rat in order to maintain body temperature during surgery and during the brief period during which the rat regained consciousness after the surgery when the inhalational anesthetic administration ceased. The protocol was approved by the Animal Care Committee, Hospital for Sick Children, Toronto, and all perioperative care, including postoperative monitoring and analgesia, was administered according to Canadian Council for Animal Care guidelines. Post-operative care included regular daily post-operative monitoring over the first week of all surgeries followed by regular monitoring by the staff of the animal facility.

In the first experiment (Experiment #1; N = 68 rats; Table 1), side-to-side autologous common peroneal (CP) cross-bridges were inserted between a donor intact tibial (TIB) nerve and a recipient denervated CP nerve stump. CP and TIB nerves were exposed in both hindlimbs through gluteal muscle-splitting incisions. The *left* CP nerve was dissected ~5–7 mm from the sciatic notch to its distal insertion into the muscles in the anterior hindlimb compartment. The CP nerve was carefully dissected free from the TIB nerve along the natural division of the two nerves as they course through the sciatic nerve. Dissection was halted at the most proximal portion of the sciatic nerve at the sciatic notch where the CP, TIB, and sural nerve fascicles were interweaved. A ~28–30 mm nerve length was harvested, cut, and kept moist in the hindlimb for later division into one to nine autologous CP side-to-side nerve cross-bridges. In the *right* experimental hindlimb, the CP nerve was transected and the proximal and distal nerve stumps were ligated. The distal CP nerve stump was laid parallel to the donor TIB nerve and the two CP nerve stumps were sutured to underlying innervated muscle to prevent nerve regeneration from the proximal to the distal nerve stump [25]. CP cross-bridges from the *left* hindlimb were

Table 1. The two sets of experiments (Exp.) in which 1–9 cross-bridges were inserted through perineural windows between the donor tibial nerve and the recipient common peroneal (CP) nerve in Exp 1, and denervated common peroneal (CP) nerve stumps were coapted three months after placing the cross-bridges in Exp. 2.

Experiment sets and Rat numbers		Number of side-to-side cross-bridges						Perineurial window radius and bridge length (mm)	
Experiments: Q & A	**Rats**	**0**	**1**	**3**	**5**	**7**	**9**	**radius**	**length**
Exp. 1A									
Does window size affect axon crossing? *Yes*, *with most axons regenerating rather than sprouting*	20	-	-	7	5	8	-	0.125	6
	12	-	6	6	-	-	-	0.250	6
Exp. 1B									
Do donor axons grow in either direction in the recipient nerve stump? *Yes*, *even when disconnected from denervated targets*	12	-	-	12	-	-	-	0.50	3.2
	6			6					
Exp. 1C									
Do more donor axons grow through bridges when window size is increased to incorporate >3 bridges? *No they do not*.	18	-	-	-	6	6	6	10.00	3.2
Exp. 2A									
Does the 'protection' by 3 cross-bridges improve nerve regeneration and muscle reinnervation after delayed repair? *Yes*, *increasing the regeneration of both motor and sensory axons 3-fold as well as increasing muscle reinnervation*	12	-	-	12	-	-	-	0.50	3.2
	12	12	-	-	-	-	-	0	3.2
Exp 2B									
Does 'protection' by >3 bridges improve this regeneration? *No*, *>3 bridges did not improve regeneration*	18	-	-	-	6	6	6	10.00	3.2

The research questions addressed are shown with the answers in italics.

doi:10.1371/journal.pone.0127397.t001

inserted into the sides of the donor TIB nerve and the recipient denervated CP nerve stump through equidistant perineurial windows placed over a 10 mm length (Fig 1A–1D). The radius of the windows was increased from ~125 to 500 μm (Table 1).

The windows were made by lifting the perineurium with a fine forceps to open and extend the incision. Their size was varied to insert cross-bridges in the following configuration: three, five, or seven 6 mm long bridges were inserted through perineurial windows (~125 μm radius, n = 20), one and three 6 mm long bridges (~250 μm radius, n = 12; Fig 1A and 1B), three 3.2 mm long bridges (~500 μm radius, n = 12; Fig 1C) and listed under Exp.1B in Table 1. To test for possible target neurotrophism, the distal end of the recipient denervated CP nerve stump was ligated in rats in which 3.2 mm long bridges were inserted through perineurial windows of a ~500 μm radius (n = 6; Fig 1D) as listed under Exp.1B in Table 1. When more than three bridges were placed, the perineurium was removed over the 10 mm length of the donor and recipient nerves. We placed five, seven, and nine 3.2 mm long cross-bridges after removing the perineurium (n = 18; Fig 1E and 1F) as listed under Exp 1C in Table 1. The autologous CP nerve cross-bridges were secured at right angles to the donor TIB nerve and the recipient denervated CP nerve stump by applying Tisseel glue (Baxter, Mississauga, Ontario; 1:1 mix of

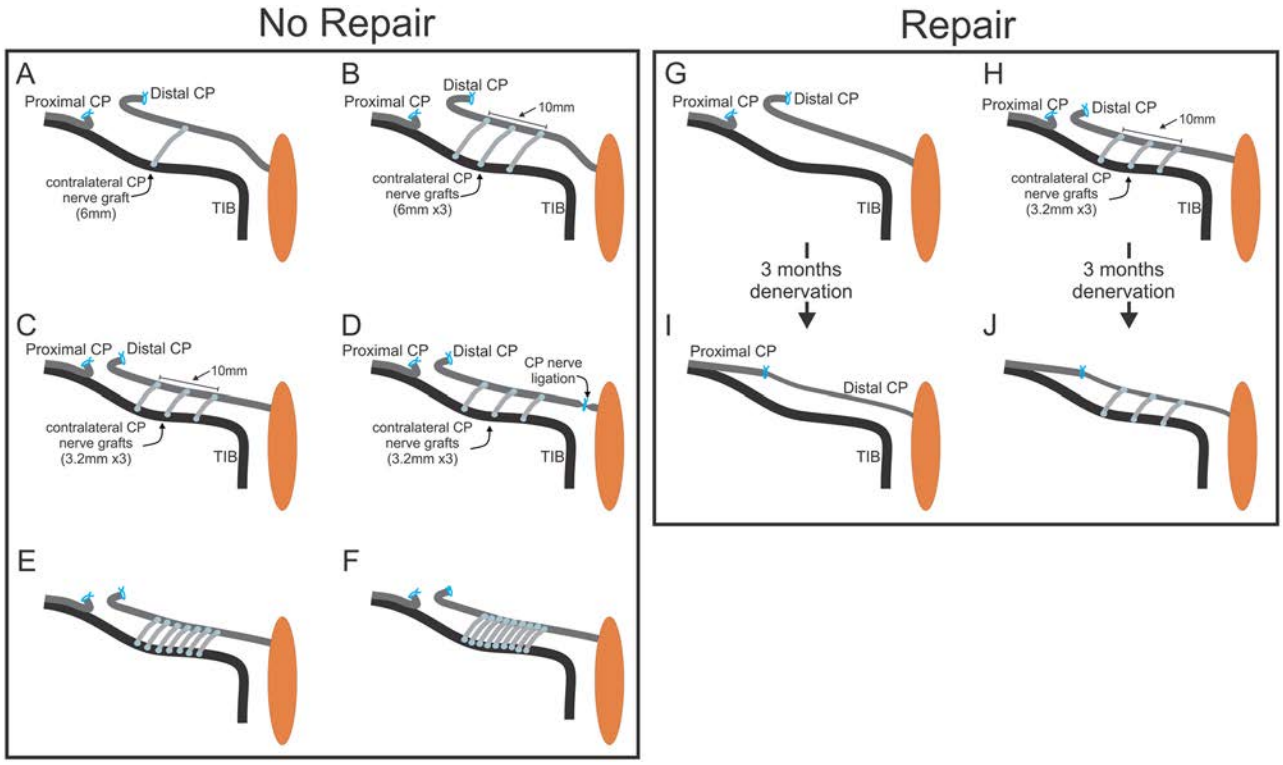


Fig 1. The surgical placement of autografts as side-to-side cross-bridges between an intact donor tibial (TIB) and a recipient denervated common peroneal (CP) distal nerve stump and the delayed coaptation of the CP nerve stumps. In the first set of experiments (No Repair: Table 1), the distal nerve stump of transected CP nerve was laid parallel to the intact TIB donor nerve for securing CP autologous cross-bridges at right angles to the nerves: 1 and 3 (5 and 7 not shown) cross-bridges 6 mm long (A,B) or 3 to 9 cross-bridges 3.2 mm in length (C-F). Perineurial windows were opened in the TIB and CP nerves to insert 1–3 bridges over a distance of 10 mm on each nerve (A-C). To examine possible neurotrophic influence of the denervated targets, the connection of the denervated CP nerve with these targets, the nerve was ligated (D). To insert more than 3 bridges of 3.2 mm length, the perineurium was removed (E-F). In a second set of experiments (Repair, Table 1), no cross-bridges were placed between the donor TIB nerve and recipient denervated CP nerve stump in a control group of rats (G) and 3–9 CP autologous cross-bridges were placed between the nerves in the experimental rat group (H) (only 3 cross-bridges shown). Three months later, the CP nerve stumps were refreshed and sutured together to encourage CP nerve regeneration through either an 'unprotected' chronically denervated CP nerve stump where no cross-bridges were placed (I) or through a CP nerve stump that was 'protected' by placing 3–9 cross-bridges between the donor TIB nerve and the denervated CP nerve stump (J).

doi:10.1371/journal.pone.0127397.g001

thrombin and fibrinogen). Thereafter the internal and external incisions were closed with 5–0 silk and 4–0 Vicryl suture, respectively.

In a second sterile surgery carried out three months later in the right experimental hindlimb, donor TIB neurons that had grown their axons into the recipient denervated CP nerve stump either side or both sides of the inserted cross-bridges were retrogradely labeled. In the rats in which 3.2 mm cross-bridges were placed (Fig 2A) as listed under Exp. 1B and C in Table 1, a 2–3 mm long CP nerve sample was taken for morphology (see below) prior to exposing the axons of the TIB neurons to a 4% solution of fluorogold (FG; Hydrostilbamidine bis(methanesulphonate), Sigma #39286) or an 8% solution of fluororuby dextran tetramethylrhodamine (FR; Molecular Probes, Eugene, OR, USA) solution. The transected tips of the donor TIB nerve and the CP nerve stump were exposed to the dyes within Vaseline wells for one hour, the dyes being randomized to the CP nerve stump either side of the cross-bridges. Thereafter the wells were removed and the exposed nerves checked for visible staining. The incision site was then closed and the rats were allowed to recover.

In the rats in which one or three 6 mm long CP autografts were placed (Fig 3A and 3B), the recipient CP distal nerve stump was exposed to one dye 10 mm distal to the cross-bridges in order to backlabel TIB neurons that sent axons into the denervated CP distal nerve stump. The donor TIB nerve was also cut 10 mm distal to the location of the cross-bridge placement for retrograde labeling with the second dye (Fig 3A). In this manner, those TIB neurons that were backlabelled with the dye applied to the recipient CP nerve alone were identified as the TIB neurons that had regenerated their axons across the bridges and into the recipient denervated CP nerve stump. Typical examples are the two middle motoneurons in the photomicrograph in Fig 3A that contain only the FR dye. Those TIB neurons that contained both dyes were neurons that had sprouted axons through the cross-bridges, retaining their axons within the donor TIB nerve distal to the cross-bridges (Fig 3A). In the same manner as for the first group of rats where donor TIB neurons that had grown their axons either side of the cross-bridges into the recipient denervated nerve stump, backlabeling was performed by exposing the transected tips of the donor TIB nerve and the CP nerve stump to the dyes for one hour. One week after retrograde labelling, rats were transcardially perfused with 4% paraformaldehyde under deep isofluorane anesthesia. The lumbosacral spinal cord and the dorsal root ganglia (DRG) at the L4-5 levels that contained the CP and TIB motor and sensory neuron pools, respectively, were surgically removed and embedded in optimum cutting temperature medium (OCT). In the right experimental hindlimb of the *Thy-1* GFP transgenic rats, the donor TIB nerve and the recipient denervated CP nerve stump that were 'bridged' by side-to-side CP nerve autografts were dissected, the extraneous connective tissue carefully removed, and the nerves embedded longitudinally in OCT and frozen at -20°C.

In a second experiment (Experiment #2; Table 1), autologous CP nerve cross-bridges were dissected from the left hindlimb and placed into the right hindlimb in a second group of 30 rats (Fig 1H) under the same aseptic conditions and using the same drugs for anesthesia and pain management. A control group of rats (n = 12) was included in which the same CP transection and ligation of the proximal and distal stumps was carried out in the right experimental hindlimb but no autologous CP cross-bridges were placed (Fig 1G) as listed in Exp. 2A in Table 1. In the second sterile surgery carried out three months later, the ligated CP nerve stumps in the experimental right hindlimb were identified and examined visually. Thereafter, the proximal nerve stump was electrically stimulated via bipolar electrodes to ensure that no axon regeneration had occurred between the ligated CP nerve stumps over the three month period. The proximal and distal CP nerve stumps were then freed and refreshed for microsurgical coaptation (Fig 1I and 1J), using 10–0 silk thread within a ~2.5 mm long Silastic tube, as described in detail previously [25]. Briefly, the two CP nerve stumps were opposed by inserting a

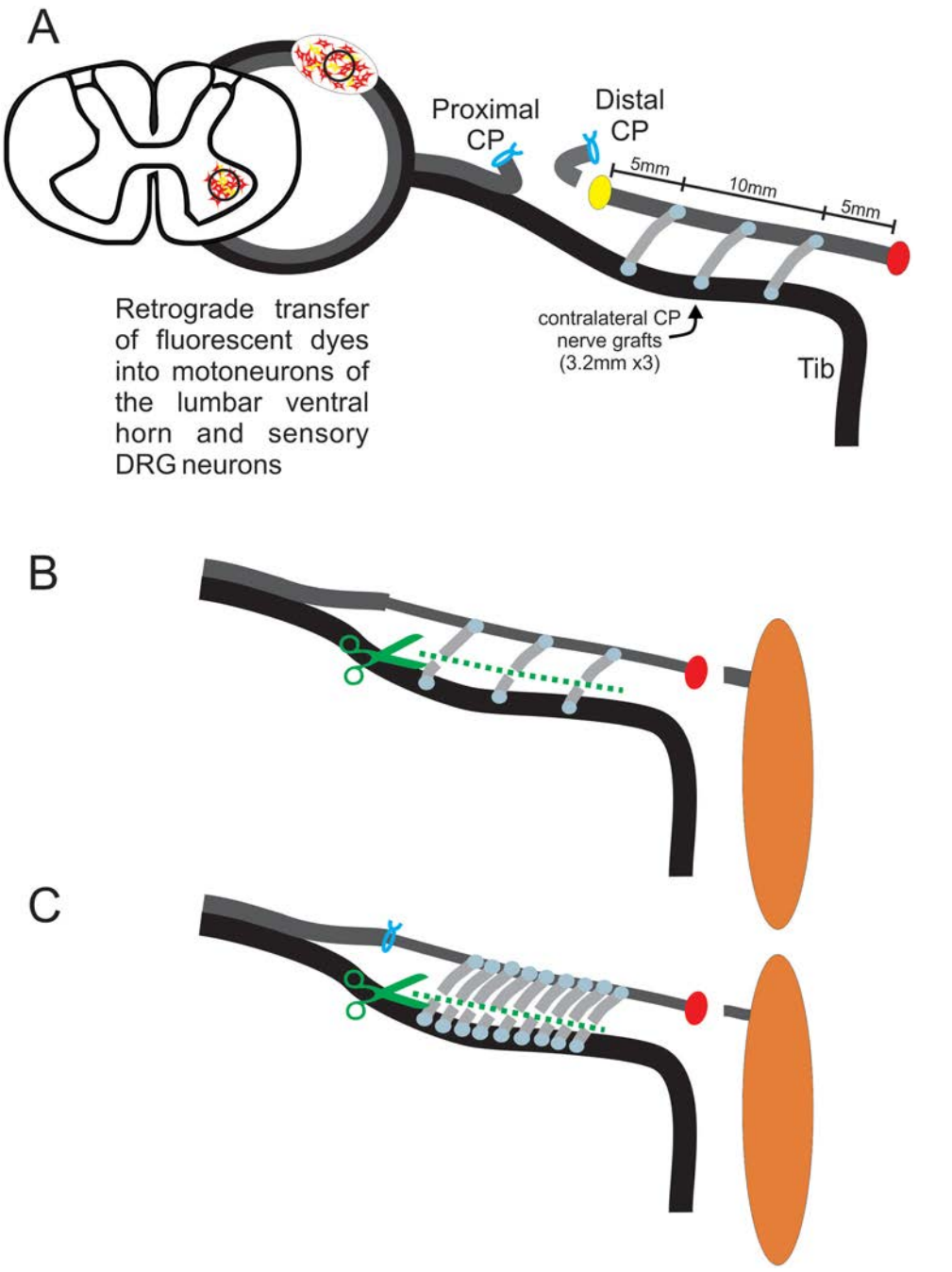


Fig 2. Retrograde labeling of motor and sensory tibial (TIB) neurons that grow axons from a donor TIB nerve into a recipient denervated common peroneal (CP) nerve and, of CP neurons that regenerate their axons after delayed CP nerve repair. In the first set of experiments (No Repair: Table 1) A. Fluorogold (FG) and fluororuby (FR) retrograde dyes were applied to the CP nerve stump 5 mm either side of 3.2 mm long cross-bridges in order to identify the TIB neurons that had grown axons through the cross-bridges into the recipient denervated CP nerve stump. B,C. In a second set of experiments (Repair, Table 1), 5 months after delayed repair of CP nerve, FG or FR was applied to the regenerated CP axons to enumerate the CP neurons that had regenerated through the denervated CP nerve stump 'protected' by 3 (B) and 9 (C) bridges, as examples. By cutting through the cross-bridges at the same time as the dye application, retrograde labelling was confined to only the CP neurons that had regenerated their axons through the cross-bridges (B, C).

doi:10.1371/journal.pone.0127397.g002

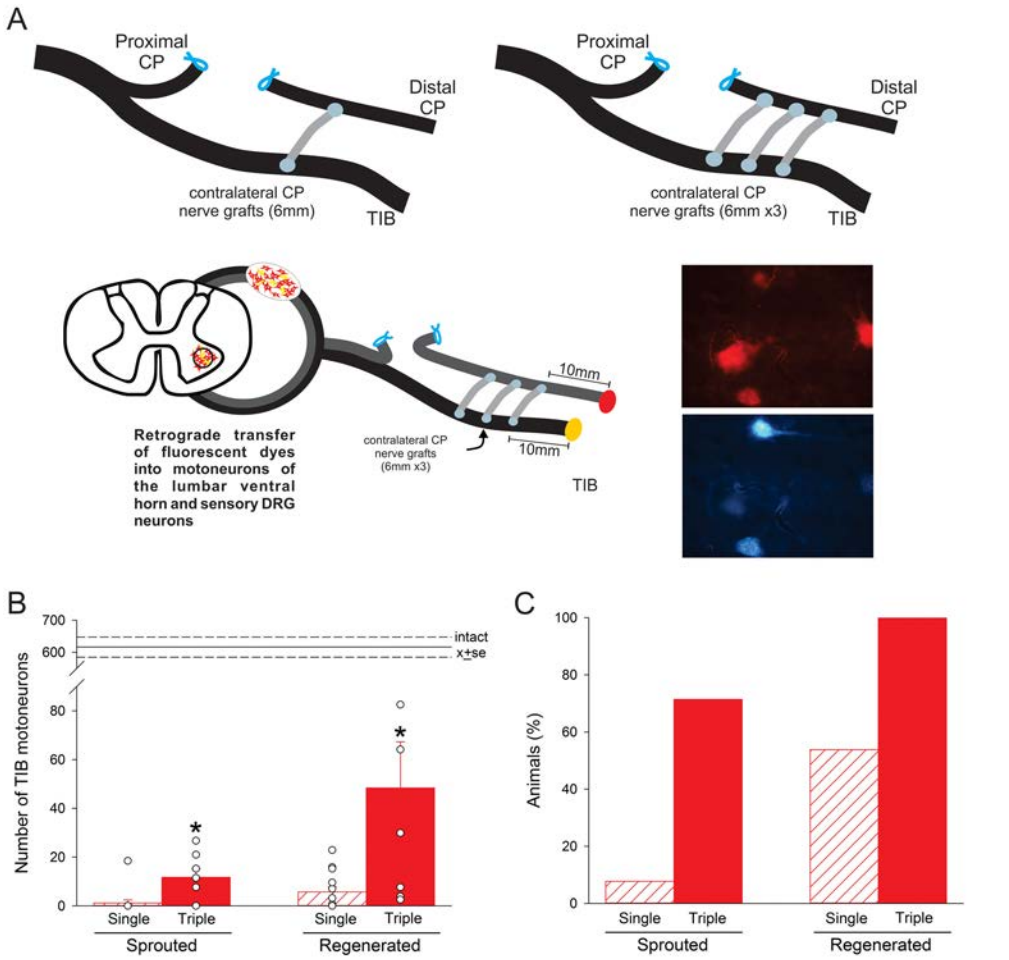


Fig 3. More donor tibial (TIB) motoneurons regenerate axons into a recipient common peroneal (CP) nerve stump when 3 rather than a single cross-bridge was secured between perineurial windows in the nerves; few motoneurons sprout axons through the cross-bridges. In the first set of experiments (No Repair: Table 1), A. 1 or 3 autologous CP nerve cross-bridges (6 mm long) were placed between a donor TIB nerve and a recipient denervated CP nerve stump via perineurial windows (with a radius of~250 μm) that were opened in both nerves. Three months later, fluorogold (FG) and fluororuby (FR) retrograde dyes were applied to the CP and TIB nerves distal to the cross-bridges in order to identify TIB motoneurons that had sprouted (containing *both* dyes) and those that had regenerated (containing only FR) axons into the recipient denervated CP distal nerve stump. B. Mean ± SE of the numbers of TIB motoneurons that sprouted and regenerated their axons into the recipient denervated CP nerve stump (data points for individual rats are shown) and C. the proportion of rats (as a percentage) in which sprouted and regenerated TIB motoneurons were found. In B. significant differences are shown by the * with more neurons sprouting *and* regenerating axons through 3 cross-bridges as compared to 1 cross-bridge.

doi:10.1371/journal.pone.0127397.g003

needle attached to the 10–0 silk thread through the center of the tube, through the perineurium of the proximal and then the distal nerve stump, and exiting the tube at the same site. The two stumps of the transected CP nerve were gently pulled together by pulling the silk suture, the apposition of the nerve stumps being aided by capillary suction within the silastic tube [25]. The suture was tied, the incisions closed, and the rats allowed to recover on a heat pad.

In a third aseptic surgery performed three months after CP microsurgical coaptation, CP neurons that had regenerated their axons across the coaptation site and beyond the cross-bridges were retrogradely with either FG or FR dyes (Fig 2B and 2C). The dye was applied to the

CP distal nerve stump for one hour, 10 mm from the most distally placed side-to-side cross-bridge and ~25 mm from the CP coaptation site. In the rats in which cross-bridges had been placed, the bridges were cut to ensure that *only* the CP neurons that had regenerated their axons through the distal CP nerve stump were backlabelled and *not* the donor TIB neurons whose axons had grown through into the denervated CP distal nerve stumps prior to the coaptation of the CP nerve stumps (Fig 2B and 2C). In the control group of rats in which no bridges were placed, the same location on the distal nerve stump was cut to apply the retrograde dyes. Surgical closure of the wound followed and the rats were allowed to recover on a heat pad. One week later, transcardial perfusion was carried out as described for Experiment #1 for dissection and removal of the lumbosacral spinal cord and the DRGs.

Data collection

Neuronal and axon counts. Fifty and 20 μm thick sagittal sections of the lumbosacral spinal cord and the DRGs, respectively, were cryosectioned for visualization and counting of 1) the donor TIB motor and sensory neurons that regenerated and/or sprouted their axons into the recipient denervated CP nerve stump in the right experimental hindlimb (Exp. 2A-C in Table 1), and 2) CP motor and sensory neurons that regenerated their axons into the chronically denervated CP nerve stump which had and had not been 'protected' by autologous CP side-to-side cross-bridges prior to delayed CP nerve repair (Exp. 2A,B in Table 1), again in the right experimental hindlimb. The sections were visualized and the retrograde labeled neurons counted under a fluorescent filter with an excitation band pass of 470–490 nm for FG and of 580–620 for FR dyes. All the backlabelled motoneurons were counted in every spinal cord section whilst DRG sensory neurons were visualized and counted on every 5th section. Only those neurons in which a distinct nucleus was visible were counted. The numbers were corrected to control for the counting of split nuclei using the method of Abercrombie [26].

A 2–3 mm length of CP nerve was excised for histomorphometry prior to backlabelling the TIB neurons in the second sterile surgery of the second experiment (Exp. 2A and B in Table 1). The nerve was fixed overnight in 2.5% gluteraldehyde solution buffered in 0.025 M cacodylate, washed, and then stored in 0.15 M cacodylate buffer. Samples were subsequently post-fixed in 2% osmium tetroxide, dehydrated in a series of graded alcohols, and embedded in EPON. Nerve cross-sections of 0.6 μm were cut through the center of the sample and stained with toluidine blue for viewing at the light microscopic level. Entire nerve cross-sections were captured at 1000x magnification (Leica DM2500) and the myelinated axons were counted using a semi-automated Matlab program [27].

Recordings of isometric force of muscles and motor units. In 12 rats, the right experimental hindlimb was prepared for recording of isometric contractions of the extensor digitorum longus (EDL) muscle under deep isofluorane anesthesia and at 37°C, five months after surgical coaptation of the CP nerve stumps with and without placement of three autologous CP cross-bridges (Fig 4 and Table 1: Exp. 2A). The femoral condyles were anchored in a custom-designed force measurement apparatus (Red Rock Inc, St. Louis, MO) and the EDL muscle tendon isolated and attached to a 2 N thin film load cell (S100, Strain Measurement Devices Inc., Meriden, CT) to record isometric force. The CP nerve distal to the site of coaptation was freed for electrical stimulation to 1) evoke EDL muscle twitch (Fig 4A) and tetanic contractions in response to supramaximal (2X threshold) bipolar stimuli, and 2) record motor unit twitch contractions in response to progressive increases of stimulus voltage from 0 V upwards with 100 μs long biphasic stimuli delivered at 0.5 Hz (Fig 4B). Motor units (MUs) were recruited in all-or-none steps of voltage to a maximum of 60% of the maximum muscle twitch force. The mean motor unit twitch force was determined by motor unit number estimation (MUNE).

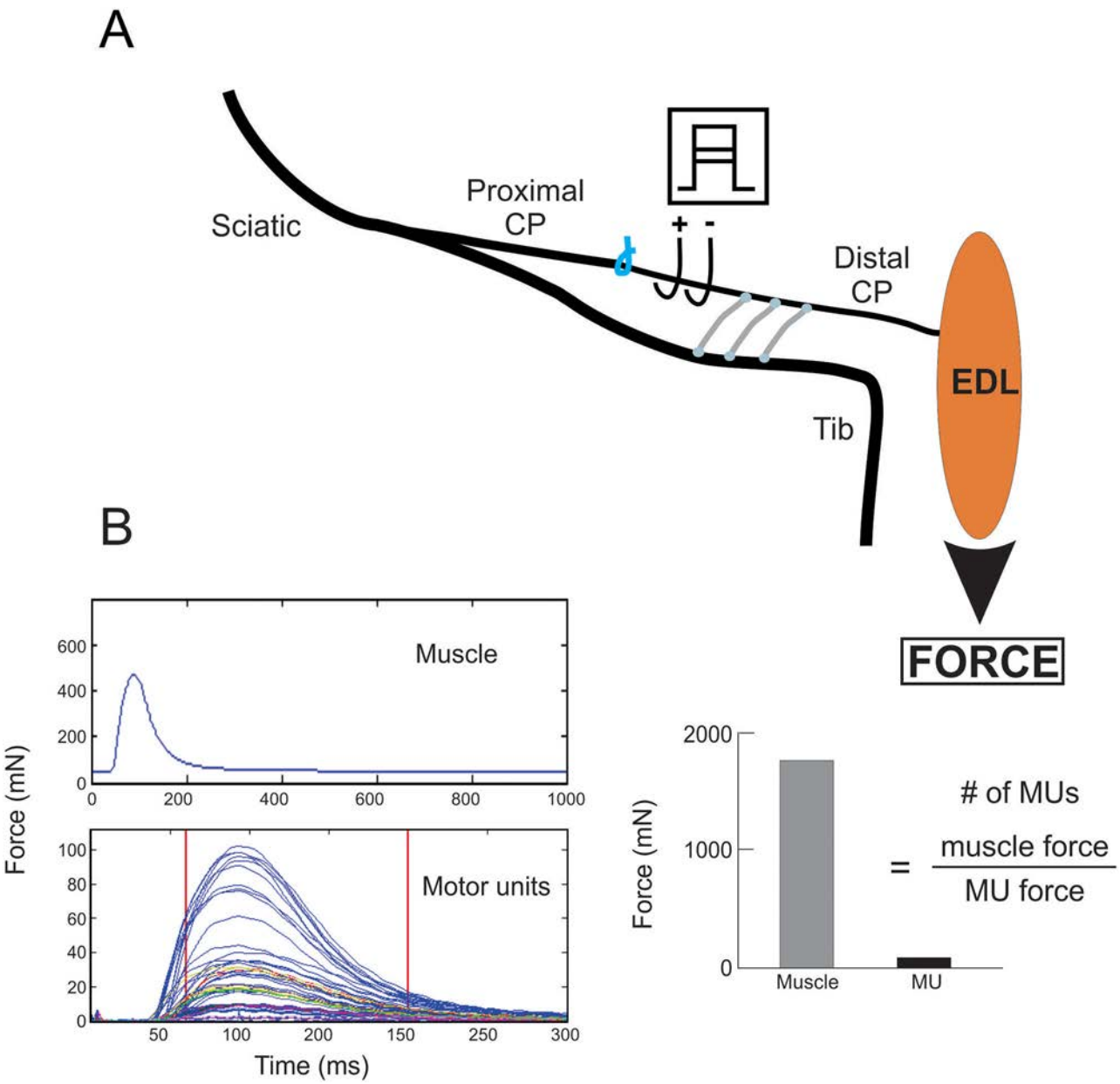


Fig 4. *In vivo* recording of muscle isometric contractile forces to determine numbers of reinnervated motor units. A. In the second set of experiments (Repair, Table 1), bipolar electrodes placed on the regenerated common peroneal (CP) nerve were used to electrically stimulate the CP nerve supramaximally to evoke extensor digitorum longus (EDL) muscle twitch (B) and tetanic isometric contractions or to stimulate the CP nerve incrementally in order to evoke all-or-none increments in twitch force. Motor unit (MU) number was calculated as the ratio of the muscle and average MU twitch forces—motor unit number estimation (MUNE).

doi:10.1371/journal.pone.0127397.g004

MUNE (number of MUs) was computed by the division of the maximal muscle twitch force divided by the mean contractile force of the motor units (Fig 4B), as described in detail previously [28,29]. MUNE provides an estimation of the number of the CP motoneurons that reinnervated the EDL muscle.

Statistics. The data are plotted with mean ± standard errors (SEs) as well as individual data points in Fig 3B. Differences between mean values were evaluated using a one-way

analysis of variance (ANOVA) followed by a post-hoc Tukey's multiple comparisons of means ($p \leq 0.05$).

Results

More neurons send axons through larger perineurial windows

Autologous common peroneal (CP) nerve cross-bridges from the left hindlimb were dissected and placed in a side-to-side fashion via perineurial windows that were opened at equal distances within a 10 mm length of the intact donor tibial (TIB) nerve and the recipient denervated CP nerve stump in the right experimental hindlimb (Fig 1). TIB axonal sprouting and/or regeneration through the cross-bridges and into the distal end of the recipient denervated CP nerve stump was/were determined three months later using retrograde dyes to backlabel motor and sensory TIB neurons (Fig 3). The TIB neurons that *regenerated* their axons into the recipient CP nerve stump were backlabelled with the dye applied to the CP nerve stump but *not* with dye applied to the donor TIB nerve. The TIB neurons that *sprouted* their axons on the other hand were backlabelled from *both* the recipient CP nerve stump and the donor TIB nerve (Fig 3A).

It was reported that the size of the perineurial window is an important determinant of how many axons regenerated through a denervated distal nerve stump inserted into the side of an intact donor nerve—an end-to-side coaptation [30–32]. We first addressed the question of how the size of the perineurial windows impacts on the crossing of donor axons into a recipient denervated nerve stump via side-to-side cross-bridges, an important question that had not been addressed previously (Exp. 1A in Table 1). When small perineurial windows of ~125 μm radius were cut in the donor TIB nerve and the recipient denervated CP nerve stump to accommodate the autologous CP nerve cross-bridges, few and variable numbers of donor TIB motoneurons (<1%) were backlabelled from the recipient denervated CP nerve stump: mean (±SE) numbers of labeled TIB motoneurons that sent axons into the CP nerve stump proximal and distal to the bridges were 8.3 ± 3.3 and 4.5 ± 1.8 (n = 7) respectively for 3 bridges, 0.5 ± 0.6 and 14.2 ± 7.9 (n = 5) respectively for 5 bridges, and 2.1 ± 1.2 and 11.0 ± 9.4 (n = 8), respectively for 7 bridges.

When wider perineurial windows were opened, significantly more donor TIB motoneurons sent their axons through three cross-bridges into the recipient denervated CP nerve stump, the mean number increasing as a linear function of the radius of the window (Fig 5). Despite considerable scatter in the numbers of TIB motoneurons that regenerating axons into the recipient CP nerve stump through one and three windows with a radius of 250 μm (Fig 3B), the mean numbers of motoneurons sending their axons through these perineurial windows were significantly greater than through smaller windows of 125 μm radius. The numbers increased further when the radius of the perineurial windows was doubled to 500 μm (Fig 5). These data demonstrate that the numbers of neurons that regenerate their axons through cross-bridges between a donor nerve and a recipient denervated nerve stump depend on the size of the perineurial windows that are opened to place the cross-bridges.

Note in Fig 3B that the number of TIB neurons that regenerated their axons through a single cross-bridge was small relative to the numbers that regenerated their axons through three cross-bridges. Moreover, TIB neurons regenerated their axons into the recipient denervated CP nerve stumps in only 50% of the rats in which a single cross-bridge was placed (Fig 3C). Relative to the number of TIB neurons regenerating their axons through one and three cross-bridges into the recipient denervated CP nerve stump, there was only ~0.16% of total TIB motoneuron pool (737 ± 16) that sprouted axons through a single bridge into the denervated CP distal nerve stump (Fig 3B). The mean number (11.7 ± 3.5) of TIB neurons that sprouted

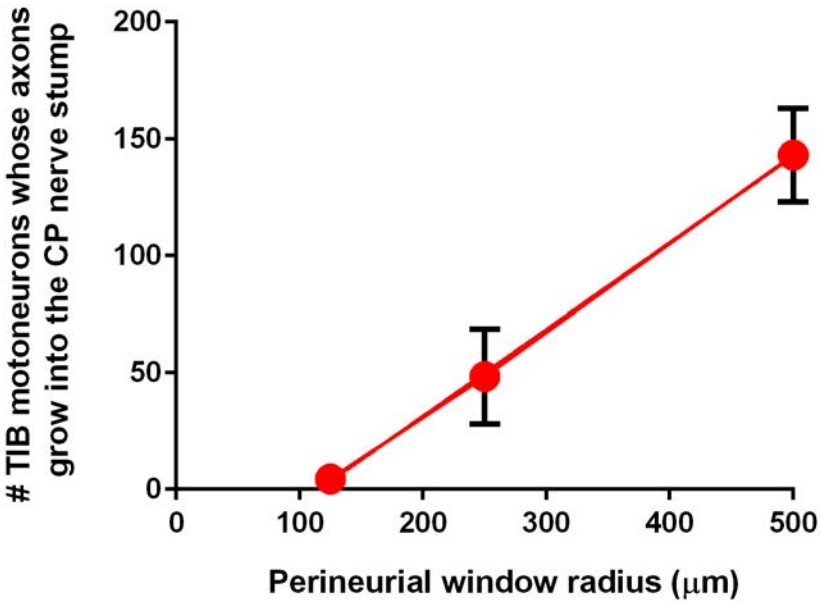


Fig 5. Linear relationship between the numbers of donor neurons sending their axons across 3 side-to-side cross-bridges and the size of the perineurial windows inserted in the nerves. Mean (±SE) numbers of tibial (TIB) motoneurons whose axons crossed 3 side-to-side cross-bridges and were backlabelled with dyes applied distal to the cross-bridges. Note that the error bars that are smaller than the size of the circular marker are not visible.

doi:10.1371/journal.pone.0127397.g005

axons increased 10-fold when three cross-bridges were placed but the proportion of 1.6% donor motoneurons that sprouted their axons was very small. These findings indicated that increasing the number of bridges was effective in promoting the regeneration and to a much lesser extent, the sprouting of donor axons through the bridges and into the recipient denervated nerve (Exp. 1A in Table 1).

Donor motor and sensory neurons send axons across side-to-side cross-bridges

In order to determine the direction of growth of donor TIB axons through three CP nerve autografts and into the recipient denervated CP nerve stump (Exp. 1B in Table 1), two different dyes were applied to the CP nerve stump 5 mm proximal and distal to three 3.2 mm long CP cross-bridges placed between the ~500 μm perineurial windows in the two nerves (Fig 2A). Donor TIB motoneurons regenerated their axons through the cross-bridges and equally well in both directions within the recipient CP nerve stump; very few neurons regenerated their axons in both directions (neurons co-labelled from dyes applied proximal and distal to the bridges) (Fig 6A and 6B). The number of TIB dorsal root ganglion (DRG) sensory neurons that regenerated their axons into the recipient denervated CP nerve stump was also not significantly different either side of the three bridges (Fig 6C). The sum of the TIB neurons that regenerated axons into the recipient denervated CP nerve stump was 335 ± 86 for the motoneurons and 2809 ± 1018 for the DRG sensory neurons (Fig 6B and 6C). These numbers correspond to ~32% and ~37% of the total number of TIB motor and sensory neurons of 900 and 8900, respectively [33].

It is unlikely that a ~35% reduction in the numbers of TIB motoneurons that retained intact axons within the donor TIB nerve would result in substantial denervation of the extensor muscles, including the triceps surae muscles that are innervated by these motoneurons. This is

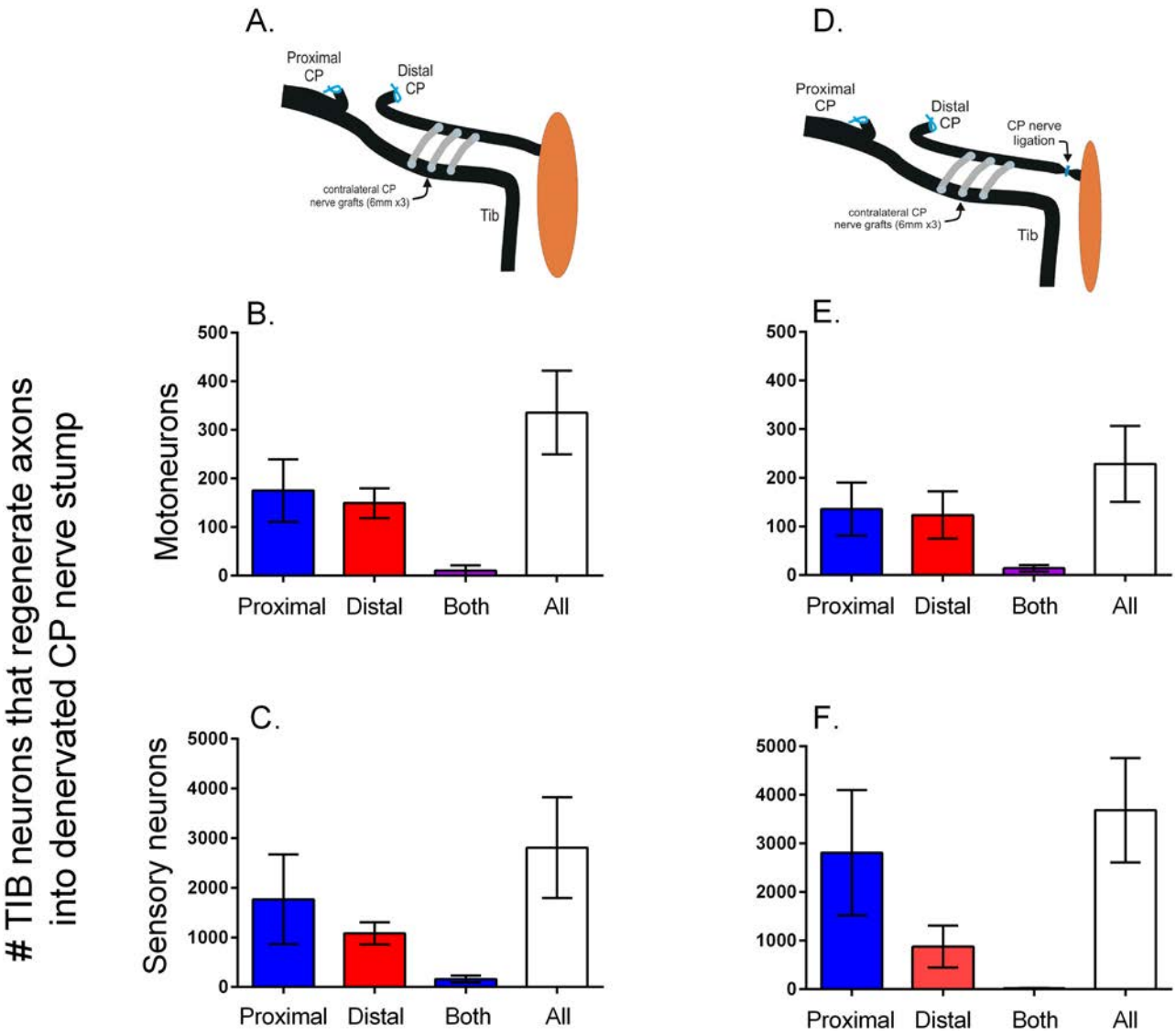


Fig 6. Donor neurons sending axons through cross-bridges proceed equally well in both proximal and distal directions in the recipient denervated nerve stump regardless of whether or not the nerve stump is in contact with denervated targets. In the first set of experiments (No Repair: Table 1), A. 3 cross-bridges of 3.2 mm length and 500 μm radius were placed between donor tibial (TIB) nerve and the recipient denervated common peroneal (CP) nerve stump. The mean numbers (±SE) of both the motor (B) and sensory (C) TIB neurons that regenerated axons into the recipient CP nerve stump proximal and distal to the bridges was the same with very few neurons sending axons in both directions. D. The ligation of the denervated CP nerve stump to isolate the stump from possible neurotrophic effects of the denervated targets, did not significantly affect the numbers of E. motor and F. sensory neurons that sent their axons in both directions, negating possible neurotrophic effects. Each of two retrograde fluorescent dyes were applied either proximal or distal to the cross-bridges to backlabel the TIB neurons as shown in Fig 2A.

doi:10.1371/journal.pone.0127397.g006

because the 4-5-fold maximal enlargement of functional motor units by axonal sprouting is sufficient to fully reinnervate these muscles [34]. Correspondingly, the average mass of the gastrocnemius muscles in the right experimental hindlimb was 1531.6 ± 53 mg. This mass was not significantly different from the average mass of the muscles of 1403.4 ± 70 mg in the left control hindlimb in which the TIB nerve was intact but CP distal nerve stump was removed to construct the autologous CP cross-bridges that were placed in the experimental right hindlimb (see Methods).

Myelinated donor TIB axons were found throughout the cross-section of the recipient CP nerve stumps both proximal and distal to the three cross-bridges placed between the donor TIB nerve and the recipient denervated CP nerve stump (Fig 7A). Intact perineurium surrounded single nerve fascicles; there appeared to be more large-diameter axons in the CP nerve stump distal to the bridges three months after placing the cross-bridges, a period of time when some cross-reinnervation of the flexor muscles by the TIB nerves occurs (unpublished observations). The number of donor TIB axons in the denervated CP nerve stump was the same proximal and distal to the cross-bridges (Fig 7C). The large variability in these numbers was consistent with the variability in the numbers of motor and sensory neurons that regenerated their axons into the CP nerve stumps, proximal and distal to the bridges (cf Fig 6B and 6C).

Ligation of the CP nerve stump distal to the last cross-bridge did not affect how many motor and sensory TIB neurons regenerated their axons proximally and/or distally into the recipient denervated CP nerve stump (Fig 6D, 6E and 6F; Exp. 1B in Table 1). The spatial distribution and the numbers of regenerated TIB nerve fibers was also unaffected both proximal and distal to the three cross-bridges (Fig 7B and 7C). These findings discounted possible neurotrophic effects of denervated targets on the direction taken by the regenerated TIB axons within the recipient denervated CP distal nerve stump. Even though there was a trend for the total *number of TIB axons* that grew into the recipient CP nerve stump to be higher than when the CP nerve stump was not ligated distally, this trend was not statistically significant (Fig 7C). The *size* of the TIB axons in the ligated distal CP nerve stump was noticeably smaller as compared to the size when the distal nerve stump was not ligated (cf Fig 7B and 7C) consistent with findings that axon diameter of regenerated axons recovers only after functional contacts are made [35].

Removing the perineurium

The connective tissue sheath of the perineurium of the donor TIB nerve and the recipient denervated CP nerve stump was intact over the 10 mm distance of insertion of three cross-bridges but it was removed to insert five, seven, and nine cross-bridges between the nerves (Fig 1; Exp. 1C in Table 1). The numbers of motor and sensory neurons that regenerating their axons through more than three cross-bridges did not increase, their numbers being the same as when three cross-bridges were placed between perineurial windows (Fig 8). The numbers of donor TIB axons that grew across the bridges into the CP nerve stump proximal and distal to the bridges were also the same, irrespective of the number of bridges (Fig 9D). However, myelinated TIB axons were found in equal numbers inside *and* outside of the original CP nerve fascicle proximal to the placement of more than three cross-bridges after stripping the perineurium (Fig 9B, 9C and 9E). This was in contrast to the containment of the donor TIB axons within the single fascicle of the recipient CP nerve stump when they regenerated their axons through perineurial windows (Fig 9A). Yet, the donor TIB axons were contained inside of the perineurium distal to the five, seven and nine cross-bridges in the CP nerve stump (Fig 9B, 9C, and 9E). Typically there were two or more fascicles in the distal CP nerve stump unlike the normal CP axon distribution within a single fascicle in the popliteal fossa.

Improved nerve regeneration through 'protected' nerve stumps after delayed repair

We had previously reported that insertion of three cross-bridges through perineurial windows with a radius of 250 μm, in the donor TIB nerve and the recipient denervated CP distal nerve stump three months before a delayed CP nerve coaptation, increased the number of CP motoneurons that regenerated their axons by a factor of 1.7-fold [12]. In this study, we inserted

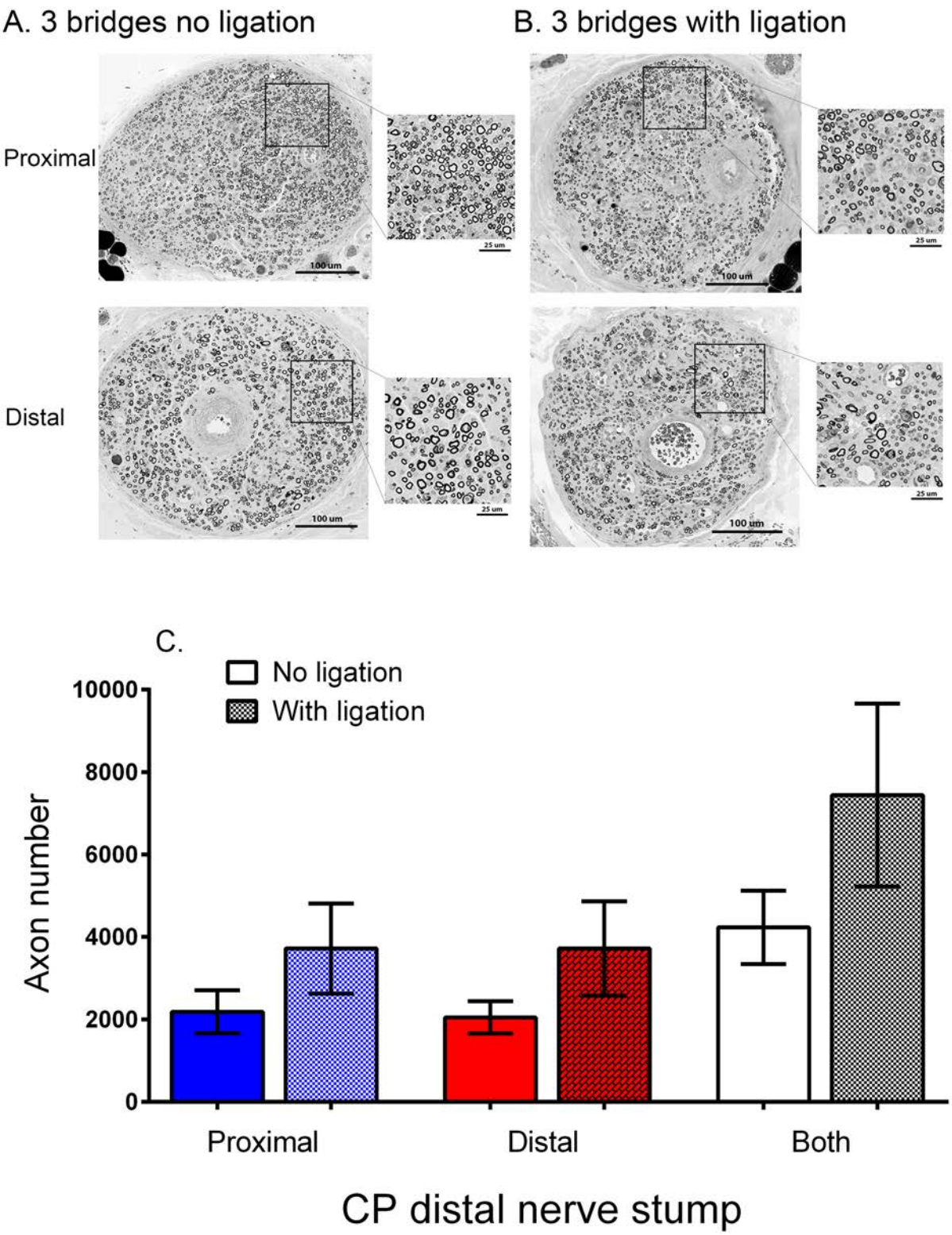


Fig 7. Donor axons regenerate and become myelinated equally well either side of cross-bridges placed between the donor tibial (TIB) nerve and the recipient denervated common peroneal (CP) whether or nor the distal nerve stump is isolated from denervated targets. A. Cross-sections of regenerated TIB axons within the recipient denervated CP nerve stump, proximal and distal to the insertion of 3 cross-bridges between the nerves 3 months previously (Experiment #1, No Repair: Table 1). TIB axons that grew within the CP nerve stump distal to the cross-bridges tended to be larger than B. those in the CP nerve stump that was ligated, consistent with findings that regenerated axons recover size only after making functional contacts. C. Mean (±SE) TIB

axon numbers in the recipient denervated CP nerve stump were the same proximal and distal to 3 cross-bridges, whether or not the CP nerve stump was isolated from denervated targets. This negates possible neurotrophic target influences on donor TIB nerves growing into a recipient denervated CP nerve stump.

doi:10.1371/journal.pone.0127397.g007

three, five, seven, and nine cross-bridges. The three bridges were placed between perineurial windows of twice the radius, namely 500 μm, and the perineurium was stripped over the 10 mm distance of the cross-bridge insertion when more than three cross-bridges were placed (Exp. 2A and B in Table 1). *All* the chronically axotomized CP motoneurons regenerated their axons through the three month chronically denervated CP nerve stump when they were 'protected' by three cross-bridges as compared to only ~33% of the motoneurons regenerating their axons through the nerve stump that was not 'protected' by cross-bridges placed between the donor TIB nerve and the denervated CP distal stump over the three month period prior to CP coaptation (Fig 10A). The chronic axotomy of the neurons and the chronic denervation of the distal nerve stumps three months prior to surgical repair account for the poor motor regeneration after delayed nerve repair [3, 7,8,25,36–38]. The same 3-fold increase in the number of chronically axotomized DRG sensory neurons that regenerated their axons after the three month delayed nerve repair of the CP nerve was also seen when three cross-bridges were placed to 'protect' the chronically denervated CP nerve stump (Fig 10B). The chronic axotomy of the sensory neurons reduced sensory nerve regeneration to 11%, a new finding that reflects the greater susceptibility of sensory neurons to axotomy [39–40]. Note that the cross-bridges were cut at the time of backlabelling the CP nerve distal to the cross-bridges so as to backlabel only the CP neurons that had regenerated their axons after the delayed nerve repair and *not* the donor TIB neurons whose axons crossed into the denervated CP distal nerve stumps via the cross-bridges (Fig 2B and 2C).

In summary, these data demonstrate that the protective effect of donor TIB axons on chronically denervated Schwann cells facilitates delayed nerve regeneration through the Schwann cells and requires that the axons are contained within the perineurium of the recipient denervated CP nerve stumps (Fig 9).

Donor axon 'protection' promotes reinnervation of denervated muscles

In order to determine whether muscle reinnervation is improved when CP axons regenerate through distal nerve stumps that were 'protected' by three cross-bridges, muscle isometric forces and the twitch forces of the muscle fibers innervated by single motor nerves, were recorded (Exp. 2A in Table 1). Typical twitch and tetanic isometric contractile forces developed by reinnervated extensor digitorum longus (EDL) muscles were evoked by electrical stimulation of the CP nerve distal to the placement of the cross-bridges. The electrical pulses were set at 2X threshold to evoke twitch and tetanic contractions in response a single pulse and to repetitive pulses at 100 Hz, respectively. The contractile forces were significantly greater in amplitude when the chronically denervated distal CP nerve stumps were 'protected' by three cross-bridges as compared to when no bridges were placed prior to the three month delayed CP nerve coaptation (Fig 11A; note that the force ranges on the Y-axis are three times greater when three cross-bridges as compared to no bridges, were placed). Mean contractile forces were significantly larger although they did not reach preoperative levels within the five months of nerve regeneration but the wet weight of the muscles recovered completely when the chronically denervated CP nerve stump was 'protected' (Fig 11B, 11C, and 11D). Of note, development of both twitch and tetanic contractions were slower in the former as compared to the latter conditions.

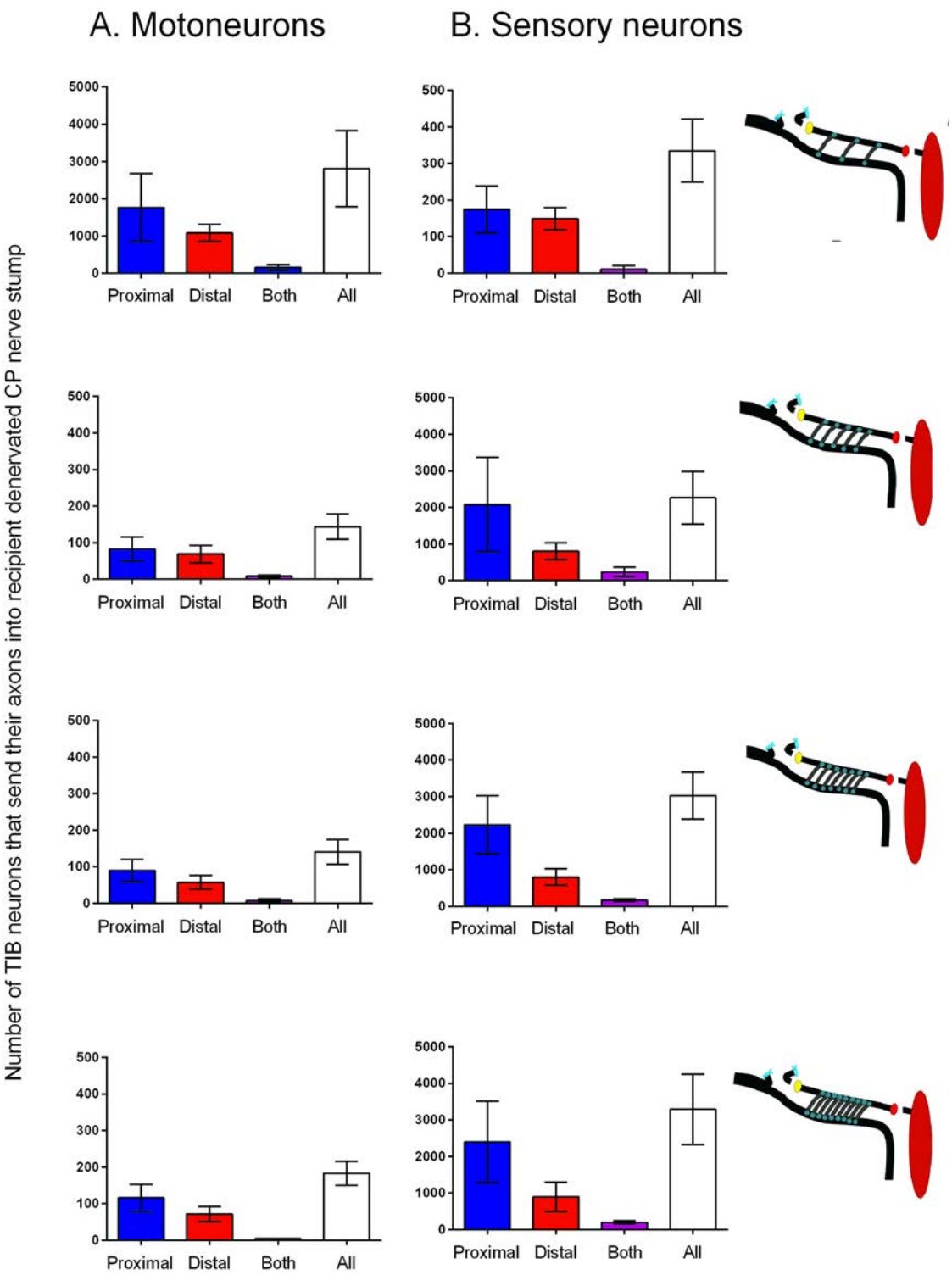


Fig 8. Donor tibial (TIB) neurons grew their axons across cross-bridges into a recipient denervated common peroneal (CP) distal nerve stump where they proceeded to grow both proximal and distal to the cross-bridges. In Experiment #1, No Repair: Table 1, motor and sensory neurons were backlabelled with two fluorescent dyes applied proximal and distal to the cross-bridges (see Fig 2A). The numbers (±SE) of TIB motoneurons and sensory neurons that regenerated their axons into the denervated CP distal nerve stump both proximal and distal to 3, 5, 7 and 9 cross-bridges (as illustrated) were not significantly different. Very few neurons regenerated axons both proximal and distal to the cross-bridges as shown by the few neurons that were double-labelled with two retrograde dyes.

doi:10.1371/journal.pone.0127397.g008

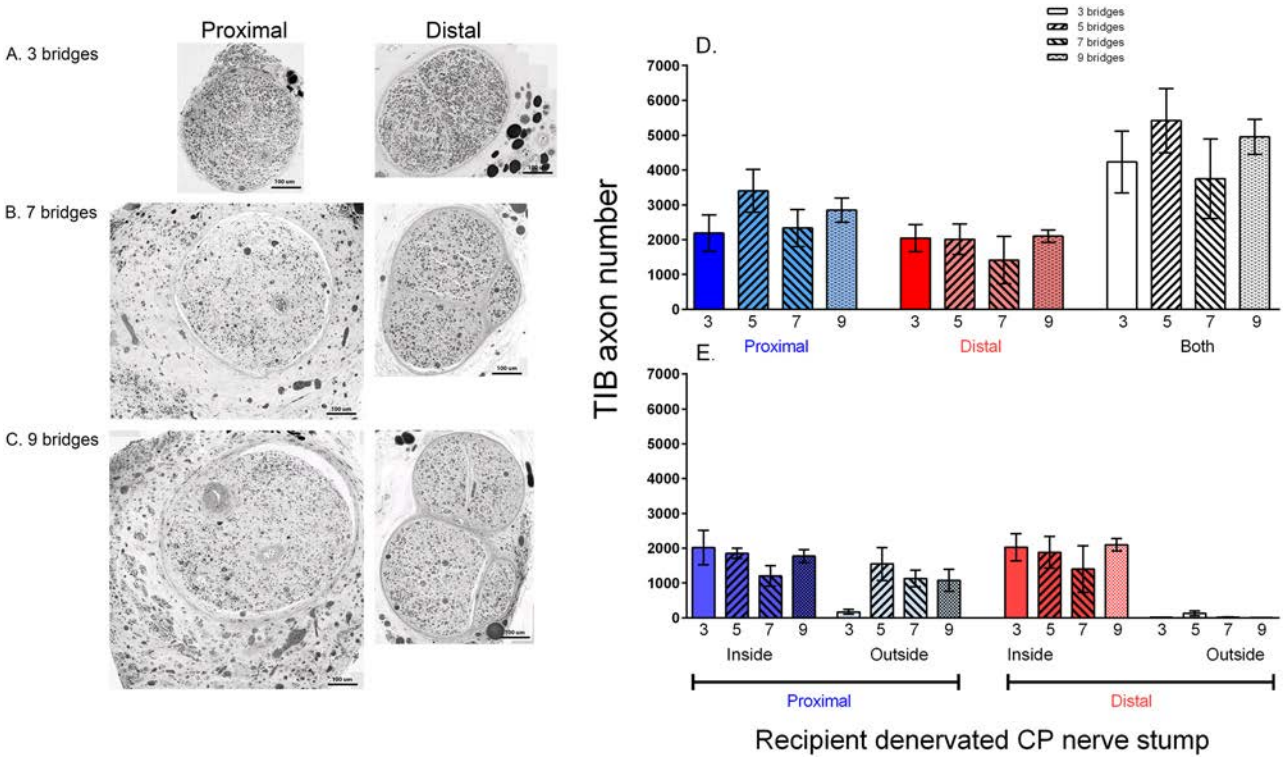


Fig 9. Regenerated tibial (TIB) axons lie outside as well as inside perineurium in the recipient common peroneal (CP) nerve stump proximal to the 10 mm length of the donor TIB nerve and the recipient CP nerve stump where the perineurium was stripped to place 5, 7, or 9 cross-bridges between the donor TIB nerve and recipient CP nerve stump. Cross-sections of the recipient denervated CP nerve either side of A. 3, B. 7 and C. 9 cross-bridges that were placed between the donor TIB nerve and recipient denervated CP nerve stump (Experiment #1, No Repair: Table 1). Regenerated and myelinated TIB axons distal to the cross-bridges were multi-fasciculated when the perineurium was removed to place 5–9 cross-bridges (B,C). D. The means (±SE) of the numbers of TIB axons that regenerated proximal and distal to the cross-bridges were not statistically different irrespective of the number of cross-bridges that were placed whilst E. the same numbers (means ± SE) of TIB axons regenerated within and outside of the perineurium of the CP nerve stump proximal but not distal to 5, 7 and 9 cross-bridges.

doi:10.1371/journal.pone.0127397.g009

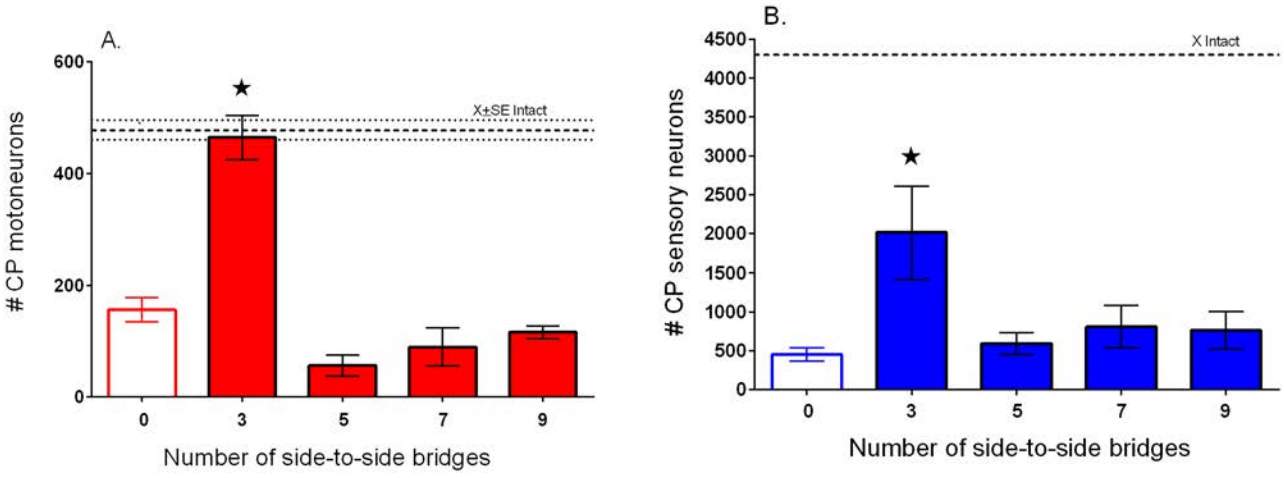


Fig 10. Three but not more cross-bridges placed between a donor tibial (TIB) nerve and a recipient denervated common peroneal (CP) nerve enhance CP motor and sensory nerve regeneration after a 3 month delayed repair of the transected CP nerve. Mean (±SE) numbers of CP A. motor and B. sensory neurons that regenerated their axons through the chronically denervated CP distal nerve stump as a function of the number of side-to-side cross-bridges placed between the donor TIB nerve and the recipient CP nerve stump prior to delayed surgical repair (coaptation) of the transected CP nerve.

doi:10.1371/journal.pone.0127397.g010

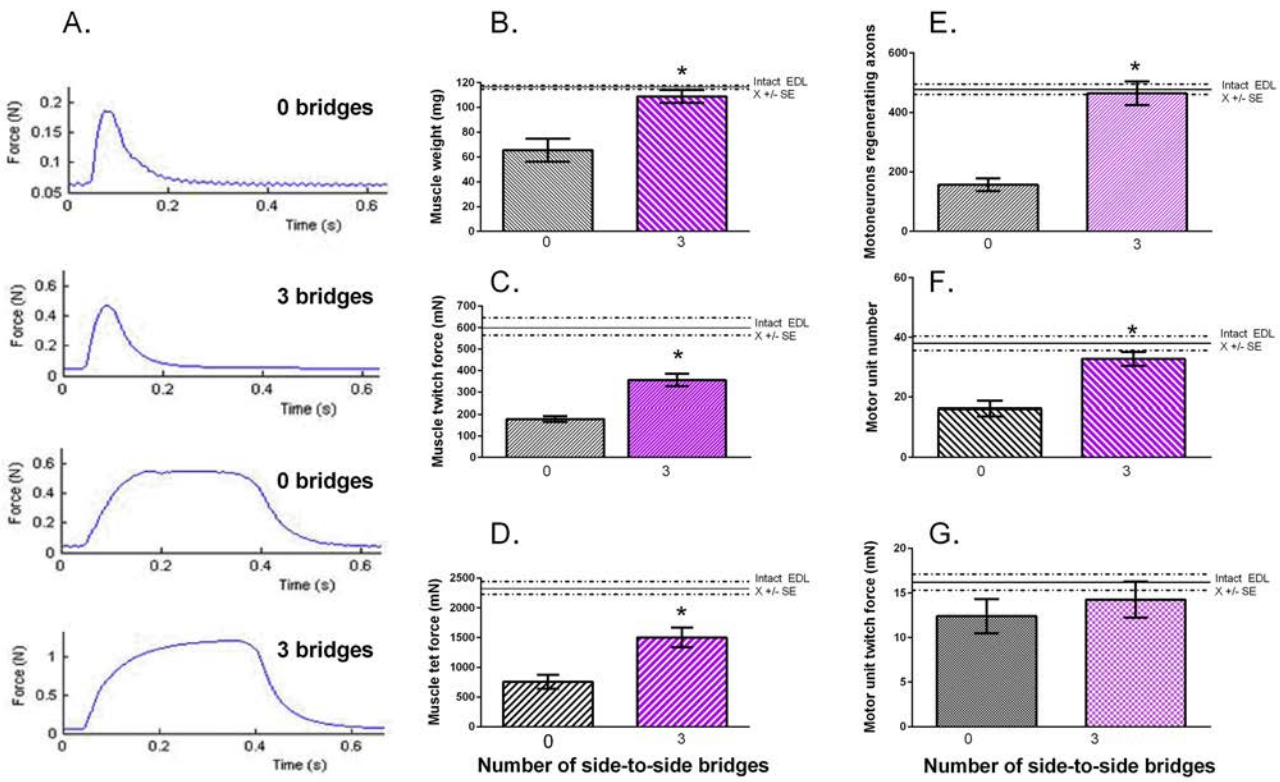


Fig 11. Donor tibial (TIB) axons 'protect' recipient denervated common peroneal (CP) nerve stumps to promote regeneration of CP axons and reinnervation of denervated muscles within 5 months after a 3 month delayed CP nerve repair. A. Examples of maximal twitch and tetanic contractions of extensor digitorum longus (EDL) muscle. These were recorded in response to 0.5 Hz and 100 Hz repetitive CP nerve stimulation at 2X threshold showing increased contractile forces when 3 as compared to 0 bridges were placed between donor TIB nerve and the recipient CP nerve stump 3 months prior to the delayed CP nerve repair (coaptation). (Note the smaller Y-axes for 0 as compared to 3 cross-bridges). The mean (±SE) values of muscle B. wet weight, C. twitch and D. tetanic forces and of the numbers of E. CP motoneurons that regenerated their axons and F. motor units (measured as shown in Fig 4) were significantly increased when 3 cross-bridges were placed as compared to no cross-bridges placed. G. The mean (±SE) values of motor unit twitch forces were not significantly different, the return of all the regenerating motor axons reinnervating all the denervated muscle fibers.

doi:10.1371/journal.pone.0127397.g011

The calculated number of reinnervated motor units [the ratio of maximal muscle and mean single motor unit twitch forces (Fig 4)] reached normal levels (Fig 11F), consistent with *all* the motoneurons regenerating axons through the CP nerve stump that was 'protected' by three cross-bridges after delayed CP nerve coaptation (Fig 11E). The mean twitch contractile forces of the reinnervated MUs were the same whether zero or three cross-bridges were placed (Fig 11G). Hence, the recording of muscle and motor unit forces validated the counts of the motoneurons that regenerated their axons after delayed nerve repair when the chronically denervated CP nerve stump was 'protected' by donor TIB axons.

Discussion

The regenerative capacity of injured neurons declines with time and distance from their denervated targets as they regenerate their axons but fail to reach their targets (chronic axotomy) and the Schwann cells in the distal nerve stumps remain chronically denervated [41]. We demonstrated here that regenerative capacity is restored by encouraging donor axons from an otherwise intact donor nerve to grow across side-to-side autologous cross-bridges into a recipient denervated distal nerve stump prior to the nerve regeneration of the original axotomized neurons. These finding have clear clinical implications for application because first, both motor

and sensory neurons demonstrate equal capacity to grow axons from a donor nerve into a recipient denervated nerve stump and second, the neurons send their axons both proximal and distal to the cross-bridges. Surgical repair of injured nerves may be delayed or, even after immediate nerve repair of brachial plexus injuries for example, regenerating nerves typically grow over long and therefore challenging distances. Under these conditions, the relatively simple surgical procedure of placement of side-to-side bridges between an adjacent intact donor nerve and a recipient denervated nerve stump would encourage the occupation of the chronically denervated nerve stumps and their 'protection' with and by donor axons during the lengthy period of growth of regenerating axons from the more proximal nerve stumps. This in turn, would enhance the passage of the regenerating axons from the proximal nerve stump and would lead in turn, to improved motor and sensory outcomes in patients.

Studies have indicated that donor axons cross an end-to-side nerve repair (end-to-side neurorrhaphy) whether or not a perineurial window is created [18,19,42]. On the other hand, other studies have suggested that perineurial windows are essential [43,44]. Histomorphological examination of axons in the denervated nerve stump showed that more axons crossed through the perineurial window and into the nerve stump when the window was widened [14,30–32]. We have in this study, examined whether this is the case for two end-to-side neurorrhaphies of autologous nerve grafts placed between a donor nerve and a recipient denervated nerve stump (side-to-side cross-bridges). The size of the perineurial windows was increased systematically to demonstrate that there is a linear relationship between the perineurial window size and the number of neurons contributing axons into the recipient denervated nerve stump (Fig 5): few if any neurons regenerated axons through very small perineurial windows and more donor neurons grew axons reliably through larger ones. Sprouting, as defined by the presence of doubly labeled neurons and was reported after end-to-side neurorrhaphy [21], was a minor contributor of donor axons through the side-to-side cross-bridges to the recipient denervated stump (Fig 3). Most of the donor TIB neurons regenerated their axons across the cross-bridges and into the recipient denervated CP nerve stump as measured and defined by their retrograde labelling from axons within the CP nerve stump and their failure to be backlabelled from the donor TIB nerve 10 mm distal to the last cross-bridge (Fig 3A). Very few donor TIB neurons were doubled-labelled from both the donor TIB nerve and the recipient denervated CP nerve stump distal to the last cross-bridge, these neurons sprouting axons through the cross-bridges and into the recipient denervated CP nerve stump (Fig 3B and 3C). Furthermore, both motor *and* sensory neurons contributed axons equally across the side-to-side bridges (Figs 6 and 8) in contrast to the poor growth of motor axons that was reported across an end-to-side neurorrhaphy [21,45], An average of ~32 and ~37% of the donor motor and sensory neurons regenerated their axons through perineurial windows with a radius of 500 μm that were opened to insert three cross-bridges between the donor tibial (TIB) nerve and the recipient common peroneal (CP) denervated nerve stump. The ~35% reduction in the number of intact TIB axons within the donor TIB nerve would not likely compromise the innervation of the extensor muscles that these axons supply. Motor nerves that retain their contact with their target muscle fibers within partially denervated muscles can sprout axons within the muscles to reinnervate denervated muscle fibers [46]. This sprouting capacity is sufficient so that great remaining intact motor nerves can effectively reinnervate *all* the muscle fibers in partially denervated muscles as long as the partial denervation does not exceed 80–85% [34,47,48]. The mass of the gastrocnemius muscles in the experimental hindlimb in which the cross-bridges were placed between the donor TIB and the denervated recipient CP nerve was the same as in the left control hindlimb. This indicates that all of the extensor muscle fibers were innervated three months after the placement of the cross-bridges. Moreover, as sprouting occurs within weeks [48], the recovery of gastrocnemius muscle weight supports the contention that the sprouting

had occurred within the muscles in response to the reduced numbers of TIB axons in the donor nerve.

Donor TIB neurons regenerated their axons across two perineurial windows from the donor nerve, through the cross-bridges, and into the recipient denervated CP nerve stump (Figs 5–9). The Schwann cells within the cross-bridges were denervated, the autologous side-to-side cross-bridges having been constructed from the denervated CP nerve harvested from the contralateral hindlimb (Fig 1). These denervated Schwann cells likely attracted and/or supported the axons growing from the donor nerve because, in their absence, axon outgrowth from a donor nerve fails [49]. Regenerating axons gradually grow across a suture site over a prolonged period of up to twenty eight days in the rat as the axons pass through disorganized arrays of extracellular laminin and other glycoproteins at the site [50,51]. Inhibitory chondroitin sulphate proteoglycans contribute to the lengthy axon outgrowth prior to their degradation [52–59]. The regenerating axons from the donor nerve likely cross perineurial windows over a similar protracted period and, indeed, we have observed this 'staggered' regeneration of axons through side-to-side cross-bridges in *Thy-1* transgenic rats [60]. During this period of time, the denervated Schwann cells within the cross-bridges enter into a growth permissive state in which they express many neurotrophic factors and p75 receptors that are permissive for axon growth [61–64]. The denervated Schwann cells will also respond to release of neuregulin, cAMP, and other mitogens from ingrowing axons by cell division [65–67]. Donor axons regenerate into the first (most proximal) cross-bridge before the second and the third such that the numbers of myelinated axons are significantly higher within the first as compared to the third bridge one month after their insertion [60]. It is possible that this proximo-distal course of the donor axons transpired because the perineurial windows were opened along the parallel course of the fibers within the nerves. When more cross-bridges were secured in the nerves whose perineurium was stripped to accommodate them, the numbers of donor axons that crossed into the recipient denervated nerve stump did not increase (Fig 9). These regenerating axons were located equally within and outside of the perineurium of the recipient distal nerve stump proximal to the cross-bridges and within perineurium distal to the bridges (Fig 9). Since all axons had crossed the first three bridges, it is likely that either the axons and/or the indwelling fibroblasts elaborated the perineurium around the axons as the axons passed through the 10 mm length of the CP nerve stump into which the cross-bridges were inserted between the donor TIB nerve and the recipient CP nerve stump. The possibility that donor axons might grow preferentially toward denervated end-organs was discounted in the experiments in which the distal end of the denervated nerve stump was ligated: equal numbers of both motor and sensory neurons sent their axons proximal and distal to the cross-bridges (Figs 6 and 7).

Three months after placing the cross-bridges, the mean number of ~4500 donor axons that occupied the recipient denervated nerve stump (Figs 7 and 9) was ~1.5 times the mean total number of ~3000 parent motor and sensory neurons that regenerated the axons (Figs 6 and 8). The ratio of ~1.5 of donor axons within the recipient nerve stump to neurons that regenerated these axons, is small when compared to the ratio of 5 of the regenerated axons distal to a nerve crush to their parent axons proximal to the crush site [68]. The fewer TIB axons that regenerated into the recipient CP denervated nerve stumps may have resulted from the progressive decline in the numbers of the denervated Schwann cells and/or their progressive atrophy after chronic denervation of the recipient denervated nerve stump. The finding that these axons were myelinated (Fig 7) is consistent with our former findings of the myelination of the few axons that succeeded in regenerating into chronically denervated nerve stumps after a delayed surgical repair [36].

It is likely that donor axons regenerate considerably more rapidly across the second as compared to the first perineurial window between each of the cross-bridges and the recipient

denervated nerve stump. From the staggered time course of axon regeneration across a suture site of ~28 days, it is likely that the first axons to regenerate across the 3.2 mm long cross-bridges would reach the second window within days. In the course of the first ten days during which the extracellular matrix becomes aligned, Schwann cells cross into the suture site and are arrayed in the Bands of Bungner that in turn, guide regenerating axons into and through the endoneurial tubes of the denervated distal nerve stump [51]. The pace of axon crossing increases so that all the neurons regenerate their axons across the suture site within three to four weeks [50]. Within the three to four week period of axon regeneration across the first suture site of the cross-bridge insertion into the donor nerve, infiltrating macrophages will clear the axonal debris in the cross-bridges that was generated by the Wallerian nerve degeneration of the axons that were isolatedfrom their neuronal cell bodies [69–78]. As a result, many of the regenerating donor axons in the cross-bridges should grow more rapidly through the second perineurial window and into the recipient denervated nerve stump. A conservative estimate for most of the donor axons to cross into the recipient denervated nerve stump would therefore be in the order of eight weeks with the result that many Schwann cells in the recipient stump would be chronically denervated prior to entry of donor axons. The progressive growth of axons across three bridges would extend this period of time for some of the donor axons with the result that the denervation period may be even longer. It is during this period of chronic denervation of the Schwann cells in the recipient denervated nerve stump that the expression of growth associated genes by the Schwann cells would decline, the neurotrophic factors and their receptors declining exponentially from a peak expression between ten and twenty days [5,6,61,62,79,80]. The exponential decline in the growth permissive state of the Schwann cells parallels the corresponding decline in the regeneration of axons [3,7–8].

The rationale of creating the side-to-side cross-bridges prior to delayed nerve repair was to prolong the permissive state of the Schwann cells by passage of donor axons into the recipient denervated nerve stump. This in turn, was to boost the capacity of the axotomized neurons to regenerate their axons within a chronically denervated nerve stump. The occupation of the distal nerve stump by donor TIB axons was increased by increasing the size of the perineurial windows cut into the donor nerve and into the recipient denervated nerve stump (Fig 5). As a result, three times as many motor and sensory CP neurons regenerated their axons into the CP distal nerve stump after delayed repair when cross-bridges were inserted through perineurial windows with a radius of 500 μm, as compared to the numbers that regenerated their axons when no cross-bridges were inserted to 'protect' the chronically denervated CP nerve stump (Fig 10). *All* CP motoneurons regenerated their axons through the 'protected' distal nerve stump when three cross-bridges were inserted through perineurial windows of a 500 μm radius as compared to the more limited 1.7-fold increase when ~50 of the TIB motoneurons sent their axons into the recipient denervated CP nerve stump through perineurial windows of half the radius, namely 250 μm (Figs 6 and 9 in [12]). The same increase was seen for the sensory neurons but, the chronic injury having reduced the regenerative capacity of the sensory neurons more drastically than for the motoneurons, the increase was short of all the sensory neurons regenerating their axons after the delayed repair (Fig 10B). The efficacy of side-to-side cross-bridges in promoting sensory nerve regeneration after delayed nerve repair is particularly striking given the more severe effect of axotomy on sensory neurons [39,40] with some ensuing cell death [81], and the lower capacity of the injured sensory neurons as compared to injured motoneurons to regenerate their axons after delayed nerve repair when no side-to-side cross-bridges were placed (Fig 10B). Reinnervated muscles recovered their former weight in concert with the regeneration of all the CP motor nerves through the denervated distal nerve stumps that were 'protected' by the cross-bridges (Fig 11B, 11E, and 11F). This was so even though the time span of five months in this study for CP nerve regeneration and muscle reinnervation after delayed

nerve coaptation was insufficient for the muscles to fully recover their contractile forces (Fig 11A, 11C, and 11D). Nonetheless, the 'protection' significantly improved the muscle contractile forces (Fig 11A, 11C, and 11D).

It is likely the donor axons that grew into the denervated nerve stump released agents such as neuregulin that promote the proliferation of the Schwann cells and their expression of regeneration associated genes. Those axons that made contact with Schwann cells were remyelinated by the Schwann cells (Figs 7 and 9), converting their gene expression from growth permissive to the myelinating phenotype [63,64,79,82–84]. Those that did not contact the Schwann cells likely sustained their expression of the regeneration associated genes, at least in part, via these same agents as well as agents that have not yet been identified. These agents in turn, supported the regeneration of axons through the denervated endoneurial sheaths after the delayed CP nerve coaptation.

In the current study, we allowed the babysitting donor axons to remain within the recipient denervated nerve stump after delayed nerve repair. This was done so as to model the clinical scenario of nerve regeneration of injured neurons being progressively compromised by chronic axotomy and chronic SC denervation over time and distance [3,7,8,41]. We transected the cross-bridges at the time of applying retrograde dyes to the regenerated axons in the CP nerve to ensure that the regenerative success of only the CP neurons, and not that of the donor TIB neurons, was determined (Fig 2). The five to nine bridges placed between the donor nerve and the recipient denervated stump that had been stripped of the perineurium did not offer the `protection`that the three cross-bridges had (Fig 10). This was likely due to insufficient donor axons occupying the endoneurial tubes of the recipient denervated nerve stump with as many axons lying outside as inside of the perineurium (Fig 9). The disrupted distal nerve stump may also have contributed to the poor regenerative success after delayed nerve repair. Under clinical human conditions in which cross-bridges may be placed between larger nerves such as the ulnar and the median nerves in the forearm after brachial plexus nerve injuries for example, it may be prudent to rotate the orientation of the cross-bridges around each of the nerves to allow for adequate 'protection' of the denervated Schwann cells in the empty endoneurial tubes.

In summary, our animal experiments systematically investigated the optimal size of perineurial windows between a donor nerve and a recipient denervated nerve stump and revealed that windows whose radii were ~3-fold larger than that of the autologous nerve cross-bridges were optimal for promoting excellent nerve repair after delayed nerve surgery.

Acknowledgments

We extend our grateful thanks first to the Canadian Institutes for Health Research (CIHR) for their award of a CIHR operating grant #253172 for this work and second to Drs. Michael Willand and Joseph Catapano for their critical reading of the manuscript.

Author Contributions

Conceived and designed the experiments: TG GHB. Performed the experiments: TG MH CAL HC JZ. Analyzed the data: TG MH CAL HC JZ. Wrote the paper: TG.

References

1. Hudson AR, Hunter D (1977) Timing of peripheral nerve repair: important local neuropathological factors. Clin Neurosurg 24: 391–405. PMID: 583689
2. Lundborg G (2004) Nerve Injury and Repair. New York: Churchill Livingstone.

3. Gordon T, Tyreman N, Raji MA (2011) The basis for diminished functional recovery after delayed peripheral nerve repair. J Neurosci 31: 5325–5334. 31/14/5325 [pii]; doi: 10.1523/JNEUROSCI.6156-10.2011 PMID: 21471367
4. Gordon T (2010) The physiology of neural injury and regeneration: The role of neurotrophic factors. J Commun Disord 43: 265–273. S0021-9924(10)00021-3 [pii]; doi: 10.1016/j.jcomdis.2010.04.003 PMID: 20451212
5. Boyd JG, Gordon T (2003) Neurotrophic factors and their receptors in axonal regeneration and functional recovery after peripheral nerve injury. Mol Neurobiol 27: 277–324. PMID: 12845152
6. Hoke A, Gordon T, Zochodne DW, Sulaiman OAR (2002) A decline in glial cell-line-derived neurotrophic factor expression is associated with impaired regeneration after long-term Schwann cell denervation. Exp Neurol 173: 77–85. PMID: 11771940
7. Fu SY, Gordon T (1995) Contributing factors to poor functional recovery after delayed nerve repair: prolonged denervation. J Neurosci 15: 3886–3895. PMID: 7751953
8. Fu SY, Gordon T (1995) Contributing factors to poor functional recovery after delayed nerve repair: prolonged axotomy. J Neurosci 15: 3876–3885. PMID: 7751952
9. Hall SM (1999) The biology of chronically denervated Schwann cells. Ann N Y Acad Sci 883: 215–233. PMID: 10586247
10. Bain JR, Veltri KL, Chamberlain D, Fahnestock M (2001) Improved functional recovery of denervated skeletal muscle after temporary sensory nerve innervation. Neurosci 103: 503–510.
11. Veltri K, Kwiecien JM, Minet W, Fahnestock M, Bain JR (2005) Contribution of the distal nerve sheath to nerve and muscle preservation following denervation and sensory protection. J Reconstr Microsurg 21: 57–70. PMID: 15672322
12. Ladak A, Schembri P, Olson J, Udina E, Tyreman N, Gordon T (2011) Side-to-side nerve grafts sustain chronically denervated peripheral nerve pathways during axon regeneration and result in improved functional reinnervation. Neurosurgery 68: 1654–1665. doi: 10.1227/NEU.0b013e31821246a8 PMID: 21346654
13. Viterbo F, Trindade JC, Hoshino K, Mazzoni A (1994) Two end-to-side neurorrhaphies and nerve graft with removal of the epineural sheath: experimental study in rats. Br J Plast Surg 47: 75–80. PMID: 8149062
14. Liu K, Chen LE, Seaber AV, Goldner RV, Urbaniak JR (1999) Motor functional and morphological findings following end-to-side neurorrhaphy in the rat model. J Orthop Res 17: 293–300. doi: 10.1002/jor.1100170220 PMID: 10221848
15. Hayashi A, Pannucci C, Moradzadeh A, Kawamura D, Magill C, Hunter DA, et al. (2008) Axotomy or compression is required for axonal sprouting following end-to-side neurorrhaphy. Exp Neurol 211: 539–550. doi: 10.1016/j.expneurol.2008.02.031 PMID: 18433746
16. Goheen-Robillard B, Myckatyn TM, Mackinnon SE, Hunter DA (2002) End-to-side neurorrhaphy and lateral axonal sprouting in a long graft rat model. Laryngoscope 112: 899–905. PMID: 12150625
17. Ray WZ, Mackinnon SE (2010) Management of nerve gaps: autografts, allografts, nerve transfers, and end-to-side neurorrhaphy. Exp Neurol 223: 77–85. doi: 10.1016/j.expneurol.2009.03.031 PMID: 19348799
18. Viterbo F, Amr AH, Stipp EJ, Reis FJ (2009) End-to-side neurorrhaphy: past, present, and future. Plast Reconstr Surg 124: e351–e358. doi: 10.1097/PRS.0b013e3181bf8471; 00006534-200912001-00009 [pii]. PMID: 19952703
19. Viterbo F, Trindade JC, Hoshino K, Mazzoni NA (1992) Latero-terminal neurorrhaphy without removal of the epineural sheath. Experimental study in rats. Rev Paul Med 110: 267–275. PMID: 1341024
20. Yuksel F, Karacaoglu E, Guler MM (1999) Nerve regeneration through side-to-side neurorrhaphy sites in a rat model: a new concept in peripheral nerve surgery. Plast Reconstr Surg 104: 2092–2099. PMID: 11149773
21. Zhang Z, Soucacos PN, Bo J, Beris AE (1999) Evaluation of collateral sprouting after end-to-side nerve coaptation using a fluorescent double-labeling technique. Microsurgery 19: 281–286. doi: 10.1002/(SICI)1098-2752(1999)19:6<281::AID-MICR5>3.0.CO;2-D [pii]. PMID: 10469443
22. Kemp SW, Phua PD, Stanoulis KN, Wood MD, Liu EH, Gordon T, et al. (2013) Functional recovery following peripheral nerve injury in the transgenic Thy1-GFP rat. J Peripher Nerv Syst 18: 220–231. doi: 10.1111/jns5.12035 PMID: 24028190
23. Magill CK, Moore AM, Borschel GH, Mackinnon SE (2010) A new model for facial nerve research: the novel transgenic Thy1-GFP rat. Arch Facial Plast Surg 12: 315–320. 12/5/315 [pii]; doi: 10.1001/archfacial.2010.71 PMID: 20855773
24. Moore AM, Borschel GH, Santosa KA, Flagg ER, Tong AY, Kasukurthi R, et al. (2012) A transgenic rat expressing green fluorescent protein (GFP) in peripheral nerves provides a new hindlimb model for the

study of nerve injury and regeneration. J Neurosci Methods 204: 19–27. S0165-0270(11)00611-X [pii]; doi: 10.1016/j.jneumeth.2011.10.011 PMID: 22027490

25. Furey MJ, Midha R, Xu QG, Belkas J, Gordon T (2007) Prolonged target deprivation reduces the capacity of injured motoneurons to regenerate. Neurosurgery 60: 723–732. PMID: 17415210
26. Abercrombie M (1946) Estimation of nuclear population from microtome sections. Anatomy Record 94: 239–247. PMID: 21015608
27. More HL, Chen J, Gibson E, Donelan JM, Beg MF (2011) A semi-automated method for identifying and measuring myelinated nerve fibers in scanning electron microscope images. J Neurosci Methods 201: 149–158. S0165-0270(11)00455-9 [pii]; doi: 10.1016/j.jneumeth.2011.07.026 PMID: 21839777
28. Major LA, Hegedus J, Weber DJ, Gordon T, Jones KE (2007) Method for counting motor units in mice and validation using a mathematical model. J Neurophysiol 97: 1846–1856. PMID: 17151224
29. Hegedus J, Putman CT, Tyreman N, Gordon T (2008) Preferential motor unit loss in the SOD1^{G93A} transgenic mouse model of amyotrophic lateral sclerosis. J Physiol 586: 3337–3351. doi: 10.1113/jphysiol.2007.149286 PMID: 18467368
30. Walker JC, Brenner MJ, Mackinnon SE, Winograd JM, Hunter DA (2004) Effect of perineurial window size on nerve regeneration, blood-nerve barrier integrity, and functional recovery. J Neurotrauma 21: 217–227. doi: 10.1089/089771504322778677 PMID: 15000762
31. Yan JG, Matloub HS, Sanger JR, Zhang LL, Riley DA, Jaradeh SS (2002) A modified end-to-side method for peripheral nerve repair: large epineurial window helicoid technique versus small epineurial window standard end-to-side technique. J Hand Surg Am 27: 484–492. PMID: 12015724
32. Oyamatsu H, Koga D, Igarashi M, Shibata M, Ushiki T (2012) Morphological assessment of early axonal regeneration in end-to-side nerve coaptation models. J Plast Surg Hand Surg 46: 299–307. doi: 10.3109/2000656X.2012.696264 PMID: 22931136
33. Schmalbruch H (1986) Fiber composition of the rat sciatic nerve. Anat Rec 215: 71–81. PMID: 3706794
34. Rafuse VF, Gordon T, Orozco R (1992) Proportional enlargement of motor units after partial denervation of cat triceps surae muscles. J Neurophysiol 68: 1261–1275. PMID: 1432083
35. Gordon T, Stein RB (1982) Time course and extent of recovery in reinnervated motor units of cat triceps surae muscles. J Physiol 323: 307–323. PMID: 7097576
36. Sulaiman OAR, Gordon T (2000) Effects of short- and long-term Schwann cell denervation on peripheral nerve regeneration, myelination, and size. GLIA 32: 234–246. PMID: 11102965
37. Boyd JG, Gordon T (2002) A dose-dependent facilitation and inhibition of peripheral nerve regeneration by brain-derived neurotrophic factor. Eur J Neurosci 15: 613–626. PMID: 11886442
38. Boyd JG, Gordon T (2001) The neurotrophin receptors, trkB and p75, differentially regulate motor axonal regeneration. J Neurobiol 49: 314–325. PMID: 11745667
39. Hoffer JA, Stein RB, Gordon T (1979) Differential atrophy of sensory and motor fibers following section of cat peripheral nerves. Brain Res 178: 347–361. PMID: 228793
40. Milner TE, Stein RB (1981) The effects of axotomy on the conduction of action potentials in peripheral sensory and motor nerve fibres. J Neurol Neurosurg Psychiatry 44: 485–496. PMID: 7276961
41. Fu SY, Gordon T (1997) The cellular and molecular basis of peripheral nerve regeneration. Mol Neurobiol 14: 67–116. PMID: 9170101
42. Viterbo F, Teixeira E, Hoshino K, Padovani CR (1998) End-to-side neurorrhaphy with and without perineurium. Sao Paulo Med J 116: 1808–1814. PMID: 10030106
43. Akeda K, Hirata H, Matsumoto M, Fukuda A, Tsujii M, Nagakura T, et al. (2006) Regenerating axons emerge far proximal to the coaptation site in end-to-side nerve coaptation without a perineurial window using a T-shaped chamber. Plast Reconstr Surg 117: 1194–1203. doi: 10.1097/01.prs.0000201460.54187.d7; 00006534-200604010-00018 [pii]. PMID: 16582786
44. Haninec P, Samal F, Tomas R, Houstava L, Dubovwy P (2007) Direct repair (nerve grafting), neurotization, and end-to-side neurorrhaphy in the treatment of brachial plexus injury. J Neurosurg 106: 391–399. doi: 10.3171/jns.2007.106.3.391 PMID: 17566208
45. Tarasidis G, Watanabe O, Mackinnon SE, Strasberg SR, Haughey BH, Hunter DA (1997) End-to-side neurorrhaphy resulting in limited sensory axonal regeneration in a rat model. Ann Otol Rhinol Laryngol 106: 506–512. PMID: 9199612
46. Gordon T, Yang JF, Ayer K, Stein RB, Tyreman N (1993) Recovery potential of muscle after partial denervation: a comparison between rats and humans. Brain Res Bull 30: 477–482. PMID: 8457897
47. Tam SL, Gordon T (2003) Mechanisms controlling axonal sprouting at neuromuscular junction. J Neurocyto Invited review. 32: 961–974. PMID: 15034279
48. Tam SL, Gordon T (2011) Axonal sprouting in health and disease. Enclyclopedia Neurosci 1–8.

49. Al-Qattan MM, Al-Thunyan A (1998) Variables affecting axonal regeneration following end-to-side neurorrhaphy. Br J Plast Surg 51: 238–242. S0007-1226(97)90188-0 [pii]; doi: 10.1054/bjps.1997.0188 PMID: 9664884

50. Brushart TM, Hoffman PN, Royall RM, Murinson BB, Witzel C, Gordon T (2002) Electrical stimulation promotes motoneuron regeneration without increasing its speed or conditioning the neuron. J Neurosci 22: 6631–6638. PMID: 12151542

51. Witzel C, Rohde C, Brushart TM (2005) Pathway sampling by regenerating peripheral axons. J Comp Neurol 485: 183–190. PMID: 15791642

52. Wang X, Hasan O, Arzeno A, Benowitz LI, Cafferty WB, Strittmatter SM (2012) Axonal regeneration induced by blockade of glial inhibitors coupled with activation of intrinsic neuronal growth pathways. Exp Neurol 237: 55–69. S0014-4886(12)00244-0 [pii]; doi: 10.1016/j.expneurol.2012.06.009 PMID: 22728374

53. Huebner EA, Strittmatter SM (2009) Axon regeneration in the peripheral and central nervous systems. Results Probl Cell Differ 48: 339–351. doi: 10.1007/400_2009_19 PMID: 19582408

54. Houle JD, Tom VJ, Mayes D, Wagoner G, Phillips N, Silver J (2006) Combining an autologous peripheral nervous system "bridge" and matrix modification by chondroitinase allows robust, functional regeneration beyond a hemisection lesion of the adult rat spinal cord. J Neurosci 26: 7405–7415. PMID: 16837588

55. Groves ML, McKeon R, Werner E, Nagarsheth M, Meador W, English AW (2005) Axon regeneration in peripheral nerves is enhanced by proteoglycan degradation. Exp Neurol 195: 278–292. PMID: 15950970

56. Zuo J, Neubauer D, Graham J, Krekoski CA, Ferguson TA, Muir D (2002) Regeneration of axons after nerve transection repair is enhanced by degradation of chondroitin sulfate proteoglycan. Exp Neurol 176: 221–228. S0014488602979227 [pii]. PMID: 12093099

57. Zuo J, Hernandez YJ, Muir D (1998) Chondroitin sulfate proteoglycan with neurite-inhibiting activity is up-regulated following peripheral nerve injury. J Neurobiol 34: 41–54. PMID: 9469617

58. Braunewell KH, Martini R, LeBaron R, Kresse H, Faissner A, Schmitz B, et al. (1995) Up-regulation of a chondroitin sulphate epitope during regeneration of mouse sciatic nerve: evidence that the immunoreactive molecules are related to the chondroitin sulphate proteoglycans decorin and versican. Eur J Neurosci 7: 792–804. PMID: 7542529

59. Udina E, Ladak A, Furey M, Brushart T, Tyreman N, Gordon T (2010) Rolipram-induced elevation of cAMP or chondroitinase ABC breakdown of inhibitory proteoglycans in the extracellular matrix promotes peripheral nerve regeneration. Exp Neurol 223: 143–152. doi: 10.1016/j.expneurol.2009.08.026 PMID: 19733561

60. Hendry JM, Alvarez-Veronesi MC, Snyder A, Gordon T, Borschel GH (2015) Side-to-side bridges support donor axon regeneration into chronically denervated nerves and are associated with characteristic changes in Schwann cell phenotype. Neurosurg in revision.

61. Brushart TM, Aspalter M, Griffin JW, Redett R, Hameed H, Zhou C, et al. (2013) Schwann cell phenotype is regulated by axon modality and central-peripheral location, and persists in vitro. Exp Neurol 247C: 272–281. S0014-4886(13)00153-2 [pii]; doi: 10.1016/j.expneurol.2013.05.007

62. Hoke A, Redett R, Hameed H, Jari R, Zhou C, Li ZB, et al. (2006) Schwann cells express motor and sensory phenotypes that regulate axon regeneration. J Neurosci 26: 9646–9655. PMID: 16988035

63. Arthur-Farraj PJ, Latouche M, Wilton DK, Quintes S, Chabrol E, Banerjee A, et al. (2012) c-Jun reprograms Schwann cells of injured nerves to generate a repair cell essential for regeneration. Neuron 75: 633–647. S0896-6273(12)00583-1 [pii]; doi: 10.1016/j.neuron.2012.06.021 PMID: 22920255

64. Jessen KR, Mirsky R, Salzer J (2008) Introduction. Schwann cell biology. GLIA 56: 1479–1480. doi: 10.1002/glia.20779 PMID: 18803316

65. Fricker FR, Bennett DL (2011) The role of neuregulin-1 in the response to nerve injury. Future Neurol 6: 809–822. PMID: 22121335

66. Fricker FR, Lago N, Balarajah S, Tsantoulas C, Tanna S, Zhu N, et al. (2011) Axonally derived neuregulin-1 is required for remyelination and regeneration after nerve injury in adulthood. J Neurosci 31: 3225–3233. 31/9/3225 [pii]; doi: 10.1523/JNEUROSCI.2568-10.2011 PMID: 21368034

67. Morrissey TK, Levi AD, Nuijens A, Sliwkowski MX, Bunge RP (1995) Axon-induced mitogenesis of human Schwann cells involves heregulin and p185erbB2. Proc Natl Acad Sci U S A 92: 1431–1435. PMID: 7877996

68. Mackinnon SE, Dellon AL, O'Brien JP (1991) Changes in nerve fiber numbers distal to a nerve repair in the rat sciatic nerve model. Muscle Nerve 14: 1116–1122. PMID: 1745287

69. Chen S, Bisby MA (1993) Long-term consequences of impaired regeneration on facial motoneurons in the C57BL/Ola mouse. J Comp Neurol 335: 576–585. PMID: 8227536

70. Beuche W, Friede RL (1984) The role of non-resident cells in Wallerian degeneration. J Neurocytol 13: 767–796. PMID: 6512566

71. Stoll G, Griffin JW, Li CY, Trapp BD (1989) Wallerian degeneration in the peripheral nervous system: participation of both Schwann cells and macrophages in myelin degradation. J Neurocytol 18: 671–683. PMID: 2614485

72. Bruck W (1997) The role of macrophages in Wallerian degeneration. Brain Pathol 7: 741–752. PMID: 9161725

73. Stoll G, Muller HW (1999) Nerve injury, axonal degeneration and neural regeneration: basic insights. Brain Pathol 9: 313–325. PMID: 10219748

74. Hirata K, Mitoma H, Ueno N, He JW, Kawabuchi M (1999) Differential response of macrophage subpopulations to myelin degradation in the injured rat sciatic nerve. J Neurocytol 28: 685–695. PMID: 10851347

75. Mueller M, Wacker K, Ringelstein EB, Hickey WF, Imai Y, Kiefer R (2001) Rapid response of identified resident endoneurial macrophages to nerve injury. Am J Pathol 159: 2187–2197. S0002-9440(10)63070-2 [pii]; doi: 10.1016/S0002-9440(10)63070-2 PMID: 11733369

76. Hirata K, Kawabuchi M (2002) Myelin phagocytosis by macrophages and nonmacrophages during Wallerian degeneration. Microsc Res Tech 57: 541–547. doi: 10.1002/jemt.10108 PMID: 12112437

77. Rotshenker S (2011) Wallerian degeneration: the innate-immune response to traumatic nerve injury. J Neuroinflammation 8: 109. 1742-2094-8-109 [pii]; doi: 10.1186/1742-2094-8-109 PMID: 21878125

78. Gaudet AD, Popovich PG, Ramer MS (2011) Wallerian degeneration: gaining perspective on inflammatory events after peripheral nerve injury. J Neuroinflammation 8: 110. 1742-2094-8-110 [pii]; doi: 10.1186/1742-2094-8-110 PMID: 21878126

79. Gordon T (2014) Neurotrophic factor expression in denervated motor and sensory Schwann cells: Relevance to specificity of peripheral nerve regeneration. Exp Neurol 254: 99–108. S0014-4886(14)00025-9 [pii]; doi: 10.1016/j.expneurol.2014.01.012 PMID: 24468476

80. You S, Petrov T, Chung PH, Gordon T (1997) The expression of the low affinity nerve growth factor receptor in long-term denervated Schwann cells. GLIA 20: 87–100. PMID: 9179594

81. McKay HA, Brannstrom T, Wiberg M, Terenghi G (2002) Primary sensory neurons and satellite cells after peripheral axotomy in the adult rat: timecourse of cell death and elimination. Exp Brain Res 142: 308–318. PMID: 11819038

82. Mirsky R, Woodhoo A, Parkinson DB, Arthur-Farraj P, Bhaskaran A, Jessen KR (2008) Novel signals controlling embryonic Schwann cell development, myelination and dedifferentiation. J Peripher Nerv Syst 13: 122–135. JNS168 [pii]; doi: 10.1111/j.1529-8027.2008.00168.x PMID: 18601657

83. Jessen KR, Mirsky R (2005) The origin and development of glial cells in peripheral nerves. Nat Rev Neurosci 6: 671–682. nrn1746 [pii]; doi: 10.1038/nrn1746 PMID: 16136171

84. Knott EP, Assi M, Pearse DD (2014) Cyclic AMP Signaling: A Molecular Determinant of Peripheral Nerve Regeneration. Biomed Res Int 2014: 651625. doi: 10.1155/2014/651625 PMID: 25177696

Enhancement of Facial Nerve Motoneuron Regeneration through Cross-Face Nerve Grafts by Adding End-to-Side Sensory Axons

Eva Placheta, M.D.
Matthew D. Wood, Ph.D.
Christine Lafontaine, M.Sc.
Edward H. Liu, M.D.
J. Michael Hendry, M.D.
Doychin N. Angelov, M.D.
Manfred Frey, M.D.
Tessa Gordon, Ph.D.
Gregory H. Borschel, M.D.

Vienna, Austria; Toronto, Ontario, Canada; and Cologne, Germany

Background: In unilateral facial palsy, cross-face nerve grafts are used for emotional facial reanimation. Facial nerve regeneration through the grafts takes several months, and the functional results are sometimes inadequate. Chronic denervation of the cross-face nerve graft results in incomplete nerve regeneration. The authors hypothesize that donor axons from regional sensory nerves will enhance facial motoneuron regeneration, improve axon regeneration, and improve the amplitude of facial muscle movement.

Methods: In the rat model, a 30-mm nerve graft (right common peroneal nerve) was used as a cross-face nerve graft. The graft was coapted to the proximal stump of the transected right buccal branch of the facial nerve and the distal stumps of the transected left buccal and marginal mandibular branches. In one group, sensory occipital nerves were coapted end-to-side to the cross-face nerve graft. Regeneration of green fluorescent protein–positive axons was imaged in vivo in transgenic *Thy1*–green fluorescent protein rats, in which all neurons express green fluorescence. After 16 weeks, retrograde labeling of regenerated neurons and histomorphometric analysis of myelinated axons was performed. Functional outcomes were assessed with video analysis of whisker motion.

Results: "Pathway protection" with sensory axons significantly enhanced motoneuron regeneration, as assessed by retrograde labeling, in vivo fluorescence imaging, and histomorphometry, and significantly improved whisker motion during video analysis.

Conclusion: Sensory pathway protection of cross-face nerve grafts counteracts chronic denervation in nerve grafts and improves regeneration and functional outcomes. (*Plast. Reconstr. Surg.* 135: 460, 2015.)



Neurobiology of Disease 37 (2010) 412–422

Contents lists available at ScienceDirect

Neurobiology of Disease

journal homepage: www.elsevier.com/locate/ynbdi

Functional over-load saves motor units in the SOD1-G93A transgenic mouse model of amyotrophic lateral sclerosis

T. Gordon [a,b,*], N. Tyreman [a,b], S. Li [a,b], C.T. Putman [a,c], J. Hegedus [a,b]

[a] Center for Neuroscience, University of Alberta, Edmonton, AB, Canada T6G 2S2
[b] Division of Rehabilitation and Physical Medicine, Faculty of Medicine, University of Alberta, Edmonton, AB, Canada T6G 2S2
[c] Exercise Biochemistry Laboratory, Faculty of Physical Education and Recreation, University of Alberta, Edmonton, AB, Canada T6G 2H9

ARTICLE INFO

Article history:
Received 15 July 2009
Revised 23 September 2009
Accepted 22 October 2009
Available online 29 October 2009

Keywords:
Amyotrophic Lateral Sclerosis
Motor Unit
Activity
Motoneuron
Denervation
Neuromuscular
Muscle
Adaptation
Transgenic
Twitch
Tetanus
Myosin

ABSTRACT

The fastest, most forceful motor units are lost progressively during asymptomatic disease in the SOD1^{G93A} transgenic mouse model of amyotrophic lateral sclerosis. As the disease progresses the surviving motor units must increase their levels of activity to sustain posture and movement. If activity-dependent conversion of motor units to more fatigue resistant types increased their resilience and hence survival, we hypothesized that an experimental increase in motor unit activity in the hindlimb muscles of the SOD1^{G93A} transgenic mouse should "save" those motor units that are normally lost in the first 90 days of age. To test this hypothesis, we partially denervated hindlimb muscles in SOD1^{G93A} and their corresponding control SOD1^{WT} transgenic mice by avulsion of either L4 or L5 spinal roots at 40 days of age. Whole muscle and single motor unit isometric twitch forces were recorded and the numbers intact motor units in fast-twitch tibialis anterior, medial gastrocnemius, extensor digitorum longus muscles and the slow-twitch soleus muscle were calculated at 90 days of age. We found that the rapid age-dependent decline in numbers of functional motor units in fast-twitch muscles of the SOD1^{G93A} transgenic mice was dramatically reduced by the functional hyperactivity in the partially denervated muscles and, that these muscles comprised a significantly higher component of type IIA and type IID/X fibers than those muscles that were innervated by nerves in intact spinal roots. We conclude that the vulnerable motor units are saved by increasing their neuromuscular activity and consequently, converting them to slower, less forceful, fatigue resistant motor units.
© 2009 Elsevier Inc. All rights reserved.

Introduction

Progressive motoneuron loss in amyotrophic lateral sclerosis (ALS) results in skeletal muscle denervation, manifesting as weakness and eventual paralysis. A mutation within the gene encoding the antioxidant enzyme cytosolic copper/zinc superoxide dismutase (SOD1) is associated with ~20% of familial ALS cases (Rosen, 1993). The SOD1^{G93A} transgenic mouse expressing the most common human mutation of a glycine to alanine conversion at the 93rd codon of SOD1 in high copy number develops symptoms and pathology similar to ALS patients (Gurney et al., 1994). The mechanisms of toxicity of the mutation remain unknown but studies of transgenic mouse lines indicate that mutant SOD1 toxicity is not related to copper-mediated catalysis of the conversion of toxic superoxide radicals to hydrogen peroxide and oxygen (Cleveland, 1999; Boillee et al., 2006). Proposed mechanisms include first, a gain of function for mSOD1 with reduced zinc binding to transform the protein into a toxic pro-oxidant and second, a propensity of a subfraction of mutant SOD1 proteins to form misfolded proteins and aggregates that saturate chaperones, inhibit proteasomes and/or interact with mitochondrial proteins (Rowland and Shneider, 2001; Boillee et al., 2006; Julien and Kriz, 2006; Rakhit et al., 2007).

Each motoneuron normally innervates tens and even thousands of muscle fibers, the neuron and its muscle fibers commonly referred to as the motor unit (MU) (Gordon et al., 2004b). Motoneurons are lost in a "die-back" manner with muscle denervation and loss of functionally intact MUs preceding loss of the axons, thinning of nerves in ventral roots, and motoneuron loss from the spinal cord (Chiu et al., 1995; Frey et al., 2000; Fischer et al., 2004; Hegedus et al., 2007; Gordon et al., 2008; Parkhouse et al., 2008). Die-back preferentially affects large motoneurons that innervate the most forceful type IIB muscle fibers (Henneman et al., 1965; Henneman and Olson, 1965; Frey et al., 2000; Pun et al., 2006; Hegedus et al., 2008), in accordance with selective vulnerability of large motor axons in sporadic ALS (Kawamura et al., 1981). Selective retardation of slow axonal transport of neurofilaments and tubulin in ALS mouse models that commonly occurs before detectable pathology results in their cellular accumulation. This may be the critical event leading to

* Corresponding author. Division of Physical Medicine and Rehabilitation/Centre for Neuroscience 525 Heritage Medical Research Centre Faculty of Medicine and Dentistry, University of Alberta Edmonton, AB, Canada T6G 2S2. Fax: +1 780 492 1617.
E-mail address: tessa.gordon@ualberta.ca (T. Gordon).
Available online on ScienceDirect (www.sciencedirect.com).

0969-9961/$ – see front matter © 2009 Elsevier Inc. All rights reserved.
doi:10.1016/j.nbd.2009.10.021

progressive strangulation of the nerves, the largest being the most vulnerable (Williamson and Cleveland, 1999).

Cellular mechanisms underlying the rapid preferential decline of the largest motor units during the asymptomatic phase in ALS are not yet understood. Dramatic loss of the most forceful MUs with the largest axons in the SOD1^{G93A} transgenic mice necessitates increased recruitment of surviving MUs and thereby, increased neuromuscular activity of the remaining pool of motoneurons and their muscle fibers (i.e. the MUs). This increased neuromuscular activity may, in turn, account for conversion of muscle fibers from IID/X to IIA phenotypes that is already apparent at 60 days of age in the TA muscle of SOD1^{G93A} mice (Hegedus et al., 2007; Hegedus et al., 2008). The motoneurons innervating type IIB and IID/X muscle fibers are the most susceptible to die-back and increased neuromuscular activity. The associated conversion of MU phenotypes with concurrent size reduction may confer some protection owing to reduced conduction velocity and axonal size (Munson et al., 1997; Havton et al., 2001). In the present study, we test the hypothesis that increased neuromuscular activity in the SOD1^{G93A} transgenic mouse model of ALS prolongs functional contact of motor axons with their skeletal muscles and promotes the retention of functional MUs. In order to increase neuromuscular activity of hindlimb muscles of the SOD1^{G93A} transgenic mouse, we used the physiological method of functional overload of hindlimb muscles by partial denervation of the hindlimbs after avulsing one of two contributing spinal roots.

Methods

Generation of SOD1^{G93A} mice

Male transgenic mice that express mutant human SOD1^{G93A} genes (B6JSL-TgN (SOD1-G93A) were purchased from Jackson Laboratories, USA. A colony was established by breeding male SOD1^{G93A} transgenic mice to non-transgenic B6JSL female mice. We identified transgenic SOD1^{G93A} mice from the offspring of these matings through standard PCR protocol for the human SOD1 performed on ear samples taken at the time of weaning (Rosen, 1993). After the pups were weaned at ~21 days of age they were separated by gender into standard rodent cages with free access to food and water. All of the experiments were approved by the University of Alberta Health Sciences Laboratory Animal Ethics committee and were carried out in accordance with the guidelines of the Canadian Council for Animal Care.

Partial denervation of hindlimb muscles

We partially denervated one hindlimb in 32 male mice (22 SOD1^{G93A} transgenic mice and 10 age-matched wild-type SOD1^{wt} control mice) at 40 days of age. Partial denervation was completed by avulsing one of two spinal roots that innervates the hindlimbs. Mice were anaesthetized by an intraperitoneal (IP) injection of an anesthetic cocktail made up of ketamine (100 mg/ml) and atravet

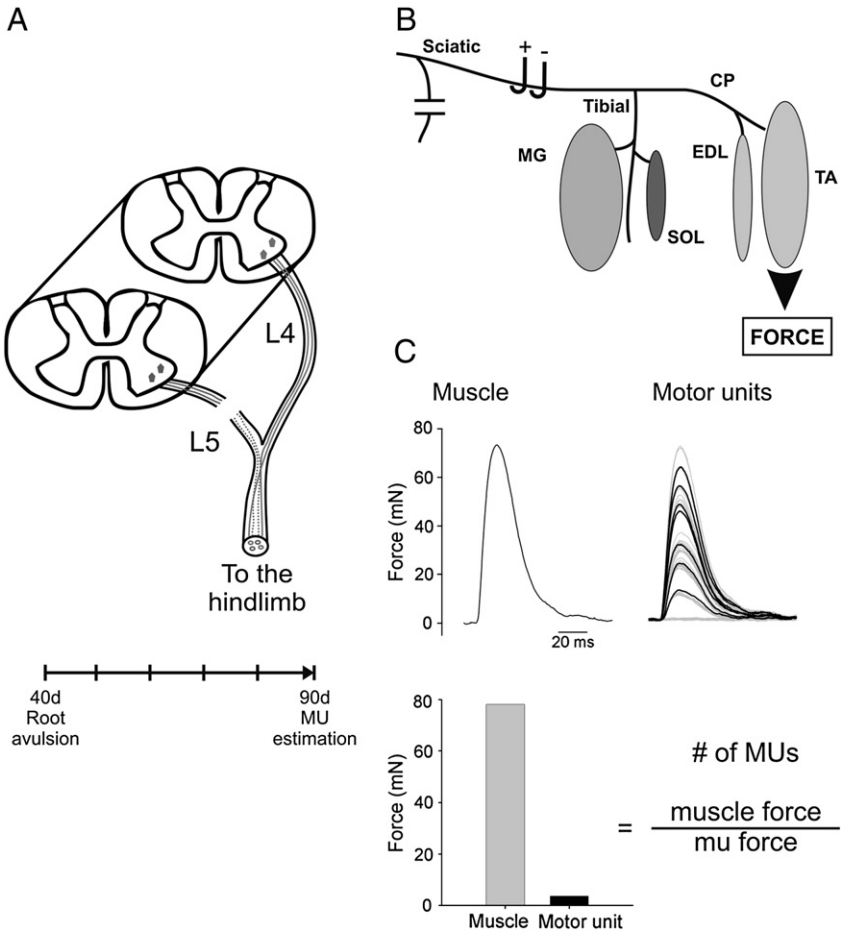


Fig. 1. (A) At 40 days of age, the muscles in one hindlimb were partially denervated by cutting one of two primary spinal roots, L4 and L5. The proximal nerve stump of the root was grasped with forceps to avulse the root, thereby preventing axon regeneration. (B) The tendons of the fast-twitch MG and slow-twitch SOL muscles of the ankle extensor group and those of the fast-twitch TA and EDL muscles of the ankle flexor group were isolated to connect to a force transducer to measure isometric contractions in response to stimulation of the sciatic nerve. (C) Isometric force was measured in response to maximum stimulation of the sciatic nerve at 1 Hz to elicit twitch contractions and to 100 Hz to elicit maximal tetanic contractions (not shown). Incremental stimulus voltage on the sciatic nerve elicited all-or-none increases in contractile force. Using a method to randomly select 15 levels of force in response to these increments, the number of motor units was estimated (MUNE) by division of the muscle and the average motor unit force. Details in the text.

(10 mg/ml) diluted in sterile saline. The dosage of the anesthetic was 17.5 ml/kg body weight for both control and $SOD1^{G93A}$ mice.

A small incision was made along the spinal cord just above the iliac crest to expose the nerves that radiate from the spinal roots. From the iliac crest, we counted the spinal roots to identify the nerves coming from the L4 and the L5 segments on the right side of the mouse (Fig. 1A). Using fine forceps and scissors, the bone around the segment of interest was cleared of muscle, and the proximal nerve stump of either the L4 or the L5 spinal root was firmly grasped and avulsed to prevent axon regeneration. The skin incision was sutured closed and the mice were allowed to recover before being returned to their cages. For the next 50 days, all experimental mice were subject to daily health checks during which their general health and mobility were evaluated.

Electrophysiological recordings

Surgery

The method used to enumerate and characterize motor units (MUs) has been described in detail (Major et al., 2007; Hegedus et al., 2009a). In brief, mice were anesthetized with the ketamine/atravet cocktail injected IP to induce surgical anesthesia. Periodically, additional doses of the cocktail were administered IP in order to maintain anesthesia throughout the experiment. The lower hindlimbs of the mice were exposed, and the tendons to the plantaris and lateral gastrocnemius muscles were identified and cut. Tendons to the soleus (SOL), medial gastrocnemius (MG), tibialis anterior (TA) and extensor digitorum longus (EDL) muscles were identified and separated. These muscles were tied individually with a 4.0 silk thread for attachment to the strain gauge (Kulite model KH-102) during recording (Fig. 1B). Following isolation of the nerves bilaterally, the sciatic nerves were exposed on both sides and wire electrodes were sutured alongside the nerves for electrical stimulation. Both hindlimbs were prepared in all mice and the non-operated side was used as a control. The hindlimbs were clamped at the knees and ankles to immobilize the legs without interfering with the blood supply to the muscles.

Isometric force recordings and MU enumeration

Isometric forces evoked from individual muscles through electrical stimulation of the sciatic nerve were amplified and digitized using Axoscope Software (version 8.0, Axon Instruments, USA). The lengths of the muscles were adjusted to yield maximal evoked isometric twitch contractile force in response to stimulation of the sciatic nerve. Maximal contractile muscle forces were recorded in response to single suprathreshold (2× threshold amplitude) stimulation of the sciatic nerve at a frequency of 0.5 Hz.

Average MU force was determined by incremental stimulation of the sciatic nerve to elicit discrete increases in MU force as described in detail previously and illustrated in Fig. 1C (Hegedus et al., 2007; Major et al., 2007; Hegedus et al., 2009a). The incremental increases in whole muscle force were recorded in response to sciatic nerve stimulation at a frequency of 0.5 Hz, and the amplitude of the stimulus pulse was manually controlled from 0 to 10 V. The all-or-none increments in muscle force were recorded and overlaid in a custom software program written in MatLab. Using this program, 8–20 increments were randomly chosen from throughout the entire range of muscle forces. We calculated average MU force as the mean force associated with these increments. In order to estimate the number of intact MUs, the whole muscle twitch contractile force was divided by the average MU force.

Determination of muscle fiber composition by SDS-PAGE and histochemistry

Myosin heavy chain (MHC) isoforms were analyzed according to Gallo et al. (2004) Briefly, muscles from both SOD^{G93A} and SOD^{WT} transgenic mice were homogenized on ice with buffer containing 100 mM $Na_4P_2O_7$ (pH 8.5), 5 mM EGTA, 5 mM $MgCl_2$, 0.3 M KCl, 10 mM DTT and protease inhibitor cocktail at 5 mg/ml concentration (CompleteTM, Roche Diagnostic, Laval, PQ, Canada). Samples were subsequently stirred for 30 min on ice followed by centrifugation at 13,400×*g* for 5 min at 4 °C. The supernatant of each sample was then isolated and diluted 1:1 with glycerol and stored at -20 °C until analyzed. Extracts were diluted to 0.1 μg/μl in modified Laemmli lysis buffer, boiled for 6 min, and cleared by centrifugation. The MHC extract in a volume of 6 μl was electrophoresed in triplicate for 24 h at constant 275 V and 12 °C on polyacrylamide gels containing glycerol. Gels were then fixed and MHC isoforms were detected by silver staining (Oakley et al., 1980). The relative proportions of MHC isoforms were determined with integrative densitometry (Syngene ChemiGenius, GeneTools, Syngene, Cambridge, UK).

Statistics

Data were considered significant if $p<0.05$, and p was determined using an independent samples *t*-test (SPSS version 14.0, 2005). Significance is denoted by stars in the figures (* for $p<0.05$ and ** for <0.01). For calculations including MU forces we tested the data set for normality using a one-sided Kolmogrov–Smirnov test. For non-normally distributed data, significance was determined using the Mann–Whitney *U*-test in the SPSS program.

Results

Many functional motor units are lost in fast-twitch muscles of $SOD1^{G93A}$ mice in the pre-symptomatic phase of disease

Functional motor units (MUs) are the motoneurons and the muscle fibers that they innervate. By isolating axons for stimulation,

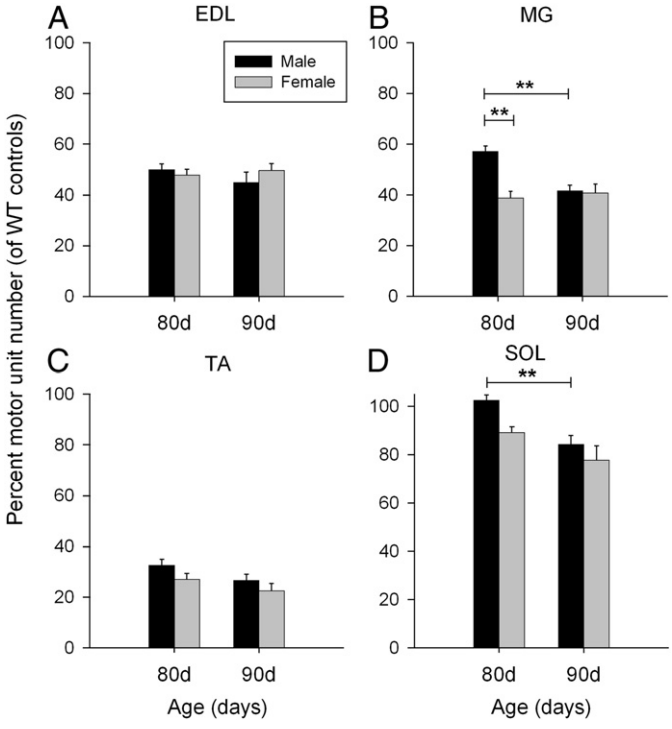


Fig. 2. The number of motor units in fast-twitch EDL, MG and TA muscles and slow-twitch SOL muscles in $SOD1^{G93A}$ transgenic mice at 80 and 90 days of age in male and female mice. The number of motor units is expressed as a percent of the number in $SOD1^{WT}$ transgenic mice. Although there was a significant decline in motor unit numbers between 80 and 90 days of age in the SOL muscle there was only a significant reduction in the MG muscle for the male mice. This gender difference not being significant over time (Hegedus et al., 2009b), both genders were used in the remaining studies of partial denervation. $^{**}p<0.01$ and $^{*}p<0.05$.

we recorded the isometric force of single MUs in normally caged SOD1^{G93A} transgenic mice. As illustrated in Figs. 1B, C, the isometric contractile force of the fast-twitch medial gastrocnemius (MG), extensor digitorum longus (EDL) and tibialis anterior (TA) muscles and the slow-twitch soleus (SOL) muscles was recorded in turn in each animal. At a frequency of 1 Hz, supramaximal stimulation of the sciatic nerve to the muscles evoked muscle twitch contractile force. Using incremental stimulation described in the Methods section, we recorded forces developed by the muscle fibers innervated by single motoneurons–single MUs. The ratio of the muscle and the mean MU twitch contractile forces provided the estimation of the number of intact MUs.

We found that the numbers of MUs rapidly declined from 40 days of age in the fast-twitch hindlimb muscles, reaching a plateau between 80 and 90 days when the mice began to show symptoms of hindlimb weakness at the onset of symptomatic disease (Chiu et al., 1995; Veldink et al., 2003; Hegedus et al., 2007). At 80 days of age, a large percentage of the intact MUs innervating the fast-twitch hindlimb muscles were already lost ($n=5$ for males, $n=8$ for females; Fig. 2). In the EDL and MG muscles, ~50% of the functional MUs remained at 80 and 90 days of age; although the percentage of functionally intact MUs that remained was significantly higher in the MG muscles in the male as compared to the female SOD1^{G93A} mice ($P<0.01$) (Figs. 2A, B), no systematic gender difference was seen during the progressive decline in MU numbers over the course of the ~140 day lifespan of the mice (Hegedus et al., 2009b). In the TA muscles of the 80 to 90 day old SOD1^{G93A} transgenic mice only ~25% of the functional MUs remained (Fig. 2C). The decline of functional MUs in the slow-twitch SOL muscle occurred later with a significant decline after 80 days of age (Fig. 2D). This is consistent with the relative saving of the type I muscle fibers during the asymptomatic phase of the disease (Gordon et al., 2005; Hegedus et al., 2007; Hegedus et al., 2009b).

Partially denervated muscles in SOD^{wt} transgenic mice enlarge their motor units to compensate for loss of intact motor units

The spinal roots that emanate from the L4 and L5 segments of the spinal cord in the mouse innervate the ankle extensor and flexor muscles of the hindlimb. Either the L4 or L5 spinal root was avulsed unilaterally at 40 days of age in SOD1^{G93A} and SOD^{wt} transgenic mice of both male and female mice to partially denervate the hindlimb muscles. Thereby neuromuscular activity in the remaining intact MUs is increased to sustain posture and movement (Einsiedel and Luff, 1994; Seburn and Gardiner, 1996; Tyc and Vrbova, 2007). In human patients with neurogenic lesions the maximal discharge rate of MUs increases as the number of MUs in the muscles decreases (Schulte-Mattler et al., 2000). Because the MU loss was the same in male and female SOD1^{G93A} transgenic mice (Hegedus et al., 2007; Hegedus et al., 2009b), our further analyses of partially denervated muscles were performed on transgenic mice of both genders.

Avulsion of the L4 spinal root in the SOD^{wt} transgenic mice reduced the mean number of intact MUs in the TA muscle from 77 to 30, a significant reduction of about 60% (Fig. 3A). Based on evidence in several animal species including cat, rat and mouse, and humans, loss of up to 80% of MUs is normally compensated for by collateral sprouting in the order of 3–8 fold to enlarge remaining intact MUs (Yang et al., 1990; Rafuse et al., 1992; Gordon et al., 1993; Tam et al., 2001; Tam and Gordon, 2003a; Gordon et al., 2004a). Collateral sprouting and reinnervation in the SOD^{wt} mice was evident as increased MU forces and preservation of total muscle contractile force even after avulsion of the L4 spinal root. Fig. 3 demonstrates a significant rightward shift of the MU force histograms to larger MU forces at 90 days of age (Fig. 3B) with a significant increase in their average MU force (Fig. 3C). Recovery of muscle twitch force was equal that in the contralateral muscles where the innervation remained intact (Fig. 3D).

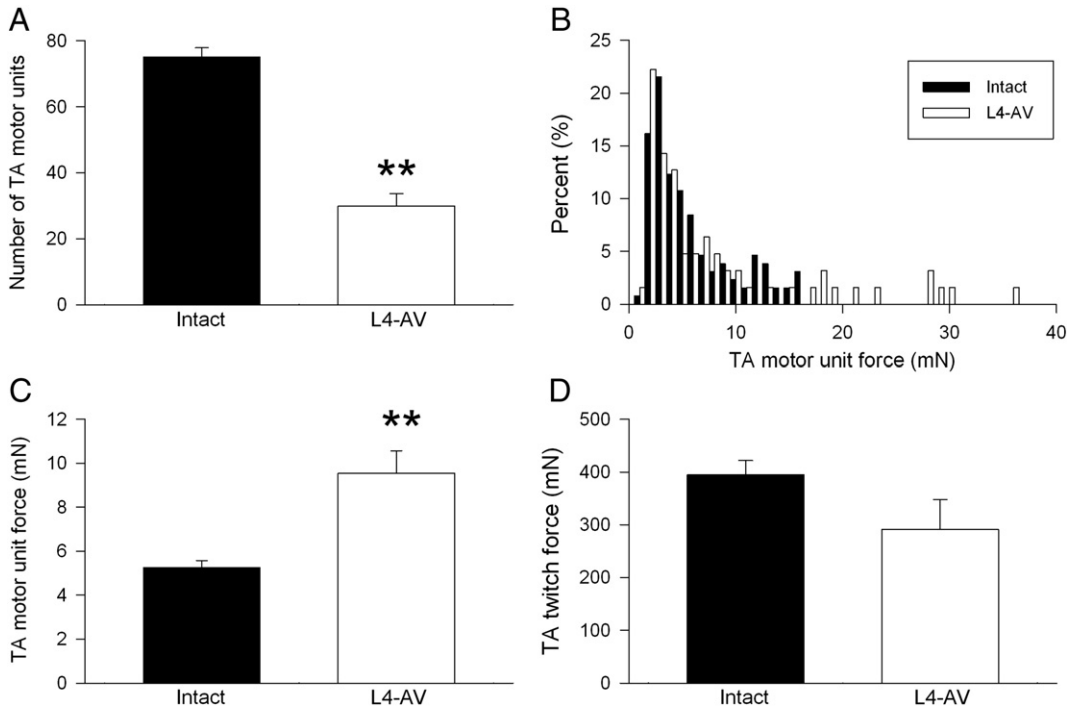


Fig. 3. The response of TA muscle in the SOD1^{WT} transgenic mouse to partial denervation by avulsion of the L4 spinal root (L4-AV). (A) The number of motor units was significantly reduced in the partially denervated TA ($p<0.01$) with a significant shift of the percentage frequency histogram (B) of motor unit forces to the right. The average increase in TA motor unit force (C) was significant and corresponded with a similar decline in numbers of intact motor units remaining in the partially denervated TA muscle. (D) As a result of the motor unit enlargement, the partially denervated TA muscle after L4 avulsion recovered whole muscle twitch force that was not significantly different from the intact contralateral TA muscle. **$p<0.01$ and *$p<0.05$.

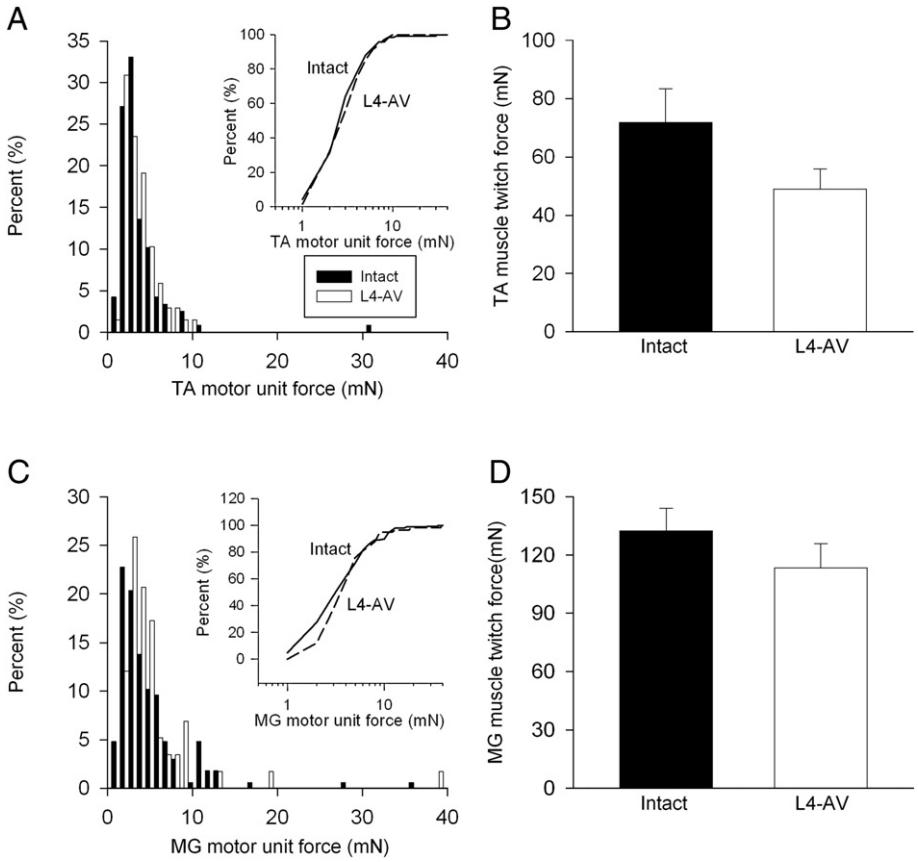


Fig. 4. Little or no enlargement of motor unit twitch contractile forces after partial denervation of the TA and MG muscles in the hindlimbs of SOD1^{G93A} transgenic mouse *but* full recovery of muscle forces despite avulsion of the L4 spinal root. In the TA (A) and MG (C) muscle there was no significant shift of the percentage frequency histograms and of the cumulative percent histogram of motor unit forces to the right, despite the significant reduction in the numbers of remaining motor units at 40 days of age that was shown in Fig. 3 and Supplementary Fig 1. Yet the muscles developed as much twitch force in response to maximal stimulation of the sciatic nerve as did the contralateral muscles that developed force in response to stimulation of *all* the motor nerves emanating from spinal roots L4 and L5 (B, D). The findings indicate that the motor units that remained after L4 spinal root avulsion survived during the next 50 days until force recording at 90 days of age.

Avulsion of L4 spinal root also reduced numbers of intact MUs in the MG muscle (Supplementary Fig. 1). Similar to the TA muscle, the force frequency histograms for the partially denervated MG muscle were shifted to the right with increased MU forces. The increased mean forces compensated for the reduced number of MUs, resulting in comparable contractile muscle force in the partially denervated and intact muscles (Supplementary Fig. 1). In contrast no significant reduction was found in SOL muscles whose motor axons exit the spinal cord in the L5 spinal root (see Fig. 5D). The EDL muscle which is similar in muscle fiber type composition as compared to the synergistic TA muscle demonstrated a similar progression and rate of MU loss. The muscle not being significantly denervated by either L4 or L5 was not studied further.

Partially denervated muscles in SOD1^{G93A} transgenic mice do NOT enlarge their surviving motor units but they develop as much force as their contralateral intact muscles

The L4 spinal root was avulsed in the SOD1^{G93A} transgenic mice, reducing the number of MUs in the muscles by the same proportion as in the SOD^{wt} mice. However, the increased MU twitch forces seen in the TA and MG muscles in the SOD^{wt} mice were *not* found in the SOD1^{G93A} transgenic mice (cf. Figs. 4 and 3, Supplementary Fig. 1). There was little or no shift of the force histograms to the right in the 90 day old SOD1^{G93A} mice after partial denervation of the muscles at 40 days of age (Figs. 4A, C). There was, however, a trend for the smaller MUs to enlarge in the MG muscles (insert in Fig. 4C) where the proportion of type I and IIA muscle fibers are higher than in the TA muscle, consistent with the known capacity of motor nerves innervating these fibers to sprout in the SOD1^{G93A} transgenic mouse muscles, unlike those innervating the larger muscle fibers (Frey et al., 2000).

Despite there being no or minimal MU enlargement, after partial denervation of the hindlimb of the SOD1^{G93A} transgenic mice, the contractile force in the partially denervated muscles was the same as that in the muscles in the contralateral intact hindlimb (Figs. 4B, D). Since muscle contractile force is the product of the number of MUs in the muscle and the force they develop (Tötösy de Zepetnek et al., 1992) and the MU forces in the partially denervated and intact muscles were not significantly different (Figs. 4A, C), we conclude that the number of MUs in fast-twitch muscles that normally decline sharply from 40 to 90 days of age (see Fig. 6) do not, all the MUs in the partially denervated muscles surviving. Thus the normal muscle contractile forces in the partially denervated TA (Figs. 3D and 5B) and MG muscles (Supplementary Fig. 1, Fig. 4D) indicate that the remaining MUs after avulsion of one spinal root, remain intact and do *not* decline in number over the 40 to 90 days as those MUs that do decline in number in the intact contralateral limb of the SOD1^{G93A} transgenic mouse (see Figs. 5–7).

Partial denervation by avulsion of the L5 spinal root produced similar results to avulsion of the L4 spinal root. L5 avulsion resulted in a significant loss of functional MUs in both the fast-twitch TA and MG muscles and the slow-twitch SOL muscle in SOD1^{G93A} transgenic and SOD^{wt} mice. Data for the TA muscle is shown in Figs. 5A–C and data for MG and SOL muscles are shown in Supplementary Figs. 2C,F. Sprouting and reinnervation in the partially denervated SOD^{wt} mice resulted in a significant rightward shift of the MU force distributions to larger forces and increases in mean MU force compared to the

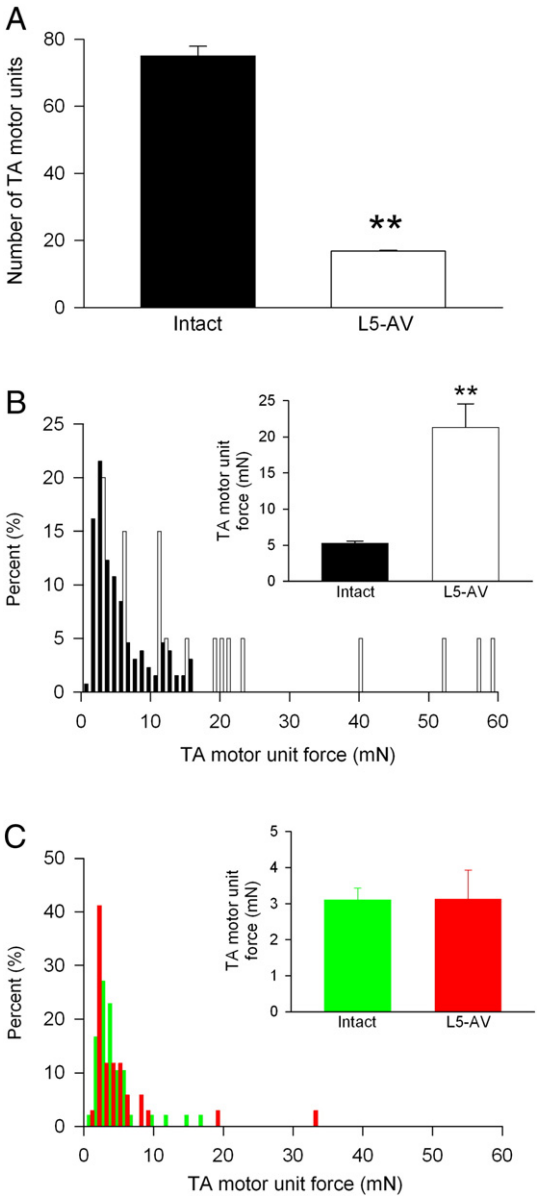


Fig. 5. Little or no enlargement of motor unit twitch contractile forces after partial denervation of the TA muscle in the hindlimbs of SOD1^{G93A} transgenic mouse following avulsion of the L5 spinal root. Avulsion of L5 spinal root significantly reduced the number of motor units in the fast-twitch TA muscle (A). The percentage frequency histograms and the cumulative percent histograms of motor unit forces in the SOD1^{WT} transgenic mice but *not* the SOD1^{G93A} transgenic mice were shifted significantly to the right for the TA muscle (cf. C with B) ($P<0.01$). **$p<0.01$ and *$p<0.05$.

intact contralateral muscles (Fig. 5B; Supplementary Fig. 2B). In contrast MU force distributions and mean MU force in SOD1^{G93A} transgenic mice were the same for the partially denervated and intact contralateral muscles (Fig. 5C; Supplementary Fig. 2C,F). The data are consistent with our previous findings that TA MU forces in the 60 day old SOD1^{G93A} mouse did not increase significantly to compensate for the age-dependent decline of ~70% in the proportion of intact MUs in the SOD1^{G93A} transgenic mice relative to the SOD^{wt} mice (Hegedus et al., 2007). While there was a trend in that study for a similar increase in MU force, the change was not significant. Since only the motoneurons that supply the small MUs with type I and IIA muscle fibers sustain their sprouting capacity in the SOD1^{G93A} transgenic mouse (Frey et al., 2000; De Winter et al., 2006; Pun et al., 2006), any enlargement of the small proportion of low force MUs with type I and IIA muscle fibers was not detected as reported earlier (Hegedus et al., 2008).

More intact motor units survive in the more active partially denervated muscles of the SOD1^{G93A} mouse to account for the sustained muscle force in the muscles

During the asymptomatic phase of disease prior to 90 days of age, there is a clear decline with age in numbers of intact MUs in the fast-twitch hindlimb muscles of SOD1^{G93A} transgenic mice (black symbols, Figs. 6A, C, E), when compared with the number of MUs in the SOD1^{WT} transgenic mice. Avulsion of the L5 spinal root removed at least 50% of the motor axons that normally innervate the TA, MG and SOL muscles in both SOD^{wt} and SOD1^{G93A} transgenic mice (Figs. 6A, C, E). Given this reduction, it follows that the predicted decline in surviving MUs in the partially denervated muscles of the SOD1^{G93A} transgenic mice should parallel the decline with age seen for each muscle in the hindlimbs supplied by intact spinal roots (gray symbols, Figs. 6A, C, E). The *actual* number of MUs counted in the muscles at 90 days of age after the L5 spinal root avulsion (at 40 days of age) was much greater than the predicted number after their age-dependent decline (open symbols, Figs. 6A, C, E). Indeed, the number of functional MUs after L5 root avulsion was the same as the number for the TA and MG muscles in the hindlimb supplied by both L4 and L5 in the unoperated contralateral hindlimb (Figs. 6B, D). In the SOL muscle, where the reduction in MU numbers after L5 root avulsion was ~35%, the numbers of MUs innervating the partially denervated muscles in the SOD^{G93A} mouse were still greater than predicted. However, the numbers were not as high as in the 90 day old muscles of hindlimbs with intact spinal roots (Fig. 6F). The significant reduction in MU numbers in muscles of the SOD^{wt} mice after L5 root avulsion contrasts with the survival of all MUs in muscles of the SOD1^{G93A} transgenic mice after the L5 avulsion days earlier (Fig. 7).

An additional comparison was made, as shown in Fig. 8 and Supplementary Fig. 3 between MU numbers expected (predicted) after the L5 root avulsion (in gray), and the actual numbers counted in the partially denervated muscles relative to the mean numbers of MUs in the SOD1^{G93A} transgenic mice with intact spinal roots. It is clear that the functional sequelae of the partial denervation of the muscles at 40 days of age sustained the survival of all the MUs that remained (Fig. 8A; Supplementary Fig. 3A,D). It was the sustained numbers of intact MUs, and not an increased force capacity of those MUs (Fig. 8B; Supplementary Fig. 3B,E) that accounted for the contractile forces of the partially denervated muscles equaling the forces of the contralateral muscles whose spinal root innervation remained intact (Fig. 8C; Supplementary Fig. 3C,F).

Partially denervated muscles of the SOD1^{G93A} mouse exhibit phenotypes of more aerobic slower muscle fibers

The selective vulnerability of MUs that contain the type IIB muscle fibers during the asymptomatic phase of disease in SOD^{G93A} transgenic mice was accompanied by increased proportions of type IIA muscle fibers but not with elimination of *all* the type IIB muscle fibers (Hegedus et al., 2007; Hegedus et al., 2008) as was previously claimed by Frey et al. (2000), De Winter et al. (2006), and Pun et al. (2006). The fiber type transition observed in TA muscles of the 60 day old SOD^{G93A} transgenic mice suggested that the increased neuromuscular activity of the surviving MUs accounted for the conversion and, perhaps, in turn, the survival of the active MUs (Hegedus et al., 2008). We asked whether the survival of all intact MUs in partially denervated muscles of the 90 day old SOD1^{G93A} transgenic mouse was accompanied by increased conversion of muscle fibers to more oxidative phenotype.

Examination of the partially denervated TA and MG muscles in the SOD^{G93A} mice showed that, indeed, the muscle fibers at 90 days of age had undergone significant transformation from predominantly type IIB and type IID/X fibers toward increased proportions of type IIA (type IIA are commonly referred to as fast-oxidative fibers) (Pette and Vrbova, 1999). These muscles also displayed increased expression of

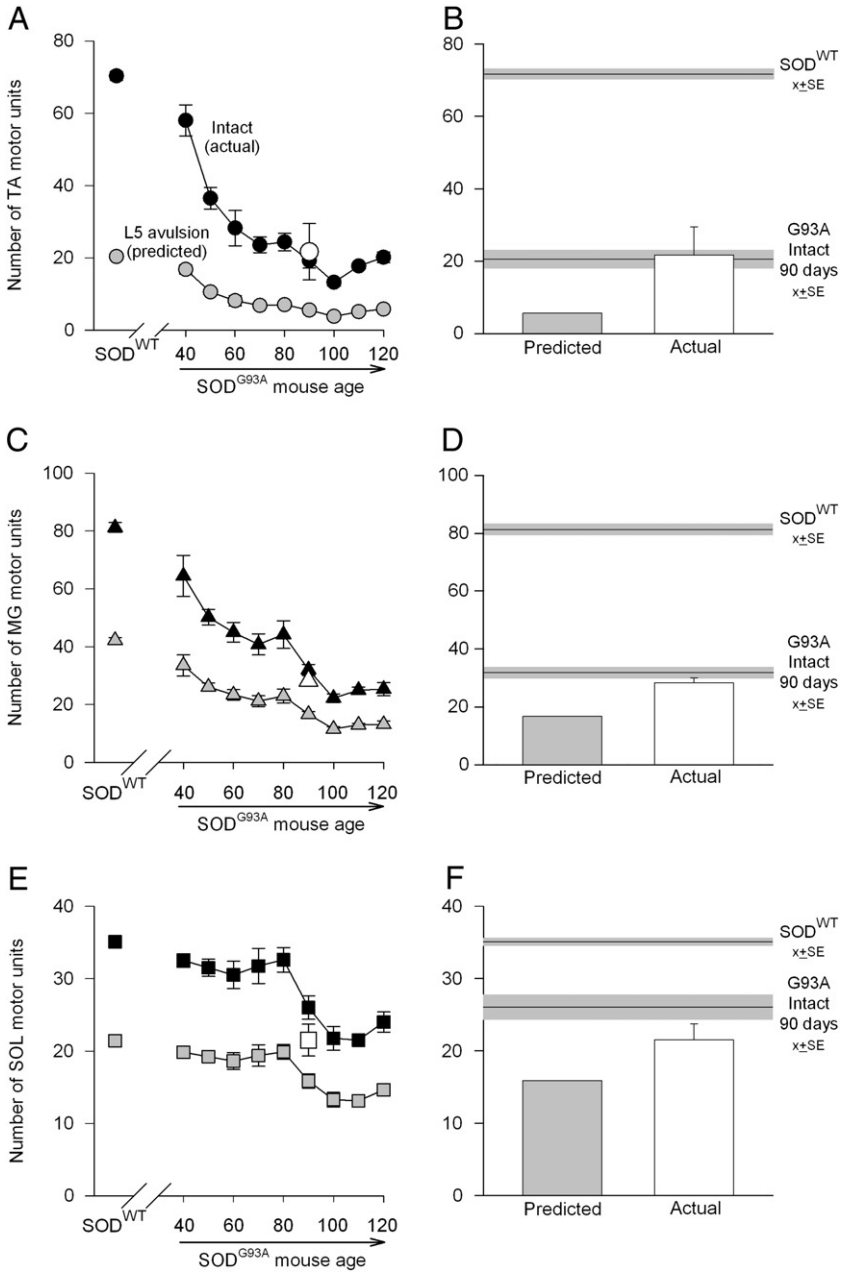


Fig. 6. The mean (+SE) numbers of motor units in partially denervated TA (A, B), MG (C, D) and SOL (E, F) muscles at 90 days of age after L5 root avulsion in SOD1^{G93A} transgenic mice, are compared with the numbers in the mice with intact spinal roots. The reduced number of motor units resulting from avulsion of L5 spinal root is shown for the SOD1^{WT} transgenic mice with the predicted number of motor units in the SOD1^{G93A} transgenic mice plotted as a function of age and compared directly with the mean (+SE) numbers of motor units (A, C, E). The histograms compare the actual motor unit numbers for the muscles with the predicted numbers and demonstrate that for the fast-twitch TA (B) and MG (D) muscles and for the slow-twitch SOL muscle (F), the actual numbers are not significantly different from the numbers recorded in muscles of the SOD1^{G93A} transgenic mice in which all spinal roots were intact (B, D, F). In panels (A, C, E) black symbols represent actual measurements, gray represent predicted measures assuming the same rate of degeneration following partial denervation, and the open symbols represent the actual values measured in partially denervated muscles at 90 days of age.

the slowest MHC-I isoform after L4 spinal root avulsion (Fig. 9). By comparison, expression of MHC-I and MHC-IIA in the EDL muscles also increased, as the fast IID/X and IIB fibers transitioned toward these slower phenotypes (Fig. 9). A trend for an increase in MHC-I were observed in the SOL muscle ($p = 0.06$), probably as this slower isoform was expressed in the IIA fibers.

Discussion

Our major finding was that increased neuromuscular activity prevents the precipitous loss of motor units (MUs) from hindlimb muscles that normally occurs during presymptomatic disease in a transgenic mouse model of ALS. Functional overload of one hindlimb in the SOD1^{G93A} mouse by cutting one of two contributing spinal roots at 40 days of age, results in survival of *all* functional MUs at 90 days as compared to ~30–60% survival without root avulsion. This supports our hypothesis that increased neuromuscular activity "saves" functionally intact MUs. Partial denervation as the model of increased neuromuscular activity, resulted in muscle fiber conversion from type IIB through IID/X to type IIA and I, providing support that these muscles experienced increased MU recruitment.

The findings are consistent with fiber conversion to more oxidative phenotype during the rapid attrition of forceful fast MUs in the SOD1^{G93A} transgenic mouse; lumbosacral motoneurons innervating the fatigable type IIB muscle fibers die-back during asymptomatic disease (Hegedus et al., 2007; Hegedus et al., 2008). Coincident

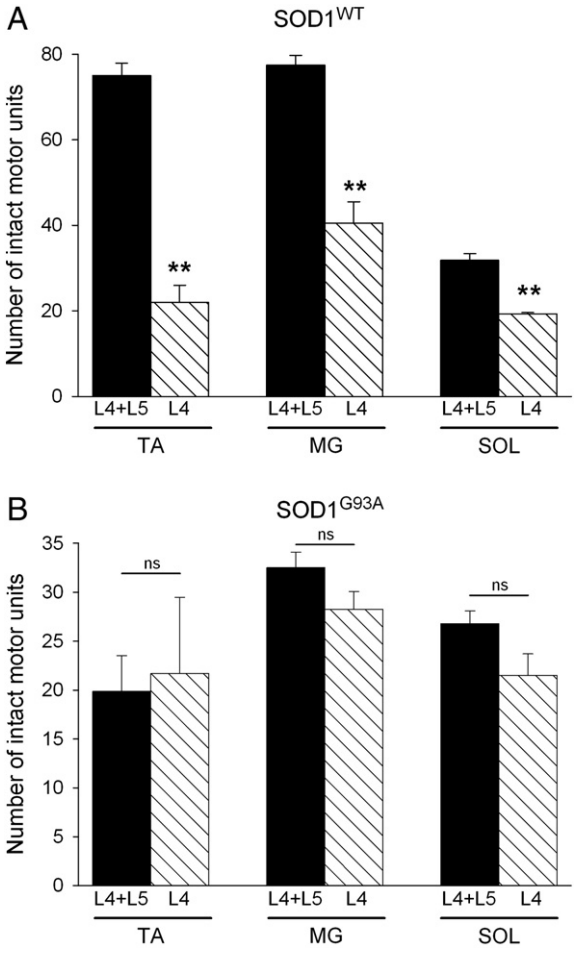


Fig. 7. Comparison of the mean (+SE) number of intact motor units and those remaining in the partially denervated muscles after cutting the L5 spinal root in hindlimb muscles in SOD1^{WT} (A) and the SOD1^{G93A} (B) transgenic mice. **$p<0.01$ and *$p<0.05$.

conversion towards slow phenotype suggested the possibility that the conversion is a positive adaptive response of reduced MU numbers to their increased neuromuscular activity. Indeed, MU numbers plateau during symptomatic disease after 90 days of age (Hegedus et al., 2007) again indicating that increased recruitment of fewer functional MUs is adaptive for survival. Indications from our time course data with the contrasting sensitivity of fast-twitch as compared to slow-twitch muscles were confirmed and expanded by our present findings of parallel conversion of muscle fiber types and 'saving' of the motoneurons innervating more fatigue resistant muscle fibers.

A proportion of muscle fibers is denervated after cutting one ventral root and intramuscular axons of the remaining intact MUs normally sprout to reinnervate denervated muscle fibers: perisynaptic Schwann cells extend processes that bridge between endplates that lead axonal sprouts to innervate denervated endplates (Son and Thompson, 1995a; Son and Thompson, 1995b; Love et al., 2003; Tam and Gordon, 2003a; Gordon et al., 2004a). Sprouting enlarges MUs by including more muscle fibers per motoneuron and in turn, increases their force output (Rafuse et al., 1992; Gordon et al., 1993; Fu and Gordon, 1995; Rafuse and Gordon, 1996a; Rafuse and Gordon, 1996b; Tam and Gordon, 2003a; Gordon et al., 2004a). The observed increased MU forces in the partially denervated muscles of the SOD^{wt} transgenic mice were directly proportional to the reductions of up to 80% in MU numbers, consistent with previous reports of MU enlargement in rodents (Havton et al., 2001; Tam and Gordon, 2003b; Gordon et al., 2004a). The sprouted axons reinnervate all denervated fibers to fully restore muscle twitch and tetanic contractions to normal levels. MU enlargement in the SOD^{wt} transgenic mice was seen in the large MG and TA muscles that were partially denervated by >50% in contrast to the SOL and EDL muscles where the resolution for MU enlargement was insufficient to detect significant increases in MU forces for <50% partial denervation (Rafuse et al., 1992).

MU enlargement was minimal in the partially denervated muscles in the SOD1^{G93A} transgenic mice in contrast to the SOD1^{WT} transgenic mice. This is consistent with immunocytochemical evidence that motor nerves innervating type IIB muscle fibers fail to sprout in the presence of the chemorepellant semaphorin 3A in the terminal Schwann cells at muscle endplates of type IIB fibers of SOD1^{G93A} transgenic mice (Frey et al., 2000; De Winter et al., 2006). Evidence of MU enlargement of less forceful MUs in fast-twitch TA and MG muscles indicated some degree of effective sprouting of the motor nerves supplying type I and IIA muscle fibers. Muscle force is the product of the number and contractile force of its component MUs (Tötösy de Zepetnek et al., 1992). Hence the finding that contractile force in TA and MG muscles in the partially denervated hindlimbs of SOD1^{G93A} transgenic mice was the same as that in the hindlimbs supplied by intact spinal roots (*despite* there being no increase in MU contractile force) was the first indication that the partial denervation of the muscles by root avulsion had "saved" the remaining MUs and prevented their progressive decline in number with age. When the L5 spinal root was avulsed for example, there was a significant reduction of 40–70% in MU numbers in the hindlimb muscles at 40 days of age. The remaining MUs in the partially denervated hindlimb muscles of

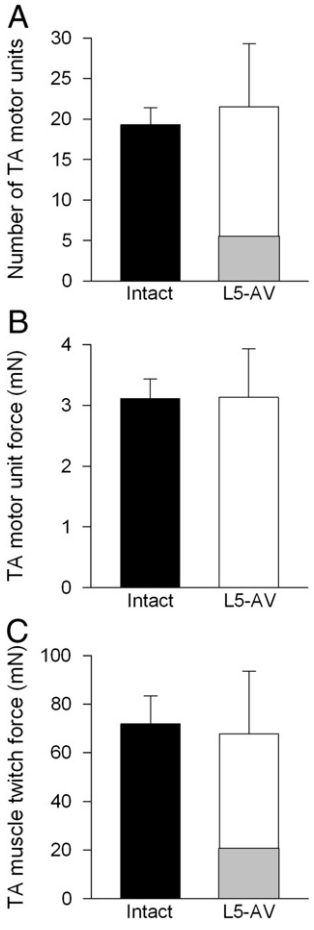


Fig. 8. Partial denervation of hindlimb muscles prevented the normal decline in the numbers of intact motor units in SOD1^{G93A} transgenic mouse. Histograms of the motor unit number + SE (A) motor unit twitch forces (B) and muscle twitch forces (C) in the tibialis anterior muscle of intact hindlimbs at 90 days of age compared with the predicted (gray bars) and the actual (white bar) number of motor units and the recorded TA motor unit and muscle twitch force after L5 spinal root avulsion (L5-AV).

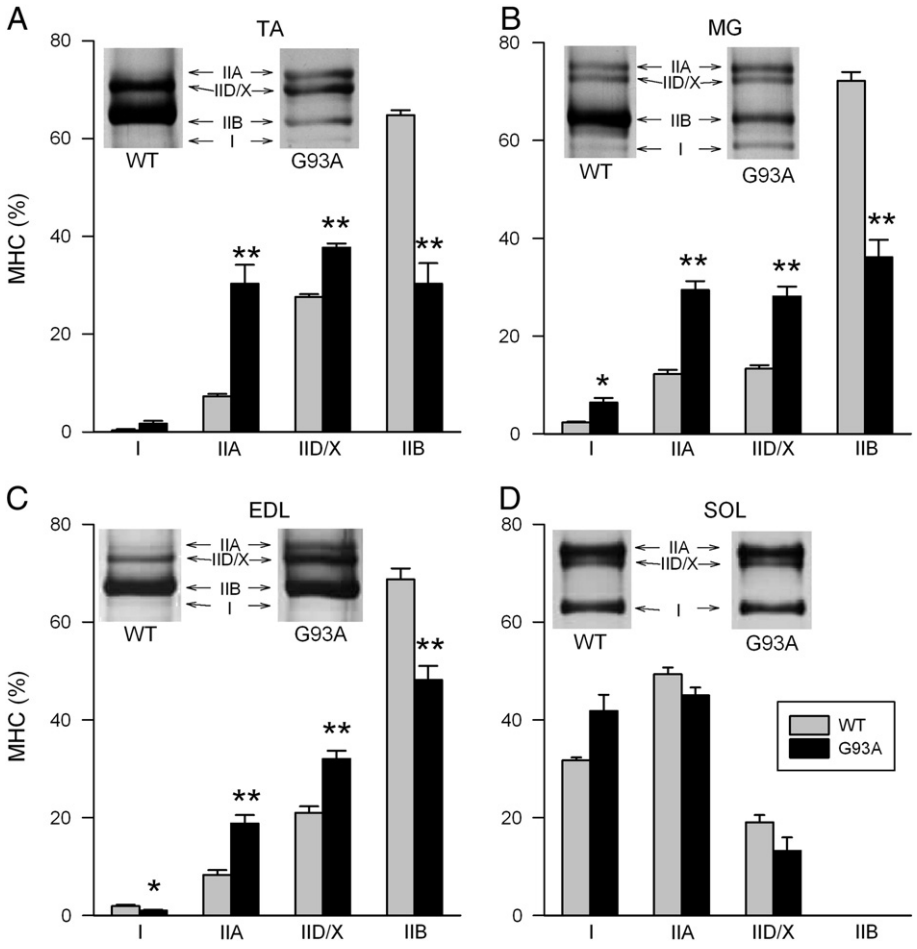


Fig. 9. Myosin heavy chain (MHC) isoforms in partially denervated TA (A), MG (B), EDL (C) and SOL (D) hindlimb muscles in SOD^{WT} and SOD^{G93A} transgenic mice at 90 days of age after avulsion of the L5 spinal root at 40 days of age. $^{**}p<0.01$ and $^{*}p<0.05$.

the $SOD1^{G93A}$ transgenic mice at the time of the avulsion all survived to 90 days of age. Importantly, the number of surviving functionally intact MUs in the partially denervated hindlimbs supplied by one of two spinal roots at 90 days of age was not significantly different from the number in the intact hindlimbs where the muscles were innervated by both spinal roots (Figs. 6 and 7). The considerable fiber type conversion from type IIB through to type IIA and I in the partially denervated muscles demonstrated that there was indeed, increased recruitment of the smaller motoneuron pool during asymptomatic disease that resulted in striking survival of functional MUs.

One cohesive explanation for the activity-induced fiber type conversion toward type IIA and I concurrent with sustained survival of MUs in the partially denervated hindlimbs of the $SOD1^{G93A}$ transgenic mouse is the evidence (1) for activity-dependent decline in axon size (Gordon et al., 1997) and (2) that more motoneurons survive in the $SOD1^{G93A}$ transgenic mouse after axotomy (Kong and Xu, 1999) when the caliber of the axons central to the site of nerve transection declines (Davis et al., 1978; Gordon, 1983; Gordon et al., 1991). Electrical stimulation of motoneurons and their muscle units for 12 h of each day promotes a type IIB to I transition in muscle fiber types and slow and less forceful muscle and MU contractions that do not fatigue. In addition, the activity induces a rapid decline in nerve conduction velocities and conversion of motoneuron electrical properties from fast to slow (Gordon et al., 1997; Munson et al., 1997; Gordon et al., 2004b). Conduction velocity is directly proportional to nerve fiber size such that the reduced conduction velocities reflect reduced size of the nerve fibers. It follows that the conversion from type IIB to IIA and I in the muscles in $SOD1^{G93A}$ transgenic mice is paralleled by changes in the motoneuron properties including reduced size of the motoneurons and their axons. Findings that axon diameters decline significantly after partial denervation (Havton et al., 2001) concur with the conclusion that the nerve fiber calibers decline in parallel with type IIB→type IIA and I muscle fiber conversion after partial denervation. Therefore, the preferential survival of the MUs with smaller axons during the lifespan of the $SOD1^{G93A}$ transgenic mouse and our new evidence for the survival of the more active MUs in partially denervated hindlimbs that convert progressively from type IIB to IIA and I, may be related, at least in part to their smaller axons. Moreover, the paradoxical finding that cutting the peripheral nerve (axotomy) in $SOD1^{G93A}$ transgenic mice actually increased the survival of ventral root axons is a second line of evidence that motoneurons with small axons survive better than larger axons in the $SOD1^{G93A}$ transgenic mouse (Kong and Xu, 1999). Consistent with these two lines of evidence, a plateau in numbers of functional MUs was reached at 100–110 days of age during the symptomatic disease after the rapid decline in MU numbers during the asymptomatic phase and progressive loss of the MUs containing the type IIB and IID/X muscle fibers (Hegedus et al., 2007). Yet reduced neurofilament content and smaller motor nerve fibers in the SOD^{G37R} transgenic mouse model of ALS where one allele of each neurofilament gene was disrupted did not alleviate motor axon loss (Nguyen et al., 2000). Alternative explanations including activity-dependent changes in gene expression in the neurons will have to be considered for the "saving" of functional motor units by partial denervation and/or axotomy. Motoneurons that supply type IIB and

IID/X muscle fibers have been referred to as vulnerable as opposed to those non-vulnerable motoneurons supplying type IIA and I fibers (Saxena et al., 2009). An exciting finding was that, in three transgenic mouse models, the vulnerable motoneurons upregulate endoplasmic reticulum (ER) stress markers prior to muscle fiber denervation while the non-vulnerable motoneurons do not. Perhaps the activity-dependent type IIB to type IIA and I by partial denervation in this study might reduce ER stress sufficiently to promote survival of functionally intact motor units. This possibility is imminently testable.

Conflicting data on the effects of imposed exercise programs on disease progression in mouse models and human ALS (Chung et al., 1992; Drory et al., 2001; Scarmeas et al., 2002; Krivickas, 2003; Chio et al., 2005; Kaspar et al., 2005) are likely explained by the different types of exercise and the effects that they mediate on muscle fiber composition. Daily amount and not pattern of activity determines muscle fiber composition: >5% daily activity converted muscle fibers from type IIB to type I, daily activity of <5% converted fibers to type IIA, and <0.5% daily activity favors type IIB fibers (Donselaar et al., 1987; Kernell et al., 1987; Kernell and Eerbeek, 1988; Gordon and Pattullo, 1993). Orderly MU recruitment from small slow fatigue resistant to the largest fatigable MUs favors isometric muscle contractions during postural movements with progressive recruitment and hence activation of the largest and fastest MUs during movements that overcome gravity and move limbs (Gordon and Pattullo, 1993; Gordon et al., 2004b). Consequently, our findings of survival of MUs with fatigue resistant muscle fibers in $SOD1^{G93A}$ transgenic mice indicate that daily low frequency activation for at least 5% of each day rather than exercises promoting brief high activation rates could benefit ALS patients by prolonging MU survival. The motor deficits and hastened disease onset in $SOD1^{G93A}$ transgenic mice that were exercised in short high intensity bursts (Mahoney et al., 2004) concur.

Acknowledgments

Our grateful thanks to the Canadian Institutes of Health Research and the Canadian Amyotrophic Lateral Sclerosis Society of Canada for their generous support of our work. We would like to thank Dr. Kelvin Jones for his much appreciated help in editing the manuscript. The word comprises a component of the PhD thesis of JH obtained from the University of Alberta. TG is an Alberta Heritage Foundation for Medical Research (AHFMR) Senior Investigator; CP is an AHFMR senior scholar.

Appendix A. Supplementary data

Supplementary data associated with this article can be found, in the online version, at doi:10.1016/j.nbd.2009.10.021.

References

Boillee, S., Vande, V.C., Cleveland, D.W., 2006. ALS: a disease of motor neurons and their nonneuronal neighbors. Neuron 52, 39–59.
Chio, A., Benzi, G., Dossena, M., Mutani, R., Mora, G., 2005. Severely increased risk of amyotrophic lateral sclerosis among Italian professional football players. Brain 128, 472–476.
Chiu, A.Y., Zhai, P., Dal Canto, M.C., Peters, T.M., Kwon, Y.W., Prattis, S.M., Gurney, M.E., 1995. Age-dependent penetrance of disease in a transgenic mouse model of familial amyotrophic lateral sclerosis. Mol. Cell. Neurosci. 6, 349–362.
Chung, J.M., Leem, J.W., Kim, S.H., 1992. Somatic afferent fibers which continuously discharge after being isolated from their receptors. Brain Res. 599, 29–33.
Cleveland, D.W., 1999. From Charcot to SOD1: mechanisms of selective motor neuron death in ALS. Neuron 24, 515–520.
Davis, L.A., Gordon, T., Hoffer, J.A., Jhamandas, J., Stein, R.B., 1978. Compound action potentials recorded from mammalian peripheral nerves following ligation or resuturing. J. Physiol. 285, 543–559.
De Winter, F., Vo, T., Stam, F.J., Wisman, L.A., Bar, P.R., Niclou, S.P., van Muiswinkel, F.L., Verhaagen, J., 2006. The expression of the chemorepellent Semaphorin 3A is selectively induced in terminal Schwann cells of a subset of neuromuscular synapses that display limited anatomical plasticity and enhanced vulnerability in motor neuron disease. Mol. Cell. Neurosci. 32, 102–117.
Donselaar, Y., Eerbeek, O., Kernell, D., Verhey, B.A., 1987. Fibre sizes and histochemical staining characteristics in normal and chronically stimulated fast muscle of cat. J. Physiol. 382, 237–254.
Drory, V.E., Goltsman, E., Reznik, J.G., Mosek, A., Korczyn, A.D., 2001. The value of muscle exercise in patients with amyotrophic lateral sclerosis. J. Neurol. Sci. 191, 133–137.
Einsiedel, L.J., Luff, A.R., 1994. Activity and motor unit size in partially denervated rat medial gastrocnemius. J. Appl. Physiol. 76, 2663–2671.
Fischer, L.R., Culver, D.G., Tennant, P., Davis, A.A., Wang, M., Castellano-Sanchez, A., Khan, J., Polak, M.A., Glass, J.D., 2004. Amyotrophic lateral sclerosis is a distal axonopathy: evidence in mice and man. Exp. Neurol. 185, 232–240.
Frey, D., Schneider, C., Xu, L., Borg, J., Spooren, W., Caroni, P., 2000. Early and selective loss of neuromuscular synapse subtypes with low sprouting competence in motoneuron diseases. J. Neurosci. 20, 2534–2542.
Fu, S.Y., Gordon, T., 1995. Contributing factors to poor functional recovery after delayed nerve repair: prolonged denervation. J. Neurosci. 15, 3886–3895.
Gallo, M., Gordon, T., Tyreman, N., Shu, Y., Putman, C.T., 2004. Reliability of isolated isometric function measures in rat muscles composed of different fibre types. Exp. Physiol. 89, 583–592.
Gordon, T., 1983. Dependence of peripheral nerves on their target organs. In: Burnstock, G, O'Brien, R, Vrbova, G (Eds.), Somatic and autonomic nerve-muscle interactions. Elsevier, Amsterdam, pp. 289–316.
Gordon, T., Pattullo, M.C., 1993. Plasticity of muscle fiber and motor unit types. Exerc. Sport Sci. Rev. 21, 331–362.
Gordon, T., Yang, J.F., Ayer, K., Stein, R.B., Tyreman, N., 1993. Recovery potential of muscle after partial denervation: a comparison between rats and humans. Brain Res. Bull. 30, 477–482.
Gordon, T., Gillespie, J., Orozco, R., Davis, L., 1991. Axotomy-induced changes in rabbit hindlimb nerves and the effects of chronic electrical stimulation. J. Neurosci. 11, 2157–2169.
Gordon, T., Tyreman, N., Rafuse, V.F., Munson, J.B., 1997. Fast-to-slow conversion following chronic low-frequency activation of medial gastrocnemius muscle in cats: 1. Muscle and motor unit properties. J. Neurophysiol. 77, 2585–2604.
Gordon, T., Hegedus, J., Tam, S.L., 2004a. Adaptive and maladaptive motor axonal sprouting in aging and motoneuron disease. Neurol. Res. 26, 174–185.
Gordon, T., Thomas, C.K., Munson, J.B., Stein, R.B., 2004b. The resilience of the size principle in the organization of motor unit properties in normal and reinnervated adult skeletal muscles. Can. J. Physiol. Pharmacol. 82, 645–661.
Gordon, T., Tam, S.L., Sharp, P.S., Hegedus, J., 2005. Progressive die-back and death of motoneurons in transgenic mouse model of ALS. Biocybern. Biomed. Eng. 25, 17–26.
Gordon, T., Ly, V., Hegedus, J., Tyreman, N., 2008. Early detection of denervated muscle fibers in hindlimb muscles after sciatic nerve transection in wild type mice and in the G93A mouse model of amyotrophic lateral sclerosis. Neurol. Res. 31, 28–42.
Gurney, M.E., Pu, H., Chiu, A.Y., Dal Canto, M.C., Polchow, C.Y., Alexander, D.D., Caliendo, J., Hentati, A., Kwon, Y.W., Deng, H.X., 1994. Motor neuron degeneration in mice that express a human Cu,Zn superoxide dismutase mutation. Science 264, 1772–1775.
Havton, L.A., Hotson, J.R., Kellerth, J.O., 2001. Partial peripheral motor nerve lesions induce changes in the conduction properties of remaining intact motoneurons. Muscle Nerve 24, 662–666.
Hegedus, J., Putman, C.T., Gordon, T., 2007. Time course of preferential motor unit loss in the SOD1(G93A) mouse model of amyotrophic lateral sclerosis. Neurobiol. Dis. 28, 154–164.
Hegedus, J., Putman, C.T., Tyreman, N., Gordon, T., 2008. Preferential motor unit loss in the $SOD1^{G93A}$ transgenic mouse model of amyotrophic lateral sclerosis. J. Physiol. 586, 3337–3351.
Hegedus, J., Jones, K.E., Gordon, T., 2009a. Development and use of the incremental twitch subtraction MUNE method in mice. Clin. Neurophysiol. Suppl. (Motor Unit Number Estimation (MUNE) and Quantitative EMG) 209–217.
Hegedus, J., Putman, C.T., Gordon, T., 2009b. Progressive motor unit loss in the G93A mouse model of amyotrophic lateral sclerosis is unaffected by gender. Muscle Nerve 39, 318–327.
Henneman, E., Olson, C.B., 1965. Relations between structure and function in the design of skeletal muscles. J. Neurophysiol. 28, 581–598.
Henneman, E., Somjen, G., Carpenter, D.O., 1965. Functional significance of cell size in spinal motoneurons. J. Neurophysiol. 28, 560–580.
Julien, J.P., Kriz, J., 2006. Transgenic mouse models of amyotrophic lateral sclerosis. Biochim. Biophys. Acta 1762, 1013–1024.
Kaspar, B.K., Frost, L.M., Christian, L., Umapathi, P., Gage, F.H., 2005. Synergy of insulin-like growth factor-1 and exercise in amyotrophic lateral sclerosis. Ann. Neurol. 57, 649–655.
Kawamura, Y., Dyck, P.J., Shimono, M., Okazaki, H., Tateishi, J., Doi, H., 1981. Morphometric comparison of the vulnerability of peripheral motor and sensory neurons in amyotrophic lateral sclerosis. J. Neuropathol. Exp. Neurol. 40, 667–675.
Kernell, D., Eerbeek, O., 1988. Different rates of long-term motor-nerve stimulation produce different effects on muscle properties. Muscle Nerve 11, 89–90.
Kernell, D., Eerbeek, O., Verhey, B.A., Donselaar, Y., 1987. Effects of physiological amounts of high- and low-rate chronic stimulation on fast-twitch muscle of the cat hindlimb: I. Speed- and force-related properties. J. Neurophysiol. 58, 598–613.
Kong, J., Xu, Z., 1999. Peripheral axotomy slows motoneuron degeneration in a transgenic mouse line expressing mutant SOD1 G93A. J. Comp. Neurol. 412, 373–380.
Krivickas, L.S., 2003. Exercise in neuromuscular disease. J. Clin. Neuromuscul. Dis. 5, 29–39.
Love, F.M., Son, Y.J., Thompson, W.J., 2003. Activity alters muscle reinnervation and terminal sprouting by reducing the number of schwann cell pathways that grow to link synaptic sites. J. Neurobiol. 54, 566–576.

Mahoney, D.J., Rodriguez, C., Devries, M., Yasuda, N., Tarnopolsky, M.A., 2004. Effects of high-intensity endurance exercise training in the G93A mouse model of amyotrophic lateral sclerosis. Muscle Nerve 29, 656–662.
Major, L.A., Hegedus, J., Weber, D.J., Gordon, T., Jones, K.E., 2007. Method for counting motor units in mice and validation using a mathematical model. J. Neurophysiol. 97, 1846–1856.
Munson, J.B., Foehring, R.C., Mendell, L.M., Gordon, T., 1997. Fast-to-slow conversion following chronic low-frequency activation of medial gastrocnemius muscle in cats: II. Motoneuron properties. J. Neurophysiol. 77, 2605–2615.
Nguyen, M.D., Lariviere, R.C., Julien, J.P., 2000. Reduction of axonal caliber does not alleviate motor neuron disease caused by mutant superoxide dismutase 1. Proc. Natl. Acad. Sci. U. S. A. 97, 12306–12311.
Oakley, B.R., Kirsch, D.R., Morris, N.R., 1980. A simplified ultrasensitive silver stain for detecting proteins in polyacrylamide gels. Anal. Biochem. 105, 361–363.
Parkhouse, W.S., Cunningham, L., McFee, I., Miller, J.M., Whitney, D., Pelech, S.L., Krieger, C., 2008. Neuromuscular dysfunction in the mutant superoxide dismutase mouse model of amyotrophic lateral sclerosis. Amyotroph. Lateral Scler. 9, 24–34.
Pette, D., Vrbova, G., 1999. What does chronic electrical stimulation teach us about muscle plasticity? Muscle Nerve 22, 666–677.
Pun, S., Santos, A.F., Saxena, S., Xu, L., Caroni, P., 2006. Selective vulnerability and pruning of phasic motoneuron axons in motoneuron disease alleviated by CNTF. Nat. Neurosci. 9, 408–419.
Rafuse, V.F., Gordon, T., 1996a. Self-reinnervated cat medial gastrocnemius muscles: I. Comparisons of the capacity of regenerating nerves to form enlarged motor units after extensive peripheral nerve injuries. J. Neurophysiol. 75, 268–281.
Rafuse, V.F., Gordon, T., 1996b. Self-reinnervated cat medial gastrocnemius muscles: II. Analysis of the mechanisms and significance of fiber type grouping in reinnervated muscles. J. Neurophysiol. 75, 282–297.
Rafuse, V.F., Gordon, T., Orozco, R., 1992. Proportional enlargement of motor units after partial denervation of cat triceps surae muscles. J. Neurophysiol. 68, 1261–1275.
Rakhit, R., Robertson, J., Velde, C.V., Horne, P., Ruth, D.M., Griffin, J., Cleveland, D.W., Cashman, N.R., Chakrabartty, A., 2007. An immunological epitope selective for pathological monomer-misfolded SOD1 in ALS. Nat. Med. 13, 754–759.
Rosen, D.R., 1993. Mutations in Cu/Zn superoxide dismutase gene are associated with familial amyotrophic lateral sclerosis. Nature 364, 362.
Rowland, L.P., Shneider, N.A., 2001. Amyotrophic lateral sclerosis. N. Engl. J. Med. 344, 1688–1700.
Saxena, S., Cabuy, E., Caroni, P., 2009. A role for motoneuron subtype-selective ER stress in disease manifestations of FALS mice. Nat. Neurosci. 12, 627–636.
Scarmeas, N., Shih, T., Stern, Y., Ottman, R., Rowland, L.P., 2002. Premorbid weight, body mass, and varsity athletics in ALS. Neurol 59, 773–775.
Schulte-Mattler, W.J., Georgiadis, D., Tietze, K., Zierz, S., 2000. Relation between maximum discharge rates on electromyography and motor unit number estimates. Muscle Nerve 23, 231–238.
Seburn, K.L., Gardiner, P.F., 1996. Properties of sprouted rat motor units: effects of period of enlargement and activity level. Muscle Nerve 19, 1100–1109.
Son, Y.J., Thompson, W.J., 1995a. Nerve sprouting in muscle is induced and guided by processes extended by Schwann cells. Neuron 14, 133–141.
Son, Y.J., Thompson, W.J., 1995b. Schwann cell processes guide regeneration of peripheral axons. Neuron 14, 125–132.
Tam, S.L., Archibald, V., Tyreman, N., Jassar, B., Gordon, T., 2001. Increased neuromuscular activity reduces sprouting in partially denervated muscles. J. Neurosci. 21, 654–667.
Tam, S.L., Gordon, T., 2003a. Mechanisms controlling axonal sprouting at neuromuscular junction. J. Neurocyto. Invited Review 32, 961–974.
Tam, S.L., Gordon, T., 2003b. Neuromuscular activity impairs axonal sprouting in partially denervated muscles by inhibiting bridge formation of perisynaptic Schwann cells. J. Neurobiol. 57, 221–234.
Tötösy de Zepetnek, J.E., Zung, H.V., Erdebil, S., Gordon, T., 1992. Innervation ratio is an important determinant of force in normal and reinnervated rat tibialis anterior muscles. J. Neurophysiol. 67, 1385–1403.
Tyc, F., Vrbova, G., 2007. Modification of motoneuron size after partial denervation in neonatal rats. Arch. Ital. Biol. 145, 337–344.
Veldink, J.H., Bar, P.R., Joosten, E.A., Otten, M., Wokke, J.H., van den Berg, L.H., 2003. Sexual differences in onset of disease and response to exercise in a transgenic model of ALS. Neuromuscul. Disord. 13, 737–743.
Williamson, T.L., Cleveland, D.W., 1999. Slowing of axonal transport is a very early event in the toxicity of ALS-linked SOD1 mutants to motor neurons. Nat. Neurosci. 2, 50–56.
Yang, J.F., Stein, R.B., Jhamandas, J., Gordon, T., 1990. Motor unit numbers and contractile properties after spinal cord injury. Ann. Neurol. 28, 496–502.